Leopoldina
Nationale Akademie
der Wissenschaften

NOVA ACTA LEOPOLDINA

Neue Folge | Band 121 | Nummer 408

# Deglacial Changes in Ocean Dynamics and Atmospheric $CO_2$

Michael Sarnthein and Gerald H. Haug (Eds.)

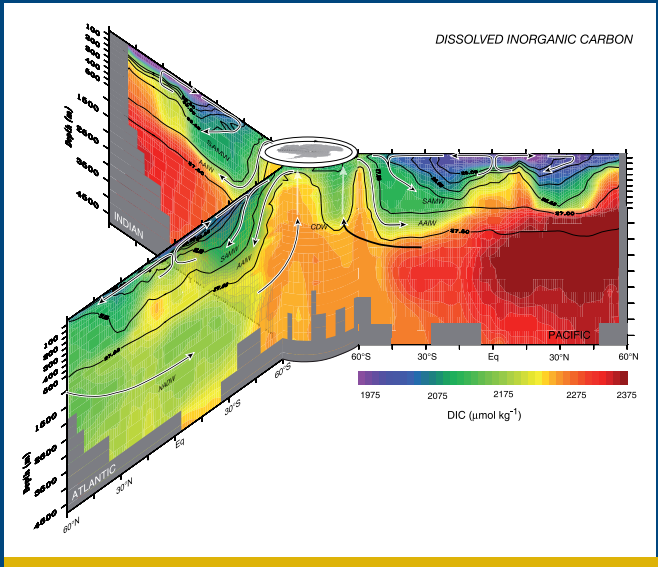


Deutsche Akademie der Naturforscher Leopoldina –
Nationale Akademie der Wissenschaften, Halle (Saale) 2015

Wissenschaftliche Verlagsgesellschaft Stuttgart

# NOVA ACTA LEOPOLDINA

Abhandlungen der Deutschen Akademie der Naturforscher Leopoldina

Herausgegeben von Jörg HACKER, Präsident der Akademie

NEUE FOLGE NUMMER 408 BAND 121


# Deglacial Changes in Ocean Dynamics and Atmospheric $CO_2$

## Modern, Glacial, and Deglacial Carbon Transfer between Ocean, Atmosphere, and Land

Leopoldina Symposium
Halle (Saale)
18 – 21 March 2015


Editors:

Michael SARNTHEIN (Kiel)
Member of the Leopoldina

Gerald H. HAUG (Zürich)
Member of the Leopoldina

In Cooperation with
Edouard BARD (Aix-en-Provence), Hubertus FISCHER (Bern),
Tatiana ILYINA (Hamburg), and Michael SCHULZ (Bremen)


With 116 Figures and 2 Tables


**Deutsche Akademie der Naturforscher Leopoldina –
Nationale Akademie der Wissenschaften, Halle (Saale) 2015
Wissenschaftliche Verlagsgesellschaft Stuttgart**

Redaktion: Dr. Michael Kaasch und Dr. Joachim Kaasch

**Die Schriftenreihe Nova Acta Leopoldina erscheint bei der Wissenschaftlichen Verlagsgesellschaft Stuttgart, Birkenwaldstraße 44, 70191 Stuttgart, Bundesrepublik Deutschland.**
**Jedes Heft ist einzeln käuflich.**

Die Schriftenreihe wird gefördert durch das Bundesministerium für Bildung und Forschung sowie das Ministerium für Wissenschaft und Wirtschaft des Landes Sachsen-Anhalt.

Cover:
Global distribution of Dissolved Inorganic Carbon. The 3-D scheme combines vertical meridional sections across the Atlantic (*left*), Pacific (*right*), and Indian Ocean (*to the back*) with the Antarctic continent in the center. Also shown are the major currents, water masses, and density layers. The interaction between the large-scale ocean circulation and the biological pump creates strong vertical and horizontal gradients, with the highest DIC concentrations found in the deep North Atlantic, while the surface ocean is generally depleted. Modifications of this strong vertical and horizontal redistribution of DIC are key for sequestering or releasing the $CO_2$ needed to drive the glacial-interglacial changes in atmospheric $CO_2$. (Author: Niki Gruber, ETH Zürich)

**Bibliografische Information der Deutschen Nationalbibliothek**
Die Deutsche Nationalbibliothek verzeichnet diese Publikation in der Deutschen Nationalbibliografie; detaillierte bibliografische Daten sind im Internet über http//dnb.ddb.de abrufbar.

Die Abkürzung ML hinter dem Namen der Autoren steht für Mitglied der Deutschen Akademie der Naturforscher Leopoldina – Nationale Akademie der Wissenschaften.


Postadresse: Jägerberg 1, 06108 Halle (Saale), Postfachadresse: 110543, 06019 Halle (Saale)
Hausadresse der Redaktion: Emil-Abderhalden-Straße 37, 06108 Halle (Saale)
Tel.: +49 345 47239134, Fax: +49 345 47239139
Herausgeber: Prof. Dr. Dr. h. c. mult. Jörg Hacker, Präsident der Deutschen Akademie der Naturforscher Leopoldina – Nationale Akademie der Wissenschaften
Printed in Germany 2015
Gesamtherstellung: Druck Zuck GmbH
ISBN: 978-3-8047-3433-3
ISSN: 0369-5034
Gedruckt auf chlorfrei gebleichtem Papier.

# Contents

**Poster**

# Introduction

About 35 years ago ice core-based records have first revealed the dramatic glacial-to-interglacial changes in the atmospheric $CO_2$ content. In view of the modern men-made rise in atmospheric $CO_2$ these natural changes ever more belong to the hottest topics in the study of the Earth's carbon cycle. Since the 1980s an enormous and rapidly ever growing wealth of scientific findings and models has been published, that uncover the role of carbon exchange between the largest reservoir on Earth, the global ocean, and those in the atmosphere and on land, studies that clearly urge for an overview and broad synthesis.

The present symposium on "Deglacial Ocean Dynamics and Atmospheric $CO_2$" has brought together a global community of almost 50 leading scientists and 20 early-career scientists, which provide a platform capable of identifying limitations in the representation of key carbon-cycle processes in models, that control the carbon exchange amongst the four major carbon pools of the Earth's surface, the ocean, atmosphere, terrestrial biosphere, and soils. As listed in the program the symposium evaluates empiric and model-based findings on changing past carbon inventories as well as on past modes, locations, and rates of carbon transfer. In particular, the carbon transfer for modern, that is 'pre-industrial', times is compared with two distinct past climate states, the Last Glacial Maximum (LGM) and deglacial times. In turn, past natural changes in carbon flux may be compared with potential man-made changes today.

A calculated transfer of ~530 Gt of $^{14}C$ depleted carbon is required to produce the deglacial coeval rise of carbon in the atmosphere and terrestrial biosphere and in soils. While a number of key processes underlying this transfer have been identified, Earth-system models are still unable to fully reproduce it. Most likely, this transfer was linked to changes in the ventilation of the deep ocean, the largest carbon pool on the Earth's surface. Accordingly, the failure to correctly represent the carbon transfer in complex models raises several **important scientific questions**, in particular, (*i*) whether deep-ocean ventilation was significantly reduced during the last glacial period, (*ii*) how and where to trace empirical evidence for a deglacial carbon release from the ocean, (*iii*) how to reconcile the carbon release with major shifts in atmospheric radiocarbon contents, and (*iv*) how to test the various alternative carbon sources and mechanisms that may have controlled the last-glacial-to-interglacial shifts in $\Delta^{14}C$ and $CO_2$, the most prominent short-term change in carbon pools over the last 100,000 years.

The present volume contains almost 70 extended abstracts on the latest state of the art in the outlined fields of $CO_2$ research. Most abstracts provide some figures and key references that may help the interested reader to enter more deeply the fields of research in question. The abstracts of oral and poster presentations are printed in alphabetic order. With regards to contents the abstract titles of oral contributions are linked to the various carbon archives in polar ice sheets, the ocean, and on land, and to various, largely overlapping scientific approaches and objectives as listed in the Conference Program at the beginning of this volume.

*Acknowledgments*

The symposium organizers acknowledge the generous support of the *Leopoldina* German National Academy of Sciences, the *Deutsche Forschungsgemeinschaft* in Bonn (DFG), the Kiel Excellence Cluster 'The Future Ocean', and *IMAGES* (International Marine Past Global Change Study). Further funds were made available by MPI Hamburg, MARUM Bremen, ETH Zürich (CH), and the Oeschger Center for Climate Change Research in Bern (CH). The publication of this volume would not have been possible without the dedicated help of Michael and Joachim Kaasch and their publisher's group at the *Leopoldina*.

Michael Sarnthein ML and Gerald H. Haug ML,
Edouard Bard, Hubertus Fischer, Tatiana Ilyina, and Michael Schulz

# Symposium Programme

## Wednesday, 18 March 2015

8:30 a.m. **Welcome**

### General and Modern-Ocean Issues

9:00 a.m. **Keynote**
**Andrew J. Watson** p. 247
College of Life and Environmental Sciences, University of Exeter
***Southern Ocean Overturning, Controlled by Wind or Buoyancy Flux? Unterstanding the Link between Antarctic Temperatures and Atmospheric $CO_2$***

9:45 a.m. **Jelle Bijma** p. 35
Marine Biogeosciences, Alfred Wegener Institute Bremerhaven
***Ocean Acidification – A Biogeological Perspective***

10:15 a.m. **Andreas Oschlies** p. 171
GEOMAR Helmholtz Centre for Ocean Research Kiel
***Robustness and Uncertainties of Current Marine Carbon Cycle Models***

10:45 a.m. Coffee Break

11:15 a.m. **Nicolas Gruber** p. 85
Institute of Biochemistry and Pollutant Dynamics, ETH Zürich
***The Global Ocean Carbon Sink: Recent Trends and Variability***

### Ice Core Records

11:45 a.m. **Jean Jouzel** p. 123
Laboratoire des Sciences du Climat et de l'Environnement, Gif-sur-Yvette
***Ice Core Records: Climate Reconstruction***

12:15 p.m. **Dominique Raynaud** p. 191
Laboratoire de Glaciologie et Géophysique de l'Environnement (LGGE) Grenoble
***The Ice Core Record of $CO_2$ – A Focus on the Climate/$CO_2$ Phase Relationship during Deglacial Transitions***

12:45 p.m. **Gerald H. Haug** p. 93
Department of Earth Sciences, Geological Institute, ETH Zürich
***The Polar Oceans during the Deglaciation***

13:15 p.m. Lunch and Coffee

14:00 p.m. **Poster** pp. 259–350

16:00 p.m. **Shaun A. Marcott** p. 149
Department of Geoscience, University of Wisconsin-Madison
***Abrupt Changes in the Global Carbon Cycle over the Past 70 ka***

16:30 p.m. **Jochen Schmitt** p. 201
Physics Institute and Oeschger Centre for Climate Change Research, University of Bern
***Atmospheric $\delta^{13}CO_2$ from Ice Cores: An Overloaded Parameter***

17:00 p.m. **Fortunat Joos** p. 117
Physics Institute and Oeschger Centre for Climate Change Research, University of Bern
***Mechanisms and Multi-Tracer Fingerprints of Past Carbon Cycle Changes in the Bern3D-LPX Model***

17:30 p.m. **Ed Brook and Thomas Bauska** p. 39
College of Earth, Ocean, and Atmospheric Sciences, Oregon State University, Corvallis, OR
***Isotopic Constraints on Greenhouse Gas Variability during the Last Deglaciation from Blue Ice Archives***

18:00 p.m. **Keynote**
**Hubertus Fischer** p. 59
Physics Institute and Oeschger Centre for Climate Change Research, University of Bern
***Latest Insights into Past Carbon Cycle Changes from $CO_2$ and $\delta^{13}C_{atm}$***

## Thursday, 19 March 2015

### N Pacific and S Ocean Records

9:00 a.m. **Keynote**
**Ralf Tiedemann** p. 229
Alfred Wegener Institute, Helmholtz Centre for Polar and Marine Research, Bremerhaven
***New Constraints on the Glacial Extent of the Pacific Carbon Pool and its Deglacial Outgassing***

9:45 a.m. **Andrea Burke** p. 49
Department of Earth and Environmental Sciences, University of St Andrews
***Radiocarbon Constraints on Southern Ocean Circulation***

10:15 a.m. **Luke C. Skinner** p. 217
Godwin Laboratory for Palaeoclimate Research, University of Cambridge, UK
***On the Glacial Ocean Circulation and its Impact on the Global Radiocarbon and Carbon Cycles***

10:45 a.m. Coffee Break

## Atlantic and Whole Ocean

11:15 a.m. **Andreas Schmittner** p. 207
College of Earth, Ocean, and Atmospheric Sciences, Oregon State University, Corvallis, OR
***Was the Early Deglacial $CO_2$ Rise Caused by a Reduction of the Atlantic Overturning Circulation?***

11:45 a.m. **Jess Adkins** p. 21
California Institute of Technology, Pasadena, CA
***Radiocarbon (and Other) Constraints on the Transition from Glacial Maximum to the Holocene***

12:15 p.m. **David J. R. Thornalley** p. 223
Woods Hole Oceanographic Institution, University College London
***Reconstructing Deglacial Circulation Changes in the Northern North Atlantic and Nordic Seas: $\Delta^{14}C$, $\delta^{13}C$, Temperature, and $\delta^{18}OSW$ Evidence***

12:45 p.m. **Gerrit Lohmann** p. 141
Alfred Wegener Institute, Helmholtz Centre for Polar and Marine Research, Bremerhaven
***Abrupt Climate Change Experiments: The Bølling/Allerød Transition***

13:15 p.m. Lunch and Coffee

14:00 p.m. **Poster** pp. 259–350

16:00 p.m. **I. Nicholas McCave** p. 155
Godwin Laboratory for Palaeoclimate Research, University of Cambridge, UK
***A Carbon Isotope Perspective on the Glacial Circulation of the Deep Southwest Pacific***

16:30 p.m. **Michael Sarnthein** p. 197
Institute for Geosciences, University of Kiel
***Benthic $^{14}C$ Ventilation Ages Record Changing Storage of Dissolved Inorganic Carbon in the Abyssal Ocean***

17:00 p.m. **James W. B. Rae** p. 187
Department of Earth and Environmental Sciences, University of St. Andrews
***Signals of $CO_2$ Destratification from Boron Isotopes***

17:30 p.m. **Karen E. Kohfeld** p. 127
School of Resource and Environmental Management, Simon Fraser University, Burnaby
***Using Paleo-Oceanographic Data Synthesis to Test Ideas about Changes in Atmospheric $CO_2$ Concentrations during Glacial Inception***

18:00 p.m. **Andrey Ganopolski** p. 75
Potsdam Institute for Climate Impact Research (PIK), Potsdam
***The Last Four Glacial $CO_2$ Cycles Simulated with the CLIMBER-2 Model***

## Öffentlicher Vortrag / Public Lecture

20:00 p. m. **Thomas Stocker**
Physics Institute, Climate and Environmental Physics,
University of Bern
***Klimawandel: Zu spät für 2 °C?***

# Friday, 20 March 2015

## Biogeochemistry and Radiocarbon

9:00 a.m. **Keynote**
**Robert F. Anderson** p. 23
Lamont-Doherty Earth Observatory, Earth Institute, Columbia University, Palisades, NY
***Ocean Stratification, Carbon Storage, and Calcite Compensation throughout the Late Pleistocene Glacial Cycles***

9:45 a.m. **Edouard Bard** p. 29
Centre de Recherche et d'Enseignement de Géosciences (CEREGE), Aix-en-Provence
***Variations of Sea-Surface $^{14}C$ Reservoir Ages (SSRA) and their Paleoclimatic Implications: From a Chronometric Problem to a New Paleoceanographic Proxy***

10:15 a.m. **Pieter M. Grootes** p. 81
Institute of Ecosystem Research, University of Kiel
***Oceanic Reservoir Ages, $^{14}C$ Concentrations, and Carbon Dynamics (also in the "Mistery Interval")***

10:45 a.m. Coffee Break

11:15 a.m. **Mathis P. Hain** p. 89
National Oceanography Centre Southampton (NOCS), University of Southampton
***Simulating Atmospheric Radiocarbon through Deglaciation***

11:45 a.m. **Stefan Mulitza** p. 167
MARUM – Center for Marine Environmental Sciences, Bremen
***Response of the Tropical Atlantic Ocean-Atmosphere System to Deglacial Changes in Atlantic Meridional Overturning***

12:15 p.m. **Enqing Huang** p. 101
School of Ocean and Earth Science, Tongji University, Shanghai, and MARUM Bremen
***Radiocarbon Distribution and Radiocarbon-Based Circulation Age of the Atlantic Ocean during the Last Glacial Maximum***

12:45 p.m. **Birgit Schneider** p. 211
Institute of Geosciences, University of Kiel
***What is Shaping the $\Delta^{14}C$-DIC Relationship in the Deep Ocean?***

13:15 p.m. Lunch and Coffee

14:00 p.m. **Open Discussion**
**(Conveners: Thomas Bauska, Philippe Ciais, and Samuel L. Jaccard)**
***Results and Limits to Reconstruct Carbon Cycle Changes***

16:00 p.m. **Samuel L. Jaccard** p. 111
Institute of Geological Sciences, Physics Institute and Oeschger Centre for Climate Change Research, University of Bern
***Deglacial Changes in Ocean (De)Oxygenation***

### Terrestrial Carbon Inventories

16:30 p.m. **Peter Köhler** p. 135
Alfred Wegener Institute, Helmholtz Centre for Polar and Marine Research, Bremerhaven
***High Latitude Impacts on Deglacial $CO_2$: Southern Ocean Westerly Winds and Northern Hemisphere Permafrost Thawing***

17:00 p.m. **Philippe Ciais** p. 55
Laboratoire des Sciences du Climat et de l'Environnement, Saclay
***An Attempt to Quantify Terrestrial Carbon Storage during the Last Glacial Maximum and the Implications for Deglaciation $CO_2$ Changes***

17:30 p.m. **Victor Brovkin** p. 43
Max Planck Institute for Meteorology, Hamburg
***The Role of the Terrestrial Biosphere in CLIMBER-2 Simulations of the Last 4 Glacial $CO_2$ Cycle***

18:00 p.m. **Martin Heimann** p. 97
Max Planck Institute for Biogeochemistry, Jena
***Constraints on Global Climate-Carbon Cycle Feedbacks on Interannual to Glacial Cycle Timescales***

19:00 p.m. Joint Dinner

## Saturday, 21 March 2015

### Hypotheses and Data for Mechanisms of Change

9:00 a.m. **Keynote**
**Axel Timmermann** p. 235
International Pacific Research Center, University of Hawaii, Honolulu, HI
***Deglacial $CO_2$/Climate Feedbacks: Models, Myths, and Misconceptions***

9:45 a.m. **Eric D. Galbraith** p. 71
Depart. of Earth and Planetary Science, McGill University, Montreal
***The Role of Air-Sea Disequilibrium in Ocean Carbon Storage and its Isotopic Composition***

## Ocean Alkalinity / Syntheses

| | | |
|---|---|---|
| 10:15 a.m. | **Klaus Wallmann**<br>GEOMAR Helmholtz Centre for Ocean Research Kiel<br>***Effects of Eustatic Sea-Level Change on Atmospheric $CO_2$ and Glacial Climate*** | p. 241 |
| 10:45 a. m. | *Coffee Break* | |
| 11:15 a. m. | **Tatiana Ilyina**<br>Max Planck Institute for Meteorology, Hamburg<br>***The Combined Effects of Changes in Ocean Chemistry, Biology, and Hydrodynamics on Alkalinity*** | p. 107 |
| 11:45 a.m. | **Alfredo Martínez-García**<br>Geological Institute, ETH Zürich<br>***Iron Fertilization of the Subantarctic Ocean during the Last Ice Age*** | p. 151 |
| 12:15 p.m. | **Didier Paillard**<br>Laboratoire des Sciences du Climat et de l'Environnement, Gif-sur-Yvette<br>***Glacial $CO_2$ as a Key to the Glacial-Interglacial Problem*** | p. 175 |
| 12:45 p.m. | **Andy Ridgwell**<br>School of Geographical Sciences, University of Bristol, UK<br>***Are the Drabbest Proxies the 'Best'? Patterns of Bulk $CaCO_3$ and Glacial Carbon Storage*** | p. 195 |
| 13:15 p.m. | Lunch and Coffee | |
| 14:00 p.m. | **Poster** | pp. 259–350 |
| 16:00 p.m. | **Laurie Menviel**<br>Climate Change Research Centre, Univ. of New South Wales, Sydney<br>***Southern Ocean Overturning Role in Modulating High Southern Latitude Climate and Atmospheric $CO_2$ on Millennial Timescales*** | p. 159 |
| 16:30 p.m. | **Jimin Yu**<br>Research School of Earth Sciences. Australian National Univ., Canberra<br>***Deep Atlantic Carbon Sequestration and Atmospheric $CO_2$ Decline during the Last Glaciation*** | p. 253 |
| 17:00 p.m. | **Tobias Friedrich**<br>International Pacific Research Center, Univ. of Hawaii, Honolulu, HI<br>***Effects of Sea-Ice and Ocean-Circulation Changes on Deglacial Deep-Ocean Radiocarbon Trends*** | p. 65 |
| 17:30 p.m. | **André Paul and Michael Schulz**<br>MARUM – Center for Marine Environmental Sciences, Univ. of Bremen<br>***Model-Based Reconstruction of the Marine Carbon Cycle during the Last Glacial Maximum*** | p. 183 |
| 18:00 p.m. | **Keynote**<br>**Daniel M. Sigman**<br>Department of Geosciences, Princeton University, Princeton, NJ<br>***Taking Stock of the Hypotheses for Polar Ocean Stratification and Carbon Dioxide Sequestration during the Last Ice Age*** | p. 213 |

**Adjourn / Farewell**

# Extended Abstracts

Nova Acta Leopoldina NF *121*, Nr. 408, 21–22 (2015)

# Radiocarbon (and Other) Constraints on the Transition from Glacial Maximum to the Holocene

Jess Adkins (Pasadena, CA, USA)

The deep ocean tracer distribution at the Last Glacial Maximum (LGM) was demonstrably different than it is today. This observation, spanning $\delta^{13}C$, $\delta^{18}O$, $\Delta^{14}C$, and a variety of other tracers, frames the ocean state at the start of the deglaciation. The evidence points towards the deep circulation occupying a 2-cell structure (sinking in the North Atlantic and in the Southern Ocean) with very little mixing between the cells. This is in contrast to today where the two cells are intimately linked by mixing in the ocean interiors and uplifting of isopycnals around Antarctica. We have proposed that these two states can be explained by an equatorward shift of the sea ice extent around Antarctica at the LGM (Ferrari et al. 2014). We have also shown that the increased stratification of the LGM deep ocean may have been largely driven by differences in salinity, with Southern Source waters being saltier than Northern Source waters. This extra salt in the deep sea can come from increased sea ice export around Antarctica. It can also come from a feedback at the land ice-ocean interface where cooling northern sourced waters leads to saltier southern sourced waters. Today the warmth of NADW leads to melting of land based ice in the Weddell Sea. Cooling NADW leads to less melting but does not change the tendency to form winter sea ice that leaves concentrated brines on the continental shelves (Miller et al. 2012).

One way to define the deglaciation is as the transition between the two deep ocean quasi steady-states. Here we propose a new 'capacitor' for the climate system, deep ocean heat storage, that could provide a key physical mechanism to explain some of the important features of deglacial climate. Through thermobaricity in seawater's equation of state (the pressure dependence of the thermal expansion coefficient), salt stratification can store heat in a water column that is locally statically stable. However, analogous to CAPE in the atmosphere, this heat energy is convectively available and can lead to large, abrupt deep-ocean mixing. Using clumped isotopes in deep-sea corals from Heinrich event 1, we have found warmer water underneath colder water, about 800 years before the Bolling-Alerod warming recorded in Greenland ice cores (Thiagarajan et al. 2014). We propose that the abrupt nature of the Bolling is due to the discharge of this deep ocean thermal capacitor, which then changes the deep circulation from a glacial to a modern pattern. We will also show new radiocarbon data from the Southern Ocean to help further constrain the role of intermediate waters in the last termination.

## *References*

Ferrari, R., Jansen, M. F., Adkins, J. F., Burke, A., Stewart, A. L., and Thompson, A. F.: Antarctic sea ice control on ocean circulation in present and glacial climates. Proc. Natl. Acad. Sci. USA *111*, 8753–8758 (2014)

Miller, M., Adkins, J. F., Menemenlis, D., and Schodlok, M. P.: The role of ice shelves in setting glacial ocean bottom water salinity. Paleoceanography *27*, doi:10.1029/2012PA002297 (2012)

Thiagarajan, N., Subhas, A. V., Southon, J. R., Eiler, J. M., and Adkins, J. F.: Abrupt pre-Bølling-Allerød warming and circulation changes in the deep ocean. Nature *511*, 75–78; doi:10.1038/nature13472 (2014)

Prof. Jess Adkins, Ph.D.
California Institute of Technology
MC 131-24
1200 E California Blvd.
Pasadena, CA 91125
USA
Phone: +1 626 3958550
E-Mail: jess@gps.caltech.edu

Nova Acta Leopoldina NF *121*, Nr. 408, 23–27 (2015)

# Ocean Stratification, Carbon Storage, and Calcite Compensation throughout the Late Pleistocene Glacial Cycles

Robert F. Anderson,[1] Katherine A. Allen,[2] Jimin Yu,[3] and Julian P. Sachs[4]

With 2 Figures

The nutrient-deepening hypothesis (Boyle 1988) posits that the restructuring of ocean water masses under ice-age environmental conditions led to the downward displacement and broadening of the zone of minimum oxygen concentrations in the ocean. A greater ice-age efficiency of the ocean's biological pump in response to a combination of enhanced ocean stratification and fertilization of the Southern Ocean with iron supplied by dust may have worked synergistically to lower the oxygen concentration in the deep sea (Anderson et al. 2014, Lamy et al. 2014, Martínez-García et al. 2014, Sigman et al. 2010). Acidification of the deep ocean by increased storage of respiratory $CO_2$ under ice-age conditions would have induced dissolution of sedimentary $CaCO_3$, raising the ocean's alkalinity and further increasing the storage of $CO_2$ by carbonate compensation (Broecker and Peng 1987). None of these conditions in isolation is sufficient to account for the observed reduction of atmospheric $CO_2$ during the late Pleistocene ice ages, by amounts ranging between 80 and 100 ppm relative to interglacial periods (Archer et al. 2000). However, in combination, these processes are thought to be capable of storing sufficient $CO_2$ in the deep sea to balance the loss of carbon from the atmosphere and the terrestrial biosphere (Peacock et al. 2006).

Any combination of physical and biogeochemical conditions that increases the efficiency of the biological pump (Volk and Hoffert 1985), so as to sequester more carbon in the deep ocean, will also reduce the dissolved $O_2$ concentration in the deep ocean (Sigman et al. 2010). A growing body of qualitative evidence points to lower dissolved $O_2$ levels in the deep ocean during the peak of the last ice age (~18–28 ka BP, Bradtmiller et al. 2010, Jaccard and Galbraith 2012, Jaccard et al. 2009). While lower deep-sea $O_2$ levels during the last ice age are now generally accepted, as yet it has not been possible to quantify the amount of additional $CO_2$ storage in the deep sea, or the contribution of this storage to ice-age atmospheric $CO_2$ levels.

Although quantitative constraints on dissolved oxygen concentrations in the past are lacking, here we illustrate the evolution of deep Pacific Ocean carbonate chemistry by making reasonable assumptions that are consistent with qualitative proxy evidence. For the central

1 Lamont-Doherty Earth Observatory of Columbia University, Palisades, New York 10964, USA.
2 Department of Marine and Coastal Sciences, Rutgers University, 71 Dudley Road, New Brunswick, New Jersey 08901, USA.
3 Research School of Earth Sciences, The Australian National University, Canberra, ACT 0200, Australia.
4 School of Oceanography, University of Washington, Seattle, WA 98195, USA.

equatorial Pacific Ocean (140°W) where we have a 500 ka record of $CaCO_3$ burial (see below), we take an ice-age bottom water oxygen concentration of 35 µmol/kg, which is consistent with the Pacific oxygen concentrations estimated by Jaccard et al. (2009). Oxygen concentrations are unlikely to have been much lower than this because we are unaware of any evidence that the deep Pacific became anoxic during the last glacial period, or even sufficiently low in dissolved oxygen to allow the proliferation of species of benthic foraminifera that thrive under low-oxygen conditions. Further assuming that bottom water was 2 °C colder than today (Elderfield et al. 2010) and that salinity increased by the global average of about 3 % due to storage of freshwater in continental ice sheets, we calculate that the bottom water would have had an initial $O_2$ concentration of 371 µmol/kg if it formed in equilibrium with the atmosphere. Under these assumptions, the apparent oxygen utilization of Pacific bottom water would have been 153 µmol/kg greater than today, which is equivalent to 108 µmol/kg greater storage of respiratory $CO_2$ using a respiratory quotient of 1.415 (Anderson 1995).

Bottom water in the central Pacific during the Last Glacial Maximum had a carbonate ion concentration that was not significantly different from that which exists today (Yu et al. 2013). The conditions that we reconstruct for the Last Glacial Maximum, with carbonate ion

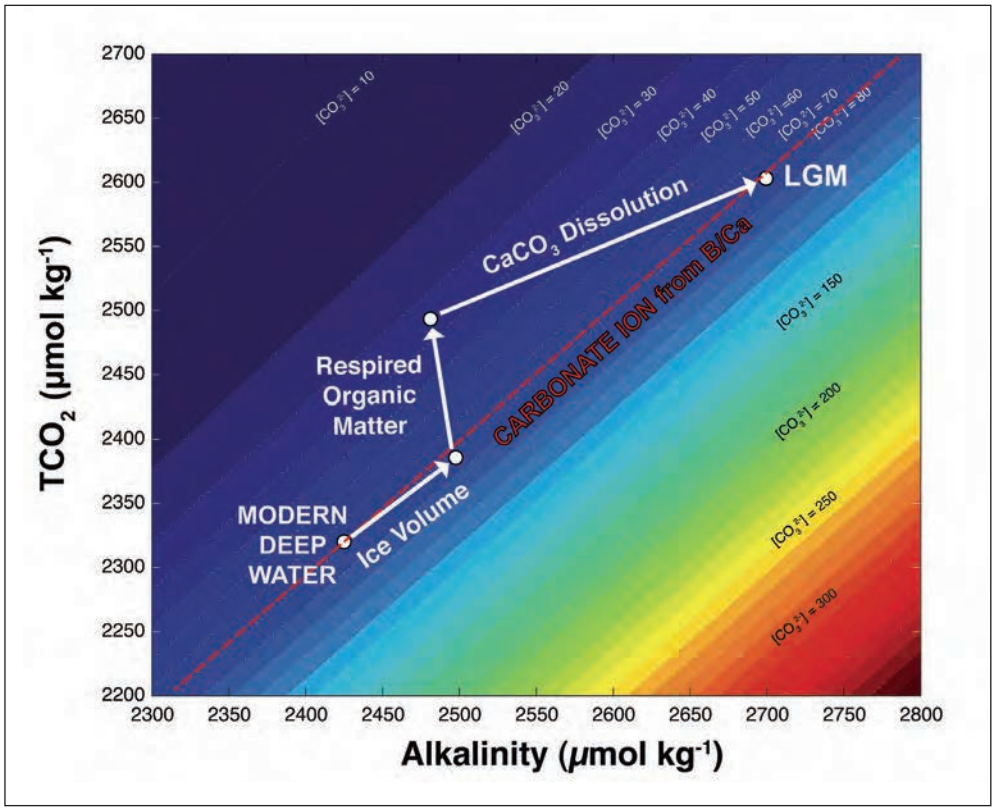


Fig. 1 Graphical illustration of the calculation of total dissolved inorganic carbon ($TCO_2$) and alkalinity in central Pacific bottom water during the peak of the last glacial period assuming a dissolved oxygen concentration of 35 µmol/kg (see main text for details and assumptions).

concentration similar to today but a respiratory $CO_2$ concentration at least 100 µmol/kg higher, requires the dissolution of substantial amounts of $CaCO_3$ to raise the alkalinity of seawater and thereby maintain a constant carbonate ion concentration ($\{CO_3^{2-}\}$ ~ DIC – ALK), where DIC is the total dissolved inorganic carbon concentration and ALK is alkalinity. With these constraints, we reconstruct the DIC and ALK of Central Pacific bottom water during the Last Glacial Maximum by working stepwise through each of the factors that would have had a significant impact on carbonate system (Fig. 1). The combined effect of greater accumulation of respiratory $CO_2$ and carbonate compensation would have created a DIC concentration ~217 µmol/kg greater than that which exists today.

Taking the illustration a step further, if half the global ocean (~$6.5 \times 10^{20}$ liters; i.e., the deep ocean) contained 108 µmol/kg more respiratory $CO_2$ than today, then this would amount to a total of 846 gigatons of carbon (GtC), sufficient to account for the carbon lost from the atmosphere (~200 GtC) and from the terrestrial biosphere (~600 GtC, Peterson et al. 2014). Of course, these values need to be refined with more detailed models, but they illustrate the potential to close the ice-age carbon budget with increased storage of $CO_2$ in the deep ocean under the combined effects of greater stratification and greater iron fertilization.

Recent success in application of B/Ca ratios as a proxy for carbonate ion concentration (Yu et al. 2013, 2014) have confirmed that $CaCO_3$ accumulation in sediments throughout the deep Indo-Pacific region is regulated primarily by changes in carbonate ion concentration (i.e., by $CaCO_3$ preservation, Anderson et al. 2008, Hodell et al. 2001). Building on this,

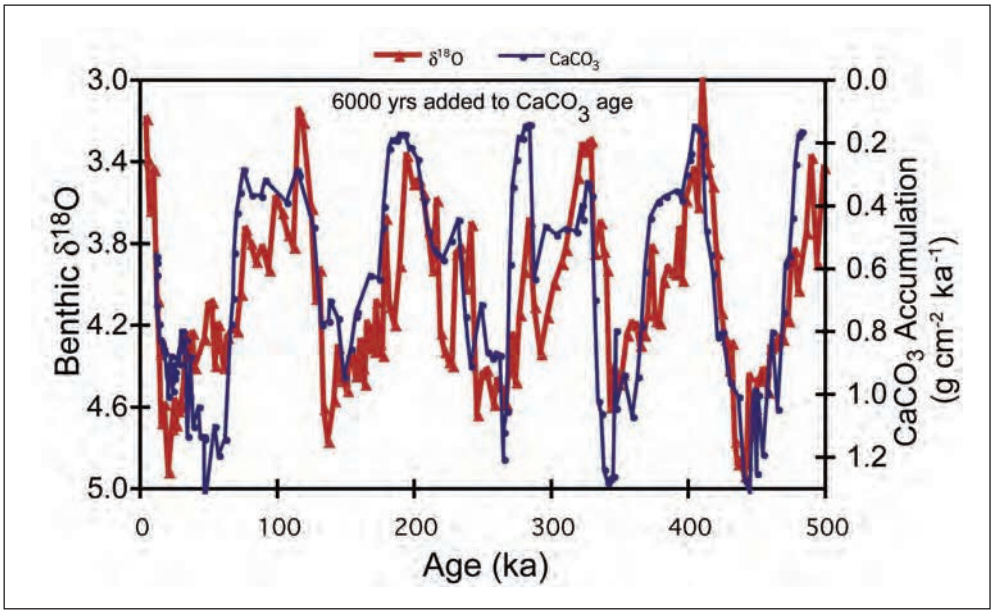


Fig. 2 A 500 ka record from TT013-PC72 (0.11°N, 139.4°W, 4298 m) in the central equatorial Pacific Ocean. The oxygen isotope composition of benthic foraminifera (Murray et al. 2000) was used to provide an age model, and to illustrate changes in global ice volume (*red curve*). The accumulation rate of $CaCO_3$ (*blue curve*) reflects past changes in deep water carbonate ion concentration (Anderson et al. 2008, Yu et al. 2013). Note the inverted axis scale; the sense is that "up" is equivalent to low carbonate ion concentration. A 6000-year lag has been added to the $CaCO_3$ record to illustrate the (potential) time scale for the deep-sea carbonate system to respond to changes in ice volume.

we use the 500 ka record of $CaCO_3$ accumulation in central equatorial Pacific sediments (TT013 PC72, 0.1°N, 140°W, Anderson et al. 2008) to compare past changes in deep-sea $\{CO_3^{2-}\}$ to global ice volume, as inferred from the $\delta^{18}O$ of *C. wuellerstorfi* in the same core.

We find a good correlation between $CaCO_3$ accumulation and $\delta^{18}O$, which is improved by imposing a 6000-year lag on the $CaCO_3$ record (Fig. 2), likely reflecting the time scale for adjustment of the ocean carbonate system to external forcing. In viewing records like this one must be mindful of the caveat that "everything correlates with everything else on 100-ka timescales" (colloquially referred to by some as the Labeyrie principle). That is, one cannot infer cause and effect from correlations like this. Nevertheless, we can be confident that deep-sea $\{CO_3^{2-}\}$ is systematically linked to global ice volume, at least throughout the Late Pleistocene. Taking a lesson from the last glacial period, we can further infer that these changes in $\{CO_3^{2-}\}$ reflect past changes in ocean stratification, the efficiency of the biological pump, and carbonate compensation.

One must also keep in mind that the carbonate ion record consists of a transient signal that follows the accumulation and release of respiratory $CO_2$ as well as a quasi-steady-state signal tied to changes in whole-ocean ALK. Future work should seek higher resolution records to better define the phase relationship between ice volume and deep-sea carbonate chemistry, together with models to resolve the transient from steady state aspects of changes in carbonate chemistry.

## *References*


Anderson, L. A.: On the hydrogen and oxygen content of marine phytoplankton. Deep-Sea Res. Part I – Oceanographic Research Papers *42*, 1675–1680 (1995)

Anderson, R. F., Barker, S., Fleisher, M., Gersonde, R., Goldstein, S. L., Kuhn, G., Mortyn, P. G., Pahnke, K., and Sachs, J. P.: Biological response to millennial variability of dust and nutrient supply in the Subantarctic South Atlantic Ocean. Phil. Trans. Royal Soc. A–Mathematical Physical and Engineering Sciences *372*; doi.org/10.1098/rsta.2013.0054 (2014)

Anderson, R. F., Fleisher, M. Q., Lao, Y., and Winckler, G.: Modern $CaCO_3$ preservation in equatorial Pacific sediments in the context of recent glacial cycles. Marine Chemistry *111*, 30–46 (2008)

Archer, D., Winguth, A., Lea, D., and Mahowald, N.: What caused the glacial/interglacial atmospheric $pCO_2$ cycles? Rev. Geophys. *38*, 159–189 (2000)

Boyle, E. A.: Vertical oceanic nutrient fractionation and glacial interglacial $CO_2$ cycles. Nature *331*, 55, 56 (1988)

Bradtmiller, L. I., Anderson, R. F., Sachs, J. P., and Fleisher, M. Q.: A deeper respired carbon pool in the glacial equatorial Pacific Ocean. Earth Planet. Sci. Lett. *299*, 417–425 (2010)

Broecker, W. S., and Peng, T. H.: The role of $CaCO_3$ compensation in the glacial to interglacial atmospheric $CO_2$ change. Global Biogeochem. Cycles *1*, 15–29 (1987)

Elderfield, H., Greaves, M., Barker, S., Hall, I. R., Tripati, A., Ferretti, P., Crowhurst, S., Booth, L., and Daunt, C.: A record of bottom water temperature and seawater $\delta^{18}O$ for the Southern Ocean over the past 440 kyr based on Mg/Ca of benthic foraminiferal Uvigerina spp. Quat. Sci. Rev. *29*, 160–169 (2010)

Hodell, D. A., Charles, C. D., and Sierro, F. J.: Late Pleistocene evolution of the ocean's carbonate system. Earth Planet. Sci. Lett. *192*, 109–124 (2001)

Jaccard, S. L., and Galbraith, E. D.: Large climate-driven changes of oceanic oxygen concentrations during the last deglaciation. Nature Geosci. *5*, 151–156 (2012)

Jaccard, S. L., Galbraith, E. D., Sigman, D. M., Haug, G. H., Francois, R., Pedersen, T. F., Dulski, P., and Thierstein, H. R.: Subarctic Pacific evidence for a glacial deepening of the oceanic respired carbon pool. Earth Planet. Sci. Lett. *277*, 156–165 (2009)

Lamy, F., Gersonde, R., Winckler, G., Esper, O., Jaeschke, A., Kuhn, G., Ullermann, J., Martínez-García, A., Lambert, F., and Kilian, R.: Increased dust deposition in the Pacific Southern Ocean during glacial periods. Science *343*, 403–407 (2014)

Martínez-García, A., Sigman, D. M., Ren, H., Anderson, R. F., Straub, M., Hodell, D. A., Jaccard, S. L., Eglinton, T. I., and Haug, G. H.: Iron fertilization of the Subantarctic Ocean during the last ice age. Science *343*, 1347–1350 (2014)

Murray, R. W., Knowlton, C., Leinen, M., Mix, A. C., and Polsky, C. H.: Export production and carbonate dissolution in the central equatorial Pacific Ocean over the past 1 Myr. Paleoceanography *15*, 570–592 (2000)

Peacock, S., Lane, E., and Restrepo, J. M.: A possible sequence of events for the generalized glacial-interglacial cycle. Global Biogeochem. Cycles *20*, GB2010; doi:2010.1029/2005GB002448 (2006)

Peterson, C. D., Lisiecki, L. E., and Stern, J. V.: Deglacial whole-ocean $\delta^{13}C$ change estimated from 480 benthic foraminiferal records. Paleoceanography *29*, 549–563 (2014)

Sigman, D. M., Hain, M. P., and Haug, G. H.: The polar ocean and glacial cycles in atmospheric $CO_2$ concentration. Nature *466*, 47–55 (2010)

Volk, T., and Hoffert, M. I.: Ocean carbon pumps: Analysis of relative strengths and efficiencies in ocean-driven atmospheric $CO_2$ changes. In: Sundquist, E. T., and Broecker, W. S. (Eds.): The Carbon Cycle and Atmospheric $CO_2$: Natural Variations Archean to Present. Vol. *32*, pp. 99–110. Washington, D. C.: American Geophysical Union 1985

Yu, J., Anderson, R. F., Jin, Z., Menviel, L., Zhang, F., Ryerson, F. J., and Rohling, E. J.: Deep South Atlantic carbonate chemistry and increased interocean deep water exchange during last deglaciation. Quat. Sci. Rev. *90*, 80–89 (2014)

Yu, J., Anderson, R. F., Jin, Z., Rae, J. W. B., Opdyke, B. N., and Eggins, S. M.: Responses of the deep ocean carbonate system to carbon reorganization during the Last Glacial–interglacial cycle. Quat. Sci. Rev. *76*, 39–52 (2013)

Prof. Robert F. Anderson, Ph.D.
Lamont-Doherty Earth Observatory
Columbia University
Earth Institute
61 Route 9W
P.O. Box 1000
Palisades, NY 10964
USA
Phone: +1 845 3658508
Fax: +1 845 3658155
E-Mail: boba@ldeo.columbia.edu

# Variations of Sea-Surface $^{14}C$ Reservoir Ages (SSRA) and their Paleoclimatic Implications: From a Chronometric Problem to a New Paleoceanographic Proxy

Edouard Bard (Aix-en-Provence, France)

With 2 Figures

Radiocarbon ages measured on shells of biological organisms growing on shallow coastlines or living among the plankton must be corrected for the difference in $^{14}C$ composition between the atmosphere and the sea surface. This problem has been clearly identified since the mid-1950s (e.g. Craig 1954), but fortuitously, the usual amplitude of the $^{14}C$ shift to be corrected for is on the order of 400 years, which, for marine carbonates, cancels out the isotopic fractionation correction embedded in the calculation of a conventional $^{14}C$ age (the $\delta^{13}C$ of the dated sample being normalized to –25 ‰).

Subsequent surveys of the sea surface reservoir age (SSRA) have demonstrated that its value is not always equal to 400 years, but that it varies between 300 and 1200 years in the modern ocean (see Fig. 1 and compilations published by Bard 1988 and Reimer and Reimer 2001). From the point of view of $^{14}C$ chronometry, the SSRA spatial variability is thus viewed as a problem which limits the accuracy of radiocarbon ages.

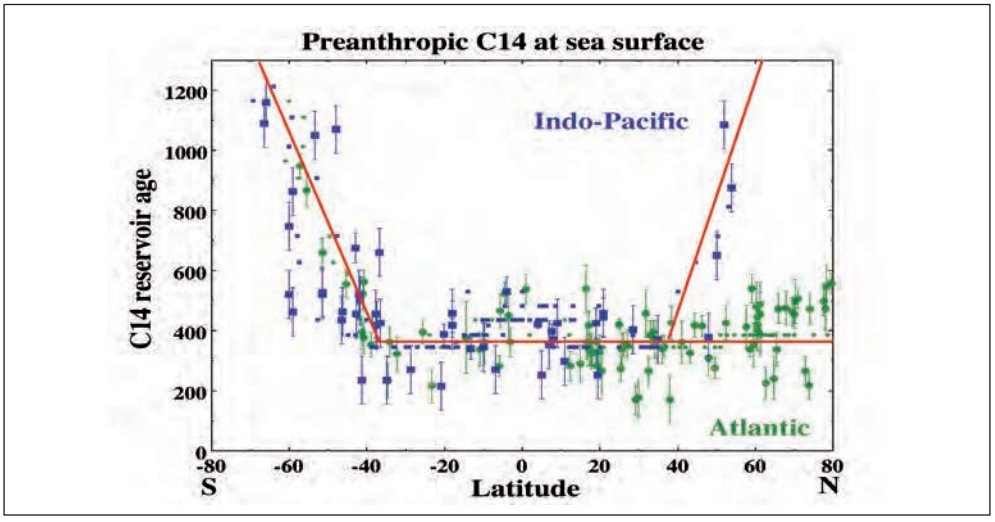


Fig. 1 Sea surface reservoir ages plotted *versus* the latitude based on direct $^{14}C$ measurements of the dissolved $TCO_2$ in surface water from the World Ocean (green labels stand for samples from the Atlantic Ocean and blue labels for those from the Indian and Pacific Oceans). These samples were collected in the 1950s before the thermonuclear bomb tests in the atmosphere (Bard 1988 and references therein).

In parallel, numerical modelling has allowed to quantify the residence time of carbon atoms in the different reservoirs of the global carbon cycle, notably in the different water masses of the World Ocean. The ocean mixed layer is a complex reservoir, sandwiched as it is between the atmosphere and the intermediate and deep ocean with its slow circulation accompanied with a significant radioactive decay of $^{14}C$ atoms. At steady state, the SSRA is thus determined by the mixing of young carbon from the atmosphere with older carbon from advected waters.

Bard (1988) performed the first systematic and quantitative study of the various causes of SSRA variations by using the box-diffusion model of Oeschger et al. (1975). It was shown that the SSRA depends on a combination of multiple parameters such as atmospheric $pCO_2$, the free ocean surface, the piston velocity for gas exchange, the solubility of $CO_2$, kinetic fractionation factors, the mixed layer depth, the mixing of the deep ocean, upwelling intensity and even transient changes of the $^{14}C$ production in the upper atmosphere. Several of these factors are directly related to climate parameters such as sea-surface temperature, wind strength, sea-ice cover.

This led Bard (1988) to propose that the SSRA should be viewed as a new paleoceanographic proxy, rather than being considered solely as an obstacle to accurate chronometry. He went further by proposing two methods to reconstruct paleo-SSRA by measuring $^{14}C$ in coeval contemporaneous marine and terrestrial organic matter which are found in association at the same site or can be linked stratigraphically by the same precise time marker, instantaneous at the geological scale. The first technique is restricted to shallow coastal sediments enabling the physical association of continental and marine material, while the second technique can be used over long distances with marine samples from the open ocean. Volcanic eruptions were identified as the best instantaneous time marker since they can be found as tephra layers in marine and lake sediments. The Vedde Ash eruption which occurred about 12,000 years ago in the middle of the Younger Dryas cold event was proposed as an ideal test case for this new proxy.

By dating planktonic foraminifera mixed with Vedde tephras at several sites from the North Atlantic, Bard et al. (1994) reported the first results using this technique and documented a significant increase of the SSRA in the middle of the Younger Dryas event (800 years as compared with a modern value of 400 years). In the wake of this initial work, several other papers have been published on SSRA variations based on tephra layers of various ages from the North-Atlantic (Austin et al. 1995, Haflidason et al. 1995, Bondevik et al. 1999, 2001, 2006, Eiriksson et al. 2000, 2004, 2011, Knudsen and Eiriksson 2002, Larsen et al. 2002, Thornalley et al. 2011b) and other locations from the World Ocean (Sikes et al. 2000, Hutchinson et al. 2004, Siani et al. 2001, 2013, Ikehara et al. 2011, Skinner et al. 2015).

Based on the tephra approach, large SSRA values of up to 2000 years have been reported for specific cold periods such as the Younger Dryas and Heinrich event 1 in the North Atlantic and Mediterranean Sea (Siani et al. 2001, Thornalley et al. 2011b). Similarly, large SSRA values in the subtropical Southern Pacific have been reconstructed for the last glacial period (Sikes et al. 2000, Skinner et al. 2015). These studies point to the possibility of SSRA change by more than 1000 years at a specific location.

Unfortunately, suitable volcanic eruptions are not that frequent and tephra layers are unevenly distributed in the sediments of the World Ocean. This has led several authors to apply usual stratigraphic techniques to date oceanic records by correlation of paleoceanographic records with other paleoclimatic records that have been dated accurately. This technique has allowed to calculate SSRA changes that are similar to or sometimes even larger than those reconstructed with the tephra method. For example, SSRA values on the order of

2000–2500 years have been reported for the Northeast Atlantic during the last deglaciation period (Waelbroeck et al. 2001, Peck et al. 2006, Thornalley et al. 2011a, Skinner et al. 2014), but a recent compilation of North-Atlantic data led to smaller values of up to 1300 years (Stern and Lisiecki 2013).

By correlating the $^{14}C$ stratigraphies directly with the $^{14}C$ calibration curve, Sarnthein et al. (2007) calculated SSRA for several sites ranging from low latitudes (South China Sea, Santa Barbara Basin) to high latitudes (Icelandic Basin, Subarctic Northwest Pacific). They reconstructed very large SSRA values of up to 2000–2500 years for the glacial period. Comparing those evaluations with present day values for the same locations translates into dramatic SSRA increases of up to greater than +1500 years for the South China Sea and of about +2000 years for the Icelandic Sea.

Kubota et al. (2014) made a recent attempt to calculate SSRA changes by compiling $^{14}C$ ages in U-Th dated coral from tropical Pacific islands. Comparison with the $^{14}C$ calibration curve led them to propose that SSRA increased by +400 years during the Heinrich 1 event, resulting in SSRA values on the order of 800 years in the tropical Pacific.

In parallel to reconstructing paleo-SSRA values from geological archives, numerical models can be used to simulate SSRA as a response to past climate changes occurring over the $^{14}C$ time range. For example, the atmospheric $CO_2$ concentration was lower during the glacial period (190 *vs*. 280 ppm) which led to an increase of the reservoir age by about +200 years for the full change between the Last Glacial Maximum and Holocene periods (Bard 1988, 1998; Fig. 2). It is generally considered that wind speeds were higher during the last glacial period as a response to a steepened temperature gradient between low and high latitudes. Increasing the wind speed velocity by 50 % on average would increase the $CO_2$ piston velocity, thereby leading to a reduction of the reservoir age by about –250 years (Bard 1988). This first-order calculation based on a box diffusion model is certainly a maximum value, as increased wind speed also favours mixing with older water from below the surface box.

In addition to these global changes, which partly cancel out, it is important to take into account the possibility of local variations in $^{14}C$ reservoir ages linked to regional paleoceanographic changes. For example, high latitudes are affected by sea-ice which limits air-sea gas exchange. Bard et al. (1994) used a 13-box model to calculate shifts of up to +350 years as a response to perennial sea-ice in the Nordic Seas.

Several modelling groups have gone farther in simulating the spatial variations of SSRA by using more complex models to mimic the ocean-atmosphere couple and its physical and biogeochemical responses (Stocker and Wright 1998, Delaygue et al. 2003, Butzin et al. 2005, Franke et al. 2008, Singarayer et al. 2008, Ritz et al. 2008, Hain et al. 2011). These models have been used to calculate global maps of the SSRA under steady state climate changes representing glacial conditions. The modelled SSRA are generally larger than for the present day ocean with increases of up to a couple of centuries at low latitudes, several centuries in the Northern latitudes and up to a millennium in the Southern Ocean.

Numerical models have also been used to calculate rapid SSRA changes linked to transient climate changes resulting from alterations of the Meridional Overturning Circulation (MOC) when it is forced with freshwater in the zones of deep-water convection. The SSRA response can be complex with transient decrease and increase, but the overall amplitude of the swings is limited to a few centuries, and even less in zones remote from the convection zones.

Overall, the SSRA changes simulated by models are smaller than the largest changes reconstructed from $^{14}C$ measurements in oceanic sediments. This contrast may be due to deficiencies

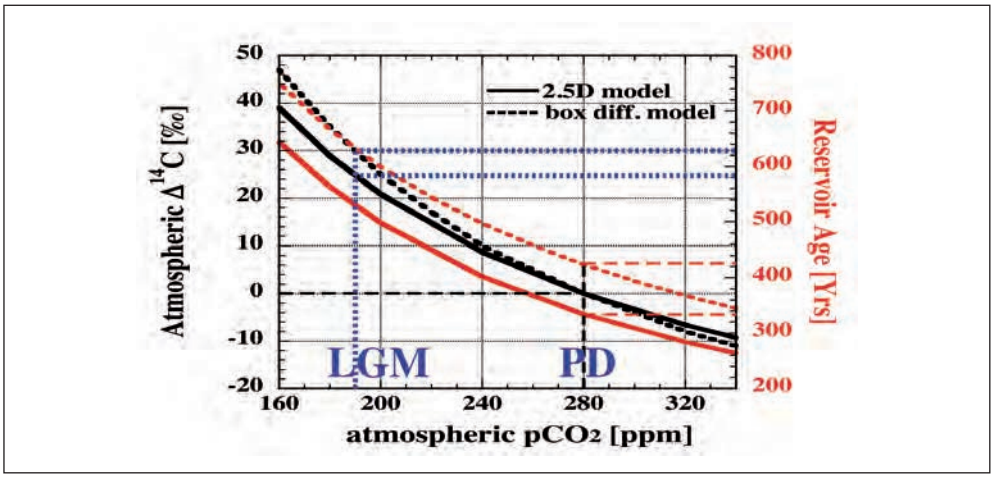


Fig. 2 Steady state calculations of the dependence between the sea surface reservoir age and the atmospheric $pCO_2$ (updated from Bard 1988, 1998 by using calculations performed by Delaygue et al. 2003 with the Bern model). PD stands for the present day preindustrial conditions and LGM for the Last Glacial Maximum.

of numerical models in capturing the exchange timescales between the main carbon reservoirs, the effects of the dynamical oceanic circulation and of altered biogeochemical cycles.

Alternatively, the discrepancy may point to unrecognized biases in the $^{14}C$ proxy data linked to subtle sedimentological or geochemical effects. For example, the reconstruction of SSRA by the different proposed methods is sensitive to phenomena such as sediment reworking, bioturbation, dissolution, and contamination coupled with abundance changes of the carrier of the $^{14}C$ signal (e.g. Bard et al. 1987, 2001, Barker et al. 2007, Broecker and Clark 2011).

I will discuss these issues in the light of the recent literature, notably by comparing the amplitude of model outputs and by assessing the possible magnitude of biases on the SSRA reconstructions based on $^{14}C$ in oceanic sediments.

## *References*

Austin, W. E. N., Bard, E., Hunt, J. B., Kroon, D., and Peacock, J. D.: The $^{14}C$ age of the Icelandic Vedde Ash: implications for Younger Dryas marine reservoir age corrections. Radiocarbon *37*, 53–62 (1995)

Bard, E.: Correction of accelerator mass spectrometry $^{14}C$ ages measured in planktonic foraminifera: Paleoceanographic implications. Paleoceanography *3*, 635–645 (1988)

Bard, E.: Geochemical and geophysical implications of the radiocarbon calibration. Geochimica et Cosmochimica Acta *62*, 2025–2038 (1998)

Bard, E.: Paleoceanographic implications of the difference in deep-sea sediment mixing between large and fine particles. Paleoceanography *16*, 235–239 (2001)

Bard, E., Arnold, M., Duprat, J., Moyes, J., and Duplessy, J. C.: Reconstruction of the last deglaciation: deconvolved records of $d^{18}O$ profiles, micropaleontological variations and accelerator mass spectrometric $^{14}C$ dating. Clim. Dynam. *1*, 101–112 (1987)

Bard, E., Arnold, M., Mangerud, M., Paterne, M., Labeyrie, L., Duprat, J., Mélières, M. A., Sonstegaard, E., and Duplessy, J. C.: The North Atlantic atmosphere-sea surface $^{14}C$ gradient during the Younger Dryas climatic event. Earth Planet. Sci. Lett. *126*, 275–287 (1994)

Barker, S., Broecker, W. S., Clark, E., and Hajdas, I.: Radiocarbon age offsets of foraminifera resulting from differential dissolution and fragmentation within the sedimentary bioturbated zone. Paleoceanography *22*, PA2205; doi:10.1029/2006PA001354 (2007)

Bondevik, S., Birks, H. H., Gulliksen, S., and Mangerud, J.: Late Weichselian marine $^{14}C$ reservoir ages at the western coast of Norway. Quat. Res. *52*, 104–114 (1999)

Bondevik, S., Mangerud, J., and Gulliksen, G.: The marine $^{14}C$ age of the Vedde Ash Bed along the west coast of Norway. J. Quat. Sci. *16*, 3–7 (2001)

Bondevik, S., Mangerud, J., Birks, H. H., Gulliksen, S., and Reimer, P.: Changes in North Atlantic radiocarbon reservoir ages during the Allerød and Younger Dryas. Science *312*, 1514–1517 (2006)

Broecker, W. S., and Clark, E.: Radiocarbon-age differences among coexisting planktic foraminifera shells: The Barker Effect. Paleoceanography *26*, PA2222; doi:10.1029/2011PA002116 (2011)

Butzin, M., Prange, M., and Lohmann, G.: Radiocarbon simulations for the glacial ocean: The effects of wind stress, Southern Ocean sea ice and Heinrich events. Earth Planet. Sci. Lett. *235*, 45–61 (2005)

Craig, H.: Carbon 13 in plants and the relationships between carbon 13 and carbon 14 variations in nature. J. Geol. *62*, 115–149 (1954)

Delaygue, G., Stocker, T. F., Joos, F., and Plattner, G. K.: Simulation of atmospheric radiocarbon during abrupt oceanic circulation changes: trying to reconcile models and reconstructions. Quat. Sci. Rev. *22*, 1647–1658 (2003)

Eiríksson, J., Knudsen, K. L., Haflidason, H., and Heinemeier, J.: Chronology of late Holocene climatic events in the northern North Atlantic based on AMS $^{14}C$ dates and tephra markers from the volcano Hekla, Iceland. J. Quat. Sci. *15*, 573–580 (2000)

Eiríksson, J., Larsen, G., Knudsen, K. L., Heinemeier, J., and Símonarson, L. A.: Marine reservoir age variability and water mass distribution in the Iceland Sea. Quat. Sci. Rev. *23*, 2247–2268 (2004)

Eiríksson, J., Knudsen, K. L., Larsen, G., Olsen, J., Heinemeier, J., Bartels-Jónsdóttir, H. B., Jiang, H., Ran, L., and Símonarson, L. A.: Coupling of palaeoceanographic shifts and changes in marine reservoir ages off North Iceland through the last millennium. Palaeogeogr., Palaeoclim., Palaeoecol. *302*, 95–108 (2011)

Franke, J., Paul, A., and Schulz, M.: Modeling variations of marine reservoir ages during the last 45,000 years. Clim. Past *4*, 125–136 (2008)

Haflidason, H., Sejrup, H. P., Klitgaard Kristensen, D., and Johnsen, S.: Coupled response of the late glacial climatic shifts of northwest Europe reflected in Greenland ice cores: evidence from the northern North Sea. Geology *23*/12, 1059–1062 (1995)

Hain, M. P., Sigman, D. M., and Haug, G. H.: Shortcomings of the isolated abyssal reservoir model for deglacial radiocarbon changes in the mid-depth Indo-Pacific Ocean. Geophys. Res. Lett. *38*, L04604; doi: 10.1029/2010GL046158 (2011)

Hutchinson, I., James, T. S., Reimer, P. J., Bornhold, B. D., and Clague, J. J.: Marine and limnic radiocarbon reservoir corrections for studies of late- and postglacial environments in Georgia Basin and Puget Lowland, British Columbia, Canada and Washington, USA. Quat. Res. *61*, 193–203 (2004)

Ikehara, K., Danhara, T., Yamashita, T., Tanahashi, M., Morita, S., and Ohkushi, K.: Paleoceanographic control on a large marine reservoir effect offshore of Tokai, south of Japan, NW Pacific, during the last glacial maximum-deglaciation, Quat. Int. *246*, 213–221 (2011)

Knudsen, K. L., and Eiríksson, J.: Application of tephrochronology to the timing and correlation of palaeoceanographic events recorded in Holocene and Late Glacial shelf sediments off North Iceland. Mar. Geol. *191*, 165–188 (2002)

Kubota, K., Yokoyama, Y., Ishikawa, T., Obrochta, S., Suzuki, A., and Larger, C.: $O_2$ source at the equatorial Pacific during the last deglaciation. Sci. Rep. *4*, 5261 (2014)

Larsen, G., Eiríksson, J., Knudsen, K. L, and Heinemeier, J.: Correlation of late Holocene terrestrial and marine tephra markers, north Iceland: implications for reservoir age changes. Polar Res. *21*, 283–290 (2002)

Oeschger, H., Siegenthaler, U., Schotterer, U., and Gugelmann, A.: A box diffusion model to study the carbon dioxide exchange in nature. Tellus *27*, 168–192 (1975)

Peck, V. L., Hall, I. R., Zahn, R., Elderfield, H., Grousset, F. E., and Scourse, J. D.: High resolution evidence for linkages between European ice sheet instability and Atlantic meridional overturning circulation. Earth Planet. Sci. Lett. *243*, 476–488 (2006)

Reimer, P. J., and Reimer, R. W.: A marine reservoir correction database and on-line interface. Radiocarbon *43*, 461–463 (2001)

Ritz, S. P., Stocker, T. F., and Müller, S. A.: Modeling the effect of abrupt ocean circulation change on marine reservoir age. Earth Planet. Sci. Lett. *268*/1, 2, 202–211 (2008)

Sarnthein, M., Grootes, P. M., Kennett, J. P., and Nadeau, M. J.: $^{14}C$ reservoir ages show deglacial changes in ocean currents. In: Schmittner, A., Chiang, J., and Hemming, S. (Eds.): Ocean Circulation: Mechanisms and Impacts. Geophys. Monograph Series *173*; pp. 175–197. Washington, DC: American Geophysical Union 2007

Siani, G., Michel, E., De Pol-Holz, R., DeVries, T., Lamy, F., Carel, M., Isguder, G., Dewilde. F., and Lourantou, A.: Carbon isotope records reveal precise timing of enhanced Southern Ocean upwelling during the last deglaciation. Nature Comm. *4*, 2758; doi: 10.1038/ncomms3758 (2013)

Siani, G., Paterne, M., Michel, E., Sulpizio, R., Sbrana, A., Arnold, M., and Haddad, G.: Mediterranean sea surface radiocarbon reservoir age changes since the last glacial maximum. Science *294*, 1917–1920 (2001)

Sikes, E. L., Samson, C. R., Guilderson, T. P., and Howard, W. R.: Old radiocarbon ages in the southwest Pacific Ocean during the last glacial period and deglaciation. Nature *405*, 555–559 (2000)

Singarayer, J. S., Richards, D. A., Ridgwell, A., Valdes, P. J., Austin, W. E. N., and Beck, J. W.: An oceanic origin for the increase of atmospheric radiocarbon during the Younger Dryas. Geophys. Res. Lett. *35*, L14707; doi:10.1029/2008GL034074 (2008)

Skinner, L., Waelbroeck, C., Scrivner, A., and Fallon, S.: Radiocarbon evidence for alternating northern and southern sources of ventilation of the deep Atlantic carbon pool during the last deglaciation. Proc. Nat. Acad. Sci. USA *111*, 5480–5484 (2014)

Skinner, L., McCave, I. N., Carter, L., Fallon, S., Scrivner, A. E., and Primeau, F.: Reduced ventilation and enhanced magnitude of the deep Pacific carbon pool during the last glacial period. Earth Planet. Sci. Lett. *411*, 45–52 (2015)

Stern, J. V., and Lisiecki, L. E.: North Atlantic circulation and reservoir age changes over the past 41,000 years. Geophys. Res. Lett. *40*, 3693–3697; doi:10.1002/grl.50679 (2013)

Stocker, T. F., and Wright, D. G.: The effect of a succession of ocean ventilation changes on $^{14}C$. Radiocarbon *40*/1, 359–366 (1998)

Thornalley, D. J. R., Barker, S., Broecker, W. S., Elderfield, H., and McCave, I. N.: The deglacial evolution of North Atlantic deep convection. Science *331*, 202–205 (2011a)

Thornalley, D. J. R., McCave, I. N., and Elderfield, H.: Tephra in deglacial ocean sediments south of Iceland: Stratigraphy, geochemistry and oceanic reservoir ages. J. Quat. Sci. *26*/2, 190–198 (2011b)

Waelbroeck, C., Duplessy, J.-C., Michel, E., Labeyrie, L., Paillard, D., and Duprat, J.: The timing of the last deglaciation in North Atlantic climate records. Nature *412*, 724–727 (2001)

Prof. Edouard Bard
CEREGE
(Aix-Marseille University
CNRS, IRD, Collège de France)
Le Trocadéro
Europole de l'Arbois BP80
13545 Aix-en-Provence Cedex4
France
Phone: +33 4 42507418
Fax: +33 4 42507421
E-Mail: bard@cerege.fr

Nova Acta Leopoldina NF *121*, Nr. 408, 35–38 (2015)

# Ocean Acidification – A Biogeological Perspective

Jelle Bijma (Bremerhaven)

With 2 Figures

When $CO_2$ is absorbed from the atmosphere into the ocean, it forms carbonic acid and lowers pH. This process is commonly referred to as ocean acidification (OA) (e.g. Gattuso and Hansson 2011). On geologic timescales, the $CO_2$ concentration in the atmosphere and the carbonate chemistry of the oceans are constantly changing and adjusting to forcing through tectonics, volcanism, weathering, biology and currently, the human race.

Relationships between the elemental and isotope composition of fossil remains and environmental parameters, so-called proxy relationships or "proxies" for short, allow to reconstruct climates of the past. Proxy evidence suggest that atmospheric $CO_2$ concentrations have been much higher than today during long warm intervals in Earth's history and that those conditions were not always harmful to e.g. calcifying organisms (e.g Hönisch et al. 2012). In fact, the name Cretaceous with its high atmospheric $pCO_2$ was coined because of its massive limestone deposits from e.g coccolithophores that build the cliffs of Dover. Hence, it is a common misconception that high atmospheric $pCO_2$, *per se*, goes hand in hand with reduced biocalcification. In fact, for most calcifying organisms the saturation state of the ocean with respect to calcium carbonate may be more important than its pH. If a carbon perturbation is slow enough, surface waters will remain supersaturated because dissolution of deep sea sediments and weathering of rock on the continent, can keep pace with the perturbation and the saturation state of the ocean with respect to calcium carbonate is well regulated (e.g. Ridgwell and Schmidt 2010). As a consequence, calcifying organisms continue to form their skeletons in a well buffered ocean even when pH is low. On the other hand, organisms that actively regulate their acid-base balance will still be under pressure at a lower pH even though the saturation state of the ocean remains high (Fig. 1), simply because they have to spend more metabolic energy on their pH regulation at the expense of other processes (Bijma et al. 2013).

There have been periods in Earth's history where we have indications that the oceans have been acidified (a lower pH than today). For instance, at the end of the Permian (e.g. Knoll et al. 2007), ca. 251 Ma ago or at the Paleocene-Eocene Thermal Maximum (PETM), 55 Ma ago. These acidification events were also triggered by a carbon perturbation but had a different origin (volcanism and methane clathrates, respectively) than today. Nevertheless, all are characterized by catastrophic extinctions and biodiversity loss. Importantly, it should be noted that OA (lowering of pH) is only one consequence of a carbon perturbation. These events are usually accompanied by global warming, stronger stratification of the ocean and a decrease of the oxygenation of the deep sea (so-called "Ocean Anoxic Events" or OAE's).

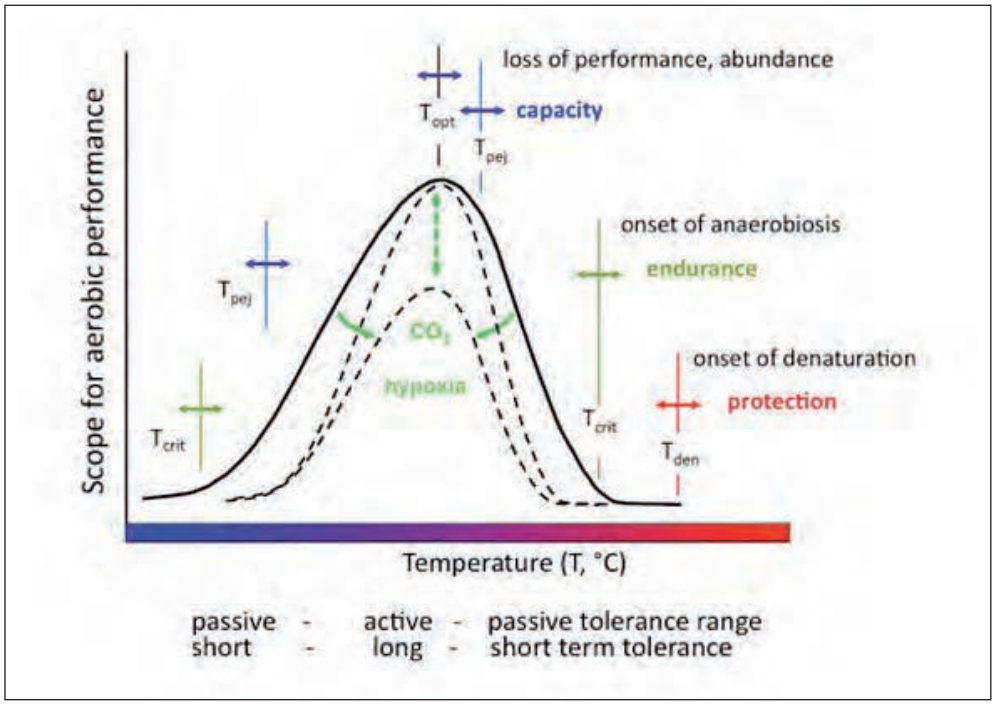


Fig. 1 The window of optimal performance of many organisms is affected by temperature, ocean carbonate chemistry and hypoxia, the three direct symptoms of a massive carbon perturbation. For animals, the concept of oxygen and capacity limited thermal tolerance (OCLTT) provides an explanation for the specialization of animals on specific, limited temperature ranges and their sensitivity to temperature extremes. Furthermore, it allows integration of other stressors on a thermal matrix of performance (see Pörtner et al. 2005, 2010).

As such, it is difficult to de-convolve the consequence of decreased pH from the plethora of associated impacts.

It is important to keep in mind that the climatic conditions prior to the above mentioned geologic events were vastly different from today. The atmospheric $pCO_2$ was high to start with, the oceans were warmer and had a different chemistry, which, by itself, had a considerable impact on the saturation state with respect to calcium carbonate. However, the most important difference between all previous geological events compared to today is the rate at which the human induced carbon perturbation proceeds (Fig. 2).

Hence, even though we do not seem to have a perfect analogue to the present day carbon perturbation, we can only expect that the consequences of man-made OA are worse than those recorded in the geological records, simply because the rate of change is unprecedented in the Earth's history, and the marine ecosystem as we know it today has mainly evolved in a time where atmospheric $CO_2$ has been low and oceans were well buffered (Bijma et al. 2013). The detailed PETM record, which is probably the best analogue, teaches us, that it might take about 100 ka for a full chemical recovery of the ocean and that biological recovery takes millions of years.

Ocean acidification is occurring today and will continue to intensify, closely tracking global $CO_2$ emissions. Given the potential threat to marine ecosystems and biodiversity and,

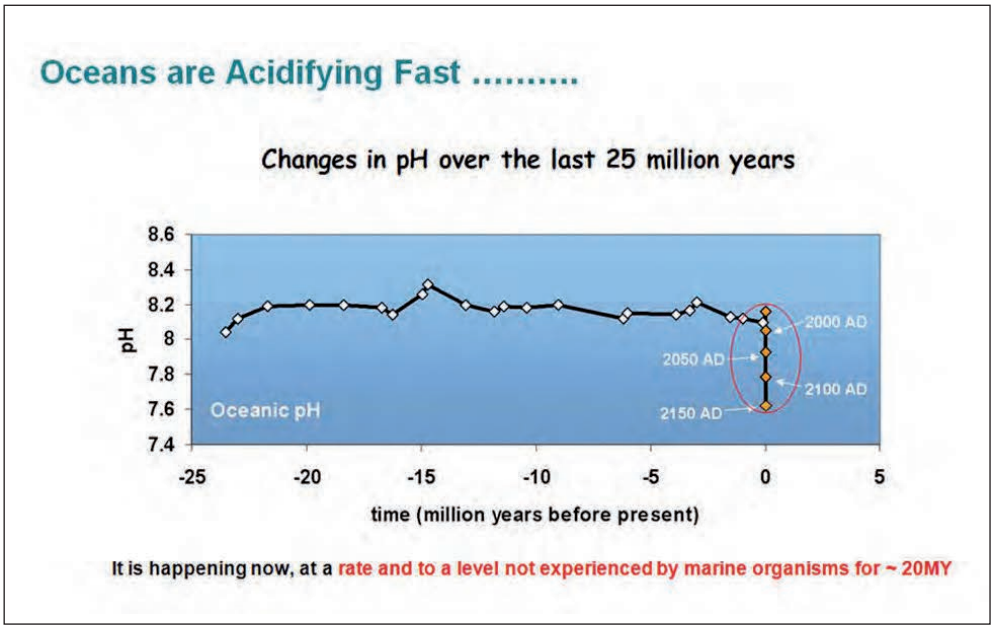


Fig. 2 The paleohistorical record of ocean pH demonstrates that present levels are unseen in the last 20 million years (after Turley et al. 2006). Note that depending on the rate (and magnitude) of a carbon perturbation, pH and the saturation state may be decoupled (slow rate) or change simultaneously (fast rate as today).

its ensuing impact on human society and economy, especially as it acts in conjunction with ocean warming, there is an urgent need for immediate action. This "double trouble" is probably the most critical environmental issue that humans will have to face in their immediate future and it might become the major socio-economic challenge of this century.

The impacts of ocean acidification are global in scope and yet some of the least understood of all climate change phenomena. Given that its effects are already measurable and that biological impacts may become dramatic within only decades, we must now accept the challenge to better coordinate and stimulate research on ocean acidification if we are to fully understand the consequences of and eventually help mitigate ocean acidification.

Understanding the risks and consequences of OA and recognizing that both OA and global warming are caused by anthropogenic $CO_2$ emissions will hopefully help to set in motion a stringent climate policy worldwide. The only solution to neutralize OA and global warming is a long-term mitigation strategy to limit future release of $CO_2$ to the atmosphere and/or enhance removal of excess $CO_2$ from the atmosphere.

## *References*

Bijma, J., Pörtner, H.-O., Yesson, C., and Rogers, A. D.: Climate change and the oceans – What does the future hold? Marine Pollution Bulletin *74*, 495–505 (2013)

Gattuso, J.-P., and Hansson, L. (Eds.): Ocean Acidification. Oxford: Oxford University Press 2011

Hönisch, B., Ridgwell, A., Schmidt, D. N., Thomas, E., Gibbs, S. J., Sluijs, A., Zeebe, R., Kump, L., Martindale, R. C., Greene, S. E., Kiessling, W., Ries, J., Zachos, J. C., Royer, D. L., Barker, S., Marchitto, T. M., Moyer, R., Pelejero, C., Ziveri, P., Foster, G. L., and Williams, B.: The geological record of ocean acidification. Science *335*, 1058–1063 (2012)

Knoll, A. H., Barnbach, R. K., Payne, J. L., Pruss, S., and Fischer, W. W.: Paleophysiology and end-Permian mass extinction. Earth Planet. Sci. Lett. *256*, 295–313 (2007)

Pörtner, H. O.: Oxygen and capacity limitation of thermal tolerance: a matrix for integrating climate related stressors in marine ecosystems. J. Exp. Biol. *213*, 881–893 (2010)

Pörtner, H. O., Langenbuch, M., and Michaelidis, B.: Synergistic effects of temperature extremes, hypoxia, and increases in $CO_2$ on marine animals: From Earth history to global change. J. Geophys. Res. *110*, C09S10; doi:10.1029/2004JC002561 (2005)

Ridgwell, A., and Schmidt, D. N.: Past constraints on the vulnerability of marine calcifiers to massive carbon dioxide release. Nature Geosci. *3*, 196–200 (2010)

Turley, C., Blackford, J. C., Widdicombe, S., Lowe, D., Nightingale, P. D., and Rees, A. P.: Reviewing the impact of increased atmospheric $CO_2$ on oceanic pH and the marine ecosystem. In: Schellnhuber, H. J., Cramer, W., Nakicenovic, N., Wigley, T., and Yohe, G. (Eds.): Avoiding Dangerous Climate Change; pp. 65–70. Cambridge, UK: Cambridge University Press 2006

Prof. Dr. Jelle Bijma
Marine Biogeosciences
Alfred Wegener Institute
Helmholtz Centre for Polar and Marine Research
Am Handelshafen 12
27570 Bremerhaven
Germany
Phone: +49 471 483118
Fax: +49 471 48311149
E-Mail: jelle.bijma@awi.de

Nova Acta Leopoldina NF *121*, Nr. 408, 39 – 42 (2015)

# Isotopic Constraints on Greenhouse Gas Variability during the Last Deglaciation from Blue Ice Archives

Ed Brook, Thomas Bauska, and Alan Mix (Corvallis, OR, USA)

With 2 Figures

Trace gas records from traditional ice cores provide vital records of changes in atmospheric composition but deep ice coring is expensive, time consuming, and sample quantities are typically limited. In some locations on the margins of Greenland and Antarctica ancient ice outcrops at the surface and can be sampled in very large quantities (Fig. 1 shows the Taylor Glacier outcrop location in Antarctica). Such samples provide the opportunity to make measurements that are otherwise difficult on traditional ice cores, for example the radiocarbon content of $CH_4$ (Petrenko et al. 2009), or high precision measurements of stable isotope ratios of trace gases (for example, recent work on the isotopic composition of $N_2O$ by Schilt et al. 2014, see Fig. 2). Ice margin samples also offer the possibility of very high-resolution sampling in key intervals.

We focus here on a complete record of $CO_2$ and $\delta^{13}C\text{-}CO_2$ for the last deglaciation obtained from the Taylor Glacier, in the Dry Valleys region of Antarctica (Fig. 1). Samples were taken by shallow (~ 4 m) coring in an ~360 m cross- glacier transect after extensive field reconnaissance and analysis of atmospheric $CH_4$ to establish the stratigraphy.

Ice ranging in age from early Holocene to Eemian outcrops at various locations on Taylor Glacier. Although the ice is deformed by folding, it is possible to reconstruct time series of gas records by correlating $CH_4$ concentration records and the $\delta^{18}O\text{-}O_2$ with well dated ice core records. We take advantage of the large sample sizes available to use a high precision dual inlet method to measure $\delta^{13}C\text{-}CO_2$ (Bauska et al. 2014) from 22–11 ka. The reproducibility of the isotope measurements is ~ 0.02 ‰. The high precision results combined with high-resolution sampling reveal more detail about carbon cycle changes than previous data sets.

In Figure 2 we plot $CO_2$ and $\delta^{13}C\text{-}CO_2$ as well as $CH_4$, $N_2O$ and $\delta^{15}N\text{-}N_2O$ (the latter three records from Schilt et al. 2014). The age scale is based on correlating $CH_4$ variations with the very well dated WAIS Divide ice core (Marcott et al. 2014) and confirmation of field results with laboratory measurements of $CH_4$, $CO_2$, $N_2O$ and $\delta^{18}O\text{-}O_2$ (Schilt et al. 2014, Baggenstos et al., in prep.) and comparison of those records with established ice core data. Corrections for gravitational fractionation are based on $\delta^{15}N\text{-}N_2$ measurements made at the Scripps Institute of Oceanography (Baggenstos and Severinghaus, in prep.).

$CH_4$ and $CO_2$ concentration trends show all of the expected abrupt changes and inflection points known from other records, allowing us to precisely date the Taylor Glacier records and place them in a global stratigraphic framework. Relative to WAIS Divide we expect (and observe) that the Taylor Glacier record is smoothed due to diffusion in the firn column because the original deposition site of Taylor Glacier ice was in a relatively lower accumulation rate region.

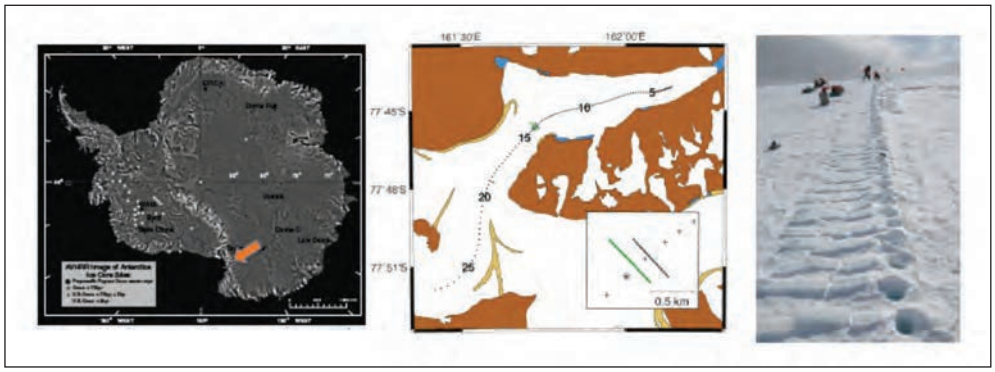


Fig. 1 *Left*: Location of Taylor Glacier blue ice outcrop, middle: sketch map of sampling region (inset shows location of sample transect (green line). *Right*: example of high resolution coring.

The high precision $\delta^{13}C$-$CO_2$ record is fully consistent with previous reconstructions but allows us to see changes on short timescales (Fig. 2). During the Last Glacial Maximum (LGM) $CO_2$ and $\delta^{13}C$-$CO_2$ were not constant; small variations (< 5 ppm and 0.08 ‰), suggest that the carbon cycle was not completely at steady state. From 18 ka to 15.5 ka $\delta^{13}C$-$CO_2$ shows a strong 0.3 ‰ decrease that corresponds to an increase in $CO_2$ of 35 ppm. We show that the decrease happened in two roughly equal steps. An initial decrease of ~0.15 ppm between 18 and 16.5 ka corresponds with the initial increase of $CO_2$ by ~ 20 ppm. At ~ 16.5 ka a rapid additional drop of $\delta^{13}C$-$CO_2$ of ~0.15 ‰ occurred over a period of several centuries, and corresponds with an additional increase of $CO_2$ by ~ 7 ppm. From 15.5 ka to 11 ka, $CO_2$ increased by 40 ppm and $\delta^{13}C$-$CO_2$ gradually increased. Superimposed on this trend is a second sharp decline in $\delta^{13}C$-$CO_2$ that started at ~12.9 ka, coincident with the start of the $CO_2$ rise during the Younger Dryas. $\delta^{13}C$-$CO_2$ reached a minimum at ~12.5 ka and recovered over the next ~1000 years.

We combine the data with carbon cycle box model experiments to examine processes that are plausibly responsible for the deglacial rise in atmospheric $CO_2$. We employ a Keeling plot technique where in a classic two-component system the y-axis intercept of a linear regression to the data ($y_0$) is the $\delta^{13}C$ signature of the reservoir controlling the atmosphere. In the more complex mixing between the atmosphere, ocean and terrestrial biosphere a carbon cycle model must be used to account for process like air-sea gas exchange and ocean mixing which can lead to a non-linear, time-variant relationship between $CO_2$ and $\delta^{13}C$-$CO_2$.

We use the model results to outline a scenario that couples deglacial climate history and our carbon cycle observations. During the early part of HS1, the collapse of AMOC (McManus et al. 2004) decreased heat transport to the North Atlantic. In response, large areas of the Northern Hemisphere (NH) cooled and Southern Hemisphere (SH) warmed, the ITCZ shifted southward and SH westerlies shifted southward or strengthened (Wang et al. 2004, Cheng et al. 2009, Denton et al. 2010). We hypothesize that a shift of the westerlies off the SH continents and/or increased SH precipitation lead to a precipitous decline in dust delivery over the Subantarctic ocean, driving the bulk of the $CO_2$ rise from about 18–15.5 ka. The southward migration of the ITCZ also lead to a drying in parts of the NH, possibly causing a reduction in land carbon, most notably around 16.5 ka when the first abrupt change in

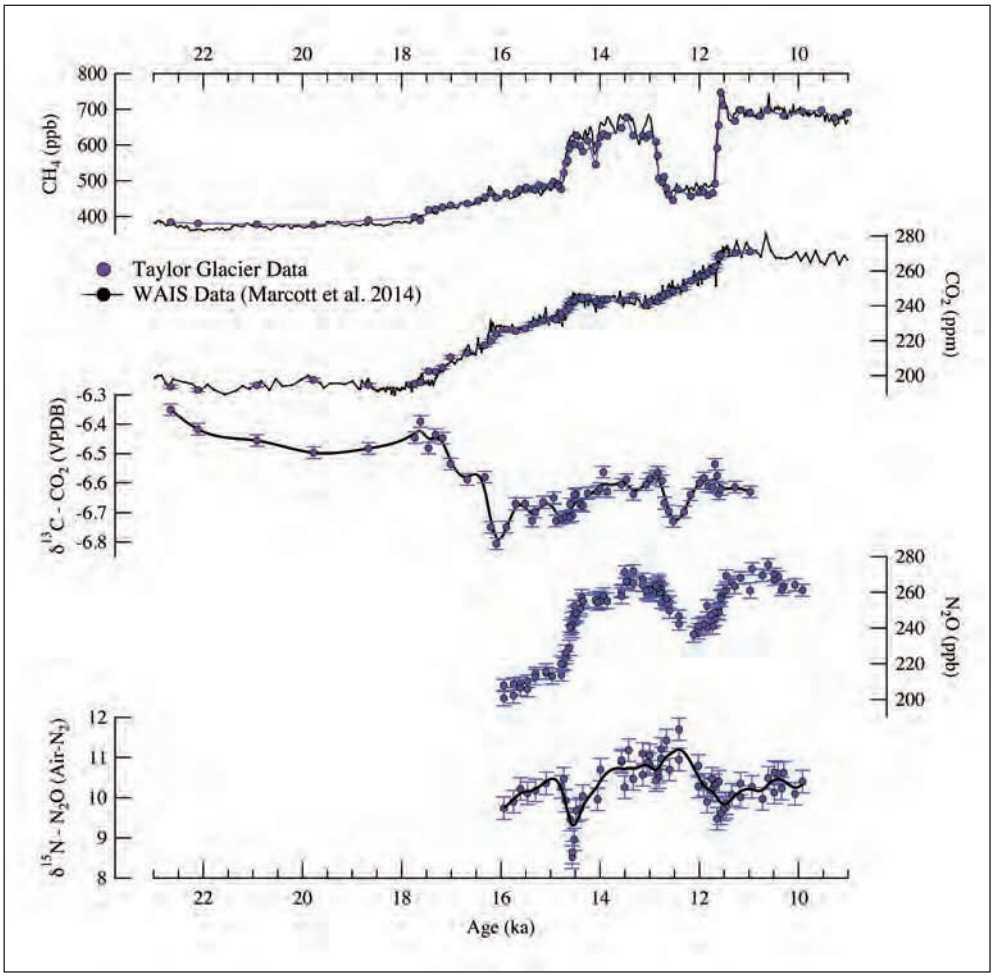


Fig. 2 Blue: $CH_4$, $CO_2$, $\delta^{13}C\text{-}CO_2$, and $\delta^{15}N\text{-}N_2O$ from the Taylor Glacier blue ice archive. $\delta^{15}N\text{-}N_2O$ results were used by SCHILT et al. (2014) to partition the $N_2O$ change in to oceanic and terrestrial sources. Terrestrial changes dominate on centennial timescales but inferred changes in marine emissions are consistent with current understanding of changes in ocean oxygenation.

$\delta^{13}C\text{-}CO_2$ occurred. Alternatively, or additionally, the changing SH westerlies around 16.5 ka leading to enhanced air-sea gas exchange and possibly greater upwelling.

During the later half of HS1, dust deposition had effectively reached interglacial levels, and the $\delta^{13}C\text{-}CO_2$ data are consistent with the $CO_2$ rise being driven mostly by warming ocean temperatures and an additional release of ocean biological carbon. However, the initial rise in $CO_2$ during the YD could have been triggered by either a second loss of land carbon or additional enhancement of SH westerlies, driven ultimately by AMOC reduction and NH cooling.

Our new data provide strong constraints on the mechanisms behind glacial-interglacial $CO_2$ variability. The $\delta^{13}C\text{-}CO_2$ record shows that most of the 75 ppm increase in atmospheric $CO_2$ could plausible be attributed to a combination of a release of organic carbon from the

ocean and rising ocean temperature, but the $CO_2$ rises occurred in a series of steps, each with a $d^{13}C$ fingerprint that suggests that different mechanisms may have been triggered at various times during the deglacial transition. Primary release of $CO_2$ accumulated in the ocean from respired organic matter occurred relatively early in the transition. Global temperature changes lagged the release of deep ocean carbon, supporting a trigger for the deglaciation in ocean circulation or ocean biological processes. At least twice during the deglaciation a rapid release of carbon depleted in $^{13}C$ to the atmosphere occurred over a few centuries, suggesting that abrupt and significant releases of $CO_2$ to the atmosphere may be common nonlinear features of Earth's carbon cycle.

## *References*


Bauska, T. K., Brook, E. J., Mix, A. C., and Ross, A.: High-precision dual-inlet IRMS measurements of the stable isotopes of $CO_2$ and the $N_2O/CO_2$ ratio from polar ice core samples. Atmospheric Measurement Techniques *7*/11, 3825–3837 (2014)

Cheng, H., Edwards, R. L., Broecker, W. S., Denton, G. H., Kong, X., Wang, Y., Zhang, R. and Wang, X.: Ice age terminations. Science *326*/5950, 248–252 (2009)

Denton, G. H., Anderson, R. F., Toggweiler, J. R., Edwards, R. L., Schaefer, J. M., and Putnam, A. E.: The last glacial termination. Science *328*/5986, 1652–1656 (2010)

Marcott, S. A., Bauska, T. K., Buizert, C., Steig, E. J., Rosen, J. L., Cuffey, K. M., Fudge, T. J., Severinghaus, J. P., Ahn, J., Kalk, M. L., Mc Connell, J. P., Sowers, T., Taylor, K. C., White, J. W., and Brook, E. J.: Centennial-scale changes in the global carbon cycle during the last deglaciation. Nature *514*/7524, 616–619 (2014)

McManus, J. F., Francois, R., Gherardi, J. M., Keigwin, L. D., and Brown-Leger, S.: Collapse and rapid resumption of Atlantic meridional circulation linked to deglacial climate changes. Nature *428*/6985, 834–837 (2004)

Petrenko, V. V., Smith, A. M., Severinghaus, J. P., Brook, E. J., Lowe, D., Riedel, K., Brailsford, G., Hua, Q., Schaefer, H., Reeh, N., Weiss, R. F., and Etheridge, D.: $^{14}CH_4$ measurements in Greenland ice: investigating last glacial termination $CH_4$ sources. Science *324*/5926, 506–508 (2009)

Schilt, A., Brook, E. J., Bauska, T. K., Baggenstos, D., Fischer, H., Joos, F., Petrenko, W., Schaefer, H., Schmidt, J., Severinghaus, J. P., Spahni, R., and Stocker, T. F.: Isotopic constraints on marine and terrestrial $N_2O$ emissions during the last deglaciation. Nature *516*/7530, 234–237 (2014)

Wang, X., Auler, A. S., Edwards, R. L., Cheng, H., Cristalli, P. S., Smart, P. L., Richards, D. A., and Shen, C. C.: Wet periods in northeastern Brazil over the past 210 kyr linked to distant climate anomalies. Nature *432*/7018, 740–743 (2004)



Prof. Ed Brook, Ph.D.
Thomas Bauska, Ph.D.
Prof. Alan Mix, Ph.D.
College of Earth, Ocean, and Atmospheric Sciences
Oregon State University
Wilkinson 130
Corvallis, OR, 97331
USA
Phone: +1 541 7378197
Fax: +1 541 7371200
E-Mail: brooke@geo.oregonstate.edu
bauskat@science.oregonstate.edu

Nova Acta Leopoldina NF *121*, Nr. 408, 43 – 47 (2015)

# The Role of the Terrestrial Biosphere in CLIMBER-2 Simulations of the Last 4 Glacial $CO_2$ Cycles

Victor Brovkin (Hamburg) and Andrey Ganopolski (Potsdam)

With 3 Figures

Terrestrial ecosystems strongly affect fluxes of heat, water, and greenhouse gases between land and atmosphere. In pre-industrial climate, vegetation biomass and mineral soils contained about 2,000 Gt of carbon, about 4 – 5 times more than the atmosphere at that time. During Last Glacial Maximum (LGM), a decrease in atmospheric $CO_2$ from 280 to 200 ppmv should have caused about 30 % decrease in plant productivity mainly due to physiological effect of $CO_2$ (reduction in water use efficiency). In addition, expansion of ice sheets and climate change led to extreme reduction of boreal and temperate forests and an increase in savannah in subtropical regions. This view is strongly supported by pollen-based reconstructions of vegetation cover. A decrease in tropical forests due to less moisture and lower $CO_2$ level was compensated by a growth of forests on exposed tropical shelves. In total, effects of climate and $CO_2$ on terrestrial vegetation should have led to a strong reduction in terrestrial carbon storage. Model-based studies suggest a decrease in land carbon in the range from 300 to 800 GtC, with a largest uncertainty coming from the changes in distribution in vegetation cover. Estimates based on marine $^{13}C$ changes are close to 500 GtC, falling in the middle of the range of the model estimates. The later do not account for the boreal peat growth during the Holocene, estimated into about 400 GtC. In total, following previous model simulations, it could about 1,000 GtC of interglacial-to-glacial difference in terrestrial carbon storage (biomass and mineral soils).

Such strong variability in land carbon does not help to explain changes in atmospheric $CO_2$ during glacial cycles as changes in land carbon counteract the atmospheric $CO_2$ drawdown during glaciation inception and $CO_2$ increase during deglaciation. Translated into atmosphere $CO_2$ changes, this would mean not very much – 20 to 30 ppm depending on the strength of the ocean carbonate compensation and weathering effect on alkalinity – but it should be added at the top of 80 to 100 ppm changes needed to be explained by the ocean carbon cycle. On a long term, it is possible for the ocean to absorb extra 1,000 GtC in addition to its huge reservoir capacity of about 40,000 GtC, but during periods of fast climate changes the ocean is too slow to explain observed fast changes in atmospheric $CO_2$. Without an extra pool capable to release 400 – 500 GtC relatively quickly, the models are unable to explain the periods of fast $CO_2$ changes.

A possible solution to this problem was recently suggested by an involvement of terrestrial carbon storage in cold environments (e.g. Ciais et al. 2012). Decomposition of organic matter is strongly temperature-dependent with an average $Q_{10}$ factor of 2, i.e. it slows down

by a factor of 2 in response to the temperature drop by 10 °C. In frozen soils, decomposition of soil carbon is negligible. A presence of ice in the soils, for example in the form of ice wedges in the permafrost soils, leads to a burial of carbon on a very long time scale until the permafrost is thawed and organic carbon is available for decomposition again. Because the glacial inception led to continuous decrease in temperature, decomposition of plant litter at the surface was slow, and most of organic was not decomposed but accumulated at the surface. The formation of permafrost led to continuous burial of carbon in the soils, which could reach tens and hundreds of kg C $m^{-2}$. Current stocks of carbon in permafrost environment are estimated in about 1,500 Gt of carbon, and these storages should be much higher during the glacial periods because significant part of permafrost was thawed during deglaciation. These processes of decomposition of frozen carbon in response to deglacial changes continue today because of thermokarst and thermal erosion which occur irregularly after surface disturbances due to surface fires or water erosion during spring snow melt. In addition, substantial part of frozen organic carbon was trapped under the ice sheets. This organics was likely transported by the ice dynamics to the edges of the ice sheets boundaries, where it could decompose quickly during abrupt warming events.

## 1. Terrestrial Carbon Model Setup

The CLIMBER-2 model is the Earth System model of intermediate complexity (Petoukhov et al. 2000). It includes all necessary components to simulate dynamics of the Earth climate and carbon cycle on multi-millennial time scale. The physical model components include dynamic-statistical atmospheric model, 3-basin zonally averaged ocean model, thermodynamic sea ice model and ice-sheet model (Ganopolski and Calov 2011). The biogeochemistry model includes terrestrial vegetation and carbon cycle model VECODE, marine biogeochemistry model including models of marine biota and deep-sea carbonate sediments, as well as a model of carbon isotopes. For glacial cycle simulations, the biogeochemistry model is updated with models of coral reef growth and terrestrial weathering (Brovkin et al. 2012). The CLIMBER-2 model has been applied for simulating paleoclimates and biogeochemistry including LGM time slice and transient biogeochemistry dynamics during the Holocene and the last glacial cycle, as well as transient changes in climate-ice sheet system over the last eight glacial cycles (Ganopolski and Calov 2011).

To address the role of permafrost carbon in the glacial $CO_2$ cycles, we updated CLIMBER-2 model with a module for carbon in permafrost, peat, and carbon buried under ice sheet. Recently, Crichton et al. (2014) included permafrost component into CLIMBER-2 framework by accounting for the permafrost extent based on the frost index and by slowing down the timescale of decomposition of the slow carbon pool. Here, we follow another approach. Instead of modifying the timescale of already existing slow carbon pool in the soil model, we introduce three new carbon pools: boreal peat, permafrost, and carbon buried under ice sheet. A simplified model of the peat growth assumes that under favourable conditions for the peat growth, a small fraction of litter is accumulated in the peat pool. This is occurring during the warm periods such as interglacials. The permafrost area is calculated based on soil temperature, and organic content of the permafrost fraction of the grid cell is allocated into the permafrost carbon pool. During the ice sheet growth, the carbon under ice sheets is re-allocated into the buried carbon. During deglaciation, this buried carbon is transformed into unfrozen

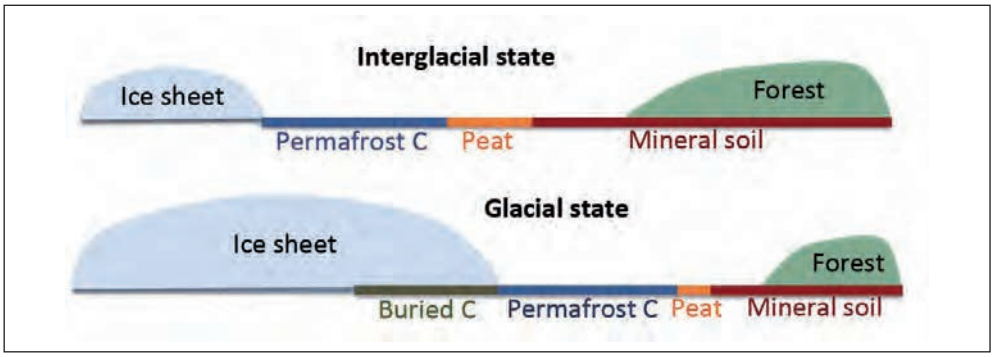


Fig. 1 A sketch of changes in soil carbon pools in regions affected by ice sheet dynamics.

soil pool from which it can relatively quickly be released to the atmosphere. The dynamics of the soil carbon pools during the glacial cycle is illustrated on Figure 1.

The physical model in glacial transient simulations is driven by changes in the orbital forcing and by reconstructed concentrations of greenhouse gases, while the carbon cycle model simulates atmospheric $CO_2$ interactively, but without feedback to the physical system. For more details of the setup of the physical model, the performance of the ocean carbon cycle model, and simulated atmospheric $CO_2$ concentration see the companion paper by Ganopolski and Brovkin in this issue.

## 2. Results

In the course of the four last glacial cycles, total terrestrial carbon storages are changing in the range of 2,700 to 3,100 GtC (Fig. 2). This variability is less than variations in particular components of the terrestrial carbon cycle. The biomass and mineral soil storages are at maximum of 1,800–2,100 GtC during interglacials, and they go down to 1,500–1,600 GtC during glacial maxima. The boreal peat storages grow up to 500 PgC at the end of interglacials or during warm interstadials, but decline to almost zero during glacial maxima. The buried carbon shows the strongest amplitude of changes of ca. 800 GtC with a rapid increase during glacial inception and a rapid decrease during deglaciation. The permafrost carbon in general follows the same dynamics as the buried carbon but shows less amplitude of changes while more abrupt reaction during periods of rapid climate changes.

During glacial inception, while biomass and mineral soil carbon decrease, terrestrial carbon storage increases due to an increase in buried and permafrost carbon (see comparison of 125 to 115 ka BP on Fig. 3). As a result, the land carbon change contributes to drawdown $CO_2$ during the period of large ice sheet initiation. This would help to start glacial inceptions in the model. At the Last Glacial Maximum, the land total storage is slightly less than at the-industrial. The fast decrease in permafrost and buried carbon during deglaciation contributes to the rapid $CO_2$ growth as the land carbon storages decrease by about 200 GtC between 20 and 10 ka BP despite of strong increase in the biomass and mineral soil carbon. At the end of the Holocene, the land carbon storage grows due to peat accumulation, and the permafrost carbon starts to increase in response to the cooling in the high northern latitudes.

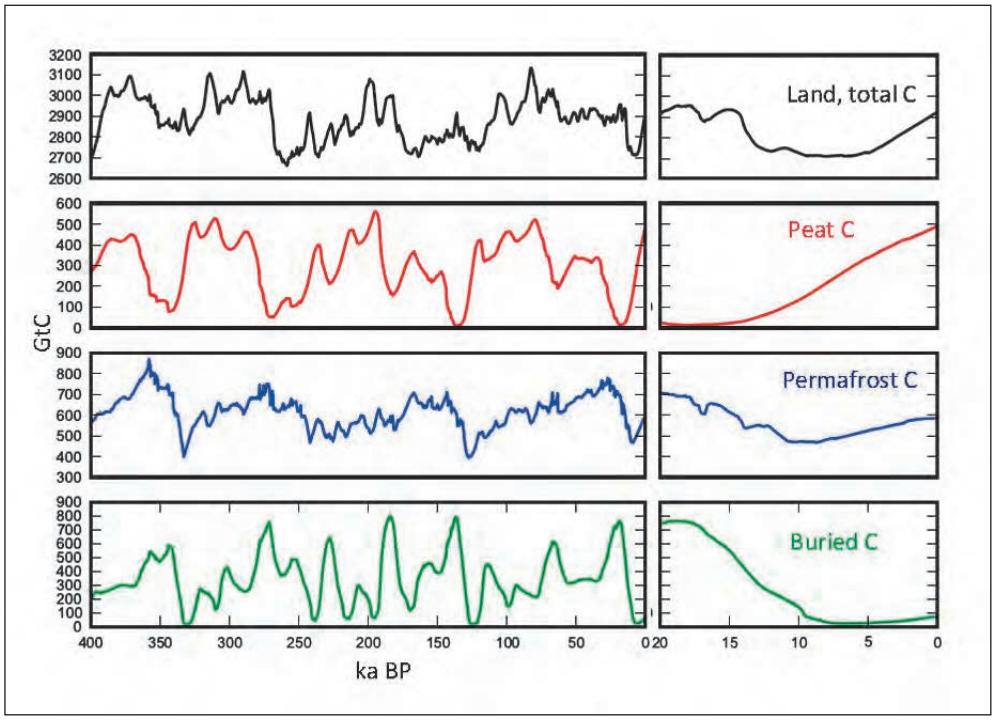


Fig. 2 Simulated changes in terrestrial carbon storages (GtC) during the last 400,000 years (*left*) and the last 20,000 years (*right*).

## 3. Conclusions

The glacial $CO_2$ cycles are shaped by changes in marine biogeochemistry which exerts control on the atmospheric $CO_2$ on multi-millennial timescale. The response of terrestrial carbon to glacial boundary conditions is usually seen as an obstacle in explaining low glacial $CO_2$ levels. By introducing new carbon pools into terrestrial carbon model, we show that dynamics of soil carbon in the regions affected by the ice sheet growth could change the view on the role of terrestrial biosphere in glacial periods. Especially during the deglaciation period, the land could act as a source of several hundred GtC to atmosphere, contrary to the conventional terrestrial biosphere models that simulate carbon storages growth during deglaciation. While development of modelling approaches to simulate permafrost carbon and carbon stored under ice sheets are still in the initial phase and their calibration is a challenge, we think that these components are an important part of explanation of the glacial $CO_2$ cycles. More efforts need to be invested into understanding of frozen carbon dynamics.

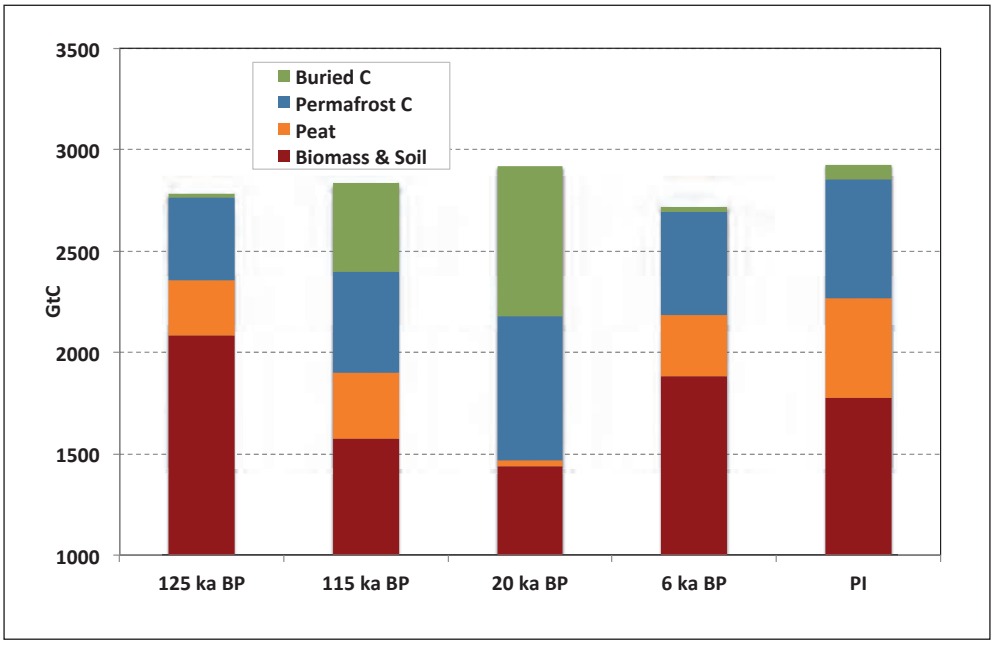


Fig. 3 Simulated land carbon storages at the last interglacial (125 ka BP), glacial inception (115 ka BP), Last Glacial Maximum (20 ka BP), mid-Holocene (6 ka BP), and pre-industrial.

## *References*


Brovkin, V., Ganopolski, A., Archer, D., and Munhoven, G.: Glacial $CO_2$ cycle as a succession of key physical and biogeochemical processes. Clim. Past *8*, 251–264 (2012)

Ciais, P., Tagliabue, A., Cuntz, M., Bopp, L., Scholze, M., Hoffmann, G., Lourantou, A., Harrison, S. P., Prentice, I. C., Kelley, D. I., Koven, C., and Piao, S. L.: Large inert carbon pool in the terrestrial biosphere during the Last Glacial Maximum. Nature Geosci. *5*, 74–79 (2012)

Crichton, K., Roche, D., Krinner, G., and Chappellaz, J.: A simplified permafrost-carbon model for long-term climate studies with the CLIMBER-2 coupled earth system model. Geosci. Mod. Dev. *7*, 3111–3134 (2014)

Ganopolski, A., and Calov, R.: The role of orbital forcing, carbon dioxide and regolith in 100 kyr cycles. Clim. Past *7*, 1415–1425 (2011)

Petoukhov, V., Ganopolski, A., Brovkin, V., Claussen, M., Eliseev, A., Kubatzki, C., and Rahmstorf, S.: CLIMBER-2: a climate system model of intermediate complexity. Part I: model description and performance for present climate. Clim. Dynam. *16*, 1–17 (2000)



Dr. Victor Brovkin
Max Planck Institute for Meteorology
Bundesstraße 53
G1717
20146 Hamburg
Germany
Phone: +49 40 41173339
Fax: +49 40 41173298
E-Mail: victor.brovkin@mpimet.mpg.de

Dr. Andrey Ganopolski
Potsdam Institute for Climate Impact Research (PIK)
P.O. Box 601203
14412 Potsdam
Germany
Phone: +49 331 2882594
Fax: +49 331 2882620
E-Mail: andrey.ganopolski@pik-potsdam.de

Nova Acta Leopoldina NF *121*, Nr. 408, 49–54 (2015)

# Radiocarbon Constraints on Southern Ocean Circulation

Andrea Burke,[1] Andrew L. Stewart,[2] Jess F. Adkins,[3] Raffaele Ferrari,[4] Malte F. Jansen,[5] Andrew F. Thompson,[3] and Laura F. Robinson[6]

With 2 Figures

The Southern Ocean is thought to play a fundamental role in driving glacial-interglacial carbon cycle changes. The reason for this is two-fold: the ice core records of atmospheric $CO_2$ and Antarctic temperature are strongly correlated, and the Southern Ocean is a region that connects the deep ocean to the surface ocean through deep water formation and sloping isopycnals in the Antarctic Circumpolar Current (ACC). Since the deep ocean is the major reservoir of carbon at the earth surface, it is likely that the change in atmospheric $CO_2$ over the deglaciation is linked to processes involving the deep ocean.

Ocean radiocarbon reconstructions provide an important record of changes in ocean circulation and $CO_2$ exchange, and are thus keys for examining the processes that led to the rapid climate and $CO_2$ shifts that characterize the last deglaciation. In this talk I will present a compilation of new and published radiocarbon data from the Southern Ocean, interpreted with help from a two-dimensional dynamical model, to examine the circulation history in this important region. The radiocarbon records are reconstructed from benthic foraminifera from sediment cores in the high latitude South Atlantic (Barker et al. 2010, Skinner et al. 2010) and deep-sea corals from the Drake Passage (Burke and Robinson 2012). In contrast to radiocarbon depth profiles in the modern Southern Ocean, these data show a significant mid-depth radiocarbon minimum during the Last Glacial Maximum (LGM) (Fig. 1). The large vertical radiocarbon gradients that characterized the LGM then disappeared during the early deglaciation, resulting in a much more homogenous radiocarbon depth profile. To first order, these results can be interpreted as increased isolation of waters at mid-depths at the LGM, and then ventilation and mixing during the early deglaciation. But what were the mechanisms that led to this glacial mid-depth radiocarbon minimum?

There are several hypotheses that invoke changes in the Southern Ocean to explain glacial-interglacial carbon cycling, and these can be roughly divided into physical and biological processes (for an extensive discussion of these see Fischer et al. [2009] and references

1 Department of Earth and Environmental Sciences, Irvine Building, University of St Andrews, St Andrews, KY16 8YG, United Kingdom; ab276@st-andrews.ac.uk.
2 Department of Atmospheric and Oceanic Sciences, UCLA, Los Angeles, CA, USA.
3 Division of Geological and Planetary Sciences, Caltech, Pasadena, CA, USA.
4 Department of Earth, Atmospheric and Planetary Sciences, MIT, Cambridge, MA, USA.
5 Department of the Geophysical Sciences, University of Chicago, Chicago, IL, USA.
6 School of Earth Sciences, University of Bristol, Bristol, United Kingdom.

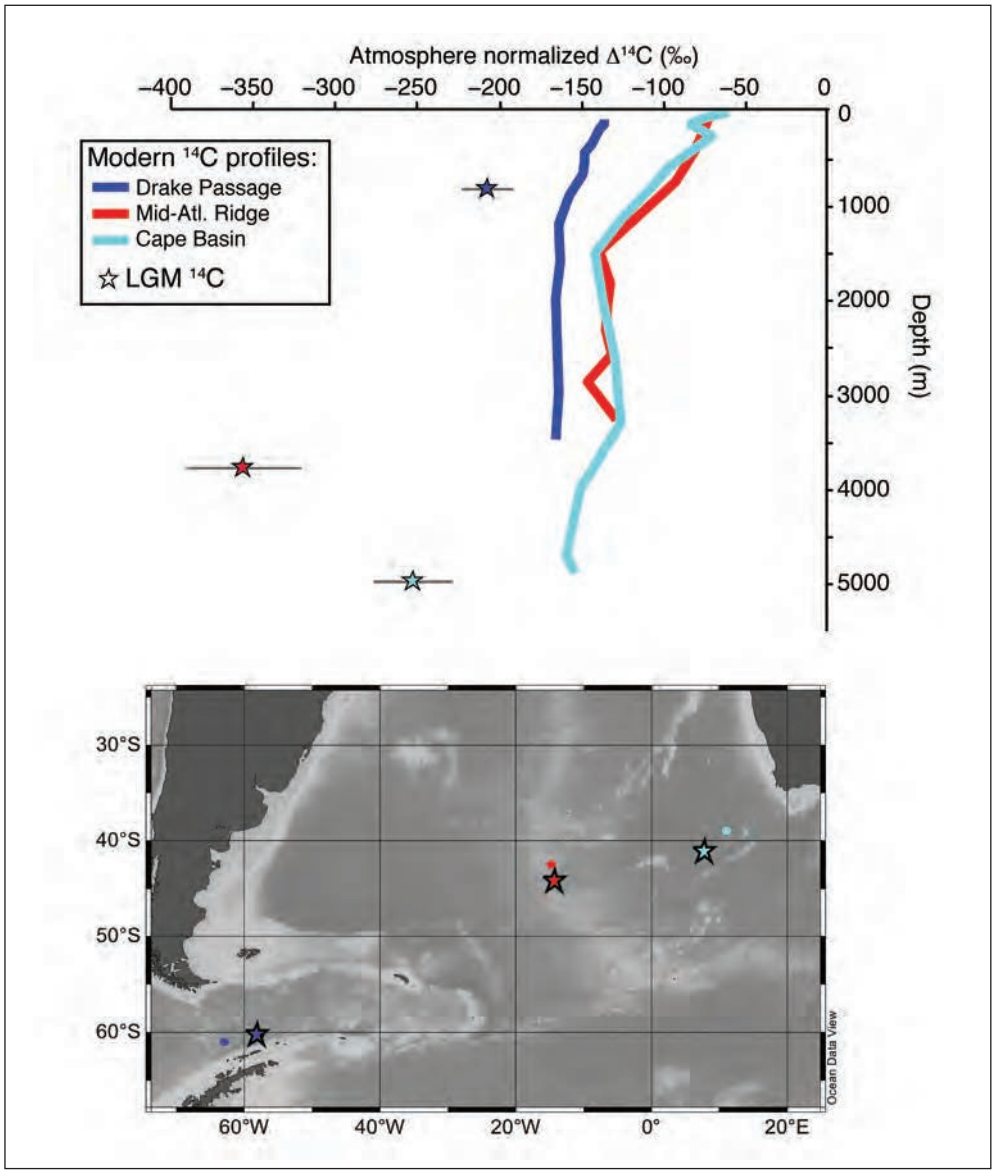


Fig. 1 From Burke et al., submitted. (*top*) Radiocarbon data plotted as atmosphere normalized $\Delta^{14}C$ from the Atlantic sector of the Southern Ocean. Modern water column data are plotted as lines and come from GLODAP (Key et al. 2004). Data reconstructed from the LGM are plotted as stars (Barker et al. 2010, Skinner et al. 2010, Burke and Robinson 2012) (*bottom*). Map showing location of sediment cores or corals (*stars*) and water column stations (*dots*).

therein). In this talk we will focus on the physical processes, namely wind and sea ice. The wind hypotheses (e.g. Toggweiler et al. 2006, Anderson et al. 2009) invoke a change in the strength or position of the westerly winds over the Southern Ocean. These hypotheses suggest

that weaker or equatorward-shifted winds during the Last Glacial Maximum would reduce Southern Ocean upwelling, thus limiting the amount of carbon that is brought to the surface ocean from the deep. Over the deglaciation, the winds either strengthened or shifted poleward with warming Antarctic temperatures, which would increase Southern Ocean upwelling and would release $CO_2$ to the atmosphere. The sea ice hypotheses (e.g. Stephens and Keeling 2000) suggests that a greater extent of sea ice in the glacial period acted to 'cap' the Southern Ocean and reduced air-sea gas exchange, which would result in lower glacial atmospheric $CO_2$ concentrations. Over the deglaciation, as Antarctic temperatures warmed and there was a reduction in sea ice extent, the Southern Ocean became 'uncapped', providing a source of $CO_2$ to the atmosphere.

Last year we put forth a hypothesis that highlighted another potential role for sea ice in glacial-interglacial climate change: it is intimately linked to the geometry of the overturning circulation (Ferrari et al. 2014) (Fig. 2). The quasi-permanent sea ice edge in the Southern Ocean is the boundary between positive and negative buoyancy forcing in the surface ocean. North of the sea ice edge, waters become less dense and flow equatorward forming the upper overturning branch, and south of the sea ice edge waters become more dense and flow poleward forming the lower overturning branch. Today the overturning circulation forms one continuous figure-eight loop. North Atlantic Deep Water flows southward in the Atlantic and upwells south of the sea ice edge, becomes more dense, and returns north in the Atlantic and Pacific basins in the lower overturning branch. Diapycnal diffusion in these ocean basins transforms water from the lower overturning branch to a density (corresponding to a depth of ~2 km) that outcrops in the ACC north of the sea ice boundary, thus closing the overturning circulation loop in the upper branch (Fig. 2). We hypothesized that the glacial expansion of sea ice (Gersonde et al. 2005) would result in a shoaling of the boundary between the upper and lower overturning branches in basins north of the ACC, away from enhanced diapycnal mixing associated with mid ocean ridges. A shoaling of the boundary above 2 km water depth would mean that the overturning circulation could not be closed by diapycnal diffusion in a single figure eight loop, and thus there would have to be two separate overturning cells, and NADW would be confined to the upper cell (Fig. 2). This geometry is consistent with $\delta^{18}O$ and $\delta^{13}C$ data from the Atlantic (e.g. Sarnthein et al. 2000, Curry and Oppo 2005, Lund et al. 2011) which show a shoaling of the boundary between northern- and southern-sourced water during the LGM. The restriction of northern-sourced water to the upper overturning branch would result in a deep southern-sourced water mass that was more isolated from the atmosphere compared to today, potentially providing a means to store more carbon in the deep.

To test our hypothesis and determine the effect of this process on glacial radiocarbon distributions, we created an idealized, 2D, residual-mean dynamical model of the global overturning circulation with a decaying tracer that is advected by the circulation to simulate radiocarbon for a comparison to published radiocarbon data (Burke et al. submitted). The model is simple and efficient, but it includes the physical and dynamical elements necessary to test our hypothesized changes in the circulation. We find that an expansion of sea ice under glacial conditions leads to a shoaled boundary between the upper and lower branches of the overturning circulation as we hypothesized, as well as a minimum in radiocarbon at mid-depths, as seen in the radiocarbon data. Thus sea ice provides a potential means by which to isolate the deep ocean and store excess carbon, without relying solely on a large reduction in air-sea gas exchange. We note that although the westerly winds hypothesis is a popular paradigm, eddy resolving models of the Southern Ocean do not show a strong sensitivity of overturning

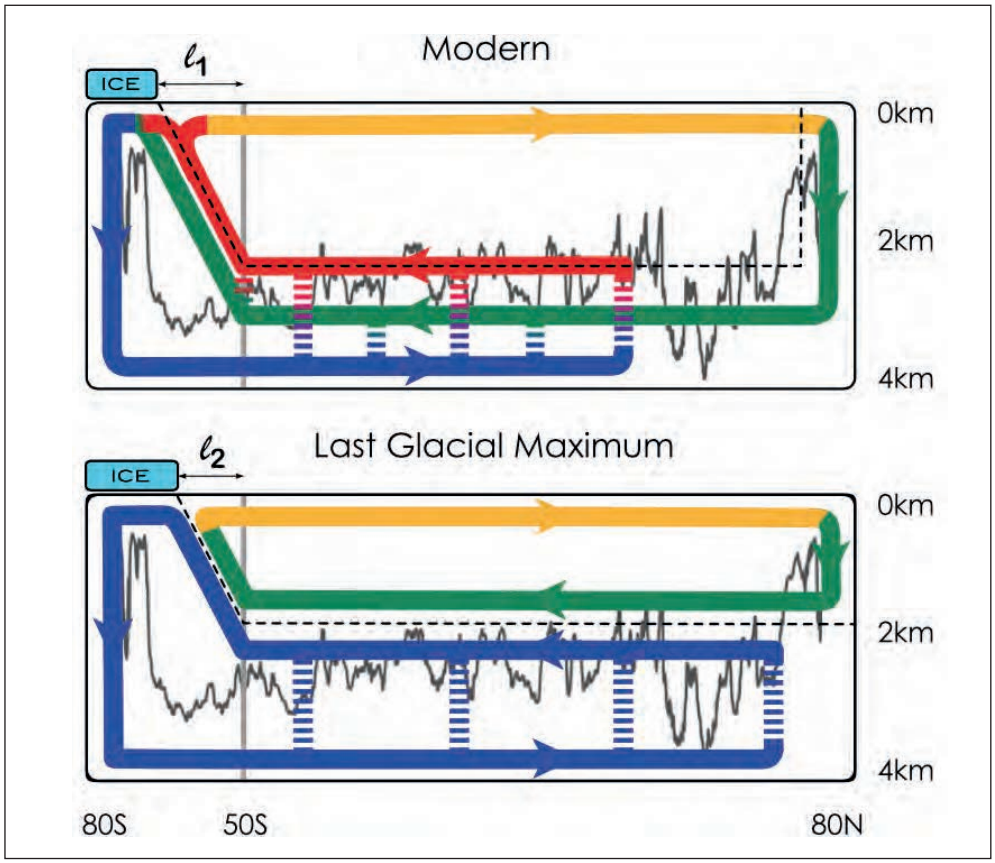


Fig. 2 (*Upper*) Schematic of the modern overturning circulation. The coloured bands are a zonally-averaged view of the major water masses, whereby green is North Atlantic Deep Water (NADW), blue is Antarctic Bottom Water (AABW), red is Pacific/Indian Deep Water (PDW/IDW), and orange is Antarctic Intermediate Water (AAIW). The dashed vertical lines represent diapycnal mixing of AABW into NADW and PDW/IDW. The dashed black line represents the boundary between the upper and lower overturning branches. The jagged gray line represents the top of major bathymetric features showing the depth beneath which mixing is enhanced. (*Lower*) Schematic of the LGM overturning circulation. The extent of sea ice is further equatorward compared to the modern. Mixing-driven upwelling of abyssal waters is confined below 2 km and it cannot lift waters high enough to upwell north of the ice line. As a result the abyssal overturning circulation closes on itself, forming two distinct cells. From Ferrari et al. 2014.

circulation to changes in winds (Munday et al. 2013), a process known as eddy saturation. Thus winds alone are not likely to cause a change the overturning circulation on glacial-interglacial timescales; a change in the surface buoyancy forcing is needed. Furthermore, our model shows that the mid-depth radiocarbon minimum is more sensitive to sea ice extent and circulation geometry than changes in wind strength.

Following our thought process forward in time from the LGM, we suggest that a consequence of a reduction in the sea ice during deglaciation would be to deepen the boundary between overturning branches, thus ending the isolation of the deep cell and transitioning

back into a circulation geometry of a figure-eight cell. This circulation restructuring due to the reduced extent of sea ice and coupled with increased gas exchange in the surface Southern Ocean, could potentially drive the changes in atmospheric $CO_2$ that have been reconstructed over this time period. A final point is that the deglaciation is not characterized by a monotonic increase in temperature and $CO_2$. Notably, the deglacial $CO_2$ rise is punctuated by a pause during the Antarctic Cold Reversal (ACR). We capture an intriguing signal in our shallow deep-sea coral radiocarbon records during this time period: a sharp decrease in radiocarbon that lasts ~ 1,000 years. We suggest that this is a result of either an increase in surface stratification or a northward shift of fronts, potentially due to a readvance of sea ice, and that this may help to explain the pause in the atmospheric deglacial $CO_2$ rise.

## *References*


Anderson, R. F., Ali, S., Bradtmiller, L. I., Nielsen, S. H. H., Fleisher, M. Q., Anderson, B. E., and Burckle, L. H.: Wind-driven upwelling in the Southern Ocean and the deglacial rise in atmospheric $CO_2$. Science *323*/5920, 1443–1448; doi:10.1126/science.1167441 (2009)

Barker, S., Knorr, G., Vautravers, M. J., Diz, P., and Skinner, L. C.: Extreme deepening of the Atlantic overturning circulation during deglaciation. Nature Geosci. *3*/8, 567–571; doi:10.1038/ngeo921 (2010)

Burke, A., and Robinson, L. F.: The Southern Ocean's role in carbon exchange during the last deglaciation. Science *335*/6068, 557–561; doi: 10.1126/science.1208163 (2012)

Curry, W. B., and Oppo, D. W.: Glacial water mass geometry and the distribution of $\delta^{13}C$ of $\Sigma CO_2$ in the western Atlantic Ocean. Paleoceanography *20*/1; doi: 10.1029/2004PA001021 (2005)

Ferrari, R., Jansen, M. F., Adkins, J. F., Burke, A., Stewart, A. L., and Thompson, A. F.: Antarctic sea ice control on ocean circulation in present and glacial climates. Proc. Natl. Acad. Sci. USA *111*/24, 8753–8758; doi: 10.1073/pnas.1323922111 (2014)

Fischer, H., Schmitt, J., Lüthi, D., Stocker, T. F., Tschumi, T., Parekh, P., Joos, F., Köhler, P., Völker, C., Gersonde, R., Barbante, C., Le Floch, M., Raynaud, D., and Wolff, E.: The role of Southern Ocean processes in orbital and millennial $CO_2$ variations – A synthesis. Quat. Sci. Rev. *1*/13; doi: 10.1016/j.quascirev.2009.06.007 (2009)

Gersonde, R., Crosta, X., Abelmann, A., and Armand, L.: Sea-surface temperature and sea ice distribution of the Southern Ocean at the EPILOG Last Glacial Maximum-a circum-Antarctic view based on siliceous microfossil records. Quat. Sci. Rev. *24*/7, 9, 869–896; doi: 10.1016/j.quascirev.2004.07.015 (2005)

Key, R. M., Kozyr, A., Sabine, C. L., Lee, K., Wanninkhof, R., Bullister, J. L., Feely, R. A., Millero, F. J., Mordy, C., and Peng, T. H.: A global ocean carbon climatology: Results from Global Data Analysis Project (GLODAP). Global Biogeochem. Cycles *18*/4; doi: 10.1029/2004GB002247 (2004)

Lund, D. C., Adkins, J. F., and Ferrari, R.: Abyssal Atlantic circulation during the Last Glacial Maximum: Constraining the ratio between transport and vertical mixing. Paleoceanography *26*/1; doi: 10.1029/2010PA001938 (2011)

Munday, D. R., Johnson, H. L., and Marshall, D. P.: Eddy saturation of equilibrated circumpolar currents. J. Phys. Oceanogr. *43*/3, 507–532 (2013)

Sarnthein, M., Stattegger, K., Dreger, D., Erlenkeuser, H., Grootes, P., Haupt, B., Jung, S., Kiefer, T., Kuhnt, W., and Pflaumann, U.: Fundamental modes and abrupt changes in North Atlantic circulation and climate over the last 60 ky – Concepts, reconstruction and numerical modeling. In: Schafer, P., Ritzrau, W., Schluter, M., and Thiede, J. (Eds.): The Northern North Atlantic: A Changing Environment. Vol. *16*; pp. 365–410. Berlin: Springer 2000

Skinner, L. C., Fallon, S., Waelbroeck, C., Michel, E., and Barker, S.: Ventilation of the deep Southern Ocean and deglacial $CO_2$ rise. Science *328*/5982, 1147–1151; doi: 10.1126/science.1183627 (2010)

Stephens, B. B., and Keeling, R. F.: The influence of Antarctic sea ice on glacial-interglacial $CO_2$ variations. Nature *404*/6774, 171–174 (2000)

Toggweiler, J. R., Russell, J. L., and Carson, S. R.: Midlatitude westerlies, atmospheric $CO_2$, and climate change during the ice ages. Paleoceanography *21*/2, doi: 10.1029/2005PA001154 (2006)

Dr. Andrea Burke
Department of Earth and Environmental Sciences
Irvine Building, University of St Andrews
St Andrews, KY16 8YG
United Kingdom
Phone: +44 1334 463910
Fax: +44 1334 463949
E-Mail: ab276@st-andrews.ac.uk

Nova Acta Leopoldina NF *121*, Nr. 408, 55–57 (2015)

# An Attempt to Quantify Terrestrial Carbon Storage during the Last Glacial Maximum and the Implications for Deglaciation $CO_2$ Changes

Philippe Ciais,[1] Dan Zhu,[1] Shushi Peng,[1] Tao Wang,[1] Gerhard Krinner,[1] Sergei A. Zimov,[2] Alessandro Tagliabue,[1] Matthias Cuntz,[3] Laurent Bopp,[1] and Colin Prentice[4]

Quantifying the state of the global carbon cycle during the Last Glacial Maximum (LGM) is needed to understand how $CO_2$ changed by some 80 ppm during the last deglaciation. Two isotopic tracers of the carbon cycle: $^{18}O$ in $O_2$ and $^{13}C$ in the oceanic and atmospheric carbon reservoirs, were used by Ciais et al. (2011) to quantify the state of the carbon cycle during the Last Glacial Maximum (LGM) some 21,000 years ago.

Using $\delta^{13}C$ measurements in the atmosphere from ice cores, and in the ocean from benthic foraminifera, we estimated the distribution of carbon into the land and ocean reservoirs during the LGM period. Our mass balance approach to bring a data driven constraint on the LGM carbon pools is derived from Bird et al. (1996). Namely, we assume that both the mass of both C and of its stable isotope $^{13}C$ in the atmosphere-land-ocean carbon system is constant between the LGM and Holocene. Parameters entering into this calculation are: (*i*) atmospheric $CO_2$ concentration and its $\delta^{13}C$ composition, which were both constrained by new ice cores measurements, (*ii*) changes in $\delta^{13}C$ of ocean dissolved carbon, that was diagnosed to 0.34 ± 0.05 ‰ using a new database of *cibicides* benthic foraminifera in 133 ocean cores, with 60 cores below 3 km depth (see http://motif.lsce.ipsl.fr ), or alternatively from an ensemble of 3D LGM ocean circulations simulations compatible with these data (Tagliabue et al. 2009) and (*iii*) the $\delta^{13}C$ of the land biosphere during the LGM and pre-industrial periods, which was tested for values ranging between 0 ‰ and 2 ‰ higher than today, according to vegetation reconstructions (Bird et al. 1996) or to land carbon model calculations. Uncertainty in each parameter was propagated to the estimates of land and ocean carbon pools.

The main results of the Ciais et al. (2011) study indicated a low terrestrial gross primary productivity (40 ± 20 Pg C $a^{-1}$) and a high marine productivity (60 ± 10 Pg C $a^{-1}$) during the LGM as compared to the pre-industrial Holocene (PIH). Moreover, the terrestrial biosphere of the LGM contained "only" 370 PgC less than during the pre-industrial Holocene, which

1 Laboratoire des Sciences du Climat et de l'Environnement, CE Orme des Merisiers, 91191 Gif sur Yvette, France; philippe.ciais@cea.fr.

2 Northeast Science Station, Pacific Institute for Geography, Russian Academy of Sciences, Cherskii 678830, Russia; sazimov55@mail.ru.

3 Helmholtz Centre for Environmental Research – UFZ, Leipzig, Germany; mcuntz@bgc-jena.mpg.de.

4 AXA Chair of Biosphere and Climate Impacts, Department of Life Sciences, Grand Challenges in Ecosystems and the Environment (Silwood Park) and Grantham Institute for Climate Change, Imperial College, London; Colin.Prentice@bristol.ac.uk.

implies both a smaller than previously thought "biosphere regrowth" storage of terrestrial carbon between LGM and PIH and a smaller "ocean loss" of carbon to the atmosphere.

Combining the two global atmospheric constraints on gross primary productivity (GPP) and global land/ocean carbon storage, with a Bayesian inversion of the area of five mega-biomes, we infer during the LGM: (*i*) a small extent of tropical forests compared to PIH, (*ii*) a large extension of cold steppe and tundra biomes with carbon-rich soils, and (*iii*) the existence of a pool of inert carbon of 2300 Pg C matched with the typical 13 C signature of organic carbon. This elusive inert organic carbon pool needed to close global mass balance of carbon and GPP, could be located in Yedoma sediments that had continuously and slowly been formed since 50,000 years BP over non-glaciated areas, in marine organic sediments, in wetlands that might have developed in the exposed continental shelves during the LGM and in peat. Yet, reconstructions of LGM biomes from Pollen data suggest that peatland extent during the LGM should be much smaller than today.

To gain insights on the location of LGM inert pool (LIP), we will present results of the simulation of soil carbon in the Northern Hemisphere buried below the active layer by cryoturbation, and of peatland potential distribution from flooded area during the LGM, using climate forcing anomalies from PMIP and the ORCHIDEE-MICTv4 land surface model that contains a specific parameterization of soil C formation and decomposition in the high-latitude frozen soils, coupled with a module simulating the effect on productivity and carbon storage of large herbivores mega-fauna present during the Pleistocene.

The LIP pool is defined to be stable with respect to the equilibrium between climate and the carbon cycle during the late glacial period, but it is not inert during the deglaciation and the Holocene when the carbon cycle was not in equilibrium with climate. In particular, the large shifts in climate and increase of atmospheric $CO_2$ from 20 to 11 ka BP, together with the disappearance of ice sheets and sea-level rise, should have an impact on the stability of the LIP.

Thus, more insights are needed about the possible dynamics of this inert pool throughout the deglaciation history and the Holocene. An attempt to quantify boreal, temperate, and tropical forest storage change between LGM and PIH and the use of additional data from peat accumulation during the Holocene lead us to infer that during the deglaciation and evidence of Yedoma degradation during the Holocene warm period suggests that the LIP lost 700 Pg C to the atmosphere and ocean between LGM and PIH. This net loss is the sum of a gross loss of 1,400 Pg C and a gross gain of 600 PgC of carbon due to slow peat accumulation since the Early Holocene. The lack of evidence for large $CO_2$ increases during the Holocene suggests that the 1,400 PgC loss should have occurred between 20,000 ka BP and the early Holocene period.

In absence of information about the timing of this large release of terrestrial carbon to the atmosphere and ocean we can only speculate on the signature of this process on observed changes in the $\delta^{13}C$ of ocean dissolved carbon, changes in $\Delta^{14}C$ of ocean dissolved carbon, in $\delta^{13}C$ of atmospheric carbon during the last glacial transition.

## *References*

Bird, M. I., Llyod, J., and Farquhar, G. D.: Terrestrial carbon-storage from the last glacial maximum to the present. Chemosphere *33*, 1675–1685 (1996)

Ciais, P., Tagliabue, A., Cuntz, M., Bopp, L., Scholze, M., Hoffmann, G., Lourantou, A., Harrison, S. P., Prentice, I. C., Kelley, D. I., Koven, C., and Piao, S. L.: Large inert carbon pool in the terrestrial biosphere during the Last Glacial Maximum. Nature Geosci. *5*/1, 74–79 (2012)

Tagliabue, A. Bopp, L., Roche, D. M., Bouttes, N., Dutay, J.-C., Alkama, R., Kageyama, M., Michel, E., and Paillard, D.: Quantifying the roles of ocean circulation and biogeochemistry in governing ocean carbon-13 and atmospheric carbon dioxide at the last glacial maximum. Clim. Past *5*, 695–706 (2009)

Philippe Ciais, Ph.D.
Laboratoire des Sciences du Climat
et de l'Environnement
CE Orme des Merisiers
91191 Gif sur Yvette
France
Phone: +33 1 69089506
Fax: +33 1 69087716
E-Mail: philippe.ciais@cea.fr

Nova Acta Leopoldina NF *121*, Nr. 408, 59 – 63 (2015)

# Latest Insights into Past Carbon Cycle Changes from $CO_2$ and $\delta^{13}C_{atm}$

Hubertus Fischer,[1, 2] Jochen Schmitt,[1,2] Robert Schneider,[1] Sarah S. Eggleston,[1] Fortunat Joos,[1] Thomas K. Bauska,[3] Shaun A. Marcott,[3,4] Edward J. Brook,[3] Peter Köhler,[2] and Jérôme Chappellaz[5]

With 2 Figures

$CO_2$ represents the most important greenhouse gas released into the atmosphere as a result of human activity. The majority of our knowledge on the increase in $CO_2$ since the start of the industrialization comes from ice cores, which complement the direct atmospheric $CO_2$ measurements obtained at Mauna Loa since the 1950s. The combined $CO_2$ record shows an unambiguous anthropogenic $CO_2$ increase over the last 150 years from 280 to about 400 ppm in 2014. Values above 300 ppm are unprecedented in the long-term ice core record covering the last 800,000 years, with natural $CO_2$ concentrations varying between interglacial and glacial bounds of about 280 and 180 ppm, respectively (Lüthi et al. 2008, Petit et al. 1999). Moreover, the increase in $CO_2$ concentrations during the last termination shows significant fine structure (Marcott et al. 2014, Monnin et al. 2001), indicating a sequence of events of $CO_2$ release to the atmosphere involving different processes acting at different points in time.

Although past atmospheric $CO_2$ concentrations are known with high precision, the causes of the observed deglacial $CO_2$ changes cannot be easily attributed quantitatively to individual processes and the cause of the glacial/interglacial 80 – 100 ppm increase of atmospheric $CO_2$ remains a hot topic of paleoclimate research. Several processes have been implied (Brovkin et al. 2012, Ciais et al. 2012, Fischer et al. 2010, Jaccard et al. 2013, Köhler and Fischer 2006, Martínez-García et al. 2009, Menviel et al. 2012, Stephens and Keeling 2000, Toggweiler et al. 2006, Tschumi et al. 2011, Watson and Garabato 2006). These include:

- Southern Ocean ventilation by wind or buoyancy feedbacks,
- Iron fertilization of the marine biosphere in the Southern Ocean,
- Changes in the re-mineralization depth of organic carbon,
- Release of permafrost carbon during the deglaciation,
- Decreased solubility due to ocean warming,
- Changes in air/sea gas exchange due to changing sea ice cover,
- Marine carbonate feedbacks.

1 Climate and Environmental Physics, Physics Institute & Oeschger Centre for Climate Change Research, University of Bern, Switzerland, hubertus.fischer@climate.unibe.ch.
2 Alfred-Wegener-Institut Helmholtz-Zentrum für Polar-und Meeresforschung (AWI), Bremerhaven, Germany.
3 College of Earth, Ocean, and Atmospheric Sciences, Oregon State University, Corvallis, OR, USA.
4 Department of Geoscience, University of Wisconsin, Madison, WI, USA.
5 Laboratoire de Glaciologie et Geophysique de l'Environment, CNRS, Grenoble, France.

However, none of these processes alone is able to explain the glacial/interglacial $CO_2$ change. Substantial progress could come from better estimates of past changes in the carbon stored by the biosphere or from using stable carbon isotopes to constrain sources and sinks of carbon and exchange processes with the atmosphere. The vast majority of the carbon cycling in the Earth system on multi-millennial timescales resides in the ocean. Accordingly, the global $\delta^{13}C$ of inorganic carbon dissolved in seawater ($\delta^{13}C_{DIC}$) may provide the best constraint on past carbon cycle changes (Goodwin et al. 2011). However, a global compilation of $\delta^{13}C_{DIC}$ from marine sediment records is hampered by insufficient spatial representation of vast ocean regions, the limited temporal resolution of many sediment records, and substantial chronologic uncertainties. The alternative, to reconstruct the mean $\delta^{13}C$ record of the well-mixed atmosphere ($\delta^{13}C_{atm}$) from the fossil air contained in Antarctic ice cores has been a long-standing

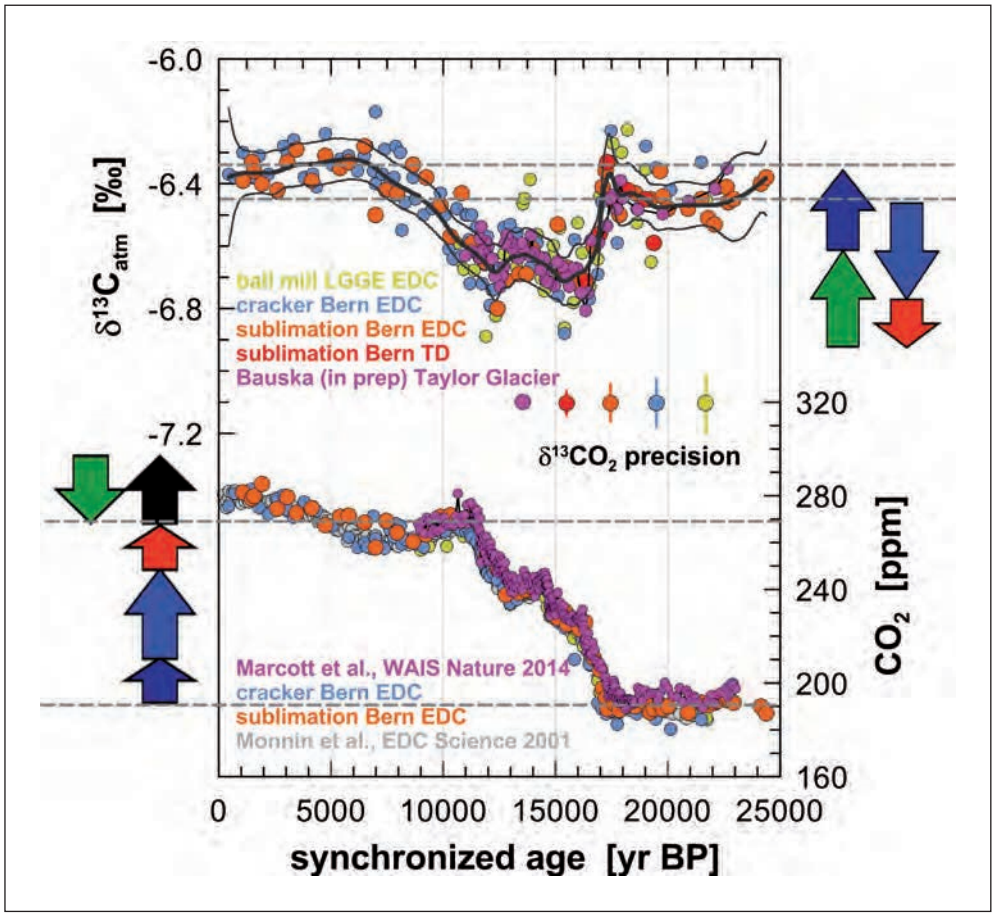


Fig. 1 Deglacial record of atmospheric changes in $CO_2$ (Marcott et al. 2014, Monnin et al. 2001) and $\delta^{13}C_{atm}$ (Schmitt et al. 2012) and Bauska et al. (in preparation). The arrows indicate the approximate glacial/interglacial changes expected from individual carbon cycle processes according to Köhler et al. 2005: Changes in sea surface temperature (*dark blue*), Southern Ocean ventilation (*blue*), iron fertilization (*red*), terrestrial biosphere regrowth (*green*) and carbonate compensation (*black*).

quest, and only latest analytical progress was able to improve the measurement error while at the same time cutting down sample size by an order of magnitude.

The new $\delta^{13}C_{atm}$ data from the air trapped in Antarctic ice cores, provides improved constraints to revisit the enigma of deglacial $CO_2$ increase (Fig. 1). Mean $\delta^{13}C_{atm}$ levels during the Last Glacial Maximum and the Holocene (as well as for MIS6 and MIS5.5) are surprisingly similar, despite different $CO_2$ concentrations and the substantially altered climate system. This supports again the notion that the $\delta^{13}C_{atm}$ record is the sum of several factors that balance each other to a large extent as shown in Figure 1. The $\delta^{13}C_{atm}$ data (Lourantou et al. 2010a, b, Schmitt et al. 2012, Schneider et al. 2013) from the last two deglaciations suggest a sequence of processes that drove atmospheric $CO_2$ changes during different stages of the transition from glacial conditions into a milder interglacial world. At the start of the transitions, upwelling of old $^{13}C$-depleted waters in the Southern Ocean increased the release of $CO_2$ to the atmosphere. This process was synchronous with a demise in iron-stimulated bioproductivity in the Southern Ocean, when atmospheric dust concentrations declined rapidly. This carbon release from the ocean was followed by the gradual growth of terrestrial carbon storage in vegetation, soil, and peatlands as evidenced by the slow $\delta^{13}C_{atm}$ increase. This process reached well into the subsequent interglacials.

While the well-studied glacial terminations indicate a release of old, isotopically depleted carbon from the deep ocean, it is not yet known unambiguously, when this carbon has been transferred to the deep ocean and where this old carbon has been stored. Again $\delta^{13}C_{atm}$ data

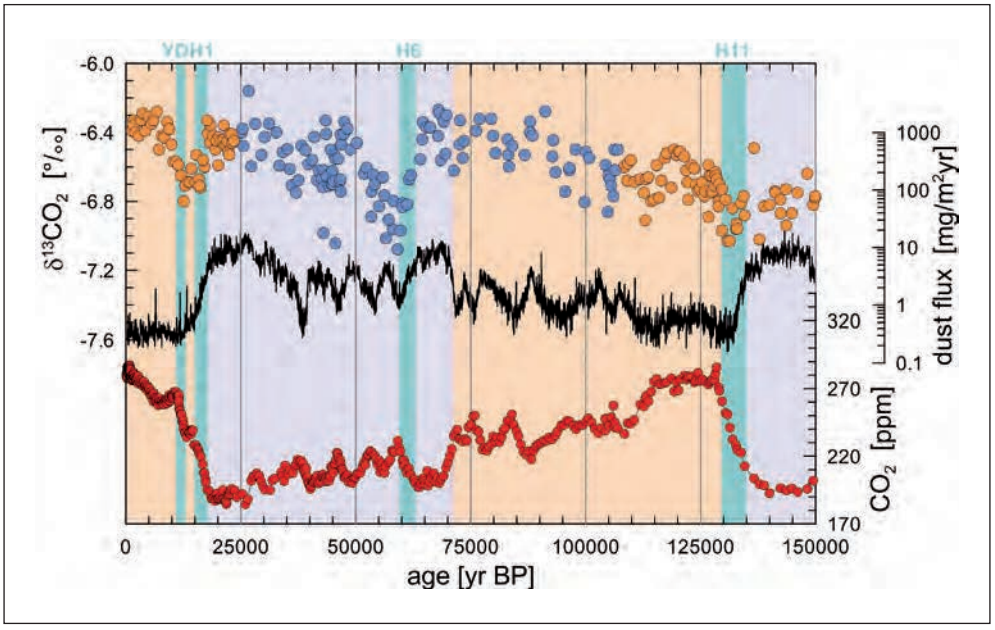


Fig. 2 Record of atmospheric $CO_2$ (Bereiter et al. 2012) and $\delta^{13}C_{atm}$ (Schmitt et al. 2012, Schneider et al. 2013) (*orange*) and Eggleston et al. (*blue*, in preparation). $\delta^{13}C_{atm}$ data points from brittle ice show negative outliers due to drill fluid contamination. The background indicates the two mode carbon cycle changes in the Southern Ocean (reduced ventilation in the Antarctic Zone [*orange*] *vs*. increased iron fertilization in the Subantarctic Zone [*light blue*] as defined by Jaccard et al. 2005).

covering the entire last glacial cycle can answer the first of these questions. Latest results from Antarctic ice cores show a gradual increase in $\delta^{13}C_{atm}$ over the entire MIS5 and 4, which culminated during an upwelling event (Anderson et al. 2009) observed at the MIS4/3 transition, similar to the one encountered during the last termination. Interestingly, during the MIS5/4 transition, when iron fertilization was most likely to set in, as indicated by the strong increase in iron bearing eolian mineral dust aerosol (Lambert et al. 2012, Martínez-García et al. 2009, Wolff et al. 2006), no clear increase in $\delta^{13}C_{atm}$ is found. This provides an experimental upper bound on the amount of $CO_2$ reduction by iron fertilization at this time. Again over MIS3 a similar long-term enrichment in $\delta^{13}C_{atm}$ is observed which ends with the upwelling event at the beginning of termination I (Anderson et al. 2009).

Superimposed on these changes in carbon storage in the abyss, a long-term trend in $\delta^{13}C_{atm}$ can also be discerned leading to 0.4 ‰ lighter values in MIS6 compared to the Last Glacial Maximum as well as in MIS5.5 compared to the Holocene. Similar offsets are also seen in marine $\delta^{13}C_{DIC}$ records suggesting long-term changes in the isotopic composition of the entire ocean/atmosphere carbon pool (Schneider et al. 2013).

## *References*


Anderson, R. F., Ali, S., Bradtmiller, L. I., Nielsen, S. H. H., Fleisher, M. Q., Anderson, B. E., and Burckle, L. H.: Wind-driven upwelling in the Southern Ocean and the deglacial rise in atmospheric $CO_2$. Science *323*, 1443–1448 (2009)

Bereiter, B., Lüthi, D., Siegrist, M., Schüpbach, S., Stocker, T. F., and Fischer, H.: Mode change of millennial $CO_2$ variability during the last glacial cycle associated with a bipolar marine carbon seesaw. Proc. Natl. Acad. Sci. USA *109*, 9755–9760 (2012)

Brovkin, V., Ganopolski, A., Archer, D., and Munhoven, G.: Glacial $CO_2$ cycle as a succession of key physical and biogeochemical processes. Clim. Past *8*, 251–264 (2012)

Ciais, P., Tagliabue, A., Cuntz, M., Bopp, L., Scholze, M., Hoffman, G., Lourantou, A., Harrison, S. P., Prentice, I. C., Kelley, D. I., Koven, C., and Piao, S. L.: Large inert carbon pool in the terrestrial biosphere during the Last Glacial Maximum. Nature Geosci. *5*, 74–79 (2012)

Fischer, H., Schmitt, J., Lüthi, D., Stocker, T. F., Tschumi, T., Parekh, P., Joos, F., Köhler, P., Völker, C., Gersonde, R., Barbante, C., Le Floch, M., Raynaud, D., and Wolff, E.: The role of Southern Ocean processes in orbital and millennial $CO_2$ variations – A synthesis. Quat. Sci. Rev. *29*, 193–205 (2010)

Goodwin, P., Oliver, K. I. C., and Lenton, T. M.: Observational constraints on the causes of Holocene $CO_2$ change. Global Biogeochem. Cycles *25*, GB3011; doi: 10.1029/2010GB003888 (2011)

Jaccard, S. L., Haug, G. H., Sigman, D. M., Pedersen, T. F., Thierstein, H. R., and Röhl, U.: Glacial/interglacial changes in Subarctic North Pacific stratification. Science *308*, 1003–1006 (2005)

Jaccard, S. L., Hayes, C. T., Martínez-García, A., Hodell, D. A., Anderson, R. F., Sigman, D. M., and Haug, G. H.: Two modes of change in Southern Ocean productivity over the past million years. Science *339*, 1419–1423 (2013)

Köhler, P., and Fischer, H.: Simulating low frequency changes in atmospheric $CO_2$ during the last 740,000 years. Clim. Past *2*, 57–78 (2006)

Köhler, P., Fischer, H., Munhoven, G., and Zeebe, R. E.: Quantitative interpretation of atmospheric carbon records over the last glacial termination. Global Biogeochem. Cycles *19*, GB4020; doi:10.1029/2004GB002345 (2005)

Lambert, F., Bigler, M., Steffensen, J. P., Hutterli, M., and Fischer, H.: Centennial mineral dust variability in high-resolution ice core data from Dome C, Antarctica. Clim. Past *8*, 609–623 (2012)

Lourantou, A., Chappellaz, J., Barnola, J.-M., Masson-Delmotte, V., and Raynaud, D.: Changes in atmospheric $CO_2$ and its carbon isotopic ratio during the penultimate deglaciation. Quat. Sci. Rev. *29*, 1983–1992 (2010a)

Lourantou, A., Lavric, J., Köhler, P., Barnola, J.-M., Paillard, D., Michel, E., Raynaud, D., and Chappellaz, J.: Constraint of the $CO_2$ rise by new atmospheric carbon isotopic measurements during the last deglaciation. Global Biogeochem. Cycles *24*, GB2015; doi:10.1029/2009GB003545 (2010b)

Lüthi, D., Le Floch, M., Bereiter, B., Blunier, T., Barnola, J.-M., Siegenthaler, U., Raynaud, D., Jouzel, J., Fischer, H., Kawamura, K., and Stocker, T. F.: High-resolution carbon dioxide concentration record 650,000–800,000 years before present. Nature *453*, 379–382 (2008)

Marcott, S. A., Bauska, T. K., Buizert, C., Steig, E. J., Rosen, J. L., Cuffey, K. M., Fudge, T. J., Severinghaus, J. P., Ahn, J., Kalk, M. L., McConnell, J. R., Sowers, T., Taylor, K. C., White, J. W. C., and Brook, E. J.: Centennial-scale changes in the global carbon cycle during the last deglaciation. Nature *514*, 616–619 (2014)

Martínez-García, A., Rosell-Melé, A., Geibert, W., Gersonde, R., Masqué, P., Gaspari, V., and Barbante, C.: Links between iron supply, marine productivity, sea surface temperature and $CO_2$ over the last 1.1 My. Paleoceanography *24*, PA1207; doi:10.1029/2008PA001657 (2009)

Menviel, L., Joos, F., and Ritz, S. P.: Simulating atmospheric $CO_2$, $^{13}C$ and the marine carbon cycle during the last glacial/interglacial cycle: possible role for a deepening of the mean remineralization depth and an increase in the oceanic nutrient inventory. Quat. Sci. Rev. *56*, 46–68 (2012)

Monnin, E., Indermühle, A., Dällenbach, A., Flückiger, J., Stauffer, B., Stocker, T. F., Raynaud, D., and Barnola, J.-M.: Atmospheric $CO_2$ concentration over the last termination. Science *291*, 112–114 (2001)

Petit, J. R., Jouzel, J., Raynaud, D., Barkov, N. I., Barnola, J.-M., Basile, I., Bender, M., Chappellaz, J., Davis, M., Delaygue, G., Delmotte, M., Kotlyakov, V. M., Legrand, M., Lipenkov, V. Y., Lorius, C., Pepin, L., Ritz, C., Saltzman, E., and Stievenard, M.: Climate and atmospheric history of the past 420,000 years from the Vostok ice core, Antarctica. Nature *399*, 429–436 (1999)

Schmitt, J., Schneider, R., Elsig, J., Leuenberger, D., Lourantou, A., Chappellaz, J., Köhler, P., Joos, F., Stocker, T. F., Leuenberger, M., and Fischer, H.: Carbon isotope constraints on the deglacial $CO_2$ rise from ice cores. Science *336*, 711–714 (2012)

Schneider, R., Schmitt, J., Köhler, P., Joos, F., and Fischer, H.: A reconstruction of atmospheric carbon dioxide and its stable carbon isotopic composition from the penultimate glacial maximum to the last glacial inception. Clim. Past *9*, 2507–2523 (2013)

Stephens, B. B., and Keeling, R. F.: The influence of Antarctic sea ice on glacial-interglacial $CO_2$ variations. Nature *404*, 171–174 (2000)

Toggweiler, J. R., Russell, J. L., and Carson, S. R.: Midlatitude westerlies, atmospheric $CO_2$, and climate change during the ice ages. Paleoceanography *21*, PA2005; doi:10.1029/2005PA001154 (2006)

Tschumi, T., Joos, F., Gehlen, M., and Heinze, C.: Deep ocean ventilation, carbon isotopes, marine sedimentation and the deglacial $CO_2$ rise. Clim. Past *7*, 771–800 (2011)

Watson, A. J., and Garabato, A. C. N.: The role of Southern Ocean mixing and upwelling in glacial-interglacial atmospheric $CO_2$ change. Tellus *58*B, 73–87 (2006)

Wolff, E. W., Fischer, H., Fundel, F., Ruth, U., Twarloh, B., Littot, G. C., Mulvaney, R., Angelis, M. de, Boutron, C. F., Hansson, M., Jonsell, U., Hutterli, M., Bigler, M., Lambert, F., Kaufmann, P., Röthlisberger, R., Steffensen, J. P., Siggaard-Andersen, M.-L., Udisti, R., Becagli, S., Castellano, E., Severi, M., Wagenbach, D., Barbante, C., Gabrielli, P., and Gaspari, V.: Southern Ocean sea ice, DMS production and iron flux over the last eight glacial cycles. Nature *440*, 491–496 (2006)

Prof. Dr. Hubertus Fischer
Climate and Environmental Physics
Physics Institute & Oeschger
Centre for Climate Change Research
University of Bern
Sidlerstrasse 5
CH-3012 Bern
Switzerland
Phone: +41 31 6318503
Fax: +41 31 6318742
E-Mail: hubertus.fischer@climate.unibe.ch

Nova Acta Leopoldina NF *121*, Nr. 408, 65 – 69 (2015)

# Effects of Sea-Ice and Ocean-Circulation Changes on Deglacial Deep-Ocean Radiocarbon Trends

Tobias Friedrich and Axel Timmermann (Honolulu, HI, USA)

With 3 Figures

The mechanisms for the orbital-scale co-variability of atmospheric $CO_2$, continental ice sheets and temperature during the Pleistocene still remain elusive. Numerous studies have demonstrated that the last glacial termination records of marine, terrestrial and atmospheric radiocarbon activity ($\Delta^{14}C$) can provide valuable insights into past ocean-ventilation changes, the exchange of carbon between the ocean and the atmosphere and the origin of a hypothetical glacial ocean-carbon reservoir (Sarnthein et al. 2013, Broecker and Barker 2007, Okazaki et al. 2012). Such a glacial ocean-carbon reservoir – created by a sluggish ocean circulation and thus a poor ventilation – should be identifiable as a large negative $\Delta^{14}C$ anomaly in benthic foraminiferal $CaCO_3$ records. Unfortunately, recent studies are inconclusive and contradictory with respect to the existence and/or a deglacial ventilation of such a reservoir. Whereas some studies clearly document regional evidence for glacial $^{14}C$-depleted deep water (Galbraith et al. 2007, Skinner et al. 2010 and others), other studies do not find such evidence (Broecker et al. 2004, Lund et al. 2011, Okazaki et al. 2012 and others).

Probably, the most controversial features found in the deglacial radiocarbon records (Fig. 1) are given by large millennial-scale excursions in radiocarbon ages during the HE1-BA-YD transition seen at Baja California (Marchitto et al. 2007), in the eastern equatorial Pacific (Stott et al. 2009), the North Pacific (Rae et al. 2014) and the Nordic Seas (Thornalley et al. 2011). These anomalies have previously been interpreted in terms of a redistribution of $^{14}C$-depleted water in the context of the ventilation of a large-scale deep-ocean carbon reservoir. The overall lack of consistency in the available $\Delta^{14}C$ records, however, suggests that local features such as regional ocean circulation changes may have contributed significantly to the temporal evolution of some $\Delta^{14}C$ records.

To test this hypothesis in the context of the Nordic Sea records (Thornalley et al. 2011) we conduct model experiments (using the LOVECLIM Earth system model) that mimic the large-scale ocean circulation changes during Heinrich event 1. A substantial weakening of the AMOC is generated and lasts for about 3,300 years which is in good agreement with the estimated duration of HE1 (Bard et al. 2000, McManus et al. 2004). As a result of the overturning circulation slowdown in the North Atlantic ventilation of the deep Arctic ocean decreases significantly (Fig. 2).

The simulated deep-ocean $\Delta^{14}C$-anomalies in the Arctic ocean reach –250–300 ‰ after about 2,500 years of the AMOC weakening. The increased residence time of the water is associated with a substantial increase in DIC and thus a surplus in carbon storage. Given that simu-

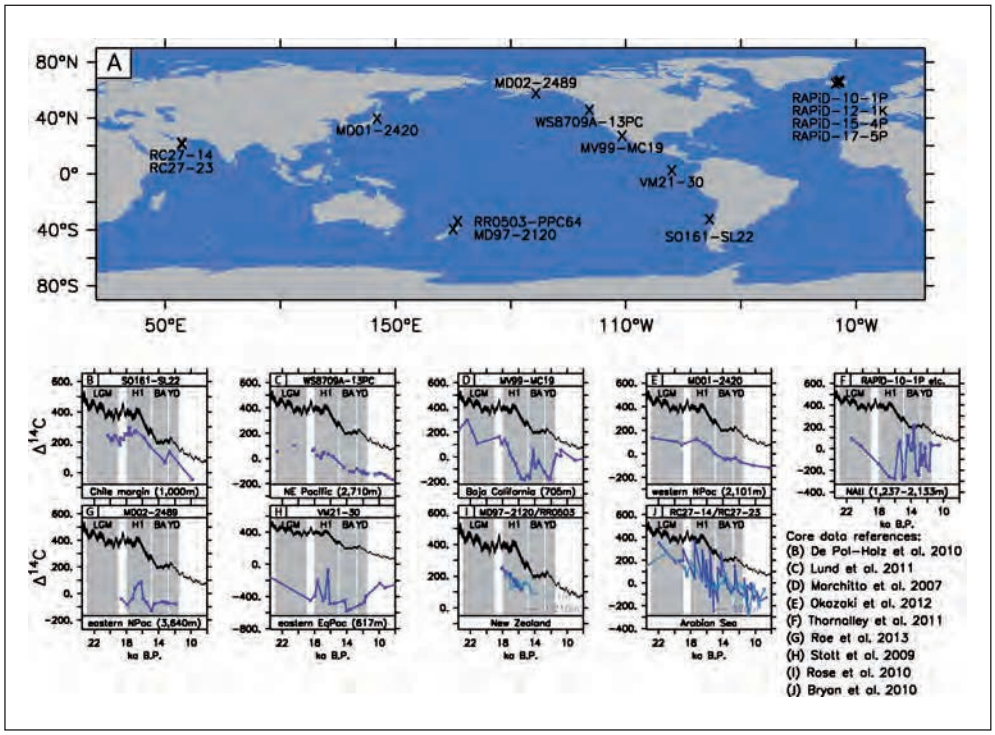


Fig. 1 Selected $\Delta^{14}C$ data from recent publications and respective core locations. The black line in the time-series panels indicates the INTCAL09 calibration curve (Reimer et al. 2009).

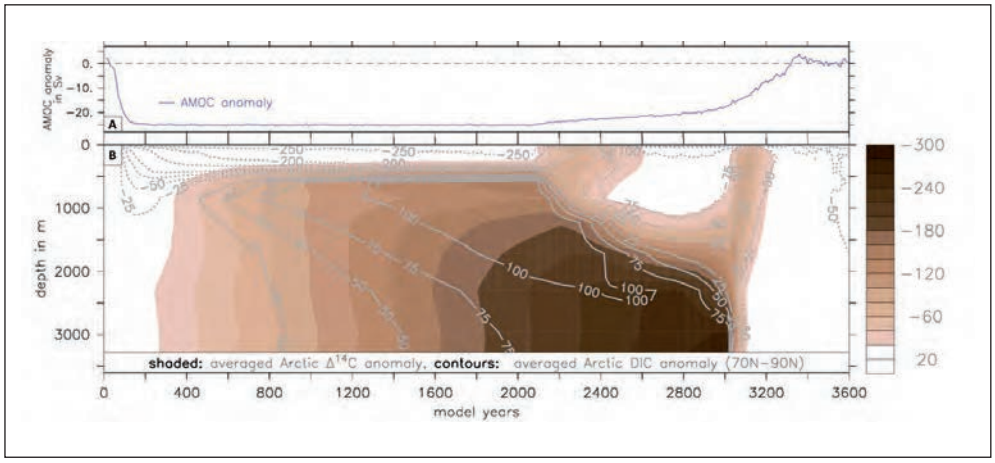


Fig. 2 (*A*) Simulated AMOC anomaly in Sv. (*B*) $\Delta^{14}C$-anomalies in ‰ (shaded) and DIC anomalies in µmol/kg (contours) horizontally averaged over Arctic ocean.

lated water mass ages in the – sea-ice covered – Arctic ocean are in the order of ~1,800–2,200 years (not shown) our preliminary results reveal that during a long-term AMOC weakening such as HE1, water mass ages in the deep Arctic ocean can reach 5,000 years and more.

We can now ask: What would happen to this extremely old water once the AMOC resumes?

Figure 2 reveals that $\Delta^{14}$C-anomalies in the Arctic ocean disappear almost immediately in the wake of the AMOC strengthening. This suggests that the old Arctic water is replaced and flushed out into the Nordic Seas. A flushing of this extremely old water in turn could potentially explain the large centennial-scale radiocarbon age variations documented by Thornalley et al. (2011). A more advanced version of the model experiment that is currently conducted has also been equipped with an artificial water mass tracer that will allow us to discern between water of Arctic and Southern Ocean origin at the Nordic Sea core locations.

Even though the consequences for the interpretation of $\Delta^{14}$C-records remain elusive at this point, our preliminary results already document some interesting conclusions:

– The Arctic ocean may have played an important role in shaping deglacial North Atlantic $\Delta^{14}$C-records but only a small role in contributing to the deglacial atmospheric $CO_2$ increase.
– Large-scale ocean circulation changes can generate regional ventilation and thus $\Delta^{14}$C-anomalies of substantial magnitude that have absolutely nothing to do with the global-scale glacial carbon reservoir.
– A regional sea-ice cover (such as simulated for the glacial Arctic) acts as a lid for air-sea gas exchange and can significantly contribute to the ageing of waters.

Figure 3 compares the simulated annual-mean Northern Hemispheric sea-ice extent for present-day and LGM conditions. Whereas under present-day conditions the sea-ice margin in the Western North Atlantic is close to Denmark Strait, the simulated sea-ice extent was significantly larger during the LGM. A similar result is obtained for the Southern Hemisphere (not shown).

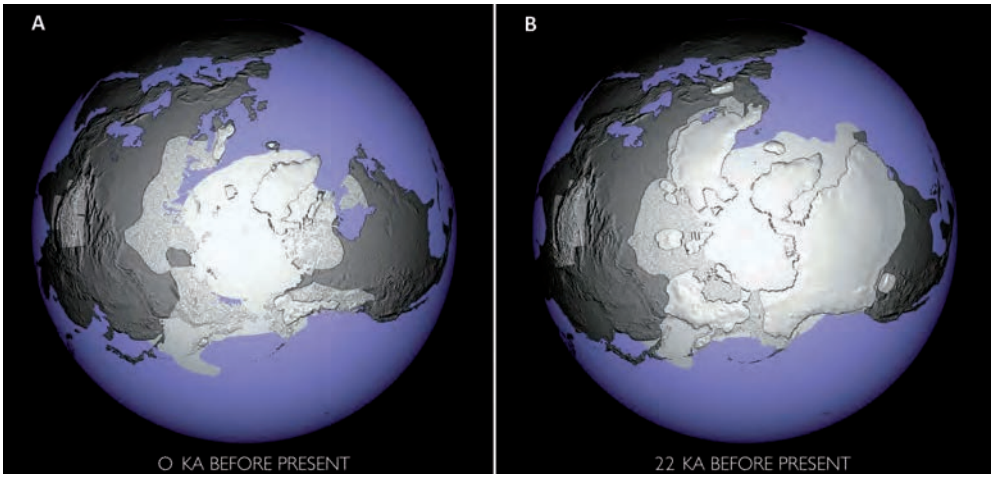


Fig. 3 Simulated sea-ice and snow cover as well as continental ice sheets for present-day (*A*) and LGM (*B*) conditions using a transient simulation of the last eight glacial cycles (Friedrich et al. 2015, in prep.).

What is the effect of this sea-ice lid on ocean ventilation and marine radiocarbon? In order to determine the magnitude of this "lid-effect" we designed and conducted model experiments in which the sea-ice cover climatologies for present-day and LGM conditions respectively are prescribed in the air-sea gas exchange parametrization of the model. This set-up allows us to solely account for the "lid-effect" whereas other critical effects of sea-ice on albedo, brine rejection, wind stress transfer and surface heat fluxes remain completely unchanged. For example, the air-sea gas exchange in a present-day simulation is diagnosed using an LGM sea-ice cover climatology and the resulting change in ocean ventilation and marine radiocarbon is documented. The interesting and surprising results will be (partly) presented during the talk.

## *References*


Bard, E., Rostek, F., Turon, J.-L., and Gendreau, S.: Hydrological impact of Heinrich events in the Subtropical Northeast Atlantic. Science *289*, 1321–1324 (2000)

Broecker, W., and Barker, S.: A 190 ‰ drop in atmosphere's $\Delta^{14}C$ during the Mystery Interval (17.5 to 14.5 kyr). Earth Planet. Sci. Lett. *256,* 90–99 (2007)

Broecker, W., Barker, S., Clark, E., Hajdas, I., Bonani, G., and Stott, L.: Ventilation of the glacial deep Pacific Ocean. Science *306*, 1169–1172 (2004)

Bryan, S. P., Marchitto, T. M., and Lehman, S. J.: The release of $^{14}C$-depleted carbon from the deep ocean during the last deglaciation: Evidence from the Arabian Sea. Earth Planet. Sci. Lett. *298*, 244–254 (2010)

De Pol-Holz, R., Keigwin, L., Southon, J., Hebbeln, D., and Mohtadi, M.: No signature of abyssal carbon in intermediate waters off Chile during deglaciation. Nature Geosci. *3*, 192–195 (2010)

Galbraith, E. D., Jaccard, S. L., Pedersen, T. F., Sigman, D. M., Haug, G. H., Cook, M., Southon, J. R., and Francois, R.: Carbon dioxide release from the North Pacific abyss during the last deglaciation. Nature *449*, 890–894 (2007)

Lund, D. C., Mix, A. C., and Southon, J.: Increased ventilation age of the deep northeast Pacific ocean during the last deglaciation. Nature Geosci. *4*, 771–774 (2011)

Marchitto, T. M., Lehman, S. J., Ortiz, J. D., Flückiger, J., and van Geen, A.: Marine radiocarbon evidence for the mechanism of deglacial atmospheric $CO_2$ rise. Science *316*, 1456–1459 (2007)

McManus, J. F., Francois, R., Gherardi, J. M., Keigwin, L. D., and Brown-Leger, S.: Collapse and rapid resumption of Atlantic meridional circulation linked to deglacial climate changes. Nature *428*, 834–837 (2004)

Okazaki, Y., Timmermann, A., Menviel, L., Harada, N., Abe-Ouchi, A., Chikamoto, M., Mouchet, A., and Asahi, H.: Deep water formation in the North Pacific during the Last Glacial termination. Science *329*, 200–204 (2010)

Okazaki, Y., Sagawa, T., Asahi, H., Horikawa, K., and Onodera, K.: Ventilation changes in the western North Pacific since the last glacial period. Clim. Past *8*, 17–24 (2012)

Rae, J. W. B., Sarnthein, M., Foster, G. L., Ridgwell, A., Grootes, P. M., and Elliot, T.: Deep water formation in the North Pacific and deglacial $CO_2$ rise. Paleoceanography *29*/6, 645–667; doi:10.1002/2013PA002570 (2014)

Reimer, P. J., Baillie, M. G. L., Bard, E., Bayliss, A., Beck, J. W., Blackwell, P. G., Bronk Ramsey, C., Buck, C. E., Burr, G. S., Edwards, R. L., Friedrich, M., Grootes, P. M., Guilderson, T. P., Hajda, I., Heaton, T. J., Hogg, A. G., Hughen, K. A., Kaiser, K. F., Kromer, B., Manning, S. W., Reimer, R. W., Richards, D. A., Scott, E. M., Southon, J. R., Staff, R. A., Turney, C. S. M., van der Plicht, J., and Weyhenmeyer, C. E.: IntCal09 and Marine09 radiocarbon age calibration curves, 0–50,000 years cal BP. Radiocarbon *51*/4, 1111–1150 (2009)

Rose, K. A., Sikes, E. L., Guilderson, T. P., Shane, P., Hill, T. M., Zahn, R., and Spero, H. J.: Upper-ocean-to atmosphere radiocarbon offsets imply fast deglacial carbon dioxide release. Nature *466*, 1093–1097 (2010)

Sarnthein, M., Schneider, B., and Grootes, P. M.: Peak glacial $^{14}C$ ventilation ages suggest major draw-down of carbon into the abyssal ocean. Clim. Past *9*, 2595–2614 (2013)

Skinner, L. C., Fallon, S., and Waelbroeck, C., Michel, E., and Barker, S.: Ventilation of the deep Southern Ocean and deglacial $CO_2$ rise. Science *328*, 1147–1151 (2010)

Stott, L., Southon, J., Timmermann, A., and Koutavas, A.: Radiocarbon age anomaly at intermediate water depth in the Pacific Ocean during the last deglaciation. Paleoceanography *24*, PA2223 (2009)

Thornalley, D. R., Barker, S., Broecker, W. S., Elderfield, H., and McCave, I. N.: The deglacial evolution of the North Atlantic deep convection. Science *331*, 202–205 (2011)

Tobias Friedrich, Ph.D.
International Pacific Research Center
School of Ocean and Earth Science and Technology
University of Hawaii
Honolulu, Hawaii 96822
USA
Phone: +1 808 9567385
Fax: +1 808 9569425
E-Mail: tobiasf@hawaii.edu

Prof. Axel Timmermann, Ph.D.
International Pacific Research Center
School of Ocean and Earth Science and Technology
University of Hawaii
Honolulu, Hawaii 96822
USA
Phone: +1 808 9562720
Fax: +1 808 9569425
E-Mail: axel@hawaii.edu

Nova Acta Leopoldina NF *121*, Nr. 408, 71–74 (2015)

# The Role of Air-Sea Disequilibrium in Ocean Carbon Storage and its Isotopic Composition

Eric D. Galbraith (Montreal, Canada)

With 3 Figures

The equilibration timescale for a nonreactive gas (such as oxygen) in the mixed layer is on the order of weeks. In contrast, $CO_2$ reacts with water, so that the dominant components of Dissolved Inorganic Carbon (DIC) are bicarbonate and carbonate. Because air-sea exchange of DIC must pass through the bottleneck of the tiny dissolved $CO_2$ pool, its equilibration is more than an order of magnitude slower than nonreactive gases, typically requiring about a year. As a result, at much of the sea surface, the concentration of DIC – and its isotopes – are significantly out of equilibrium with the atmosphere. Modification of this disequilibrium could have played a significant role in glacial-interglacial changes – both in well-recognized, and obscure, ways.

The concentration of DIC in any parcel of water at the sea surface can be conceptualized as the sum of two components (Fig. 1). The first, and by far dominant component, is the saturation concentration, $DIC_{sat}$. This concentration is determined by the temperature, salinity, and alkalinity of the water, as well as the partial pressure of $CO_2$ in the overlying atmosphere ($pCO_2$). The difference between the saturation concentration and the actual concentration is defined as the 'disequilibrium' DIC, $DIC_{diseq}$. Models suggest that the global preindustrial $DIC_{diseq}$ was fairly small, less than 3 % of $DIC_{sat}$ (Ito and Follows 2013). However, this is partly due to the cancellation between the large positive $DIC_{diseq}$ of the Southern Ocean, where $CO_2$-rich deep waters are brought only briefly to the surface before sinking, and negative $DIC_{diseq}$ in the North Atlantic, where waters are undersaturated due to cooling and biological uptake prior to sinking. The global $DIC_{diseq}$ was almost certainly larger during the LGM.

The most well-known mechanism by which $DIC_{diseq}$ could have contributed to glacial carbon storage was suggested by Keeling and Stephens (2001). Because sea-ice gets in the way of air-sea exchange, an expansion of Antarctic sea ice across the Southern Ocean surface would have significantly increased the already large $DIC_{diseq}$ concentration of Southern Ocean waters. This must have occurred, although it is difficult to quantify due to uncertainties in the reconstructions of glacial sea ice extent and difficulty in simulating the dynamics of sea ice, the mixed layer, and deep water formation in the Southern Ocean.

Two additional factors could have further increased the global inventory of $DIC_{diseq}$ during the LGM. *First*, because most of the $DIC_{diseq}$ in the Southern Ocean surface is inherited from upwelled waters, themselves enriched in carbon by the soft-tissue pump during their sojourn in the abyss, any mechanism that increases the store of soft-tissue-pump carbon in the deep Southern Ocean (such as iron fertilization or deep remineralization) would have enhanced

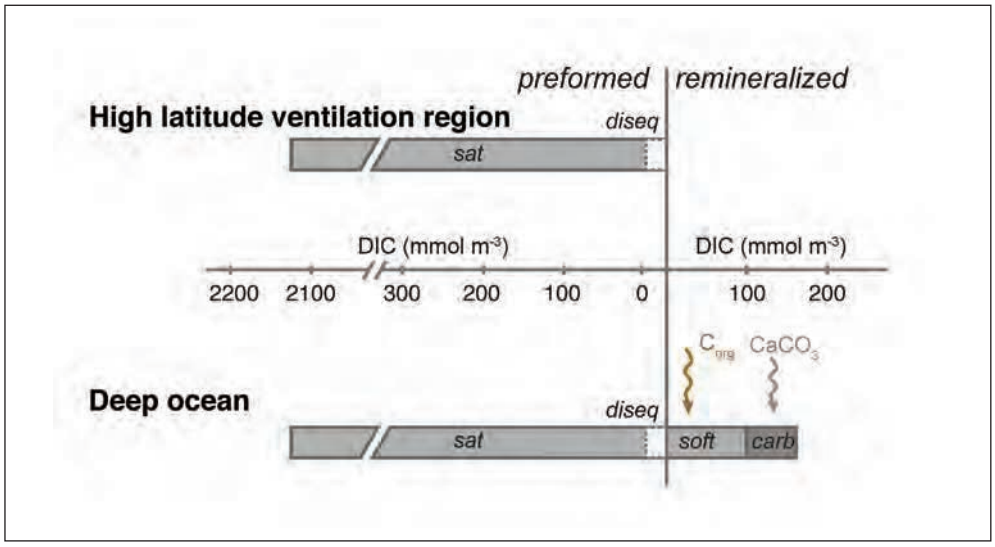


Fig. 1 DIC components at the surface (preformed) and in the subsurface (remineralized). Modified after Galbraith and Jaccard 2015.

$DIC_{diseq}$. *Second*, a change in global water mass distribution, such as the 'standing volume effect' of Skinner (2009), could have increased the global amount of $DIC_{diseq}$ by expanding the volume of deep waters occupied by Southern-sourced waters rich in $DIC_{diseq}$.

The $pCO_2$ effect also has implications for the distributions of carbon isotopes in the ocean during the glacial and deglaciation. Because they are ratios, the equilibration timescale for $\delta^{13}C$ and $\Delta^{14}C$ is approximately one order of magnitude longer than for DIC itself, and varies linearly with $DIC/CO_2$. This implies that the equilibration timescale for $\delta^{13}C$ and $\Delta^{14}C$ was a remarkable ~50 % longer during the LGM than it was during the preindustrial. This enhanced disequilibrium would have impacted each isotope system in its own way, as evaluated using a global 3-dimensional ocean model by Galbraith et al. (in review).

For radiocarbon, the slow equilibration caused by low glacial $pCO_2$ would have caused $^{14}C$ to build up in the atmosphere, all else being equal. The model simulations suggest this effect alone would have raised atmospheric $\Delta^{14}C$ by ~30 ‰ (Fig. 2). As a result, the reservoir ages of the global ocean surface would have been, fairly uniformly, ~250 years higher than preindustrial during the LGM. The $pCO_2$ effect would have varied linearly with $1/CO_2$ over the deglaciation. Meanwhile, expanded sea ice could have greatly slowed radiocarbon uptake by Southern Ocean surface waters, thereby decreasing the radiocarbon content of deep Southern Ocean waters even with no change in circulation rates.

For the stable carbon isotopes, the model suggests that enhanced disequilibrium due to the $pCO_2$ effect would have caused glacial Southern Ocean waters – charged with a heavy burden of poorly equilibrated, low-$\delta^{13}C$ respired carbon – to have become lower in $\delta^{13}C$. As a result, the internal oceanic gradients of $\delta^{13}C$ would have been amplified, increasing the difference between North Atlantic and Southern Ocean waters on the order of 0.2 ‰ (Fig. 3). This effect would have contributed to the enhanced $\delta^{13}C$ contrast between Northern and Southern source waters in the Atlantic (Curry and Oppo 2005). Again, expanded sea ice in the South-

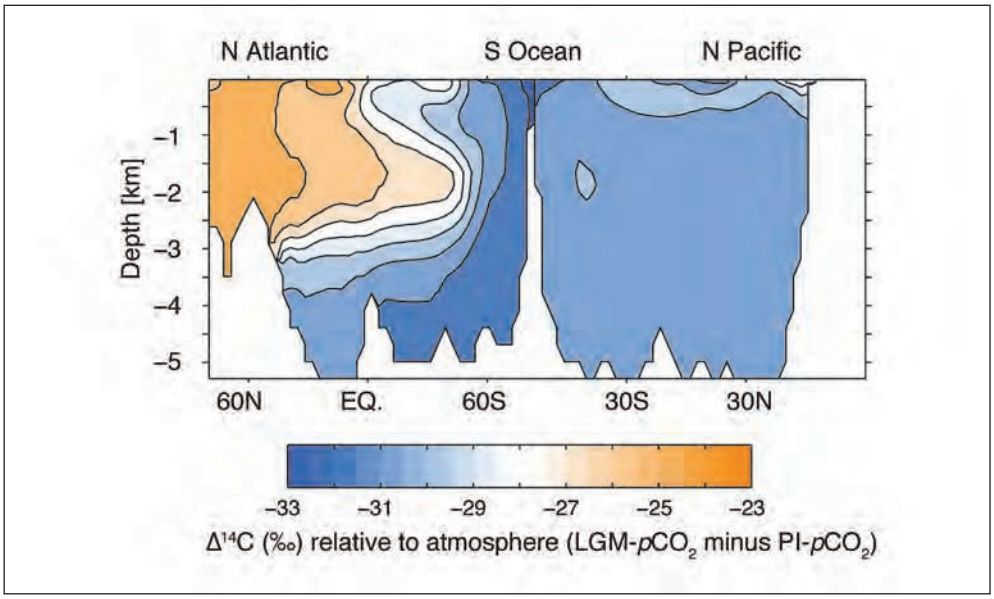


Fig. 2 Simulated glacial-interglacial changes in oceanic $\Delta^{14}C$, relative to the atmosphere, due only to the $pCO_2$ effect on air-sea exchange. Modified after GALBRAITH et al. (in review).

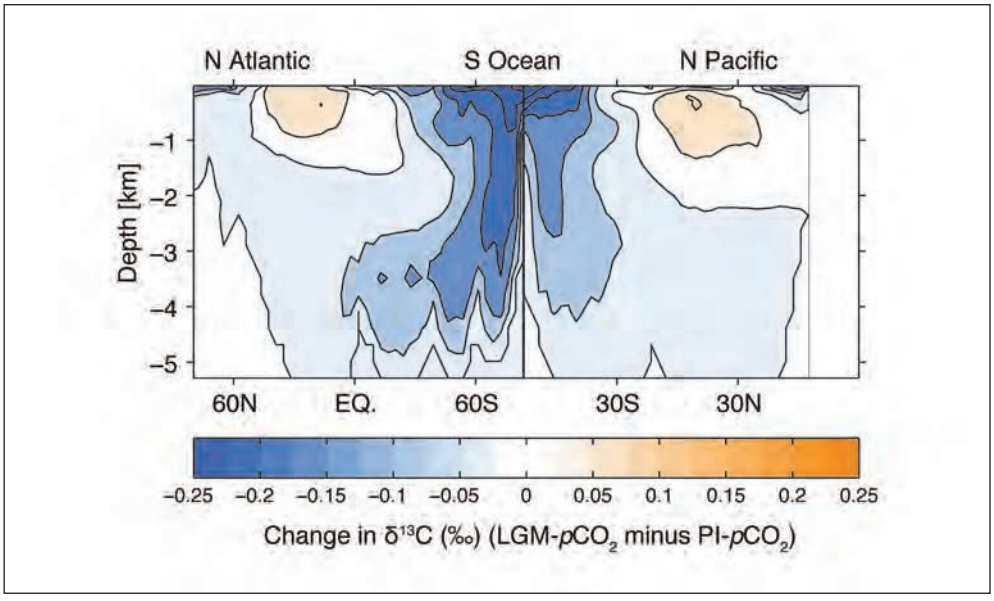


Fig. 3 Simulated glacial-interglacial changes in oceanic $\delta^{13}C$, relative to the atmosphere, due only to the $pCO_2$ effect on air-sea exchange. Modified after GALBRAITH et al. (in review).

ern Ocean would likely have exacerbated the disequilibrium, further decreasing the $\delta^{13}C$ of Southern Ocean waters.

It is important to point out that the $pCO_2$ effect on the disequilibrium of the carbon isotopes is resolved in models that include carbon speciation and changes in $pCO_2$. However, the fact that the effect is often unrecognized, and interacts with other mechanisms of glacal-interglacial change, can obscure its role. In addition, it is difficult to reconstruct $DIC_{diseq}$ from observational records, hampering its identification in glacial $CO_2$ dynamics.

During the deglaciation, the retreat of Southern Ocean sea ice and ~50 ppm rise of $pCO_2$ during the interval 17.5 to 14.5 ka would have greatly reduced the air-sea disequilibrium of DIC and its isotopes. Among other effects, this would have shifted low $\delta^{13}C$ out of the Southern Ocean and into the upper ocean and atmosphere, amplifying the effect of a simultaneous weakening of the soft tissue pump.

## *References*

Curry, W. B., and Oppo, D.: Glacial water mass geometry and the distribution of $\delta^{13}C$ of $\Sigma CO_2$ in the western Atlantic Ocean. Paleoceanography *20*, doi:10.1029/2004PA001021 (2005)

Galbraith, E. D., and Jaccard, S. L.: Deglacial weakening of the oceanic soft tissue pump: global constraints from sedimentary nitrogen isotopes and oxygenation proxies. Quat. Sci. Rev. *109*, 38–48 (2015)

Galbraith, E., Kwon, E. Y., Bianchi, D., Hain, N. P., and Sarmiento, J.: The impact of atmospheric $pCO_2$ on carbon isotope ratios of the atmosphere and ocean. Global Biochem. Cycles (in review)

Ito, T., and Follows, M. J.: Air-sea disequilibrium of carbon dioxide enhances the biological carbon sequestration in the Southern Ocean. Global Biogeochem. Cycles *27*/4, 1129–1138 (2013)

Keeling, R. F., and Stephens, B. B.: Antarctic sea ice and the control of Pleistocene climate instability. Paleoceanography *16*/1, 112–131 (2001)

Skinner, L.: Glacial-interglacial atmospheric $CO_2$ change: a possible standing volume effect on deep-ocean carbon sequestration. Clim. Past *5*/3, 537–550 (2009)

Prof. Eric Galbraith, Ph.D.
McGill University
Department of Earth and Planetary Science
3450 University St.
Montreal, Quebec
Canada H3A 2A7
Phone: +1 514 3983677
E-Mail: eric.galbraith@mcgill.ca

Nova Acta Leopoldina NF *121*, Nr. 408, 75–79 (2015)

# The Last Four Glacial $CO_2$ Cycles Simulated with the CLIMBER-2 Model

Andrey Ganopolski (Potsdam) and Victor Brovkin (Hamburg)

With 2 Figures

Antarctic ice cores reveal that atmospheric $CO_2$ concentrations, at least during the past 800 ka, varied synchronously with global ice volume and the magnitude of glacial-interglacial $CO_2$ concentration variations reached 100 ppm. It has been shown in a number of studies with climate-ice sheet models (e.g. Ganopolski and Calov 2011) that glacial cycles represent a strongly nonlinear response of the climate-cryosphere system to the astronomical forcing, primarily, through the variations of summer insolation in boreal latitudes of the Northern Hemisphere. At the same time, atmospheric $CO_2$ concentration represents an important internal positive feedback which strongly amplifies the longest (100 ka) component of glacial climate variability and translates globally regional climate signal from waning and waxing ice sheets. Explanation of full magnitude of glacial-interglacial variations of atmospheric $CO_2$ concentrations and the link between ice sheets evolution and $CO_2$ concentration still remain major scientific challenges. Most of previous studies addressed possible mechanisms of glacial $CO_2$ drawdown, and only few (e.g. Brovkin et al. 2012) attempted to explain $CO_2$ dynamics during entire glacial cycle, including glacial termination. Proposed mechanisms of the glacial-interglacial $CO_2$ variability include: change in the ocean temperature and volume, redistribution of different waters masses, change in ventilation of the deep and intermediate ocean, change in ocean alkalinity, biological productivity and several other mechanisms. Although paleoclimate records provide some useful constraints, the relative role of different mechanisms is still debated.

## 1. The Model and Experimental Setup

For our analysis we use the Earth system model of intermediate complexity CLIMBER-2 (Petoukhov et al. 2000). CLIMBER-2 includes a 2.5-dimensional statistical-dynamical atmosphere model, a 3-basin zonally averaged ocean model coupled to a thermodynamic sea ice model, the 3-dimensional thermomechanical ice sheet model SICOPOLIS, the dynamic model of the terrestrial vegetation VECODE and the global carbon cycle model. The carbon cycle model includes land carbon, oceanic geochemistry, a model for marine biota, and a sediment model (Brovkin et al. 2007, 2012). Weathering rates scale to runoff from the land surface, the coral reef growth depends on the sea level rise. The scale of nutrients utilization in sub-Antarctic ocean is proportional to the dust deposition over the Southern Ocean. Volcanic outgassing has been assumed to be constant through the glacial cycles. The model

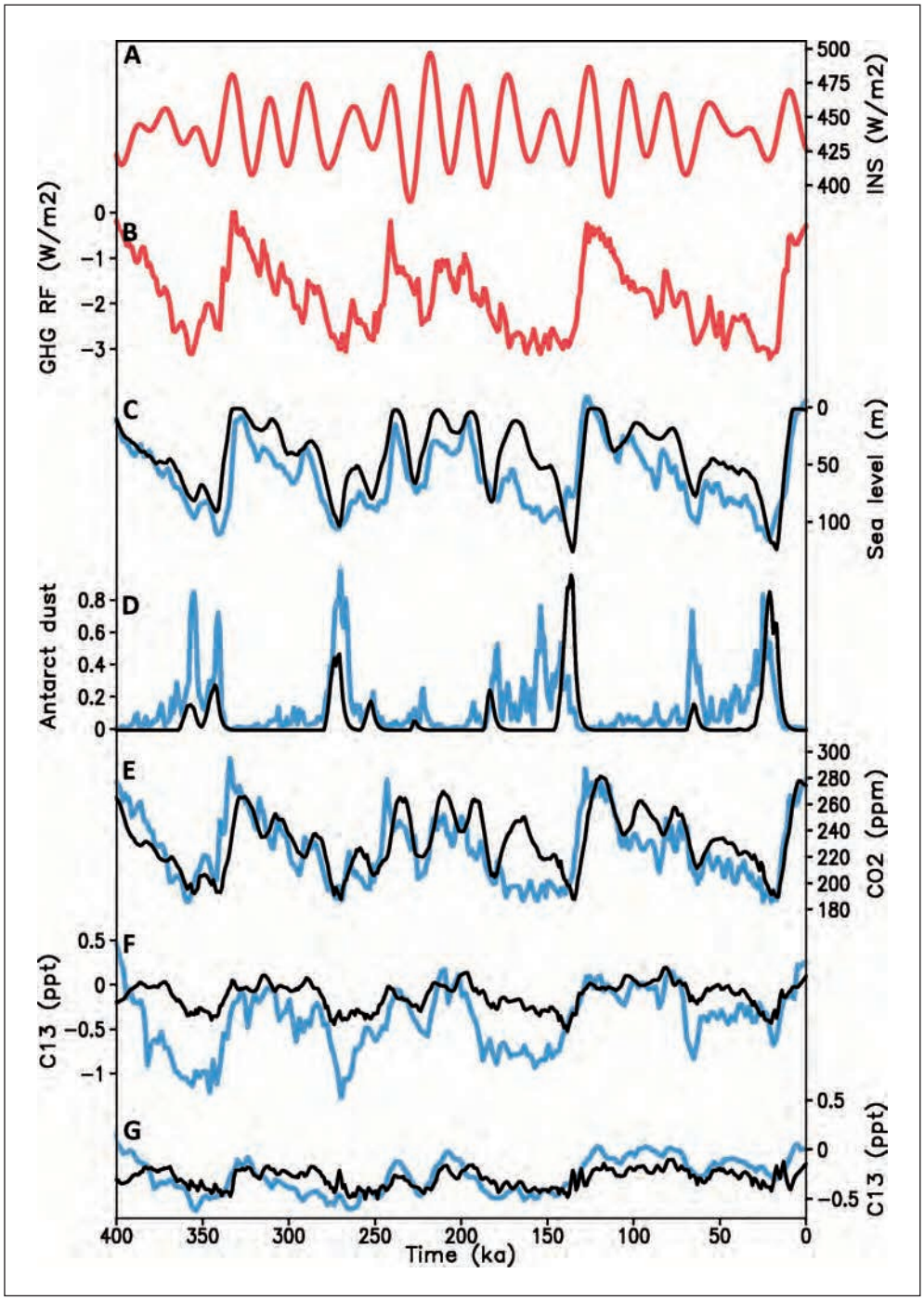


Fig. 1 Transient simulations of the last four glacial cycles forced by orbital variations and observed concentration of well-mixed GHGs. (*A*) Maximum summer insolation at 65°N; (*B*) radiative forcing (relative to preindustrial) of

also includes the dust cycle model which simulates atmospheric dust loading and dust deposition rate. The later affects surface albedo of snow and iron fertilization effect in the South Ocean. Different components of the model have different spatial resolution. Atmosphere and ice sheets are coupled bi-directionally using a physically based energy balance approach (Ganopolski et al. 2010). Ice sheet model is only applied to the Northern Hemisphere. The contribution of the Antarctic ice sheet to global ice volume is assumed to be constant during glacial cycles and equal to 10 %. The CLIMBER-2 model in different configurations has been used for numerous studies of past and future climates, in particular, simulations of glacial cycles (Ganopolski et al. 2010, Ganopolski and Calov 2011) and carbon cycle operation during the last glacial cycle (Brovkin et al. 2007, 2012).

In our experiment, we prescribed temporal variations in astronomical parameters (eccentricity, precession and obliquity). Similarly to Brovkin et al. (2012) atmospheric $CO_2$ calculated by the carbon cycle module was not used as radiative forcing for the climate model component, which instead was forced by the prescribed equivalent $CO_2$ concentration, which accounts for the radiative forcing of three major greenhouse gases – carbon dioxide, methane and nitrous oxide. Their concentrations are taken from the Antarctic ice cores. Similarly, $CO_2$ fertilization effect on vegetation was computed using reconstructed $CO_2$ concentration. Therefore, there is no feedback of the simulated atmospheric $CO_2$ concentration to climate. Unlike our previous work (Brovkin et al. 2012), "Antarctic" dust deposition rate, which is used in the parameterization of the iron fertilization effect in the Southern Ocean, was not prescribed but simulated by the model. As the initial conditions we use the final state of the climate-cryosphere system which was obtained from our earlier simulation of the last glacial cycle. The model was run from 400 ka BP until the present.

## 2. Results

Simulations of the climate system response to orbital forcing and prescribed $CO_2$ concentration are described in detail in Ganopolski and Calov (2011). Simulated ice sheets volume, their spatial distribution and other climate characteristics are in reasonably good agreement with paleoclimate reconstructions (see Fig. 1). Simulated glacial cycles are characterized by global surface air temperature variations of about 5 °C, maximum sea level drops by more than 100 m and tripling of the sea ice area in the Southern Ocean during the glacial maxima. Simulated $CO_2$ concentration closely follows global ice volume variations. The model correctly reproduces the magnitude of glacial-interglacial $CO_2$ variability of about 80 ppm. At the same time, the model underestimates the rate of $CO_2$ rise during glacial terminations and fails to simulate short $CO_2$ "overshoots" seen in the ice core records at the onset of MIS7 and MIS9 interglacials. Comparison of simulated deep ocean $\delta^{13}C$ with paleoclimate reconstructions show that the model correctly simulates larger $\delta^{13}C$ variability in the deep Atlantic compare to the deep Pacific but underestimates the magnitude of glacial-interglacial $\delta^{13}C$ variability, especially in the Atlantic. Under glacial condition the model simulates shoaling of

well-mixed GHGs; (*C*) global ice volume expressed in sea level equivalent; (*D*) Antarctic dust deposition rate in arbitrary units; (*E*) atmospheric $CO_2$ concentration; (*F*) deep South Atlantic $\delta^{13}C$; (*G*) deep North Pacific $\delta^{13}C$. Black line – modelling results, blue line – empirical data, red line – prescribed forcings.

the Atlantic meridional overturning circulation (Fig. 2*A*, *B*). As the result, the deep Atlantic under glacial conditions is filled with poorly ventilated water masses of southern origin (Fig. 2*C*). Because the dissolved inorganic carbon content of southern-source water is higher than that of North Atlantic deep water, carbon storage in the deep ocean increases significantly under glacial conditions (Fig. 2*D*).

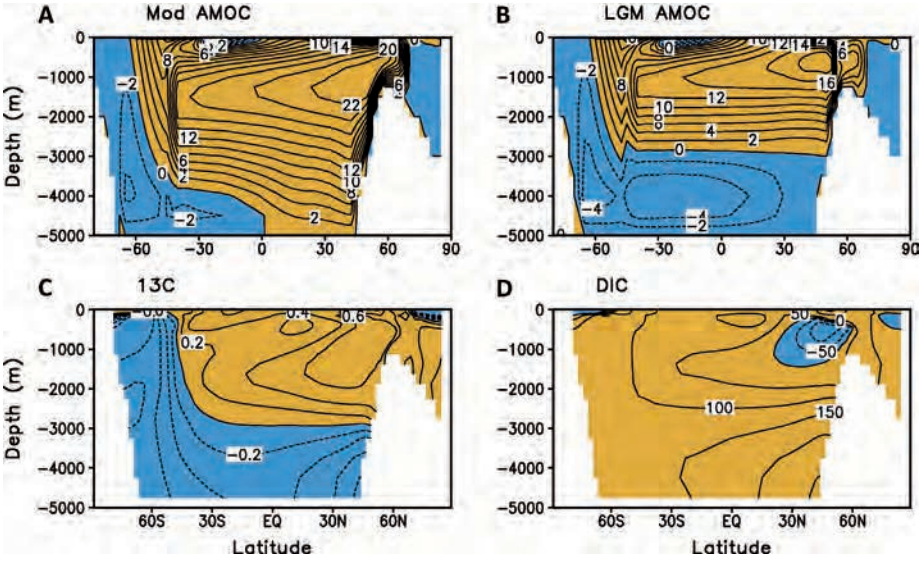


Fig. 2 Glacial-interglacial change in the Atlantic meridional overturning circulation (AMOC), dissolved inorganic carbon (DIC) and $\delta^{13}C$. (*A*) Modern AMOC (Sv); (*B*) glacial AMOC (Sv); (*C*) difference between glacial and interglacial Atlantic $\delta^{13}C$ (‰); (*D*) difference between glacial and interglacial Atlantic DIC (μmol/kg).

According to our modelling results, physical mechanisms – reduction in SSTs and changes in "standing volume" (i.e. redistribution between water masses of southern and northern origin, Brovkin et al. 2012) in response to the expansion of ice sheets and the resulting lowering of sea level – lead to the initial drop of $CO_2$ during each glacial inception. Enhanced stratification and more extensive glacial sea ice cover in the Southern Ocean also contribute to glacial $CO_2$ drawdown by reducing $CO_2$ outgassing in the Southern Ocean. This initial drop in $CO_2$ concentration is amplified by the $CaCO_3$ cycle and is followed by an increased build-up of ocean alkalinity during the rest of the glacial cycles, as exposed tropical shelves serve as a source of $CaCO_3$ to the ocean, and $CaCO_3$ burial is shifted from shallow waters to the deep sea. Increased nutrient utilization in the Southern Ocean plays an important role towards the end of each glacial cycle by contribution of up to 20 ppm to the $CO_2$ decline. The role of the land carbon is discussed in the companion paper by Brovkin and Ganopolski in this issue.

## 3. Conclusions

We present here the first simulations of the last four glacial cycles with interactive ice sheet and carbon cycle models. The model is able to reproduce the major aspects of glacial-interglacial variability, including temporal dynamics of atmospheric $CO_2$ concentration. At the same time, the model underestimates the rate of $CO_2$ rise during glacial termination and lacks $CO_2$ "overshoots" observed at the beginning of several interglacials. These problems may be related to the intrinsic limitations of zonally averaged ocean model or some missing processes. Our modelling results demonstrate that the carbon cycle remains out of equilibrium during glacial cycles which makes initialization of a carbon cycle model serious problem. In this study, we did not consider the feedback from simulated atmospheric $CO_2$ to the physical climate model because climate component of CLIMBER-2 was forced by prescribed equivalent $CO_2$ concentration. The next step will be simulation of glacial cycles driven solely by orbital forcing.

### *References*

Brovkin, V., Ganopolski, A., Archer, D., and Rahmstorf, S.: Lowering of glacial atmospheric $CO_2$ in response to changes in oceanic circulation and marine biogeochemistry. Paleoceanography *22*, PA4202; doi:10.1029/2006PA001380 (2007)

Brovkin, V., Ganopolski, A., Archer, D., and Munhoven, G.: Glacial $CO_2$ cycle as a succession of key physical and biogeochemical processes. Clim. Past *8*, 251–264 (2012)

Ganopolski, A., and Calov, R.: The role of orbital forcing, carbon dioxide and regolith in 100 kyr cycles. Clim. Past *7*, 1415–1425 (2011)

Ganopolski, A., Calov, R., and Claussen, M.: Simulation of the last glacial cycle with a coupled climate ice-sheet model of intermediate complexity. Clim. Past *6*, 229–244 (2010)

Petoukhov, V., Ganopolski, A., Brovkin, V., Claussen, M., Eliseev, A., Kubatzki, C., and Rahmstorf, S.: CLIMBER-2: a climate system model of intermediate complexity. Part I: model description and performance for present climate. Clim. Dynam. *16*, 1–17 (2000)

Dr. Andrey Ganopolski
Potsdam Institute for Climate Impact Research (PIK)
P.O. Box 601203
Telegrafenberg A62
14412 Potsdam
Germany
Phone: +49 331 2882594
Fax: +49 331 2882620
E-Mail: andrey.ganopolski@pik-potsdam.de

Dr. Victor Brovkin
Max Planck Institute for Meteorology
Bundesstraße 53
G1717
20146 Hamburg
Germany
Phone: +49 40 41173339
Fax: +49 40 41173298
E-Mail: victor.brovkin@mpimet.mpg.de

Nova Acta Leopoldina NF *121*, Nr. 408, 81–84 (2015)

# Oceanic Reservoir Ages, $^{14}C$ Concentrations, and Carbon Dynamics (also in the "Mistery Interval")

Pieter M. Grootes and Michael Sarnthein ML (Kiel)

With 2 Figures

Although the fact that the surface ocean is depleted in $^{14}C$ relative to the atmosphere is well known, it has not been easy to determine the natural degree of depletion due to the disturbance of the atmospheric $^{14}C$ content by atmospheric nuclear weapons tests started in 1954. Initial information, largely derived from paired marine/terrestrial samples providing mostly near-coastal coverage, indicated a globally averaged $^{14}C$ depletion of the surface ocean by about 5 % with some local deviations. This depletion is similar to the one reached after 400 years of decay from atmospheric concentration, and customarily $^{14}C$ depletions are reported as apparent decay ages, the "reservoir ages". Since transport of $^{14}C$ from its production at the stratosphere/troposphere transition to its decay in the (deep) ocean leads to differences in $^{14}C$ concentration between the well-mixed atmosphere and different oceanic reservoirs, this description as an apparent age is misleading, especially for the surface ocean where the $^{14}C$ concentration reflects the balance between ocean-atmosphere exchange and oceanic mixing instead of decay. Considering the paucity of data, the $^{14}C$ depletion/reservoir age was assumed to be constant over time, at least for the Holocene. The analytical capabilities of accelerator mass spectrometry (AMS) have, however, increasingly documented oceanic $^{14}C$ depletions changing with location and time. These changes reflect the atmospheric production of $^{14}C$ as well as the dynamics of the carbon cycle in the ocean and atmosphere. The $^{14}C$ record of planktonic and benthic foraminifera in sediments thus holds important information on the behaviour of these systems in the past.

As the ocean reservoirs, especially the deep ocean, contain large amounts of carbon (>90 % of the active carbon of the global carbon cycle resides as DIC in the ocean), their reservoir ages are considered to be fairly stable. Thus, indications of large, rapid changes in ocean reservoir age are often seen as problematic. Yet, the difference in $^{14}C$ concentration between an oceanic reservoir and the atmosphere, that is the apparent oceanic reservoir age, may vary significantly with changes in the $^{14}C$ concentration in the atmosphere – that contains less than 2 % of the active carbon – without a significant change in the $^{14}C$ concentration of the oceanic reservoir (Fig. 1). Such atmospheric changes may be due to $^{14}C$ production and/or oceanic outgassing. Thus the $^{14}C$ concentration of a surface ocean reservoir cannot be used as a stand-alone indicator of ocean dynamics, but requires complementary information on atmospheric and oceanic mixing for its interpretation (Fig. 2).

To develop radiocarbon calibration beyond the range of tree rings, it was assumed that $^{14}C$ concentrations in the surface ocean closely follow those in the atmosphere with a constant, though locally different, offset expressed as reservoir age. This approach is still used for

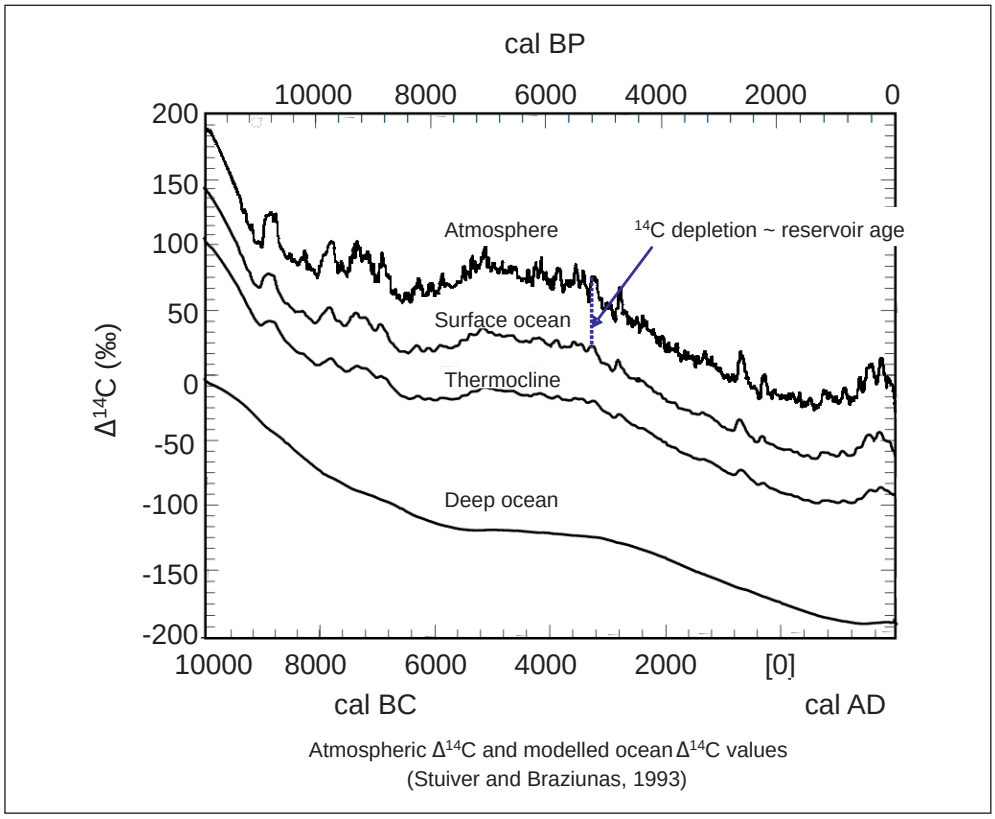


Fig. 1 Atmospheric $\Delta^{14}C$ (bidecadal values) used as input for the model calculations and calculated surface ocean (0–75 m), thermocline (75–1000 m), and deep ocean (1000–3800 m) $\Delta^{14}C$ values. The oceanic $^{14}C$ depletion relative to the atmosphere is often reported as an apparent reservoir age.

IntCal 2013, where the meanwhile documented variability in reservoir ages is treated as extra uncertainty in the data or, in some cases, leads to the exclusion of the data from the calibration data set (Reimer et al. 2013). Following this reasoning, one may assume that the fine structure of the atmospheric $^{14}C$ record over time – with periodic increases and decreases in atmospheric $^{14}C$ concentration reflected by steep parts ("jumps") and "flat" parts ("plateaus") in the age calibration curve – can also be observed in the $^{14}C$ record of the undisturbed surface ocean. Thus, tuning a suite of $^{14}C$ age plateaus and jumps in the planktonic $^{14}C$ record of a sediment core to the corresponding suite of age plateaus in the atmosphere can provide both absolute ages and reservoir ages (Sarnthein et al. 2007). By now, the deglacial sections of 14 sediment records from key sites in the ocean circulation have been tuned (Sarnthein et al. 2015, and unpublished data) to the varve counted Suigetsu record of past atmospheric $^{14}C$ concentrations (Bronk Ramsey et al. 2012). For the sediment records concerned, the varve counted timescale appears preferable to the modelled Suigetsu timescale that is generally used. Yet, the varve counted Suigetsu timescale creates in the deglacial some, as yet unresolved, problems with calibration data derived from carbonates. The tuning has revealed surprisingly high and variable reservoir ages for the surface as well as the deep ocean, ranging from 100 to

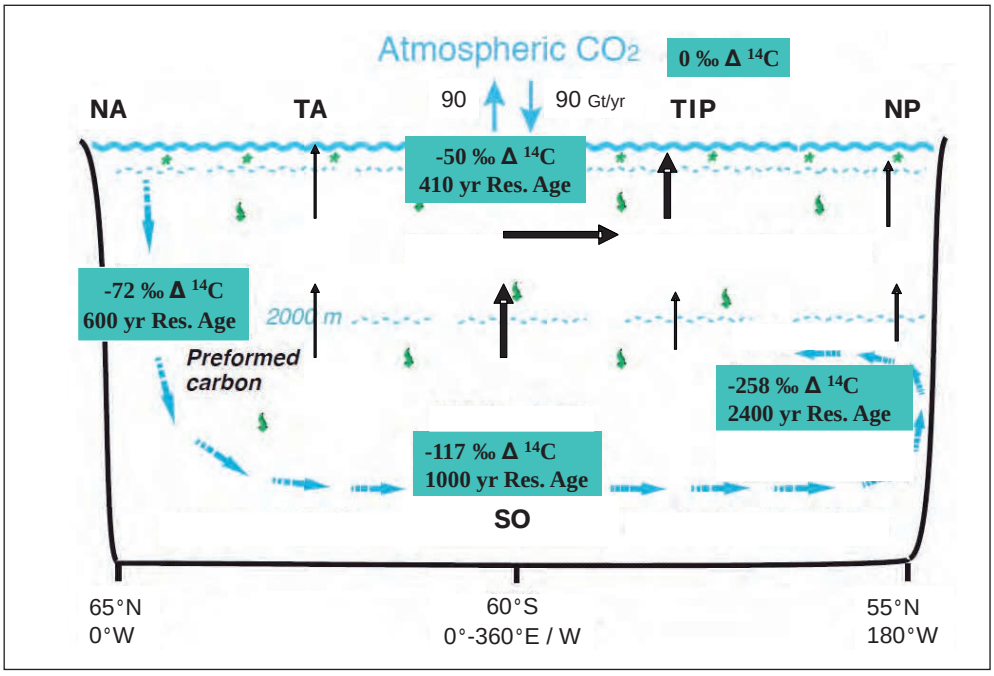


Fig. 2 Simplified scheme of the meridional overturning circulation (*blue arrows*) and accompanying changes in $^{14}C$ concentration in the modern ocean. The $^{14}C$ ages and carbon contents are subject to a delicate balance between (*i*) the gradual aging of preformed carbon from the northern North Atlantic (NA) *via* the Southern Ocean (SO) up to the subpolar North Pacific (NP) and (*ii*) the incremental absorption of young biogenic organic and inorganic carbon supplied by the biological pump from the sea surface. Vertical mixing (*black arrows*) brings intermediate and deep waters depleted in $^{14}C$ to the surface. TA indicates Tropical Atlantic, TIP the Tropical Indo-Pacific.

2500 years. To obtain the $^{14}C$ concentration of the local surface or deep ocean, the atmospheric $^{14}C$ concentration of the time needs to be multiplied by the fraction of atmospheric $^{14}C$ indicated by the reservoir age. As the atmospheric $^{14}C$ concentration during the LGM was quite high and the deglacial showed a variable and strongly decreasing concentration, the $^{14}C$ concentration changes calculated for the oceanic reservoirs are generally far more modest and are easy to reconcile with the general understanding of carbon dynamics in the ocean.

## *References*

Bronk Ramsey, C., Staff, R. A., Bryant, C. L., Brock, F., Kitagawa, H., van der Plicht, J., Schlolaut, G., Marshall, M. H., Brauer, A., Lamb, H. F., Payne, R. L., Tarasov, P. E., Haraguchi, T., Gotanda, K., Yonenobu, H., Yokoyama, Y., Tada, R., and Nakagawa, T.: A complete terrestrial radiocarbon record for 11.2 to 52.8 kyr B.P. Science *338*, 370–374 (2012)

Reimer, P. J., Bard, E., Bayliss, A., Beck, J. W., Blackwell, P. G., Bronk Ramsey, C., Buck, C. E., Cheng, H., Edwards, R. L., Friedrich, M., Grootes, P. M., Guilderson, T. P., Hajdas, I., Hatté, C., Heaton, T. J., Hoffmann, D. I., Hogg, A. G., Hughen, K. A., Kaiser, K. F., Kromer, B., Manning, S. W., Niu, M., Reimer, R. W., Richards, D. A., Scott, E. M., Southon, J. R., Staff, R. A., Turney, C. S. M., and van der Plicht, J.: INTCAL13 and MARINE13 radiocarbon age calibration curves, 0–50,000 years cal. BP. Radiocarbon *55*/4, 1869–1887 (2013)

Sarnthein, M., Grootes, P. M., Kennett, J. P., and Nadeau, M.-J.: $^{14}$C Reservoir ages show deglacial changes in ocean currents and carbon cycle. In: Schmittner, A., Chiang, J. C. H., and Hemming, S. R. (Eds.): Ocean Circulation: Mechanisms and Impacts – Past and Future Changes of Meridional Overturning. Geophys. Monograph *173*, pp. 175–196. AGU. Wash. D.C.; doi: 10.1029/173GM13 (2007)

Sarnthein, M., Balmer, S., Grootes, P. M., and Mudelsee, M.: Planktic and benthic $^{14}$C reservoir ages for three ocean basins, calibrated by a suite of $^{14}$C plateaus in the glacial-to-deglacial Suigetsu atmospheric $^{14}$C record. Radiocarbon (2015, in press)

Stuiver, M., and Braziunas, T. F.: Modeling atmospheric C-14 influences and C-14 ages of marine samples to 10,000 BC. Radiocarbon *35*/1, 137–189 (1993)

Prof. Dr. Pieter M. Grootes
University of Kiel
Institute of Ecosystem Research
Olshausenstraße 40
24098 Kiel
Germany
Phone: +49 431 8801229
Fax: +49 431 8804083
E-Mail: pgrootes@ecology.uni-kiel.de

Prof. Dr. Michael Sarnthein
University of Kiel
Institute for Geosciences
Ludewig-Meyn-Straße 10
24118 Kiel
Germany
Phone: +49 431 8802882
Fax: +49 431 8804376
E-Mail: ms@gpi.uni-kiel.de

Nova Acta Leopoldina NF *121*, Nr. 408, 85 – 88 (2015)

# The Global Ocean Carbon Sink: Recent Trends and Variability

Nicolas Gruber, Dominic Clement, Thomas Frölicher,
Alexander Haumann, and Peter Landschützer (Zürich, Switzerland)

With 1 Figure

The increasing load of anthropogenic $CO_2$ in the Earth System and the substantial amount of climate variability and change continues to challenge our understanding of the contemporaneous global ocean carbon sink, thereby providing us many lessons for our quest to explain the glacial-interglacial changes in atmospheric $CO_2$. Of particular interest are the changes in the Southern Ocean carbon sink, i.e., the region that remains at the forefront in any attempt to quantify how the ocean controlled the atmospheric $CO_2$ evolution over the last 20,000 years. The Southern Ocean is also pivotally important in current times, being responsible for more than 40 % of the global uptake of anthropogenic $CO_2$ (Mikaloff-Fletcher et al. 2006) despite covering only 30 % of the global ocean south of 30°S. Further, models suggest that it takes up three quarters of the total excess heat generated by the increasing levels of greenhouse gases in the atmosphere (Frölicher et al. in press), making it a key control valve not only for the past, but also for the present climate. While the annual rate of ocean uptake has increased considerably over the last few decades, as expected based on the substantial increase in atmospheric $CO_2$, there is considerable concern that this sink might saturate or even reverse in response to future climate change. In fact, several model-based studies have pointed out that this saturation might be occurring already in the Southern Ocean, as its sink strength began to slow down in the last two to three decades relative to expectations (Le Quéré et al. 2007, Lovenduski et al. 2008). These studies attributed this saturation to a southward movement and intensification of the westerly winds in the Southern Hemisphere, causing an increase in the upwelling of deeper waters that are naturally enriched in inorganic carbon, leading to an enhanced outgassing of this "natural" $CO_2$. This wind-driven mechanism has a direct analog to some of the proposed mechanisms for the glacial-interglacial $CO_2$ change (e.g. Anderson et al. 2009). However, while this proposed slow-down of the Southern Ocean carbon sink has been identified in several model studies including those that interpret atmospheric $CO_2$ gradients, it has not been corroborated with *in-situ* observations, nor is it clear whether this was a temporary "hiatus" from which the ocean recovered since then, or a progression toward a new low-uptake state.

Here, we use two novel sets of observations in order to assess the recent evolution of the oceanic sink for atmospheric $CO_2$ with an emphasis on the Southern Ocean. These two sets of very complimentary observations are: (*i*) surface ocean observations of the partial pressure of $CO_2$ (Bakker et al. 2014), from which monthly resolved global air-sea $CO_2$ fluxes can be estimated for the period from 1982 onward (Landschützer et al. 2014, Rödenbeck et al.

2014), and (*ii*) ocean interior observations of dissolved inorganic carbon and ancillary properties, from which the accumulation of anthropogenic $CO_2$ between the 1990s and the mid-2000s can be derived (Clement et al. in prep., Gruber et al. in prep.). The ocean interior results suggest a global increase in the anthropogenic $CO_2$ inventory of about 34±7 Pg C between 1994 and 2006, largely consistent with expectations based the increase in atmospheric $CO_2$ (Mikaloff-Fletcher et al. 2006). In contrast, the cumulative air-sea $CO_2$ flux over this period amounts to only about 19±4 Pg C. The large discrepancy can be resolved when considering that the $CO_2$ flux across the air-sea interface also contains a "natural" $CO_2$ flux component associated (*i*) with the steady-state outgassing of carbon stemming from the carbon input by rivers (about ~5 Pg C) and (*ii*) climatic perturbations (~5 Pg C). In fact, the surface ocean observations suggest that most of this lower than expected uptake between 1994 and 2006 stems from the Southern Ocean, whose sink strength was particularly weak in the 1990s, supporting the model based studies (Fig. 1). Interestingly, over the same period the thermocline of the temperate latitudes of the Southern Hemisphere accumulated a lot of anthropogenic $CO_2$, implying a strong uptake of anthropogenic $CO_2$ in the Southern Ocean. This apparent paradox can be resolved by considering that the enhanced upwelling and general vertical overturning in the Southern Ocean induced by the intensification of the westerly winds not only enhances the loss of natural $CO_2$ to the atmosphere, but also tends to enhance the uptake of anthropogenic $CO_2$ and its subsequent transport northward *via* mode and intermediate waters.

However, since ~2002, the situation in the Southern Ocean appears to have reversed (Fig. 1). We interpret this reinvigoration of the Southern Ocean carbon sink to be likely caused by a reorganization of the Southern Ocean westerly wind belt, which became more zonally asymmetric since 2002, with more cyclonically dominant conditions in the Pacific sector, and more anti-cyclonically dominant conditions in the Atlantic. As result, colder than normal air was advected from the Antarctic continent over the Pacific sector, and warmer than normal air advected from subtropical latitudes over the Atlantic and part of the Indian sector. The de-stratification effect of the cooling in the Pacific sector might have been partially compensated by a simultaneous freshening caused by the increased glacial melt water fluxes from Antarctica and increased northward transport of sea-ice and its subsequent melting. This likely kept the efficiency of the biological pump high, and avoided the build-up of high levels of dissolved inorganic carbon (DIC), which would have driven the surface ocean partial pressure of $CO_2$ ($pCO_2$) up. In the Atlantic and Indian sector, the atmospheric circulation changes likely caused also a southward deflection of the major fronts and a deepening of the thermocline, leading to the upwelling of warmer waters with lower than normal DIC. This reduction in DIC more than compensated the warming, keeping surface ocean $pCO_2$ well below that of the atmosphere. Thus, the cooling driven $pCO_2$ trend in the Pacific, and the dissolved inorganic carbon-driven trend in the Atlantic and Indian Ocean worked in tandem to prevent the partial pressure of $CO_2$ to increase across the entire Southern Ocean, thus enhancing the uptake of atmospheric $CO_2$ nearly everywhere.

The reasons underlying the development of a more asymmetric circulation pattern in the Southern Hemisphere are not fully understood yet, but could be associated with the more prevalent La Niña conditions in the equatorial Pacific since the early 2000. This is arguably speculative, but if it is indeed the case that changes in tropical climate can trigger changes in the Southern Ocean carbon sink, then entirely new scenarios for how the Earth System evolved out of the Last Glacial Maximum are conceivable, i.e., scenarios that involve teleconnection pattern between the tropics and the high latitudes with strong impacts on the Southern Ocean carbon window.

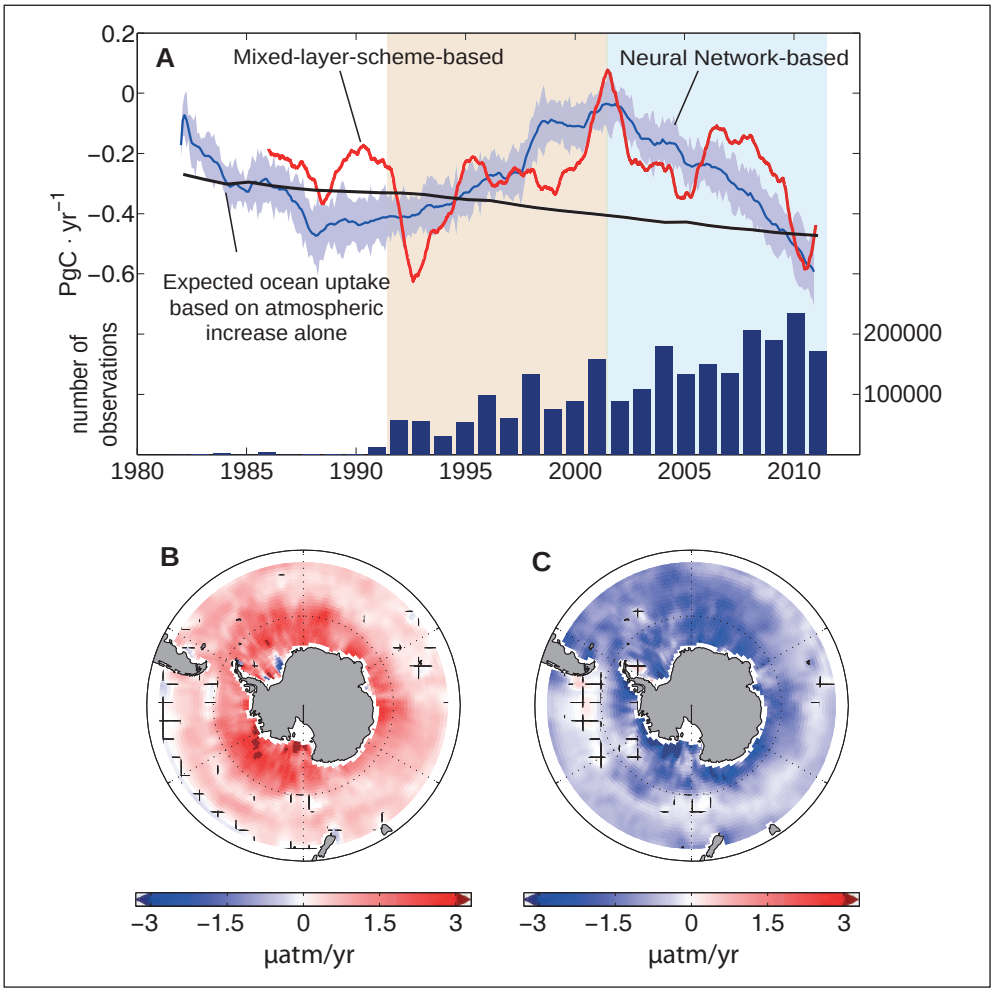


Fig. 1 Evolution of the Southern Ocean carbon sink over the last two decades. (*A*) Timeseries of the net air-sea $CO_2$ flux for the region south of 30°S. Shown are the neural network-based estimates of Landschützer et al. (2014) and the mixed-layer scheme-based estimates of Rödenbeck et al. (2014) together with a model-based estimate of the evolution of the sink in the absence of any climate variability. (*B*) Number oft observations in the SOCAT2 data base south of 44°S. (*C*) Spatial pattern of the linear trend in the air-sea $pCO_2$ difference for the 1990–2001 period based on the Landschützer et al. estimates. (*C*) as (*B*), except for the 2002–2011 period. The hatching masks trend estimates that are not statistically significant.

## *Acknowledgements*

We thank the numerous scientists and technicians who collected the observations, quality controlled them, and made them available publicly. In particular, we thank Dr. Dorothee Bakker and her team for her efforts to build the SOCAT $pCO_2$ database, and Dr. Are Olsen and his team for creating the GLODAP2 database.

## *References*

Anderson, R. F., Ali, S., Bradtmiller, L. I., Nielsen, S. H. H., Fleisher, M. Q., Anderson, B. E., and Burckle, L. H.: Wind-driven upwelling in the Southern Ocean and the deglacial rise in atmospheric $CO_2$. Science *323*, 1443–1448; doi:10.1126/science.1167441 (2009)

Bakker, D. C. E., Pfeil, B., Smith, K., Hankin, S., Olsen, A., Alin, S. R., Cosca, C., Harasawa, S., Kozyr, A., Nojiri, Y., O'Brien, K. M., Schuster, U., Telszewski, M., Tilbrook, B., Wada, C., Akl, J., Barbero, L., Bates, N. R., Boutin, J., Bozec, Y., Cai, W.-J., Castle, R. D., Chavez, F. P., Chen, L., Chierici, M., Currie, K., Baar, H. J. W. de, Evans, W., Feely, R. A., Fransson, A., Gao, Z., Hales, B., Hardman-Mountford, N. J., Hoppema, M., Huang, W.-J., Hunt, C. W., Huss, B., Ichikawa, T., Johannessen, T., Jones, E. M., Jones, S. D., Jutterström, S., Kitidis, V., Körtzinger, A., Landschützer, P., Lauvset, S. K., Lefèvre, N., Manke, A. B., Mathis, J. T., Merlivat, L., Metzl, N., Murata, A., Newberger, T., Omar, A. M., Ono, T., Park, G.-H., Paterson, K., Pierrot, D., Ríos, A. F., Sabine, C. L., Saito, S., Salisbury, J., Sarma, V. V. S. S., Schlitzer, R., Sieger, R., Skjelvan, I., Steinho, T., Sullivan, K. F., Sun, H., Sutton, A. J., Suzuki, T., Sweeney, C., Takahashi, T., Tjiputra, J., Tsurushima, N., van Heuven, S. M. A. C., Vandemark, D., Vlahos, P., Wallace, D. W. R., Wanninkhof, R., and Watson, A. J.: An update to the surface ocean $CO_2$ atlas (SOCAT version 2). Earth System Science Data *6*/1, 69–90; doi:10.5194/essd-6-69-2014 (2014)

Landschützer, P., Gruber, P. N., Bakker, D. C. E., and Schuster, U.: Recent variability of the global ocean carbon sink. Global Biogeochem. Cycles *28*/9, 927–949; doi:10.1002/2014GB004853 (2014)

Le Quéré, C., Rödenbeck, C., Buitenhuis, E. T., Conway, T. J., Langenfelds, R., Gomez, A., Labuschagne, C., Gomez, A., Labuschagne, C., Ramonet, M., Nakazawa, T., Metzl, N., Gillett, N., and Heimann, M.: Saturation of the Southern Ocean $CO_2$ sink due to recent climate change. Science *316*/5832, 1735–1738; doi:10.1126/science.1136188 (2007)

Lovenduski, N. S., Gruber, N., and Doney, S. C.: Toward a mechanistic understanding of the decadal trends in the Southern Ocean carbon sink. Global Biogeochem. Cycles *22*/3, 1–9; doi:10.1029/2007GB003139 (2008)

Mikaloff-Fletcher, S. E., Gruber, N., Jacobson, A. R., Doney, S. C., Dutkiewicz, S., Gerber, M., Follows, M., Joos, F., Lindsay, K., D. Menemenlis, D., Mouchet, A., S. A. Müller, S. A., and Sarmiento, J. L.: Inverse estimates of anthropogenic $CO_2$ uptake, transport, and storage by the ocean. Global Biogeochem. Cycles *20*/2; doi:10.1029/2005GB002530 (2006)

Rödenbeck, C., Bakker, D. C. E., Metzl, N., Olsen, A., Sabine, C., Cassar, N., Reum, F., Keeling, R. F., and Heimann, M.: Interannual sea–air $CO_2$ flux variability from an observation-driven ocean mixed-layer scheme. Biogeosciences *11*/2, 4599–4613; doi:10.5194/bg-11-4599-2014 (2014)

Prof. Dr. Nicolas Gruber
ETH Zürich
Institute of Biochemistry and Pollutant Dynamics
Environmental Physics Group
CHN E 31.2
Universitätstrasse 16
8092 Zürich
Schweiz
Phone: +41 44 6320352
Fax: +41 44 6321691
E-Mail: nicolas.gruber@env.ethz.ch

Nova Acta Leopoldina NF *121*, Nr. 408, 89–91 (2015)

# Simulating Atmospheric Radiocarbon through Deglaciation

Mathis P. Hain (Southampton, UK), Daniel M. Sigman (Princeton, NJ, USA), and Gerald H. Haug ML (Zürich, Switzerland)

The radiocarbon ($^{14}C$) isotopic composition of atmosphere and ocean have long been a target of climate research because they record changes in ocean circulation and carbon cycle across the end of the last ice age, the largest climate transition in recent geologic times. The general notion is that during glacial times $CO_2$ was sequestered in the deep ocean, where it was isolated from $^{14}C$ resupply from cosmogenic $^{14}C$ production and has to loose much of its radiocarbon content to decay. During deglaciation this sequestration of carbon was upended by changes in the carbon cycle and ocean circulation, thereby releasing the previously isolated low-$^{14}C$ $CO_2$ back to the atmosphere. Changes in the Southern Ocean utilization and transport of nutrients are thought to be central to the glacial sequestration of carbon at depth and the deglacial release of $CO_2$ from the ocean (e.g., Sigman et al. 2010, Hain et al. 2010, 2013), but sensitivity experiments with a carbon cycle box model show that these processes would have surprisingly little effect on the $^{14}C/C$ (i.e., $\Delta^{14}C_{atm}$) ratio of $CO_2$ in the atmosphere (Hain et al. 2014).

In the context of the atmospheric $CO_2$ $\Delta^{14}C_{atm}$ changes since the last ice age, two episodes of sharp $\Delta^{14}C_{atm}$ decline have been related to either the venting of deeply sequestered low-$^{14}C$ $CO_2$ through the Southern Ocean surface or the abrupt onset of North Atlantic Deep Water (NADW) formation. In model simulations using an improved reconstruction of cosmogenic $^{14}C$ production, Atlantic circulation change and Southern Ocean $CO_2$ release both contribute to the overall deglacial $\Delta^{14}C_{atm}$ decline, but only the onset of NADW can reproduce the sharp $\Delta^{14}C_{atm}$ declines (Hain et al. 2014). This finding suggests that millennial-timescale variations of $\Delta^{14}C_{atm}$ during the deglaciation are a sensitive recorder of changes in global circulation patterns, with only a modest imprint arising from changes in the carbon cycle that are responsible for the deglacial ocean release of $CO_2$ to the atmosphere.

If ocean circulation is indeed the primary driver of millennial-timescale $\Delta^{14}C_{atm}$ variations, the exact timing of the changes in $\Delta^{14}C_{atm}$ may hold important information on the climate dynamics that are operating during glacial terminations. Along these lines, the onset of both episodes sharp $\Delta^{14}C_{atm}$ decline precedes the canonical timing of abrupt Northern Hemisphere warming by about 500 years. Thus, to fully simulate $\Delta^{14}C_{atm}$ data requires an additional process that immediately precedes the onsets of NADW formation. We hypothesize that these "early" $\Delta^{14}C_{atm}$ declines record the thickening of the ocean's thermocline, giving rise to an expansion of buoyant body of water that constitutes the subtropical gyres at the expense of the volume of deep water. Due to the large differential in $^{14}C/C$ between upper ocean and

deep waters we estimate that $\Delta^{14}C_{atm}$ declines 12 ‰ per 100 m of thermocline thickening/pycnocline deepening. This implied change in the density structure and circulation of the ocean is consistent with simple physical models (e.g. Gnanadesikan 1999) and it arises in general circulation models in response to forced shutdown of NADW and/or changes in the Southern Hemisphere westerly winds (e.g. Zhang 2007, Chang et al. 2008, Mignone et al. 2006, Lauderdale et al. 2013) – such as reconstructed for Heinrich stadial 1 and the Younger Dryas preceding the onset of NADW formation. Based on these findings, we suggest that the onset of the sharp $\Delta^{14}C_{atm}$ decline records an imbalance in the ocean's buoyancy budget that progressively modifies the ocean's density structure so as to set up the subsequent abrupt re-initiation of NADW formation (Hain et al. 2014).

## *References*


Chang, P., Zhang, R., Hazeleger, W., Wen, C., Wan, X. Q., Ji, L., Haarsma, R. J., Breugem, W. P., and Seidel, H.: Oceanic link between abrupt changes in the North Atlantic Ocean and the African monsoon. Nature Geosci. *1*, 444–448 (2008)

Gnanadesikan, A.: A simple predictive model for the structure of the oceanic pycnocline. Science *283*, 2077–2079 (1999)

Hain, M. P., Sigman, D. M., and Haug, G. H.: Carbon dioxide effects of Antarctic stratification. North Atlantic Intermediate Water formation, and subantarctic nutrient drawdown during the last ice age: Diagnosis and synthesis in a geochemical box model. Global Biogeochem. Cycles *24* (2010)

Hain, M. P., Sigman, D. M., and Haug, G. H.: The biological pump in the past. In: Mottl, M. J. (Ed.): Treatise in Geochemistry. 2nd ed. doi:10.1016/B978-0-08-095975-7.00618-5. Amsterdam (etc.): Elsevier 2013

Hain, M. P., Sigman, D. M., and Haug, G. H.: Distinct roles of the Southern Ocean and North Atlantic in the deglacial atmospheric radiocarbon decline. Earth Planet. Sci. Lett. *394*, 198–208; doi:10.1016/j.epsl.2014.03.020 (2014)

Lauderdale, J. M., Garabato, A. C. N., Oliver, K. I. C., Follows, M. J., and Williams, R. G.: Wind-driven changes in Southern Ocean residual circulation, ocean carbon reservoirs and atmospheric $CO_2$. Clim. Dynam. *41*, 2145–2164 (2013)

Mignone, B. K., Gnanadesikan, A., Sarmiento, J. L., and Slater, R. D.: Central role of Southern Hemisphere winds and eddies in modulating the oceanic uptake of anthropogenic carbon. Geophys. Res. Lett. *33*/5 (2006)

Sigman, D. M., Hain, M. P., and Haug, G. H.: The polar ocean and glacial cycles in atmospheric $CO_2$ concentration. Nature *466*, 47–55 (2010)

Zhang, R.: Anticorrelated multidecadal variations between surface and subsurface tropical North Atlantic. Geophys. Res. Lett. *34*/6 (2007)



Mathis P. Hain, Ph.D.
University of Southampton
Ocean and Earth Science
National Oceanography Centre Southampton
University of Southampton Waterfront Campus
European Way
NOCS/564/20
Southampton SO14 3ZH
United Kingdom
Phone: +44 23 80592011
Fax: +44 23 80593059
E-Mail: m.p.hain@soton.ac.uk

Prof. Daniel M. Sigman, Ph.D.
Princeton University
Department of Geosciences
M52 Guyot Hall
Princeton, NJ 08544
USA
Phone: +1 609 2582194
E-Mail: sigman@princeton.edu

Prof. Dr. Gerald H. Haug
ETH Zürich
Department of Earth Sciences
Geological Institute
NO G 51.1
Sonneggstrasse 5
8092 Zürich
Schweiz
Phone: +41 44 6328610
Fax: +41 44 6321080
E-Mail: gerald.haug@erdw.ethz.ch

Nova Acta Leopoldina NF *121*, Nr. 408, 93–96 (2015)

# The Polar Oceans during the Deglaciation

Gerald H. Haug ML,[1] Anja Studer,[1,2] Abby Ren,[2] Sascha Serno,[3] Samuel L. Jaccard,[4] Alfredo Martínez-García,[1] Robert F. Anderson,[3] Gisela Winckler, Rainer Gersonde,[5] Ralf Tiedemann,[5] and Daniel M. Sigman[2]

With 2 Figures

We argue for a pervasive link between cold climates and polar ocean stratification (Haug et al. 1999, Sigman et al. 2004, 2007). In both the Subarctic North Pacific and the Antarctic Zone of the Southern Ocean, ice ages were marked by low productivity (Fig. 1 and 2, Jaccard et al. 2010, 2013). The accumulated evidence from sediment cores points to an increase in density stratification that reduced the supply of nutrients from the ocean interior into the sunlit surface in both of these regions. The last ice age was associated with stratification of the Antarctic and the subarctic North Pacific, and it can be argued that the well-known glacial decrease in North Atlantic Deep Water indicates a similar stratification of the North Atlantic. This link also applies to longer timescales, including the onset of extensive Northern Hemisphere glaciation 2.7 million years ago, which was concurrent with stratification of the Subarctic North Pacific and the Southern Ocean. The generality of the cooling/stratification connection calls for a general mechanism. Such a mechanism is provided by the non-linear relationship between the temperature of seawater and its density: Cooling of the ocean will decrease the role that temperature plays in the density structure of the polar water column, allowing the freshwater cap that is always present in the polar regions to cause greater density stratification, allowing the freshwater cap to intensify further. Nutrient-rich polar ocean regions such as the Antarctic and the Subarctic Pacific represent a "leak" in the biological pump, allowing deeply sequestered carbon dioxide to escape back into the atmosphere, and stratification of these regions largely stops that leak. Thus, the link between climate cooling and the stratification of nutrient-rich polar regions represents a positive feedback in the climate system, raising atmospheric carbon dioxide during warm periods and reducing it during cold periods.

1 Department of Earth Sciences, ETH Zürich, Zürich, Switzerland.
2 Department of Geosciences, Princeton University, Princeton, USA.
3 Lamont-Doherty Earth Observatory, Columbia University, Palisades, USA.
4 Institute of Geological Sciences, University of Bern, Bern, Switzerland.
5 Alfred Wegener Institute for Polar and Marine Research, Bremerhaven, Germany.

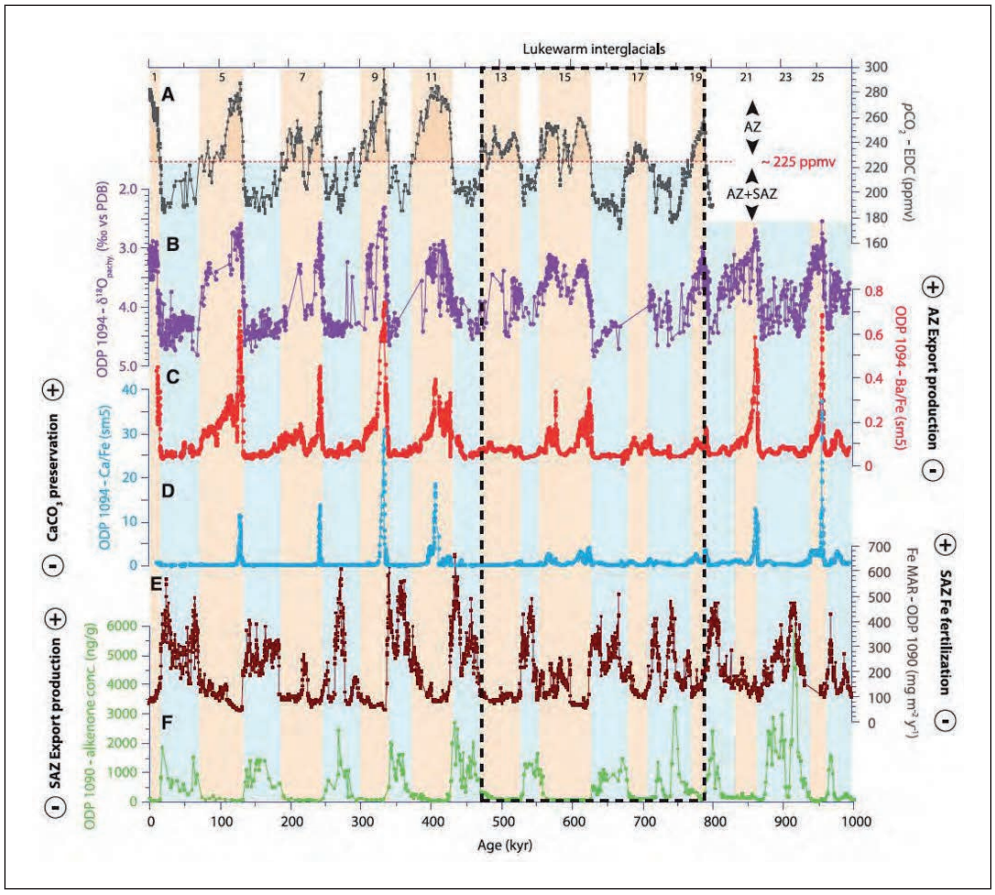


Fig. 1 Records of (*A*) atmospheric $pCO_2$ (Lüthi et al. 2008), (*B*) ODP 1094 planktic foraminifera $\delta^{18}O$, (*C*) ODP 1094 Ba/Fe (data smoothed by a five-point running mean), (*D*) ODP 1094 Ca/Fe (data smoothed by a five-point running mean), (*E*) Fe flux to subantarctic core ODP1090, and (*F*) ODP 1090 sedimentary alkenone concentration covering the past 1 Ma. Red/grey shadings highlight intervals were Antarctic (AZ)/subantarctic (SAZ) processes, respectively, are dominantly controlling the partitioning of $CO_2$ between the ocean interior and the atmosphere (from Jaccard et al. 2013).

During the last ice age, opal accumulation (and Ba/Al) in the Antarctic (Fig. 1) and the Subarctic North Pacific (Fig. 2) has been much slower than it is during the current interglacial period, suggesting less biological production and a reduced rain of biogenic material to the seafloor during glacial times. In the same glacial-age Antarctic and Subarctic North-Pacific sediments, the $^{15}N/^{14}N$ ratio of diatom-bound organic matter is markedly higher, which suggests that nutrient consumption (the ratio nutrient uptake to nutrient supply) was greater during ice ages. Taking these observations together, it can be argued that the glacial Antarctic and Subarctic North-Pacific surface was more isolated from the nutrients and carbon of deep Antarctic water, or, more physically, that the surface of the "polar twins", the Antarctic and Subarctic North-Pacific, was stratified during the last ice age.

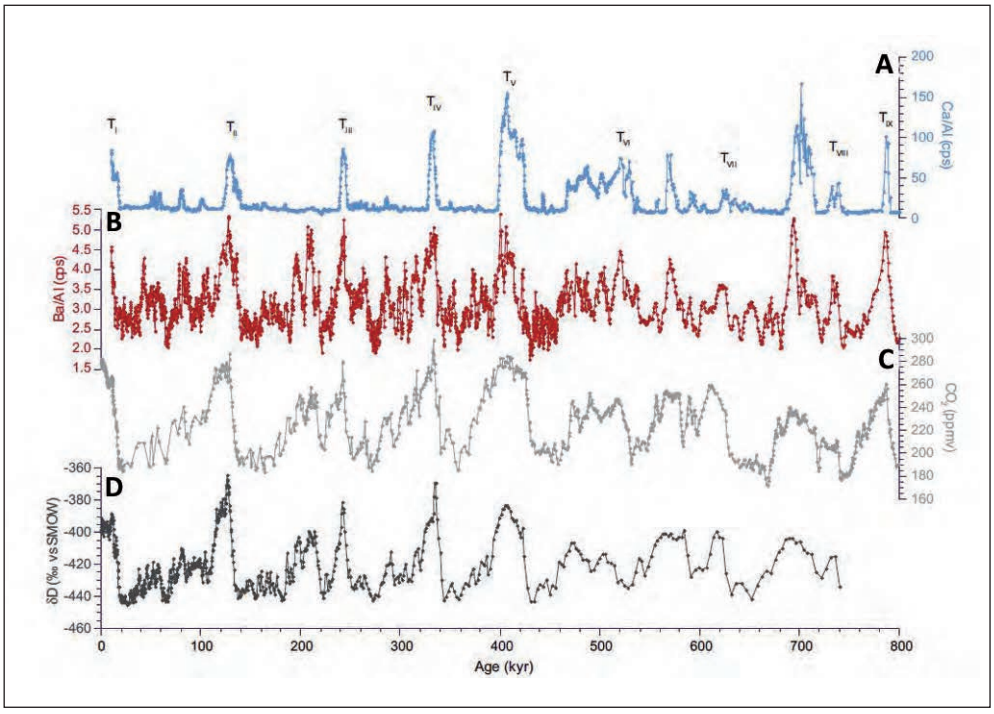


Fig. 2 Ca/Al (*A*) and Ba/Al (*B*) records from subarctic North Pacific ODP Site 882 compared to the EDC deuterium (dD) (*C*) (Jouzel et al. 2007) and $CO_2$ (Lüthi et al. 2008) (*D*) records during the past 800 ka. Glacial terminations are indicated using Roman numerals in subscript (from Jaccard et al. 2010).

Over the last deglaciation, the Southern Ocean is considered the dominant source of the atmospheric $CO_2$ rise with the Southern Hemisphere warming driving physical and biogeochemical changes in the Southern Ocean that vented $CO_2$ to the atmosphere starting at 17.6 ka. However, cooling or stalled warming characterized the Southern Ocean during the Bølling/Allerød period and the post-Younger Dryas period. Detailed reconstructions of $CO_2$ over the deglaciation show ~15 ppm maxima corresponding with the Bølling/Allerød period and the post-Younger Dryas period. Both periods were characterized by Northern Hemisphere warming, including the subarctic North Pacific. Biogenic productivity proxies and nitrogen isotopic evidence indicate that, beginning at the Bølling/Allerød and after the Yougner Dryas, the Subarctic North Pacific underwent a marked increase in vertical mixing within the upper ocean, leading to the modern condition of incomplete consumption of the nutrient supply. Biogenic opal flux and calcium carbonate data indicate that, during the Bølling/Allerød period and possibly in the post-Younger Dryas interval as well, vertical mixing reached so deeply in the Subarctic North Pacific that deeply sequestered $CO_2$ would have been vented to the atmosphere. Thus, overturning the Subarctic North Pacific may explain the atmospheric $CO_2$ peaks corresponding to Northern Hemisphere warming events, just as the Southern Ocean has vented $CO_2$ to the atmosphere during its own periods of warming.

## *References*

Haug, G. H., Sigman, D. M., Tiedemann, R., Pedersen, T. F., and Sarnthein, M.: Onset of permanent stratification in the subarctic Pacific. Nature *401*, 779–782 (1999)

Jaccard, S. L., Hayes, C. T., Martínez-García, A., Hodell, D. A., Anderson, R. F., Sigman, D. M., and Haug, G. H.: The roles of the Antaractic and Subantarctic zones in ocean productivity and atmospheric $CO_2$ over the million years. Science *339*, 1419–1423 (2013)

Jaccard, S. L., Galbraith, E. D., Sigman, D. M., and Haug, G. H.: A pervasive link between Antarctic ice core and subarctic Pacific sediment records during the past 800 kyrs. Quat. Sci. Rev. *29*, 206–212 (2010)

Lüthi, D., Le Floch, M., Bereiter, B., Blunier, T., Barnola, J.-M., Siegenthaler, U., Raynaud, D., Jouzel, J., Fischer, H., Kawamura, K., and Stocker, T. F.: High-resolution carbon dioxide concentration record 650,000–800,000 year before present. Nature *453*, 379–382 (2008)

Sigman, D. M., Boer, A. M. de, and Haug, G. H.: Antarctic stratification, atmospheric water vapor, and Heinrich events: A hypothesis for late Pleistocene deglaciations. In: Schmittner, A., Chiangm, J. H. C., and Hemming, S. R. (Eds.): Past and Future Changes of the Oceanic Meridional Overturning Circulation: Mechanisms and Impacts. AGU Geophys. Monograph *173*, 335–350 (2007)

Sigman, D. M., Jaccard, S. L., and Haug, G. H.: Polar ocean stratification in a cold climate. Nature *428*, 59–63 (2004)

Prof. Dr. Gerald H. Haug
ETH Zürich
Department of Earth Sciences
Geological Institute
NO G 51.1
Sonneggstrasse 5
8092 Zürich
Schweiz
Phone: +41 44 6328610
Fax: +41 44 6321080
E-Mail: gerald.haug@erdw.ethz.ch

Nova Acta Leopoldina NF *121*, Nr. 408, 97–99 (2015)

# Constraints on Global Climate-Carbon Cycle Feedbacks on Interannual to Glacial Cycle Timescales

Martin Heimann (Jena)

With 2 Figures

The climate system and the global carbon cycle constitute a tightly coupled system: changes in atmospheric carbon dioxide concentration ($CO_2$) modify the radiative balance of the atmosphere which impact the climate at the surface of the Earth, while changes in climate impact the major sources and sinks of $CO_2$ on land and in the ocean which control the atmospheric $CO_2$ concentration level. Figure 1 shows a conceptual view of this system, whereby only the "fast" components are considered, i.e. $CO_2$ in the atmosphere, dissolved carbon in the ocean in inorganic and organic forms, carbon stored in terrestrial vegetation and soil. The "slow" carbon cycle, i.e. carbon cycling with the lithosphere through volcanism, erosion and sedimentation on timescales of 100,000 years and more are neglected.

Currently, this system is massively perturbed by the anthropogenic inputs of $CO_2$ from the burning of fossil fuels and changes in land use (a. o. deforestation). In the past, however, this system was primarily perturbed by natural changes in radiative forcing, such as the ice-age

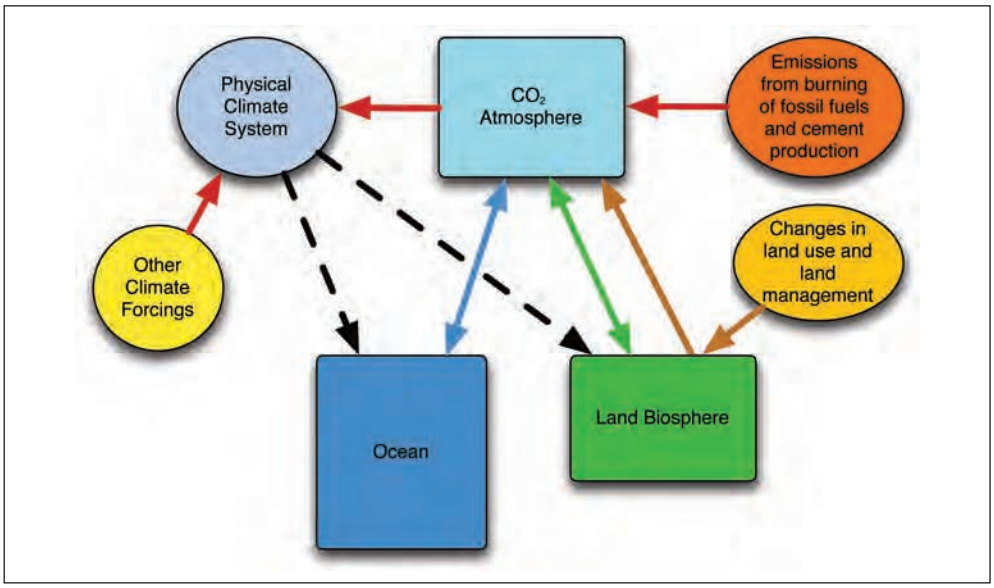


Fig. 1 Schematic of the coupled global climate – global carbon cycle system

cycles. Which sign has and how strong is the feedback loop in this system? i. e. how strongly is a perturbation of the system amplified or damped if the feedback loop is included or not? This question has been addressed in FRIEDLINGSTEIN et al. (2003), who defined the terrestrial $g_L$ and oceanic $g_O$ climate sensitivity as the amount of carbon gained or lost from these reservoirs for a global average temperature increase of 1K in the absence of any other perturbation. Likewise, the geochemical carbon cycle sensitivities $b_L$ and $b_O$ were defined as the land and oceanic carbon reservoir changes to an atmospheric change in $CO_2$ concentration of 1 ppm. Using this concept, a simple mathematical representation of the coupled system feedback loop is readily derived. This concept has been extensively used to analyse comprehensive global coupled carbon cycle – climate model simulations over the industrial period until the year 2100; e.g. for the C4MIP models (FRIEDLINGSTEIN et al. 2006) and the more recent CMIP5 models (ARORA et al. 2013, FRIEDLINGSTEIN et al. 2014). In general, these models show overall a positive feedback, however, with a large variability of responses mostly with respect to the response of the terrestrial carbon system. It is therefore of critical importance to explore the range of possible constraints provided by observations of carbon cycle – climate variations in the past.

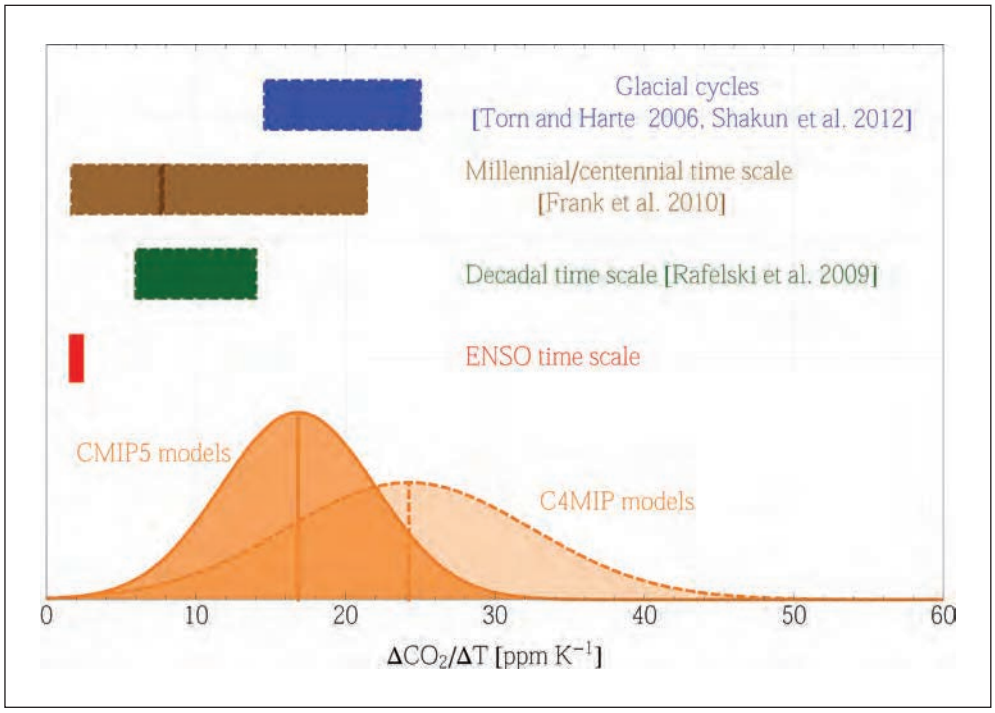


Fig. 2 Apparent carbon cycle – climate sensitivity (change in atmospheric $CO_2$ per 1 K change in global temperature) estimated from different climate records and models. *Upper part*: observational estimates as a function of time scale; *lower part*: calculated sensitivity from C4MIP and CMIP5 models.

Using a simple theoretical perturbation analysis framework, it is easy to show that the magnitudes of the climate ($g_L$, $g_O$) and the carbon cycle ($b_L$, $g_O$) sensitivities and the combined feedback factor are strongly dependent on the timescale of the perturbation. While these sensi-

tivities are not directly observable (however they can be determined of models by perturbation simulation experiments), observations of past variations of atmospheric $CO_2$ and concurrent estimates of global average temperature changes provide a constraint on the "apparent carbon cycle – climate sensitivity" S, which is defined here as the change in global $CO_2$ per change in temperature for a given climate variation. S can be derived from the individual carbon reservoir sensitivities ($g_L$, $g_O$, $b_L$, $b_O$) defined above and is also a function of timescale of the perturbation. Figure 2 shows in the upper part a summary of observational evidence from the literature of S as a function of time scale (indicated on the y-axis), from interannual variations to glacial-interglacial cycles. In the lower part of Figure 2 are shown the distributions of estimates of S from the C4MIP and CMIP5 model simulations, which pertain to a 50–100 year timescale.

The observational estimates of the apparent carbon cycle – climate system sensitivity exhibit higher values for longer timescales. This is evident given that the dynamics of the more inert carbon pools on land (e. g. deeper soils, permafrost) and in the ocean (e.g. deeper waters, surface sediments) can only be excited if a perturbation last longer. For the current climate change problem, this analysis indicates that observational evidence on the carbon cycle – climate sensitivity is at the lower end of the C4MIP and the CMIP5 models. On the other hand, in the present framework the estimates from the observed estimates of the glacial – interglacial changes in $CO_2$ and temperature provide an upper bound on the carbon cycle – climate sensitivity. Exploring further observational constraints on S and its underlying terrestrial and oceanic sensitivities as a function of time scale constitutes an important goal for carbon cycle – climate research.

## *References*


Arora, V. K., Boer, G. J., Friedlingstein, P., Eby, M., Jones, C. D., Christian, J. R., Bonan, G., Bopp, L., Brovkin, V., Cadule, P., Hajima, T., Ilyiana, T., Lindsay, K., Tjiputra, J. F., and Wu, T.: Carbon-concentration and carbon-climate feedbacks in CMIP5 Earth System models. J. Climate *26*, 5289–5314 (2013)

Frank, D. C., Esper, J., Raible, C. C., Buentgen, U., Trouet, V., Stocker, B., and Joos, F.: Ensemble reconstruction constraints on the global carbon cycle sensitivity to climate. Nature *463*, 527–530 (2010)

Friedlingstein, P., Cox, P., Betts, R. A., Bopp, L., Bloh, W. von, Brovkin, V., Cadule, P., Doney, S., Eby, M., and Fung, I.: Climate–carbon cycle feedback analysis: Results from the C4MIP model intercomparison. J. Climate *19*, 3337–3353 (2006)

Friedlingstein, P., Dufresne, J. L., Cox, P. M., and Rayner, P. J.: How positive is the feedback between climate change and the carbon cycle. Tellus *55*, 692–700 (2003)

Friedlingstein, P., Meinshausen, M., Arora, V. K., Jones, C. D., Anav, A., Liddicoat, S. K., and Knutti, R.: Uncertainties in CMIP5 climate projections due to carbon cycle feedbacks. J. Climate *27*, 511–526 (2014)

Rafelski, L. E., Piper, S. C., and Keeling, R. F.: Climate effects on atmospheric carbon dioxide over the last century. Tellus B *61*, 718–731 (2009)

Shakun, J. D., Clark, P. U., He, F., Marcott, S. A., Mix, A. C., Liu, Z., Otto-Bliesner, B., Schmittner, A., and Bard, E.: Global warming preceded by increasing carbon dioxide concentrations during the last deglaciation. Nature *484*, 49–54 (2012)

Torn, M. S., and Harte, J.: Missing feedbacks, asymmetric uncertainties, and the underestimation of future warming. Geophys. Res. Lett. *33*, L10703; doi:10.1029/2005GL025540 (2006)



Prof. Dr. Martin Heimann
Max Planck Institute for Biogeochemistry
Postfach 100164
07701 Jena
Germany

Phone: +49 3641 576350
Fax: +49 3641 577300
E-Mail: martin.heimann@bgc-jena.mpg.de

Nova Acta Leopoldina NF *121*, Nr. 408, 101–105 (2015)

# Radiocarbon Distribution and Radiocarbon-Based Circulation Age of the Atlantic Ocean during the Last Glacial Maximum

Enqing Huang,[1, 2] Luke C. Skinner,[3] Stefan Mulitza,[1] André Paul,[1] and Michael Schulz[1]

With 3 Figures

Although the volume and the distribution of water masses in the glacial Atlantic has been well established using benthic foraminiferal $\delta^{13}C$ and Cd/Ca, no robust results have been obtained regarding the ventilation age of glacial deep Atlantic. The $^{14}C$ age of a water mass has been suggested as promising proxy for the deep ocean circulation rate. The preformed $^{14}C$ of deep waters would decay at a known rate once they are isolated from the atmosphere and being transferred into the ocean interior. In practice, however, the application of B–P age ($^{14}C$ age difference between paired planktonic and benthic foraminifera) or deep water $\Delta^{14}C$ for reconstructing past ocean circulation age has long been hindered for several reasons. *First*, surface reservoir ages at core locations could differ from those at deep water formation areas, and both kinds of reservoir ages are temporally variable. *Second*, deep water at a given location and depth in the Atlantic is usually a mixture of water masses from several sources with different initial $^{14}C$ ages, and the mixing ratio is also temporally variable. Only when water-mass sources and their initial ages can be reconstructed, and the mixing ratio of different water masses at a given location and water depth can be estimated by using an independent conservative water-mass tracer, the ocean circulation age could then be inferred.

We combine existing results with newly measured $^{14}C$ ages of paired benthic and planktonic foraminifera from 28 sediment cores (Fig. 1) to map the seawater $\Delta^{14}C$ distribution at the Last Glacial Maximum (LGM, 24–18 ka BP) in the Atlantic Ocean. We further attempt to calculate the circulation age of the glacial Atlantic through assuming seawater $\delta^{13}C$ as a largely pseudo-conservative tracer in the LGM Atlantic.

In the upper 1500 m the mean $\Delta\Delta^{14}C$ value (the $\Delta^{14}C$ difference between deep water $\Delta^{14}C$ and the contemptuous atmospheric $\Delta^{14}C$) of all LGM reconstructions is –170 ‰, which is 65 ‰ less than the pre-bomb mean value (Fig. 2). Below 1500 m, the majority of the LGM $\Delta\Delta^{14}C$ reconstructions range between –220 ‰ and –310 ‰. The mean value of all LGM $\Delta\Delta^{14}C$ reconstructions below 1500 m is –275 ‰, nearly 190 ‰ less than the pre-bomb value. Taken together, the LGM $\Delta\Delta^{14}C$ above 1500 m and below 1500 m show a much stronger gradient relative to that of the pre-bomb era.

1 MARUM – Center for Marine Environmental Sciences and Faculty of Geosciences, University of Bremen, Bremen, Germany.
2 School of Ocean and Earth Science, Tongji University, Shanghai (China).
3 Godwin Laboratory for Palaeoclimate Research, Department of Earth Sciences, University of Cambridge, Cambridge (UK).

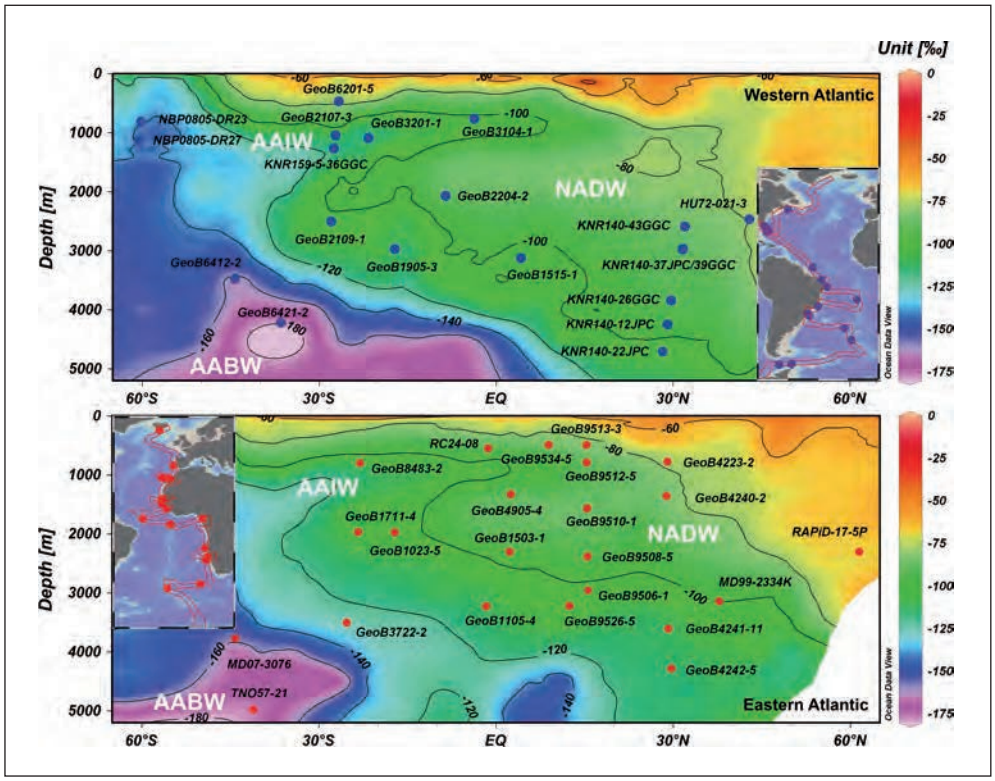


Fig. 1 Vertical distribution of the Atlantic sediment cores with the LGM seawater radiocarbon reconstructions. Meridional sections of seawater $\Delta^{14}C$ (after correction of the bomb effect) along the western and the eastern Atlantic are derived from the gridded GLODAP dataset. The position of the two sections is indicated in enclosed panels.

Circulation ages of the LGM Atlantic are estimated based on three assumptions. *First*, the majority of the LGM Atlantic was filled with waters from three sources, i.e. glacial North Atlantic Deep Water (GNADW), glacial Antarctic Intermediate Water (GAAIW) and glacial Antarctic Bottom Water (GAABW). *Second*, $\delta^{13}C$ and $\Delta\Delta^{14}C$ end-member values of GNADW, GAAIW and GAABW were constant or showed limited changes over a few thousand years prior to the LGM and within the LGM. The initial $^{14}C$ age of GNADW is taken from the simulation output (Butzin et al. 2005, Franke et al. 2008), while that of GAAIW is based on deep water coral reconstructions from the Drake Passage (Burke and Robinson 2012). The initial $^{14}C$ age of GAABW is the mean value of reconstructions from cores MD07-3076 and TNO57-21 (Barker et al. 2010, Skinner et al. 2010). *Third*, we assume that seawater $\delta^{13}C$ can be considered as largely pseudo-conservative tracer in the Atlantic during the LGM. This assumption is only justified if the replenishment of deep waters was accomplished relatively rapidly, such that the remineralization of sinking organic particles did not significantly alter the seawater $\delta^{13}C$ signature.

When plotting all results in a $\delta^{13}C$-$\Delta\Delta^{14}C$ diagram (Fig. 3), we find that the glacial AAIW values happen to lie on the mixing line between the GNADW and GAABW. Except for a few outliers, the vast majority of reconstructions fall along the mixing line within uncertainties.

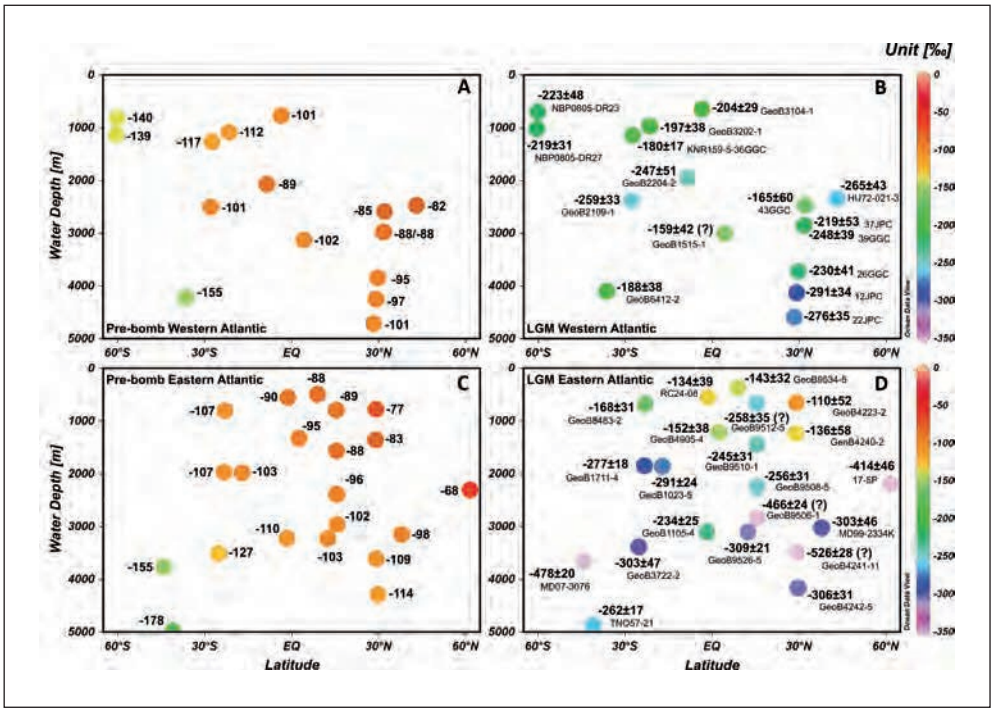


Fig. 2 Comparison of the pre-bomb $\Delta\Delta^{14}C$ values (*A* and *C*) with the LGM reconstructions (*B* and *D*) at a set of Atlantic core locations. The LGM $\Delta\Delta^{14}C$ value at each other is the mean result of several samples, and the associated uncertainty represents ±1 sigma standard error. Question marks indicate data excluded from the final analyses. The LGM water depths of all sediment cores are adjusted by –120 m.

This strongly suggests that the reconstructed $\Delta\Delta^{14}C$ signals hold significant information on mixing but only little information on circulation ages. The current dataset suggest that circulation ages of the majority of the deep Atlantic (> 1500 m) are less than 400 years during the LGM (Fig. 3), which is comparable to or even slightly less than pre-bomb value of 200 – 400 years. This implies a fast glacial deep water circulation rate, which also supports our assumption of taking $\delta^{13}C$ as a pseudo-conservative tracer.

A strong ocean circulation during the LGM could actually explain a large number of observations. The chemical gradient between the upper and the lower Atlantic, shown by the vertical distribution of seawater $\delta^{13}C$, Cd/Ca and $\Delta\Delta^{14}C$ data, is the most robust characteristic of the glacial Atlantic. To sustain such a strong gradient, besides that end-member values of the LGM AABW and NADW are significantly different, either a strong export of the LGM AABW and NADW or a very limited mixing across the NADW/AABW boundary or a combination of both is also required. Indeed, the transport to vertical diffusivity ratio of AABW in the southwestern Atlantic is estimated to be an order of magnitude larger during the LGM than the Holocene (Hoffman and Lund 2012). Given that the vertical mixing in the LGM Ocean interior is probably strengthened due to the generally enhanced wind field and the greater tidal mixing in deep basins (Wunsch 2003), a strengthening of the water mass export is a more likely explanation for the presence of the chemical gradient.

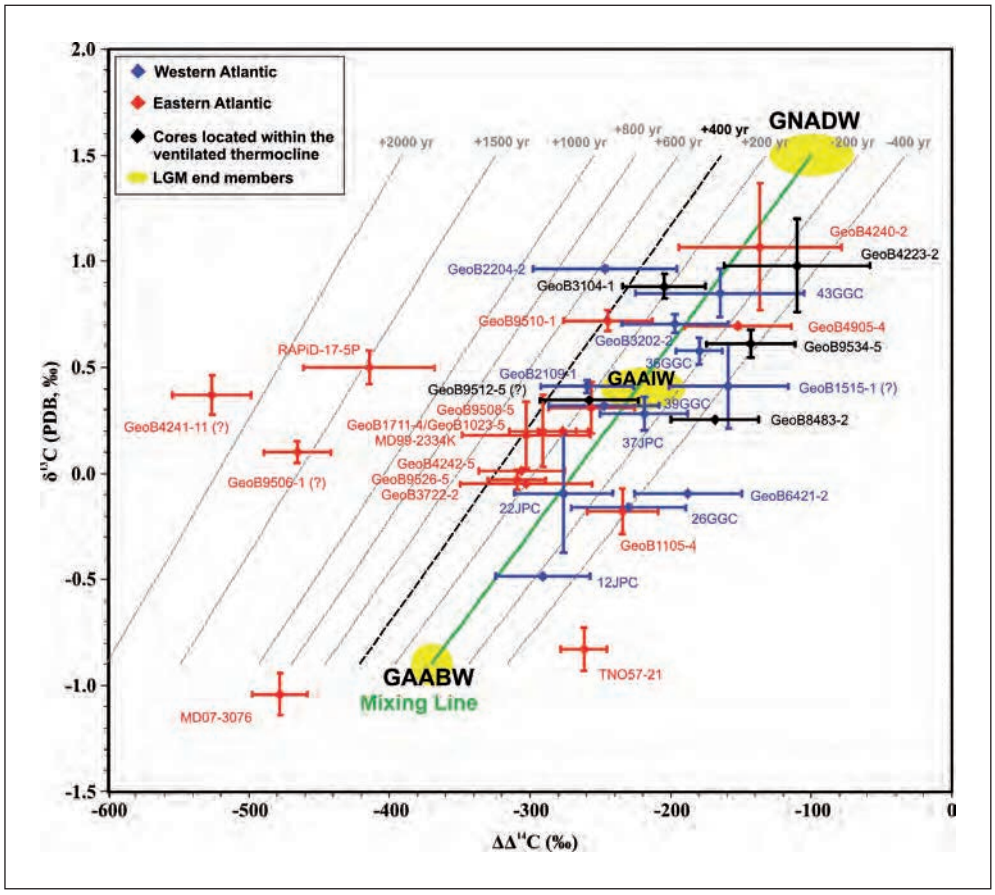


Fig. 3 The $\delta^{13}C$-$\Delta\Delta^{14}C$ diagram of the LGM bottom waters at a set of Atlantic sediment cores and water masses from three end members. Blue and red diamonds are data from the western and the eastern Atlantic, respectively. Black diamonds denote sediment cores located within the ventilated thermocline, where bottom waters are possibly influenced by subducted waters from other sources besides the GNADW and GAAIW. Error bars represent ±1 sigma standard deviation for $\delta^{13}C$ and ±1 sigma standard error for $\Delta\Delta^{14}C$. The green line is the mixing line between the GNADW and GAABW. Dashed lines represent contours with the constant radiocarbon age offset from the mixing line when assuming that $\delta^{13}C$ is a conservative tracer.

## *References*


Barker, S., Knorr, G., Vautravers, M. J., Diz, P., and Skinner, L. C.: Extreme deepening of the Atlantic overturning circulation during deglaciation. Nature Geosci. *3*, 567–571 (2010)

Burke, A., and Robinson, L. F.: The Southern Ocean's role in carbon exchange during the last deglaciation. Science *335*, 557–561 (2012)

Butzin, M., Prange, M., and Lohmann, G.: Radiocarbon simulations for the glacial ocean: The effects of wind stress, Southern Ocean sea ice and Heinrich events. Earth Planet. Sci. Lett. *235*, 45–61 (2005)

Franke, J., Paul, A., and Schulz, M.: Modeling variations of marine reservoir ages during the last 45000 years. Clim. Past *4*, 125–136 (2008)

Hoffman, J. L., and Lund, D. C.: Refining the stable isotope budget for Antarctic Bottom Water: New foraminiferal data from the abyssal southwest Atlantic. Paleoceanography *27*, PA1213; doi:10.1029/2011PA002216 (2012)

Skinner, L. C., Fallon, S., Waelbroeck, C., Michel, E., and Barker, S.: Ventilation of the deep southern ocean and deglacial $CO_2$ rise. Science *328*, 1147–1151 (2010)

Wunsch, C.: Determining paleoceanographic circulations, with emphasis on the Last Glacial Maximum. Quat. Sci. Rev. *22*, 371–385 (2003)

Enqing Huang
Room 316
School of Ocean and Earth Science
Tongji University
1239 Siping Road
200092, Shanghai
China
E-Mail: ehuang@tongji.edu.cn

Nova Acta Leopoldina NF *121*, Nr. 408, 107–110 (2015)

# The Combined Effects of Changes in Ocean Chemistry, Biology, and Hydrodynamics on Alkalinity

Tatiana Ilyina (Hamburg)

With 1 Figure

Seawater total alkalinity (TA; determined by the charge imbalance of the conservative ions in seawater) and total dissolved inorganic carbon ($TCO_2$; the sum of carbon species) control the variations of $pCO_2$ in seawater, which in turn directly determine the air – sea exchange of $CO_2$. Because TA and $TCO_2$ are conserved during mixing and are unaffected by changes in temperature and pressure (Zeebe and Wolf-Gladrow 2001), they are key parameters of the marine carbonate system used as state variables in models of ocean biogeochemistry. Oceanic TA is altered by three main processes, being (*i*) changes in freshwater fluxes, such as precipitation/evaporation, riverine discharge of fresh water, ice growth and melting, (*ii*) production of $CaCO_3$ by calcifying organisms (e.g. coccolithophorids, corals, foraminifera) and $CaCO_3$ dissolution in the water column and deep-sea sediments; and (*iii*) production and remineralization of organic matter by microalgae. Increase in the surface ocean TA enhances the oceanic uptake of atmospheric $CO_2$, while decreasing TA lowers the oceanic capacity to take up and store carbon. Changes in seawater TA by a variety of mechanisms are thought to be responsible for modulating the variations of atmospheric $CO_2$ along glacial-interglacial timescales (e.g. Rickaby et al. 2010, Kleypas 1997, Archer and Maier-Reimer 1994). Enhancement of TA has been proposed as a mean of deliberate manipulation of climate (Köhler et al. 2013, Ilyina et al. 2013a). Therefore, understanding the spatiotemporal distribution of TA changes is critical to grasp the oceanic capacity to uptake and store carbon. Furthermore, dissolution of $CO_2$ in seawater does not change TA, but may affect processes controlling its cycling. Hence, it is also interesting to study TA in the context of climate change, i. e. in a rising $CO_2$ ocean.

Projections of future climate change calculated within the 5$^{th}$ Phase of the Coupled Model Intercomparison Project (CMIP5) with the Max Planck Institute's Earth system model (MPI-ESM, Giorgetta el al. 2013) will be presented. CMIP5 experiments examined here include a historical run covering the period 1850–2005 and three future climate change scenarios referred to as extended concentration pathways (ECPs) running from the year 2006 until 2300. These ECPs follow the standard RCP scenarios in terms of the achieved radiative forcing of 8.5, 4.5, and 2.6 W m$^{-2}$ by the end of the 21$^{st}$ century with simple stabilization assumptions for the atmospheric $CO_2$ concentrations made onwards. Such extended future climate change projections ran only in the low resolution model version (LR) of MPI-ESM driven by prescribed atmospheric $CO_2$ concentrations. The oceanic biogeochemistry component of MPI-ESM is the model HAMOCC (Ilyina et al. 2013b) which runs as a subroutine of the OGCM MPIOM. The horizontal resolution of the oceanic component of MPI-ESM-LR is about 1.5°.

The model HAMOCC simulates inorganic carbon chemistry (Maier-Reimer and Hasselmann 1987) and uses an extended NPZD-type description of marine biology (Six and Maier-Reimer 1996) in which phytoplankton and zooplankton dynamics depend on temperature, solar radiation, and co-limiting nutrients (phosphate, nitrate, iron, silicate). HAMOCC uses one phytoplankton type for primary production but separates two types of planktonic shell materials (opal and calcium carbonate shells, respectively), which are exported from the euphotic zone with different sinking rates. TA in the model is the sum of carbonate, borate alkalinities, and water dissociation products. TA is altered during production and dissolution of $CaCO_3$. Dissolution of $CaCO_3$ is a function of the carbonate ion and the calcium ion concentrations, as well as temperature and pressure dependent stoichiometric constant, and is driven by the deviation from the saturation state. Biogenic calcite particles, produced in the euphotic zone, precipitate if seawater is supersaturated with respect to $CaCO_3$ and start dissolving if the water column or the sediment pore-water is undersaturated with respect to $CaCO_3$. Seasonal growth of phytoplankton increases TA, while aerobic remineralization of organic matter decreases it. Additionally, TA is altered during denitrification. The model HAMOCC also includes a sediment module (Heinze et al. 1999) which calculates formation and dissolution of sediments basically simulating the same biogeochemical processes as in the water column. Globally uniform weathering fluxes are prescribed over the simulation period.

Both the physical and the biogeochemical state of the oceans are undergoing major changes as a result of global warming and ocean acidification (*IPCC* 2013). These ongoing changes perturb fundamental mechanisms that act to modify TA in the ocean. Yet, resulting changes in TA are not intuitively projected. In our simulations, changes in the distribution of TA are calculated in response to the intensified hydrological cycle, reorganization of the circulation patterns, changes in biological processes and carbonate chemistry. Consistent with these, both positive and negative anomalies are projected in TA (Fig. 1). Because changes in TA are closely related to changes in salinity, TA anomalies at the surface resemble the patterns of salinity anomalies. Weaker correlation between anomalies in surface salinity and TA is found in the equatorial Pacific and in the Indian Ocean. These areas of the global ocean are characterized by higher primary production, including production of $CaCO_3$, relative to other oceanic areas. In response to a decreased nutrients supply to the surface, the primary production and corresponding export production of organic matter and $CaCO_3$ is reduced. Furthermore, only rather small changes in salinity are projected in these regions of the ocean. Hence, changes in TA here are driven by changes in biological processes. In the subsurface and deep ocean, effects of changes in production and dissolution of $CaCO_3$ on changes in TA are not pronounced in our projections, as the ocean stays largely supersaturated with respect to $CaCO_3$ over the simulated time range. The contribution of carbonate dissolution becomes prominent on longer temporal scales (Ilyina and Zeebe 2012). Additionally, reduced production of $CaCO_3$ due to ocean acidification can have a significant effect on the precipitation of $CaCO_3$ and thereby modify the global distribution of TA (e. g. Ilyina et al. 2009). Regionally, subsurface TA anomalies are also driven by changes in organic matter remineralization by respiration and denitrification.

In summary, we show that changes in seawater TA can modulate oceanic uptake of carbon. Furthermore, our results indicate that TA is projected to undergo changes, which should not be ignored when diagnosing the oceanic capacity to take up and store carbon in future projections, as well as in calculations of air-sea $CO_2$ exchange on glacial-interglacial time-

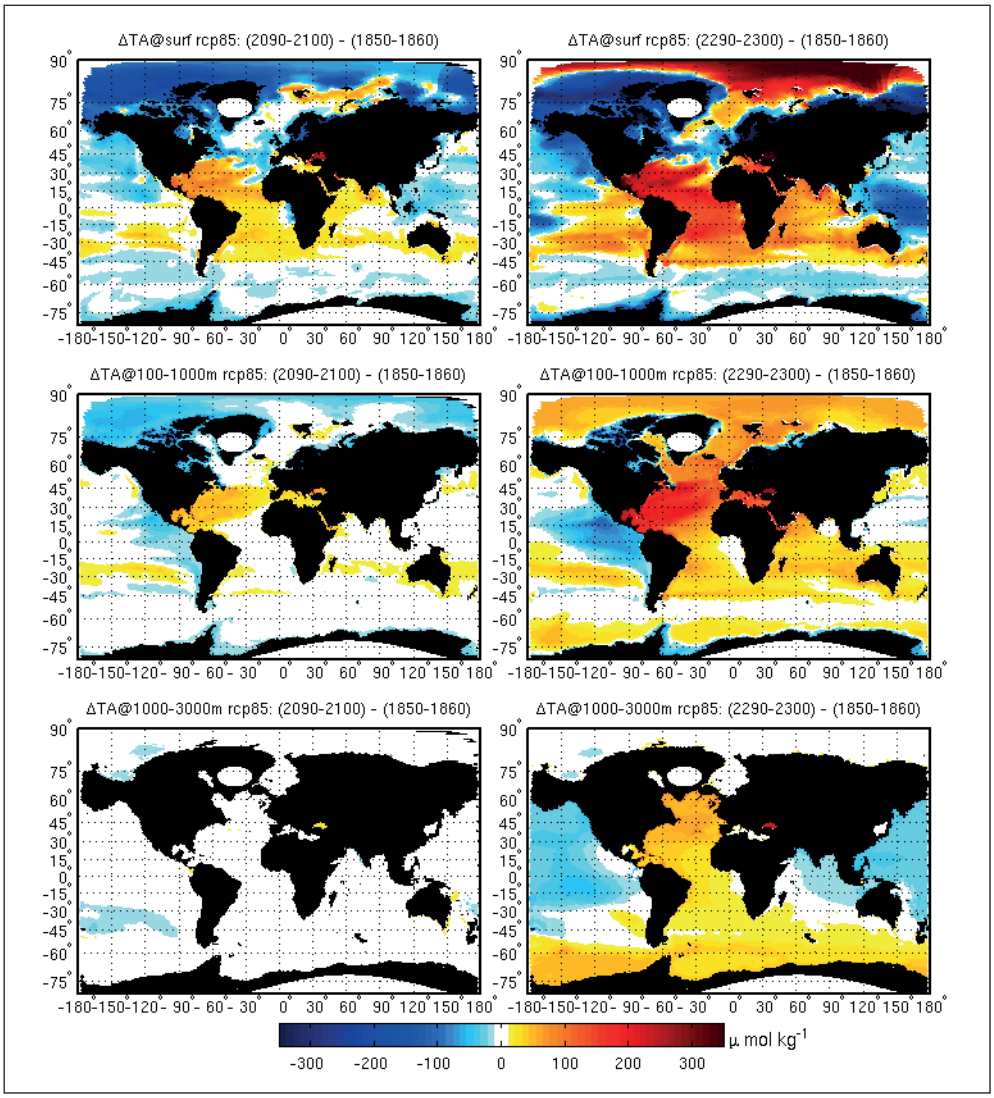


Fig. 1 Changes in TA μmol $kg^{-1}$ for the scenario RCP8.5 in 2090–2100 relative to 1850–1860 at the ocean surface, averaged over the upper 100–1000 m, and over the depth of 1000–3000 m.

scales. Finally, we show that changes in mixing/ventilation, production and dissolution of $CaCO_3$, remineralization of organic matter by aerobic and anaerobic processes, and sedimentary fluxes act in concert to contribute to the projected changes in TA. Thus, these processes have to be included prognostically in modelling studies.

## *References*


Archer, D., and Maier-Reimer, E.: Effect of deep-sea sedimentary calcite preservation on atmospheric $CO_2$ concentration. Nature *367*, 260–264 (1994)

Giorgetta, M. A., Jungclaus, J., Reick, C. H., Legutke, S., Bader, J., Böttinger, J., Brovkin, B., Crueger, T., Esch, M., Fieg, K., Glushak, K., Gayler, V., Haak, H., Hollweg, H. D., Ilyina, T., Kinne, S., Kornblueh, L., Matei, D., Mauritsen, T., Mikolajewicz, U., Mueller, W., Notz, D., Pithan, F., Raddatz, T., Rast, S., Redler, R., Roeckner, E., Schmidt, H., Schnur, R., Segschneider, J., Six, K. D., Stockhause, M., Timmreck, C., Wegner, J., Widmann, H., Wieners, K. H., Claussen, M., Marotzke, J., and Stevens, B.: Climate and carbon cycle changes from 1850 to 2100 in MPI-ESM simulations for the coupled model intercomparison project phase 5. J. Adv. Model. Earth Systems doi:10.1002/jame.20038 (2013)

Heinze, C., Maier-Reimer, E., Winguth, A. M. E., and Archer, D.: A global oceanic sediment model for long-term climate studies. Global Biogeochem. Cycles *13*/1, 221–250; doi:10.1029/98GB02812 (1999)

Ilyina, T., and Zeebe, R. E.: Detection and projection of carbonate dissolution in the water column and deep-sea sediments due to ocean acidification. Geophys. Res. Lett. *39*/6, doi:10.1029/2012GL051272 (2012)

Ilyina, T., Zeebe, R. E, Maier-Reimer, E., and Heinze, C.: Early detection of ocean acidification effects on marine calcification. Global Biogeochem. Cycles *23*/1, doi:10.1029/2008GB003278 (2009)

Ilyina, T., Wolf-Gladrow, D., Munhoven, G., and Heinze, C.: Assessing the potential of calcium-based artificial ocean alkalinization to mitigate rising atmospheric $CO_2$ and ocean acidification. Geophys. Res. Lett. *40*, 1–6; doi:10.1002/2013GL057981 (2013a)

Ilyina, T., Six, K. D., Segschneider, J., Maier-Reimer, E., Li, H., and Núñez-Riboni, I.: Global ocean biogeochemistry model HAMOCC: Model architecture and performance as component of the mpi-earth system model in different CMIP5 experimental realizations. J. Adv. Model. Earth Systems *5*/2, 287–315; doi:10.1029/2012MS000178 (2013b)

*IPCC*: Climate Change 2013: The Physical Science Basis. Contribution of Working Group I to the Fifth Assessment Report of the Intergovernmental Panel on Climate Change. 1535 pp. Cambridge (UK), New York (NY, USA): Cambridge University Press 2013

Kelypas, J. A.: Modeled estimates of global reef habitat and carbonate production since the last glacial maximum. Paleoceanography *12*/4, 533–545 (1997)

Köhler, P., Abrams, J. F., Völker, C., Hauck, J., and Wolf-Gladrow, D. A.: Geoengineering impact of open ocean dissolution of olivine on atmospheric $CO_2$, surface ocean pH and marine biology. Environm. Res. Lett. *8*/1, 014009 (2013)

Maier-Reimer, E., and Hasselmann, K.: Transport and storage of $CO_2$ in the ocean – An inorganic ocean-circulation carbon cycle model. Clim. Dyn. *2*, 63–90 (1987)

Rickaby, R. E. M., Elderfield, H., Roberts, N., Hillenbrand, C.-D., and Mackensen, A.: Evidence for elevated alkalinity in the glacial southern ocean. Paleoceanography *25*/1, PA1209; doi:10.1029/2009PA001762 (2010)

Six, K. D., and Maier-Reimer, E.: Effects of plankton dynamics on seasonal carbon fluxes in an ocean general circulation model. Global Biogeochem. Cycles *10*, 559–583 (1996)

Zeebe, R., and Wolf-Gladrow, D.: $CO_2$ in Seawater: Equilibrium, Kinetics, Isotopes. Vol. *65*. Amsterdam (etc.): Elsevier Science 2001



Dr. Tatiana Ilyina
Max Planck Institute for Meteorology
Bundesstraße 53
20146 Hamburg
Germany
Phone: +49 40 41173164
Fax: +49 40 41173298
E-Mail: tatiana.ilyina@mpimet.mpg.de

Nova Acta Leopoldina NF *121*, Nr. 408, 111–115 (2015)

# Deglacial Changes in Ocean (De)Oxygenation

Samuel L. Jaccard (Bern, Switzerland) and Eric D. Galbraith (Montreal, Canada)

Oxygen is supplied to seawater by marine photosynthesis and exchange with the atmosphere, and consumed by the respiration of organic matter in the ocean interior. Both sides of this relationship are thus dependent on physical ocean circulation: oxygen supply is determined by the physical transport of oxygenated waters from the mixed layer into the ocean subsurface, while organic matter export relies on the physical circulation to supply the surface ocean with nutrients. Thus, the occurrence of oxygen-depleted (hypoxic) waters is inextricably linked to ocean circulation, both through the supply and demand of oxygen. In addition, the oxygen flux is physically dependent on the combined effects of the temperature dependence of oxygen solubility and the degree of saturation at the surface, crucially influenced by wind and sea-ice processes. All of these factors are linked to the sea surface conditions in the high latitude source areas where the thermocline is ventilated. It is expected that as these regions warm, large-scale deoxygenation of the upper oceans will ensue. Recent observations appear to confirm this prediction, though these changes remain subtle in the face of natural decadal variability (Ito and Deutsch 2010). Paleoceanographic records extend beyond the noise of recent decadal variability, to provide an independent perspective on the links between climate and hypoxia.

A number of factors should have conspired to increase the oxygenation of the upper ocean during the last ice age. First, lower temperatures would have increased oxygen solubility, while strong winds at high-latitudes would have helped to equilibrate the surface waters and contributed to vigorous thermocline ventilation. In addition, global cooling would have enhanced the vertical transport of carbon from the surface to the deep ocean, due to the overall temperature dependence on the remineralization rate of sinking organic matter (Matsumoto 2007). The nutrient inventory of the upper ocean indeed appears to have been lower (Sigman and Haug 2003), which would have decreased the demand for oxygen through remineralization in much of the upper ocean. Consistent with this, paleoceanographic proxy records from near oxygen minimum zones have been interpreted as showing generally higher oxygen concentrations during the Last Glacial Maximum (LGM; Galbraith et al. 2004). Importantly, the deep ocean (below ~2.5 km) appears to have been different, with lower oxygen concentrations during the LGM, consistent with greater respired carbon storage there (Jaccard and Galbraith 2012, Jaccard et al. 2014 and references therein).

In order to elucidate the global evolution of ocean oxygenation throughout the deglaciation, we compiled available records of the four most commonly measured sedimentary

proxies of low-oxygen concentrations (Jaccard and Galbraith 2012, Jaccard et al. 2014). Three of these (redox-sensitive trace metal concentrations, benthic faunal assemblages and sedimentary laminations) are sensitive to oxygen concentrations at the sediment-water interface of the sediment core site. In addition, we include bulk sedimentary $\delta^{15}N$ (Galbraith et al. 2013), which is enriched by denitrification in the cores of oxygen minimum zones, from which it spreads by mixing and advection to adjacent regions where it can be recorded in sedimentary organic matter.

The deglacial transition at the end of the last ice age involved a warming of the global surface ocean by approximately 2 ºC (Shakun et al. 2012), similar to the magnitude of anthropogenic warming, but over a period of more than 10,000 years. Chronicling the deglacial progression between the LGM and Holocene requires a temporal framework. The oxygen-sensitive proxies are therefore analysed according to the sense of change between the four well-recognized intervals of the last deglaciation (Jaccard and Galbraith 2012, Jaccard et al. 2014). First among these, during the LGM to the Heinrich stadial 1 (HS1) transition, a coherent deoxygenation occurs in the upper 1000 m of the eastern tropical Pacific. In contrast, all available proxies show that oxygenation increased throughout the Arabian Sea during the LGM to HS1 transition. Meanwhile, none of the numerous records from north of 20 °N in the Pacific show any sign of change, nor do trace metal records from the SE Pacific. Foraminiferal abundances in the North Atlantic registered a coeval deoxygenation, though the degree of oxygen depletion there was relatively minor (to near the threshold of hypoxia, but not significantly beyond). Subsequently, the transition from HS1 to the Bølling-Allerød/Antarctic Cold Reversal (BA/ACR) saw an extremely widespread decrease in oxygenation throughout the Indo-Pacific that extended as deep as 3000 m. The only exceptions to this are among the eastern tropical Pacific sites that experienced the early deoxygenation during the LGM to HS1 transition. Globally, this transition represents the lion's share of the deglacial upper-ocean deoxygenation, given that the northern Pacific and Indian Oceans include the vast majority of the world's hypoxic waters. In most sediment records with high temporal resolution, this transition occurs very quickly. Finally, and perhaps most surprisingly, the BA/ACR to Holocene transition involved a coherent increase in oxygenation throughout most of the low-oxygen waters of the Indo-Pacific, particularly the North Pacific. This late deglacial increase in oxygenation is apparent in all available records, with no apparent dependence on water depth. In fact, the increase of oxygenation between the BA/ACR and the Holocene is more consistent among records than is the overall LGM to Holocene upper-ocean deoxygenation. The dramatic coherency of regional changes in upper-ocean oxygenation that occurred between the deglacial intervals shows that deoxygenation varied more strongly on a millennial timescale than it did on the longer, glacial-interglacial timescale. Ocean oxygenation, therefore, did not respond linearly to changes in global temperature, particularly given that the LGM to BA/ACR change involved only a fraction of the total glacial-interglacial temperature increase, and the large HS1 to BA/ACR transition involved warming only in the Northern Hemisphere. So what drove these clear, millennial-timescale changes in oxygenation?

As discussed above, the two possible causes are changes in the oxygen supply rate, and changes in subsurface respiration rates. During HS1, oxygen supply might have been expected to decrease in waters ventilated by the Southern Ocean, due to warming at high southern latitudes, while oxygen supply to the North Pacific may have increased due to wind-driven changes in circulation (Meissner et al. 2005). Meanwhile, weakening of the monsoonal

upwelling may have reduced export in the Arabian Sea (Altabet et al. 2002), even while increased trade winds enhanced upwelling in the Eastern tropical Pacific (Kienast et al. 2006). Additionally, changes in the density structure of the ocean (Schmittner et al. 2007) or the strength of the Southern westerlies (Anderson et al. 2009) may have increased the supply of nutrients to the eastern tropical Pacific during HS1 (Robinson et al. 2007). The lack of apparent LGM to HS1 change in the North Pacific may indicate either that oxygenation changes there were indeed minimal, or that hypoxia was entirely absent during the LGM and therefore could not become any less extensive during HS1, so that increased oxygenation was not recorded by the proxies. During the transition to the BA/ACR, when the Northern Hemisphere warmed abruptly, decreased oxygen solubility would have been accompanied by an invigoration of the global overturning circulation that increased the nutrient supply to the surface ocean (Schmittner et al. 2007). Thus, during the deglacial transitions, it seems likely that changes in both oxygen supply and oxygen consumption would have contributed to the observed patterns, due to coupled changes in oceanic and atmospheric circulation, intimately linked to the large-scale overturning of the ocean.

Although the overall deoxygenation of the upper Indo-Pacific during the first half of the deglaciation is in keeping with the expectation of less oxygen in a warmer ocean, the sense of change between the BA/ACR and the Holocene is not. Despite the persistence of relatively large ice sheets and global average temperatures that were still well below modern, the northern Indo-Pacific hypoxic zone appears to have contracted following the BA/ACR. Given that the colder subducting waters would have had higher saturation oxygen concentrations than today, the consumption of oxygen must have been higher. Two mechanisms are proposed for this.

*First*, a deglacial trend from low preformed nutrients to high preformed nutrients could have coincided with rapid oxygen supply to the deep ocean and/or the Southern Hemisphere, so that a large burden of remineralization was focused in the upper portion of the northern Indo-Pacific; all else being equal, this would imply that the preformed nutrient inventory of the ocean increased following the BA/ACR, which is consistent with nitrogen isotope records from the Southern Ocean and subarctic Pacific (Galbraith et al. 2013 for a review). *Second*, it is possible that the consumption rate of oxygen decreased from the BA/ACR to the Holocene due to a deglacial decrease of global nutrient inventories. It has been argued that the nitrogen and phosphorus inventories of the global ocean were 10–25 % higher during the glacial period, due to reduced removal of nitrogen and phosphorus through denitrification and apatite burial, respectively (Deutsch et al. 2004, Ganeshram et al. 2002). It has been reasoned that the reduction of these nutrient inventories was a response to the warmer conditions of the Holocene, limiting the global export production to that which could be respired given the global oxygen supply, thereby preventing widespread anoxia (Lenton and Watson 2000). This suggestion is consistent with proxy evidence that export flux in the North Pacific was particularly high during the BA/ACR (Kohfeld and Chase 2011) though testing the idea with export proxies is problematic, since the regional demand for oxygen is integrated over large areas and cannot be reliably inferred from a few points.

Forecasting the evolution of oceanic oxygen concentrations over the upcoming centuries will require a thorough understanding of the physical ocean response to anthropogenic forcing, as well as the changes in respiration rates that will result. Although the geological archive from the last deglaciation cannot directly help with these predictions, it presents emphatic evidence that the evolution of oxygenation will not be a straightforward function of

temperature, and that we may be in for surprises. Improved constraints on the deglaciation will require new palaeo-proxies that can quantify changes in dissolved oxygen and respired carbon concentrations, as well as greater spatial coverage.

## *References*


Altabet, M. A., Francois, R., Murray, D. E., and Prell, W. L.: The effect of millennial-scale changes in Arabian Sea denitrification on atmospheric $CO_2$. Nature *415*, 159–162 (2002)

Anderson, B. A., Ali, S., Bradtmiller, L. I., Nielsen, S. H. H., Fleisher, M. Q., Anderson, B. E., and Burckle, L. H.: Wind-driven upwelling in the Southern Ocean and the deglacial rise in atmospheric $CO_2$. Science *323*, 1443–1448 (2009)

Deutsch, C., Sigman, D. M., Thunell, R. C., Meckler, A. N., and Haug, G. H.: Isotopic constraints on glacial/interglacial changes in the oceanic nitrogen budget. Global Biogeochem. Cycles *18*, doi:10.1029/2003GB002189 (2004)

Galbraith, E. D., Kienast, M., Pedersen, T. F., and Calvert, S. E.: Glacial-interglacial modulation of the marine nitrogen cycle by oxygen supply to intermediate waters. Paleoceanography *19*, doi:1029/2003PA001000 (2004)

Galbraith, E. D., Kienast, M., Albuquerque, A. L., Altabet, M. A., Batista, F., Bianchi, D., Calvert, S. E., Contreras, S., Crosta, X., De Pol-Holz, R., Dubois, N., Etourneau, J., Francois, R., Hsu, T.-C., Ivanochko, T., Jaccard, S. L., Kao, S.-J., Kiefer, T., Kienast, S., Lehmann, M. F., Martinez, P., McCarthy, M., Meckler, A. N., Mix, A., Möbius, J., Pedersen, T. F., Pichevin, L., Quan, T. M., Robinson, R. S., Ryabenko, E., Schmittner, A., Schneider, R., Schneider-Mor, A., Shigemitsu, M., Sinclair, D., Somes, C., Studer, A. S., Tesdal, J.-E., Thunell, R., and Terence Yang, J.-Y.: The acceleration of oceanic denitrification during deglacial warming. Nature Geosci. *6*, 579–584 (2013)

Ganeshram, R. S., Pedersen, T. F., Calvert, S. E., and Francois, R.: Reduced nitrogen fixation in the glacial ocean inferred from changes in marine nitrogen and phosphorus inventories. Nature *415*, 156–159 (2002)

Ito, T., and Deutsch, C.: A conceptual model for the temporal spectrum of oceanic oxygen variability. Geophys. Res. Lett. *37*, doi:10.1029/2009GL041595 (2010)

Jaccard, S. L., Galbraith, E. D., Frölicher, T. L., and Gruber, N.: Ocean (de)oxygenation across the last deglaciation: Insights for the future. Oceanography *27*/1, 26–35 (2014)

Jaccard, S. L., and Galbraith, E. D.: Large climate-driven changes of oceanic oxygen concentrations during the last deglaciation. Nature Geosci. *5*, 151–156 (2012)

Kienast, M., Kienast, S. S., Calvert, S. E., Eglinton, T. I., Mollenhauer, G., Francois, R., and Mix, A. C.: Eastern Pacific cooling and Atlantic overturning circulation during the last deglaciation. Nature *443*, 846–849 (2006)

Kohfeld, K. E., and Chase, Z.: Controls on deglacial changes in biogenic fluxes in the north Pacific Ocean. Quat. Sci. Rev. *30*, 3350–3363 (2011)

Lenton, T. M., and Watson, A. J.: Redfield revisited: 1. Regulation of nitrate, phosphate and oxygen in the ocean. Global Biogeochem. Cycles *14*, 225–248 (2000)

Matsumoto, K.: Biology-mediated temperature control on atmospheric $pCO_2$ and ocean biogeochemistry. Geophys. Res. Lett. *34*, doi:10.1029/2007GL031301 (2007)

Meissner, K. J., Galbraith, E. D., and Völker, C.: Denitrification under glacial and interglacial conditions: A physical approach. Paleoceanography *20*, doi:10.1029/2004PA001083 (2005)

Robinson, R. S., Mix, A., and Martinez, P.: Southern Ocean control on the extent of denitrification in the southeast Pacific over the last 70 ka. Quat. Sci. Rev. *26*, 201–212 (2007)

Sigman, D. M., and Haug, G. H.: Biological pump in the past. In: Elderfield, H. (Ed.): The Oceans and Marine Geochemistry. Treatise on Geochemistry. Vol. *6*, pp. 491–528. Oxford: Elsevier Pergamon 2003

Shakun, J. D., Clark, P. U., He, F., Marcott, S. A., Mix, A. C., Liu, Z., Otto-Bliesner, B., Schmittner, A., and Bard, E.: Global warming preceded by increasing carbon dioxide concentrations during the last deglaciation. Nature *484*, 49–55 (2012)

Schmittner, A., Galbraith, E. D., Hostetler, S. W., Pedersen, T. F., and Zhang, R.: Large fluctuations of dissolved oxygen in the Indian and Pacific oceans during Dansgaard-Oeschger oscillations caused by variations of North Atlantic Deep Water subduction. Paleoceanography *22*, doi:10.1029/2006PA001384 (2007)

Prof. Samuel L. Jaccard, Ph.D.
University of Bern
Institute of Geological Sciences and
Oeschger Center for Climate Change Research
Baltzerstrasse 1+3
CH-3012 Bern
Switzerland
Phone: +41 31 6314568
E-Mail: samuel.jaccard@geo.unibe.ch

Prof. Eric D. Galbraith, Ph.D.
McGill University
Department of Earth and Planetary Science
3450 University St.
Montreal, Quebec
Canada H3A 2A7
Phone: +1 514 3983677
E-Mail: eric.galbraith@mcgill.ca

Nova Acta Leopoldina NF *121*, Nr. 408, 117–121 (2015)

# Mechanisms and Multi-Tracer Fingerprints of Past Carbon Cycle Changes in the Bern3D-LPX Model

Fortunat Joos, Renato Spahni, Benjamin D. Stocker,[1] Raphael Roth, Laurie Menviel,[2] Sarah S. Eggleston, Hubertus Fischer, and Jochen Schmitt (Bern, Switzerland)

With 2 Figures

Proxy information from ice cores, marine sediments, peat, and other archives demonstrate a fascinating spatio-temporal evolution of the coupled climate and biogeochemical system on orbital-to-decadal timescales. However, we are still far from a complete understanding of the drivers, mechanisms, and feedbacks governing past changes in the Earth System. This is partly related to limited modelling capacities. While traditional and highly stylized box models are relatively easy to construct and can be run over many thousand years, they lack physical and biogeochemical realism and spatial resolution. On the other hand, the community is just starting to perform single runs with comprehensive state-of-the-art Earth System Models over several millennia as they are costly to apply. In addition, these models often miss representations of important components for long-term $CO_2$ variations such as ocean sediments or peat. Earth System Models of Intermediate Complexity can fill the gap by providing spatially-explicit information, e.g. by resolving tracer gradients in ocean sediments or north-south movements in the distribution of peatlands over glacial-interglacial cycles, the possibility to run sensitivity simulations over hundred thousands of years and to include representations for many tracers and isotopes.

In the presentation, results from transient simulations over glacial-interglacial periods and of illustrative sensitivity experiments with the Bern3D-LPX climate-carbon cycle model will be discussed. A focus is on mechanisms governing past variations in atmospheric $CO_2$ and the associated spatial and temporal imprints (Fig. 1) on carbon isotopes, deep-ocean carbonate ion concentrations, the export of biogenic particles, and on peatland distribution and carbon storage in the land biosphere. Results are compared to proxies from marine, ice, peat, and other archives. In the following, we provide a brief overview of the Bern-LPX model and summarize some recent publications based on Bern3D-LPX results.

## 1. Model and Mechanisms

The Bern3D-LPX model couples an atmosphere energy balance model with a 3-dimensional geostrophic-frictional balance ocean model, and a sea ice module with representations of the terrestrial and oceanic biogeochemical cycles, including ocean sediments. The ocean module

1 Now at Department of Life Sciences, Imperial College London (UK).
2 Now at Climate Change Research Centre, University of New South Wales (Australia).

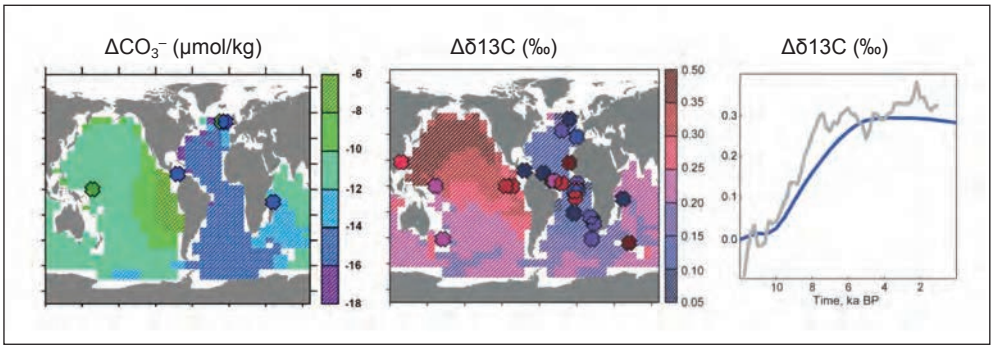


Fig. 1 An illustration of spatio-temporal tracer dynamics in the ocean (Menviel and Joos 2012). Change in deep ocean carbonate concentration (*left*) and $\delta^{13}C$ (*middle*) as simulated by the Bern3D model and reconstructed from sediment cores (symbols) over the last 10,000 years. The right panel shows the simulated $\delta^{13}C$ evolution (*blue*) and as reconstructed from the available $\delta^{13}C$ sediment data.

includes the tracers dissolved inorganic and organic carbon, alkalinity, phosphate, oxygen, silica, iron, the carbon isotopes $^{13}C$ and $^{14}C$, isotopes of neodymium, protactinium, and thorium, nitrous oxide, and CFCs and considers biological production, dissolution, and sedimentation of opal, calcium carbonate, and organic particles. The LPX land module is a dynamic global vegetation model that simulates the dynamics of vegetation cover, albedo changes, peat and wetland area extent, carbon and nitrogen fluxes and stocks, land-atmosphere fluxes of carbon dioxide, methane and nitrous oxide, anthropogenic land use including shifting cultivation, and fire (Stocker et al. 2013).

Mechanisms of glacial-interglacial $CO_2$ change investigated with the Bern3D-LPX model include among others changes in Southern Ocean overturning, in North Atlantic Deep Water formation, iron fertilization of marine phytoplankton, changes in ocean phosphate inventory, changes in the remineralization depth of organic matter and calcium carbonate particles, changes in the distribution of peatland and changes in peat carbon stocks, or volcanic outgassing of $CO_2$. An important aspect is that the inclusion of an ocean sediment module and of weathering and burial fluxes allows for multi-millennial scale changes in the total inventories of carbon, alkalinity, nutrients and isotopes in the ocean-atmosphere-land biosphere system and for associated millennial-scale adjustment processes including a newly identified "organic matter-nutrient-sediment feedback".

## 2. Deglacial $CO_2$, Southern Ocean Ventilation, and the Influence of Volcanism

Tschumi et al. 2011 examined the sensitivity of atmospheric $CO_2$, its carbon isotope composition, and oceanic properties to changes in deep ocean ventilation, the ocean carbon pumps, and sediment formation in the Bern3D ocean-sediment carbon cycle model. The results provide support for the hypothesis that a break up of Southern Ocean stratification and invigorated deep ocean ventilation were the dominant drivers for the early deglacial $CO_2$ rise of 35 ppm between the Last Glacial Maximum and 14.6 ka BP. Another rise of 10 ppm until the end of the Holocene is attributed to carbonate compensation responding to the early deglacial change in ocean circulation. A multi-proxy analysis which indicates that an acceleration of

deep ocean ventilation during early deglaciation is not only consistent with recorded atmospheric $CO_2$ but also with the reconstructed opal sedimentation peak in the Southern Ocean at around 16 ka BP, the record of atmospheric $\delta^{13}C$-$CO_2$, and the reconstructed changes in the Pacific $CaCO_3$ saturation horizon. A limitation is that our coarse resolution model does not properly represent near-coast convective processes in the Southern Ocean and is only able to simulate a slowly-ventilated deep ocean when forced with unrealistic boundary conditions.

Huybers and Langmuir (2009) proposed that an increase in volcanic activity provoked by ice sheet melting contributed substantially to the deglacial $CO_2$ increase. Roth and Joos (2012) evaluated their volcanic $CO_2$ emission scenarios in the Bern3D carbon cycle-climate model. The simulated increase of atmospheric $CO_2$ peaks around 6 ka BP at 46 ppm for the central scenario and with a range between 13 and 142 ppm. Modelled carbonate ion concentration in the deep ocean decreases and the calcite saturation horizon shoals on global average by 440 m (150 to 1500 m). The comparison of our model results and available proxy evidence suggests a small role for volcanic carbon emissions in regulating glacial–interglacial $CO_2$ variations, but uncertainties prevent a firm conclusion. A problem with the volcanic emission hypothesis is in the timing of emissions which peak in the early Holocene, a period of decreasing atmospheric $CO_2$.

## 3. Glacial-Interglacial Changes in $CO_2$

Menviel et al. (2012) transiently simulated changes in atmospheric $CO_2$ and climate over the last glacial-interglacial cycle for a range of forcing scenarios. A third of the glacial-interglacial atmospheric $CO_2$ change can be explained by relatively well-established forcings such as temperature, salinity, a shallowing and weakening of the Atlantic Meridional Overturning Circulation, iron fertilization of the marine biosphere by aeolian dust input and land carbon inventory changes. A hypothetical 10 % increase in the oceanic phosphate inventory decreases atmospheric $CO_2$ by 50 ppm during the glaciation, however, due to the long residence time of phosphorus in the ocean and the long timescales of ocean sediment interactions it only contributes to a 5 ppmv increase between 20 and 0 ka BP. A deepening of particulate organic matter remineralization can effectively lower $pCO_2$ during the glaciation, however, it leads to a significant increase in deep carbonate ion concentration and to changes in export production which are in poor agreement with paleo-proxies. The parameterization of brine rejection around Antarctica could lead to 10–20 ppmv change in $CO_2$, but its timing casts doubt onto its effectiveness in forcing $CO_2$ variations over the last glacial-interglacial cycle. Variations in the Atlantic Meridional Overturning, including its collapse and recovery, only slightly modulate atmospheric $CO_2$ over the glacial period and the last termination and are, in contrast to recent suggestions, not responsible for the bulk of the modelled deglacial $CO_2$ rise.

The role of changes in the marine remineralization of particulate organic matter (POM) and calcium carbonate has been further investigated. Roth et al. (2014) mapped the responses to changes in remineralization length scales with the Bern3D ocean-sediment model for atmospheric $CO_2$, $\delta^{13}C$ and tracer fields for which observations and palaeoproxies exist (Fig. 2). Results show that the "sediment burial-nutrient feedback" amplifies the response in atmospheric $CO_2$ by a factor of four to seven. A transient imbalance between the weathering flux and the burial of organic matter and calcium carbonate leads to sustained changes in the ocean's inventory of phosphate, carbon, carbon isotopes, and alkalinity and in turn in surface

nutrient availability, marine productivity, and atmospheric $CO_2$ and $\delta^{13}CO_2$. It takes decades to centuries to reorganize tracers and fluxes within the ocean, many millennia to approach equilibrium for burial fluxes, while $\delta^{13}C$ signatures are still changing 200,000 years after the perturbation. The results highlight the role of organic matter burial for both $CO_2$ and $\delta^{13}C$ and the substantial impacts of seemingly small changes in POM remineralization on atmospheric $CO_2$ and $\delta^{13}C$. More general, weathering-burial feedbacks can effectively and strongly enhance the impact of changes in marine biological processes on atmospheric $CO_2$ and could had contributed to the long-term $CO_2$ decrease from interglacial to glacial maximum conditions. However, the multi-millennial timescales of the amplification imply little importance of this feedback for glacial terminations with comparably short duration.

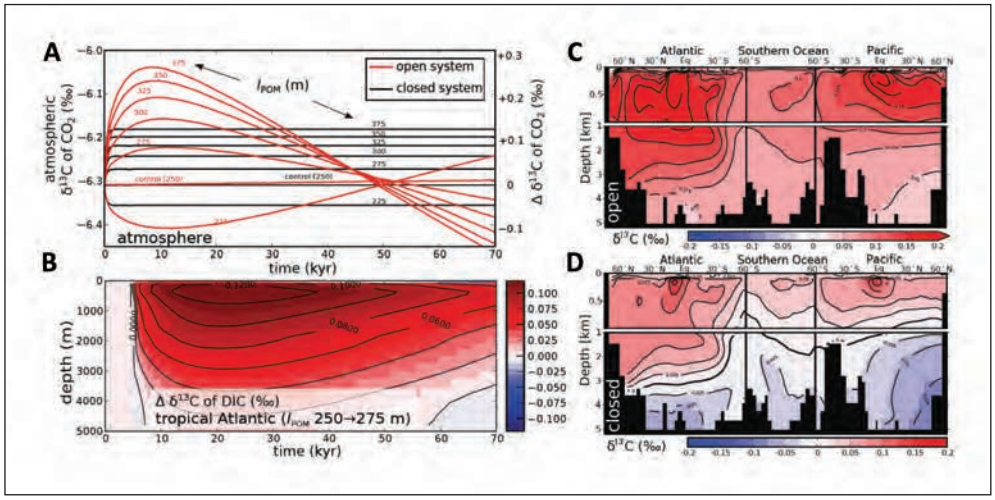


Fig. 2 An illustration of the multi-millennial timescales associated with imbalances in the weathering and burial of organic material. Results are from experiments where a step-like change in the remineralization length-scale of particulate organic matter (POM) is prescribed at time 0 (Roth et al. 2014). (*A*) Evolution of $\delta^{13}C$ in the atmosphere for the closed system (no sediment, no burial; *black*) and open system (*red*); labels indicate the prescribed remineralization depth after the step change. (*B*) Hovmöller diagram of the change in $\delta^{13}C$ of DIC averaged over the tropical Atlantic and (*C*, *D*) anomaly in $\delta^{13}C$ of DIC after 15 ka in the open and closed systems in a transect through the Atlantic, Southern and Pacific oceans and when remineralization depth is increased from 250 to 275 m. The burial-weathering feedback leads to a temporary increase in the mean ocean $\delta^{13}C$ signature as indicated by the red colours in (*C*), whereas the within ocean reorganization leads to a $\delta^{13}C$ enrichment in the upper ocean and depletion below.

## 4. Deglacial Changes in Global Peatlands

Peatlands currently store about 550 GtC and are a major component of the land carbon cycle. Predicting the spatio-temporal dynamics of global peatlands is the key to understand their role under past and future climate change. LPX-Bern, including the module to simulate peat carbon and peat area dynamically (Spahni et al. 2013, Stocker et al. 2014), was forced with varying climate boundary conditions as simulated for the transition from the Last Glacial Maximum (LGM) to today. This reveals the spatial dynamics of peatlands in response to climatic shifts, ice sheet retreat, and sea level rise. In line with maps of pollen records of sphag-

num cores, a northward shift of peatlands is simulated over the past 20,000 years. A large expansion of the total peatland area is simulated for the Eurasian continent. In South-East Asia, tropical peatlands, wide-spread at the LGM, are simulated to have been submerged by rising sea levels. Our results suggest that C stored in peatlands was around present-day levels at the LGM, dropped during the deglaciation and accumulated gradually at higher latitudes under the more stable climatic conditions during the Holocene.

## *References*


Huybers, P., and Langmuir, C.: Feedback between deglaciation, volcanism, and atmospheric $CO_2$, Earth Planet. Sci. Lett. *286*, 479–491; doi:10.1016/j.epsl.2009.07.014 (2009)

Menviel, L., and Joos, F.: Toward explaining the Holocene carbon dioxide and carbon isotope records: Results from transient ocean carbon cycle-climate simulations. Paleoceanography *27*, PA1207; doi:10.1029/2011pa002224 (2012)

Menviel, L., Joos, F., and Ritz, S. P.: Simulating atmospheric $CO_2$, $^{13}C$ and the marine carbon cycle during the last glacial–interglacial cycle: possible role for a deepening of the mean remineralization depth and an increase in the oceanic nutrient inventory. Quat. Sci. Rev. *56*, 46–68; doi:10.1016/j.quascirev.2012.09.012 (2012)

Roth, R., and Joos, F.: Model limits on the role of volcanic carbon emissions in regulating glacial-interglacial $CO_2$ variations. Earth Planet. Sci. Lett. *329*/330, 141–149; doi:10.1016/j.epsl.2012.02.019 (2012)

Roth, R., Ritz, S. P., and Joos, F.: Burial-nutrient feedbacks amplify the sensitivity of atmospheric carbon dioxide to changes in organic matter remineralisation. Earth Syst. Dynam. *5*, 321–343; doi:10.5194/esd-5-321-2014 (2014)

Spahni, R., Joos, F., Stocker, B. D., Steinacher, M., and Yu, Z. C.: Transient simulations of the carbon and nitrogen dynamics in northern peatlands: from the Last Glacial Maximum to the 21st century. Clim. Past *9*, 1287–1308; doi:10.5194/cp-9-1287-2013 (2013)

Stocker, B. D., Roth, R., Joos, F., Spahni, R., Steinacher, M., Zaehle, S., Bouwman, L., Xu, R., and Prentice, I. C.: Multiple greenhouse-gas feedbacks from the land biosphere under future climate change scenarios. Nature Clim. Change *3*, 666–672; doi:10.1038/nclimate1864; http://www.nature.com/nclimate/journal/v3/n7/abs/nclimate1864.html#supplementary-information (2013)

Stocker, B. D., Spahni, R., and Joos, F.: DYPTOP: a cost-efficient TOPMODEL implementation to simulate subgrid spatio-temporal dynamics of global wetlands and peatlands. Geosci. Model Dev. Discuss. *7*, 4875–4930; doi:10.5194/gmdd-7-4875-2014 (2014)

Tschumi, T., Joos, F., Gehlen, M., and Heinze, C.: Deep ocean ventilation, carbon isotopes, marine sedimentation and the deglacial $CO_2$ rise. Clim. Past *7*, 771–800; doi:10.5194/cp-7-771-2011 (2011)



Prof. Dr. Fortunat Joos
Climate and Environmental Physics
Physics Institute and
Oeschger Centre for Climate Change Research
University of Bern
Sidlerstrasse 5
CH-3012 Bern
Switzerland
Phone: +41 31 6314461
Fax: +41 31 6318742
E-Mail: joos@climate.unibe.ch

Nova Acta Leopoldina NF *121*, Nr. 408, 123–126 (2015)

# Ice Core Records: Climate Reconstruction

Jean JOUZEL (Gif-sur-Yvette, France)

With 2 Figures

Since about 60 years, water stable isotopes, $\delta^{18}O$ and $\delta D$ (more recently $\delta^{17}O$) are key tools to reconstruct climate parameters from polar ice cores giving access to continuous and very detailed paleoclimate series from Greenland and Antarctica. This includes information about the mean annual local temperature, $T_s$, and – assuming that it is linked to the derivative of the saturation vapour pressure – about the precipitation rate which is a key parameter for ice core dating. It also includes information about the oceanic origin of the precipitation (e.g. from the deuterium-excess).

Temperature reconstruction is based on the linear relationship between annual values of $\delta D$ and $\delta^{18}O$ and $T_s$, particularly well observed in polar regions and well explained by both simple and complex isotopic models. In a conventional approach, the present-day spatial relationship between the isotopic concentration of the precipitation ($\delta D$ or $\delta^{18}O$ which can indifferently be used as paleothermometers) and $T_s$, defined over a certain region, is assumed to hold in time throughout this region. Of course the fact that present-day isotope concentrations and local temperatures are correlated is not sufficient to validate this critical assumption. Such factors as the evaporative origin and the seasonality of precipitation can also affect $\delta D$ and $\delta^{18}O$. If these factors change markedly under different climates, the spatial slope can no longer be taken as a reliable surrogate of the temporal slope for interpreting the isotopic signal. For example, there is now ample evidence that temporal slopes are considerably lower (by up to a factor of 2) than the observed present-day spatial slope, for Greenland sites.

In this review, we will focus on the temperature interpretation of the large isotopic shifts associated with glacial-interglacial changes and on the detailed recontructions of deglacial periods. We will examine the complementarity between water isotopes (Fig. 1) and other approaches such as borehole paleothermometry, changes in the isotopic composition of nitrogen in the entrapped air bubbles and information derived from difference in firn diffusion of $\delta D$ and $\delta^{18}O$ (Fig. 2). We will also discuss how this information is used for estimating accumulation changes and for ice core dating.

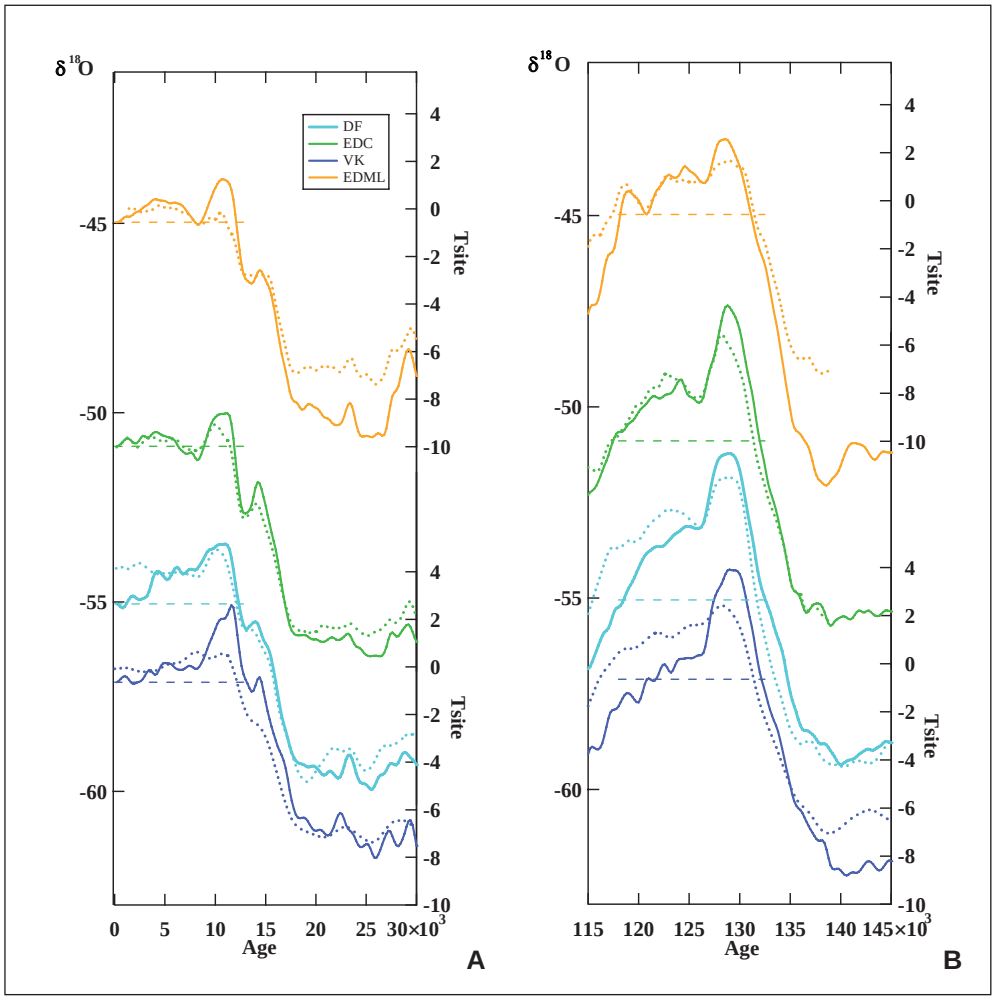


Fig. 1 Comparison between the initial isotopic records (‰, left axis) and the site temperature (°C, right axis, same temperature scaling for all records) estimated after correction for sea water isotopic composition and moisture source correction taking into account deuterium excess data, for EDC and EDML (Stenni et al. 2010), Vostok (Vimeux et al. 2001) and Dome F (Uemura et al. 2004, Kawamura et al. 2007). The resolution of the Tsite records varies between 200 years (EDC and EDML), 300 years (DF) and 400 years (Vostok). They have been normalized with respect to the last millennium and smoothed using a binomial filter to highlight only multi millennial trends. (*A*) Current interglacial, and (*B*) Last interglacial. With this approach, strong increases in deuterium excess during interglacials at Vostok and DF (not shown here) appear to account for long term interglacial isotopic decreases.

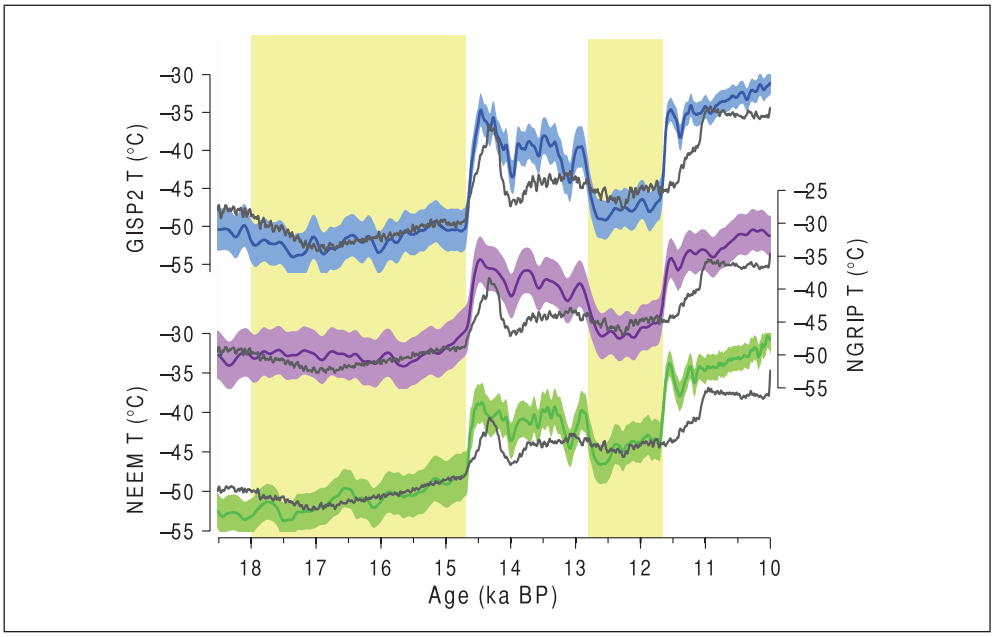


Fig. 2 Greenland temperature reconstructions with 1 s uncertainty envelope for GISP2 (*blue*), NGRIP (*purple*), NEEM (*green*), and CCSM3 GCM output (*gray*) adapted from Buizert et al. (2014).

## *References*


Buizert, C., Gkinis, V., Severinghaus, J. P., He, F., Lecavalier, B. S., Kindler, P., Leuenberger, M., Carlson, A. E., Vinther, B., Masson-Delmotte, V., White, J. W. C., Liu, Z., Otto-Bliesner, B., and Brook, E. J.: Greenland temperature response to climate forcing during the last deglaciation. Science *345*/6201, 1177–1180 (2014)

Gkinis, V.: Water isotope diffusion rates from the NorthGRIP ice core for the last 16000 years: glaciological implications. Earth Planet. Sci. Lett. *405*, 132–141 (2014)

Jouzel, J.: Water stable isotopes: atmospheric composition and applications in ice core studies. In: Keeling, R. F. (Ed.), and Holland, H. D., and Turekian, K. K. (Exec. Eds.): The Atmosphere. Treatise of Geochemistry. Vol. *5*. 5.08, 214-2562013, 214–256. Amsterdam: Elsevier Ltd. 2014

Kawamura, K., Parrenin, F., Lisiecki, L., Uemura, R., Vimeux, F., Severinghaus, J. P., Hutterli, M. A., Nakazawa, T., Aoki, S., Jouzel, J., Raymo, M. E., Matsumoto, K., Nakata, H., Motoyama, H., Fujita, S., Goto-Azuma, K., Fujii, Y., and Watanabe, O.: Northern Hemisphere forcing of climatic cycles in Antarctica over the past 360,000 years. Nature *448*, 912–915 (2007)

Masson-Delmotte, V., Buiron, D., Ekaykin, A., Frezzotti, M., Gallée, H., Jouzel, J., Krinner, G., Landais, A., Motoyama, H., Oerter, H., Pol, K., Pollard, D., Ritz, C., Schlosser, E., Sime, L. C., Sodemann, H., Stenni, B., Uemura, R., and Vimeux, F.: A comparison of the present and last interglacial periods in six Antarctic ice cores. Clim. Past *7*/2, 397–423; doi:10.5194/cp-7-397-2011 (2011)

Parrenin, F., Masson-Delmotte, V., Köhler, P., Raynaud, D., Paillard, D., Schwander, J., Barbante, C., Landais, A., Wegner, A., and Jouzel, J.: Synchronous change in atmospheric $CO_2$ and Antarctic temperature during the last deglacial warming. Science *339*, 1060–1063; doi:10.1126/science.1226368 (2013)

Stenni, B., Masson-Delmotte, V., Selmo, E., Oerter, H., Meyer, H., Röthlisberger, R., Jouzel, J., Cattani, O., Falourd, S., Fischer, H., Hoffmann, G., Iacumin, P., Johnsen, S. J., Minster, B., and Udisti, R.: The deuterium excess records of EPICA Dome C and Dronning Maud Land ice cores (East Antarctica). Quat. Sci. Rev. *29*, 146–159 (2010)

Uemura, R., Yoshida, N., Kurita, N., Nakawo, M., and Watanabe, O.: An observation-based method for reconstructing ocean surface changes using a 340,000 year deuterium excess record from the Dome Fuji ice core, Antarctica. Geophys. Res. Lett. *31*, L13216; doi:10.1029/2004GL019954 (2004)

Vimeux, F., Masson, V., Delaygue, G., Jouzel, J., Petit, J.-R., and Stievenard, M.: A 420,000 year deuterium excess record from East Antarctica: Information on past changes in the origin of precipitation at Vostok. J. Geophys. Res. *106*, 31863–31873 (2001)

Prof. Dr. Jean Jouzel
Laboratoire des Sciences du Climat
et de l'Environnement
(IPSL, CEA-CNRS-UVSQ, Bt 701)
Point Courrier 129
CEA – Orme des Merisiers
91191 Gif/Yvette, Cedex
France
Phone: +33 1 69087713
Fax: +33 1 69087716
E-Mail: jean.jouzel@lsce.ipsl.fr

Nova Acta Leopoldina NF *121*, Nr. 408, 127–134 (2015)

# Using Paleo-Oceanographic Data Synthesis to Test Ideas about Changes in Atmospheric $CO_2$ Concentrations during Glacial Inception

Karen E. Kohfeld (Burnaby, Canada) and Zanna Chase (Hobart, Australia)

With 1 Figure

Several hypotheses have been put forth to explain the 80–100 ppm change in atmospheric carbon dioxide concentrations that has occurred consistently on glacial-interglacial timescales over the past 800,000 years (Sigman et al. 2010). A combination of process-based modelling and paleo-environmental data from the geological record suggest that while changes in ocean biology have likely played a role as an important feedback mechanism, changes in marine biology alone cannot explain the full glacial-interglacial change in atmospheric carbon dioxide concentrations (Kohfeld et al. 2005, Kohfeld and Ridgwell 2009). This result points towards an important, triggering role of physical changes in the global ocean as a main driver of changes in atmospheric carbon dioxide concentrations, in particular during the earliest part of the glacial cycle.

A number of hypotheses have involved physical mechanisms as the key drivers of glacial interglacial changes in atmospheric carbon dioxide concentrations including: sea ice expansion (Stephens and Keeling 2000, Ferrari et al. 2014), polar surface water stratification (Francois et al. 1997, Sigman et al. 2004), change in the position and intensity of Southern Hemisphere westerly winds (Toggweiler et al. 2006, Anderson et al. 2009) and changes in the degree of deep-ocean mixing leading the deep-ocean stratification (Adkins et al. 2002, Watson and Naveiro-Garabato 2006, Adkins 2013, De Boer and Hogg 2014). While many of the hypotheses focus on changes in physical oceanographic conditions that may have occurred between the Last Glacial Maximum (hereafter LGM, ~19–23 ka) and the Holocene, only a few (Adkins 2013, Timmermann et al. 2014, Peacock et al. 2006, Ganopolski and Brovkin 2014) consider the change in environmental conditions during glacial inception. The $CO_2$ record from Antarctic ice cores demonstrates that atmospheric $CO_2$ had decreased by 34–45 ppmv between 80–110 ka, a change that represents 40–55 % of the total glacial-interglacial signal. The goal of this presentation is to consider the implications of the timing of hypothesized changes in physical processes during glacial inception. In other words, is there evidence that any of these physical changes occurred early enough in the glacial cycle to enhance the uptake of $CO_2$ by the world's oceans during glacial inception?

To understand conditions during glacial inception, we use compilations of sea-surface temperature (SST) reconstructions, polar planktonic oxygen isotope data, and existing compilations of carbon isotope data from foraminifera (Oliver et al. 2010) for sites with data that extend from 130,000 years ago to today. We compiled sea surface temperature data reconstructed using alkenone (49 sites), Mg/Ca ratios (15 sites), and faunal assemblage reconstruc-

tions (planktonic foraminifera, diatoms, and radiolarian, 55 sites) from 117 deep-sea cores distributed between 57°N and 57°S. To gain an understanding of how conditions may have been changing in the high polar latitudes, we supplemented these SST reconstructions with oxygen isotope data from planktonic foraminifera from high-latitude sites between 50 and 72°N (15 sites) and between 50 and 68°S (4 sites).

We examine conditions for several time periods during glacial inception that represent different levels of atmospheric $CO_2$ changes: Stage 5e (120–130 ka), Stage 5d (100–110 ka), Stage 5a (80–90 ka), Stage 4 (60–70 ka) and the Marine Isotope Stage 2 (here defined as 18–28 ka). For the sake of comparison we averaged information over 10,000 years for each interval. We compare these data with evidence for changes in sea level (Waelbroeck et al. 2002), orbital insolation forcing (Berger and Loutre 1991), ice core temperature estimates (Jouzel et al. 2007), and proxies of sea ice extent (Wolff et al. 2010). In all cases, we assess the conditions at Stages 5d, 5a, and 4 by comparing them with the total magnitude of change between Stage 5e and the LGM (Stage 2, 18–28 ka), which we take as indicative of the full glacial signal.

As a first order approximation, averaging the SST changes at all 117 sites suggests temperatures were on the order of 1.5°C cooler during Stage 5d compared with Stage 5e, a change that represents just over 1/3 of the total Stage 5e-LGM temperature change. A simple calculation (using CO2SYS), based on this preliminary estimate of whole-ocean temperature change, suggests that the effect of temperature on the solubility of $CO_2$ could account for on the order of 18 ppm reduction in atmospheric $CO_2$ by Stage 5d. It is worth noting that the global SST reduction is likely an underestimate because of under-representation of oceanic regions poleward of 55° latitude. At the same time, SSTs in high-latitude polar regions will undoubtedly be constrained by freezing temperatures, which could reduce the effect of this bias on the global temperature change. Using the sea level approximation of Waelbroeck et al. (2002), we estimate that the effect of ice volume on global salinity had only reached 30 % of its interglacial-glacial total impact, which would have added about 2 ppmv of $CO_2$ to the atmosphere. Combining these two effects results in 16 ppmv reduction, or roughly half of the total observed 34 ppmv change in atmospheric $CO_2$, by Stage 5d. Release of terrestrial carbon would offset this figure, and based on the sea-level reconstruction (Waelbroeck et al. 2002) we estimate the decrease in the terrestrial biosphere by Stage 5d to cause an increase in atmospheric $CO_2$ of 4.5 ppmv, or 30 % of the 15 ppmv glacial-interglacial increase in $pCO_2$ driven by terrestrial carbon release (Sigman and Boyle 2000). Thus the combined reduction in atmospheric $CO_2$ attributable to changes in sea-surface temperature, salinity, and the terrestrial biosphere is on the order of ~11 ppmv.

In terms of the spatial patterns in cooling, the high latitude and tropical regions did not cool equally during glacial inception (Fig. 1). Not only did the tropics (40°S and 40°N) cool less overall during the glacial cycle, the proportion of the total observed cooling during glacial inception (Stage 5d) was only a small fraction (–0.7 °C, or about 25 %) of the total observed cooling between Stage 5e and the LGM. The same can be said of SSTs reconstructed in the northern high latitudes (40–57°N), which show a slow response early during glacial inception. In contrast, cooling in the Southern Hemisphere south of 40°S – as recorded in SSTs and in the EPICA Dome C ice core – kept pace with $CO_2$ reductions. In fact, 50–65 % of the total Stage 5e-LGM cooling had already occurred in the high-latitude Southern Hemisphere by Stage 5d, when 34 ppmv (41 %) of the glacial-interglacial $CO_2$ reduction had occurred (Fig. 1).

Taken alone, the reconstructed temperature response suggests that physical changes in the Southern Hemisphere preceded the response observed in the Northern Hemisphere. However,

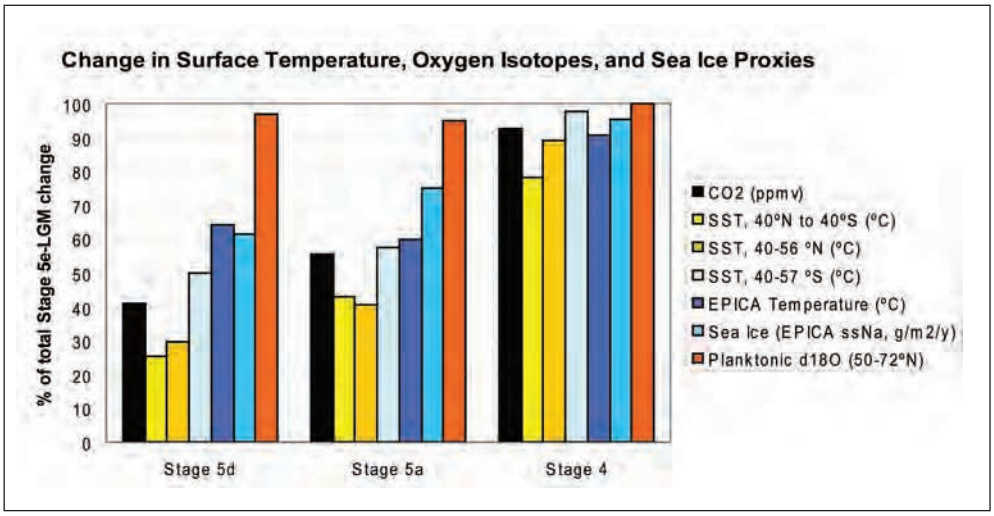


Fig 1 Changes in atmospheric carbon dioxide (*black*); sea-surface temperatures for 40°S-40°N (*yellow*), 40–56°N (*light orange*), 40–57°S (*light blue*); EPICA surface temperature (*dark blue*), EPICA sea salt Sodium (ssNa) as a proxy for sea ice extent (*turquoise*), and the $\delta^{18}O$ of polar planktonic foraminifera from 50–72°N in the North Atlantic Ocean (*red-orange*) during Stage 5d (100–110 ka), Stage 5a (80–90 ka), and Stage 4 (60–70 ka). Changes are expressed as the percent of the total change estimated for each proxy between Stage 5e (120–130 ka) and the Last Glacial Maximum (LGM, here estimated as 18–28 ka).

these estimates of changes in the global average temperature do not include a representation of SSTs poleward of 56° latitude in both hemispheres. We can supplement existing sea-surface temperature estimates in polar regions using oxygen isotope data from planktonic foraminifera from 15 sites between 50°N and 72°N in the North Atlantic Ocean. After removing an estimate of ice volume, these records suggest that, on average, oxygen isotope values of planktonic foraminifera increased by approximately 0.70 ‰ between Stage 5e and Stage 5d, a change that could equate to several degrees of cooling, and represents more than 90 % of the total Stage 5e-LGM change. Interpreting the $\delta^{18}O$ of polar planktonic foraminifera is complicated by influences such as seawater salinity and foraminiferal vital effects (e.g., depth habitat and season of growth). However, interpreting this regional change as a substantial decrease in temperature during glacial inception is supported by recent high-resolution faunal reconstructions from two sites at 55 and 61°N in the North Atlantic (Mokeddem et al. 2014), suggesting that the vast majority of the cooling in the high-latitude North Atlantic had likely already occurred by Stage 5d, 100,000 years ago.

This evidence for early cooling in the high latitude North Atlantic region could provide support for the hypothesis of Adkins (2013), who suggests that early cooling of North Atlantic Deep Water (NADW) in the formation region during glacial inception could serve as the precursor to the change in the density balance between NADW and Antarctic Bottom Water (AABW). Adkins (2013) suggests that when the pre-cooled NADW was upwelled along the coast of Antarctica, it reduced the melting of land ice and its associated freshwater contribution to AABW. As a result, a colder, more saline AABW could have been formed, the density of NADW was decreased relative to the more saline AABW, and deep water stratification was initiated. Reductions in summer insolation forcing in the Northern Hemisphere precedes that

of the Southern Hemisphere between Stages 5e and 5d (Berger and Loutre 1991), which would be consistent with a Northern Hemisphere initiation of cooling that is observed in the planktonic oxygen isotope data and would support this hypothesis.

One potential implication of this hypothesis is that the cooling of North Atlantic SSTs – and their subsequent influence on the salinity and density of AABW – should lead to the initiation of deep-ocean stratification that allowed for trapping of carbon dioxide in the deep ocean, resulting in changes in the distribution of the $\delta^{13}C$ of benthic foraminifera. Is this change observed? Examination of the $\delta^{13}C$ data from the Atlantic Ocean (Oliver et al. 2010) demonstrates that evidence for substantial AABW expansion does not occur until Stage 4. We can reach two possible conclusions from this observation: (*i*) that deep-water stratification does not occur until Stage 4; or (*ii*) that deep-water stratification only becomes detectable in $\delta^{13}C$ data when complementary, surface water productivity changes amplify the deep water signal in the South Atlantic through nutrient trapping.

Combining evidence from multiple proxies may be useful in resolving this question. Interpreting $\delta^{13}C$ purely as a water mass tracer is complicated by the effects of air-sea gas exchange, productivity, and sea-ice on C isotope fractionation. In contrast, Nd isotope ratios in seawater are minimally affected by mass-dependent fractionation, and are therefore almost conservative, with the potential to serve as robust circulation tracer (Friedrich et al. 2014). We are aware of only two Nd isotope studies covering the first half of the last glaciation. By measuring benthic oxygen isotopes, C isotopes and Nd isotopes in the same South Atlantic core (4981 m water depth), Piotrowsky et al. (2004) demonstrate a clear sequence of events at the stage 5/4 transition. They find ice-sheet growth and deep water cooling happens first (as shown by benthic $\delta^{18}O$), followed by a large decrease in benthic $\delta^{13}C$, which is then followed by a shift in Nd isotopes. These records strongly suggest the decrease in $\delta^{13}C$ observed in this core, and indeed in the larger compilation (Oliver et al. 2010), is driven by non-circulatory effects related to reorganization of the carbon cycle. The change in thermohaline circulation, as recorded by Nd isotopes, clearly occurs after the change in the carbon cycle, at around the start of Stage 4. Similarly, Böhm et al. (2014) show, using $^{231}Pa/^{230}Th$ ratios and Nd isotope ratios, that the AMOC operated in the 'warm', or 'on' mode throughout much of the last glacial cycle, with the influence of NADW at Bermuda Rise beginning to decrease only around 50 ka, and reaching a minimum at the peak of the last glacial period. More records of Nd isotope composition at the 5/4 transition are needed to verify this conclusion, but together the Nd and $\delta^{13}C$ data suggest that the initial cooling of the NADW was not sufficient to invoke the change in deep water density structure implied by Adkins' hypothesis by Stage 5d, and that deep water stratification only begins to play a significant role in reducing atmospheric $CO_2$ during Stage 4.

In this case, other mechanisms are needed to explain the ~22 ppm decrease in $CO_2$ up to Stage 4 not explained by temperature, salinity, and terrestrial carbon. What do the data suggest together? SST records south of 40°S, along with EPICA Dome C surface temperature and non-sea-salt Calcium data (indicative of sea-ice extent) (Wolff et al. 2010), all suggest that the Southern Hemisphere temperature and sea ice responses kept pace with changes in Southern Hemisphere summer insolation changes at 60°S (Fig. 1). Furthermore, temperature reconstructions suggest that meridional temperature gradients were enhanced during Stage 5d relative to Stage 5e, consistent with insolation forced modelling simulations of glacial inception (Timmermann et al. 2014). According to these simulations, stronger meridional temperature gradients led to stronger westerly winds, which would not support westerly wind

weakening as a dominant mechanism during Stage 5d. Southern Hemisphere sea-ice extent had already increased considerably by the end of Stage 5d (~60 % of the total Stage 5e-LGM change), and therefore may have contributed to reduction of atmospheric $CO_2$ by reducing air-sea gas exchange (Stephens and Keeling 2000). Another possibility is that polar surface stratification may have been initiated at this time, either in response to decreased salinity, and/or due to the "equation of state" mechanism, where seawater density is less sensitive to temperature, and more sensitive to salinity, and low temperatures (Sigman et al. 2010). The few Southern Hemisphere sites poleward of 50°S used in this study suggest little or no change in the $\delta^{18}O$ planktonic foraminifera. Once ice volume effects are accounted for, the average change is actually slightly negative. This could be a result of no observed temperature change, or temperature decreases that are coupled with changes in the $\delta^{18}O$ of sea water (which could result from freshwater inputs). With only four data points it is difficult to interpret this information as a regionally extensive signal. However, evidence for expanded sea ice (Wolff et al. 2010) and reduced opal fluxes (Jaccard et al. 2013) could provide indirect support for enhanced surface water stratification. In sum, although the existing data are somewhat indirect and inconclusive, there is some evidence pointing to the expansion of sea ice cover and the initiation of surface water stratification in the Southern Hemisphere as dominant contributors to $CO_2$ drawdown early in the glacial inception during Stage 5d.

Another interesting characteristic of the SST data presented here is that spatially, the maximum cooling is found in the Subantarctic Zone already during Stage 5d. In previous data syntheses, this maximum cooling was found to be coincident with large changes in biogenic export production during the LGM (Kohfeld et al. 2013). These authors proposed that the strong coincidence of the zone of maximum cooling and biological productivity suggested that productivity changes were linked to physical circulation changes. In contrast, recent work (Jaccard et al. 2013, Martínez-García et al. 2014) has suggested that the productivity response that is observed in the Subantarctic zone is probably driven by iron fertilization. The region-wide SST reconstruction in this study demonstrates that a large fraction of the cooling of the Subantarctic Zone had already occurred prior to any evidence for large productivity increases in the Subantarctic Zone. Thus, regardless of the source of the iron reaching the Subantarctic zone, this combined evidence supports the idea that biogeochemical (Fe) rather than physical conditions drove increases in the Subantarctic Zone productivity after Stage 5a.

In summary, this study uses a new compilation of SST reconstruction from 117 deep-sea cores, polar planktonic oxygen isotope data from 19 high-latitude sites, existing compilations of carbon isotope data from foraminifera (Oliver et al. 2010), for sites with data from 130,000 years ago to today, to assess changes in physical oceanographic conditions during glacial inception. When combined with proxies of surface temperature and sea-ice extent from the EPICA Dome C ice core (Jouzel et al. 2007, Wolff et al. 2010), this analysis reveals several interesting points. *First*, surface temperature reconstructions all suggest that substantial cooling had already begun in both the northern and southern high-latitudes between Stage 5e and Stage 5d, 130–100 ka, while low-latitude temperatures had not changed substantially. The largest fraction of the total glacial-interglacial temperature change is observed in the high-latitude North Atlantic Ocean, as evidenced from oxygen isotope records from polar planktonic foraminifera. This cooling, coupled with estimated changes in ocean salinity and the terrestrial biosphere, likely result in a ~11 ppmv reduction in $CO_2$ by Stage 5d. *Second*, while the large temperature changes reconstructed for the high-latitude North Atlantic provide support for a North Hemisphere trigger for deep-ocean circulation changes

that led to deep-ocean stratification during Stage 5d, evidence for deep-ocean stratification is not strongly detectable either the in the $\delta^{13}C$ of benthic foraminifera or the existing Nd isotope data from deep-sea cores. This could suggest that other physical mechanisms (such as sea-ice expansion and surface water stratification) play an early role in reducing atmospheric $CO_2$ prior to Stage 5d, with deep-ocean stratification playing a larger role at the onset of Stage 4. Finally, the juxtaposition of substantial (~2 °C) cooling prior to the onset large increases in productivity in the Subantarctic Zone support previous assertions that biogeochemical rather than physical changes are responsible for the increases in Subantarctic productivity, which likely contributed to changes in atmospheric carbon dioxide after Stage 4.

## *Acknowledgments*

We gratefully acknowledge the researchers who published the original data used in this study as well as the people and funding agencies that support the PANGAEA and NOAA NGDC Paleoclimatology data archives, which make access to these data possible. KEK is supported by NSERC Discovery Grant and NSERC Canada Research Chair programs. Zanna Chase is supported by an Australian Research Council Future Fellowship.

## *References*

Adkins, J. F.: The role of deep ocean circulation in setting glacial climates. Paleoceanography *28*, 539–561 (2013)

Adkins, J. F., McIntyre, K., and Schrag, D. P.: The salinity, temperature and $\delta^{18}O$ content of the glacial deep ocean. Science *298*, 1769–1773 (2002)

Anderson, R. F., Ali, S., Bradtmiller, L. I., Nielsen, S. H. H., Fleisher, M. Q., Anderson, B. E., and Burckle, L. H.: Wind-driven upwelling in the Southern Ocean and the deglacial rise in atmospheric $CO_2$. Science *323*, 1443–1448 (2009)

Berger, A., and Loutre, M. F.: Insolation values for the climate of the last 10 million years. Quat. Sci. Rev. *10*, 297–317 (1991)

Boer, A. M. de, and Hogg, A. M.: Control of the glacial carbon budget by topographically induced mixing. Geophys. Res. Lett. *41*, 4277–4284; doi:10.1002/2014GL059963 (2014)

Böhm, E., Lippold, J., Gutjahr, M., Frank, M., Blaser, P., Antz, B., Fohlmeister, J., Frank, N., Andersen, M. B., and Deininger, M.: Strong and deep Atlantic meridional overturning circulation during the last glacial cycle. Nature *517*, 73–76 (2014)

Ferrari, R., Jansen, M. F., Adkins, J. F., Burke, A., Stewart, A. L., and Thompson, A. F.: Antarctic sea ice control on ocean circulation in present and glacial climates. Proc. Natl. Acad. Sci. USA *111*, 8753–8758 (2014)

Francois, R., Altabet, M. A., Yu, E.-F., Sigman, D. M., Bacon, M. P., Frank, M., Bohrmann, G., Bareille, G., and Labeyrie, L. D.: Contribution of Southern Ocean surface-water stratification to low atmospheric $CO_2$ concentrations during the last glacial period. Nature *389*, 929–935 (1997)

Friedrich, T., Timmermann, A., Stichel, T., and Pahnke, K.: Ocean circulation reconstructions from $\varepsilon_{Nd}$: A model-based feasibility study. Paleoceanography *29*, 1003–1023 (2014)

Ganopolski, A., and Brovkin, V.: Simulation of Quaternary glacial cycles with fully interactive carbon cycle. Geophys. Res. Abstracts *16*, EGU2014 (2014)

Jaccard, S. L., Hayes, C. T., Martínez-García, A., Hodell, D. A., Anderson, R. F., Sigman, D. M., and Haug, G. H.: Two modes of change in Southern Ocean productivity over the past million years. Science *339*, 1419–1423 (2013)

Jouzel, J., Masson-Delmotte, V., Cattani, O., Dreyfus, G., Falourd, S., Hoffmann, G., Minster, B., Nouet, J., Barnola, J. M., Chappellaz, J., Fischer, H., Gallet, J. C., Johnsen, S., Leuenberger, M., Loulergue, L., Luethi, D., Oerter, H., Parrenin, F., Raisbeck, G., Raynaud, D., Schilt, A., Schwander, J., Selmo, E., Souchez, R., Spahni, R., Stauffer, B., Steffensen, J. P., Stenni, B., Stocker, T. F., Tison, J. L., Werner, M., and Wolff, E. W.: Orbital and millennial Antarctic climate variability over the past 800,000 years. Science *317*, 793–796 (2007)

Kohfeld, K. E., Graham, R. M., Boer, A. M. de, Sime, L. C., Wolff, E. W., Le Quéré, C., and Bopp, L.: Southern Hemisphere westerly wind changes during the Last Glacial Maximum: paleo-data synthesis. Quat. Sci. Rev. *68*, 76–96 (2013)

Kohfeld, K. E., Le Quéré, C., Anderson, R. F., and Harrison, S. P.: Role of marine biology in glacial-interglacial $CO_2$ cycles. Science *308*, 74–78 (2005)

Kohfeld, K. E., and Ridgwell, A.: Glacial-interglacial variability in atmospheric $CO_2$. In: Le Quéré, C., and Saltzman, E. (Eds.): Surface Ocean/Lower Atmosphere Processes. Geophys. Monograph Series *37*, doi: 10.1029/2008GM000845. Washington, DC: American Geophysical Union 2009

Martínez-García, A., Sigman, D. M., Ren, H., Anderson, R. F., Straub, M., Hodell, D. A., Jaccard, S. L., Eglinton, T. I., and Haug, G. H.: Iron fertilization of the subantarctic ocean during the last ice age. Science *343*, 1347–1359 (2014)

Mokeddem, Z., McManus, J. F., and Oppo, D. W.: Oceanographic dynamics and the end of the last interglacial in the subpolar North Atlantic. Proc. Natl. Acad. Sci. USA *111*, 11263–11266 (2014)

Oliver, K. I. C., Hoogakker, B. A. A., Crowhurst, S., Henderson, G. M., Rickaby, R. E. M., Edwards, N. R., and Elderfield, H.: A synthesis of marine sediment core $\delta^{13}C$ data over the last 150 000 years. Clim. Past *6*, 645–673 (2010)

Peacock, S., Lane, E., and Restrepo, J. M.: A possible sequence of events for the generalized glacial-interglacial cycle. Global Biogeochem. Cycles *20*, GB2010; doi:2010.1029/2005GB002448 (2006)

Piotrowski, A. M., Goldstein, S. L., Hemming, S. R., and Fairbanks, R. G.: Intensification and variability of ocean thermohaline circulation through the last deglaciation. Earth Planet. Sci. Lett. *225*, 205–220 (2004)

Sigman, D. M., and Boyle, E. A.: Glacial/interglacial variations in atmospheric carbon dioxide. Nature *407*, 859–869 (2000)

Sigman, D. M., Hain, M. P., and Haug, G. H.: The polar ocean and glacial cycles in atmospheric $CO_2$ concentration. Nature *466*, 47–55 (2010)

Sigman, D. M., Jaccard, S. L., and Haug, G. H.: Polar ocean stratification in a cold climate. Nature *428*, 59–63 (2004)

Stephens, B. B., and Keeling, R. F.: The influence of Antarctic sea ice on glacial-interglacial $CO_2$ variations. Nature *404*/6774, 171–174 (2000)

Timmermann, A., Friedrich, T., Timm, O. E., Chikamoto, M. O., Abe-Ouchi, A., and Ganopolski, A.: Modeling obliquity and $CO_2$ effects on Southern Hemisphere climate during the past 408 ka. J. Climate *27*, 1863–1875 (2014)

Toggweiler, J. R., Russell, J. L., and Carson, S. R.: Midlatitude westerlies, atmospheric $CO_2$, and climate change during the ice ages. Paleoceanography *21*/2, doi:10.1029/2005PA001154 (2006)

Waelbroeck, C., Labeyrie, L., Michel, E., Duplessy, J. C., McManus, J. F., Lambeck, K., Balbon, E., and Labracherie, M.: Sea-level and deep water temperature changes derived from benthic foraminifera isotopic records. Quat. Sci. Rev. *21*, 295–305 (2002)

Watson, A. J., and Naveiro Garabato, A. C.: The role of Southern Ocean mixing and upwelling in glacial-interglacial atmospheric $CO_2$ change. Tellus *58*B, 73–87 (2006)

Wolff, E. W., Barbante, C., Becagli, S., Bigler, M., Boutron, C. F., Castellano, E., Angelis, M. de, Federer, U., Fischer, H., Fundel, F., Hansson, M., Hutterli, M., Jonsell, U., Karlin, T., Kaufmann, P., Lambert, F., Littot, G. C., Mulvaney, R., Röthlisberger, R., Ruth, U., Severi, M., Siggaard-Andersen, M. L., Sime, L. C., Steffensen, J. P., Stocker, T. F., Traversi, R., Twarloh, B., Udisti, R., Wagenbach, D., and Wegner, A.: Changes in environment over the last 800,000 years from chemical analysis of the EPICA Dome C ice core. Quat. Sci. Rev. *29*, 285–295 (2010)

Prof. Karen E. Kohfeld, Ph.D.
School of Resource and Environmental Management
Simon Fraser University
8888 University Drive
Burnaby, BC, V5A 1S6
Canada
Phone: +1 778 7824651
Fax: +1 778 7824968
E-Mail: kohfeld@sfu.ca

Zanna Chase, Ph.D.
Institute for Marine and Antarctic Studies
University of Tasmania
Private Bag 129
Hobart, Tasmania, 7001
Australia
Phone: +61 3 6226 8596
Fax: +61 3 6226 2937
E-Mail: zanna.chase@utas.edu.au

Nova Acta Leopoldina NF *121*, Nr. 408, 135–140 (2015)

# High Latitude Impacts on Deglacial $CO_2$: Southern Ocean Westerly Winds and Northern Hemisphere Permafrost Thawing

Peter Köhler, Christoph Völker, Gregor Knorr (Bremerhaven), and Edouard Bard (Aix-en-Provence, France )

With 2 Figures

Climate in the high latitudes changed massively during the last deglaciation. Temperature rose due to the polar amplification more than twice as much as in the global mean leading predominately to the shrinking of various parts of the cryosphere: decline of northern hemispheric (NH) land ice sheets and permafrost thawing, and a reduction in sea ice extent in both hemispheres. It is thus a rather natural choice to also analyse how changes in these polar regions might influence the global carbon cycle and atmospheric $CO_2$. Here we use carbon cycle models to analyse two examples of the impact of high latitude climate change on deglacial $CO_2$: (*i*) changes in the position of the westerly winds in the Southern Ocean during the Last Glacial Maximum (LGM) (based on Völker and Köhler 2013); (*ii*) Northern Hemisphere permafrost thawing at the onset of the Bølling/Allerød (B/A) around 14.6 ka ago (based on Köhler et al. 2014).

## 1. Southern Ocean Westerly Winds

The synchronicity of changes in atmospheric $CO_2$ and Antarctic temperature found in ice cores (e.g. Parrenin et al. 2013) has led to hypotheses which suggest Southern Ocean processes as causes for a dominant part of the observed deglacial rise in atmospheric $CO_2$. Toggweiler et al. (2006) e.g. proposed that changes in the Southern Hemispheric (SH) belt of westerly winds are the cause for a dominant part of the observed deglacial $CO_2$ rise. The reasoning of Toggweiler et al. (2006) is that nowadays Southern Hemispheric westerly winds lead to the upwelling of carbon-rich waters *via* a northward Ekman transport. If this westerly-induced upwelling is reduced (either by a northward shift or a reducing of the strength of the westerlies), less carbon-rich water is brought to the surface. As a consequence, net oceanic carbon uptake would drag $CO_2$ from the atmosphere to the surface of the Southern Ocean, where it would finally be transported to the abyss with deep waters formed around Antarctica. Toggweiler et al. (2006) argued about latitudinal shifts in the wind belt (equatorward during colder climates) while they performed simulation scenarios in which the strength, not the position of the SH westerly winds, was modified under the assumption that the effect of both on atmospheric $CO_2$ might be similar. In Völker and Köhler (2013) we provided a sensitivity test of the westerly wind hypothesis in which various shortcomings of the original study or its successors (Menviel et al. 2008, Tschumi et al. 2008, d'Orgeville et al. 2010, Lee et

al. 2011) are overcome: We used a (*i*) full ocean general circulation model (the MITgcm) (*ii*) including a fully prognostic sea ice model and applied (*iii*) LGM background conditions using (*iv*) a realistic bathymetry. In doing so, the potential role of the different carbon pumps on atmospheric $CO_2$ can be elucidated. In detail, we shifted the Southern Ocean westerly winds both southward and northward by up to 10°.

We find (Fig. 1) that a southward (northward) shift in the westerly winds leads to an intensification (weakening) of no more than 10 % of the Atlantic meridional overturning circulation (AMOC). This response of the ocean physics to shifting winds agrees with other studies starting from preindustrial background climate, but the responsible processes are different. In our setup, changes in AMOC seemed to be more pulled by upwelling in the south than pushed by buoyancy changes and subsequent downwelling in the north, opposite to what previous studies with different background climate are suggesting. The net effects of the changes in ocean circulation lead to a rise in atmospheric $pCO_2$ of less than 10 µatm for both northward and southward shift in the winds. For northward shifted winds the zone of upwelling of carbon- and nutrient-rich waters in the Southern Ocean is expanded, leading to more $CO_2$ outgassing to the atmosphere but also to an enhanced biological pump in the subpolar region. For southward shifted winds the upwelling region contracts around Antarctica, leading to less nutrient export northward and thus a weakening of the biological pump. These model results do not support the idea that shifts in the westerly wind belt play a dominant role in coupling atmospheric $CO_2$ rise and Antarctic temperature during deglaciation suggested by the ice core data.

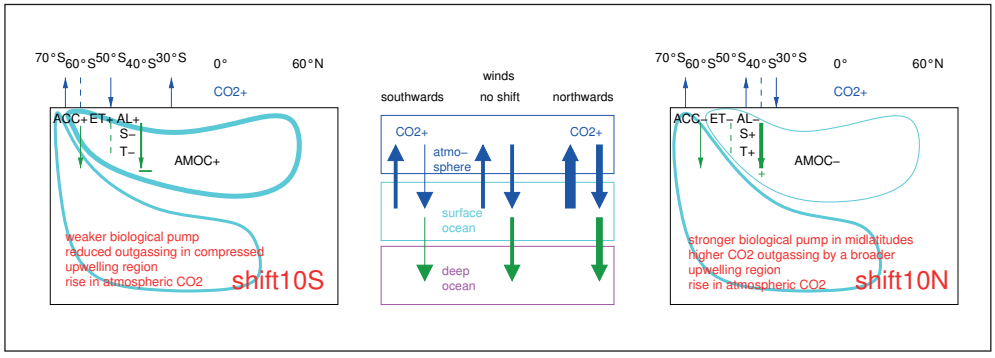


Fig. 1 Conceptual view of how changes in the SH winds influence the ocean circulation and the carbon cycle (after Völker and Köhler 2013). Impact of Southern Ocean westerly winds shifted (*left*) 10°S, and (*right*) 10°N as function of latitude. (*Middle*) Condensed changes in the carbon cycle comparing the LGM simulations. Strength of the biological pump (*green*) and of the gas exchange (*blue*) depict how carbon varies between atmosphere, surface, and deep ocean. ACC: Antarctic Circumpolar Current, ET: Ekman transport, and AL: Agulhas leakage.

According to our results, the impact of changes in the SH westerlies on ocean circulation and on atmospheric $CO_2$ during the deglaciation might have been as follows: Independent estimates (Kohfeld et al. 2013) suggest that the SH westerly wind belt was probably shifted to the north by no more than 5° in the LGM. In the atmospheric forcing of our LGM simulation the maximum in zonal wind stress was already shifted north by 4°. We, therefore, argue that starting from our LGM reference simulation, a southward shift of the westerly winds by 5° is the closest analogue to what might have happened in the past during termination I. These

changes in the SH winds probably evolved slowly over the whole deglaciation, not abrupt in a short time window of a few centuries. It might thus explain only a small part of less than 10 % of the deglacial AMOC enhancement and a rise in atmospheric $CO_2$ by 7 µatm. Thus, it becomes clear that SH westerly wind belt variation was not the dominant process which tightly couples atmospheric $CO_2$ and high-latitude SH temperature during terminations or even over whole glacial cycles.

## 2. Northern Hemisphere Permafrost Thawing

One of the most abrupt and yet unexplained past rises in atmospheric $CO_2$ (10 ppmv in two centuries in the EPICA Dome C [EDC] ice core) occurred in quasi-synchrony with abrupt northern hemispheric warming into the Bølling/Allerød, about 14.6 ka ago. In Köhler et al. (2014) we used a U/Th-dated record of atmospheric $\Delta^{14}C$ from Tahiti corals to provide an independent and precise age control for this $CO_2$ rise. We also used model simulations to show that the release of old (nearly $^{14}C$-free) carbon can explain these changes in $CO_2$ and $\Delta^{14}C$. The $\Delta^{14}C$ record provides an independent constraint on the amount of carbon released (125 PgC). We suggest, in line with observations of atmospheric $CH_4$ and terrigenous biomarkers, that thawing permafrost in high northern latitudes could have been the source of carbon, possibly with contribution from flooding of the Siberian continental shelf during meltwater pulse 1A. Our findings highlight the potential of the permafrost carbon reservoir to modulate abrupt climate changes *via* greenhouse-gas feedbacks. These calculations and conclusions were challenged by the new $CO_2$ data (Marcott et al. 2014) from the West Antarctic Ice Sheet Divide Ice Core (WDC), which have a higher temporal resolution. We therefore revised our carbon release experiments (Fig. 2) in order to meet these new WDC $CO_2$ data. We furthermore used a new age distribution during gas enclosure in ice which includes the most recent understanding of firn densification. We then can align EDC and WDC $CO_2$ data and propose a peak amplitude in atmospheric $CO_2$ of about 15 ppmv around 14.6 ka BP corresponding to a C pulse of 85 PgC released in 200 years (0.425 PgC per year). This is 68 % of the initial suggested strength of the C pulse of 125 PgC, that then led to a peak amplitude in true atmospheric $CO_2$ of 22 ppmv. $CO_2$ data from other ice cores suggest that the amplitude in atmospheric $CO_2$ was in-between both these scenarios. The revised scenario proposes a carbon release that is still large enough to explain the atmospheric $\Delta^{14}C$ anomaly of –(50–60) ‰ in 200–250 years derived from Tahiti corals. However, in the revised scenario the released carbon needs to be essentially free of $^{14}C$, while in the previously suggested scenario there was still the possibility that the released carbon still contained some $^{14}C$ and had a difference in the $\Delta^{14}C$ signature to the atmosphere $\Delta(\Delta^{14}C)$ of –700 ‰. The previous scenario, therefore, contained a larger possibility that the released carbon might eventually been released from the deep ocean. The revised interpretation proposed here strengthens the idea that the carbon was released from permafrost thawing, since this had more likely a nearly $^{14}C$-free signature than any other known source. We therefore conclude, that the new WDC $CO_2$ data are not in conflict with our permafrost thawing hypothesis, but indicate only that the magnitude of the released carbon might have been smaller than initially suggested.

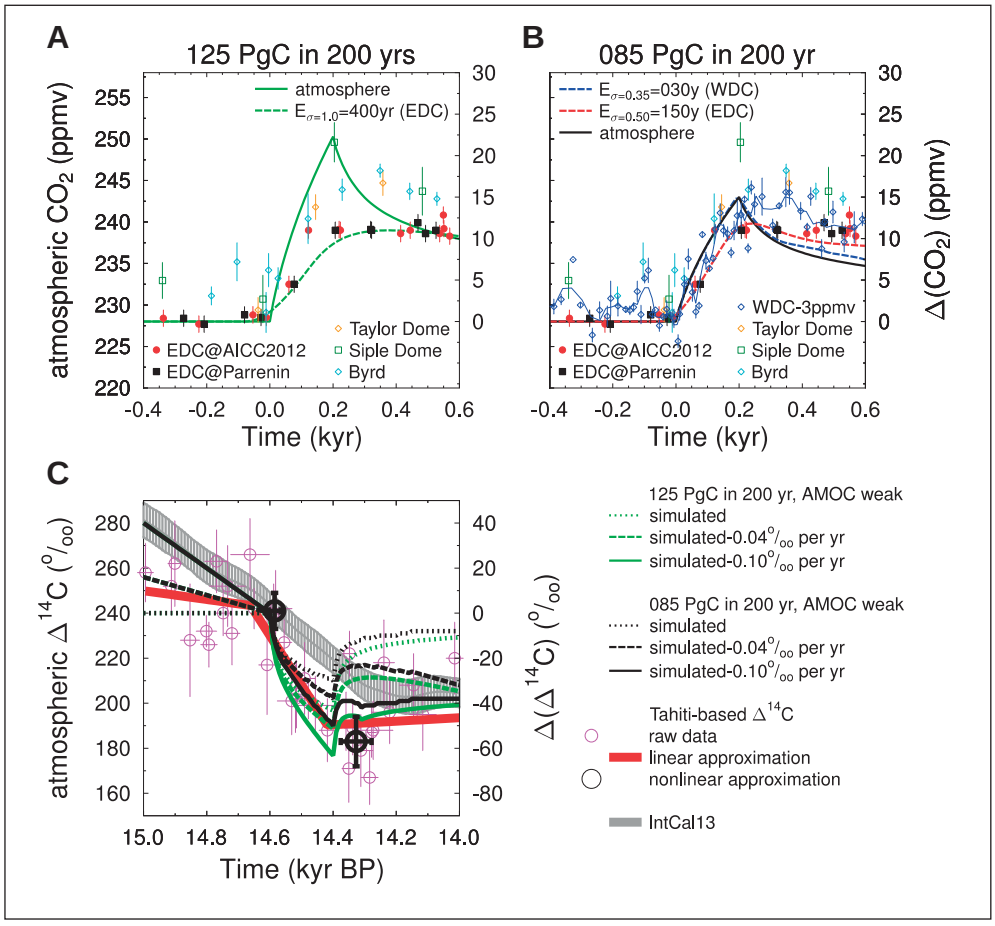


Fig. 2 Simulated atmospheric $CO_2$ and $\Delta^{14}C$ anomalies around 14.6 ka BP following the idea of NH permafrost thawing (Köhler et al. 2014). True atmospheric $CO_2$ as simulated by either a carbon release of (*A*) 125 PgC or (*B*) 85 PgC. Signal filtered with the log-normal function with a mean width E of (*A*) 400 years to mimic gas enclosure in EDC or by (*B*) 30 and 150 years to mimic gas enclosure in WDC or EDC, respectively, following the newly proposed age distribution characteristics of the OSU firn densification model (Mitchell et al. 2013, Marcott et al. 2014). Shape of the log-normal filter function is determined by the parameter σ given in the subscript to E with σ = 1.0 being the previous standard choice leading to a long-tailed filter function, while new evidences point to a more narrow age distribution, thus to σ<1.0 (*A*): Ice core $CO_2$ data (±1SD) from EDC (Schmitt et al. 2012, Monnin et al. 2001, Lourantou et al. 2010) on two different chronologies (Parrenin et al. 2013, Veres et al. 2013) AICC2012 and Parrenin, Taylor Dome on revised age model (Smith et al. 1999, Ahn et al. 2004), Siple Dome (Ahn et al. 2004), Byrd on age model GICC05 (Neftel et al. 1988, Pedro et al. 2012). (*B*): Additionally to $CO_2$ data in (*A*) the new WDC $CO_2$ data (Marcott et al. 2014) are plotted as individual data points and as 3-point-running mean (*blue line*), both shifted by –3 ppmv. All $CO_2$ time series in (*A*, *B*) are shifted to have the beginning of the abrupt $CO_2$ rise at t = 0 ka. (*C*): Impacts of both scenarios of a carbon release event around 14.6 ka BP on atmospheric $\Delta^{14}C$, including transient background anomalies and compared with the Tahiti-based $\Delta^{14}C$ signal (start and stop of $\Delta^{14}C$ anomaly given by bold black circles, mean±1SD) derived in Köhler et al. (2014) from the data published in Durand et al. (2013) (magenta circles, mean±1SD) and how this disagrees with the IntCal13 stack (Reimer et al. 2013).

## *References*


Ahn, J., Wahlen, M., Deck, B. L., Brook, E. J., Mayewski, P. A., Taylor, K. C., and White, J. W. C.: A record of atmospheric $CO_2$ during the last 40,000 years from the Siple Dome, Antarctica ice core. J. Geophys. Res. *109*, D13 305; doi:10.1029/2003JD004415 (2004)

Durand, N., Deschamps, P., Bard, E., Hamelin, B., Camoin, G., Thomas, A. L., Henderson, G. M., Yokoyama, Y., and Matsuzaki, H.: Comparison of $^{14}C$ and U-Th ages in corals from IODP #310 cores offshore Tahiti. Radiocarbon *55*, 1947–1974; doi:10.2458/azu_js_rc.v55i2.16134 (2013)

d'Orgeville, M., Sijp, W. P., England, M. H., and Meissner, K. J.: On the control of glacial-interglacial atmospheric $CO_2$ variations by the Southern Hemisphere westerlies. Geophys. Res. Lett. *37*, L21703; doi:10.1029/2010GL045261 (2010)

Köhler, P., Knorr, G., and Bard, E.: Permafrost thawing as a possible source of abrupt carbon release at the onset of the Bølling/Allerød. Nature Comm. *5*, 5520; doi:10.1038/ncomms6520 (2014)

Kohfeld, K. E., Graham, R. M., Boer, A. M. de, Sime, L. C., Wolff, E. W., Le Quéré, C., and Bopp, L.: Southern Hemisphere westerly wind changes during the Last Glacial Maximum: paleo-data synthesis. Quat. Sci. Rev. *68*, 76–95; doi:10.1016/j.quascirev.2013.01.017 (2013)

Lee, S.-Y., Chiang, J. C. H., Matsumoto, K., and Tokos, K. S.: Southern Ocean wind response to North Atlantic cooling and the rise in atmospheric $CO_2$: Modeling perspective and paleoceanographic implications. Paleoceanography *26*, PA1214; doi:10.1029/2010PA002004 (2011)

Lourantou, A., Lavrič, J. V., Köhler, P., Barnola, J.-M., Paillard, D., Michel, E., Raynaud, D., and Chappellaz, J.: Constraint of the $CO_2$ rise by new atmospheric carbon isotopic measurements during the last deglaciation. Global Biogeochem. Cycles *24*, GB2015; doi: 10.1029/2009GB003545 (2010)

Marcott, S. A., Bauska, T. K., Buizert, C., Steig, E. J., Rosen, J. L., Cuffey, K. M., Fudge, T. J., Severinghaus, J. P., Ahn, J., Kalk, M. L., McConnell, J. R., Sowers, T., Taylor, K. C., White, J. W. C., and Brook, E. J.: Centennial scale changes in the global carbon cycle during the last deglaciation. Nature *514*, 616–619; doi:10.1038/nature13799 (2014)

Menviel, L., Timmermann, A., Mouchet, A., and Timm, O.: Climate and marine carbon cycle response to changes in the strength of the southern hemispheric westerlies. Paleoceanography *23*, PA4201; doi:10.1029/2008PA001604 (2008)

Mitchell, L., Brook, E., Lee, J. E., Buizert, C., and Sowers, T.: Constraints on the late Holocene anthropogenic contribution to the atmospheric methane budget. Science *342*, 964–966; doi:10.1126/science.1238920 (2013)

Monnin, E., Indermühle, A., Dällenbach, A., Flückiger, J., Stauffer, B., Stocker, T. F., Raynaud, D., and Barnola, J.-M.: Atmospheric $CO_2$ concentrations over the last glacial termination. Science *291*, 112–114; doi:10.1126/science.291.5501.112 (2001)

Neftel, A., Oeschger, H., Staffelbach, T., and Stauffer, B.: $CO_2$ record in the Byrd ice core 50,000-5,000 years BP. Nature *331*, 609–611 (1988)

Parrenin, F., Masson-Delmotte, V., Köhler, P., Raynaud, D., Paillard, D., Schwander, J., Barbante, C., Landais, A., Wegner, A., and Jouzel, J.: Synchronous change in atmospheric $CO_2$ and Antarctic temperature during the last deglacial warming. Science *339*, 1060–1063; doi:10.1126/science.1226368 (2013)

Pedro, J. B., Rasmussen, S. O., and van Ommen, T. D.: Tightened constraints on the time-lag between Antarctic temperature and $CO_2$ during the last deglaciation. Clim. Past *8*, 1213–1221; doi:10.5194/cp-8-1213-2012 (2012)

Reimer, P. J., Bard, E., Bayliss, A., Beck, J. W., Blackwell, P. G., Bronk Ramsey, C., Buck, C. E., Cheng, H., Edwards, R. L., Friedrich, M., Grootes, P. M., Guilderson, T. P., Haflidison, H., Hajdas, I., Hatté, C., Heaton, T. J., Hoffmann, D. L., Hogg, A. G., Hughen, K. A., Kaiser, K. F., Kromer, B., Manning, S. W., Niu, M., Reimer, R. W., Richards, D. A., Scott, E. M., Southon, J. R., Staff, R. A., Turney, C. S. M., and van der Plicht, J.: IntCal13 and Marine13 radiocarbon age calibration curves 0–50,000 years cal BP. Radiocarbon *55*, 1869–1887; doi:10.2458/azu_js_rc.55.16947 (2013)

Schmitt, J., Schneider, R., Elsig, J., Leuenberger, D., Lourantou, A., Chappellaz, J., Köhler, P., Joos, F., Stocker, T. F., Leuenberger, M., and Fischer, H.: Carbon isotope constraints on the deglacial $CO_2$ rise from ice cores. Science *336*, 711–714; doi:10.1126/science.1217161 (2012)

Smith, H. J., Fischer, H., Wahlen, M., Mastroianni, D., and Deck, B.: Dual modes of the carbon cycle since the Last Glacial Maximum. Nature *400*, 248–250 (1999)

Toggweiler, J. R., Russell, J. L., and Carson, S. R.: Midlatitude westerlies, atmospheric $CO_2$, and climate change during the ice ages. Paleoceanography *21*, PA2005; doi:10.1029/2005PA001154 (2006)

Tschumi, T., Joos, F., and Parekh, P.: How important are Southern Hemisphere wind changes for low glacial carbon dioxide? A model study. Paleoceanography *23*, PA4208; doi:10.1029/2008PA001592 (2008)

Veres, D., Bazin, L., Landais, A., Toyé Mahamadou Kele, H., Lemieux-Dudon, B., Parrenin, F., Martinerie, P., Blayo, E., Blunier, T., Capron, E., Chappellaz, J., Rasmussen, S. O., Severi, M., Svensson, A., Vinther, B., and Wolff, E. W.: The Antarctic ice core chronology (AICC2012): an optimized multi-parameter and multi-site dating approach for the last 120 thousand years. Clim. Past *9*, 1733–1748; doi: 10.5194/cp-9-1733-2013 (2013)

Völker, C., and Köhler, P.: Responses of ocean circulation and carbon cycle to changes in the position of the Southern Hemisphere westerlies at Last Glacial Maximum. Paleoceanography *28*, 726–739; doi:10.1002/2013PA002556 (2013)

Dr. Peter Köhler
Dr. Christoph Völker
Dr. Gregor Knorr
Alfred Wegener Institute
Helmholtz Centre
for Polar and Marine Research
P.O. Box 12 01 61
27515 Bremerhaven
Germany
Phone: +49 471 48311687
Fax: +49 471 48311149
E-Mail: peter.koehler@awi.de

Prof. Edouard Bard
CEREGE
(Aix-Marseille University
CNRS, IRD, Collège de France)
Le Trocadéro
Europole de l'Arbois BP80
13545 Aix-en-Provence Cedex4
France
Phone: +33 4 42507418
Fax: +33 4 42507421
E-Mail: bard@cerege.fr

Nova Acta Leopoldina NF *121*, Nr. 408, 141–147 (2015)

# Abrupt Climate Change Experiments: The Bølling/Allerød Transition

Gerrit Lohmann, Xu Zhang, and Gregor Knorr (Bremerhaven)

With 3 Figures

## 1. Introduction

Within glacial periods, and especially well documented during the last one, there are dramatic climate transitions, including high latitude temperature changes approaching the same magnitude as the glacial cycle itself with world-wide teleconnections, recorded in archives from the polar ice caps, high to middle latitude marine sediments, lake sediments, and continental loess sections (e.g. Bender et al. 1999). Flohn (1986) proposed as a concept of abrupt climate change to include both singular events and catastrophes such as extreme El Niños, as well as discontinuities in paleoclimate indices. One hypothesis for explaining deglacial as well as Dansgaard-Oeschger climatic transitions is that the Atlantic meridional overturning circulation (AMOC) flips between different modes, with warm intervals reflecting periods of strong deep water formation in the northern North Atlantic and *vice versa* (Ganopolski and Rahmstorf 2001). As an alternative approach, one can estimate the underlying dynamics with its bifurcation directly from data (Kwasniok and Lohmann 2009). Several hypotheses of the ocean dynamics during the terminations are discussed (in the following sections 2–5), including the effect of global warming (sections 2, 4, 5), freshwater history (sections 2, 3, 5), ice sheet height (section 4), and orbital forcing (section 5). For section 2 we use an ocean general circulation model (OGCM) coupled to an energy balance of the atmosphere. For sections 3–5, we apply the Earth system model COSMOS consisting of an AOGCM including interactive vegetation for the glacial dynamics.

## 2. Deglacial Warming Induces an Abrupt AMOC Transition

The question is what causes the abrupt warming at the onset of the Bølling as seen in the Greenland ice cores. There is a clear antiphasing seen in the deglaciation interval between 20 and 10 ka ago: During the first half of this period, Antarctica steadily warmed, but little change occurred in Greenland. Then, at the time when Greenland's climate underwent an abrupt warming, the warming in Antarctica stopped. Knorr and Lohmann (2007) describe how global warming (which may be induced by greenhouse gases and feedbacks) can induce a rapid intensification of the ocean circulation (Fig. 1*A*, *B*). The basic mechanism is related to a release of convectively unstable warm subsurface water in the northern North Atlantic. Sub-

sequently, a sudden increase of the northward heat transport draws more heat from the south, and leads to a strong warming in the north. This 'heat piracy' from the South Atlantic has been formulated by Crowley (1992). A logical consequence of this heat piracy is the Antarctic Cold Reversal (ACR) during the Northern Hemisphere warm Bølling/Allerød. Figure 1*C* shows that an abrupt onset of the AMOC is triggered by a continuous global background warming during the deglaciation with a typical hysteresis behaviour.

Figure 1*C*, *D* emphasizes the combined effect of hosing and AMOC strengthening due to global warming. The hosing provides only a second-order effect, only affecting the timing of the transition. In MWP1, the release of the MPW-1A to the North Atlantic retards the

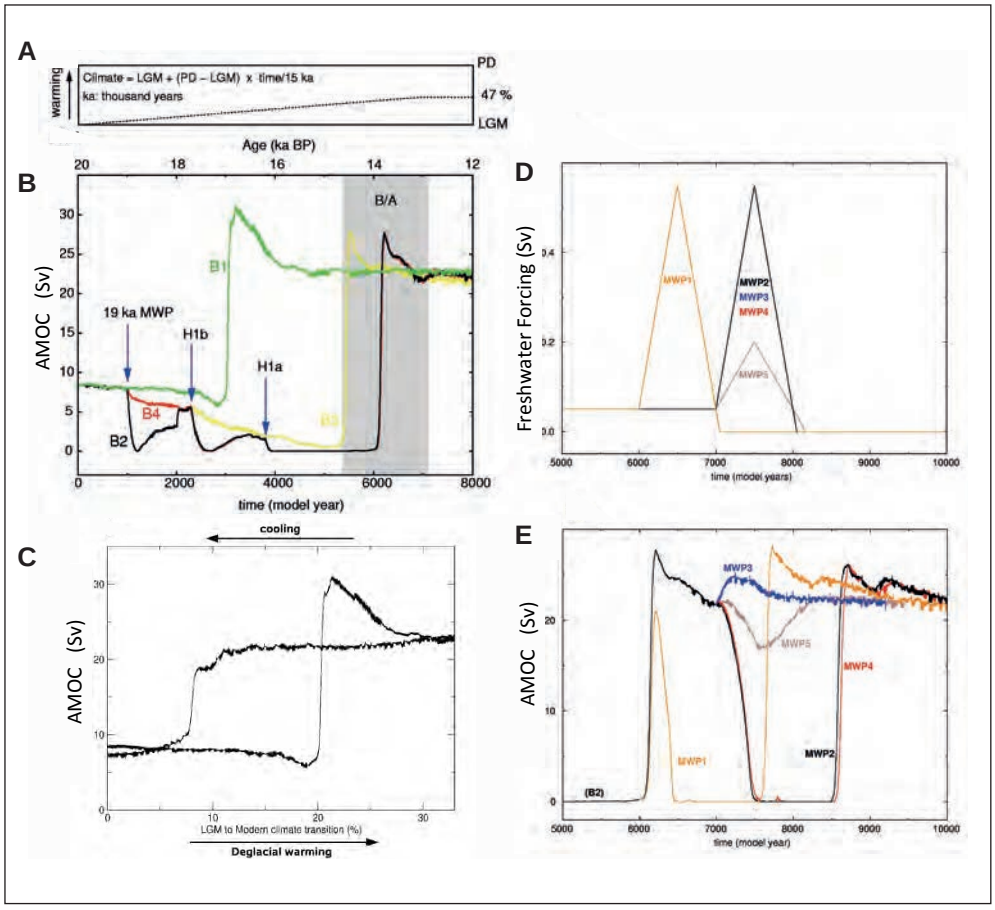


Fig. 1 Temporal changes in the global background climate and AMOC. The background climate conditions are linearly interpolated between glacial and modern conditions. All experiments start from the glacial equilibrium and the gradual warming is stopped after 7000 model years (*A*). (*B*) The green curve (B1) represents the experiment without any deglacial freshwater pulses. Experiments B2 (*yellow curve*), B3 (*red curve*), and B3 (*green curve*), exhibit different successions of deglacial meltwater pulse scenarios to the North Atlantic. The beginning of the respective freshwater perturbations is indicated by the blue arrows. (*C*) Hysteresis diagram based on B1. (*D*, *E*) Temporal signature of the different meltwater scenarios (see text in section 2). Panels (*A*), (*B*), (*C*) are from Knorr and Lohmann 2007. Model is of intermediate complexity: LSG-EBM (Prange et al. 2003, Knorr and Lohmann 2003).

abrupt AMOC amplification by about one decade, but does not inhibit the amplification of the AMOC. The rising freshwater flux of MWP-1A causes a drop back to the "off-mode" simultaneously to the maximum meltwater magnitude. The AMOC remains stalled until the warming proceeds to more than 50 % of the total termination 1 warming at 7500 years. In experiment MWP2 the MWP-1A is released 1000 years later than in MWP1, and the AMOC is also suppressed to the "off-mode", and the recovery to an interstadial AMOC occurs 500 years after the cessation of MWP-1A within a century. The application of MWP-1A in the Weddel Sea results in a slight increase of the NADW export in experiment MWP3. The division of the meltwater inflow to both, the North Atlantic and the Weddel Sea in MWP4 also ceases NADW export to the South Atlantic for about 1000 years with a minimal retarded model response compared to MWP2. The application of a weaker meltwater pulse than in MWP4 temporarily reduces, but does not shut-down the AMOC in MWP5.

## 3. Northern and Southern Hosing and Overshoot in the AMOC

A quite different concept is that deglacial meltwater may induce a Northern Hemisphere warming after the meltwater has stopped. A freshwater hosing of 0.2 Sv (1 Sv = $10^6$ $m^3/s$) has been applied for 150 years in the North Atlantic (NA) in the Ice-Rafted Debris (IRD) belt in the North Atlantic Ocean (40°N–55°N) or in Southern Ocean (SO) in the region (52°–62°S, 40°W–62°W), respectively (Fig. 2). The NA hosing experiment indicate an AMOC reduction, but the following recovery stages after 250 years exhibit a clear overshoot (Fig. 2*A*). One can subdivide the underlying dynamics of the overall recovery into two stages: one directly following the end of the freshwater perturbation that describes the initial resumption and a superposed phase that coincides with the AMOC overshoot dynamics (Gong et al. 2013, Zhang et al. 2013). The deep water formation in the South Labrador Sea reduces to 4–7 Sv, and a shutdown of deep water formation in the GIN Sea is diagnosed. Subsequently, an instant restart of deep water formation in the South Labrador Sea is triggered, whereas the restart in the GIN Sea occurs 30 years later. The corresponding trigger mechanism is related to a modified salinity stratification and subsurface warming that quickly build up during the freshwater perturbation. The surface anomaly in surface temperature is shown in Figure 2*B*. The SO hosing provides almost no change in AMOC (Fig. 2*A*), and the surface temperature signature shows only a minor cooling after 150 years in the North Atlantic (not shown). Roche et al. (2010) explored the impact of freshwater pulses with respect to different geographical locations. Liu et al. (2009) showed in their experiments covering the deglaciation that a Bølling-type overshoot can be obtained when the freshwater hosing history has been prescribed in such a way that the reconstructed temperatures and AMOC are resembled.

## 4. Influence of $CO_2$ and Northern Hemisphere Ice Sheet Height

During times when the ice sheets were at intermediate ice-sheet volume, large millennial-scale warmings are accompanied by increases in atmospheric carbon dioxide with a global-scale impact (Schulz et al. 1999). Here, we show the role of $CO_2$ changes on AMOC during times of intermediate glacial ice volume (Zhang et al. 2014). A transient simulation in which we linearly increase atmospheric $CO_2$ concentration from 185 to 205 ppm within 500 years, under an

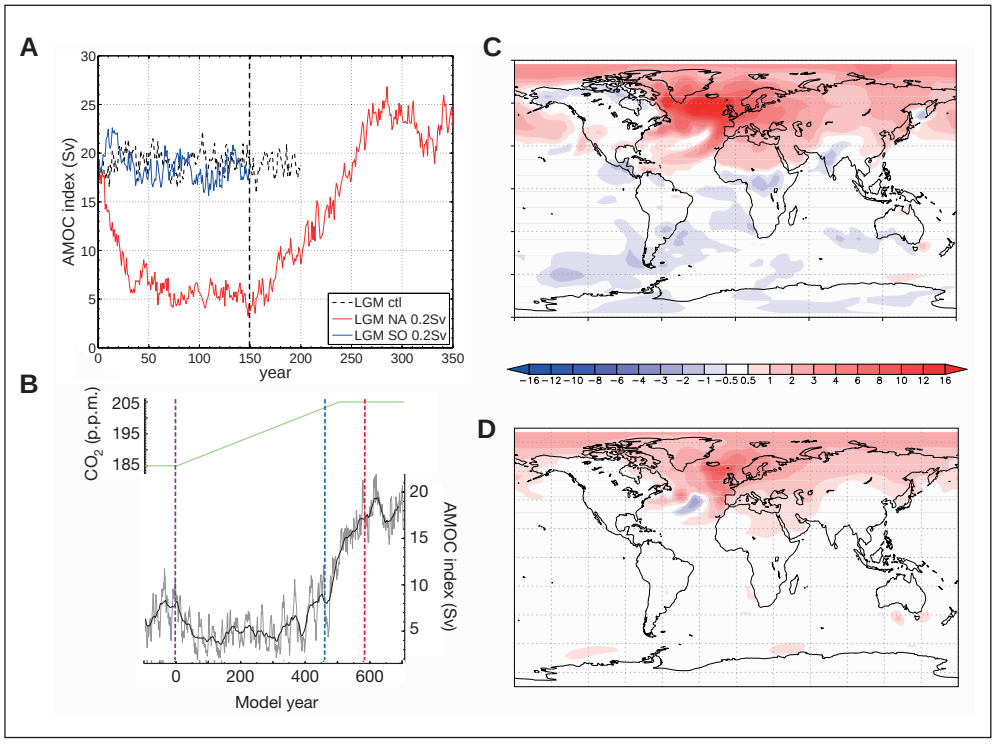


Fig. 2 (*A*) AMOC response to freshwater hosing of 0.2 Sv in the North Atlantic Ocean (NA) or in Southern Ocean (SO), respectively. The NA hosing experiment indicate an AMOC reduction, but the following recovery stages after 250 years exhibit a clear overshoot (*B*). (*C*) Transient $CO_2$ forcing and AMOC response. Bold lines show the 30-year running mean of the original data (grey lines). The vertical purple, blue and red dotted lines represent the starting points for the transient simulations, abrupt AMOC transitions and cooling in the Southern Hemisphere, respectively. Negative model years indicate the control simulation of a glacial state, but with 40 % Northern Hemisphere ice sheet height which is close to the height threshold. (*D*) Surface temperature anomaly between year 600–700 (warming) and 300–400 (cooling) of panel (*C*). Model: Fully coupled AOGCM COSMOS in T31 resolution (References in Zhang et al. 2013). Panels (*C*), (*D*) are from Zhang et al. 2014.

intermediate ice sheet height (40 % of the Last Glacial Maximum ice-sheet level), indicates an abrupt onset of AMOC (Fig. 2*C*) and thus surface temperature in the North Atlantic (Fig. 2*D*). The surface temperature in Figure 2*D* is shown as anomaly between the model year 600–700 (warming) and 300–400 (cooling) in this simulation (Fig. 2*C*). The response can be understood in terms of a transition in a bistable system with respect to the ice sheet height (Zhang et al. 2014). The ice sheet height seems to be an important background parameter for multiple equilibria of the AMOC and millennial variability at intermediate ice-sheet height. For the termination, it is most likely a second-order effect since the lowered ice sheet will weaken the AMOC.

## 5. Influence of Southern Hosing, $CO_2$, and Orbital Forcing

Additional hypotheses related to Southern Hemisphere hosing from the Antarctic Ice Sheet (AIS) and warming are tested for deglaciation. Freshwater enters into the Southern Ocean where freshwater input at 21–14 ka before present (ka in the following) is linearly scaled by the reconstructed IBRD flux (Weber et al. 2014). To determine the effect of different freshwater sources, three transient freshwater forcing experiments were conducted under glacial background conditions (DG1, 2, 3). Freshwater flux is added to the coastal areas of East AIS (0°–180°E) and West AIS (120°W–60°W). In DG1, the forcing is assumed to originate from the East AIS. In DG2, East (West) AIS forcing is used for the period 21–15 ka (15–14 ka). DG3 assumes East AIS forcing at 21–16 ka and West AIS forcing at 16–14 ka. Two other experiments (DG2C and DG2CO) were conducted to examine the effect of $CO_2$ (DG2C) as well as a combination of $CO_2$ and orbital forcing (DG2CO) on AMOC and surface temperature (Fig. 3). DG2C and DG2CO show almost the same signature in time and space indicating that the $CO_2$ effect is stronger than the effect by insolation. Figure 3*D*, *E* shows the surface temperature anomaly between 14.7–14.6 ka (warming in the north, Figure 3*A*) and 15.55–15.4 ka (cooling in the north, Fig. 3*A*) in simulations DG2 and DG2CO, respectively.

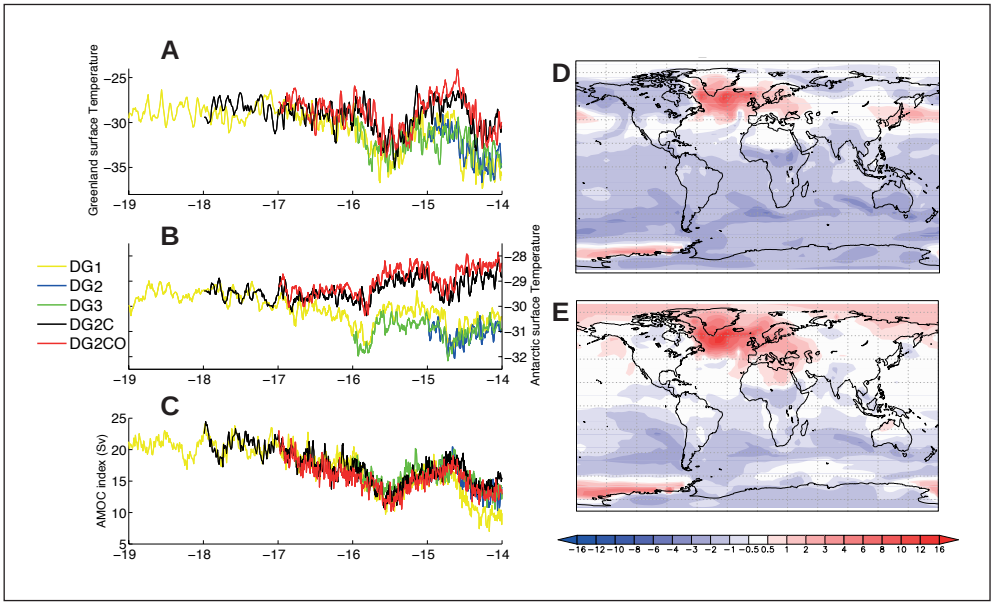


Fig. 3 (*A*, *B*, *C*) Temperature and AMOC response to external forcing. The freshwater is determined by assuming that 50% of the maximum sea level rates during MWP1A (40 mm/year) originated from Antarctica. The corresponding peak freshwater forcing around Antarctica reaches values of 0.23 Sv (Weber et al. 2014). DG1: the freshwater forcing is assumed to originate from the East AIS. DG2: East (West) AIS forcing is used for the period 21–15 ka (15–14 ka). DG3: East AIS forcing at 21–16 ka and West AIS forcing at 16–14 ka. In DG2C, varied $CO_2$ concentrations were prescribed for the period 18–14 ka. Orbital forcing covering the period from 17–14 ka were additionally used in DG2CO. (*D*, *E*) shows the surface temperature anomaly between 14.7–14.6 ka and 15.55–15.4 ka in simulations DG2 (*D*) and DG2CO (*E*). Model: Fully coupled AOGCM COSMOS in T31 resolution.

Figure 3*C* indicates an AMOC increase for all of the scenarios prior to 14.7~14.6 ka which we may call the Bølling transition. It can be shown that cooling over Antarctic (Fig. 3*B*) strongly depends on the timing of freshwater injection (during 14.7–14.6 ka) when there is a strong meltwater pulse. This SO meltwater pulse will cease the AMOC strength after a delay when the freshwater signal transports to the North Atlantic. Thus, the warming over Greenland during 14.7–14.6 ka is not related to the contemporary SO meltwater pulse, but to the absence of SO freshwater forcing prior to this time. It is worth noting that these runs were accelerated by factor of 5, implying the simulated warming in our runs may not directly represent the real Bølling warming.

Location shifts of freshwater injection around Antarctic can explain the warming along the west coast of Antarctic in Figure 3*D*, *E*. For the water around Antarctica, Weber et al. (2014) found a more pronounced halocline during periods of strong freshwater forcing as the main cause for the subsurface warming in the Southern Ocean during deglaciation. Such subsurface warming may have induced instabilities in the coupled atmosphere-ocean-ice system which could be important for ice-shelf instabilities and shall be investigated in the future.

## 6. General Conclusions

The forcing and feedback mechanisms during the termination have not fully been explored. More model experiments yield more complex views, which are sometimes even contradictory. Robust features seem to be: Global warming induces stronger AMOC, Northern Hemisphere freshwater hosing weakens AMOC with a potential temperature and AMOC overshoot, Southern Hemisphere hosing shows a moderate weakening of AMOC after a delay of the order of 100 years, higher Northern Hemisphere ice sheet height produces stronger AMOC. These principle features shall be tested for different model with different levels of complexity. It is important to explore the phase space of abrupt climate changes like the deglaciation, and to explore the separation between first and second order effects (Lohmann 2014). This is also important to understand past warm climate states where models show a mismatch with the data, e.g. for the Holocene (Lohmann et al. 2013, Liu et al. 2014) or the Pliocene (Salzmann et al. 2013). This indicates that at least some underlying assumptions might need to be revisited, reflecting phase three of Kuhn's (1962) theory of scientific development.

### *References*

Bender, M., Malaize, B., Orchardo, J., Sowers, T., and Jouzel, J.: High precision correlations of Greenland and Antarctic ice core records over the last 100 kyr. In: Clark, P. U., Webb, R. S., and Keigwin, L. D. (Eds.): Mechanisms of Global Climate Change at Millennial Time Scales. Geophys. Monogr. Ser. *112*, 149–164. Washington DC: AGU 1999

Crowley, T. J.: North Atlantic deep water cools the Southern Hemisphere. Paleoceanography *7*, 489–497 (1992)

Flohn, H.: Singular events and catastrophes now and in climatic history. Naturwissenschaften *73*, 136–149 (1986)

Ganopolski, A., and Rahmstorf, S.: Rapid changes of glacial climate simulated in a coupled climate model. Nature *409*, 153–158 (2001)

Gong, X., Knorr, G., Lohmann, G., and Zhang, X.: Dependence of abrupt Atlantic meridional ocean circulation changes on climate background states. Geophys. Res. Lett. *40*/14, 3698–3704; doi:10.1002/grl.50701 (2013)

Knorr, G., and Lohmann, G.: Southern Ocean origin for resumption of Atlantic thermohaline circulation during deglaciation. Nature *424*, 532–536 (2003)

Knorr, G., and Lohmann, G.: Transitions in the Atlantic thermohaline circulation by global deglacial warming and melt-water pulses. Geochem. Geophys. Geosyst. doi:10.1029/2007GC001604 (2007)

Kuhn, T. S.: The Structure of Scientific Revolutions. International Encyclopedia of Unified Science. Vol. II, No. 2. Chicago: University of Chicago Press [1]1962, [4]2012

Kwasniok, F., and Lohmann, G.: Deriving dynamical models from paleoclimatic records: application to glacial millennial-scale climate variability. Phys. Rev. E *80*/6, 066104; doi:10.1103/PhysRevE.80.066104 (2009)

Liu, Z., Otto-Bliesner, B. L., He, F., Brady, E. C., Tomas, R., Clark, P. U., Carlson, A. E., Lynch-Stieglitz, J., Curry, W., Brook, E., Erickson, D., Jacob, R., Kutzbach, J., and Cheng, J.: Transient simulation of last deglaciation with a new mechanism for Bølling-Allerød warming. Science *325*/5938, 310–314; doi:10.1126/science.1171041 (2009)

Liu, Z., Zhu, J., Rosenthal, Y., Zhang, X., Otto-Bliesner, B., Timmermann, A., Smith, R. S., Lohmann, G., Zheng, W., and Timm, O. E.: The Holocene temperature conundrum. Proc. Natl. Acad. Sci. USA *111*/34, 3501–3505; doi:10.1073/pnas.1407229111 (2014)

Lohmann, G.: Abrupt climate change modeling. In: Encyclopedia of Complexity and Systems Science; pp. 1–30; doi:10.1007/978-3-642-27737-5_1-5. New York: Springer 2014

Lohmann, G., Pfeiffer, M., Laepple, T., Leduc, G., and Kim, J.-H.: A model-data comparison of the Holocene global sea surface temperature evolution. Clim. Past *9*, 1807–1839; doi:10.5194/cp-9-1807-2013 (2013)

Prange, M., Lohmann, G., and Paul, A.: Influence of vertical mixing on the thermohaline hysteresis: Analyses of an OGCM. J. Phys. Oceanogr. *33*/8, 1707–1721 (2003)

Roche, D. M., Wiersma, A. P., and Renssen, H.: A systematic study of the impact of freshwater pulses with respect to different geographical locations. Clim. Dyn. *34*/7–8, 997–1013; doi:10.1007/s00382-009-0578-8 (2010)

Salzmann, U., et al.: How well do models reproduce warm terrestrial climates of the Pliocene? Nature Clim. Change doi:10.1038/nclimate2008 (2013)

Schulz, M., Berger, W. H., Sarnthein, M., and Grootes, P. M.: Amplitude variations of 1470-year climate oscillations during the last 100,000 years linked to fluctuations of continental ice mass. Geophys. Res. Lett. *26*/22, 3385–3388 (1999)

Weber, M. E., Clark, P. U., Kuhn, G., Timmermann, A., Sprenk, D., Gladstone, R., Zhang, X., Lohmann, G., Menviel, L., Chikamoto, M. O., Friedrich, T., and Ohlwein, C.: Millennial-scale variability in Antarctic ice-sheet discharge during the last deglaciation. Nature *510*, 134–138; doi:10.1038/nature13397 (2014)

Zhang, X., Lohmann, G., Knorr, G., and Purcell, C.: Abrupt glacial climate shifts controlled by ice sheet changes. Nature *512*, 290–294; doi:10.1038/nature13592 (2014)

Zhang, X., Lohmann, G., Knorr, G., and Xu, X.: Different ocean states and transient characteristics in Last Glacial Maximum simulations and implications for deglaciation. Clim. Past *9*, 2319–2333; doi:10.5194/cp-9-2319-2013 (2013)

Prof. Dr. Gerrit Lohmann
Alfred Wegener Institute
Helmholtz Centre for Polar an Marine Research
Building F-301
Bussestraße 24
27570 Bremerhaven
Germany
Phone: +49 471 48311758
Fax: +49 471 48311149
E-Mail: gerrit.lohmann@awi.de

Nova Acta Leopoldina NF *121*, Nr. 408, 149–150 (2015)

# Abrupt Changes in the Global Carbon Cycle over the Past 70 ka

Shaun A. Marcott,[1] Edward J. Brook,[2] Thomas K. Bauska,[2]
Rachael H. Rhodes,[2] and Michael Kalk[2]

Two long-standing questions in carbon cycle dynamics are what caused the glacial-to-interglacial rise in atmospheric carbon dioxide ($CO_2$) and the millennial scale variations during Marine Isotope Stage 3 (MIS 3). The enduring paradigm is that the underlying processes are related to the Southern Ocean, and operate at millennial (or longer) timescales, which is largely based on the strong covariance of $CO_2$ with Antarctic temperature. We present a $CO_2$ record spanning the last glacial and deglacial periods from the West Antarctic Ice Sheet Divide ice core (WDC), which has a sampling resolution of 25–150 years. Our work provides new evidence that a centennial scale component of atmospheric $CO_2$ variability exists during both the $CO_2$ rise of the last termination, and the more rapid oscillations of MIS 3.

$CO_2$ varied in three distinct modes (Monnin et al. 2001, Marcott et al. 2014) during the last termination: a relatively gradual mode on the order of 10 ppm per millennia, a relatively rapid mode of approximately 10–15 ppm per century, and a stable mode where $CO_2$ did not change for 1–2 ka. The rapid increases in $CO_2$ were also accompanied by rapid 50–200 ppb increases/decreases in $CH_4$, potentially linking the changes to a common causal mechanism, such as the rate of Atlantic meridional overturning circulation (AMOC). During MIS 3 similar centennial and millennial changes occur in $CO_2$ as recorded at WDC, complimenting existing datasets from other sites around Antarctica (Indermühle et al. 2000, Loulergue et al. 2007, Ahn and Brook 2008, Ahn et al. 2012, Bereiter et al. 2012), but recorded at much higher temporal resolution. Notably, the rapid changes in both $CO_2$ and $CH_4$ observed during Heinrich stadial (HS) 1 of the last deglacial also occur during HS 4 and 5, but are seemingly absent in the other HS's, thus complicating a simple AMOC or ice rafting episode connection. During the slower, millennial scale $CO_2$ changes of MIS 3, we also find that the relative peak $CO_2$ values tend to lag nearly all of the Antarctic isotope maxima (AIM) events by approximately 300–600 years, and that the canonical "A" type structure of the $CO_2$ changes in MIS 3 is not faithfully reproduced at WDC. Many of the signals appear more saw-toothed in form. This is likely due to the comparatively higher accumulation and minimal smooth at WDC compared to previous reconstructions.

What is clear from our new WDC data is that natural $CO_2$ can change very rapidly (~10 ppm in 100–200 years), which is not fully captured by existing Earth System models.

1 Department of Geoscience, University of Wisconsin-Madison, 1215 W Dayton St., Madison, WI, USA.
2 College of Earth, Ocean, and Atmospheric Sciences, Oregon State University, 104 COAS Admin. Build., Corvallis, OR, USA.

Our understanding of how atmospheric $CO_2$ behaves under natural forcings therefore needs refining. What is less clear is the suite of mechanisms that initiate and modulate these changes over the last 70 ka. It is tempting to explore links to AMOC, given the observations from the last termination and some HSs of MIS 3 where both $CO_2$ and $CH_4$ rapidly change at times when AMOC is also changing. In other instances, this simple relationship breaks down or is obscured by other processes that influence the carbon cycle. Our talk will highlight our new data and provide potential hypothesis for our new observations.

## *References*

Ahn, J., and Brook, E. J.: Atmospheric $CO_2$ and climate on millennial time scales during the last glacial period. Science *322*, 83–85 (2008)

Ahn, J., Brook, E. J., Schmittner, A., and Kreutz, K.: Abrupt change in atmospheric $CO_2$ during the last ice age. Geophys. Res. Lett. *39*, doi:10.1029/2012GL053018 (2012)

Bereiter, B., Lüthi, D., Siegrist, M., Schüpbach, S., Stocker, T. F., and Fischer, H.: Mode change of millennial $CO_2$ variability during the last glacial cycle associated with a bipolar marine carbon seesaw. Proc. Natl. Acad. Sci. *109*/*25*, 9755–9760 (2012)

Indermühle, A., Monnin, E., Stauffer, B., Stocker, T. F., and Wahlen, M.: Atmospheric $CO_2$ concentration from 60 to 20 kyr BP from the Taylor Dome ice core, Antarctica. Geophys. Res. Lett. *27*/5, 735–738 (2000)

Loulergue, L., Parrenin, F., Blunier, T., Barnola, J.-M., Spahni, R., Schilt, A., Raisbeck, G., Chappellaz, J., and others: New constraints on the gas age-ice age difference along the EPICA ice cores, 0–50 kyr. Clim. Past Discuss. *3*/2, 435–467 (2007)

Marcott, S. A., Bauska, T. K., Buizert, C., Steig, E. J., Rosen, J. L., Cuffey, K. M., Fudge, T. J., Severinghaus, J. P., Ahn, J., Kalk, M. L., McConnell, J. R., Sowers, T., Taylor, K. C., White, J. W. C. and Brook, E. J.: Centennial-scale changes in the global carbon cycle during the last deglaciation: Nature *514*/7524, 616–619; doi:10.1038/nature13799 (2014)

Monnin, E., Indermühle, A., Dällenbach, A., Flückiger, J., Stauffer, B., Stocker, T. F., Raynaud, D., and Barnola, J.-M.: Atmospheric $CO_2$ concentrations over the last glacial termination: Science *291*, 112–114 (2001)

Prof. Shaun A. Marcott, Ph.D.
Department of Geoscience
University of Wisconsin-Madison
1215 W Daytin St., Weeks Hall
Madison WI 53706
USA
Phone: +1 608 262 2368
Fax: +1 608 262 0693
E-Mail: smarcott@wisc.edu

Nova Acta Leopoldina NF *121*, Nr. 408, 151–154 (2015)

# Iron Fertilization of the Subantarctic Ocean during the Last Ice Age

Alfredo Martínez-García,[1] Daniel M. Sigman,[2] Haojia Ren,[3]
Robert F. Anderson,[4] Marietta Straub,[1] David A. Hodell,[5]
Samuel L. Jaccard,[6] Timothy I. Eglinton, and Gerald H. Haug ML[1]

With 2 Figures

The concentration of major inorganic nutrients nitrate and phosphate is perennially high in one quarter of the surface ocean. However, despite this excess of macronutrients, iron availability limits phytoplankton growth in the Southern Ocean, the equatorial Pacific and the subarctic North Pacific. The Southern Ocean is the largest of these high-nutrient low-chlorophyll (HNLC) regions and therefore represents the area of the ocean where variations in iron availability can have the largest impact on Earth's carbon cycle through its fertilizing effect on marine ecosystems.

Combining his discovery of iron limitation in the modern Southern Ocean, and the first observations of increased glacial dust deposition recorded in Antarctic ice cores, John H. Martin proposed the "iron hypothesis": that iron fertilization of the ice age Southern Ocean caused an increase in productivity, which increased the rain of organic carbon into isolated deep waters and thus contributed to the reduction in atmospheric $CO_2$ observed during ice ages (Martin 1990).

Paleoceanographic records from the Subantarctic Atlantic have revealed a remarkable correlation between phytoplankton productivity and aeolian iron flux (Kumar et al. 1995, Martínez-García et al. 2009) supporting the iron hypothesis. In the context of the observed coupling between higher dust flux, and increased Subantarctic productivity, the key test for the iron hypothesis in the Subantarctic is whether surface nutrient concentrations declined. If the ice age increase in Subantarctic productivity was due to iron fertilization, then the "major" nutrients nitrate and phosphate in surface waters would have been more completely consumed in the production of phytoplankton biomass, thereby lowering their concentrations in the Subantarctic surface. Changes in the completeness of nitrate consumption by phytoplankton (and thus surface nitrate concentration) can be reconstructed using the isotopes of nitrogen because isotope fractionation during the assimilation of nitrate by phytoplankton leads to a $\delta^{15}N$ increase in Subantarctic surface nitrate and biomass N as nitrate consumption progresses (Altabet and Francois 1994, DiFiore et al. 2006).

1 Geological Institute, ETH Zurich, Sonneggstrasse 5, 8092 Zurich, Switzerland.
2 Department of Geosciences, Princeton University.
3 Research Center for Environmental Changes, Academia Sinica, Taiwan.
4 Lamont-Doherty Earth Observatory, Columbia University.
5 Department of Earth Sciences, University of Cambridge, UK.
6 Institute of Geological Sciences and Oeschger Center for Climate Change Research, University of Bern.

In a sediment core from the Subantarctic Atlantic (ODP Site1090, Fig. 1), we analysed foraminifera-bound nitrogen isotopes to reconstruct ice age changes in surface nitrate concentration in concert with millennial-scale $^{230}$Th-normalized fluxes of iron and productivity proxies, providing the first comprehensive paleoceanographic test of John Martin's ice age "iron hypothesis" (Martínez-García et al. 2014). The data shows that peak glacial times and millennial cold events were nearly universally associated with increases in dust flux, export production, and nutrient consumption (the last indicated by higher FB-$\delta^{15}$N) (Fig. 2). This combination of changes is uniquely consistent with ice age iron fertilization of the Subantarctic Atlantic.

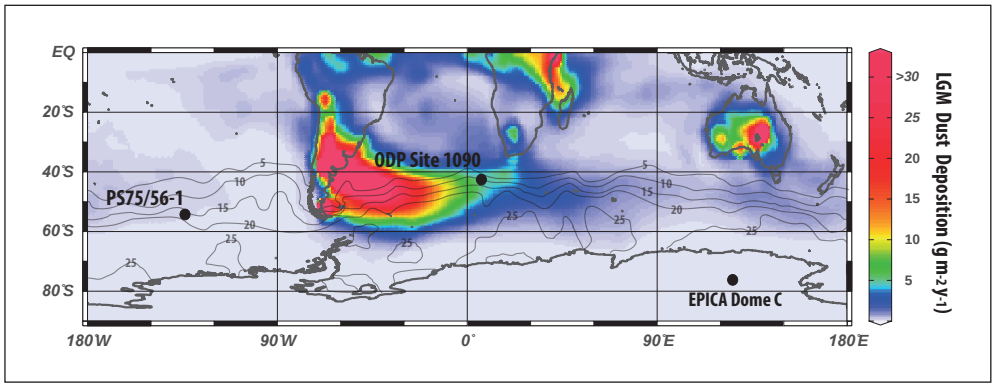


Fig. 1 Location of Ocean Drilling Program (ODP) Site 1090 and PS75/56-1 relative to modern nitrate concentration and ice age dust deposition. Black contours indicate climatological surface nitrate concentration in austral summer (December to February, in micromolar) (Garcia et al. 2010). Colours depict model-reconstructed dust deposition during the Last Glacial Maximum (in g/m$^2$/y) (Mahowald et al. 2006). (Adapted from Martínez-García et al. 2014.)

The strengthening of the biological pump associated with the observed increase in nutrient consumption during the high-dust intervals of the last two ice ages can explain up to ~40 ppm of the $CO_2$ decrease that characterizes the transitions from mid-climate states to full ice age conditions. In addition, our data indicate that the connection of dust flux, productivity, and nutrient consumption applies to millennial-scale oscillations within the last ice age, providing a new explanation for the observed atmospheric $CO_2$ changes during these climate oscillations.

Fig. 2 Records of Subantarctic dust-borne iron flux, phytoplankton productivity, surface nitrate consumption, and atmospheric $CO_2$ over the last glacial cycle. (*A*) Atmospheric $CO_2$ concentrations measured in Antarctic ice cores (Ahn and Brook 2008, Bereiter et al. 2012, Petit et al. 1999). The pink shaded area highlighting the decline in atmospheric $CO_2$ that correlates with large dust flux, productivity and nutrient consumption increases. (*B*) *G. bulloides* FB-d$^{15}$N (red circles) and $^{230}$Th-normalized iron flux from ODP Site 1090 (black line), calculated using the $^{230}$Th-normalized mass flux measured in the parallel core TN057-6. (*C*) $^{230}$Th-normalized alkenone flux from TN057-6 (0–90 ka) and ODP Site 1090 (90–160 ka). TN057-6 alkenone concentrations are from Sachs and Anderson 2003. (D) Dust flux at Antarctic ice core EPICA Dome C (EDC) (Lambert et al. 2012). (Adapted from Martínez-García et al. 2014.)

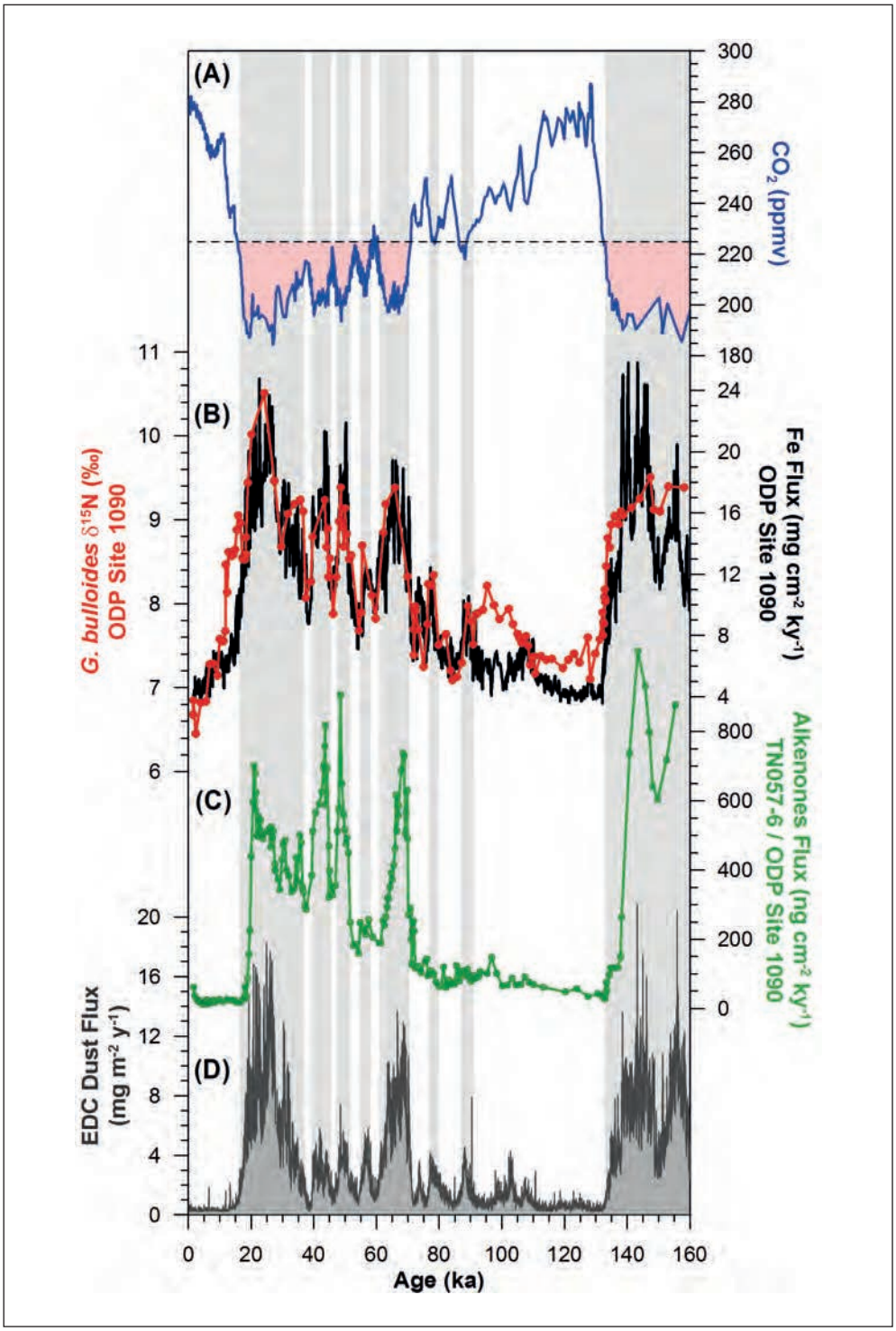
(A)
(B)
(C)
(D)
CO2 (ppmv)
300
280
260
240
220
200
180
G. bulloides δ15N (‰)
ODP Site 1090
11
10
9
8
7
6
Fe Flux (mg cm-2 ky-1)
ODP Site 1090
24
20
16
12
8
4
Alkenones Flux (ng cm-2 ky-1)
TN057-6 / ODP Site 1090
800
600
400
200
0
EDC Dust Flux
(mg m-2 y-1)
20
16
12
8
4
0
0
20
40
60
80
100
120
140
160
Age (ka)

The analysis of foraminifera-bound nitrogen isotopes, dust and productivity proxies in a core located in the Subantarctic Pacific (PS75/56-1, Fig. 1) will soon allow us to evaluate the impact of iron fertilization in this sector of the Southern Ocean characterized by lower ice age dust fluxes.

## *References*


Ahn, J., and Brook, E. J.: Atmospheric $CO_2$ and climate on millennial time scales during the last glacial period. Science *322*, 83–85 (2008)

Altabet, M. A., and Francois, R.: Sedimentary nitrogen isotopic ratio as a recorder for surface ocean nitrate utilization. Global Biogeochem. Cycles *8*/1, 103–116 (1994)

Bereiter, B., Lüthi, D., Siegrist, M., Schüpbach, S., Stocker, T. F., and Fischer, H.: Mode change of millennial $CO_2$ variability during the last glacial cycle associated with a bipolar marine carbon seesaw. Proc. Natl. Acad. Sci. USA *109*, 9755–9760 (2012)

DiFiore, P. J., Sigman, D. M., Trull, T. W., Lourey, M. J., Karsh, K., Cane, G., and Ho, R.: Nitrogen isotope constraints on subantarctic biogeochemistry. J. Geophys. Res. *111*, C08016; doi:10.1029/2005JC003216 (2006)

Garcia, H. E., Locarnini, R. A., Boyer, T. P., and Antonov, J. I.: Nutrients (phosphate, nitrate, and silicate). In: Levitus, S. (Ed.): World Ocean Atlas 2009. Vol. 4, pp. 398. Washington: U.S. Government Printing Office 2010

Kumar, N., Anderson, R. F., Mortlock, R. A., Froelich, P. N., Kubik, P., Dittrichhannen, B., and Suter, M.: Increased biological productivity and export production. The glacial Southern-Ocean. Nature *378*, 675–680 (1995)

Lambert, F., Bigler, M., Steffensen, J. P., and Hutterli, M.: Centennial mineral dust variability in high-resolution ice core data from Dome C, Antarctica. Clim. Past *8*, 609–623 (2012)

Mahowald, N. M., Muhs, D. R., Levis, S., Rasch, P. J., Yoshioka, M., Zender, C. S., and Luo, C.: Change in atmospheric mineral aerosols in response to climate: Last glacial period, preindustrial, modern, and doubled carbon dioxide climates. J. Geophys. Res. *111*, D10202 (2006)

Martin, J.: Glacial-interglacial $CO_2$ change: The iron hypothesis. Paleoceanography *5*, 1–13 (1990)

Martínez-García, A., Rosell-Melé, A., Geibert, W., Gersonde, R., Masqué, P., Gaspari, V., and Barbante, C.: Links between iron supply, marine productivity, sea surface temperature, and $CO_2$ over the last 1.1 Ma. Paleoceanography *24*, PA1207 (2009)

Martínez-García, A., Sigman, D. M., Ren, H., Anderson, R. F., Straub, M., Hodell, D. A., Jaccard, S. L., Eglinton, T. I., and Haug, G. H.: Iron fertilization of the Subantarctic Ocean during the last ice age. Science *343*, 1347–1350 (2014)

Petit, J. R., Jouzel, J., Raynaud, D., Barkov, N. I., Barnola, J. M., Basile, I., Bender, M., Chappellaz, J., Davis, M., Delaygue, G., Delmotte, M., Kotlyakov, V. M., Legrand, M., Lipenkov, V. Y., Lorius, C., Pepin, L., Ritz, C., Saltzman, E., and Stievenard, M.: Climate and atmospheric history of the past 420,000 years from the Vostok ice core, Antarctica. Nature *399*, 429–436 (1999)

Sachs, J. P., and Anderson, R. F.: Fidelity of alkenone paleotemperatures in southern Cape Basin sediment drifts. Paleoceanography *18*/4, 1082; doi:10.1029/2002PA000862 (2003)



Dr. Alfredo Martínez-García
Geological Institute
ETH Zürich
NO G53.1
Sonneggstrasse 5
8092 Zürich
Switzerland
Phone: +41 44 6324696
Fax: +41 44 6321080
E-Mail: alfredo.martinez-garcia@erdw.ethz.ch

Nova Acta Leopoldina NF *121*, Nr. 408, 155–157 (2015)

# A Carbon Isotope Perspective on the Glacial Circulation of the Deep Southwest Pacific

I. Nicholas McCave (Cambridge, UK)

With 2 Figures

In a depth transect from 1200 m to 4900 m in the SW Pacific east of New Zealand, benthic carbon and oxygen isotopic profiles reflect the structure of water masses at present and inferred for the past. Between Holocene and Last Glacial Maximum (LGM) these have retained a constant structure of Lower Circumpolar Deep Water-Upper Circumpolar Deep Water/ North Pacific Deep Water-Antarctic Intermediate Water (LCDW, UCDW, NPDW, AAIW) with little apparent change in the depths of water mass boundaries between glacial and interglacial states (Fig. 1). Among the lowest values of LGM benthic $\delta^{13}C$ in the world ocean (–1.03 ‰ based on *Cibicidoides wüllerstorfi*) occur here at ~2200 m. Comparable values occur in the Atlantic sector of the Southern Ocean (Hodell et al. 2006), while those from the North Pacific are distinctly higher, suggesting that the Southern Ocean, not Glacial NPDW was the source for the unventilated/nutrient-enriched water seen here. Oxygen and carbon isotopic data are compatible with a glacial cold deep water mass of high salinity, but lower nutrient content (or better ventilated), below ~3400 m depth. A stratum ~1500–2000 m thick of old (ventilation age ~2.7 ka *vs.* 1.6 ka at present [Skinner et al. 2015]), nutrient-rich water (mean $\delta^{13}C$ of – 0.84 ‰) entering the Pacific during the LGM is indicated by these data. This contrasts with the South Atlantic where unventilated/nutrient-enriched water with $\delta^{13}C$ ~ 0.9 ‰ extends down to the sea bed. The Ross Sea is the most likely source of the ventilated glacial deep water with $\delta^{13}C$ of – 0.31 ‰ entering the Pacific below ~3500 m.

McCave et al. (2008) regarded the S Atlantic as the major source for the low $\delta^{13}C$ water flowing in the ACC over the major sills above 3500 m depth around Kerguelen and the Macquarie-Balleny Ridges to arrive east of New Zealand in the deep western boundary current (DWBC). The top of this water mass at Chatham Rise was ~ 2000m (Fig. 1, 2). Neutral density surfaces slope downwards to the north, so that, presuming a similarly shaped glacial density structure (*c.f.* Ferrari et al. 2014), this low $\delta^{13}C$ water, mixing with higher $\delta^{13}C$ Ross Sea Bottom Water (RSBW) would become the bottom and deep water north of the equator, occupying much of the North Pacific, albeit with higher $\delta^{13}C$ (Fig. 2). For a 50/50 RSBW/ UCDW mixture that would be 0.58 ‰, but data from the mid-latitude N Pacific gives values of ~0.2 ‰ (Herguera et al. 1992, Matsumoto et al. 2002), less even than the RSBW inflow value at Chatham rise (Fig. 1), so there remains an unresolved problem in relating the inflow to the interior of the deep N Pacific. The 2000 m boundary to the top of this low $\delta^{13}C$ water appears to be universal (Atlantic and Pacific) and justified on theoretical grounds (Curry and Oppo 2005, Herguera et al. 1992, Ferrari et al. 2014). Flow speed results from both the Indian Ocean and SW Pacific DWBCs indicate little change in the flow, which could be interpreted as flux, between glacial and the present (McCave et al. 2008, Thomas et al. 2007). The present inflow in the Pacific DWBC is ~ 16 Sv (Whitworth et al. 1999).

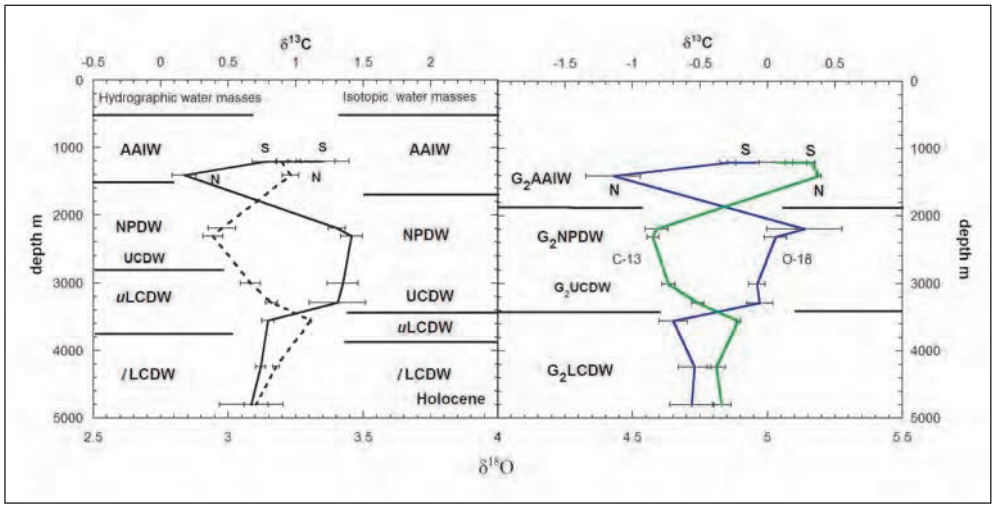


Fig. 1 Averaged depth profiles of $\delta^{18}O$ and $\delta^{13}C$ for the SW Pacific down the north side of Chatham Rise (40°–42°S; 178°E–168°W). *Left*, Holocene; *right*, LGM. Oxygen, blue; carbon, green. No corrections for relation to modern water values or glacial terrigenous carbon influence have been applied. Note that the scale for $\delta^{18}O$ runs continuously across the whole diagram with each panel 1.5 ‰ wide, and that the scale for $\delta^{13}C$ is such that each panel is 3 ‰ wide. N and S for AAIW sites refer to positions north and south of Chatham Rise.

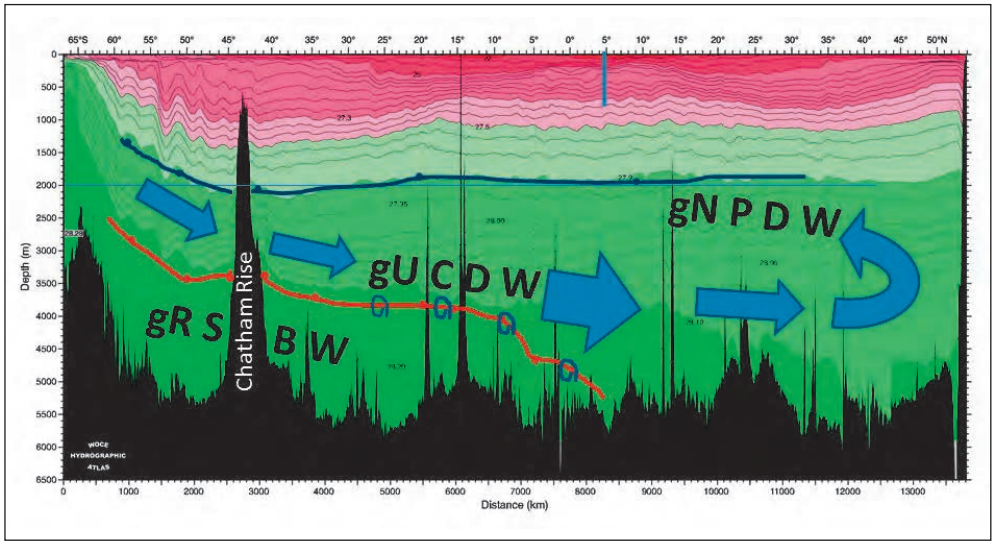


Fig. 2 Glacial water masses deduced for the Chatham rise transect superimposed on the neutral density field ($\gamma^n$) of the N–S western Pacific WOCE line P15 along 170°W (Talley 2007). The top of the low $\delta^{13}C$ watermass at 2000 m (gUCDW) is continued to the north at the same level, but the base at ~3400 m is shown descending to the north along present $\gamma^n$ of 28.14 kg/m$^3$. Below that is glacial Ross Sea Bottom Water (gRSBW) with mixing symbols along the upper interface. It is presumed that a similar transformation to North Pacific Deep Water occurred in the glacial as at present (gNPDW), the Pacific being a 'dead-end' ocean. The possibility of a North Pacific convection cell leading to intermediate water production is not shown.

## *References*


Curry, W. B., and Oppo, D. W.: Glacial water mass geometry and the distribution of $\delta^{13}C$ of $\Sigma CO_2$ in the western Atlantic Ocean. Paleoceanography *20*, PA1017 (2005)

Ferrari, R., Jansen, M. F., Adkins, J. F., Burke, A., Stewart, A. L., and Thompson, A. F.: Antarctic sea ice control on ocean circulation in present and glacial climates. Proc. Natl. Acad. Sci. USA *111*/24, 8753–8758 (2014)

Herguera, J. C., Jansen, E., and Berger, W. H.: Evidence for a bathyal front at 2000 m depth in the glacial Pacific, based on a depth transect on Ontong Java plateau. Paleoceanography *7*, 273–288 (1992)

Hodell, D. A., Venz, K. A., Charles, C. D., and Ninnemann, U. S.: Pleistocene vertical carbon isotope and carbonate gradients in the south Atlantic sector of the Southern Ocean. Geochem. Geophys. Geosyst. *4*/1004; doi:10.1029/2002GC000367 (2003)

Matsumoto, K., Oba, T., Lynch-Stieglitz, J., and Yamamoto, H.: Interior hydrography and circulation of the glacial Pacific Ocean. Quat. Sci. Rev. *21*, 1693–1704 (2002)

McCave, I. N., Carter, L., and Hall, I. R.: Glacial-interglacial changes in water mass structure and flow in the SW Pacific Ocean. Quat. Sci. Rev. *27*, 1886–1908 (2008)

Skinner, L. C., McCave, I. N., Carter, L., Fallon, S., Scrivner, A. E., and Primeau, F.: Reduced ventilation and enhanced magnitude of the deep Pacific carbon pool during the last glacial period. Earth Planet. Sci. Lett. *411*, 45–52 (2015)

Talley, L. D.: Hydrographic Atlas of the World Ocean Circulation Experiment (WOCE). Vol. 2: Pacific Ocean. (Series eds. by M. Sparrow, P. Chapman and J. Gould). 326 pp. Southampton, U. K.: International WOCE Project Office 2007

Thomas, A. L., Henderson, G. M., and McCave, I. N.: Constant bottom-water flow into the Indian Ocean for the past 140 ka indicated by sediment $^{231}Pa/^{230}Th$ ratios. Paleoceanography *22*, PA4210 (2007)

Whitworth, T., Warren, B. A., Nowlin, W. D., Rutz, S. B., Pillsbury, R. D., and Moore, M. I.: On the deep western-boundary current in the Southwest Pacific Basin. Progr. Oceanogr. *43*, 1–54 (1999)



Prof. I. Nicholas McCave, Sc.D.
University of Cambridge
Godwin Laboratory for Palaeoclimate Research
Department of Earth Sciences
Downing Street
Cambridge, CB2 3EQ
UK
Phone: +44 1223 333422
Fax: +44 1223 333450
E-Mail: mccave@esc.cam.ac.uk

Nova Acta Leopoldina NF *121*, Nr. 408, 159–166 (2015)

# Southern Ocean Overturning Role in Modulating High Southern Latitude Climate and Atmospheric $CO_2$ on Millennial Timescales

Laurie Menviel,[1] Paul Spence,[1] Nick Golledge,[2] and Matthew H. England[1]

With 3 Figures

## 1. Introduction

During the last glacial period and particularly Marine Isotope Stage 3, North Atlantic Deep Water (NADW) formation weakened significantly on a millennial timescale leading to Greenland stadials (Kissel et al. 2008). Ice core records reveal that each Greenland stadial is associated with a warming over Antarctica, so-called Antarctic Isotope Maximum (AIM) (*EPICA and Community Members* 2006). Recent ice core records further suggest that atmospheric $CO_2$ increased with Antarctic temperature only during the long Greenland stadials, i.e. the Heinrich stadials (Ahn and Brook 2014).

Under present day conditions, the formation of NADW leads to an equatorward ocean heat transport in the South Atlantic. Previous studies (Stocker 1998) suggested that the bipolar seesaw pattern in surface air temperature during AIM was due to a heat redistribution in the Atlantic basin: as NADW weakens its associated northward heat transport also reduces. However, idealized experiments performed with coupled Atmosphere-Ocean General Circulation Models featuring a significant NADW weakening only display a small warming (0.5–1 ºC) over Antarctica if any (Kageyama et al. 2012), in contrast with estimates for the large AIM (e.g. AIM12 and AIM8).

Antarctic Bottom Waters (AABW), presently formed under sea-ice on the Antarctic continental shelf, are an integral part of the global oceanic circulation and make significant contribution to deep ocean ventilation (Orsi et al. 2002). Due to difficulties in estimating past Southern Ocean ventilation, possible changes in AABW during the last glacial period and the deglaciation have received little attention.

Performing transient simulations of MIS3 with prognostic atmospheric $CO_2$ and comparing our results with paleoproxy records we suggest that enhanced AABW transport could have played a significant role in shaping the large AIM and the associated atmospheric $CO_2$ increase (Menviel et al. 2015). High resolution simulations of the Antarctic ice sheet further show that weakened AABW during the Antarctic Cold Reversal could have accelerated the retreat of the West Antarctic Ice Sheet (Golledge et al. 2014).

1 Climate Change Research Centre, University of New South Wales ARC Centre of Excellence for Climate System Science, Sydney, NSW 2052, Australia.

2 Antarctic Research Centre, Victoria University of Wellington, Wellington 6140, New Zealand.

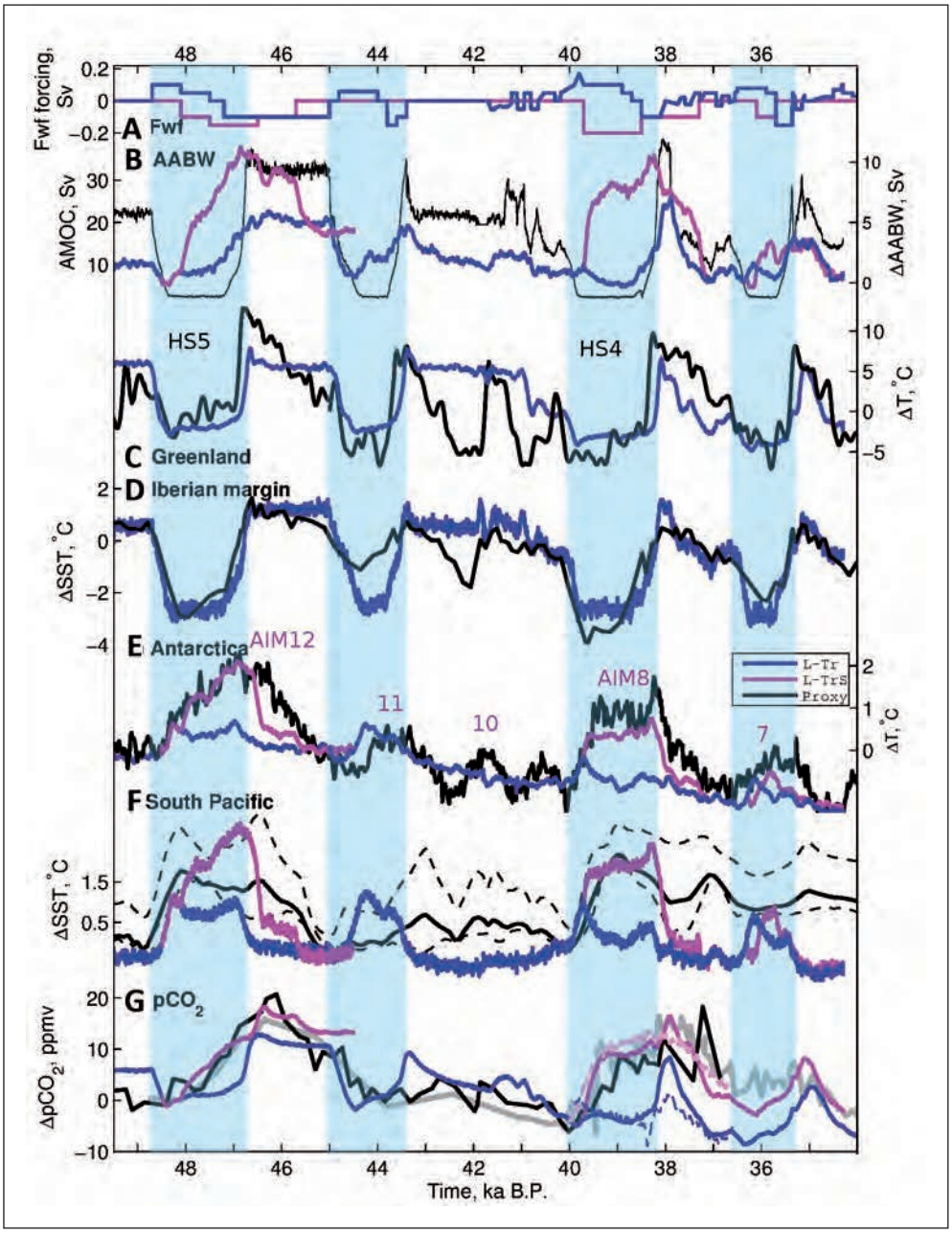


Fig. 1 Results of transient MIS3 simulations performed with LOVECLIM. Standard transient simulation (L-Tr, blue) and transient simulation with enhanced AABW (L-TrS, magenta) performed with LOVECLIM (Menviel et al. 2015) compared to paleoproxy records (black). Timeseries of (*A*) applied North Atlantic (blue) and Southern Ocean (magenta) freshwater forcing (Sv); (*B*) simulated maximum meridional overturning circulation in the North Atlantic (Sv, black) and simulated changes in Antarctic Bottom Water (AABW, Sv); (*C*) simulated NE Greenland air temperature anomalies (40ºW–10ºE, 66ºN–85ºN) compared to the NGRIP temperature reconstruction (Huber et al. 2006) on the GICC05 timescale (Svensson et al. 2008); (*D*) simulated SST anomalies (ºC) off the Iberian

## 2. Methodology

We perform transient simulations spanning the period 50–34 ka BP with two Earth System Models (LOVECLIM and the UVic ESCM) to understand the possible link between changes in NADW, changes in high latitude Southern Hemispheric climate and evolution of atmospheric $CO_2$.

The transient experiments are run with continuously varying orbital and ice sheet forcing (topography and albedo) and with prognostic atmospheric $CO_2$. As both models do not include an interactive ice sheet, the impact on oceanic circulation of the time-evolution of ice sheet growth and freshwater release is simulated by applying a freshwater forcing to the North Atlantic region.

Moderate changes in the mid/high Southern latitudes hydrological cycle can significantly impact surface salinity. As the atmospheric models used here are simple, it is thus possible that our standard experiments might not capture the past variability of AABW accurately. Additional transient experiments are performed, in which a salt flux is added over the Southern Ocean during Heinrich stadials 5 and 4, corresponding to AIM12 and AIM8 respectively.

Given the importance of mesoscale eddies for meridional heat transport in the Southern Ocean, we further investigate the relationship between enhanced AABW formation and SST changes using a global eddy-permitting ocean sea-ice model (GFDL-MOM025). From a present-day control run, a 40 years long simulation is performed with 0.5 psu increase in the sea surface salinity restoring climatology within 4º latitude of the Antarctic coastline.

## 3. Impact of AABW Changes during Heinrich Stadials 5 and 4

The simulated NADW weakening during MIS3 yield a 9 ºC surface air temperature decrease over Greenland and a ~3 ºC sea surface cooling off the Iberian margin (Fig. 1) during Heinrich stadials, in good agreement with paleoproxy records (Huber et al. 2006, Martrat et al. 2007, Menviel et al. 2014a).

However, we find that changes in NADW alone are not sufficient to explain the temperature anomaly estimated from Antarctic ice cores during the largest AIM (namely AIM12 and AIM8). In both models, NADW cessation leads to ~0.6 ºC air temperature increase over Antarctica, which is in reasonable agreement with Antarctic temperature anomaly estimates for AIM10 and AIM7 but is less than half of the estimated anomaly for the large AIM (i.e. AIM12 and AIM8) (Fig. 1).

---

margin (15ºW–8ºW, 37ºN–43ºN) compared to alkenone-based SST anomalies from marine sediment core MD01-2444 (Martrat et al. 2007) on the GICC05 timescale; (*E*) air temperature anomalies (ºC) averaged over Antarctica (90ºS–75ºS) compared to temperature anomaly estimates from EPICA Dome C ice core (Jouzel et al. 2007) on the EDC3 time-scale (Parrenin et al. 2007); (*F*) SST anomalies averaged over the South Pacific Ocean (120ºE–285ºE, 55ºS–35ºS) compared to a SST anomaly composite from South Pacific marine sediment cores (Pahnke et al. 2003, Kaiser et al. 2005, Caniupan et al. 2011, Lopes Dos Santos et al. 2013). Dashed black lines represent the +1 and –1 standard deviation of the composite; (*G*) simulated atmospheric $CO_2$ (ppmv) anomalies compared to $pCO_2$ anomalies measured in EDML and Talos Dome ice cores (Bereiter et al. 2012, black) and Siple Dome ice core (Ahn and Brook 2014, grey). Dashed blue and magenta lines represent experiments respectively similar to L-Tr and L-TrS but with fully coupled changes in terrestrial carbon.

Stronger AABW during AIM12 and AIM8 doubles the simulated warming at high Southern latitude thus leading to ~1.5 ºC temperature increase over Antarctica in better agreement with paleoproxy records (Fig. 1, Menviel et al. 2015).

The robustness of this southern warming response is tested using an eddy-permitting coupled ocean sea-ice model (GFDL-MOM025). We find that stronger Antarctic Bottom Water formation contributes to Southern Ocean surface warming by increasing the Southern Ocean meridional heat transport (Menviel et al. 2015).

In the standard MIS3 transient experiments, NADW weakening decreases the ventilation in the Atlantic, thus increasing the Dissolved Inorganic Carbon (DIC) content in that basin (Fig. 2). A strengthening of North Pacific Deep Water (NPDW) increases the ventilation of the Pacific above ~2000m depth, which decreases the DIC content in that region. The net

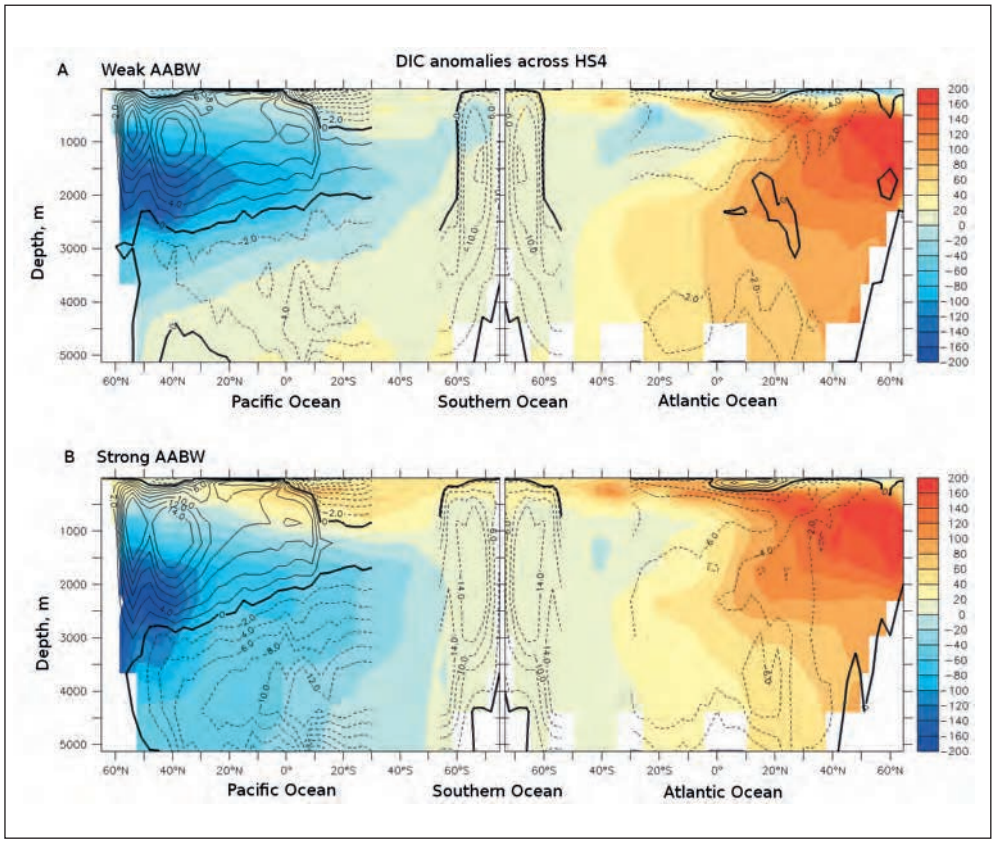


Fig. 2 Dissolved Inorganic Carbon (DIC) anomalies (µmol/L) across HS4 (39.1 ka BP compared to 39.9 ka BP) as simulated in transient experiments performed with LOVECLIM (Menviel et al. 2015) and averaged over (*left*) the Pacific and (*right*) Atlantic basins. (*A*) Results of standard transient experiment (L-Tr) and (*B*) results of transient experiment with enhanced AABW (L-TrS). Overlaid is the overturning streamfunction (Sv).

result is a slight atmospheric $CO_2$ decrease during a shutdown of NADW formation. This is in contrast with the atmospheric $CO_2$ increases observed during the first parts of AIM12 (~47.6 ka BP) and AIM8 (~39.8 ka BP), which occur during periods of weak NADW formation (HS5 and HS4, respectively).

Transient experiments in which AABW is enhanced display a ~13 ppmv atmospheric $CO_2$ increase during HS5 and HS4 in better agreement with ice core records. Enhanced AABW formation is shown to effectively ventilate the deep Pacific carbon, bringing DIC rich waters to the surface of the Southern Ocean and leading to $CO_2$ outgassing into the atmosphere (Fig. 2, MENVIEL et al. 2014b).

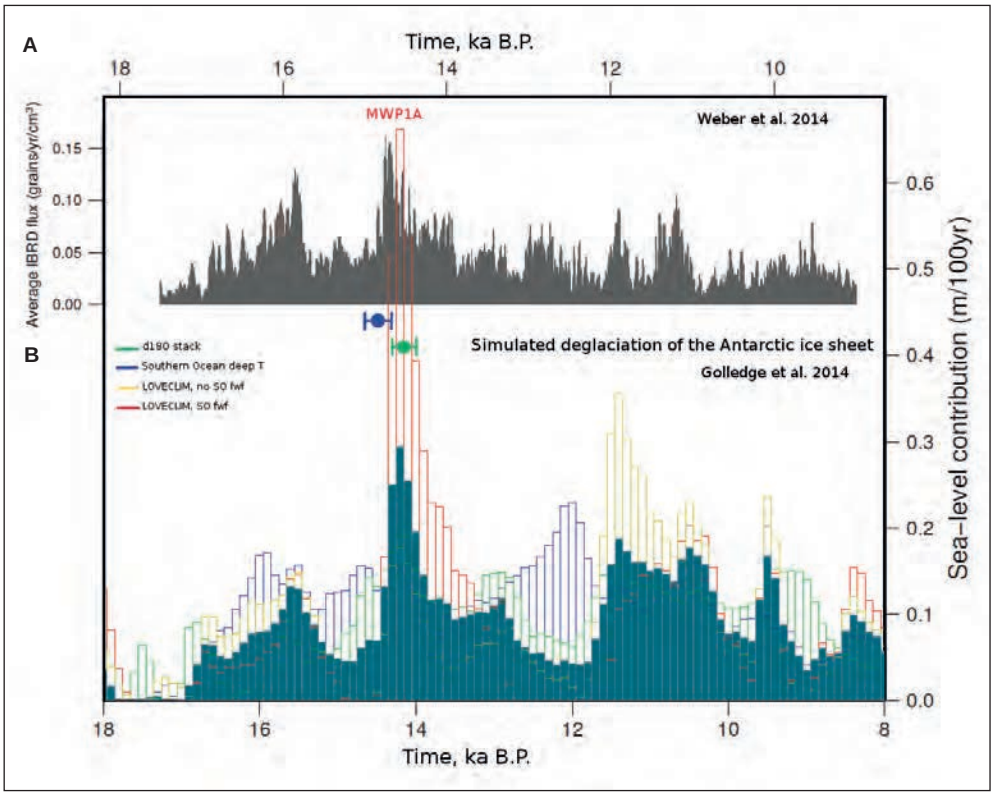


Fig. 3 (*A*) Stack of iceberg-rafted debris flux measured in marine sediment cores from the Scotia Sea (WEBER et al. 2014) compared to (*B*) Sea-level contribution through the period 18–8 ka BP, binned at 100-year intervals simulated by a high resolution Antarctic Ice Sheet model for group means and ensemble mean (solid grey). Experiments are forced with ocean heat fluxes based on a benthic $\delta^{18}O$ global stack (green), a Southern Ocean deep temperature record (blue), a transient simulation of the deglaciation (yellow) and a transient simulation of the deglaciation which includes weak AABW formation at the time of the Antarctic Cold Reversal (red) (GOLLEDGE et al. 2014). The blue and green circles represent the timing of meltwater pulses 1*A* as estimated by DESCHAMP et al. 2012 and LUI et al. 2004.

## 4. AABW Changes during the Last Deglacation

Transient simulations of the last deglaciation performed with LOVECLIM have shown that a weakening of AABW formation at the end of Heinrich stadial 1 would lead to cooling over Antarctica and at the surface of the Southern Ocean, thus initiating the Antarctic Cold Reversal (Menviel et al. 2011). Increased Southern Ocean stratification during times of weak AABW induces a subsurface warming in the Southern Ocean (Menviel et al. 2010).

Using a high resolution Antarctic ice sheet model (PISM), we show that this subsurface warming can thermally erode grounded marine-based ice and instigate a positive feedback that further accelerate the ice-sheet retreat (Golledge et al. 2014). Coincident with iceberg-rafted debris records from the Scotia Sea (Weber et al. 2014, Fig. 3), we simulate up to 4 m rise in sea level equivalent during the broad period of meltwater pulse 1A (15–13 ka BP), mainly due to a retreat of the West Antarctic Ice Sheet in the Weddell Sea and Antarctic Peninsula sectors.

## 5. Summary

We suggest that strong Antarctic Bottom Water formation during HS5 and HS4 could enhance the bipolar seesaw effect and lead to a warming of Antarctica and the Southern Ocean in better agreement with paleoproxy records. In addition strong AABW can effectively ventilate the deep Pacific Ocean and release oceanic carbon into the atmosphere, thus leading to atmospheric $CO_2$ increase during HS5 and HS4 (AIM12 and AIM8, respectively, Menviel et al. 2015).

Conversely, weak AABW formation between 14.8 and 13 ka BP would lead to a cooling at high Southern latitudes, which could explain the Antarctic Cold Reversal. The associated Southern Ocean stratification induces a subsurface warming, which leads to an accelerated deglacial retreat of the West Antarctic ice sheet (Golledge et al. 2014).

Enhanced AABW formation during Greenland stadials could be due to changes in surface buoyancy forcing over the Southern Ocean and/or to stronger/poleward shifted southern hemispheric westerlies. The amplitude of the Greenland stadial, the origin and timing of the meltwater pulse/iceberg discharge as well as the background climatic conditions might further modulate the AABW response.

### *References*

Ahn, J., and Brook, E. J.: Siple Dome ice reveals two modes of millennial $CO_2$ change during the last ice age. Nature Comm. *5*, doi:10.1038/ncomms4723 (2014)

Bereiter, B., Lüthi, D., Siegrist, M., Schüpbach, S., Stocker, T. F., and Fischer, H.: Mode of change of millennial $CO_2$ variability during the last glacial cycle associated with a bipolar marine carbon seesaw. Proc. Natl. Acad. Sci. USA *109*, 9755–9760; doi:10.1073/pnas.1204069109 (2012)

Caniupan, M., Lamy, F., Lange, C. B., Kaiser, J., Arz, H., Kilian, R., Baeza Urrea, O., Aracena, C., Hebbeln, D., Kissel, C., Laj, C., Mollenhauer, G., and Tiedemann, R.: Millennial-scale sea surface temperature and Patagonian Ice Sheet changes off southernmost Chile (53°S) over the past 60 kyr. Paleoceanography *26*, doi:10.1029/2010PA002049 (2011)

Deschamps, P., Durand, N., Bard, E., Hamelin, B., Camoin, G., Thomas, A. L., Henderson, G. M., Okuno, J., and Yokoyama, Y.: Ice-sheet collapse and sea-level rise at the Bolling warming 14,600 years ago. Nature *483*, doi:10.1038/nature10902 (2012)

*EPICA and Community Members*: One-to-one coupling of glacial climate variability in Greenland and Antarctica. Nature *444*, 195–198 (2006)

Golledge, N. R., Menviel, L., Carter, L., Fogwill, C. J., England, M. H., Cortese, G., and Levy, R. H.: Antarctic contribution to meltwater pulse 1A from reduced Southern Ocean overturning. Nature Comm. *5*, doi:10.1038/ncomms6107 (2014)

Huber, C., Leuenberger, M., Spahni, R., Flückiger, J., Schwander, J., Stocker, T. F., Johnsen, S., Landais, A., and Jouzel, J.: Isotope calibrated Greenland temperature record over Marine Isotope Stage 3 and its relation to $CH_4$. Earth Planet. Sci. Lett. *243*, 504–519 (2006)

Jouzel, J., Masson-Delmotte, V., Cattani, O., Dreyfus, G., Falourd, S., Hoffmann, G., Minster, B., Nouet, J., Barnola, J. M., Chappellaz, J., Fischer, H., Gallet, J. C., Johnsen, S., Leuenberger, M., Loulergue, L., Luethi, D., Oerter, H., Parrenin, F., Raisbeck, G., Raynaud, D., Schilt, A., Schwander, J., Selmo, E., Souchez, R., Spahni, R., Stauffer, B., Steffensen, J. P., Stenni, B., Stocker, T. F., Tison, J. L., Werner, M., and Wolff, E. W.: Orbital and millennial Antarctic climate variability over the past 800,000 years. Science *317*, 793–796 (2007)

Kageyama, M., Merkel, U., Otto-Bliesner, B., Prange, M., 2, Abe-Ouchi, A., Lohmann, G., Ohgaito, R., Roche, D. M., Singarayer, J., Swingedouw, D., and Zhang, X.: Climatic impacts of fresh water hosing under Last Glacial Maximum conditions: a multi-model study. Clim. Past *9*, 935–953 (2012)

Kaiser, J., Lamy, F., and Hebbeln, D.: A 70-kyr sea surface temperature record off Southern Chile. Paleoceanography *20*, PA4009; doi:10.1029/2004PA001146 (2005)

Kissel, C., Laj, C., Piotrowski, A. M., Goldstein, S. L., and Hemming, S. R.: Millennial-scale propagation of Atlantic deep waters to the glacial Southern Ocean. Paleoceanography *23*, doi:10.1029/2008PA001624 (2008)

Liu, J. P., and Milliman, J. D.: Reconsidering melt-water pulses 1A and 1B: global impacts of rapid sea-level rise. J. Ocean Univ. China *3*, 183–190 (2004)

Lopes Dos Santos, R. A., Spooner, I., Barrows, T. T., Deckker, P. de, Damsté, J. S. S., and Schouten, S.: Comparison of organic ($U^K37$, $TEX^H$ 86, LDI) and faunal proxies (foraminiferal assemblages) for reconstruction of late Quaternary sea surface temperature variability from offshore southeastern Australia. Paleoceanography *28*, doi:10.1002/palo.20035 (2013)

Martrat, B., Grimalt, J. O., Shackleton, N. J., Abreu, L. de, Hutterli, M. A., and Stocker, T. F.: Four climate cycles of recurring deep and surface water destabilizations on the Iberian margin. Science *317*, 502–507 (2007)

McManus, J. F., Francois, R., Gherardi, J. M., Keigwin, L. D., and Brown-Leger, S.: Collapse and rapid resumption of Atlantic meridional circulation linked to deglacial climate changes. Nature *428*, 834–837 (2004)

Menviel, L., Timmermann, A., Elison Timm, O., and Mouchet, A.: Climate and biogeochemical response to a rapid melting of the West Antarctic Ice Sheet during interglacials and implications for future climate. Paleoceanography *25*, 1–12 (2010)

Menviel, L., Timmermann, A., Elison Timm, O., and Mouchet, A.: Deconstructing the last glacial termination: the role of millennial and orbital-scale forcings. Quat. Sci. Rev. *30*, 1155–1172 (2011)

Menviel, L., Timmermann, A., Friedrich, T., and England, M. H.: Hindcasting the continuum of Dansgaard-Oeschger variability: Mechanisms, patterns and timing. Clim. Past *10*, 63–77 (2014a)

Menviel, L., England, M. H., Meissner, K. J., Mouchet, A., and Yu, J.: Atlantic-Pacific seesaw and its role in outgassing $CO_2$ during Heinrich events. Paleoceanography *29*, doi:10.1002/2013PA002542 (2014b)

Menviel, L., Spence, E., and England, M. H.: Contribution of enhanced Antarctic Bottom Water formation to Antarctic warm events and millennial-scale atmospheric $CO_2$ increase. Earth Planet. Sci. Lett. *413*, 37–50 (2015)

Orsi, A. H., Smethie, W. M., and Bullister, J. L.: On the total input of Antarctic waters to the deep ocean: A preliminary estimate from chlorofluorocarbon measurements. J. Geophys. Res. *107*/C8, 3122; doi:10.1029/2001JC000976 (2002)

Pahnke, K., Zahn, R., Elderfield, H., and Schulz, M.: 340,000-year centennial-scale marine record of Southern Hemisphere climatic oscillation. Science *301*, 948–952 (2003)

Parrenin, F., Barnola, J. M., Beer, J., Blunier, T., Castellano, E., Chappellaz, J., Dreyfus, G., Fischer, H., Fujita, S., Jouzel, J., Kawamura, K., Lemieux-Dudon, B., Loulergue, L., Masson-Delmotte, V., Narcisi, B., Petit, J.-R., Raisbeck, G., Raynaud, D., Ruth, U., Schwander, J., Severi, M., Spahni, R., Steffensen, J. P., Svensson, A., Udisti, R., Waelbroeck, C., and Wolff, E.: The EDC3 chronology for the EPICA Dome C ice core. Clim. Past *3*, 485–497 (2007)

Stocker, T. F.: The seesaw effect. Science *282*, 61–62 (1998)

Svensson, A., Andersen, K. K., Bigler, M., Clausen, H. B., Dahl-Jensen, D., Davies, S. M., Johnsen, S. J., Muscheler, R., Parrenin, F., Rasmussen, S. O., Röthlisberger, R., Seierstad, I., Steffensen, J. P., and Vinther, B. M.: A 60,000 year Greenland stratigraphic ice core chronology. Clim. Past *4*, 47–57 (2008)

Weber, M. E., Clark, P. U., Kuhn, G., Timmermann, A., Sprenk, D., Gladstone, R., Zhang, X., Lohmann, G., Menviel, L., Chikamoto, M. O., Friedrich, T., and Ohlwein, C.: Millennial-scale variability in Antarctic ice-sheet discharge during the last deglaciation. Nature *510*, 134–138 (2014)

Dr. Laurie Menviel
Climate Change Research Centre
University of New South Wales
ARC Centre of Excellence for Climate System Science
Level 4, Mathews Building
Sydney, NSW 2052
Australia
Phone: +61 2 9385 8488
Fax: +61 2 9385 8969
E-Mail: l.menviel@unsw.edu.au

Nova Acta Leopoldina NF *121*, Nr. 408, 167–169 (2015)

# Response of the Tropical Atlantic Ocean-Atmosphere System to Deglacial Changes in Atlantic Meridional Overturning

Stefan Mulitza,[1] Cristiano M. Chiessi,[2] Jörg Lippold,[3] Jean Lynch-Stieglitz,[4] Andreas Mackensen,[5] André Paul,[1] Matthias Prange,[1] Rodrigo Portilho Ramos,[1] Anna Paula S. Cruz,[6] Enno Schefuss,[1] Tilmann Schwenk,[1] Michael Schulz,[1] Ralf Tiedemann[5], Ines Voigt,[1] Martin Werner,[5] and Yancheng Zhang[1]

With 1 Figure

An important feature of the present-day circulation in the Atlantic is the cross-equatorial flow of warm and shallow waters from the South Atlantic into the North Atlantic. Much of this transport is maintained at the western boundary through the North Brazil Current, which is regarded as the major upper component of the modern Atlantic Meridional Overturning Circulation (AMOC) (Zhang et al. 2011). The associated heat transport into the North Atlantic promotes a northerly location of the Intertropical Convergence (ITCZ) (Marshall et al. 2014) and the associated rainfall maximum for much of the year. At the southern and northern limits of the ITCZ semi-arid conditions prevail in Northeast Brazil (Nordeste) and the Sahel.

Across the equator, the northward flow with the western boundary current is compensated through the southward flow of North Atlantic Deep Water (NADW) as the lower branch of the AMOC. This water mass is collectively formed from surface waters sinking in the Greenland, Iceland, Norwegian, and Labrador seas and is identifiable as a tongue of nutrient poor and $^{13}C$ rich water extending southward in the deep Atlantic (Kroopnick 1985). Nutrient-rich and low $\delta^{13}C$ Antarctic Bottom Water (AABW) formed in the Southern Ocean is penetrating northward below the NADW.

Since the AMOC underwent substantial variations during the last deglaciation (McManus et al. 2004), high-resolution sediment records from ocean margin settings offer the opportunity to study interactions between ocean circulation, continental climate and the carbon cycle. We present two previously unpublished sediment cores recently retrieved off NE Brazil (GeoB16202-2 and GeoB16206-1, ~2°S, 2248 m and 1367 m water depth) and one sediment core from the continental margin off NW Africa (GeoB9508-5, ~16°N, 2384 m water depth) (Fig. 1) covering the last deglaciation (Mulitza et al. 2008). Age models of all cores are based on calibrated AMS radiocarbon dates and show highly resolved deglacial sections with sedimentation rates up to 1 mm/year during Heinrich stadial 1 due to intensified terrigenous input. XRF elemental ratios of bulk sediments and δD of plant wax (Niedermeyer et al. 2009) have been used to characterize terrestrial climate. Protactinium/Thorium (Pa/Th) ratios

1 MARUM – Center for Marine Environmental Sciences, University of Bremen, Germany.
2 School of Arts, Sciences and Humanities, University of São Paulo, Brazil.
3 University of Bern, Institute of Geological Sciences, Switzerland.
4 School of Earth and Atmospheric Sciences, Georgia Institute of Technology, Atlanta, USA.
5 Alfred Wegener Institute for Polar and Marine Research, Bremerhaven, Germany.
6 Fluminense Federal University, Niterói, Rio de Janeiro, Brazil.

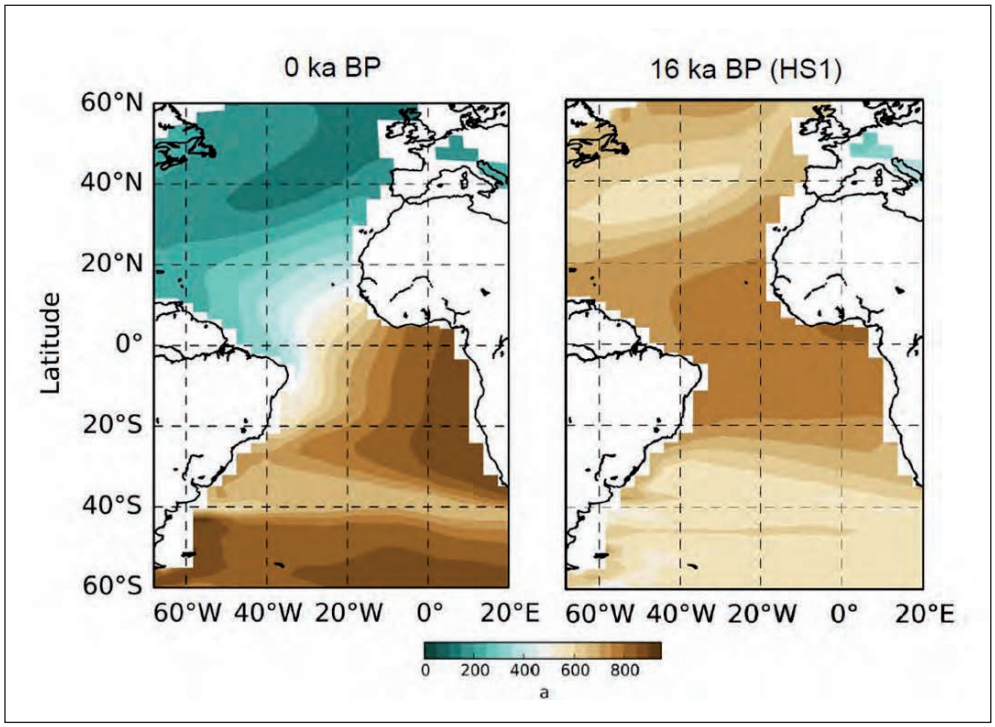


Fig. 1 Core locations and ideal age (1112.51 m depth) for the control run (0 ka BP) and Heinrich stadial 1 (16 ka BP) from climate model simulations of Liu et al. (2009). Ideal age (Thiele and Sarmiento 1990) is a tracer that is advected and mixed in the same way as temperature and salinity and records time since contact with the surface. The model data suggest the development of an equatorial tongue with high ideal ages with AMOC slowdown during Heinrich stadial 1.

on bulk sediments and carbon isotopes ratios of benthic foraminifera have been used to infer the state of the AMOC and deep water nutrient content.

During Heinrich stadial 1, when the AMOC was substantially reduced due to meltwater input to the North Atlantic, we observe dry conditions in the Sahel and wet conditions in NE Brazil consistent with a southward displacement of the marine ITCZ. Off NE Brazil, contemporaneous changes in Pa/Th ratios and δD of plant waxes indicate that both AMOC strength and precipitation were tightly coupled over Heinrich stadial 1, with increasing precipitation during AMOC slowdown. We show that this response pattern agrees with the results of climate model simulations (Liu et al. 2009, Merkel et al. 2010), which suggests that the southward displacement of the long-term mean position of the ITCZ is directly linked to the magnitude of the AMOC slowdown.

Carbon isotope ratios measured on single shells of the benthic foraminifer *Cibicidoides* spp. show lowest values during Heinrich stadial 1 and the Younger Dryas in all cores. Generally, carbon isotope ratios are in perfect tune with Pa/Th measured on the deeper core which suggests a strong nutrient enrichment in deep- and intermediate waters during times of AMOC slowdown. At the intermediate water depth site, carbon isotope ratios during Heinrich stadial 1 reach values as low as –1 ‰. Since this extreme depletion seems to be restricted to

the tropical Atlantic, we suggest that a local remineralisation of organic matter and nutrient enrichment with a sluggish circulation and/or a potential southward and downward extension of the poor-ventilated equatorial shadow zone are, at least partially, contributing to depleted values at intermediate water depths (Fig. 1).

## *References*


Kroopnick, P. M.: The distribution of C-13 $\Sigma CO_2$ in the world oceans. Deep-Sea Res. Part A–Oceanogr. Res. Pap. *32*, 57–84 (1985)

Liu, Z., Otto-Bliesner, B. L., He, F., Brady, E. C., Tomas, R., Clark, P. U., Carlson, A. E., Lynch-Stieglitz, J., Curry, W., Brook, E., Erickson, D., Jacob, R., Kutzbach, J., and Cheng, J.: Transient simulation of last deglaciation with a new mechanism for Bølling-Allerød warming. Science *325*, 310–314 (2009)

Marshall, J., Donohoe, A., Ferreira, D., and McGee, D.: The ocean's role in setting the mean position of the Inter-Tropical Convergence Zone. Clim. Dynam. *42*, 1967–1979 (2014)

McManus, J. F., Francois, R., Gherardi, J. M., Keigwin, L. D., and Brown-Leger, S.: Collapse and rapid resumption of Atlantic meridional circulation linked to deglacial climate changes. Nature *428*, 834–837 (2004)

Merkel, U., Prange, M., and Schulz, M.: ENSO variability and teleconnections during glacial climates. Quat. Sci. Rev. *29*, 86–100 (2010)

Mulitza, S., Prange, M., Stuut, J. B., Zabel, M., Dobeneck, T. von, Itambi, A. C., Nizou, J., Schulz, M., and Wefer, G.: Sahel megadroughts triggered by glacial slowdowns of Atlantic meridional overturning. Paleoceanography *23*, PA4206; doi:10.1029/2008PA001637 (2008)

Niedermeyer, E. M., Prange, M., Mulitza, S., Mollenhauer, G., Schefuss, and Schulz, M.: Extratropical forcing of Sahel aridity during Heinrich stadials. Geophys. Res. Lett. *36*, L20707; doi:10.1029/2009GL039687 (2009)

Thiele, G., and Sarmiento, J. L.: Tracer dating and ocean ventilation. J. Geophys. Res. – Oceans *95*, 9377–9391 (1990)

Zhang, D., Msadek, R., McPhaden, M. J., and Delworth, T.: Multidecadal variability of the North Brazil Current and its connection to the Atlantic meridional overturning circulation. J. Geophys. Res. – Oceans *116*, doi:10.1029/2010JC006812 (2011)



Dr. Stefan Mulitza
University of Bremen
MARUM – Center for Marine Environmental Sciences
Postfach 330 440
28334 Bremen
Germany
Phone: +49 421 21865536
Fax: +49 421 21865505
E-Mail: smulitza@marum.de

Nova Acta Leopoldina NF *121*, Nr. 408, 171–173 (2015)

# Robustness and Uncertainties of Current Marine Carbon Cycle Models

Andreas Oschlies (Kiel)

Numerical biogeochemistry-circulation models are essential tools for exploring ideas, testing hypotheses, and making inferences about the possible past and future evolution of climate and the Earth system. Results of such models are used not only for academic purposes, but are also used to inform society and decision makers. It is therefore mandatory that we aim for a good understanding of the robustness and uncertainties of the results of such models. This is not an easy task as current state-of-the-art models are complex systems, composed of many different modules describing different components of the Earth system, with different modules often developed for different purposes, and each one having numerous input parameters that are difficult to constrain from observations. A complete sensitivity or uncertainty analysis of such complex models is not routinely done, and this study will describe first attempts to evaluate the robustness and uncertainty of marine carbon cycle components of current Earth system models.

We begin with the question of how we can assess whether a given model is any good. For different research questions "good" will have different meanings, and in the context of the large-scale and long-timescale carbon cycle, patterns of observed biogeochemical tracer distributions may serve as a reasonable reference that a "good" model should be able to reproduce. Observations are available mostly for the current state of the ocean, and one has to keep in mind that a reasonable simulation of the present state does not automatically imply that the same model will provide reasonable simulations of different climate states. A reasonable simulation of present-day biogeochemical tracer distributions may, however, be regarded as a necessary test that any high-quality model has to pass. To this extent we have developed a computationally efficient testbed for marine biogeochemical models that can, *via* the transport matrix method (Khatiwala 2007), be integrated for several thousand years per day (Kriest et al. 2010, 2012). In this scheme, a seasonally cycling steady-state circulation field is employed to transport passive tracers and to spin up the biogeochemical model for a range of different parameter combinations or initial conditions. One interesting preliminary result is that for typical models of one or two nutrients, dissolved organic matter, one phytoplankton and one zooplankton compartment, the model-derived steady state is independent of the chosen initial tracer distributions as long as total phosphorus is kept constant. This suggests some robustness of model results, although this finding has been difficult to generalize given the strong nonlinearities in biogeochemical model formulations and the associated potential for bifurcations and multiple steady states. The result is, however, good news for any paleo

modelling studies that usually have to start from initial conditions about which we have very little prior knowledge (though even our prior knowledge about the ocean's phosphorus content at different times might be very limited, Wallmann 2012).

In general, the outcome of biogeochemical model integrations will depend on both ocean circulation and biogeochemical process descriptions. The attribution of any model-data misfits to either of these is therefore not straightforward. An encouraging finding is that initial model evaluations suggest that even different circulation fields result in very similar biological model parameters that yield smallest model-data misfits with respect to global distributions of nutrients and oxygen (Kriest and Oschlies 2013). Less encouraging is that a range of models, ranging from conceptually simple nutrient-restoring models to state-of-the-art multi-nutrient multi-plankton functional type models, seems to yield very similar root-mean-square misfits to observed global distributions of phosphate and oxygen (Kriest et al. 2012). If these results are confirmed for different circulation fields and fully optimized biogeochemical model parameters, the biogeochemical model development of the last decades appears to have had essentially no effect on the ability of the different models to reproduce observed distributions of these biogeochemical tracers. Overall, all models investigated can at least simulate global tracer distributions better than a random model, with most explanatory power being found for the distributions of nutrients and oxygen in the vertical. This vertical distribution is highly relevant for the ocean-atmosphere partitioning of carbon, which is of particular interest for research topics such as glacial cycles.

While an evaluation of models with respect to their ability to reproduce the current state of the ocean is, in principle, possible and straightforward, uncertainties in the simulated sensitivity of the different models with respect to environmental change are much more difficult to assess. Specifically tuned models that yield very similar fits to present-day tracer distributions can simulate changes in simulated primary production of even opposite sign in response to global warming (Taucher and Oschlies 2011). Changes in simulated export production and air-sea fluxes of $CO_2$ appear, however, more robust with respect to changes in biogeochemical parameters. Analysis of the way current biogeochemical models simulate the marine nitrogen cycle suggest far less robust results with respect to its sensitivity to changes in redox conditions or oceanic nutrient supply from land or from the atmosphere (Landolfi et al. 2013). It is shown that typical formulations used to describe marine nitrogen fixation and its response to nitrogen loss processes *via* denitrification and anammox can yield counterintuitive results of net losses of marine fixed nitrogen upon addition of new nitrogen to large parts of the tropical oceans. Changes in redox conditions associated with oxygen minimum zones can also affect the cycling of iron and phosphorus, with potentially large impacts on oceanic nutrient inventories and the global carbon cycle. Such processes are not generally represented in state-of-the-art models such as those used in the Coupled Model Intercomparison Project Phase 5 (CMIP5), which formed the basis of the model simulations used in the recent 5$^{th}$ IPCC Assessment Report. A neglect or misrepresentation of such processes that can change the marine nutrient inventory can introduce substantial uncertainty in model projections of past or future climates that is difficult to quantify. A better process understanding and case studies involving observed changes ranging from paleoevents to interannual or seasonal variability appears promising for providing better constraints on models and estimated uncertainties.

While assessing models *via* metrics evaluating large-scale patterns of model-data misfits can provide reasonable information about the models' ability to simulate the current state of

the ocean, the investigation of individual processes is advocated to gain more confidence into the models' applicability for extrapolations to past and future environmental conditions.

## *References*

Khatiwala, S.: A computational framework for simulation of biogeochemical tracers in the ocean. Global Biogeochem. Cycles *21*/3, GB3001 (2007)

Kriest, I., Khatiwala, S., and Oschlies, A.: Towards an assessment of simple global marine biogeochemical models of different complexity. Progr. Oceanogr. *86*/3–4, 337–360 (2010)

Kriest, I., Oschlies, A., and Khatiwala, S.: Sensitivity analysis of simple global marine biogeochemical models. Global Biogeochem. Cycles *26*/2, GB2029 (2012)

Kriest, I., and Oschlies, A.: Swept under the carpet: organic matter burial decreases global ocean biogeochemical model sensitivity to remineralization length scale. Biogeosciences *10*/12, 8401–8422 (2013)

Landolfi, A., Dietze, H., Koeve, W., and Oschlies, A.: Overlooked runaway feedback in the marine nitrogen cycle: the vicious cycle. Biogeosciences *10*/3, 1351–1363 (2013)

Taucher, J., and Oschlies, A.: Can we predict the direction of marine primary production change under global warming? Geophys. Res. Lett. *38*/2, L02603 (2011)

Wallmann, K.: Phosphorus imbalance in the global ocean? Global Biogeochem. Cycles *24*/4, GB4030 (2010)

Prof. Dr. Andreas Oschlies
GEOMAR Helmholtz Centre for Ocean Research Kiel
and University of Kiel
Düsternbrooker Weg 20
24105 Kiel
Germany
Phone: +49 431 6001936
Fax: +49 431 6004469
E-Mail: aoschlies@geomar.de

Nova Acta Leopoldina NF *121*, Nr. 408, 175–181 (2015)

# Glacial $CO_2$ as a Key to the Glacial-Interglacial Problem

Didier Paillard (Gif-sur-Yvette, France)

With 2 Figures

The notion of climate change appeared in the mid-nineteenth century with the discovery of ice ages. Already at that time, the atmospheric concentration in carbon dioxide was suspected to affect climate, and on these premises Arrhenius (1896) estimated that glacial $CO_2$ levels should be about 40 % lower than preindustrial levels. Though based on some erroneous radiative data and modelling, this appears today as an incredibly good prediction, which stands as a reminder of the clear impact of $CO_2$ concentrations on glacial climate. Since the nineteenth century, a central question in climatology has been to understand the respective roles of the astronomical forcing and of greenhouse gas changes on the ice age problem. It is worth emphasizing that this question is far from being settled in spite of the tremendous progresses achieved in observing and simulating the present day climate. Indeed, if in the twentieth century, advances in geochronology have proved unambiguously that ice ages are paced by the astronomical forcing (Hays et al 1976), the mechanisms involved are unclear, in particular concerning the largest 100 ka variations.

The detailed chronology of events during the last deglaciation shows that $CO_2$ had already increased by about 50–60 ppm at 14.6 ka BP while the ice-sheets had not changed much (see Fig. 1). A direct consequence is the clear lead in the rise of southern or tropical temperatures over Northern Hemisphere ones (e.g. Shakun et al. 2012). This has long been recognized as a possible "upset" for the Milankovitch theory. Indeed, the astronomical forcing on Earth's climate is very weak, but can, nevertheless, affect significantly the ice-sheets: indeed their mass balance depends largely on local, seasonal, insolation forcing, which experiences sizeable variations through time. As a result, the astronomical theory tells us that ice-sheet changes are driving global climatic changes, in particular through their large albedo effect. This stands in sharp contrast with the geochemical theory of ice ages, based on $CO_2$, which states on the contrary, that global climatic changes should drive the evolution of ice-sheets. Obviously, the succession of events observed during the last deglaciation is not consistent with a simple astronomical causation, but in strong favour of a $CO_2$ induced termination. Terminations are occurring more or less every 100 ka, a periodicity that cannot be easily explained by the astronomical forcing. The fact that they are systematically associated with a large atmospheric $CO_2$ increase is another strong indication of the role of greenhouse gases in the 100-ka problem.

The lack of a well-accepted theory of the glacial carbon cycle is currently the main missing piece in the puzzle of Quaternary climates. Many possible physical and biogeochemical

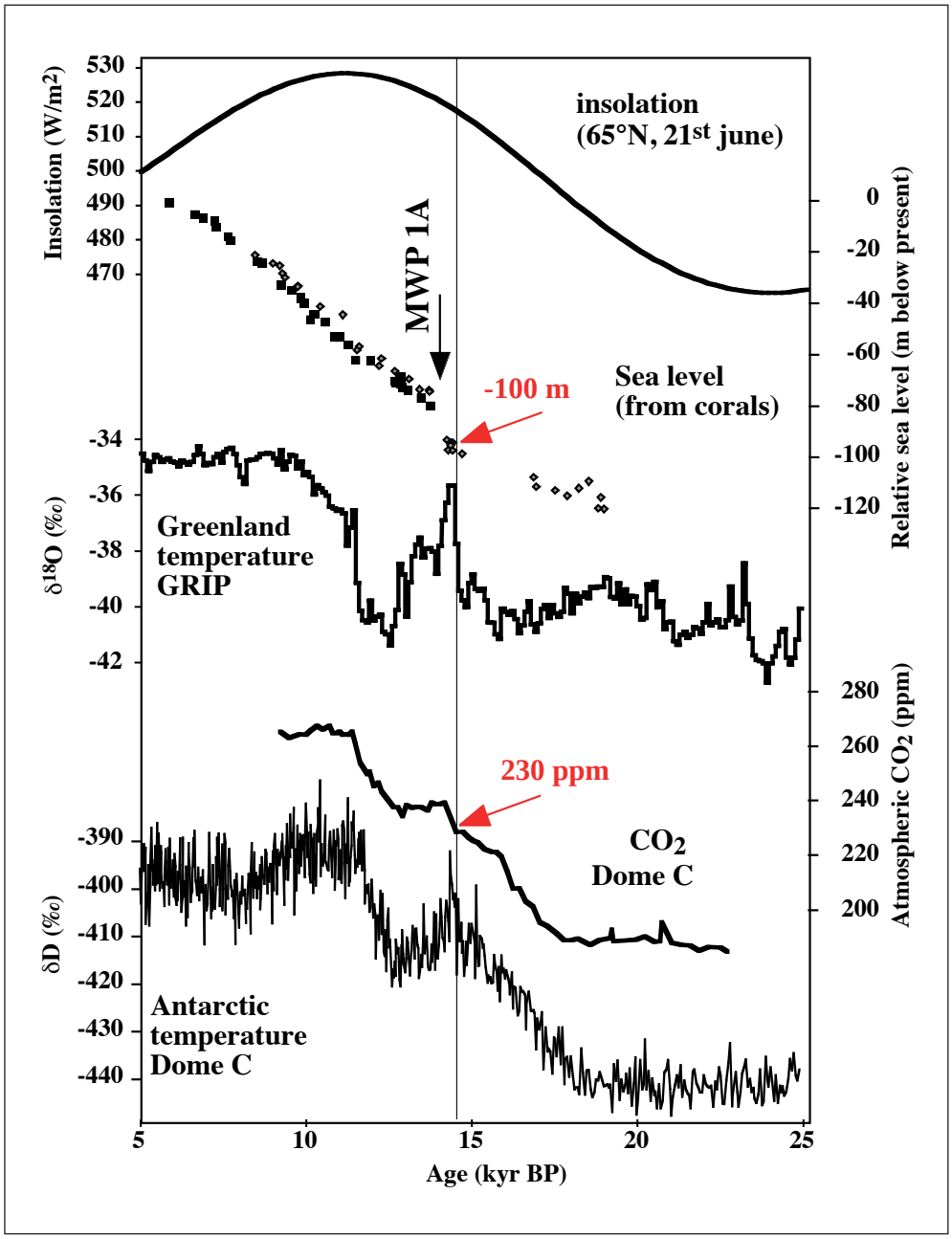


Fig. 1 From top to bottom: insolation at 65°N at the june solstice (Laskar et al. 2004); sea level records (Fairbanks 1989, Bard et al. 1996), Greenland $\delta^{18}O$ record as a proxy of Northern Hemisphere climate (Dansgaard et al. 1993); atmospheric $CO_2$ (Monnin et al. 2001) and antarctic $\delta D$ as a proxy of Southern Hemisphere climate (Stenni et al. 2001). At the onset of the Bølling-Allerød, about 14.6 ka BP, the sea level is within glacial values, while atmospheric $CO_2$ has increased by about 50 ppm. More generally, the Southern Hemisphere warms several thousands of years before the Northern Hemisphere one.

processes have been suggested (e.g. Archer et al. 2000, Sigman and Boyle 2000) but there is currently no consensus on the most important ones. Most likely, the deep ocean contained more carbon during glacial times since this is the only large carbon reservoir involved within the timescales of interest. Most likely also, the Southern ocean is the key area, since the evolution of atmospheric $CO_2$ closely parallels the evolution of Southern records, as examplified by the strong correlation between $pCO_2$ and temperature reconstructions over Antarctica (Petit et al. 1999, Lüthi et al. 2008). Most studies are trying to simulate the carbon cycle during the Last Glacial Maximum with the hope of obtaining atmospheric levels about 100 ppm lower than during pre-industrial times, as recorded in ice cores. In other words, most studies are trying to explain lower $pCO_2$ as a consequence of cold, ice-sheet induced, climate. But as outlined above, we know quite well the succession of events, at least during the deglaciation, and the causal link between ice-sheets and carbon appears to be just the opposite. What is needed is a mechanism for lowering $CO_2$ that breaks down more or less at the Last Glacial Maximum, because of the glacial maximum. In other words, the key question might not be "why is $pCO_2$ lower during glacial times", but "why does $pCO_2$ rise just after glacial maxima". This point of view offers quite severe constraints on the possible mechanisms involved.

This idea was developed in a conceptual model of ice ages (Paillard and Parrenin 2004) that represents in a consistent way the evolution of both ice sheet volume and $pCO_2$, but also their lead-lag relationship as emphasized above. This model allows to understand ice ages as a relaxation oscillation, something often recognized as possibly the best framework for explaining the qualitative features observed in the Quaternary climatic evolution. The critical trigger in this relaxation is represented by glacial maxima causing a large $CO_2$ release. In this model, the following physical explanation is proposed: glacial $CO_2$ is stored in the deep ocean thanks to the formation of cold-salty bottom waters on the Antarctic continental shelves. This mechanism breaks down naturally when the Antarctic ice-sheet reaches its maximum extent, quite probably a few millennia within or after the Last Glacial Maximum, mainly as a response of sea level drop.

Since the publication of this concept, several new pieces of information are strongly supporting this idea. In particular, a key ingredient is a lower atmospheric $CO_2$ caused by the formation of cold and salty bottom waters around Antarctica. This mechanism was tested in a model of intermediate complexity (CLIMBER2) by Bouttes et al. (2010, 2011, 2012). In this implementation, a prescribed fraction of the salt rejected by sea ice formation around Antarctica is transported directly in the bottom ocean. This crude parameterization aims at representing the accumulation of cold and salty waters on the continental shelves, that sink as bottom gravity currents along the topography down to the abyss. In this model, the standard level of glacial $CO_2$ (in the absence of salty bottom water formation) is about 15 ppm higher than preindustrial one (280 ppm), mostly due to the reduction of the terrestrial biosphere. When the salt fraction that sinks to the bottom increases to about 60 %, the atmospheric $CO_2$ is reduced by 50 ppm (in the more diffusive ocean version model) or by 80 ppm (in the less diffusive ocean version model). Interestingly, this has strong implication on deep ocean properties. Indeed, deep Southern ocean waters become significantly saltier, in agreement with sediment pore data (Adkins et al. 2002). The $\delta^{13}C$ of deep southern ocean also becomes significantly lower (Bouttes et al. 2011), thus explaining the deep $\delta^{13}C$ values measured in benthic foraminifera over the past decades (e.g. Duplessy et al. 1988, Curry et al. 2005). Interestingly, the concentrations of both atmospheric and oceanic $^{14}C$ are also well represented by this model (Mariotti et al. 2013). It is therefore extremely encouraging that this simple

"salty bottom water" mechanism is able to reproduce quantitatively not only the atmospheric $CO_2$ but also the large scale distributions of its major isotopes.

A key question in climate sciences is the predictive power of models. In the transient simulations of the deglacial $CO_2$ (Bouttes et al. 2012), an interesting feature is the synchroneity of the initial temperature and $CO_2$ increases. At that time, it was generally believed that temperature should lead slightly, by a few centuries, the $CO_2$ increase, mostly by extrapolating results from Caillon et al. (2003) obtained on termination 3. Still, in our scenario, the stopping of "salty bottom water" down-flow results in a destratification of the Southern Ocean that leads both to an increase of $CO_2$ and a decrease of sea-ice extent. In this mechanism, temperatures around Antarctica and $CO_2$ are therefore strongly linked together, and react simultaneously. Interestingly, this synchronicity at the start of the $CO_2$ rise around 18 ka BP, was recently confirmed (Parrenin et al. 2013). *A posteriori*, it can be said that our "salty bottom water" or "brines" hypothesis made an unexpected prediction.

Recent observations of dense salty water formation on the continental shelves of Antarctica associated with sea ice brine rejection (Ohshima et al. 2013) gives undoubtedly some support to the hypothesis outlined above, since this processes contribute today to some non-negligible part of AABW (Meredith 2013). Such a mode of bottom water formation is likely to be much more important in a colder climate, when sea ice formation is likely to be enhanced. As mentioned above, at the glacial maximum the Antarctic ice-sheet covers a significant part of the continental shelf and this mechanism breaks down. A key open question is the dynamics of the gravity currents that transport these salty shelf waters down to the bottom of the Southern Ocean (Foldvik et al. 2004, Ohshima et al. 2013). Unfortunately, these processes are not well understood, and not well represented by current state-of-the-art climate models. Another important mechanism is the basal melting under the ice shelves that provides today a significant amount of fresh water to the continental shelf waters, thus reducing their density and their ability to contribute to bottom water formation. More generally, the coupling between the ocean and basal melting appears today to be widely distributed around Antarctica and more important than previously acknowledged (Rignot et al. 2013). According to regional ocean model studies of the caverns beneath Antarctic ice shelves, reducing the ice basal melting would greatly enhance the formation of bottom waters (Hellmer 2004) which would again become more dense and saltier. This is likely to occur during glacial periods thus favouring salty AABW formation and lower $pCO_2$. If the mechanisms outlined above clearly need further confirmations, many indications from paleoclimatic data, from present day observations, from regional modelling and from intermediate complexity models, altogether seem to confirm the initial hypothesis.

As outlined by the example of Arrhenius mentioned above, it is not unusual that an "oversimplified model" can provide accurate predictions, while much better, more physically based ones – like in the Ångström (1900) paper – are unable to reach similar conclusions. Paleoclimatologists proved that Arrhenius' predictions were basically right, even if this model had some serious flaws. In the same spirit, it was suggested that scientists should predict past atmospheric $CO_2$ before it was measured over the eight climatic cycles of Epica Dome C (Wolff et al. 2005). Though there was no clearer winner or loser out of this exercise (Hopkin 2005), this was quite rich in outlining some necessary key assumptions. Similarly, predicting today the $CO_2$ beyond the last million years is a challenging exercise. As explained above, predictions on the relative timing of events, before it has been ascertained by observations, should be also a more usual target for climate and carbon models that simulate the

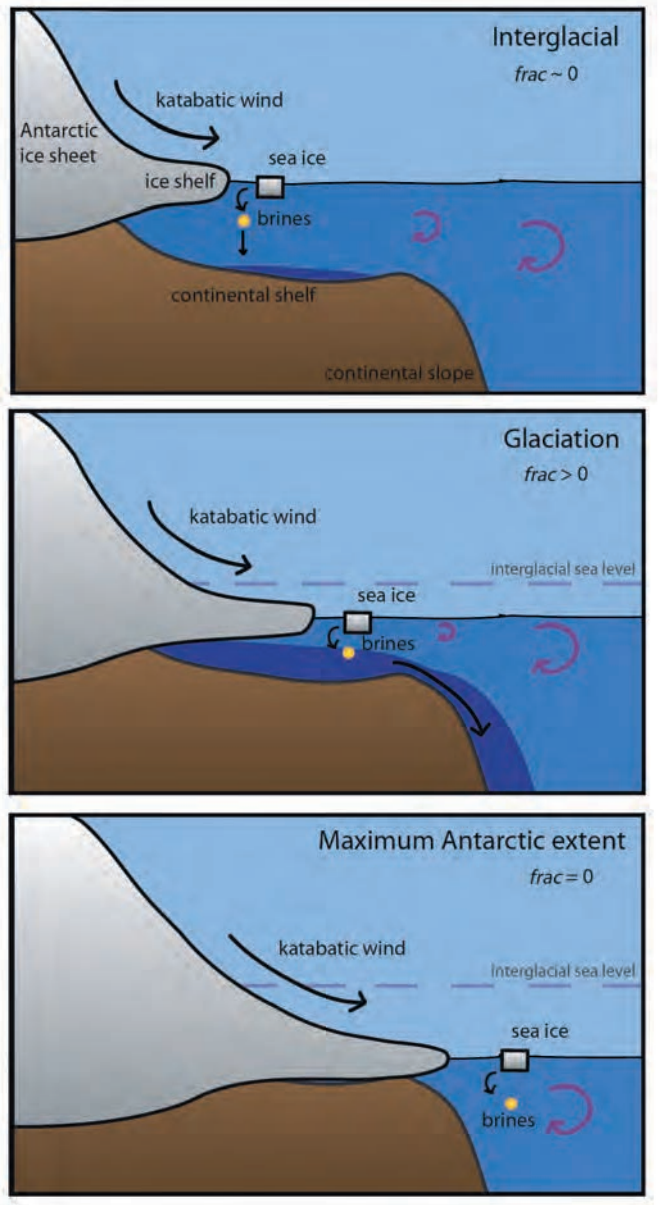


Fig. 2 Scheme of the mechanism (Paillard and Parrenin 2004). *Top*: current situation, where salty waters from brine rejection are mostly mixed with open ocean waters. *Middle*: with lower sea-level, more intense sea ice formation, less ice shelf melting, it is likely that the salty waters will overspill down to the bottom of the Ocean. *Bottom*: shortly after the glacial maximum in the north, Antarctica will reach its maximum area and will cover a substantial part of the continental shelves (schemes from Bouttes et al. 2012). The critical parameter is the fraction ("frac") of salty "brine" waters reaching the bottom of the Ocean.

past. Indeed, the dynamics of events is a much more stringent constraint on processes than the simulation of steady-states or snapshots, as usually performed in state-of-the-art model experiments.

The very strong correlation observed in Antarctic cores between southern temperatures and $CO_2$ is a solid indication that Quaternary $CO_2$ changes are tightly linked to physical changes in the Southern Ocean, and quite probably in a rather direct and simple way. The "salty bottom water" or "brines" hypothesis exposed over the last ten years offers a rather simple explanation of most observational evidences, both on the glacial-interglacial timescale and on the best century-resolved ice cores chronologies. Recent physical oceanographic data tend to prove the validity of the concept. It seems therefore that we are getting closer to a more complete understanding of the dynamics of glacial cycles that includes the dynamics of the carbon cycle. By building such a synthesis between the astronomical theory and the geochemical theory of ice ages (Paillard 2015), we would at last provide a framework for the largest, well-documented, recent climatic changes, which are Quaternary cycles.

## *References*


Adkins, J. F., McIntyre, K., and Schrag, D.: The salinity, temperature and $\delta^{18}O$ of the glacial deep ocean. Science *298*, 1769–1773 (2002)

Ångström, K.: Ueber die Bedeutung des Wasserdampfes und der Kohlensäure bei der Absorption der Erdatmosphäre. Annalen der Physik *3*, 720–732 (1900)

Archer, D., Winguth, A. M. E., Lea, D. W., and Mahowald, N. M.: What caused the glacial/interglacial atmospheric $pCO_2$ cycles? Rev. Geophys. *38*, 159–189 (2000)

Arrhenius, S.: On the influence of carbonic acid in the air upon the temperature of the ground. Philos. Mag. *41*, 237–276 (1896)

Bard, E., Hamelin, B., Arnold, M., Montaggioni, L., Cabioch, G., Faure, G., and Rougerie, F.: Deglacial sea-level record from Tahiti corals and the timing of global meltwater discharge. Nature *382*, 241–244 (1996)

Bouttes, N., Paillard, D., and Roche, D. M.: Impact of brine-induced stratification on the glacial carbon cycle. Clim. Past. *6*, 575–589 (2010)

Bouttes, N., Paillard, D., Roche, D. M., Brovkin, V., and Bopp, L.: Last Glacial Maximum $CO_2$ and $\delta^{13}C$ successfully reconciled. Geophys. Res. Lett. *38*, 1–5 (2011)

Bouttes, N., Paillard, D., Roche, D. M., Waelbroeck, C., Kageyama, M., Lourantou, A., Michel, E., and Bopp, L.: Impact of oceanic processes on the carbon cycle during the last termination. Clim. Past. *8*, 149–170 (2012)

Caillon, N., Severinghaus, J., Jouzel, J., Barnola, J.-M., Kang, J., and Lipenkov, V.: Timing of atmospheric $CO_2$ and antarctic temperature changes across termination III. Science *299*, 1728–1731 (2003)

Curry, W., and Oppo, D.: Glacial water mass geometry and the distribution of $\delta^{13}C$ of $\Sigma CO_2$ in the western Atlantic Ocean. Paleoceanography *20*, PA1017, 269–305 (2005)

Duplessy, J.-C., Shackleton, N., Fairbanks, R., Labeyrie, L., Oppo, D., and Kallel, N.: Deepwater source variations during the last climatic cycle and their impact on the global deepwater circulation. Paleoceanography *3*, 343–360 (1988)

Fairbanks, R. G.: A 17,000-year glacio-eustatic sea level record: influence of glacial melting rates on the Younger Dryas event and deep ocean circulation. Nature *342*, 637–642 (1989)

Foldvik, A., Gammelsrod, T., Osterhus, S., Fahrbach, E., Rohardt, G., Schroder, M., Nicholls, K. W., Padman, L., and Woodgate, R. A.: Ice shelf water overflow and bottom water formation in the southern Weddell Sea. J. Geophys. Res.–Oceans *109*, C02015 (2004)

Hays, J., Imbrie, J., and Shackleton, N.: Variations in the earth's orbit: pacemakers of the ice ages. Science *194*, 1121–1132 (1976)

Hellmer, H.: Impact of Antarctic ice shelf basal melting on sea ice and deep ocean properties. Geophys. Res. Lett. *31*, 1–4 (2004)

Hopkin, M.: Antarctic ice puts climate predictions to the test. Nature *438*, 536–537 (2005)

Lüthi, D., Le Floch, M., Bereiter, B., Blunier, T., Barnola, J.-M., Siegenthaler, U., Raynaud, D., Jouzel, J., Fischer, H., Kawamura, K., and Stocker, T. F.: High-resolution carbon dioxide concentration record 650,000–800,000 years before present. Nature *453*, 379–382 (2008)

Mariotti, V., Paillard, D., Roche, D., Bouttes, N., and Bopp, L.: Simulated last glacial maximum $\Delta^{14}C_{atm}$ and the deep glacial ocean carbon reservoir. Radiocarbon *55*, 1595–1602 (2013)

Meredith, M.: Oceanography: replenishing the abyss. Nature Geosci. *6*, 166–167 (2013)

Monnin, E., Indermühle, A., Dällenbach, A., Flückiger, J., Stauffer, B., Stocker, T. F., Raynaud, D., and Barnola, J.-M.: Atmospheric $CO_2$ concentrations over the last glacial termination. Science *291*, 112–114; doi:10.1126/science.291.5501.112 (2001)

Ohshima, K. I., Fukamachi, Y., Williams, G. D., Nihashi, S., Roquet, F., Kitade, Y., Tamura, T., Hirano, D., Herraiz-Borreguero, L., Field, I., Hindell, M., Aoki, S., and Wakatsuchi, M.: Antarctic bottom water production by intense sea-ice formation in the Cape Darnley polynya. Nature Geosci. *6*, 235–240 (2013)

Paillard, D.: Quaternary glaciations: from observations to theories. Quat. Sci. Rev. *107*, 11–24 (2015)

Paillard, D., and Parrenin, F.: The Antarctic ice-sheet and the triggering of deglaciations. Earth Planet. Sci. Lett. *227*, 263–271 (2004)

Parrenin, F., Masson-Delmotte, V., Kohler, P., Raynaud, D., Paillard, D., Schwander, J., Barbante, C., Landais, A., Wegner, A., and Jouzel, J.: Synchronous change of atmospheric $CO_2$ and antarctic temperature during the last deglacial warming. Science *339*, 1060–1063 (2013)

Petit, J.-R., Jouzel, J., Raynaud, D., Barkov, N., Barnola, J.-M., Basile, I., Bender, M., Chappellaz, J., Davis, M., Delaygue, G., Delmotte, M., Kotlyakov, V. M., Legrand, M., Lipenkov, V., Lorius, C., Pepin, L., Ritz, C., Saltzman, E. S., and Stievenard, M.: Climate and atmospheric history of the past 420,000 years from the Vostok ice core, Antarctica. Nature *399*, 429–436 (1999)

Rignot, E., Jacobs, S., Mouginot, J., and Scheuchl, B.: Ice-shelf melting around Antarctica. Science *341*, 266–270 (2013)

Shakun, J. D., Clark, P. U., He, F., Marcott, S. A., Mix, A., Liu, Z., Otto-Bliesner, B., Schmittner, A., and Bard, E.: Global warming preceded by increasing carbon dioxide concentrations during the last deglaciation. Nature *484*, 49–54 (2012)

Sigman, D., and Boyle, E.: Glacial/interglacial variations in atmospheric carbon dioxide. Nature *407*, 859–869 (2000)

Stenni, B., Masson-Delmotte, V., Johnson, S., Jouzel, J., Longinelli, A., Monnin, E., Röthlisberger, R., and Selmo, E.: An oceanic cold reversal during last deglaciation. Science *293*, 2074–2077 (2001)

Wolff, E., Kull, C., Chappellaz, J., Fischer, H., Miller, H., Stocker, T. F., Watson, A. J., Flower, B., Joss, F., Köhler, P., Matsumoto, K., Monnin, E., Mudelsee, M., Paillard, D., and Shackleton, N.: Modeling past atmospheric $CO_2$: Results of a challenge. Eos *86*, 341–345 (2005)

Dr. Didier Paillard
Laboratoire des Sciences du Climat et
de l'Environnement
Orme des Merisiers
Centre de Saclay
91191 Gif-sur-Yvette
France
Phone: +33 1 69089467
Fax: +33 1 69087716
E-Mail: didier.paillard@lsce.ipsl.fr

Nova Acta Leopoldina NF *121*, Nr. 408, 183–186 (2015)

# Model-Based Reconstruction of the Marine Carbon Cycle during the Last Glacial Maximum

André Paul, Takasumi Kurahashi-Nakamura,
Stefan Mulitza, and Michael Schulz (Bremen)

With 1 Figure

Based on sediment data for the Atlantic Ocean during the Last Glacial Maximum (LGM, 19 to 23 thousand years before present [ka BP]) it has been suggested that the analogue of modern North Atlantic Deep Water (NADW) was shallower than today (Duplessy et al. 1988, Labeyrie et al. 1992, Sarnthein et al. 1994 – but compare to Gebbie 2014). However, no firm conclusion has been reached yet regarding the strength of the ventilation of the deep Atlantic Ocean during this time period: Was it weaker, as strong as today or even stronger? A reliable reconstruction of the ocean state during the LGM is important because it forms the initial conditions for the sequence of changes in the climate and the carbon cycle during the last deglaciation and until today.

In order to produce a quantitative reconstruction of the global ocean state during the LGM, we combine the sediment data with a numerical model and apply data assimilation methods that allow to systematically (or even automatically) vary selected model parameters in order to minimize the misfit between the data and the model (cf. Kurahashi-Nakamura et al. 2014). The sediment data that we consider are carbon isotopic ratios $^{13}C/^{12}C$ ($\delta^{13}C$) and $^{14}C/^{12}C$ ($\Delta^{14}C$) of fossil shells of benthic foraminifera, from which we can estimate water properties such as the carbon isotopic ratios of dissolved inorganic carbon ($\delta^{13}C_{DIC}$ and $\delta^{14}C_{DIC}$).

We apply the MIT general circulation model (MITgcm, Marshall et al. 1997, http://mitgcm.org/) in two different configurations with either a simplified parameterization of $\delta^{13}C_{DIC}$ for the abyssal ocean (valid for depths larger than 1000 m, cf. Marchal and Curry 2008), or an implementation of $\delta^{13}C_{DIC}$ and $\delta^{14}C_{DIC}$ based on the MITgcm carbon cycle component (the so-called "DIC package", Dutkiewicz et al. 2005a, b). The more complex model includes fractionation processes during photosynthesis and air-sea gas exchange. It is furthermore fitted with additional passive tracers such as iron (which serves as a micronutrient), radiocarbon and ideal age. Surface boundary conditions for the LGM are derived from a coupled atmosphere-ocean general circulation model (Merkel et al. 2010).

For the modern ocean, we use the corrected GEOSECS data (Kroopnick 1983, 1985), pre-WOCE (World Ocean Circulation Experiment) surface $\delta^{13}C_{DIC}$ by Gruber and Keeling (2001) and a recent compilation of data from the WOCE/GLODAP era by Schmittner et al. (2013). For the LGM ocean, we employ the compilation of benthic foraminiferal $\delta^{13}C$ data by Hesse et al. (2011).

In comparing the model output to the sparse and partly noisy modern and paleo data, we take special care and aim at avoiding any kind of interpolation (cf. Guiot et al. 1999).

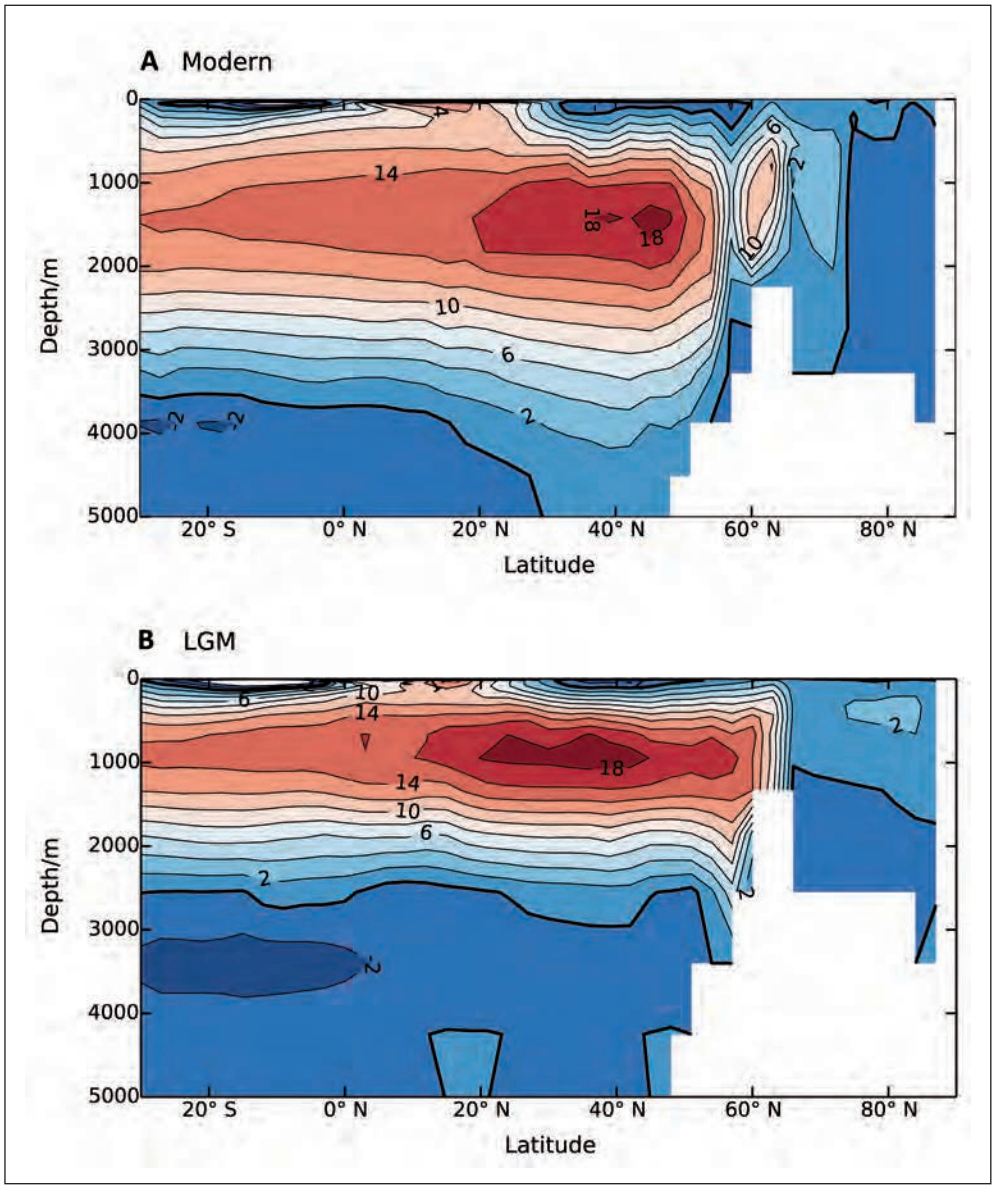


Fig. 1 Atlantic meridional overturning circulation visualized in terms of a streamfunction (in units of Sv, 1 Sv = $10^6$ $m^3$ $s^{-1}$) for (*A*) the optimized modern and (*B*) the optimized LGM ocean states. Positive values denote clockwise, negative values anti-clockwise circulation.

We test the sensitivity of the carbon isotope distributions to the formulation of fractionation during photosynthesis and check the model results against the data for the modern ocean (surface and deep $\delta^{13}C_{DIC}$ and radiocarbon). Using the simplified parameterization of $\delta^{13}C_{DIC}$, we demonstrate that we can successfully fit the MITgcm to the modern as well as the LGM data, obtaining a mean residual of 0.31 ‰ for the optimized modern ocean state and 0.28 ‰ for the optimized LGM ocean state. Comparing the LGM to the modern state, our results point to a shallower (by more than 500 m) NADW (in contrast to Gebbie 2014) and a ventilation of the deep Atlantic Ocean of similar strength (Fig. 1, cf. Huang et al. this volume).

## *References*


Duplessy, J. C., Shackleton, N. J., Fairbanks, R. G., Labeyrie, L., Oppo, L., Kallel, D., and Kallel, N.: Deepwater source variations during the last climatic cycle and their impact on the global deepwater circulation. Paleoceanography *3*, 343–360 (1988)

Dutkiewicz, S., Sokolov, A., Scott, J., and Stone, P.: A three-dimensional ocean-seaice-carbon cycle model and its coupling to a two-dimensional atmospheric model: uses in climate change studies. Report No. *122*, MIT Joint Program of the Science and Policy of Global Change, Cambridge, MA, http://globalchange.mit.edu/files/document/MITJPSPGC_Rpt122.pdf, 2005 (2005a)

Dutkiewicz, S., Follows, M. J., and Parekh, P.: Interactions of the iron and phosphorous cycles: A three-dimensional model study. Global Biogeochem. Cycles *19*, GB10121; doi:10.1029/2004GB002342 (2005b)

Gebbie, G.: How much did Glacial North Atlantic Water shoal? Paleoceanography *29*, 190–209; doi:10.1002/2013PA002557 (2014)

Gruber, N., and Keeling, C. D.: An improved estimate of the isotopoc air-sea disequilibrium of $CO_2$: Implications for the oceanic uptake of anthropogenic $CO_2$. Geophys. Res. Lett. *28*, 555–558 (2001)

Guiot, J., Boreux, J. J., Braconnot, P., and Torre, T.: Data-model comparison using fuzzy logic in paleoclimatology. Clim. Dynam. *15*, 569–581 (1999)

Hesse, T., Butzin, M., Bickert, T., and Lohmann, G.: A model-data comparison of $\delta^{13}C$ in the glacial Atlantic Ocean. Paleoceanography *26*, PA3220; doi:10.1029/2010PA002085 (2011)

Huang, E., Skinner, L. C., Mulitza, S., Paul, A., and Schulz, M. (this volume): Radiocarbon distribution and radiocarbon-based circulation age of the Atlantic Ocean during the Last Glacial Maximum.

Kroopnick, P. M.: The distribution of C-13 in the dissolved carbon dioxide of the ocean. Corrected data set (appendix). Exxon Production Research Company, PO Box 2189, Houston, Texas 77001, USA (1983)

Kroopnick, P. M.: The distribution of $^{13}C$ of $\Sigma CO_2$ in the world oceans. Deep-Sea Res. *32*, 57–84 (1985)

Kurahashi-Nakamura, T., Losch, M., and Paul, A.: Can sparse proxy data constrain the strength of the Atlantic meridional overturning circulation? Geoscientif. Model Developm. *7*, 419–432 (2014)

Labeyrie, L. D., Duplessy, J. C., Duprat, J., Juillet-Lekclerc, A., Moyes, J., Michel, E., Kallel, N., and Shackleton, N. J.: Changes in the vertical structure of the North Atlantic Ocean between glacial and modern times. Quat. Sci. Rev. *11*, 401–413 (1992)

Marchal, O., and Curry, W. B.: On the abyssal circulation in the glacial Atlantic. J. Phys. Oceanogr. *38*, 2014–2037; doi:10.1175/2008JPO3895.1 (2008)

Marshall, J., Adcroft, A., Hill, C., Perelman, L., and Heisey, C.: A finite-volume, incompressible Navier Stokes model for studies of the ocean on parallel computers. J. Geophys. Res. *102*, 5753–5766; doi:10.1029/96JC02775 (1997)

Merkel, U., Prange, M., and Schulz, M.: ENSO variability and teleconnections during glacial climates. Quat. Sci. Rev. *29*, 86–100 (2010)

Sarnthein, M., Winn, K., Jung, S. J. A., Duplessy, J. C., Labeyrie, L., Erlenkeuser, H., and Ganssen, G.: Changes in east Atlantic deepwater circulation over the last 30,000 years: Eight time slice reconstructions. Paleoceanography *9*, 209–267 (1994)

Schmittner, A., Gruber, N., Mix, A. C., Key, R. M., Tagliabue, A., and Westberry, T. K.: Biology and air sea gas exchange controls on the distribution of carbon isotope ratios ($\delta^{13}C$) in the ocean. Biogeosciences *10*, 5793–5816; doi:10.5194/bg-10-5793-2013 (2013)

Dr. André Paul
MARUM – Center for Marine Environmental Sciences
and Faculty of Geosciences
University of Bremen
PO Box 330 440
28334 Bremen
Germany
Phone: +49 421 21865450
Fax: +49 421 2189865450
E-Mail: apaul@marum.de

Nova Acta Leopoldina NF *121*, Nr. 408, 187–190 (2015)

# Signals of $CO_2$ Destratification from Boron Isotopes

James W. B. Rae,[1] Gavin L. Foster,[2] Laura F. Robinson,[3] Andy Ridgwell,[4] and Jess F. Adkins[5]

With 2 Figures

The size and tempo of deglacial $CO_2$ rise requires $CO_2$ to be released form the deep ocean to the atmosphere (Broecker 1982, Sigman and Boyle 2000). Records of deep-ocean $CO_2$ chemistry should thus offer a counterpart to the ice core records of the atmosphere, and may allow us to constrain the source of the $CO_2$ and the mechanisms of its release.

Here we present records of deep ocean carbonate chemistry using the boron isotope composition of benthic foraminifera (Rae et al. 2011) and deep-sea corals (Anagnostou et al. 2012, McCulloch et al 2012). The boron isotope proxy takes advantage of the pH dependent speciation of boric acid and borate ion, the isotope fractionation between these molecules, and the observation that only the borate ion is incorporated into growing marine carbonates (Hemming and Hanson 1992, Fig. 1). As a result the boron isotope composition of marine carbonates can act as a proxy for the pH of the ocean water in which they grew (Hönisch and Hemming 2005, Foster 2008, Henehan et al. 2013).

pH is only one parameter of the ocean carbonate system, a full determination of which requires 2 parameters to be known. However pH – and $\delta^{11}B$ of borate – is extremely closely linked with $[CO_2]$ and $[CO_3^{2-}]$, and all of these parameters are controlled (at a given temperature, salinity, and pressure) by the ratio of the two master variables, alkalinity (ALK) and dissolved inorganic carbon (DIC). Thus we can use $\delta^{11}B$ data to constrain deglacial changes in the characteristics of the carbonate system.

The simplest change in deep ocean carbonate chemistry expected over the deglaciation is loss of DIC to the atmosphere. In the absence of other processes, this should raise deep ocean pH and $[CO_3^{2-}]$. However, it is unlikely that DIC loss occurred in isolation, and other processes may also affect the ocean carbonate system. Thus, although knowledge of the carbonate chemistry of the deep ocean will help inform us about the mechanisms taking place during ocean-atmosphere $CO_2$ exchange, we shouldn't expect deep ocean $\delta^{11}B$ records to be a simple mirror image of the ice cores.

1 Department of Earth and Environmental Sciences, University of St Andrews, St Andrews, United Kingdom.
2 Ocean and Earth Science, National Oceanography Centre Southampton, University of Southampton, Southampton, United Kingdom.
3 School of Earth Sciences, University of Bristol, Bristol, United Kingdom.
4 School of Geographical Sciences, University of Bristol, Bristol, United Kingdom; Department of Earth Sciences, University of California at Riverside, Riverside, CA, USA.
5 California Institute of Technology, MC 131-24, Pasadena, CA, USA.

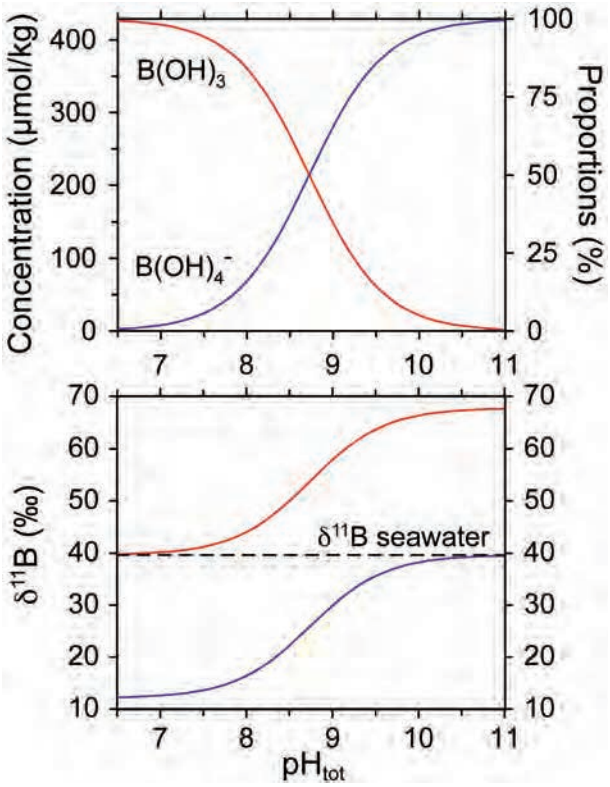


Fig. 1 The boron isotope proxy for pH. The proportion of the two molecular species of boron in seawater, boric acid and the borate ion, varies as a function of pH (*top panel*). As there is a significant isotopic fractionation between these species and the sum of their isotopes must give $\delta^{11}B$ of seawater, the isotopic composition of either species is a function of pH (*bottom panel*).

Despite the potential for different controls on deep $CO_2$ chemistry, our $\delta^{11}B$ record from deep-sea corals at mid-depths of the Drake Passage shows a pattern of pH change remarkably similar to what might be predicted from simple conceptual models. During the LGM these sites are bathed in low pH waters, show high pH excursion during the deglaciation, and recover to intermediate pH values in the Holocene. This is consistent with increased DIC storage at these depths during the LGM, $CO_2$ loss to the atmosphere over the deglaciation, and recovery *via* carbonate compensation, which acts as a net sink of ALK/DIC.

Deep ocean (>3000 m) $\delta^{11}B$ records show a more unexpected story. At three different sites – two in the deep Southern Ocean, and one in the deep North Pacific (Rae et al. 2014) – we observe excursions to low pH during intervals of $CO_2$ rise in HS1 and the YD. These signals cannot be explained with simple models of DIC loss, nor by changes in productivity or burial of $CaCO_3$. Notably, however, these pH minima occur at times of increased ventilation, as indicated by local changes in $^{14}C$ (Skinner et al. 2010, Rae et al. 2014). εNd data in our S Atlantic cores indicate that these ventilation changes are unlikely to be driven by input of water masses of

different provenance (see also Skinner et al. 2013). Instead, the change in $^{14}C$ at similar εNd indicates that the $\delta^{11}B$ data are more likely explained by mixing of carbon-rich waters through the Southern Ocean water column.

Despite the fact that deep Southern Ocean waters show a decrease in pH during intervals of $CO_2$ rise this does not preclude them from being a significant source of $CO_2$. It merely means that the signal of DIC loss is overcome by the mixing in of low-pH waters from other depths in the water column. Loss of DIC from deep waters is indeed reflected in a rapid rise in pH at the end of the mixing episode: once low-pH waters stop being transferred to depth, the removal of $CO_2$ from these deep waters allows them to recover to higher pH values than before these events.

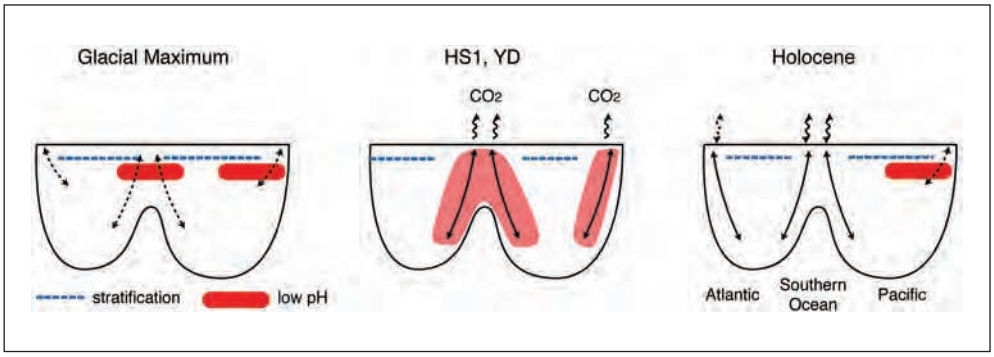


Fig. 2 Cartoon of stratification and pH at the LGM, during periods of deglacial $CO_2$ rise, and in the Holocene. In a stratified water column, low-pH waters are found at intermediate depths, due to remineralization of organic carbon to DIC. Upon destratification, these low-pH waters will be mixed throughout the water column. This may explain the low-pH excursions seen in our deep ocean $\delta^{11}B$ records during times of $CO_2$ rise, and the corresponding increase in $\delta^{11}B$ seen at mid depths.

## *References*

Anagnostou, E., Huang, K. F., You, C. F., Sikes, E. L., and Sherrell, R. M.: Evaluation of boron isotope ratio as a pH proxy in the deep sea coral Desmophyllum dianthus: Evidence of physiological pH adjustment. Earth Planet. Sci. Lett. *349*/350, 251–260 (2012)

Broecker, W. S.: Glacial to interglacial changes in ocean chemistry. Progr. Oceanogr. *11*, 151–197 (1982)

Burke, A., and Robinson, L. F.: The Southern Ocean's role in carbon exchange during the last deglaciation. Science *335*, 557–561 (2012)

Foster, G.: Seawater pH, $pCO_2$ and $[CO_3^{2-}]$ variations in the Caribbean Sea over the last 130 kyr: A boron isotope and B/Ca study of planktic foraminifera. Earth Planet. Sci. Lett. *271*, 254–266 (2008)

Haug, G. H., and Sigman, D. M.: Palaeoceanography: Polar twins. Nature Geosci. *2*, 91–92 (2009)

Hemming, N. G., and Hanson, G. N.: Boron isotopic composition and concentration in modern marine carbonates. Geochimica et Cosmochimica Acta *56*, 537–543 (1992)

Henehan, M. J., Rae, J. W. B., Foster, G. L., Erez, J., Prentice, K., Kucera, M., Bostock, H. C., Martinez-Boti, M. A., Milton, J. A., Wilson, P. A., Marshall, B., and Elliott, T.: Calibration of the Boron Isotope Proxy in the Planktic Foraminiferan *Golbigerinoides ruber* (d'Orbigny) for use in palaeo-$CO_2$ reconstruction. Earth Planet. Sci. Lett. *364*, 111–122 (2013)

Hönisch, B., and Hemming, N. G.: Surface ocean pH response to variations in $pCO_2$ through two full glacial cycles. Earth Planet. Sci. Lett. *236*/1, 2, 305–314 (2005)

McCulloch, M., Trotter, J., Montagna, P., Falter, J., Dunbar, R., Freiwald, A., Försterra, G., López Correa, M., Maier, C., Rüggeberg, A., and Taviani, M.: Resilience of cold-water scleractinian corals to ocean

acidification: Boron isotopic systematics of pH and saturation state up-regulation. Geochimica et Cosmochimica Acta *87*, 21–34 (2012)

Rae, J. W. B., Foster, G. L., Schmidt, D. N., and Elliott, T.: Boron isotopes and B/Ca in benthic foraminifera: Proxies for the deep ocean carbonate system. Earth Planet. Sci. Lett. *302*, 403 – 413 (2011)

Rae, J. W. B., Sarnthein, M., Foster, G. L., Ridgwell, A., Elliott, T., and Grootes, P.: Deepwater formation in the North Pacific and deglacial $CO_2$ rise. Paleoceanography *29*/6, 645 – 667 (2014)

Sigman, D. M., and Boyle, E. A.: Glacial/interglacial variations in atmospheric carbon dioxide. Nature *407*, 859 – 869 (2000)

Skinner, L., Fallon, S., Waelbroeck, C., Michel, E., and Barker, S.: Ventilation of the deep Southern Ocean and deglacial $CO_2$ Rise. Science *328*, 1147–1151 (2010)

Skinner, L. C., Scrivner, A. E., Vance, D., Barker, S., Fallon, S., and Waelbroeck, C.: North Atlantic versus Southern Ocean contributions to a deglacial surge in deep ocean ventilation. Geology *41*/6, 667–670 (2013)

Dr. James Rae
University of St Andrews
Department of Earth and Environmental Sciences
Irvine Building, Room 502
St Andrews, KY16 9AL, Scotland
UK
Phone: +44 1334 463910
Fax: +44 1334 463949
E-Mail: jwbr@st-andrews.ac.uk

Nova Acta Leopoldina NF *121*, Nr. 408, 191–193 (2015)

# The Ice Core Record of $CO_2$ – A Focus on the Climate/$CO_2$ Phase Relationship during Deglacial Transitions

Dominique Raynaud,[1] Frederic Parrenin,[1] Patricia Martinerie,[1] Jérôme Chappellaz,[1] and Amaelle Landais[2]

With 1 Figure

The Antarctic ice contains the purest and most direct record of past atmospheric $CO_2$ and can also provide a reliable record of Antarctic/austral high latitude temperature (see Jean Jouzel presentation). Ice cores drilled until now cover 800,000 years of history in Antarctica and allow us to better know glacial-interglacial cycles, which characterize this period. While the main driver of glacial-interglacial variations lies in changes in the Earth's orbit around the Sun, the response of the climate system involves interplay between changes in ice sheets, lands, oceans, and the atmosphere, modulating natural variations in greenhouse gas concentrations in the atmosphere. On the whole, Antarctic temperatures were warm during periods of high $CO_2$ concentrations and cold during periods of low $CO_2$ concentrations.

But this correlation does not allow us to disentangle the causal link between $CO_2$ and temperature: was it the greenhouse effect due to $CO_2$, which induced a warming, or was it the warming, which induced the increase in $CO_2$? A supplementary clue comes from the sequence of events between $CO_2$ and temperature. In particular, an essential prerequisite for understanding the role of atmospheric $CO_2$ during past deglacial transitions is to know its phase relationship with climate.

The problem is not trivial because, while Antarctic temperatures are recorded at the surface of ice sheets, atmospheric gases such as $CO_2$ are trapped at about 100 m depth – depending on site conditions – at the base of the firn where the bubbles close off, this depth being dependent of past climatic conditions. Monnin et al. (2001), using a model of this lock-in depth during the past, concluded that $CO_2$ had started to rise 800 ± 600 years after Antarctic temperature (as deduced from the EDC deuterium record) at the end of the last ice age. This result, which is in agreement with an earlier study on the Vostok and Taylor Dome ice cores, could support a scenario where the initial release of $CO_2$ into the atmosphere has been a consequence of the initial warming at high southern latitudes.

Parrenin et al. (2013) have revised this $CO_2$/Antarctic temperature lead/lag estimate by inferring the air lock-in depth from isotope 15 of nitrogen in air bubbles, which is enriched proportionally to the firn thickness. They also applied an innovative statistical method to

1 Laboratoire de Glaciologie et Géophysique de l'Environnement (LGGE), Le Centre National de la Recherche Scientifique (CNRS) / Université Joseph Fourier (UJF), Grenoble, France.

2 Institut Pierre Simon Laplace (IPSL), Laboratoire des Sciences du Climat et de l'Environnement (LSCE), Commissariat à l'énergie atomique et aux énergies alternatives (CEA) – Le Centre National de la Recherche Scientifique (CNRS) – l'Université de Versailles Saint-Quentin (UVSQ), Gif-sur-Yvette, France.

determine the Antarctic temperature and its lead/lag to $CO_2$. They determined that $CO_2$ and Antarctic temperature increased at the same time at the end of the last ice age, within 200 years (Fig. 1). This finding now makes it likely that $CO_2$ was responsible, at least partly, of the Antarctic warming at the end of the last ice age. New data and climate model experiments are necessary to disentangle the different contributors of this past natural global warming.

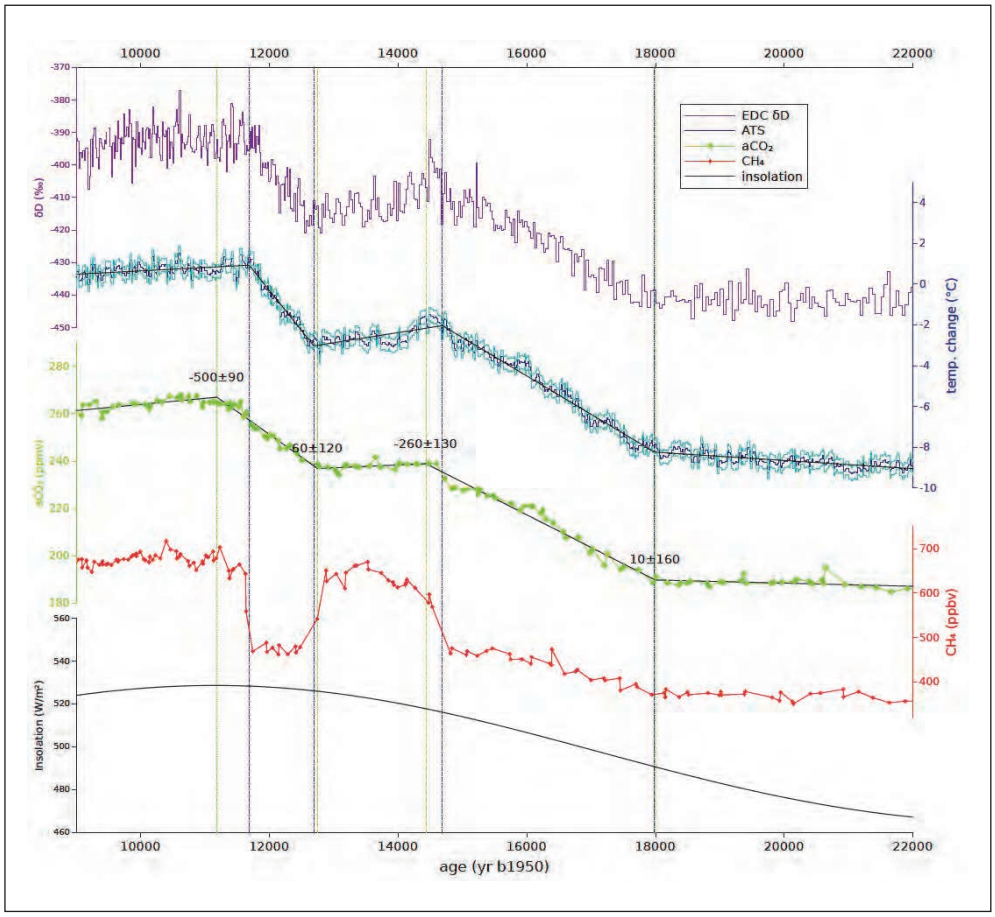


Fig. 1 Various climatic time series over termination 1. *From top to bottom*: δD from EDC (purple); Stack Antarctic temperature (dark blue); Atmospheric $CO_2$ concentrations (light green); Atmospheric $CH_4$ (taken as a proxy for Northern Hemisphere climate, red); Summer insolation (65°N, black) (adapted from Parrenin et al. 2013).

Landais et al. (2013) also investigated the changes in $CO_2$ and Antarctic temperature during transition T2, the previous glacial-interglacial transition, roughly 136 ka ago. They found that $CO_2$ and Antarctic temperature started increasing in phase around 136 ka ago but they also found a two-phase change in $CO_2$, Antarctic temperature and global climate during the course of the deglaciation.

Finally, when interpreting the ice core $CO_2$ records in terms of atmospheric trends we should take into account the fact that a significant smoothing effect of the initial atmospheric signal can occur when the atmospheric perturbation occurs at the same time scale as the gas trapping duration at the base of the firn. This is likely the case for the four events occurring during the last glacial-interglacial transition, T1 (Fig. 1). We are now trying to quantify their corresponding smoothing effect and we hope to be able to present the results during the symposium.

## *References*

Landais, A., Dreyfus, G., Capron, E., Jouzel, J., Masson-Delmotte, V., Roche, D. M., Prié, F., Caillon, N., Chappellaz, J., Leuenberger, M., Lourantou, A., Parrenin, F., Raynaud, D., and Teste, G.: Two-phase change in $CO_2$, Antarctic temperature and global climate during termination II. Nature Geosci. *6*, 1062–1065, 10.1038/NGEO1985 (2013)

Monnin, E., Indermühle, A., Dällenbach, A., Flückiger, J., Stauffer, B., Stocker, T. F., Raynaud, D., and Barnola, J.-M.: Atmospheric $CO_2$ concentrations over the last glacial termination. Science *291*, 112–114 (2001)

Parrenin, F., Masson-Delmotte, V., Köhler, P., Raynaud, D., Paillard, D., Schwander, J., Barbante, C., Landais, A., Wegner, A., and Jouzel, J.: Synchroneous change of atmospheric $CO_2$ and Antarctic temperature during the deglacial warming. Science *339*, 1060–1063 (2013)

Dr. Dominique Raynaud
Laboratoire de Glaciologie et Géophysique de l'Environnement
54, rue Molière
BP 96
38402 Saint-Martin d'Hères cedex
France
Phone: +33 4 76824252
Fax: +33 4 76824201
E-Mail: raynaud@lgge.obs.ujf-grenoble.fr

Nova Acta Leopoldina NF *121*, Nr. 408, 195–196 (2015)

# Are the Drabbest Proxies the 'Best'? Patterns of Bulk $CaCO_3$ and Glacial Carbon Storage

Andy Ridgwell (Bristol, UK)

With 1 Figure

Despite the proliferation of increasingly fancy paleoceanographic proxies over the past decade or so, our 'best' (most informative) single source of information regarding the past state of the global carbon cycle is arguably the observed distribution and temporal change in $CaCO_3$ preserved in open ocean marine sediments (Fig. 1). The preservation of biogenic $CaCO_3$ deposited to the seafloor sensitivily depends on the overlying carbonate ion concentration ($[CO_3^{2-}]$), which we would like to know from a glacial $CO_2$ perspective, and ocean floor depth, which fortunately does not change with time at any great rate. $[CO_3^{2-}]$, in turn, tells us something of the circulation of the deep ocean in addition to the overlying DIC and ALK concentrations (and hence carbon storage). In combination with relatively 'pure' (fancy) tracers of ocean circulation such as $^{144}Nd$, plus gradients in benthic $\delta^{13}C$ that reflects circulation as well as enhancement in DIC due to the action of the biological pump, it should in theory be possible to extract deep ocean $CO_2$ storage from wt% $CaCO_3$ (3 proxies and 3 variables). (?) Conversely, the relative data-richness of available wt% $CaCO_3$ and $\delta^{13}C$ observations might helpfully (statistically) be employed to fill in the gaps of the sparser but fancier $^{144}Nd$. $CaCO_3$ preservation, however, also depends on the total flux of $CaCO_3$ and POC, which is less convenient from a number of free parameters perspective, although these are both variables of glacial-interglacial carbon cycle change we would also like to know more about. If it were possible also to solve for the $CaCO_3$ and POC fluxes consistent with wt% $CaCO_3$ we would have most of the glacial $CO_2$ picture.

The potential of extensive and mature datasets such as of wt% $CaCO_3$ seems obvious, which begs the question of why it has not been more frequently and critically used to understand the glacial state. One does, however, need to be able to achieve a reasonable spatial resolution and distribution of sediment composition in a numerical model to quantitatively assimilate the data and hence likely requiring a 3D ocean circulation based model. The computational expense associated with a typical ~20–50 ka equilibrium time of deep-sea sediment composition is then partly the reason why (the other being researcher seduction by the newer proxies). An equilibrium time comparable to or exceeding the transition time between different Marine Isotope Stages then raises the question of just how representative either late Holocene or peak LGM data time-slice (Fig. 1) really are in the first place. More likely is that lower wt% and low accumulation rate sites are relatively close to equilibrium with respect to the ocean at the nominal time-slice age, whilst higher wt% locations are less so. One way forward is to run a model dynamically forward in time and characterize the time-response of

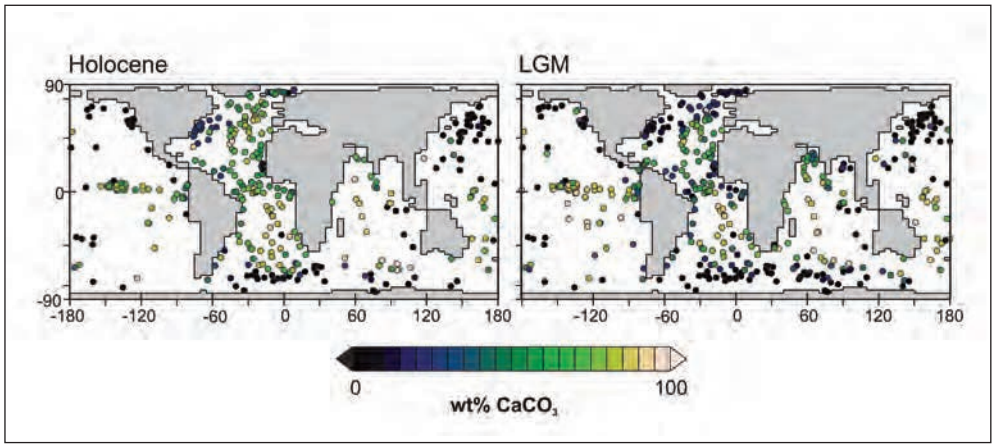


Fig. 1 Core-top (~Holocene) and LGM age observations of the global distribution of wt% $CaCO_3$ in marine sediments (Archer 1996, Catubig et al. 1998)

marine sediment composition and particularly of wt% $CaCO_3$ to quantify the degree to which different sedimentary environments record the overlying environment. At the same time, by incorporating a tracer of 'time' in the sediments, such as $\Delta^{14}C$ or $\delta^{18}O$, one can elucidate the degree to which sediment 'age' is even synchronous with the ocean. The lower wt% sites whose bulk composition better reflects time-variations in ocean chemistry may then turn out to fail to record time adequately.

So this is what I shall present – an Earth system model ('cGENIE') based exploration of the spatial and temporal dynamics of our 'best' proxy for glacial-interglacial changes in the global carbon cycle – wt% $CaCO_3$.

## *References*

Archer, D.: An atlas of the distribution of calcium carbonate in sediments of the deep sea. Global Biogeochem. Cycles *10*/1, 159–174 (1996)

Catubig, N. R., Archer, D. E., Francois, R., deMenocal, P., Howard, W., and Yu, E.-F.: Global deep-sea burial rate of calcium carbonate during the last glacial maximum. Paleoceanography *13*/3, 298–310; doi:10.1029/98PA00609 (1998)

Prof. Andy Ridgwell, Ph.D.
School of Geographical Sciences
University of Bristol
Office G10aN
University Road
Clifton, Bristol, BS8 1SS
UK
Phone: +44 117 9546858
Fax: +44 117 9287878
E-Mail: andy@seao2.org

Department of Earth Sciences
University of California at Riverside
900 University Ave
Riverside CA 92521
USA

Nova Acta Leopoldina NF *121*, Nr. 408, 197–200 (2015)

# Benthic $^{14}C$ Ventilation Ages Record Changing Storage of Dissolved Inorganic Carbon in the Abyssal Ocean

Michael Sarnthein ML,[1] Pieter M. Grootes,[2] Birgit Schneider,[1] and Klaus Wallmann[3] (Kiel)

With 3 Figures

As widely agreed, the abyssal ocean absorbed large quantities of atmospheric and terrestrial carbon during the Last Glacial Maximum (LGM). Past changes in the carbon uptake of the deep ocean were linked to various factors, in particular, to the transit time of ocean deep waters. The (apparent) $^{14}C$ ventilation age ($\Delta\Delta^{14}C$) of *modern* ocean waters below 2000 m depth directly parallels the concentration of dissolved inorganic carbon (DIC) (Fig. 1*A*) (Sarnthein et al. 2013). Modern $^{14}C$ ventilation ages increase from about 600 up to 2400 $^{14}C$ year with increasing distance from the deep water source. This aging of deep waters by 1800 $^{14}C$ year matches an increase by 230 mmol DIC/kg $H_2O$ at the terminus of the 'global conveyor belt' in the Pacific, on average 1.22 mmol DIC/kg per 1 ‰ decrease in $\Delta\Delta^{14}C$. In view of the deep-ocean volume >2000 m w.d., which represents ~50 % of the total ocean, an average concentration of 1 mmol DIC/kg corresponds to 8.5 Gt C (Amante and Eakins 2009, and GLODAP data). Hence the regression slope of Figure 1*A* implies that the modern abyssal ocean is receiving ~1.1 Gt C per $^{14}C$ year deep water transit time (Fig. 2).

Modern $\Delta\Delta^{14}C$ distributions of the four largest ocean basins show regression slopes that vary from –1.27 to –1.49 mmol DIC/kg per ‰ $\Delta\Delta^{14}C$ (Fig. 1*B*). Only the data from the northwestern Indian Ocean and the Pacific sector of the Southern Ocean deviate from this general trend, presumably because of aberrant local export productivity and carbon fluxes. Thus, most regression slopes are comparable over most parts of the modern ocean, despite different water mass conversion and circulation conditions in the different ocean basins. On the basis of this general homogeneity Sarnthein et al. (2013) proposed as a working hypothesis that the modern regression of DIC *vs*. $\Delta\Delta^{14}C$ may be long-term persistent over glacial-to-interglacial times and also incorporate the LGM slope variability. The hypothesis included various tacit assumptions: (*i*) The LGM overall geometry of thermohaline overturning circulation was basically similar to today, although AABW had likely expanded in the bottommost ocean during glacial times. (*ii*) The NADW and AABW in the Southern Ocean do not differ significantly in terms of the DIC/$\Delta\Delta^{14}C$ relationship, since AABW consists largely of 'recycled' NADW. (*iii*) Global export production was widely constant (Sigman and Boyle 2000), thus decoupled from the transit time of ocean overturning circulation, and (*iv*) ocean intermediate

1 Institute for Geosciences, University of Kiel, Olshausenstraße 40, 24098 Kiel, Germany.
2 Institute of Ecosystem Research, University of Kiel, Olshausenstraße 40, 24098 Kiel, Germany.
3 GEOMAR Helmholtz Centre for Ocean Research Kiel, Wischhofstraße 1–3, 24148 Kiel, Germany.

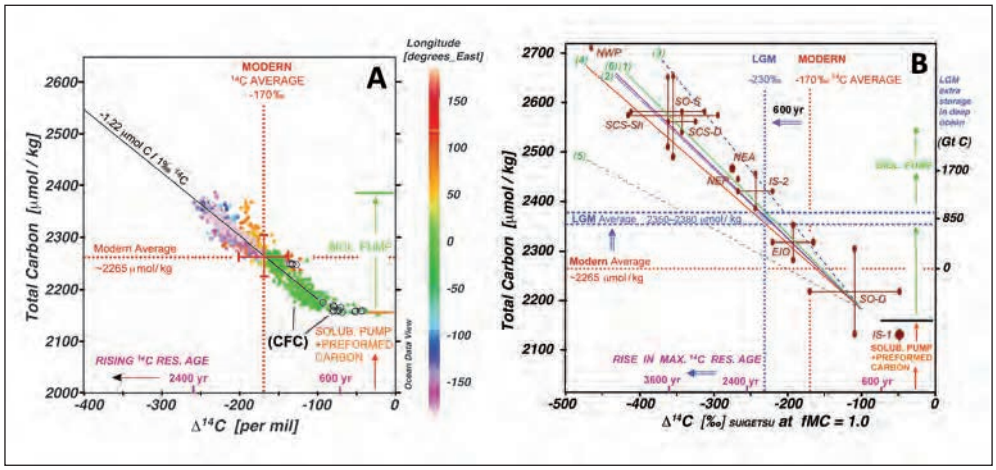


Fig. 1 (*A*) Ratio of total dissolved inorganic carbon (DIC) per kg *vs*. benthic $\Delta_{paleo}{}^{14}C$ and $^{14}C$ ventilation age for Fraction of modern carbon (fMC) = 1 of ocean waters below >2000 m w. d. (Sarnthein et al. 2013). Modern, volumetrically unweighted GLODAP data (Key et al. 2004) for longitudes of the Atlantic (green), the western (orange) and eastern Indian Ocean and Pacific (pink and blue). Standard deviation is ±32.8 ‰ for $\Delta^{14}C$ and ±40.2 µmol/kg for DIC. Black open circles mark deep waters with chlorofluorocarbon (CFC) concentrations >0.1 pmol/kg as tracer of modern anthropogenic influence in the northern North Atlantic and Weddell Sea Bottom Water (orange dots). Modern ventilation ages of 600 to 2400 $^{14}C$ years average at 1500 $^{14}C$ years = –170 ‰ $\Delta^{14}C$. (*B*). LGM regional estimates and LGM variability ranges of DIC – $\Delta^{14}C$ and age ratio (red oval dots) constrained for several ocean key regions: EIO = Eastern Indian Ocean; IS-1 = Icelandic Sea Mode 1; IS-2 = Icelandic Sea Mode 2; NEA = Northeast Atlantic; NEP = Northeast Pacific; NWP = Northwest Pacific; SCS-S = shallow South China Sea; SCS-D = deep South China Sea; SO-D = deep Southern Ocean; SO-S = shallow Southern Ocean (Sarnthein et al. 2013). Estimates were calculated using the assumption of stable regional regression slopes (compare Fig. 3). Green numbers at upper left refer to the Atlantic (1), Southern Ocean (Atlantic and Indian sectors) (2), western Indian Ocean (3), eastern Indian Ocean (4), Southern Ocean (Pacific sector) (5), and Pacific (6). Regression slopes are –1.49 µmol/kg/$\Delta^{14}C$ (1), –1.43 µmol/kg/$\Delta^{14}C$ (2), –1.87 µmol/kg/$\Delta^{14}C$ (3), –1.27 µmol/kg/$\Delta^{14}C$ (4), –0.79 µmol/kg/$\Delta^{14}C$ (5), –1.44 µmol/kg/$\Delta^{14}C$ (6). Following Fig. 1*A*, $\Delta^{14}C$ values for intra-LGM age differences between atmosphere and deep water (= apparent benthic ventilation ages) and related DIC values are calculated for 'paleo' fraction of Modern Carbon (fMC) = 1. LGM ventilation ages show average end members of <500 $\Delta^{14}C$ years in the Icelandic Sea and ~3600 $^{14}C$ years in the Southern Ocean, 5000 $^{14}C$ years in the Northwest Pacific and result in an overall conservative arithmetic mean of 2100 $^{14}C$ years equal to –230 ‰ of fMC. Blue values (µmol/kg) show mean DIC contents of the deep ocean, estimated for a mean LGM ventilation age of 2100 $^{14}C$ years. Gt C scale at upper right labels total DIC mass in the LGM ocean, stored in addition to the modern 38,100 Gt DIC, with 1 µmol DIC/kg corresponding to 8.5 Gt C in the total ocean at >2000 m w.d.. Biol. Pump = 'Biological Pump', Solub. Pump = 'Solubility Pump'. Blue arrows display Holocene-to-LGM shifts.

waters comprise approximately the same volume as deep waters, hence form an integral part of the ocean carbon inventory, the magnitude of which may occasionally alternate with that of deep waters.

Wallmann (2014) and Wallmann et al. (ms subm. 2015) now generated a 24-box earth-system model which provides a first opportunity to test the outlined hypothesis of a largely persistent DIC *vs*. $\Delta\Delta^{14}C$ slope over glacial-to-inter–glacial times (Fig. 3). The output data modelled for modern deep water boxes closely match the values averaged for water samples from pertinent deep water boxes, since the model circulation was tuned until the tracer data of the ocean were closely reproduced. The tuned model produces a regression

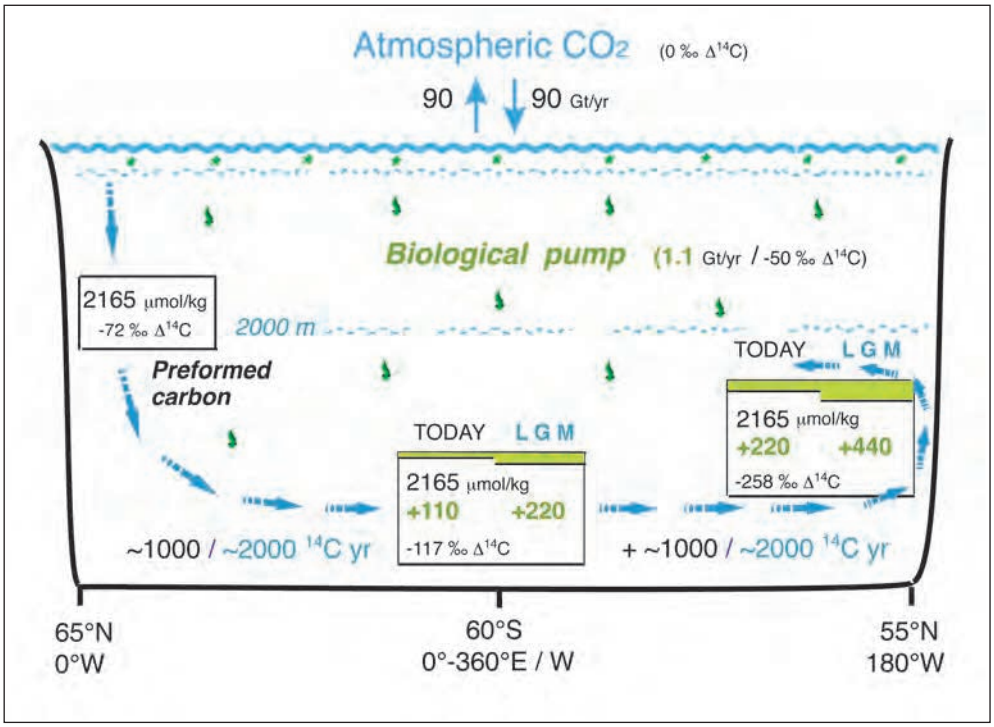


Fig. 2 Scheme of the carbon inventory of ocean deep water for modern and LGM times (Sarnthein et al. 2013). The $^{14}C$ ages and carbon contents are subject to a delicate balance between (*i*) the gradual aging of preformed carbon from the northern North Atlantic (black DIC values) up to the subpolar North Pacific and (*ii*) the incremental absorption of young biogenic organic and inorganic carbon (green DIC values) supplied by the biological pump from the sea surface. During the LGM the average transit time (blue age values) was prolonged, hence the global effect of the biological pump possibly doubled.

slope for the LGM that indeed comes close to the modern slope. This match fully confirms our hypothesis of a long-term largely persistent DIC *vs*. $\Delta\Delta^{14}C$ slope for the global ocean, that also applied for the LGM. It corroborates the value of benthic $^{14}C$ ventilation ages for quantifying oceanic carbon storage over time. The model also reveals a ~ –50-‰ shift in $\Delta^{14}C$ of the intercept with the DIC value determined by preformed carbon and solubility pump on the x-axis, which may suggest the influence of increased input of fossil carbonate dissolved in the deep ocean, in part possibly the result of reworked shelf carbonates during times of low sea level (Wallmann et al. ms subm. 2015). On the basis of this model test we feel encouraged to conclude that past changes in the $^{14}C$ transit time, that reflect changes in the circulation velocity of ocean deep waters (Fig. 2), were fully sufficient to accommodate more than the carbon released by the interglacial-to-peak glacial shift in atmospheric $CO_2$. Additional amounts of carbon were transferred from intermediate to deep ocean waters. In total, the mean DIC modelled for eleven LGM boxes lies near 2450 mmol/kg, that is consistent with 2350–2380 mmol/kg deduced from a fragmentary set of empiric data, which suggested a peak glacial carbon drawdown of ~850 Gt C into the abyssal ocean.

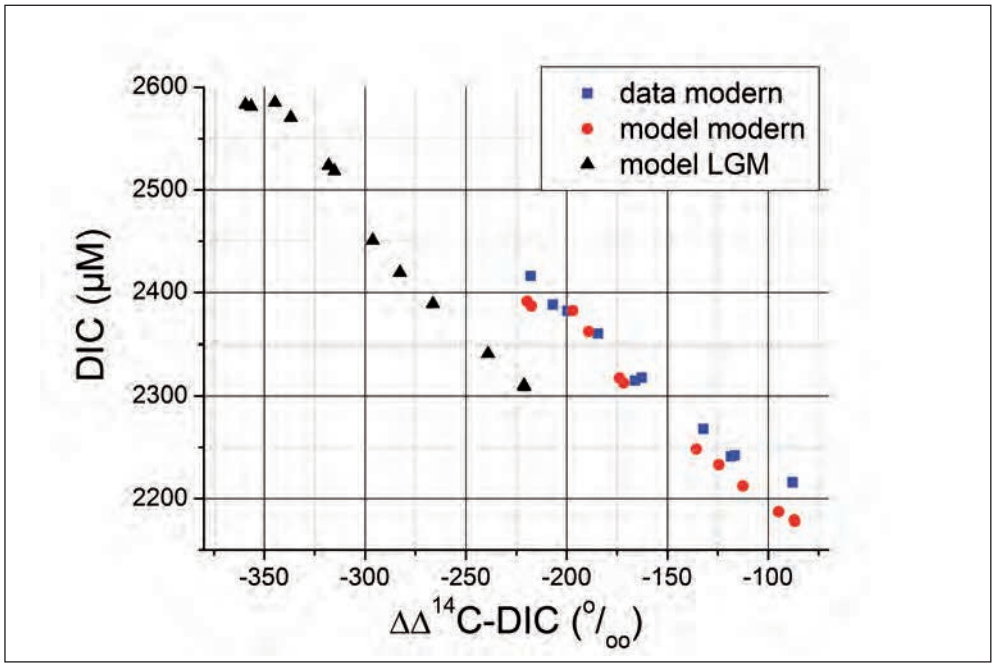


Fig. 3 DIC *vs*. difference between radiocarbon in seawater DIC and atmospheric $CO_2$ ($\Delta\Delta^{14}$C-DIC) at >2000 m water depth (Wallmann et al., subm. 2015). Different from the unweighted data in Fig. 1 (Sarnthein et al. 2013) the 'data' in this figure are weighted mean values for deep water and bottom water boxes derived from water column measurements, thus produce a different, that is, a steepened regression slope. LGM refers to model results at 21 ka BP.

## *References*

Amante, C., and Eakins, B. W.: ETOPO1 1 Arc-minute global relief model: Procedures, data sources and analysis. NOAA Techn. Memorandum NESDIS NGDC-24, 19 pp. (2009)

Key, R. M., Kozyr, A., Sabine, C. L., Lee, K., Wanninkhof, R., Bullister, J. L., Feely, R. A., Millero, F. J., Mordy, C., and Peng, T.-H.: A global ocean carbon climatology: Results from Global Data Analysis Project (GLODAP). Global Biogeochem. Cycles *18*, GB4031; doi:10.1029/2004GB002247 (2004)

Sarnthein, M., Schneider, B., and Grootes, P. M.: Peak glacial $^{14}$C ventilation ages suggest major draw-down of carbon into the abyssal ocean. Clim. Past *9*, 2595–2614; doi:10.5194/cp-9-1-2013 (2013)

Sigman, D. M., and Boyle, E.: Glacial/interglacial variations in atmospheric carbon dioxide. Nature *407*, 859–869 (2000)

Wallmann, K.: Is late Quaternary climate change governed by self-sustained oscillations in atmospheric $CO_2$? Geochimica et Cosmochimica Acta *132*, 413–439 (2014)

Wallmann, K., Schneider, B., and Sarnthein, M.: Effects of eustatic sea-level change on atmospheric $pCO_2$ and seawater composition over the last 130,000 years. Ms. subm. to Clim. Past Discuss. (2015)

Prof. Dr. Michael Sarnthein
Institute for Geosciences
University of Kiel
Olshausenstraße 40
24098 Kiel
Germany

Phone: +49 431 8802882
Fax: +49 431 8804376
E-Mail: ms@gpi.uni-kiel.de

Nova Acta Leopoldina NF *121*, Nr. 408, 201–206 (2015)

# Atmospheric $\delta^{13}CO_2$ from Ice Cores: An Overloaded Parameter

Jochen Schmitt, Sarah S. Eggleston, Fortunat Joos, and Hubertus Fischer (Bern, Switzerland)

With 2 Figures

$CO_2$ measurements on ice cores during the 1980s revealed for the first time that atmospheric $CO_2$ levels during the Last Glacial Maximum (LGM) were considerably lower than for the preindustrial Holocene (Neftel et al. 1982). Quickly, the paleo-community started an ongoing endeavour to explain the mechanisms behind the low glacial $CO_2$ levels and how the system returned to the interglacial state.

This presentation provides an overview how the stable carbon isotope composition of atmospheric $CO_2$ ($\delta^{13}C_{atm}$) contributed to this quest. It will be shown that $\delta^{13}C_{atm}$ can be a powerful parameter to differentiate between processes, if boundary conditions are well constrained or can at least assumed to be rather constant. The Holocene represents such a case of still manageable boundary conditions. Since a large suite of terrestrial and marine processes may affect $\delta^{13}C_{atm}$, it can quickly turn into an 'overloaded parameter' when applied to more complex settings. The transient and simultaneous sequence of processes during deglaciations as well as the low-frequency variations over the last 160 ka are examples, in which $\delta^{13}C_{atm}$ serves as an *inter alia* parameter to properly arrange the pieces of the carbon cycle puzzle.

Since the ocean is by far the largest reservoir capable to transferring sufficient carbon on timescales of millennia into the atmosphere, the processes in the ocean itself are on the top agenda to explain the glacial $CO_2$ level. Already in the late 1980s carbon isotope inventory changes of the global ocean based on benthic foraminifera indicated that the terrestrial carbon storage was reduced during the LGM (Duplessy et al. 1988). Consequently, a potential increase in the land carbon storage could already be ruled out to explain glacial $CO_2$ levels. Until then the key question has been where and by which processes the ocean stored the extra $CO_2$. Newer studies confirmed a whole-ocean $\delta^{13}C$ change of ~ 0.4 ‰ (Ciais et al. 2012). Like the ice core archive, marine sediment cores allow a large suite of parameters to be analysed. However, unlike the restricted geographical options of ice core drill sites, sediment cores have the advantage that they can be obtained, in principle, from any marine region and depth range.

Based on these rich archives and backed by the modelling community, an ever-increasingly detailed picture was drawn, the past circulation, the biogeochemical processes in the water column, and the terrestrial processes. Very early in this joint effort, $\delta^{13}C_{atm}$ was identified as a powerful parameter to constrain processes of the global carbon cycle (Friedli et al. 1984). To first order, each of the main active carbon reservoirs (dissolved inorganic carbon [DIC] in the ocean, organic carbon on land and in the ocean, atmospheric $CO_2$) has a distinct $\delta^{13}C$ signature. Organic carbon produced by terrestrial photosynthesis is ~ 20 ‰ lighter compared to

the atmosphere, which is itself ~ 7 ‰ lighter than the ocean DIC. The primary strength of the archive atmosphere (archived *via* firnification to glacier ice) lies in its integrating properties. The $CO_2$ exchange fluxes between the atmosphere, and both the surface ocean and the terrestrial biosphere are characterized by strong seasonal cycles superimposed by a large spatial heterogeneity. Atmospheric $CO_2$ integrates over any involved processes in space and time. The bubble enclosure process in polar firn columns leads to a further smoothing generating a signal of typically centennial means of southern hemispheric air. Pioneering studies revealed that $\delta^{13}C_{atm}$ varied during the Holocene and over the deglaciation and allowed for the first tentative interpretations on the causes of the observed $CO_2$ changes. For the Holocene $CO_2$ rise Indermühle et al. 1999 suggested that a climate induced change in the terrestrial carbon reservoir contributed in addition to marine processes. However, the measurement precision and temporal resolution achieved at that time allowed for neither a robust interpretation nor significant constraints of the temporal evolution of the processes (Broecker and Clark 2003). Incited by Broecker and Clark (2003), the ice-core community had to come up with better $\delta^{13}C_{atm}$ data. Only after major analytical hurdles were mastered, the Holocene $CO_2$ evolution could be revisited with a new $\delta^{13}C_{atm}$ record (Elsig et al. 2009). Based on this $\delta^{13}C_{atm}$ evolution and assumptions regarding the land carbon uptake during the deglaciation, the authors concluded that the early Holocene $CO_2$ drop was driven by land carbon uptake as evidenced by a $\delta^{13}C_{atm}$ rise. By contrast, the post-8000 year $CO_2$ rise cannot be explained by a corresponding release of isotopically light land carbon, but its origin lies more in the readjustment of the marine carbonate chemistry and coral reef formation. This finding supports marine studies proposing a reduction of the carbonate ion concentration (Broecker and Clark 2003), and thus conflicts with an extensive release of land carbon from early human activity (Ruddiman 2003). The study of Elsig et al. (2009) is a classic either-or example where $\delta^{13}C_{atm}$ served as a decisive parameter to discriminate among conflicting theories. This kind of 'double deconvolution' analysis was possible because the boundary conditions during the Holocene (ocean circulation, sea surface temperature, and general climate conditions) have not changed much. In contrast to the puzzling Holocene $CO_2$ rise, the route of interpretation of our follow-up study (Schmitt et al. 2012) reaching back to the LGM was different. There is consensus among modelling and proxy studies that during the deglaciation a suite of carbon cycle processes acted in conjunction and often with opposing $\delta^{13}C$ signs, ruling out single-type explanations (e. g. Köhler et al. 2005). Only the prominent early drop in $\delta^{13}C_{atm}$, associated with the $CO_2$ rise between 18 and 16 ka, could be safely associated with a net $CO_2$ outgassing from $CO_2$-oversaturated Southern Ocean water. Pointing to the synchronous rise in opal flux (Anderson et al. 2000), we implicitly suggested that a change in ocean dynamics caused both the $CO_2$ rise and the $\delta^{13}C_{atm}$ drop. Yet, from $\delta^{13}C_{atm}$ alone we cannot rule out an alternative scenario, where the Southern Ocean $CO_2$ outgassing results rather from a drop in dust-derived iron input. In this case, the surface ocean becomes $CO_2$-oversaturated with respect to the atmosphere as the biological pump driving the export production is iron limited (Martin 1990). In fact, Broecker and McGee (2013) correctly point to the fact that the drop in dust flux is coeval with at least the first $CO_2$ rise and the $\delta^{13}C_{atm}$ response of a reduced export production would be lighter $\delta^{13}C_{atm}$ values as well. In their summary on the challenges to interpret $\delta^{13}C_{atm}$ Broecker and McGee (2013) acknowledge that $\delta^{13}C_{atm}$ is still a key parameter, but if applied to the complex setting of glacial/interglacial $CO_2$ changes, the boundary conditions for $\delta^{13}C_{atm}$ have to be well quantified. One of these boundary conditions sketched in this "roadmap to interpret $\delta^{13}C_{atm}$" is the temperature field of the surface ocean. Due to the equilibrium fractionation during the air-sea gas exchange, atmospheric $CO_2$ becomes de-

pleted in the heavy carbon isotope by ~ 8 ‰ compared to DIC. Unfortunately, the fractionation factor is temperature dependent and decreases with temperature by ~ 0.1 ‰ per °C. As the transient $\delta^{13}C_{atm}$ changes over the deglaciation are only 0.3 ‰, a 3 °C SST change would already generate the same $\delta^{13}C_{atm}$ variability. To account for this temperature effect and thus "unload" the overloaded $\delta^{13}C_{atm}$ signal, Schmitt et al. (2012) applied a first-order correction using proxy SST reconstructions as used in BICYCLE (Köhler et al. 2005). The temperature correction lowers the $\delta^{13}C_{atm\ tcorr}$ signal for the Holocene by ~ 0.3 ‰, resulting in a Holocene level that is lower than that is seen in the LGM (Fig. 1). Note, in the original $\delta^{13}C_{atm}$ record the Holocene level is comparable to the LGM. In a next step we want to use the inferred changes in the land carbon stocks of ~ 300–700 PgC derived from the whole-ocean $\delta^{13}C_{DIC}$ change of 0.34 ‰ (Ciais et al. 2012). As the land biosphere took up 300–700 PgC after the LGM, all active carbon pools became heavier by 0.34 ‰. In other words, after accounting for temperature effects and land carbon storage we end up again with roughly comparable values for LGM and Holocene. Yet, the $\delta^{13}C_{atm}$ puzzle is not solved. During the LGM, the global ocean had to store more $CO_2$ (parts from the atmosphere and the land carbon change) in its interior rather than close to the surface to sustain low $pCO_2$ at the sea surface. In the modern ocean, this vertical DIC gradient is associated with a corresponding $\delta^{13}C_{DIC}$ gradient, i.e. deep water with remineralized organic carbon has lighter $\delta^{13}C_{DIC}$ than the DIC at the surface. Therefore, an increased carbon storage in the deep ocean during the LGM would have increased the vertical $\delta^{13}C_{DIC}$ gradient, thus leading to heavier $\delta^{13}C_{DIC}$ values at the sea surface. As the surface ocean $\delta^{13}C_{DIC}$ is tightly coupled with $\delta^{13}C_{atm}$, $\delta^{13}C_{atm}$ will follow and become heavier as well. During the deglaciation, the two prominent processes to explain a large part of the $CO_2$ rise – the increased Southern Ocean ventilation and the drop in export production due to reduced iron input – both decrease the vertical $\delta^{13}C_{DIC}$ gradient. Consequently, surface $\delta^{13}C_{DIC}$ and thus $\delta^{13}C_{atm}$ are then expected to be lighter during the Holocene. However, the Holocene $\delta^{13}C_{atm}$ is equal or even slightly heavier than during the LGM, pointing to a missing process, or badly constrained boundary conditions (Broecker and McGee 2013). Clearly, these rough estimates are meant for illustrative purposes only. Models of intermediate complexity have already been applied to this kind of problem set (e.g. Menviel et al. 2012) and are covered in detail in this Volume (e.g. Joos et al., Köhler et al.).

While the carbon cycle processes discussed above already provide a challenge for the paleo-community, interpretations using $\delta^{13}C_{atm}$ on longer timescales require yet additional processes to be included. As shown in Figure 2, the mean levels for MIS 6 and the LGM are markedly different, which is mirrored by the subsequent interglacials Holocene and MIS 5.5 as well (Lourantou et al. 2010, Schneider et al. 2013). One could try explain the 0.4 ‰ lighter $\delta^{13}C_{atm}$ values for the MIS 6/5 interval within the frame of the already discussed processes. Yet, there is little evidence in the records to propose e.g. major differences in ocean circulation or SST between MIS 6 and 2 to explain the 0.4 ‰ offset. Rather, it is more likely that the carbon isotopic composition of the entire marine carbon pool drifted towards heavier values over the last 160 ka as indicated in marine compilations (Oliver et al. 2010). In fact, the mean residence time of carbon in the global ocean is on the order of the duration of a glacial cycle. The main carbon fluxes into the atmosphere-ocean system are volcanic $CO_2$ emissions, carbonate weathering, and oxidation of sedimentary organic carbon. Carbon leaves the system mainly as marine sediments in form of buried carbonate sediments along with refractory organic carbon. As in the case of the aforementioned carbon cycle processes, any of these input and output fluxes is subject to temporal changes in both the mass flux and its carbon isotopic signature. As these fluxes are necessarily small compared to the large gross

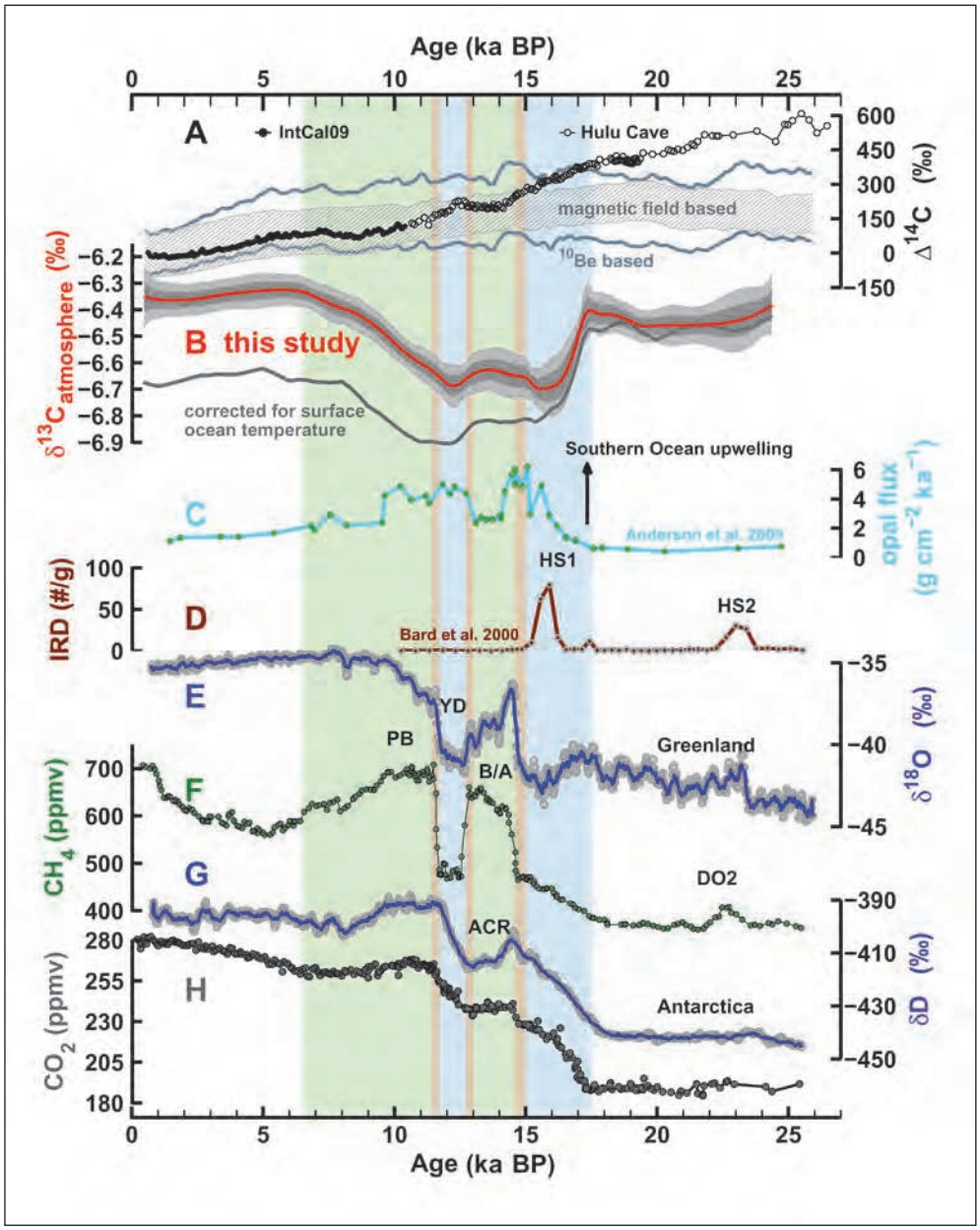


Fig. 1 Ice core reconstructions and marine records illustrating the evolution of major components of the Earth climate system over the past 24,000 years (original figure taken from SCHMITT et al. 2012). Panel *B*: Monte Carlo average of the evolution of $\delta^{13}C_{atm}$ before SST correction (red line represents the MCA; 2σ and 1σ envelopes are in gray) and after SST correction (gray line). Further descriptions and references can be found in the original paper. Green bars indicate intervals with a strong net terrestrial carbon buildup; blue bars indicate intervals where sequestered deep ocean $CO_2$ was released back to the atmosphere.

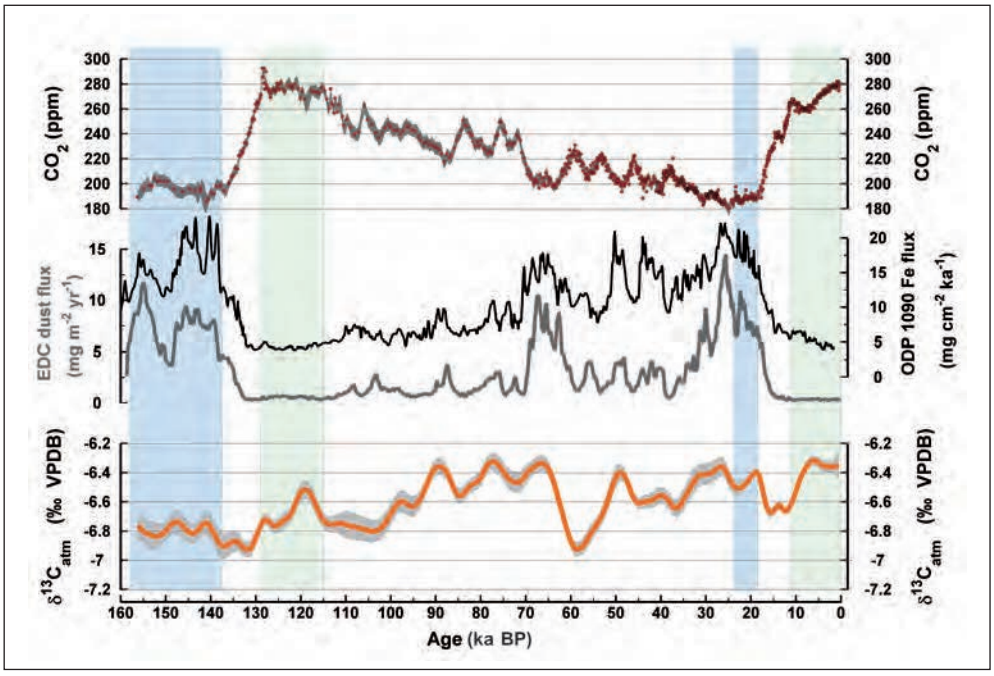


Fig. 2 Evolution of $\delta^{13}C_{atm}$ (Monte Carlo spline and 1σ error estimate of the combined data sets of Schmitt et al. (2012), Schneider et al. (2013), and recent measurements, Eggleston et al. (in preparation) (covering MIS4 and MIS3) and atmospheric $CO_2$, as well as EDC dust flux (Lambert et al. 2012) and iron deposition flux at ODP 1090 (Martínez-García et al. 2014) in the Southern Ocean region. Blue bars mark time intervals with full glacial conditions at the LGM and MIS6. Green bars mark interglacial conditions.

fluxes and sporadic, such in the case of the eruptive volcanic emission, these fluxes and their respective $\delta^{13}C$ values are poorly known. Schneider et al. (2013) discussed some of the possible options to explain the 0.4 ‰ difference, for example an increase in the terrestrial carbon storage *via* peat/yedoma during MIS 5. Indeed, the gradual $\delta^{13}C$ rise during large parts of the MIS 5 interval and well into MIS 4 could point to this direction (Fig. 2).

In summary, $\delta^{13}C_{atm}$, which can be reconstructed from polar ice over the last 800 ka, constitutes a valuable constraint for the global carbon cycle puzzle. As a globally integrated parameter and additionally temporally smoothed by the firn enclosure process, it may circumvent some of the weaknesses of more regional marine and terrestrial proxies. Ice cores directly provide a globally-averaged, low-pass filtered archive for $\delta^{13}C_{atm}$. However, to fully exploit this parameter, the individual contributions of many processes have to be better quantified using new measurements and proxies, as well as better representation in models.

## *References*

Anderson, R. F., Ali, S., Bradtmiller, L. I., Nielsen, S. H. H., Fleisher, M. Q., Anderson, B. E., and Burckle, L. H.: Wind-driven upwelling in the Southern Ocean and the deglacial rise in atmospheric $CO_2$. Science *323*, 1443–1448; doi:10.1126/science.1167441 (2009)

Broecker, W. S., and Clark, E.: Holocene atmospheric $CO_2$ increase as viewed from the seafloor. Global Biogeochem. Cycles *17*, 1052; doi:10.1029/2002GB001985 (2003)

Broecker, W. S., and McGee, D.: The $^{13}C$ record for atmospheric $CO_2$: What is it trying to tell us? Earth Planet. Sci. Lett. *368*, 175–182; doi:10.1016/j.epsl.2013.02.029 (2013)

Ciais, P., Tagliabue, A., Cuntz, M., Bopp, L., Scholze, M., Hoffmann, G., Lourantou, A., Harrison, S. P., Prentice, I. C., Kelley, D. I., Koven, C., and Piao, S. L.: Large inert carbon pool in the terrestrial biosphere during the Last Glacial Maximum. Nature Geosci. *5*, 74–79; doi:10.1038/ngeo1324 (2012)

Duplessy, J. C., Shackleton, N. J., Fairbanks, R. G., Labeyrie, L., Oppo, D., and Kallel, N.: Deepwater source variations during the last climatic cycle and their impact on the global deepwater circulation. Paleoceanography *3*, 343–360; doi:10.1029/PA003i003p00343 (1988)

Elsig, J., Schmitt, J., Leuenberger, D., Schneider, R., Eyer, M., Leuenberger, M., Joos, F., Fischer, H., and Stocker, T. F.: Stable isotope constraints on Holocene carbon cycle changes from an Antarctic ice core. Nature *461*, 507–510; doi:10.1038/nature08393 (2009)

Friedli, H., Moor, E., Oeschger, H., Siegenthaler, U., and Stauffer, B.: $^{13}C/^{12}C$ ratios in $CO_2$ extracted from Antarctic ice. Geophys. Res. Lett. *11*, 1145–1148 (1984)

Indermühle, A., Stocker, T. F., Joos, F., Fischer, H., Smith, H. J., Wahlen, M., Deck, B., Mastroianni, D., Tschumi, J., Blunier, T., Meyer, R., and Stauffer, B.: Holocene carbon-cycle dynamics based on $CO_2$ trapped in ice at Taylor Dome Antarctica. Nature *398*, 121–126 (1999)

Köhler, P., Fischer, H., Munhoven, G., and Zeebe, R. E.: Quantitative interpretation of atmospheric carbon records over the last glacial termination. Global Biogeochem. Cycles *19*, GB4020; doi:10.1029/2004GB002345 (2005)

Lambert, F., Bigler, M., Steffensen, J. P., Hutterli, M., and Fischer, H.: Centennial mineral dust variability in high-resolution ice core data from Dome C, Antarctica. Clim. Past *8*, 609–623; doi:10.5194/cp-8-609-2012 (2012)

Lourantou, A., Chappellaz, J., Barnola, J. M., Masson-Delmotte, V., and Raynaud, D.: Changes in atmospheric $CO_2$ and its carbon isotopic ratio during the penultimate deglaciation. Quat. Sci. Rev. *29*, 1983–1992; doi:10.1016/j.quascirev.2010.05.002 (2010)

Martin, J. H.: Glacial-interglacial $CO_2$ change: the iron hypothesis. Paleoceanography *5*, 1–1313; doi:10.1029/PA005i001p00001 (1990)

Martínez-García, A., Sigman, D. M., Ren, H., Anderson, R. F., Straub, M., Hodell, D. A., Jaccard, S. L., Eglinton, T. I., and Haug, G. H.: Iron fertilization of the subantarctic ocean during the last ice age. Science *343*, 1347–1359; doi:10.1126/science.1246848 (2014)

Menviel, L., Joos, F., and Ritz, S. P.: Simulating atmospheric $CO_2$, $^{13}C$ and the marine carbon cycle during the Last Glacial–Interglacial cycle: possible role for a deepening of the mean remineralization depth and an increase in the oceanic nutrient inventory. Quat. Sci. Rev. *56*, 46–68; doi:10.1016/j.quascirev.2012.09.012 (2012)

Neftel, A., Oeschger, H., Schwander, J., Stauffer, B., and Zumbrunn, R.: Ice core sample measurements give atmospheric $CO_2$ content during the past 40,000 yr. Nature *295*, 220–223 (1982)

Oliver, K. I. C., Hoogakker, B. A. A., Crowhurst, S., Henderson, G. M., Rickaby, R. E. M., Edwards, N. R., and Elderfield, H.: A synthesis of marine sediment core $\delta^{13}C$ data over the last 150 000 years. Clim. Past. *6*, 645–673; doi:10.5194/cp-6-645-2010 (2010)

Ruddiman, W. F.: The anthropogenic greenhouse era began thousands of years ago. Climatic Change *61*, 261 (2003)

Schmitt, J., Schneider, R., Elsig, J., Leuenberger, D., Lourantou, A., Chappellaz, J., Köhler, P., Joos, F., Stocker, T. F., Leuenberger, M., and Fischer, H.: Carbon isotope constraints on the deglacial $CO_2$ rise from ice cores. Science *336*, 711–714; doi:10.1126/science.1217161 (2012)

Schneider, R., Schmitt, J., Köhler, P., Joos, F., and Fischer, H.: A reconstruction of atmospheric carbon dioxide and its stable carbon isotopic composition from the penultimate glacial maximum to the last glacial inception. Clim. Past. *9*, 2507–2523; doi:10.5194/cp-9-2507-2013 (2013)

Dr. Jochen Schmitt
Climate and Environmental Physics
Physics Institute and
Oeschger Centre for Climate Change Research
University of Bern
Sidlerstrasse 5
CH-3012 Bern
Switzerland
Phone: +41 31 6318639
Fax: +41 31 6318742
E-Mail: schmitt@climate.unibe.ch

Nova Acta Leopoldina NF *121*, Nr. 408, 207–210 (2015)

# Was the Early Deglacial $CO_2$ Rise Caused by a Reduction of the Atlantic Overturning Circulation?

Andreas Schmittner[1] and David C. Lund[2]

With 3 Figures

The reason for the initial rise of atmospheric $CO_2$ during the last deglaciation remains unknown. Most recent hypotheses invoke Southern Hemisphere processes such as shifts in mid-latitude westerly winds. Coeval changes in the Atlantic Meridional Overturning Circulation (AMOC) remain poorly quantified and their relation to the $CO_2$ increase is not understood. Here we compare simulations from a global, coupled climate-biogeochemistry model that includes a detailed representation of stable carbon isotopes $\delta^{13}C$ with a synthesis of high-resolution $\delta^{13}C$ reconstructions from deep-sea sediments and ice core data. In response to a prolonged AMOC shutdown initialized from a pre-industrial state (Fig. 1), modelled $\delta^{13}C$ of Dissolved Inorganic Carbon ($\delta^{13}C_{DIC}$) decreases in most of the surface ocean and the subsurface Atlantic, with largest amplitudes (more than 1.5 ‰) in the intermediate depth North Atlantic (Fig. 2).

It increases in the intermediate and abyssal South Atlantic, as well as in the subsurface Southern, Indian and Pacific oceans. The modelled pattern is similar and highly correlated with the available foraminiferal $\delta^{13}C$ data spanning the late Last Glacial Maximum (LGM, ~ 19.5–18.5 ka BP) to the late Heinrich stadial event 1 (HS1, ~16.5–15.5 ka BP), but the model overestimates $\delta^{13}C_{DIC}$ reductions in the North Atlantic (Fig. 3). Possible reasons for the model-sediment data differences are discussed. Changes in remineralized $\delta^{13}C_{DIC}$ dominate the total $\delta^{13}C_{DIC}$ variations in the model but preformed contributions are not negligible. Simulated changes in atmospheric $CO_2$ and its isotopic composition ($\delta^{13}C_{CO2}$) agree well with ice core data (Fig. 1). Modelled effects of AMOC induced wind changes on the carbon and isotope cycles are small, suggesting that Southern Hemisphere westerly wind effects may have been less important for the global carbon cycle response during HS1 than previously thought. Our results indicate that during the early deglaciation the AMOC decreased for several thousand years. We propose that the observed early deglacial rise in atmospheric $CO_2$ and the decrease in $\delta^{13}C_{CO2}$ may have been dominated by an AMOC induced decline of the ocean's biologically sequestered carbon storage.

1 College of Earth, Ocean, and Atmospheric Sciences, Oregon State University, Corvallis, OR, USA.
2 Department of Marine Sciences, University of Connecticut, Groton, CT, USA.

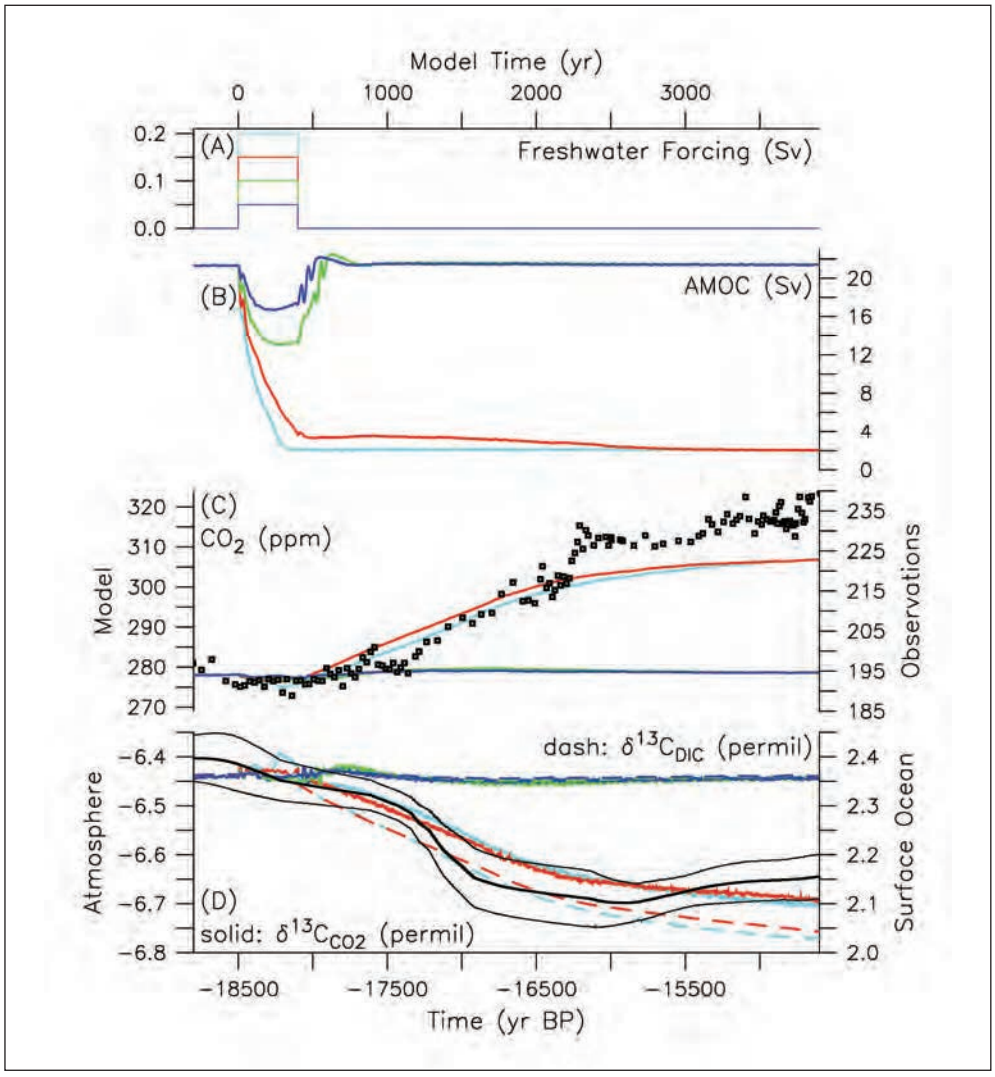


Fig. 1 Time series of (*A*) North Atlantic freshwater forcing, (*B*) AMOC response, (*C*) atmospheric $CO_2$ concentrations, (*D*) $\delta^{13}C$ of atmospheric $CO_2$ (solid, left axis) and global mean surface ocean $\delta^{13}C_{DIC}$ (dashed, right axis) for four model simulations (color lines). Symbols in (*C*) and thick black curve (error estimates are indicated by thin lines) in (*D*) show ice core measurements (Marcott et al. 2014, Schmitt et al. 2012), respectively (*bottom* and *right* in (*C*) axes).

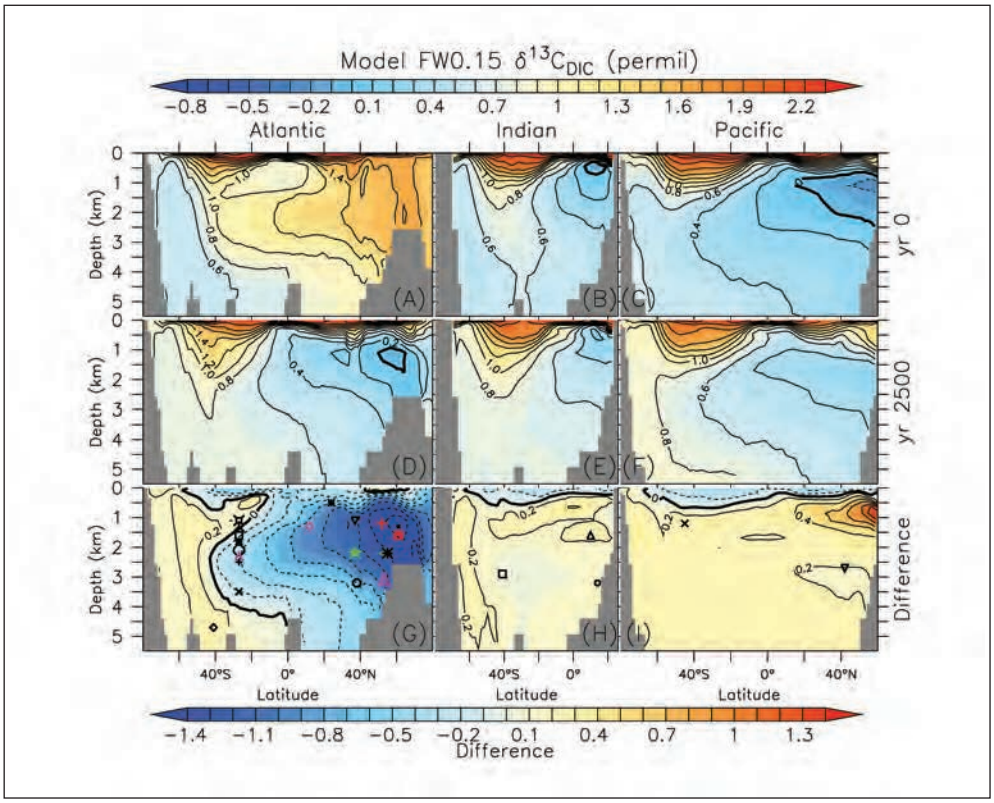


Fig. 2 Zonally averaged distributions of $\delta^{13}C_{DIC}$ (color shading and black isolines) as a function of latitude and depth simulated by model FW0.15 (red lines in Fig. 1) in the Atlantic (*left*), Indian (*center*) and Pacific (*right*) ocean basins at model years 0 (*A–C*) and 2500 (*D–F*; *A–F* use top colour scale), and the difference (*G–I*; bottom colour scale). Symbols in bottom panels denote locations of observations.

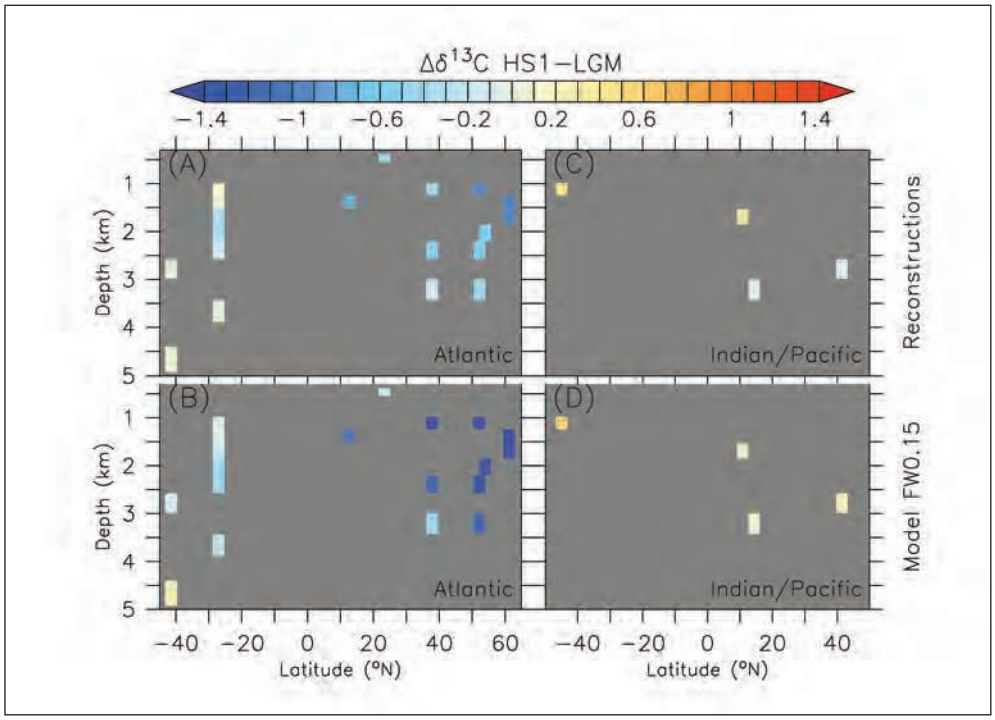


Fig. 3 HS1 minus LGM difference in $\delta^{13}C_{DIC}$ in the Atlantic (*left*) and Indian/Pacific (*right*) basins from our high-resolution synthesis of reconstructions averaged on the model grid (*top*) compared to model FW0.15 results (bottom; averages of model years 2000 to 3000 minus averages of model years –1000 to 0.).

## *References*

Marcott, S. A., Bauska, T. K., Buizert, C., Steig, E. J., Rosen, J. L., Cuffey, K. M., Fudge, T. J., Severinghaus, J. P., Ahn, J., Kalk, M. L., McConnell, J. R., Sowers, T., Taylor, K. C., White, J. W. C., and Brook, E. J.: Centennial-scale changes in the global carbon cycle during the last deglaciation. Nature *514*, 616–619; doi:10.1038/nature13799 (2014)

Schmitt, J., Schneider, R., Elsig, J., Leuenberger, D., Lourantou, A., Chappellaz, J., Köhler, P., Joos, F., Stocker, T. F., Leuenberger, M., and Fischer, H.: Carbon isotope constraints on the deglacial $CO_2$ rise from ice cores. Science *336*, 711–714; doi:10.1126/science.1217161 (2012)

Prof. Andreas Schmittner, Ph.D.
College of Earth, Ocean, and Atmospheric Sciences
Oregon State University
104 CEOAS Admin Bldg
Corvallis, OR 97331
USA
Phone: +1 541 7379952
Fax: +1 541 7372064
E-Mail: aschmitt@coas.oregonstate.edu

Nova Acta Leopoldina NF *121*, Nr. 408, 211–212 (2015)

# What is Shaping the $\Delta^{14}$C-DIC Relationship in the Deep Ocean?

Birgit Schneider and Michael Sarnthein ML (Kiel)

With 1 Figure

The deep ocean provides the largest reservoir of carbon relevant for the climate system. Understanding its sensitivity to perturbations in climate and/or the global carbon cycle gives important insights into mechanisms controlling atmospheric $CO_2$. Below 2000 m water depth, modern observations show a clear, almost linear, relationship between the $\Delta^{14}$C ventilation age and the concentration of dissolved inorganic carbon (DIC; Fig. 1). According to these observations an increase of 1.22 µmol/kg DIC equates to 1 ‰ reduction in $\Delta^{14}$C. Taking into account the ocean's volume this regression slope corresponds to a flux of 1.1 GtC/yr into the deep ocean. With the help of the regression of $\Delta^{14}$C *vs*. potential alkalinity (POTALK ≈ alkalinity + nitrate) this flux can be separated into 0.64 GtC/a from the remineralization of organic matter and 0.45 GtC/a from the dissolution of particulate inorganic carbon (PIC), which is in good agreement with results from sediment trap data (Antia et al. 2001) and inverse modelling (Schlitzer 2002).

In the present study, we are using results of ocean biogeochemical model simulations to analyse how the shape of the regression line depends on the interplay of marine biological production and ventilation time of the deep ocean. Our focus is on changes in (*i*) the ventilation time, which is expected to affect the extension of the data cloud towards more or less depleted $\Delta^{14}$C values, and (*ii*) the export of particulate organic and inorganic matter, which is expected to drive the slope of the regression line. Our results will be of particular relevance for the understanding of past climates, especially with regard to the oceanic storage of atmospheric carbon during the last glacial.

*References*

Antia, A. N., Koeve, W., Fischer, G., Blanz, T., Schulz-Bull, D., Scholten, J., Neuer, S., Kremling, K., Kuss, J., Peinert, R., Hebbeln, D., Bathmann, U., Conte, M., Fehner, U., and Zeitschel, B.: Basin-wide particulate carbon flux in the Atlantic Ocean: Regional export patterns and potential for atmospheric $CO_2$ sequestration. Global Biogeochem. Cycles *15*/4, 845–862 (2001)

Key, R. M., Kozyr, A., Sabine, C. L., Lee, K., Wanninkhof, R., Bullister, J. L., Feely, R. A., Millero, F. J., Mordy, C., and Peng, T.-H.: A global ocean carbon climatology: Results from Global Data Analysis Project (GLODAP). Global Biogeochem. Cycles *18*, GB4031; doi:10.1029/2004GB002247 (2004)

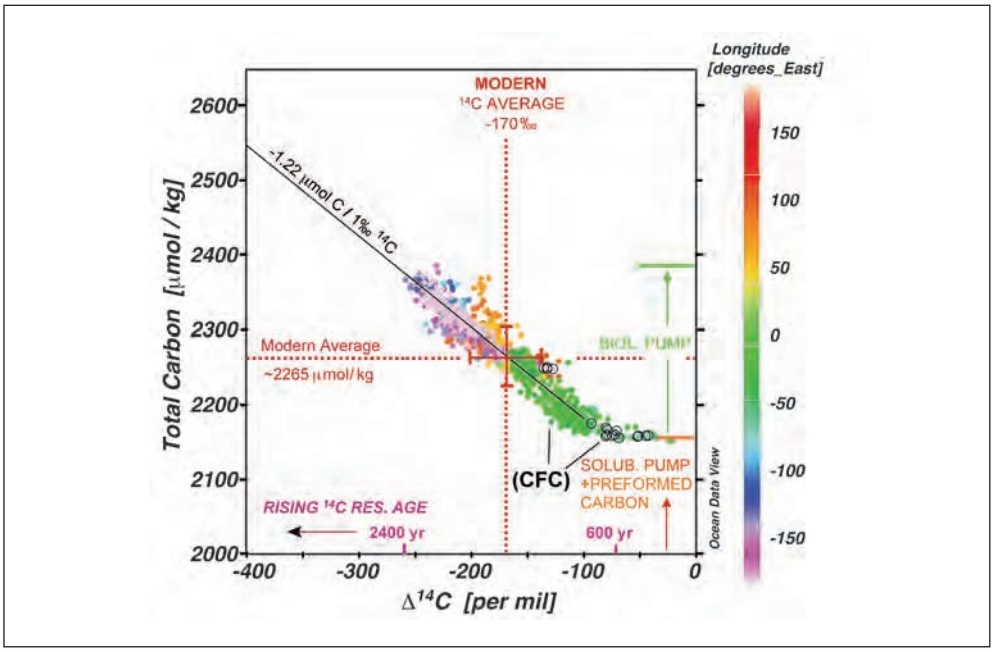


Fig. 1 Ratio of total dissolved inorganic carbon (DIC) µmol per kg *vs*. benthic $\Delta^{14}C$ and $^{14}C$ ventilation age for Fraction of modern carbon (fMC) = 1 of ocean waters below >2000 m w.d. (Sarnthein et al. 2013). Modern, volumetrically unweighted GLODAP data (Key et al. 2004) for longitudes of the Atlantic (green), the western (orange) and eastern Indian Ocean and Pacific (pink and blue). Standard deviation is ± 32.8 ‰ for $\Delta^{14}C$ and ± 40.2 µmol/kg for DIC. Black open circles mark deep waters with chlorofluorocarbon (CFC) concentrations >0.1 pmol/kg as tracer of modern anthropogenic influence in the northern North Atlantic and Weddell Sea Bottom Water (orange dots). Modern ventilation ages of 600 to 2400 $^{14}C$ year average at 1500 $^{14}C$ year = –170 ‰ $\Delta^{14}C$.

Sarnthein, M., Schneider, B., and Grootes, P. M.: Peak glacial $^{14}C$ ventilation ages suggest major draw-down of carbon into the abyssal ocean. Clim. Past *9*, 2595–2614; doi:10.5194/cp-9-1-2013 (2013)

Schlitzer, R.: Carbon export fluxes in the Southern Ocean: results from inverse modelling and comparison with satellite-based estimates. Deep-Sea Res. II *49*, 1623–1644; doi:10.1016/S0967-0645(02)00004-8 (2002)

Prof. Dr. Birgit Schneider
Institute of Geosciences
University of Kiel
Ludewig-Meyn-Straße 10
Room 14
24118 Kiel
Germany
Phone: +49 431 8803254
Fax: +49 431 8801912
E-Mail: bschneider@gpi.uni-kiel.de

Nova Acta Leopoldina NF *121*, Nr. 408, 213–216 (2015)

# Taking Stock of the Hypotheses for Polar Ocean Stratification and Carbon Dioxide Sequestration during the Last Ice Age

Daniel M. Sigman (Princeton, NJ, USA)

A comprehensive oceanic explanation for the lower atmospheric $CO_2$ concentrations observed during ice ages must have at least two components. *First*, a mechanism is required by which orbital change or a proximal atmospheric/Earth surface response to this orbital change alters the physics and/or biology of the ocean. *Second*, those ocean physical and biological changes must drive a redistribution of carbon and alkalinity in the ocean/atmosphere system that lowers the concentration of atmospheric $CO_2$.

To date, there has been more work on the second of these components: the nature of glacial/interglacial Southern Ocean changes and their implications for atmospheric $CO_2$. In the context of Southern Ocean-related explanations, the $CO_2$ response to a given physical or biological change in the ocean is accessible with existing concepts and models, although with uncertainties related to our incomplete understanding of modern ocean processes. As an example, in the 1990s, it was observed that different types of models, box models and ocean general circulation models, indicate very different $CO_2$ sensitivities to a given ocean change. This is now known to relate to a coherent difference between model types in the degree to which the surface waters contributing to deep water formation approach air/sea $CO_2$ exchange equilibrium prior to entering the ocean interior. A high degree of equilibration applies to box models because the surface waters are injected into the subsurface from a spatially expansive, homogenous surface layer. General circulation models, in contrast, tend to be characterized by highly localized open ocean convection, which limits the time for water passing through the surface to undergo air/sea $CO_2$ exchange. Given our poor understanding of the processes that contribute to the Southern Ocean ventilation of the ocean interior, it is not clear which of these two cases is closer to reality. Here, box model estimates of $CO_2$ effects are used.

A reduction in Antarctic overturning ("Antarctic stratification") or a sea ice-driven reduction in sea/air gas exchange are two Antarctic ventilation-related mechanisms for lowering ice age $CO_2$ that have strong geochemical similarities; we refer to them here as the Antarctic "ventilation barrier" mechanisms, as they essentially reduce the role that the Antarctic plays in ventilating the deep ocean. There is evidence for Antarctic stratification: paleoproductivity proxies indicate that export production was reduced while nitrogen isotope measurements of diatom-bound organic matter indicate an increased degree of nitrate consumption, which together require a decline the gross rate of deep nitrate supply to the surface ocean. Sea ice driven reduction in gas exchange is more difficult to evaluate. Given evidence for summertime melt-back even during glacial maxima, this mechanism would apply if only the most polar

Antarctic surface is important for $CO_2$ gas exchange in the waters that sink into the subsurface. In box models (and in general circulation models with fast gas exchange), the Antarctic ventilation barrier mechanisms, acting in isolation or together, can lower carbon dioxide by roughly 40 ppm, although greater $CO_2$ declines are possible with extreme (i.e. seemingly unrealistic) applications of the mechanisms. This limited amplitude of $CO_2$ drawdown applies because the Antarctic barrier mechanisms strengthen the carbonate pump (the sequestration of alkalinity in the ocean interior), which partially offsets the $CO_2$ reducing effects of the soft-tissue pump (the sequestration of organic carbon-derived DIC in the ocean interior as well as the increase in ocean alkalinity that this triggers).

Southern Ocean nutrient drawdown is an additional mechanism for lowering $CO_2$ that, in contrast to the barrier mechanisms, is not opposed by the carbonate pump. Nitrogen isotope data from diatom microfossil-bound organic matter indicate an increased degree of nitrate consumption in the Antarctic during ice ages. However, as described above, this occurred in context of substantial ice age declines in the gross nutrient supply from below, which indicates less surface/deep ocean exchange of water in the ice age Antarctic. Accordingly, the $CO_2$ effect of increased Antarctic nutrient consumption may have been muted by the reduced role of the Antarctic in ventilating the global deep ocean. Including a higher degree of nutrient consumption in the context of Antarctic stratification only reduces $CO_2$ by roughly an additional 10 ppm (i.e. to a total Antarctic biogeochemical effect of 50 ppm). An alternative description of this trade-off is that, if one were to decrease Antarctic overturning in the context of the high degree of nitrate consumption that appears to have applied to the glacial Antarctic, atmospheric $CO_2$ would change relatively little, possibly even rising. In essence, the modern interglacial Antarctic leak of deeply sequestered, respired $CO_2$ to the atmosphere can be turned off only once.

In the Subantarctic Zone, a remarkable correspondence is observed of higher dust-derived iron flux, export production based on opal and alkenone flux, and increased nitrate consumption based on nitrogen isotope measurements of foraminifera-bound organic matter. These coincident changes are consistent with dust-borne iron fertilization as the dominant ice age change. This process would have lowered atmospheric $CO_2$ partly by the same general increased $CO_2$ storage in the ocean interior that applies to Antarctic stratification and nutrient consumption changes described above. In addition, Subantarctic iron fertilization would have been particularly effective at raising ocean alkalinity by (*i*) shifting the ocean $CO_2$ storage into the deepest ocean, and (*ii*) possibly decreasing low latitude $CaCO_3$ production. Observational constraints on the lysocline depth and low latitude productivity during ice ages appear to constrain the strength of the $CO_2$ drawdown associated with Subantarctic iron fertilization change to roughly 40 ppm.

Thus, the combination of Antarctic and Subantarctic changes is needed to achieve the full (80–100 ppm) ice age $CO_2$ decline. North Atlantic overturning changes are also relevant in these calculations (and tend to contribute modestly to the $CO_2$ decline when paired with the Southern Ocean changes), but they do not change qualitatively the conclusions regarding what is required from the Southern Ocean to reach ice age $CO_2$ levels. In the context of the progressive $CO_2$ decline of the last ice age, the data indicate that Antarctic changes began at the end of the previous interglacial (the MIS 5e/5d transition, at 110 ka), while Subantarctic iron fertilization did not begin in earnest until the MIS 5a/4 transition (at 70 ka).

Above, a set of Southern Ocean physical and biological changes are outlined that are implicated by data and together have the capacity to lower $CO_2$ to near ice age observations.

However, the community lacks an understanding of the potential causes for both the implied Antarctic barrier mechanisms and the increase in Subantarctic dust supply during ice ages. Thus, even if the evidence for these Southern Ocean changes were to become incontrovertible, conceptual gaps stand in the way of a theory of glacial cycles that includes Southern Ocean-driven $CO_2$ change. The talk will specifically consider the proposals for how orbital or resulting climate changes might result in Antarctic stratification, one of the Antarctic barrier mechanisms described above. Proposals to date for ice age Antarctic stratification include (*i*) a decline in westerly wind-driven upwelling (Toggweiler et al. 2006), (*ii*) a decline in abyssal mixing (Watson and Garabato 2006, Ferrari et al. 2014, De Boer and Hogg 2014), (*iii*) a decline in the capacity of temperature to drive polar ocean overturning (Sigman et al. 2004, De Boer et al. 2007), and (*iv*) an expansion of the seasonal sea ice cycle (Bouttes et al. 2010). These will be reviewed, highlighting key strengths, weaknesses, and questions. The relationship of each proposed mechanism to the possibility of sea ice cover-driven limitation of air/sea $CO_2$ exchange will also be considered.

A case will be made that subarctic North Pacific observations call for similar biogeochemical behaviour of the Antarctic and subarctic North Pacific over glacial/interglacial cycles. This is somewhat surprising, given that the two regions have very different boundary conditions. While both regions experience net wind-driven upwelling and have haloclines, the differences in basin geometry yield different strengths of upwelling as well as different consequences. The southern westerly winds and the Antarctic Circumpolar Current are largely unimpeded by continental barriers, and surface water sent northward across the open channel of the Southern Ocean cannot be easily replaced by surface currents along continental margins; these conditions do not apply to the North Pacific. Moreover, the vertical density structure of the two regions has very different outcomes for deep ocean ventilation by the two regions, with the Antarctic forming both intermediate and deep water at globally significant rates and the more strongly stratified subarctic North Pacific forming only a modest amount of intermediate water. Given these differences, it would seem possible to hone in on their shared aspects to distinguish among physical explanations for the apparent reduction in surface/deep exchange during cold climates that appears to characterize both regions. This exercise motivates a new, admittedly speculative proposal for the mechanism of Antarctic and subarctic North Pacific stratification during ice ages, which will be presented in the latter part of the talk.

## *References*


Boer, A. M. de, Sigman, D. M., Toggweiler, J. R., and Russell, J. L.: Effect of global ocean temperature change on deep ocean ventilation. Paleoceanography *22*/2, PA2210; doi:10.1029/2005pa001242 (2007)

Boer, A. M. de, and Hogg, A.: Control of the glacial carbon budget by topographically induced mixing. Geophys. Res. Lett. *41*, 4277–4284; doi:10.1002/2014GL059963 (2014)

Bouttes, N., Paillard, D., and Roche, D. M.: Impact of brine-induced stratification on the glacial carbon cycle. Clim. Past *6*/5, 575–589; doi:10.5194/cp-6-575-2010 (2010)

Ferrari, R., Jansen, M. F., Adkins, J. F., Burke, A., Stewart, A. L., and Thompson, A. F.: Antarctic sea ice control on ocean circulation in present and glacial climates. Proc. Natl. Acad. Sci. USA *111*/24, 8753–8759; doi:10.1073/pnas.1323922111 (2014)

Sigman, D. M., Jaccard, S. L., and Haug, G. H.: Polar ocean stratification in a cold climate. Nature *428*/6978, 59–63 (2004)

Toggweiler, J., Russell, J., and Carson, S.: Midlatitude westerlies, atmospheric $CO_2$, and climate change during the ice ages. Paleoceanography *21*/2, PA2005; doi:10.1029/2005PA001154 (2006)

Watson, A. J., and Garabato, A. C. N.: The role of Southern Ocean mixing and upwelling in glacial-interglacial atmospheric $CO_2$ change. Tellus Series B–Chemical and Physical Meteorology *58*/1, 73–87; doi:10.1111/j.1600-0889.2005.00167.x (2006)

Prof. Daniel M. Sigman, Ph.D.
Princeton University
Department of Geosciences
M52 Guyot Hall
Princeton, NJ 08544
USA
Phone: +1 609 2582194
Fax: +1 609 2585275
E-Mail: sigman@princeton.edu

Nova Acta Leopoldina NF *121*, Nr. 408, 217–222 (2015)

# On the Glacial Ocean Circulation and its Impact on the Global Radiocarbon and Carbon Cycles

Luke C. Skinner,[1] Emma Freeman,[1] François Primeau,[2] and Adam E. Scrivner[1]

With 2 Figures

Our current perspective on the large-scale overturning circulation of the global ocean at the height of the last glacial period, or Last Glacial Maximum (LGM), is perhaps almost comparable to that of the contemporary ocean circulation in the early 1960s. At that time, Walter Munk, in a classic paper focusing on the large-scale overturning circulation of the Pacific Ocean interior (Munk 1966), postulated that the overturning of the ocean might be conceptualized as being achieved through a balance of downward diffusion (e.g. of buoyancy) *versus* a slow upward advection of mass. Munk (1966) used sparse Pacific water column radiocarbon data available at the time (along with information from more detailed temperature and salinity data) to show that property profiles in the Pacific interior were indeed compatible with a consistent set of vertical fluxes and stabilities (i.e. degrees of stratification), and with the notion of a large-scale overturning maintained by a balance of vertical diffusion and upwelling. Property profiles for the Pacific interior were thus given by a set of (abyssal) 'recipes' that were developed by Munk (1966) and that were declared to be appropriate and consistent parameterisations of the processes responsible for overturning in the Pacific interior, but no more than that: they were 'recipes' not fully physical explanations. Indeed, some caveats and clarifications are in order at this stage. Firstly, by now it has become apparent that the constant vertical diffusivity ($\kappa$) of ~$1\times10^{-4}$ $m^2s^{-1}$ estimated by Munk (1966) is about an order of magnitude too high for the bulk of the ocean interior, where $\kappa \sim 0.1\times10^{-4}$ $m^2s^{-1}$ or less is observed, and that much higher vertical diffusivity (by as much as two orders of magnitude, $\kappa$ ~$100\times10^{-4}$ $m^2s^{-1}$) can be found concentrated in regions of highly variable bottom topography. Nevertheless, it has been argued that the original value for $\kappa \sim 0.1\times10^{-4}$ $m^2s^{-1}$ may still hold as a global average (Munk and Wunsch 1998) that is representative of a combination of widespread lower values over most of the ocean interior and higher values concentrated in very localized regions of intensified vertical mixing (over perhaps only ~1 % of the ocean). Furthermore, it is also clear that if the 'abyssal recipes' of Munk (1966) do indeed succeed in representing the interior property profiles of the modern ocean in a consistent manner, it must be because they manage to parameterize the effects of two 'drivers' of the overturning circulation: diapycnal/isopycnal mixing (i.e. due to the energy provided for small scale motions in

1 Godwin Laboratory for Palaeoclimate Research, Department of Earth Sciences, University of Cambridge, Cambridge, CB2 3EQ, United Kingdom.

2 Department of Earth System Science, University of California, Irvine, CA, USA.

the ocean interior by winds and tides), and direct energy input to the large-scale overturning from winds in the Southern Ocean in particular (KUHLBRODT et al. 2004).

Regardless of the link between the 'abyssal recipes' of MUNK (1966) and the real physical processes they might hope to represent, it can be clearly shown that it is impossible to reconcile the circulation that prevails in the modern Atlantic interior with that in the modern Pacific interior without using very different 'ingredients' in the abyssal recipe for each basin (i.e. different diffusion/advection ratios, and different absolute vertical diffusivity values in particular). This is shown in Figure 1, which shows the root mean square (RMS) errors for fitting the abyssal (radiocarbon) recipe of MUNK (1966) to (bomb-corrected) modern radiocarbon data from relatively sparse sediment core locations in the Atlantic and Pacific. This analysis requires the assumption of a constant ratio of vertical diffusivity to upwelling ($\kappa/\omega$), and the modern value of $\kappa = 0.77$ estimated by MUNK (1966) from temperature/salinity profiles is used here in a first instance. The analysis also requires the stipulation of radiocarbon ventilation ages at the top and bottom of the domain (here defined at 0 m and –5000 m). What emerges from Figure 1 is that the Atlantic requires the supposition of a much lower value for $\lambda$, and therefore a higher value of vertical diffusivity ($\kappa$) given a fixed ratio of $\kappa/\omega$, since:

$$\kappa = \frac{4\mu_c(\kappa/\omega)^2}{\lambda^2-1} \qquad [1]$$

Although the precise physical significance of a higher "modelled $\kappa$" in the modern Atlantic *versus* the modern Pacific is not easy to infer directly from this 'abyssal recipes' analysis alone, it is not very difficult to map this clear demonstration of very different circulation regimes in the modern Atlantic and Pacific basins onto what we already know about the hydrography and dynamics in these two basins today (TALLEY et al. 2011).

This analysis becomes less trivial and more interesting when we shift our gaze to the glacial ocean. Figure 1 also shows the RMS errors for abyssal recipe solutions that best fit compiled published and unpublished estimates of ocean *versus* atmosphere radiocarbon disequilibria in the LGM Atlantic and Pacific (SKINNER and FREEMAN et al. in preparation). Figure 2 shows the 'ventilation age' profiles (i.e. bottom-water *versus* atmosphere radiocarbon disequilibria, $\delta^{14}R_{B\text{-}Atm}$, expressed in terms of equivalent decay ages in $^{14}C$-years) that are produced by the best-fit abyssal recipes for the modern- and LGM Atlantic and Pacific. What emerges in Figures 1 and 2 is that the LGM abyssal recipe solutions for the Atlantic and Pacific: (*i*) more closely resemble each other, in clear contrast to the modern situation; and (*ii*) imply globally, and especially in the Atlantic, a generally lower value of modelled 'vertical diffusivity', $\kappa$ (it can also be shown that a better fit is obtained for a doubling of the diffusion to advection ratio, $\kappa/\omega$, precisely as suggested previously by LUND et al. 2011).

Arguably, both of these observations are highly significant, even if it must be stressed that a clearly defined dynamical interpretation of these results is not at all obvious at this stage. Three key points emerge from the results in Figures 1 and 2, in decreasing order of robustness:

– They demonstrate almost unequivocally that the circulation of the glacial Atlantic was very different from the modern (in a dynamical sense that cannot be argued to be an artefact of e.g. non-conservative biological effects, as for an analysis of stable carbon isotopes for example (GEBBIE 2014).
– They further imply that the circulation of the glacial Atlantic was rather more similar to that of the modern Pacific (the details of which are more readily guessed from hydro-

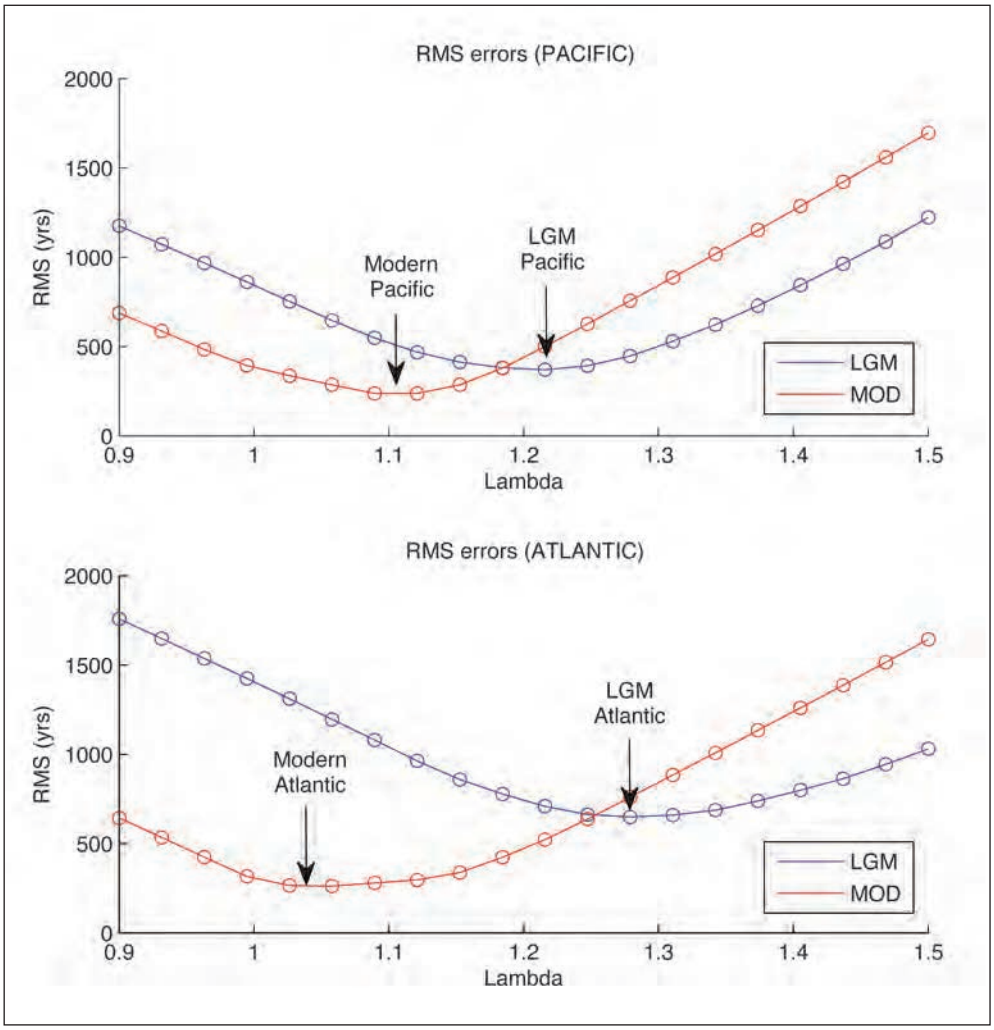


Fig. 1 Average RMS errors, as a function of lambda (λ) associated with abyssal recipe solutions for the radiocarbon profiles of the Atlantic and Pacific for κ/ω = 0.77, as compared to sparse modern and LGM radiocarbon data from sediment core locations (Skinner et al., in preparation). In the modern ocean, $\lambda_{Atlantic} < \lambda_{Pacific}$, (i.e. modelled vertical diffusivity, κ, is higher in the modern Atlantic), whereas in the LGM ocean the λ for both basins increases and $\lambda_{Atlantic} > \lambda_{Pacific}$, (i.e. modelled κ decreases overall and is even lower in the glacial Atlantic than the glacial Pacific).

graphic surveys and analyses of the modern Pacific (Talley et al. 2011), or from theoretical arguments (Ferrari 2014), than from the abyssal 'recipe' proposed here).

– If the details of the glacial radiocarbon data are taken at face value, it is apparent that the abyssal recipe that best reproduces the glacial Pacific radiocarbon profile also suggests a decrease in the modelled vertical diffusivity in that basin, and an approximate doubling of the ratio of diffusivity to upwelling, κ/ω, as previously suggested on the basis of stable isotope profiles in the glacial Atlantic (Lund et al. 2011).

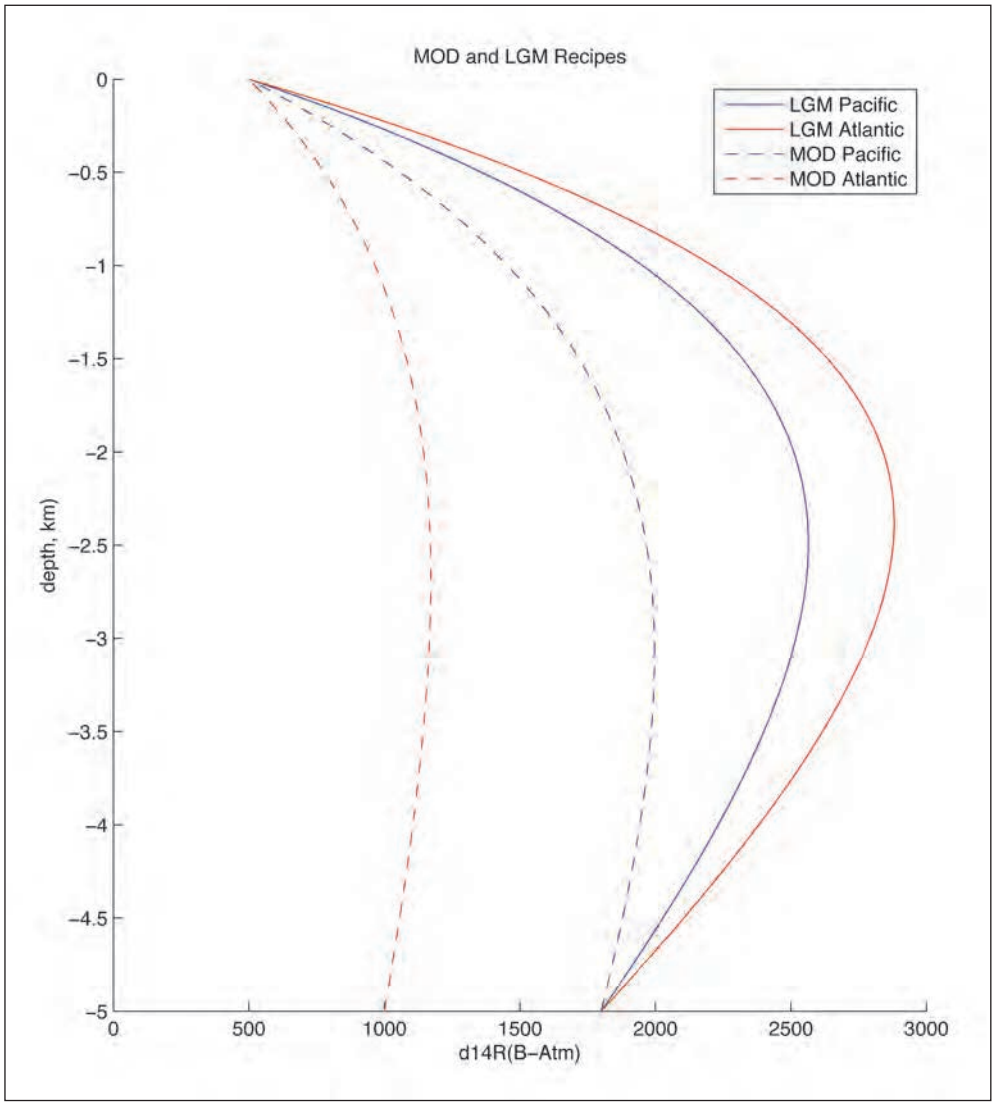


Fig. 2 Abyssal recipe solutions, giving vertical radiocarbon profiles in the modern and LGM Atlantic and Pacific basins (based on defined values at 0 and –5 km, on assumed κ/ω values and on the corresponding λ value that yields the minimum RMS in Figure 1). The vertical radiocarbon 'age' profile for the LGM Atlantic resembles (and indeed overreaches) that for the LGM Pacific, in clear contrast to the modern situation. In both cases, significantly higher radiocarbon ages appear to have been reached, as compared to the modern ocean. A 'Pacific-style' circulation thus appears to have replaced the modern Atlantic circulation at the LGM.

Our claim is therefore that a specific kind of change in the global overturning circulation, with the Atlantic adopting a Pacific-style circulation, might be inferred from emerging LGM radiocarbon data. A second proposition that extends from this is that the inferred change in the overturning circulation, with the Atlantic resembling the modern Pacific, had the effect

of increasing the global average ocean-atmosphere radiocarbon disequilibrium (i.e. ventilation age). A simple geometrical average of LGM 'ventilation age' estimates, as well as more sophisticated interpolation methods (Skinner et al., in preparation), suggest a ~600 $^{14}$C year equivalent increase in the global average ocean-atmosphere radiocarbon disequilibrium, consistent with other estimates (Sarnthein 2013).

In order to assess what impact this would have had on the marine carbon cycle, and more specifically on atmospheric $CO_2$, a linear scaling argument based on modern relationships might be advanced (Sarnthein 2013). Alternatively, a simple conceptual framework can be considered, in which the average radiocarbon age of the ocean (relative to the atmosphere) is set by the degree of mixing between the ocean interior and a well-equilibrated surface mixed layer, which also interacts with biological export from the mixed layer to set the partitioning of carbon and alkalinity between the deep ocean and the surface mixed layer. Analytical solutions within this conceptual framework can only be obtained if certain parameters are fixed. Three parameters in particular turn out to be primary determinants of the response of atmospheric $CO_2$ to a less vertically mixed ocean: (*i*) the initial age of the ocean interior prior to the change in mixing (the impact of an aging ocean on atmospheric $CO_2$ diminishes with increasing age, since typically $\delta^2CO_2/\delta(age)^2 > 0$); (*ii*) the ratio of alkalinity to organic carbon that is exported by biology to the deep ocean (a very high degree of alkalinity trapping in the deep ocean can result in increased atmospheric $CO_2$ for a less vertically mixed ocean); and (*iii*) the nutrient restoring capacity of biology in the mixed layer (i.e. the sensitivity of export productivity to nutrient supply from below, *via* vertical mixing with the deep ocean). The importance of the latter two factors have been noted previously in the literature (Hain et al. 2011, Kwon, et al. 2011); however, the conceptual framework outlined here serves to underline in a simple and generalized manner the importance of assessing these three parameters in the context of past (glacial-interglacial) ocean circulation change. Indeed, with reasonable guesses for these three parameters, the proposed simple analytical framework can successfully reproduce the results of more sophisticated intermediate complexity GCM simulations (Tschumi et al. 2011), and would suggest that a ~600 $^{14}$C year aging of the glacial ocean specifically due to a reduction in the efficiency of vertical mixing might have accounted for as much as 60 ppmv of the 90 ppmv change in atmospheric $CO_2$ between the LGM and the late Holocene. These preliminary results might therefore deserve further attention, and might emphasize the potential value of more reconstructions of the glacial ocean radiocarbon distribution.

## *References*

Ferrari, R., Jansen, M. F., Adkins, J. F., Burke, A., Stewart, A. L., and Thompson, A. F.: Antarctic sea ice control on ocean circulation in present and glacial climates. Proc. Natl. Acad. Sci. USA *111*, 8753–8758; doi:10.1073/pnas.1323922111 (2014)

Gebbie, G.: How much did Glacial North Atlantic Water shoal? Paleoceanography *29*, 190–209; doi:10.1002/2013pa002557 (2014)

Hain, M. P., Sigman, D. M., and Haug, G. H.: Carbon dioxide effects of Antarctic stratification, North Atlantic Intermediate Water formation, and subantarctic nutrient drawdown during the last ice age: Diagnosis and synthesis in a geochemical box model. Global Biogeochem. Cycles *24*, doi:Gb4023 10.1029/2010gb003790 (2011)

Kuhlbrodt, T., Griesel, A., Montoya, M., Levermann, A., Hofmann, M., and Rahmstorf, S.: On the driving processes of the Atlantic meridional overturning circulation. Rev. Geophys. *45*, 1–32 (2004)

Kwon, E. Y., Sarmiento, J. L., Toggweiler, J. R., and DeVries, J. R.: The control of atmospheric $pCO_2$ by ocean ventilation change: The effect of the oceanic storage of biogenic carbon. Global Biogeochem. Cycles *25*, GB3026; doi:10.1029/2011GB004059 (2011)

Lund, D. C., Adkins, J. F., and Ferrari, R.: Abyssal Atlantic circulation during the Last Glacial Maximum: Constraining the ratio between transport and vertical mixing. Paleoceanography *26*, Pa1213; doi:10.1029/2010pa001938 (2011)

Munk, W.: Abyssal recipes. Deep-Sea Res. *13*, 707–730 (1966)

Munk, W., and Wunsch, C.: Abyssal recipes II: energetics of tidal and wind mixing. Deep-Sea Res. I *45*, 1977–2010 (1998)

Sarnthein, M., Schneider, B., and Grootes, P. M.: Peak glacial 14-C ventilation ages suggest major draw-down of carbon into the abyssal ocean. Clim. Past Discuss. *9*, 925–965 (2013)

Talley, L. D., Pickard, G. L., Emery, W. J., and Swift, J. H.: Descriptive Physical Oceanography. Amsterdam: Elsevier $^{6}$2011

Tschumi, T., Joos, T., Gehlen, T., and Heinze, C.: Deep ocean ventilation, carbon isotopes, marine sedimentation and the deglacial $CO_2$ rise. Clim. Past *7*, 771–800 (2011)

Dr. Luke C. Skinner
University of Cambridge
Godwin Laboratory for Palaeoclimate Research
Department of Earth Sciences
Downing Site / N339
Cambridge, CB2 3EQ
UK
Phone: +44 1223 764912
Fax: +44 1223 333450
E-Mail: lcs32@cam.ac.uk

Nova Acta Leopoldina NF *121*, Nr. 408, 223–228 (2015)

# Reconstructing Deglacial Circulation Changes in the Northern North Atlantic and Nordic Seas: $\Delta^{14}C$, $\delta^{13}C$, Temperature and $\delta^{18}OSW$ Evidence

David J. R. Thornalley (London, UK)

With 1 Figure

Ice-core records have revealed that atmospheric $CO_2$ has varied during glacial-interglacial by ~90 ppm, with rapid increases in atmospheric $CO_2$ occurring during deglaciations. It is widely accepted that changes in the amount of carbon stored in the deep ocean play a leading role in explaining these cycles, primarily because of the size of the deep ocean carbon reservoir (~60 times that of the atmosphere) and the millennial timescales on which it interacts with the atmosphere (Sigman et al. 2010). To gain an understanding of how changes in deep ocean carbon storage may have controlled past variations in atmospheric $CO_2$, we ideally require robust and detailed proxy records of the properties and ventilation pathways of the deep ocean across glacial-interglacial transitions. The deep ocean is ventilated in the high latitudes, where dense isopycnals outcrop at the sea surface. Therefore to help understand deep ocean-atmosphere exchange we require reconstructions of past hydrographic changes at these high latitude ventilation sites. Furthermore, constraints on the timing and phasing of deglacial changes in these regions enable us to evaluate hypotheses regarding the underlying mechanisms of the glacial termination.

I will present a suite of multiproxy deglacial records from one of the regions of deep ocean ventilations: the high latitude North Atlantic and Nordic Seas. These data enable the reconstruction of past ventilation rates as well as the physical properties of the surface and deep ocean. There are several lines of enquiry that will be addressed through these new datasets: (*i*) What was the cause and mechanism(s) involved in the appearance of a highly $^{14}C$-depleted water mass in the mid-depth northern North Atlantic during deglaciation? (*ii*) To what extent can this water mass explain changes in mid-depth ocean properties further south, in the subtropical North Atlantic and South Atlantic? (*iii*) What was the timing and nature of ocean reorganizations within the northern North Atlantic during Heinrich stadial 1 and what role, if any, did this play in the early deglacial rise of atmospheric $CO_2$?

(*i*). New benthic radiocarbon reconstructions from a site at 2.7 km depth in the Norwegian Sea reveal the formation of an aged deep water mass within the glacial Arctic Mediterranean (AM), with a ventilation age of up to 10,000 years. Despite such an old ventilation age, $\delta^{13}C$ and nutrient reconstructions do not suggest substantial remineralization of organic matter occurred, likely owing to low surface productivity and export of AM waters at shallow and intermediate depths. A simple box model exercise confirms the feasibility of obtaining such old ventilation ages within the AM, as long as rates of deep water renewal remained less than ~0.1 Sv for the glacial and deglaciation. It is hypothesized that gradual filling of the AM with

a dense water mass occurred throughout MIS2, resulting in aging of the water column and a sharp radiocarbon front developing between well ventilated intermediate waters and the underlying aged deeper waters. Ultimately, overflow of this aged water over the Iceland-Scotland Ridge occurred during HS1 and throughout the deglaciation, influencing the northern North Atlantic. The chemical properties of this deep AM water mass, alongside those of the open deep Atlantic can explain the deglacial $\Delta^{14}C$-$\delta^{13}C$ signals reconstructed south of Iceland (Thornalley et al. 2011). Further supporting evidence for the filling and overflow of this aged water from the Nordic Seas during HS1 has been observed at an intermediate depth core in the Faroe-Shetland Channel region (Rasmussen et al., AGU Fall 2014 Meeting, and personal communication).

New multi-proxy temperature reconstructions (benthic foram Mg/Ca and clumped isotopes) from the deep Norwegian Sea also reveal glacial temperatures that were 2–3 °C warmer than modern. This is consistent with the absence of deep convection, which today cools the deep Nordic Seas to temperatures below –1 °C. The warmer deep Norwegian Sea may have been caused by either a deep inflow of warm Atlantic water and/or by geothermal heating. The shift from a warm to cold deep Nordic Seas began during HS1 and the timing of the deep ocean heat release and surface records indicating input of substantial meltwater are consistent with a role for this deep ocean heat release in melting of sea-ice and surrounding ice sheets.

(*ii*) Temperature, $\delta^{18}$Osw and radiocarbon reconstructions from south of Iceland reveal a complex pattern of hydrographic change during the deglacial, and most notably during HS1. The signature of the aged deep water from the Nordic Seas can be detected south of Iceland during HS1 in multiple proxies. Yet HS1 also contains prominent intervals of better ventilation. One such event (~15–15.5 ka) is also associated with a warming from ~0–1 °C to 4–5 °C at 1.2 km depth. Given that identical physical and chemical properties are reconstructed in both planktic and benthic foraminifera at this time, we hypothesize that this interval represents a period of regional intermediate-deep water formation that also entrained aged water from the Nordic Seas. I will compare the timing and changing hydrography of this event to assess the extent to which it may explain hydrographic changes reconstructed further south in the Atlantic.

A brief interval of particularly strong ventilation occurred ~16–16.5 ka, which is also detected in the deep Nordic Seas. This benthic radiocarbon event has importance for constraining the timing of benthic $\delta^{18}O$ and $\delta^{13}C$ changes in the subpolar North Atlantic because it occurs at the onset of major shifts in benthic and planktic $\delta^{18}O$ and $\delta^{13}C$ within the same cores. Traditionally, constraining the age of the HS1 benthic $\delta^{18}O$ and $\delta^{13}C$ isotope change in this region has been hampered by uncertainty in the planktic $^{14}C$ reservoir age. Notwithstanding the possibility that this event is an artefact of bioturbation (although replication in two cores and other lines of evidence suggest this is unlikely), the young benthic radiocarbon ages at 16–16.5 ka provide an upper (i.e. oldest) age constraint on the timing of the major isotopic shift during HS1 in these cores. Supporting evidence for a relatively young age (<17 ka) of the timing of the HS1 benthic isotope event in the northern North Atlantic is also provided by new planktic radiocarbon dates in additional cores. In light of these suggestions on the timing of regional isotopic events in the northern North Atlantic, I will explore the relative timing of HS1 benthic isotopic events throughout the North and South Atlantic.

Finally, the data from south of Iceland and the Nordic Seas suggests that intermediate and deep water formation may have been highly variable during HS1. This apparent variability would undermine the rationale behind producing single time-slice composites of HS1, e.g.

(Tessin and Lund 2012), and invalidate interpretations based on a single mode of circulation during HS1.

(*iii*) The brief interval of particularly strong ventilation at ~16–16.5 ka also coincides with surface warming events recorded further south in the subpolar North Atlantic (Fig. 1). It is therefore plausible that there was a brief reinvigoration of deep water formation in the North-east Atlantic at ~16–16.5 ka. This observation may have implications for our understanding of the mechanisms of deglacial atmospheric $CO_2$ rise.

During the deglaciation, proxy and modelling studies have established the simplified paradigm (Rahmstorf 2002) that the North Atlantic ocean switched between a relatively deep, modern-like, mode of NADW formation during warm intervals (the Holocene, 0–11.7 ka and Bølling Allerød, BA, 13–14.7 ka), to a shallower 'cold' mode, in which Antarctic Bottom Water (AABW) replaced water of northern origin below ~2–2.5 km (e. g., the Last Glacial Maximum, LGM, ~19–23 ka). In addition, during intervals of intense ice-rafting and freshwater input such as Heinrich stadial 1 (HS1, ~14.7–19 ka) and the Younger Dryas (YD, 11.7–13 ka), it is hypothesized that convection in the North Atlantic further shoaled and weakened in response to freshwater input to the North Atlantic ('Off mode'; Fig. 1). Changes in the relative proportions of NADW *vs.* AABW affects the amount of carbon stored in the deep ocean, because of their varying preformed [DIC] and physical properties. For example, it is thought that the glacial Atlantic Ocean contained a larger volume of high [DIC], cold AABW, enabling greater carbon storage in the deep ocean, helping lower atmospheric $CO_2$ (Brovkin et al. 2012).

Another important deep ocean control on atmospheric $CO_2$ is the amount of $CO_2$ that 'leaks' out of the deep ocean through upwelling in the Southern Ocean. It is hypothesized that ventilation of the deep Southern Ocean was reduced during the LGM through a range of physical and biogeochemical processes, thereby decreasing the Southern Ocean $CO_2$ 'leak'. This enabled greater storage of carbon in the deep ocean, thus helping lower atmospheric $CO_2$ concentration (Sigman et al. 2010). Employing this mechanism, numerous studies have suggested that the deglacial rise in atmospheric $CO_2$ occurred *via* enhanced upwelling in the Southern Ocean e.g. (Anderson et al. 2009). Previous ice-core reconstructions of atmospheric $CO_2$ suggested that the deglacial increase occurred predominantly through two gradual rises, during HS1 and the YD, likely in response to North Atlantic ice-rafting and freshwater events altering the overturning circulation (Denton et al. 2010). However, the new higher resolution atmospheric $CO_2$ reconstruction from the WD ice core (Fig. 1*D*; courtesy of Marcott and Brook, OSU)) reveals an alternate picture of the deglacial rise in atmospheric $CO_2$: in addition to a gradual rise in $CO_2$ during early HS1 and the YD (18–16.5 ka; 13–11.7 ka; solid grey arrows), there were three abrupt 'jumps' in $CO_2$ of ~10–15 ppm (black arrows), followed by millennial-scale plateaus (dashed grey arrows), resulting in a more step-like curve, in which up to ~40ppm of the ~90ppm deglacial rise in atmospheric $CO_2$ occurred as abrupt 'jumps'. The 'jumps' occur at the onset of the BA and Holocene, as well as at ~16.3 ka. The onset of the BA and Holocene are widely accepted as intervals of reinvigoration of NADW (Rahmstorf 2002), begging the question, was the jump at 16.3 ka also associated with an (albeit brief) interval of strong convection in the North Atlantic? I hypothesize that the onset of deep convection led to a rapid replacement of the previously poorly ventilated, DIC-rich deep Atlantic ocean, by low [DIC], warm and salty NADW, that caused the observed abrupt increases in atmospheric $CO_2$. Recharging of deep Atlantic $CO_2$ storage likely occurred during subsequent intervals of reduced NADW formation, resulting in the atmos-

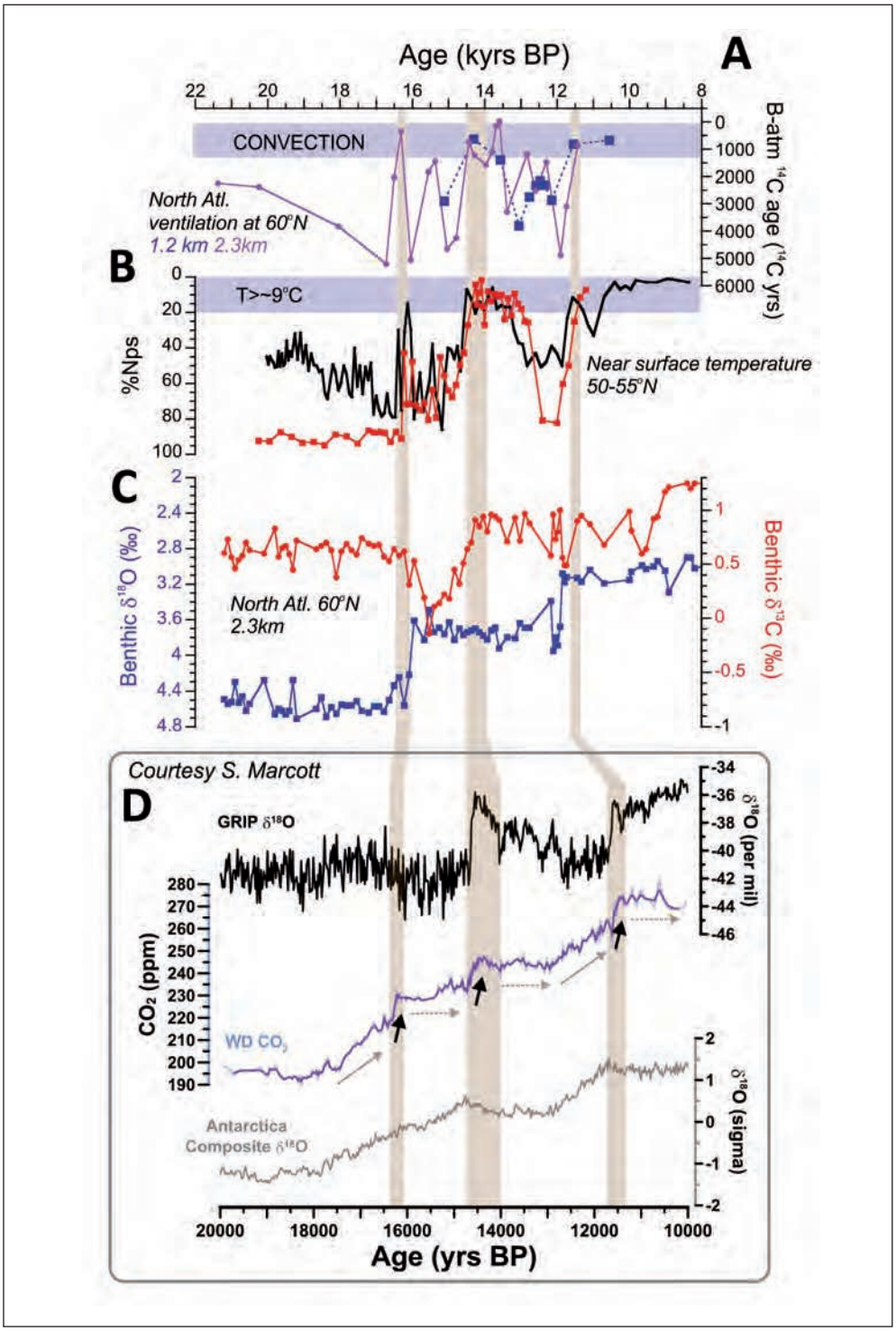
Age (kyrs BP)
A
22
20
18
16
14
12
10
8
CONVECTION
North Atl.
ventilation at 60°N
1.2 km 2.3km
B-atm $^{14}$C age ($^{14}$C yrs)
0
1000
2000
3000
4000
5000
6000
B
T>~9°C
%Nps
0
20
40
60
80
100
Near surface temperature
50-55°N
C
Benthic $\delta^{18}$O (‰)
2
2.4
2.8
3.2
3.6
4
4.4
4.8
North Atl. 60°N
2.3km
Benthic $\delta^{13}$C (‰)
1
0.5
0
-0.5
-1
Courtesy S. Marcott
D
GRIP $\delta^{18}$O
$\delta^{18}$O (per mil)
-34
-36
-38
-40
-42
-44
-46
$CO_2$ (ppm)
280
270
260
250
240
230
220
210
200
190
WD $CO_2$
Antarctica
Composite $\delta^{18}$O
$\delta^{18}$O (sigma)
2
1
0
-1
-2
20000
18000
16000
14000
12000
10000
Age (yrs BP)

pheric $CO_2$ plateaus. A similar mechanism has been invoked to explain transient increases in atmospheric $CO_2$ during the onset of the Dansgaard-Oeshger warm events of Marine Isotope Stage 3 (30–60 ka) (Bereiter et al. 2012). Although a wide range of behaviour is displayed by different models, several previous studies have suggested that, by itself, the replacement of SSW by NADW can cause a rise in atmospheric $CO_2$ of up to ~10–30 ppm e.g. (Schulz et al. 2001, Brovkin et al. 2012). Initial constraints on North Atlantic deep convection, from south of Iceland and the Nordic Seas (Fig 1*A*, *B*), support this hypothesis, but to gain confidence that this is a robust feature, further measurements are required.

To trace the extent of the 16–16.5 ka convection event in the subpolar Northeast Atlantic, I have analysed benthic $\delta^{13}C$ and benthic-planktic $^{14}C$ ages in the high sedimentation rate core OCE-326-GGC14, from 3.5 km depth in the Northwest Atlantic, during HS1. These data do not suggest that the deep North Atlantic was subject to a strong ventilation event from 16–16.5 ka, in line with other existing proxy data. It is therefore likely that ventilation was restricted to the mid-depth ocean, weakening the supporting case for this event playing a role in the atmospheric $CO_2$ jump at 16.3 ka. Yet it remains intriguing that there were clearly important hydrographic reorganizations occurring within the subpolar North Atlantic at this time, warranting continued investigation into the cause of the Northeast Atlantic ventilation and surface warming signals and any possible link to atmospheric $CO_2$ change.

## *References*


Anderson, R. F., Ali, S., Bradtmiller, L. I., Nielsen, S. H. H., Fleisher, M. Q., Anderson, B. E., and Burckle, L. H.: Wind-driven upwelling in the Southern Ocean and the deglacial rise in atmospheric $CO_2$. Science *323*, 1443–1448; doi: 10.1126/science.1167441 (2009)

Bereiter, B., Lüthi, D., Siegrist, M., Schupbach, S., Stocker, T. F., and Fischer, H.: Mode change of millennial $CO_2$ variability during the last glacial cycle associated with a bipolar marine carbon seesaw. Proc. Natl. Acad. Sci. USA *109*, 9755–9760; doi:10.1073/pnas.1204069109 (2012)

Brovkin, V., Ganopolski, A., Archer, D., and Munhoven, G.: Glacial $CO_2$ cycle as a succession of key physical and biogeochemical processes. Clim. Past *8*, 251–264; doi:10.5194/cp-8-251–2012 (2012)

Denton, G. H., Anderson, R. F., Toggweiler, J. R., Edwards, R. L., Schaefer, J. M., and Putnam, A. E.: The last glacial termination. Science *328*, 1652–1656; doi:10.1126/science.1184119 (2010)

Lagerklint, I. M., and Wright, J. D.: Late glacial warming prior to Heinrich event 1: The influence of ice rafting and large ice sheets on the timing of initial warming. Geology *27*, 1099–1102 (1999)

Peck, V. L., Hall, I. R., Zahn, R., Elderfield, H., Grousset, F., Hemming, S. R., and Scourse, J. D.: High resolution evidence for linkages between NW European ice sheet instability and Atlantic Meridional Overturning Circulation. Earth Planet. Sci. Lett. *243*, 476–488 (2006)

Rahmstorf, S.: Ocean circulation and climate during the past 120,000 years. Nature *419*, 207–214 (2002)

Schulz, M., Seidov, D., Sarnthein, M., and Stattegger, K.: Modeling ocean-atmosphere carbon budgets during the Last Glacial Maximum-Heinrich 1 meltwater event-Bolling transition. Int. J. Earth Sci. *90*, 412–425 (2001)


Fig. 1 Open ocean deep convection produces waters that have a small $^{14}C$ offset from the contemporaneous atmosphere, allowing past intervals of convection to be identified. Existing data from the high latitude North Atlantic is shown in (*A*) (Thornalley et al. 2011), suggesting a deep convection occurred at ~16–16.5 ka, during the early BA (~14.5–14.0 ka), and the Holocene (11.7–0 ka). (*B*) The convection event at 16–16.5 ka also coincides with near-surface warming in the subpolar North Atlantic (Peck et al. 2006, Lagerklint and Wright 1999); (*C*) as well as marking the onset the major benthic $\delta^{13}C$ and $\delta^{18}O$ in the mid-depth subpolar North Atlantic (data from RAPiD-17-5P). (*D*) WD ice-core atmospheric $CO_2$ reconstruction (purple), with Greenland (GRIP) and Antarctic $\delta^{18}O$ shown for reference – figure courtesy of S. Marcott (OSU).

Sigman, D. M., Hain, M. P., and Haug, G. H.: The polar ocean and glacial cycles in atmospheric $CO_2$ concentration. Nature *466*, 47–55; doi:10.1038/nature09149 (2010)

Tessin, A. C., and Lund, D. C.: Isotopically depleted carbon in the mid-depth South Atlantic during the last deglaciation. Paleoceanography *28*/2, 296–306; doi:10.1002/palo.20026 (2012)

Thornalley, D. J. R., Barker, S., Broecker, W., Elderfield, H., and McCave, I. N.: The deglacial evolution of North Atlantic deep convection. Science *331*, 202–205; doi: 10.1126/science.1196812 (2011)

David J. R. Thornalley
Department of Geology and Geophysics
Woods Hole Oceanographic Institution
Woods Hole, MA 02543
USA

and

Department of Geography
University College London
Pearson Building
Gower Street
London WC1E 6BT
UK
Phone: +44 20 76790506
Fax: +44 20 76790565
E-Mail: d.thornalley@ucl.ac.uk

Nova Acta Leopoldina NF *121*, Nr. 408, 229–233 (2015)

# New Constraints on the Glacial Extent of the Pacific Carbon Pool and its Deglacial Outgassing

Ralf Tiedemann,[1] Thomas A. Ronge,[1] Frank Lamy,[1] Peter Köhler,[1]
Matthias Frische,[2] Ricardo De Pol-Holz,[3] Katharina Pahnke,[4]
Brent V. Alloway,[5] Lukas Wacker,[6] and John Southon[7]

With 2 Figures

The analysis of air, trapped in Antarctic ice core records, documents an increase of atmospheric $CO_2$ by ~90 ppmv during the last deglacial transition, from 18.5–11 ka. Parallel to this, the record of atmospheric radiocarbon activities ($\Delta^{14}C$) reveals a significant decrease that was most pronounced during Heinrich stadial 1 (HS 1; ~ 17.5–14.7 ka; Parrenin et al. 2013, Reimer et al. 2013). The contemporaneous pattern of both records implies an associated underlying mechanism combining the rise of atmospheric $CO_2$ to the release of a radiocarbon-depleted reservoir. Because the ocean contains up to 60-times more carbon than the entire atmosphere (Broecker 1982) it has the potential to drive the atmospheric $CO_2$-pattern. Therefore, the release of $^{14}C$-depleted $CO_2$ from an old deep water carbon pool is thought to explain a substantial part of the atmospheric $CO_2$ variabilities (Skinner et al. 2010). Indeed, several studies show the presence of old $^{14}C$-depleted deep waters during the last glacial in the North and South Pacific as well as in the South Atlantic (Burke and Robinson 2012, Sarnthein et al. 2013, Sikes et al. 2000, Skinner et al. 2010) and propose the storage of $CO_2$ in the deep glacial ocean.

The upwelling systems in the Southern Ocean are considered to represent the pathway of this old $CO_2$ from the deep water toward the atmosphere (Marchitto et al. 2007). Around Antarctica, carbon rich Circumpolar Deep Waters are upwelled and hence make contact with the atmosphere. After the process of air-sea gas-exchange, the upwelled waters are mixed and provide a major source for newly formed Antarctic Intermediate Water (AAIW; Talley 2013). Due to this circulation pattern, AAIW can spread the information of upwelling of old water masses (high $CO_2$ and low $^{14}C$) into the Atlantic, Pacific and Indian Oceans. In order to localize and time the export of upwelled deep waters from the Southern Ocean, several (in

1 Alfred Wegener Institute, Helmholtz Centre for Polar and Marine Research, Bremerhaven, and University of Bremen, Am Alten Hafen 26, 27568 Bremerhaven, Germany.
2 GEOMAR Helmholtz Centre for Ocean Research, Kiel, Germany.
3 Departamento de Oceanografía and Center for Climate and Resilience Research (CR)$^2$, Universidad de Concepción, Chile.
4 Max Planck Research Group – Marine Isotope Geochemistry, Institute for Chemistry and Biology of the Marine Environment, Carl von Ossietzky University, Oldenburg, Germany.
5 School of Geography, Environment and Earth Sciences, Victoria University, Wellington, New Zealand.
6 Laboratory of Ion Beam Physics (HPK), Eidgenössische Technische Hochschule, Zürich, Switzerland.
7 School of Physical Science, University of California, Irvine, CA, USA.

parts contradicting) studies have analyzed the $^{14}C$-history of intermediate-water records (De Pol-Holz et al. 2010, Marchitto et al. 2007). However, the dimension of the glacial carbon pool as well as its evolution over time and its pathways towards the surface and ultimately towards the atmosphere still remain a matter of an ongoing debate.

The aim of our study is to present a new perspective on this topic by using a water mass transect of several sediment cores instead of only one record as most of the proceeding studies have done. We analysed six sediment cores from the Bounty Trough east of New Zealand that cover the water masses from the AAIW down to the Lower Circumpolar Deep Water (LCDW; 835 – 4339 m water depth; Fig. 1). These records were supplemented by another record that was retrieved from 3613 m water depth more than 4000 km away from New Zealand at the East Pacific Rise (Fig. 1, *top*). Our sediment core transect enables the reconstruction of $^{14}C$ over the last 30,000 years for multiple levels of the Southern Ocean's water column. As it is shown in Figure 1 (*bottom*), we can record $^{14}C$-depleted deep-waters moving towards the south, as well as newly formed intermediate and bottom waters moving towards the north, which carry the information of deep water upwelling and air-sea gas exchange. To facilitate the direct comparison of the atmospheric $\Delta^{14}C$ record to the water mass ventilation, we reconstructed the $\Delta^{14}C$ history of all sediment cores. Depicted as a $\Delta\Delta^{14}C$ notation (direct offset of the water mass to the atmospheric record), low values indicate old, weakly ventilated waters, while higher values indicate better-ventilated younger waters (Fig. 2, top).

During the last glacial our $\Delta\Delta^{14}C$ reconstructions indicate a significant radiocarbon depletion in the Circumpolar Deep Waters between ~2000 and ~4300 m water depth (Fig. 2). Contemporaneous, the intermediate-waters were significantly better ventilated (Fig. 2) indicating a strong glacial stratification separating the intermediate-waters from the underlying deep waters. Furthermore, it is noteworthy that we didn't find the lowest ventilation towards the bottom but at ~ 2500 m water depth with better ventilated waters above and below, indicating mixing processes with better ventilated water masses. In a similar way, the $\delta^{13}C$ reconstructions of McCave et al. (2008) north of our research area, also locate weakly ventilated waters between 2000 and 3500 m water depth. The extreme mid-water $^{14}C$ depletion yielding $\Delta\Delta^{14}C$ values as low as –1000 ‰ is corroborated by the previous findings of Sikes et al. (2000), who reported glacial values of – 870 ‰ in the Bounty Trough at ~2700 m water depth. Our open ocean record from the East Pacific Rise (Fig. 1, top) traces the radiocarbon depleted waters more than 4000 km away from the Bounty Trough, showing that these values do not only represent a local phenomenon off New Zealand but that a widespread expansion of old ($^{14}C$-depleted) waters prevailed in the glacial South Pacific between ~2500 and ~3600 m water depth. Furthermore, $^{14}C$-depleted water masses can be traced through the Drake Passage (Burke and Robinson 2012) and into the South Atlantic (Skinner et al. 2010).

The glacial $\Delta\Delta^{14}C$ pattern shown in Figure 2 (*top*) resembles in a striking way the modern distribution of $\Delta^{14}C$ in the Pacific Ocean (Fig. 1, *bottom*), with good ventilated intermediate-waters, increasing $^{14}C$ depletion below in UCDW, the highest depletion (oldest an $CO_2$-richest waters) between 2500 and 3600 m and better ventilated waters below, towards the bottom. For this reason and because previous studies have also found radiocarbon depleted waters in the glacial North Pacific (Sarnthein et al. 2013), our data may represent the glacial return flow of old Pacific Deep Water in analogy to the modern deep water circulation as it is shown in Figure 1 (*bottom*).

To facilitate a pronounced deep water $^{14}C$ depletion, the deep South Pacific must have had limited access to the surface and the atmosphere in consequence of enhanced ocean stratifi-

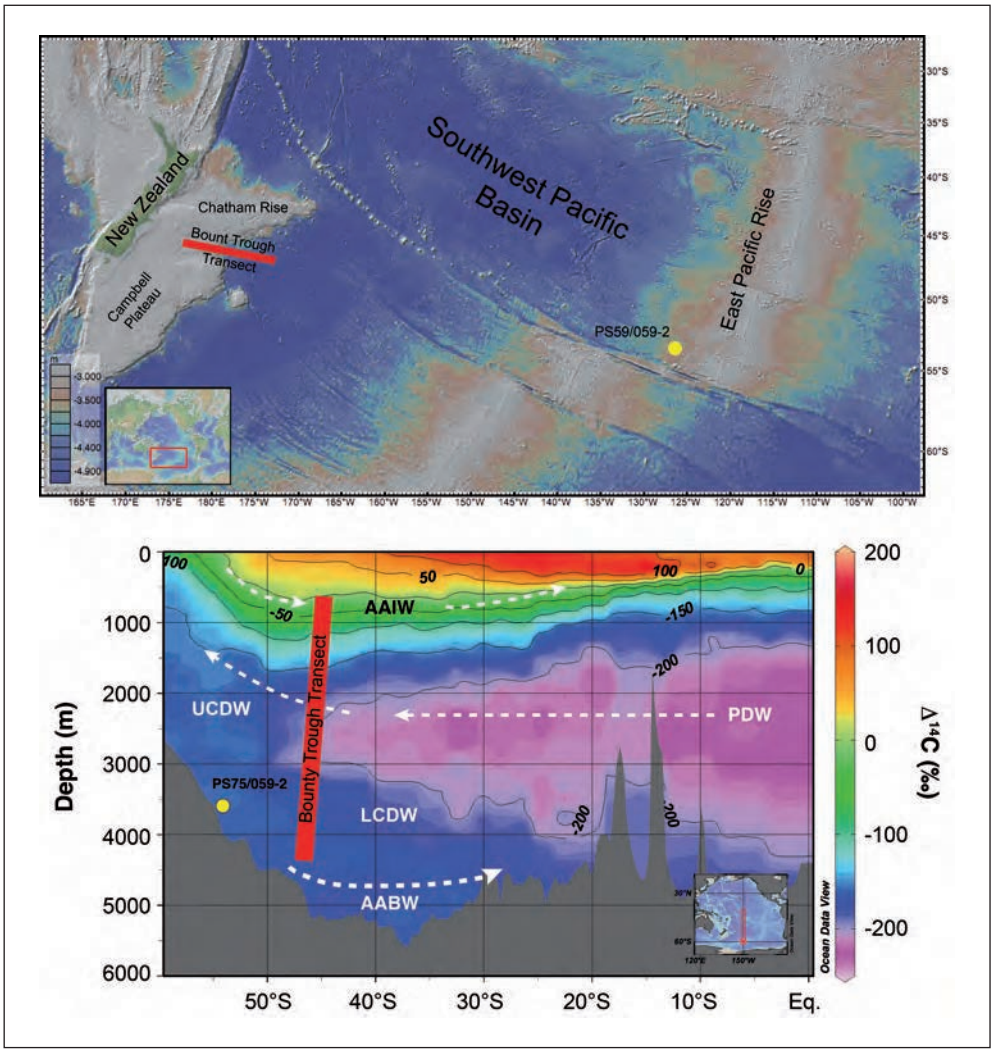


Fig. 1 (*Top*) Overview map of the southwest Pacific, indicating our research area in the Bounty Trough (red bar) and at the East Pacific Rise (yellow dot). (*Bottom*) Modern $\Delta^{14}C$ concentrations of the South Pacific. The area covered by the Bounty Trough sediment core transect is marked by the red bar. The sediment core from the East Pacific rise is indicated by a yellow circle (~ 152°W; Key et al. 2004). Antarctic Intermediate Water (AAIW); Upper and Lower Circumpolar Deep Water (UCDW and LCDW); Antarctic Bottom Water (AABW); Pacific Deep Water (PDW).

cation. Throughout the glacial expanded Antarctic sea-ice conditions (Gersonde et al. 2005) and changes in the Southern westerly wind belt (Kohfeld et al. 2013) may have hampered the upwelling of old deep waters around the Antarctic continent. Also, enhanced buoyancy-differences by increased deep water salinity (Adkins 2013) and freshening of intermediate-waters (Saenko et al. 2001) increased the stratification and inhibited the communication between the deep ocean and the surface.

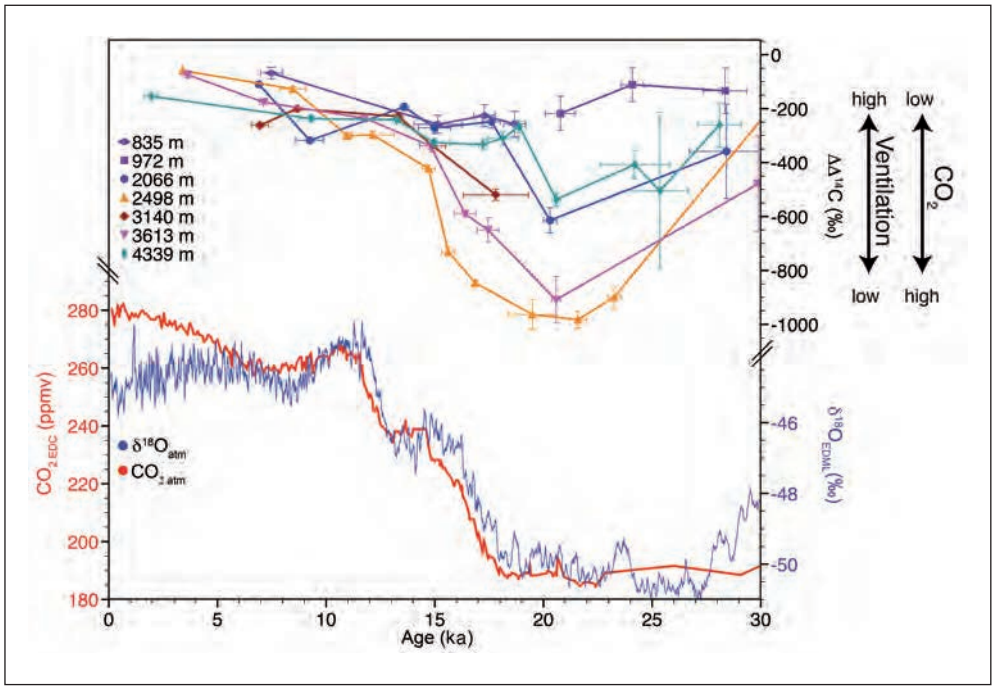


Fig. 2 (*Top*) $\Delta\Delta^{14}C$ values (offset of measured $\Delta^{14}C$ to the contemporaneous atmosphere) of the SW-Pacific. (*Bottom*) Antarctic $\delta^{18}O$ record EDML (blue; *EPICA Community Members* 2006) and atmospheric $CO_2$ EDC (red; Parrenin et al. 2013).

Parallel to the observed rise in atmospheric $CO_2$ and Antarctic temperatures, the ventilation of the deep Pacific at 2500 m significantly increases during termination 1 (Fig. 2) and point towards a transfer of old $CO_2$ from the depth towards the surface. This $CO_2$ release reduced the deep water to atmosphere offset from glacial values of about –1000 ‰ $\Delta\Delta^{14}C$ to ~ –200‰ during the Holocene. During this period of pronounced upwelling, AAIW $\Delta\Delta^{14}C$ decreases only slightly (this study; Rose et al. 2010). Therefore, we propose that the excess of upwelled $^{14}C$-depleted $CO_2$ was not substantially incorporated in newly formed AAIW, but that it was directly transported towards the atmosphere, contributing to the observed rise of atmospheric $CO_2$. At the end of termination 1 (~11.5 ka), uniform $\Delta\Delta^{14}C$ values throughout the water column mark the end of the Pacific outgassing period.

## *References*

Adkins, J. F.: The role of deep ocean circulation in setting glacial climates. Paleoceanography *28*, 539–561 (2013)

Broecker, W.: Glacial to interglacial changes in ocean chemistry. Progr. Oceanogr. *11*, 151–197 (1982)

Burke, A., and Robinson, L. F.: The Southern Ocean's role in carbon exchange during the last deglaciation. Science *335*, 557–561 (2012)

De Pol-Holz, R., Keigwin, L. D., Southon, J., Hebbeln, D., and Mohtadi, M.: No signature of abyssal carbon in intermediate waters off Chile during deglaciation. Nature Geosci. *3*, 192–195 (2010)

*EPICA Community Members*: One-to-one coupling of glacial climate variability in Greenland and Antarctica. Nature *444*/9, 195–198 (2006)

Gersonde, R., Crosta, X., Abelmann, A., and Armand, L.: Sea-surface temperature and sea ice distribution of the Southern Ocean at the EPILOG Last Glacial Maximum – a circum-Antarctic view based on siliceous microfossil records. Quat. Sci. Rev. *24*, 869–896 (2005)

Key, R. M., Kozyr, A., Sabine, C. L., Lee, K., Wanninkhof, R., Bullister, J. L., Feely, R. A., Millero, F. J., Mordy, C., and Peng, T.-H.: A global ocean carbon climatology: Results from Global Data Analysis Project (GLODAP). Global Biochem. Cycles *18*, 1–23 (2004)

Kohfeld, K. E., Graham, R. M., Boer, A. M. de, Sime, L. C., Wolff, E. W., Le Quéré, C., and Bopp, L.: Southern Hemisphere westerly wind changes during the Last Glacial Maximum: paleo-data synthesis. Quat. Sci. Rev. *68*, 76–95 (2013)

Marchitto, T. M., Lehman, S. J., Ortiz, J. D., Flückinger, J., and van Geen, A.: Marine radiocarbon evidence for the mechanism of deglacial atmospheric $CO_2$ rise. Science *316*, 1456–1459 (2007)

McCave, I. N., Carter, L., and Hall, I. R.: Glacial-interglacial changes in water mass structure and flow in the SW Pacific Ocean. Quat. Sci. Rev. *27*, 1886–1908 (2008)

Parrenin, F., Masson-Delmotte, V., Köhler, P., Raynaud, D., Paillard, D., Schwander, J., Barbante, C., Landais, A., Wegner, A., and Jouzel, J.: Synchronous change of atmospheric $CO_2$ and Antarctic temperature during the last deglacial warming. Science *339*, 1060–1063 (2013)

Reimer, P. J., et al.: IntCal13 and Marine13 radiocarbon age calibration curves 0-50,000 years Cal BP. Radiocarbon *55*/4, 1869–1887 (2013)

Rose, K. A., Sikes, E. L., Guilderson, T. P., Shane, P., Hill, T. M., Zahn, R., and Spero, H. J.: Upper-ocean-to-atmosphere radiocarbon offsets imply fast deglacial carbon dioxide release. Nature *466*, 1093–1097 (2010)

Saenko, O. A., and Weaver, A. J.: Importance of wind-driven sea ice motion for the formation of Antarctic Intermediate Water in a global climate model. Geophys. Res. Lett. *28*/21, 4147–4150 (2001)

Sarnthein, M., Schneider, B., and Grootes, P. M.: Peak glacial $^{14}C$ ventilation ages suggest major draw-down of carbon into the abyssal ocean. Clim. Past *9*, 929–965 (2013)

Sikes, E. L., Samson, C. R., Gullderson, T. P., and Howard, W. R.: Old radiocarbon ages in the southwest Pacifc Ocean during the last glacial period and deglaciation. Nature *405*, 555–559 (2000)

Skinner, L. C., Fallon, S., Waelbroeck, C., Michel, E., and Barker, S.: Ventilation of the deep Southern Ocean and deglacial $CO_2$ rise. Science *328*, 1147–1151 (2010)

Talley, L. D.: Closure of the global overturning circulation through the Indian. Pacific, and Southern Oceans: Schematics and transports. Oceanography *26*/1, 80–97 (2013)

Prof. Dr. Ralf Tiedemann
Alfred Wegener Institute
Helmholtz Centre for Polar and Marine Research
Am Alten Hafen 26
27568 Bremerhaven
Germany
Phone: +49 471 48311200
Fax: +49 471 48311149
E-Mail: Ralf.Tiedemann@awi.de

Nova Acta Leopoldina NF *121*, Nr. 408, 235–239 (2015)

# Deglacial $CO_2$/Climate Feedbacks: Models, Myths, and Misconceptions

Axel Timmermann and Tobias Friedrich (Honolulu, HI, USA)

With 3 Figures

The fact that glacial/interglacial $CO_2$ variations are orbitally paced implies the existence of a universal climate/carbon cycle feedback mechanism that operated during all glacial terminations, and not only during the last one. This means that the specifics of the millennial-scale forcing during the last glacial termination, which were very different from the ones during previous terminations, most likely played only a secondary role for the $CO_2$ change. We propose that the deglacial $CO_2$ rise would have even happened without the Heinrich 1 and Younger Dryas freshwater forcing events and associated AMOC responses. The secondary role of millennial scale variability in the reorganization of the carbon cycle is illustrated during termination 2, which started with a $CO_2$ rise at 138 ka and was followed by a single Heinrich event (H11) several thousand years later. These facts suggest that we need to focus more on an understanding of how orbital forcing affects the climate system and subsequently the carbon cycle. In our view, the millennial-scale analysis of deglacial $CO_2$ trends is a dead end.

Assuming that a significant fraction of deglacial $CO_2$ was vented physically from the Southern Ocean during all glacial terminations, we can ask: What are the key orbital-scale drivers of oceanic and atmospheric variability in the Southern Hemisphere?

A popular hypothesis is that glacial/interglacial $CO_2$ changes were driven by changes in the Southern Hemisphere westerlies. Several studies (Toggweiler et al. 2006, Anderson et al. 2009, Denton et al. 2010) postulated that a deglacial poleward shift of Southern Hemisphere westerlies and an increase of Southern Ocean upwelling, triggered the atmospheric $CO_2$ increase during termination 1 and a positive feedback that further amplified the wind anomalies. To test this idea, our presentation will provide a detailed analysis of the orbital pacemaking of Southern Hemisphere winds using a series of AGCM time-slice and transient EMIC experiments covering the past 4 glacial cycles. We find that the transient experiments conducted with the EMIC LOVECLIM simulate a Southern Hemisphere climate in close agreement with ice core data (Deuterium, Deuterium excess, sea-salt and dust fluxes). This realistic climate trajectory exhibits wind variations that are strongly driven by obliquity forcing, but very little sensitivity to greenhouse gas changes. Strong obliquity weakens the meridional temperature gradient and the surface Southern Hemisphere westerlies (Fig. 1, upper panel). In fact past glacial terminations were consistently characterized by transitions from weak obliquity (strong surface westerlies) forcing to strong obliquity values (weaker westerlies), consistent with the cold/warm orbit transition hypothesis. According to climate models of varying complexity, the obliquity-driven changes of the Southern Hemisphere westerlies

were very small (± 5 %) and were very likely insufficient to drive major $CO_2$ changes. Moreover, changes in the latitude of the surface westerlies are much more controlled by the sea-ice extent than by the direct obliquity forcing. Therefore, the previously hypothesized $CO_2$/westerly wind scenario which assumes that intensifying and poleward shifting westerlies during termination 1, which were partly connected to Northern Hemispheric millennial-scale processes, sucked up carbon-rich waters is inconsistent with physical modelling evidence, a plethora of paleo-climate proxy studies (e.g. KOHFELD et al. 2013 for overview) and also with dust data from Antarctic ice cores, which suggest stronger winds under glacial conditions.

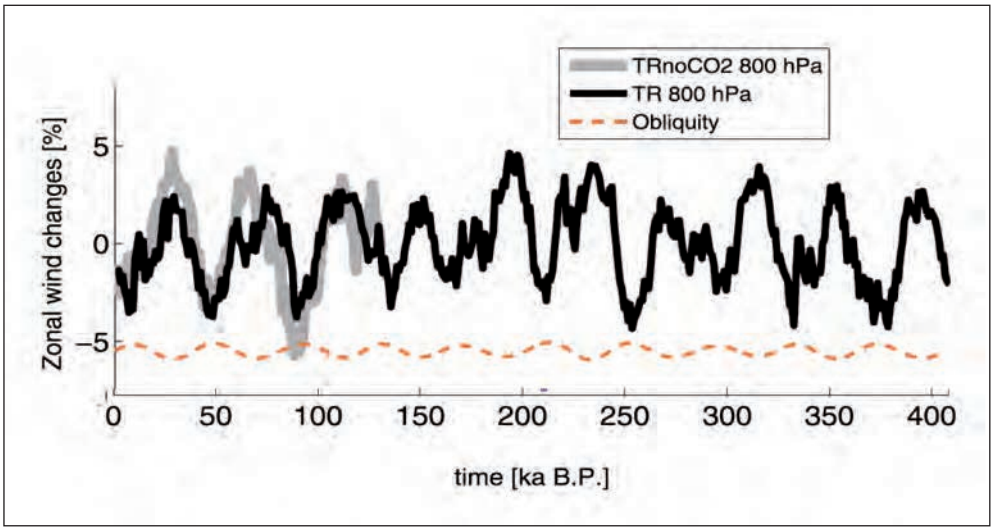


Fig. 1 Black: Simulated relative 800 hPa wind changes (percent) in transient LOVECLIM simulation forced by time-varying boundary conditions (TIMMERMANN et al. 2014). Gray: same as black but for model experiment that uses constant atmospheric $CO_2$ concentrations. Orange line, obliquity changes (arbitrary units).

A key element of the Southern Ocean/climate system is sea-ice, which influences surface albedo, air-sea gas exchange, momentum- and heat exchange. Its equatorward export controls buoyancy forcing of the Southern Ocean, the establishment of meridional salinity gradients, stratification and the production of Antarctic Bottom Water. Furthermore, sea-ice influences biological productivity. With impacts on so many carbon-cycle relevant physical and biological processes, it is paramount to understand how sea-ice responds to orbital forcing.

As shown in previous studies, the reconstructed and simulated sea-ice extent in the Southern Hemisphere strongly correlates with the fixed season spring insolation (equivalent to Southern Hemisphere summer length). This forcing is synchronous with the Northern Hemisphere summer insolation changes, which contribute to the waxing and waning of Northern Hemisphere ice-sheets. Thus, similar local forcings in Northern and Southern Hemisphere can cause respective ice-sheet and sea-ice variations, that vary in unison. Furthermore, as demonstrated in a recent study (HEINEMANN et al. 2014) orbitally-paced ocean/carbon cycle variations in the Southern Hemisphere, which may have contributed to the glacial/interglacial $CO_2$ change, would have further intensified the variations in Northern Hemispheric ice volume (Fig. 2).

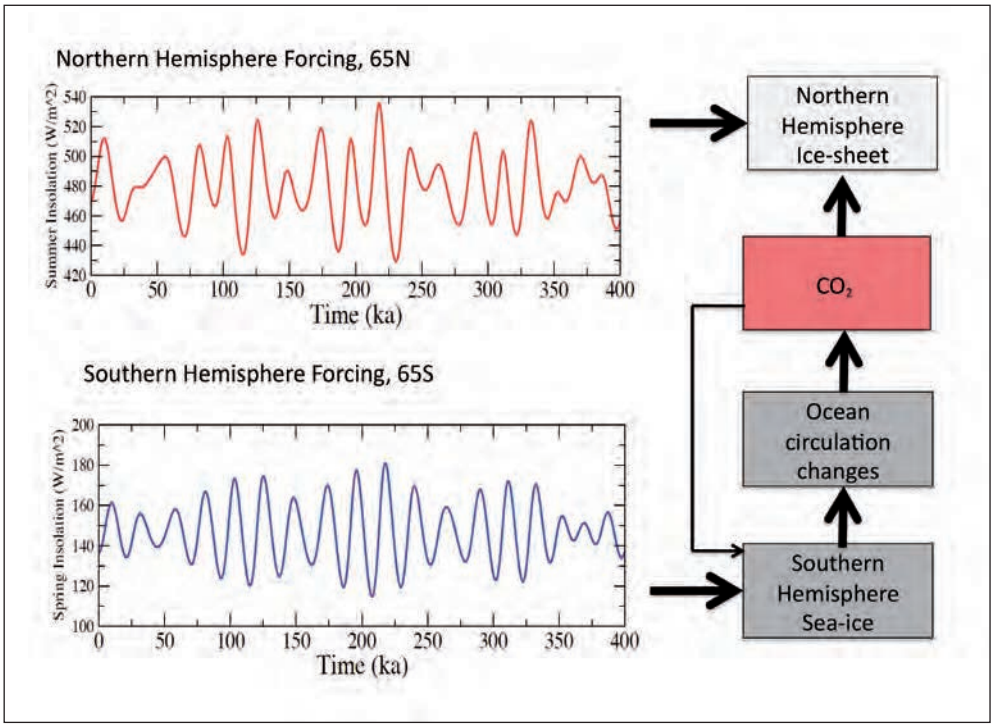


Fig. 2 Schematic of orbital synchronization between Southern Hemisphere sea-ice, atmospheric $CO_2$ and Northern Hemisphere ice-sheet variations.

Using a realistic transient climate model simulation over the past 784 ka, we present further analysis of how orbital forcing influenced sea-ice extent and in particular the efficacy of Ekman pumping in the Southern Ocean – in the presence of near-constant Southern Hemisphere westerlies (Fig. 1). Even though, Ekman pumping is only one contribution to the Southern Hemisphere upwelling, it is an important one, that can be subject to massive changes in the presence of sea-ice changes.

Ekman pumping velocities for the open ocean are usually calculated as

$$w^{AO}_e = r^{-1} [\partial_x(t^{AO}_y/f) - \partial_y(t^{AO}_x/f)], \quad [1]$$

where r represents the water density, $t^{AO}_{x,y}$ the zonal and meridional stress components between atmosphere and ocean, f the Coriolis parameter and $\partial_{x,y}$ the partial derivatives in x and y direction. The atmosphere-ocean stress vector is denoted here as $\mathbf{t}^{AO}=(t^{AO}_x,t^{AO}_x)$. In partially sea-ice covered areas, however, with a sea-ice fraction of a, such as the Southern Ocean, one has to take into account also the stress between sea-ice and ocean, which can be calculated from

$$\mathbf{t}_{IO} = \mathbf{C}_{IO}\, \mathbf{r}\, |\mathbf{u}_i - \mathbf{u}_o|\, (\mathbf{u}_i - \mathbf{u}_o), \quad [2]$$

with $C_{IO}$=0.0055 representing a drag coefficient and $\mathbf{u}_i$, $\mathbf{u}_o$ the ice and ocean velocities, respectively. Here we calculate the Ekman pumping below partially covered sea-ice areas from the output provided by the 784 ka transient LOVCLIM simulation using

$$w^N_e = r^{-1} [\partial_x(t^N_y/f) - \partial_y(t^N_x/f)], \quad [3]$$

$$\text{with } \mathbf{t^N} = a\,\mathbf{t_{IO}} + (1\text{-}a)\,\mathbf{t^{AO}}. \quad [4]$$

We define an Ekman pumping efficacy $E_e$ as $E_e = w^N_e / w^{AO}_e$ which characterizes the ratio of the wind-stress curl that is available for Ekman pumping in the ocean in sea-ice covered regions.

The Ekman pumping efficacy is smaller than 1 ($E_e$<1) in regions of sea-ice convergence or divergence, such as the Ross and Weddell Seas (Goosse and Fichefet 1999). As already proposed in Goosse and Fichefet (1999), extended Southern Hemisphere sea-ice coverage under glacial conditions may lead to a sea-ice-induced damping of the Southern Hemisphere upwelling, even when the mean winds remain the same. Here we pursue this idea further to identify potential causes for orbital-scale variations in ocean ventilation and $CO_2$. Under present-day conditions most of the carbon-rich waters upwell south of the Antarctic Polar Front.

As shown in Figure 3, over the last 350 ka the efficacy of Ekman pumping varied by a factor of 2.5 during glacial terminations, in unison with austral spring insolation changes, simulated sea-ice coverage and EPICA sea-salt fluxes (Wolff et al. 2006). Phases of high (low) eccentricity and high (low) amplitude precessional cycles in austral spring insolation correspond to interglacial (glacial) conditions and high (low) atmospheric $CO_2$, thus suggesting the presence of a nonlinear climate-carbon cycle rectification mechanism in the Southern Hemisphere. Here we propose that the orbital-modulation of sea-ice coverage and related Southern Ocean Ekman pumping may have partly controlled the upwelling of carbon-rich

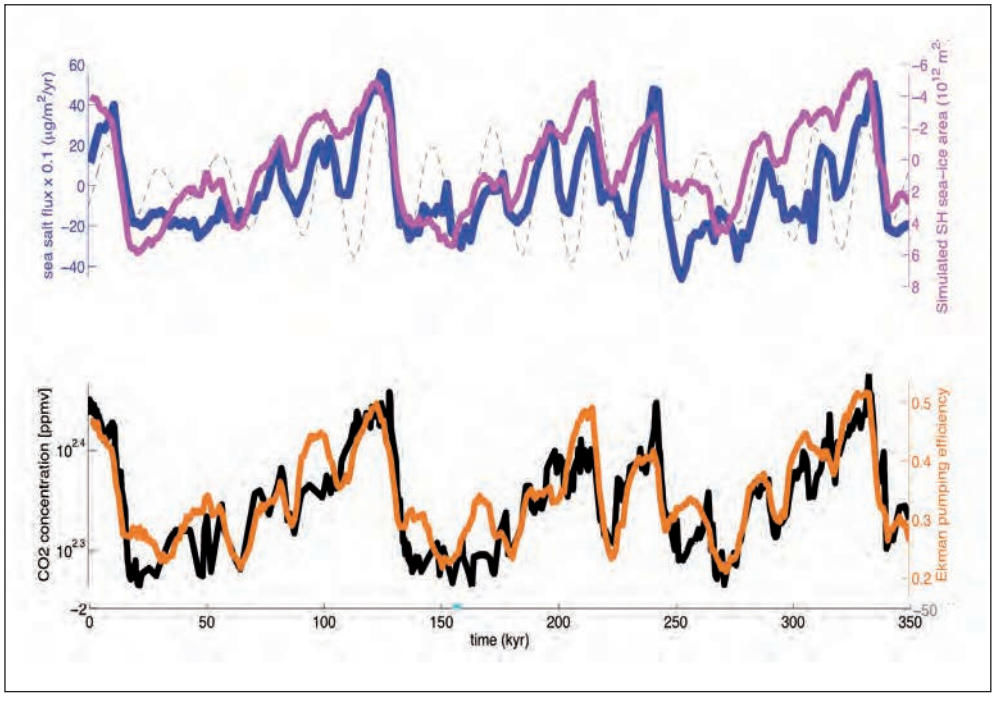


Fig. 3 Simulated Southern Hemisphere sea-ice area (magenta) in transient LOVECLIM simulation compared with EPICA sea-seal flux. Black: EPICA $CO_2$ concentrations and simulated Ekman pumping efficacy (orange) in LOVECLIM transient simulation south of Antarctic Polar front.

waters and in turn the degassing of $CO_2$ into the atmosphere. This process may be further amplified by the sea-ice control on air-sea gas exchange (Stephens and Keeling 2000). These processes will control the upwelling branch of deep ocean $CO_2$. However, in order to develop a more complete picture of $CO_2$ fluxes it is important to also study the buoyancy-driven downwelling/sinking branch, which can sequester carbon in the deep ocean in glacial times. After all, we are interested in tiny $CO_2$ flux imbalances during glacial terminations and their control by physical and biological processes. The presentation will conclude with an assessment of the role of sea-ice export on Southern Ocean surface ocean stratification, on the formation of AABW and on the physical pump.

Our new results demonstrate that orbitally-paced sea-ice variations may have played a fundamental role in interglacial/glacial variability of atmospheric $CO_2$ concentrations.

## *References*


Anderson, R. F., Ali, S., Bradtmiller, L. I., Nielsen, S. H. H., Fleisher, M. Q., Anderson, B. E., and Burckle, L. H.: Wind-driven upwelling in the Southern Ocean and the deglacial rise in atmospheric $CO_2$. Science, *323*/5920, 1443–1448 (2009)

Denton, G. H., Anderson, R. F., Toggweiler, J. R., Edwards, R. L., Schaefer, J. M., and Putnam, A. E.: The last glacial termination. Science *328*/5986, 1652–1656 (2010)

Goosse, H., and Fichefet, T.: Importance of ice-ocean interactions for the global ocean circulation: A model study. J. Geophys. Res. *104*/C10, 23337–23355 (1999)

Heinemann, M., Timmermann, A., Timm, O. E., Saito, F., and Abe-Ouchi, A.: Deglacial ice sheet meltdown: orbital pacemaking and $CO_2$ effects. Clim. Past *10*/4, 1567–1579 (2014)

Kohfeld, K., Graham, R., Boer, A. de, Sime, L., Wolff, E., Le Quéré, C., and Bopp, L.: Southern Hemisphere westerly wind changes during the Last Glacial Maximum: paleo-data synthesis. Quat. Sci. Rev. *68*, 76–95 (2013)

Stephens, B. B., and Keeling, R. F.: The influence of Antarctic sea ice on glacial-interglacial $CO_2$ variations. Nature *404*/6774, 171–174 (2000)

Timmermann, A., Friedrich, T., Timm, O. E., Chikamoto, M. O., Abe-Ouchi, A., and Ganopolski, A.: Modeling obliquity and $CO_2$ effects on Southern Hemisphere climate during the past 408 ka. J. Clim. *27*/5, 1863–1875 (2014)

Toggweiler, J. R., Russel, J. L., and Carson, S. R.: Midlatitude westerlies, atmospheric $CO_2$, and climate change during the ice ages. Paleoceanography *21*, doi: 10.1029/2005PA001154 (2006)

Wolff, E. W., Fischer, H., Fundel, F., Ruth, U., Twarloh, B., Littot, G. C., Mulvaney, R., Rothlisberger, R., Angelis, M. de, Boutron, C. F., Hansson, M., Jonsell, U., Hutterli, M. A., Lambert, F., Kaufmann, P., Stauffer, B., Stocker, T. F., Steffensen, J. P., Bigler, M., Siggaard-Andersen, M. L., Udisti, R., Becagli, S., Castellano, E., Severi, M., Wagenbach, D., Barbante, C., Gabrielli, P., and Gaspari, V.: Southern Ocean sea-ice extent, productivity and iron flux over the past eight glacial cycles. Nature *440*/7083, 491–496 (2006)



Prof. Axel Timmermann, Ph.D.
International Pacific Research Center
School of Ocean and Earth Science
and Technology
University of Hawaii
Honolulu, Hawaii 96822
USA
Phone: +1 808 9562720
Fax: +1 808 9569425
E-Mail: axel@hawaii.edu

Tobias Friedrich, Ph.D.
International Pacific Research Center
School of Ocean and Earth Science
and Technology
University of Hawaii
Honolulu, Hawaii 96822
USA
Phone: +1 808 9567385
Fax: +1 808 9569425
E-Mail: tobiasf@hawaii.edu

Nova Acta Leopoldina NF *121*, Nr. 408, 241–245 (2015)

# Effects of Eustatic Sea-Level Change on Atmospheric $CO_2$ and Glacial Climate

Klaus Wallmann (Kiel)

With 3 Figures

## 1. Introduction

The accumulation of continental ice sheets removes large volumes of water from the glacial oceans and induces a significant drop in eustatic sea-level. These glacial changes affect the oceans in multiple ways (Broecker 1982). They decrease the ocean volume, enhance seawater salinity, increase seawater $\delta^{18}O$ values, expose large shelf areas, and induce a steepening of ocean margins. The displacement of ocean margins into steeper terrain reduces the depositional area for the burial of particulate organic matter (POM) and neritic carbonate (Fig. 1).

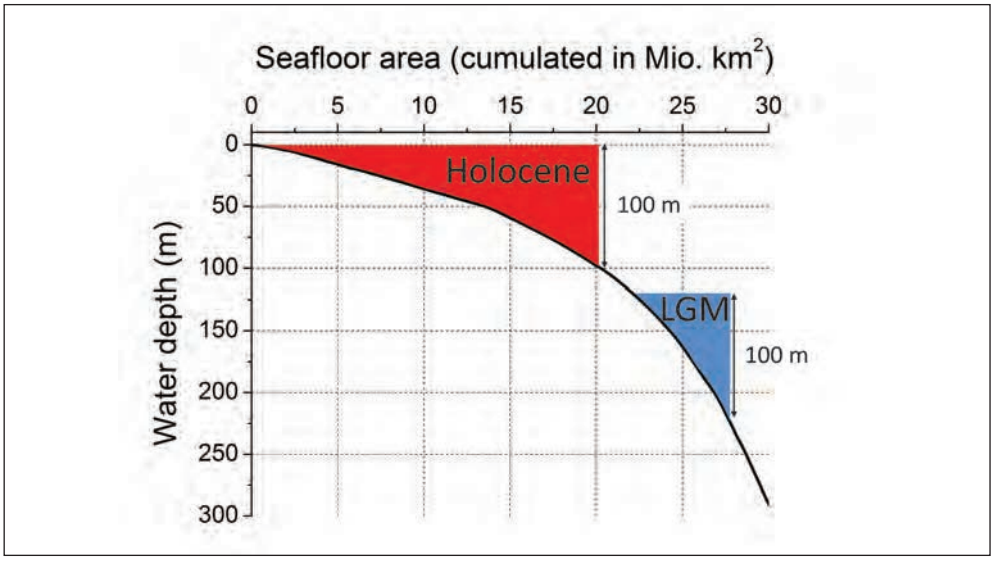


Fig. 1 Morphology of the global ocean margin. The black line is the cumulated seafloor area as derived from the high-resolution ETOPE 1 grid. The ocean margin at 0–100 m water depth is indicated for the modern ocean (red area) and for the LGM when the sea-level was lowered by 120 m (blue area). The model presented in this paper considers that the deposition and accumulation of neritic carbonate and marine particulate organic matter are diminished during glacial sea-level low-stands due to the steepening of ocean margins.

The carbon and phosphorus budgets of the global ocean are significantly affected by the glacial marine regression and the decrease in margin area since the accumulation of neritic carbonate on the inner shelf and the burial of POM on the shelf and upper slope act as major C and P sinks. The glacial decrease in shelf carbonate burial is a major driver of ocean chemistry and atmospheric $pCO_2$ change since neritic carbonates contribute ≥ 50 % to the carbonate accumulation at the global seafloor. The shelf and upper slope are key areas for POM burial. More than 80 % of the global POM accumulation occurs in these margin environments. POM burial is focused to margin areas at shallow water depths (<1000 m) since rapid POM degradation in the water column inhibits POM deposition further offshore and at larger water depths. Since POM burial is the major sink for dissolved phosphorus ($PO_4$) in the global ocean, the glacial decrease in POM burial induces an expansion of the marine $PO_4$ inventory and an increase in marine export production which may contribute significantly to the glacial draw-down of atmospheric $pCO_2$ (Broecker 1982). $^{13}C$ was observed in benthic foraminifera (Broecker 1982). While some earth system models consider the glacial decrease in neritic carbonate accumulation, the effects of sea-level change on POM burial and the marine $PO_4$ inventory are largely ignored in state-of-the-art models even though the glacial increase in the standing stock of $PO_4$ enhances the $CO_2$ transfer into the ocean's interior and acts as a powerful positive feedback mechanism that may induce self-sustained oscillations in atmospheric $pCO_2$ on glacial-interglacial timescales (Wallmann 2014). This contribution aims to convince the community that the glacial marine regression reduces POM burial at continental margins and is thus a major driver for the glacial $pCO_2$ draw-down.

## 2. Methods

A simple earth system model is developed to simulate global carbon and phosphorus cycling over the late Quaternary. It is focused on the geological cycling of C and P *via* continental weathering, volcanic and metamorphic degassing, hydrothermal processes and burial at the seabed. An ocean box model is embedded in this geological model where the global ocean is represented by surface water, thermocline and deep water boxes. Concentrations of dissolved phosphorus, dissolved inorganic carbon, and total alkalinity are calculated for each box. The partial pressure of $CO_2$ in the atmosphere ($pCO_{2A}$) is determined by exchange processes with the surface ocean and the continents. It serves as key prognostic model variable and is assumed to govern surface temperatures and global sea-level. The model is formulated as autonomous system, in which the governing equations have no explicit time-dependence (Wallmann 2014).

## 3. Results and Discussions

The model results are shown in Figure 2. The model was run without any form of external forcing. It reflects the internal non-linear dynamics of the earth system as implemented in the model system. Atmospheric $pCO_2$ is calculated as the key prognostic variable. It determines eustatic sea-level, global surface temperatures ($T_A$), the nutrient utilization in the Southern Ocean ($k_{EXP}$), the regeneration depths of organic matter in the water column ($f_{DPOPI}$) and vertical mixing between the deep ocean and the thermocline ($F_{WDI}$). The draw-down of $pCO_2$ at the glacial inception is driven by the imbalance in the carbonate system.

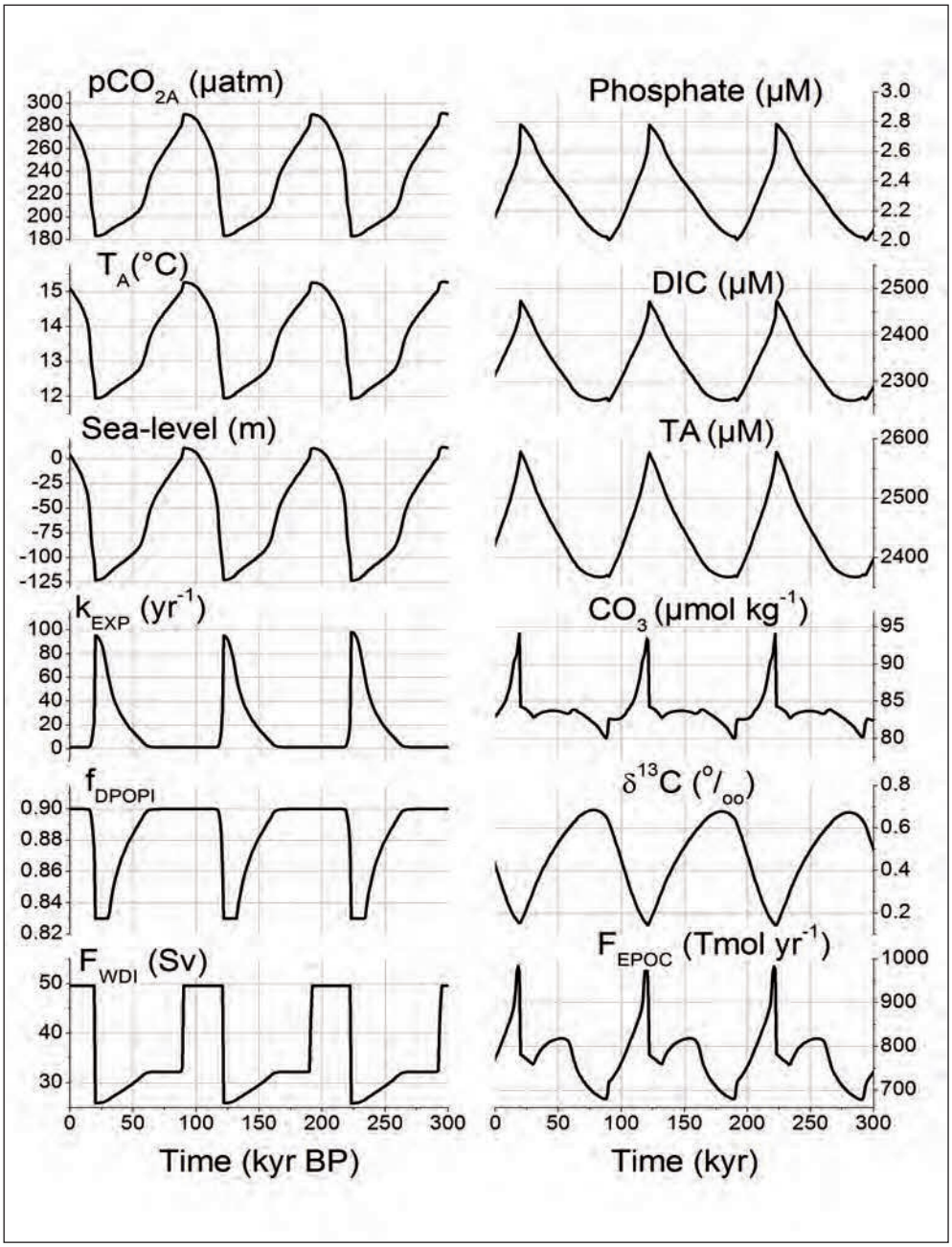


Fig. 2 100-ka cycle as calculated by the model over the last 300 ka 2014 (Wallmann 2014). See text for further explanations.

Carbonate burial exceeds the riverine flux of alkalinity (TA) into the ocean and induces a drop in the carbonate ion concentration of the deep ocean ($CO_3$). Atmospheric $CO_2$ declines over this initial period since less pelagic carbonate is preserved in the deep ocean. The subsequent glacial draw-down of $pCO_2$ is driven by a number of positive feedbacks. The sea-level fall induced by the $pCO_2$ drop reduces the burial of neritic carbonate and POM at continental margins such that the dissolved phosphate ($PO_4$) and TA inventory of the global ocean increase over time. The $PO_4$ increase promotes export production and intensifies the transfer of $CO_2$ from the atmosphere into the ocean's interior *via* the biological pump. The decrease in deep ocean ventilation supports the sequestration of $CO_2$ while the biological pump is further strengthened by the rise in dust input and nutrient utilization in the Southern Ocean. Atmospheric $pCO_2$ is lowered by ca. 100 µatm *via* these positive feedback mechanisms. The glacial

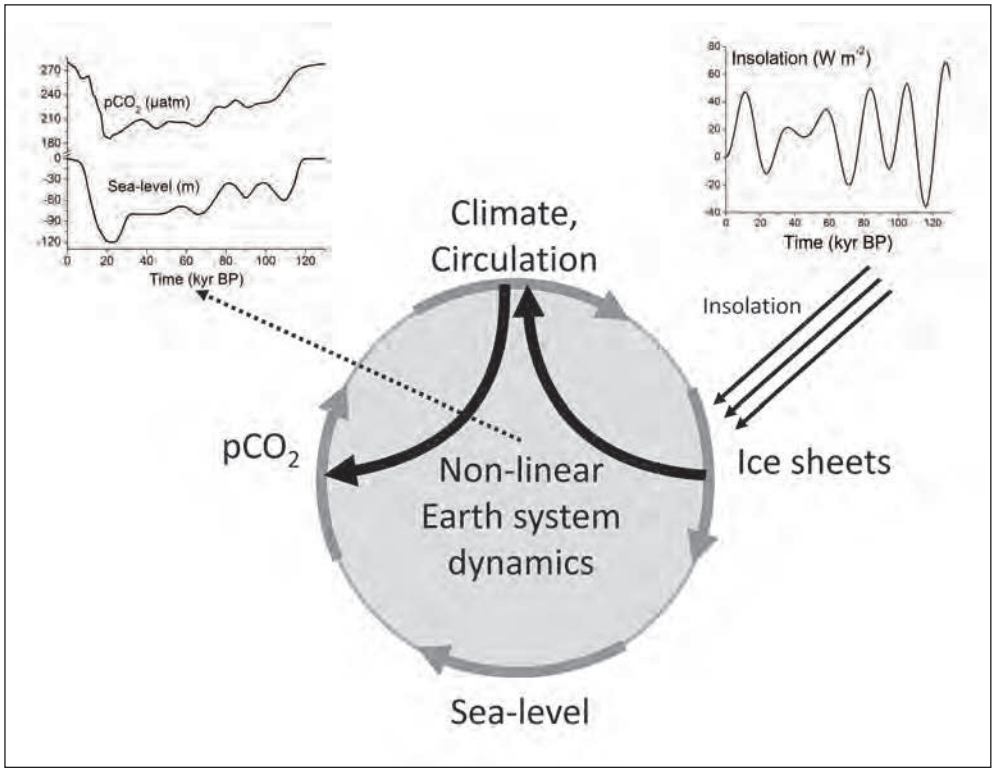


Fig. 3 Key elements of the 100 ka cycle. Summer insolation at high northern latitudes (June insolation at 60°N, diagram in the upper right corner) affects the growth and melting of continental ice sheets and thereby eustatic sea-level change. Glacial regressions reduce the burial of marine phosphorus and neritic carbonate at the steepening ocean margins while burial is enhanced by the flooding of the continental shelf during deglacial transgressions. The glacial draw-down of atmospheric $pCO_2$ and its deglacial rise are strongly supported by these changes in phosphorus and carbonate burial. The cycle is closed by atmospheric $pCO_2$ affecting global climate and thereby the volume of continental ice sheets. It is accelerated and further strengthened by additional positive feedbacks: Ice sheets affect the Earth's albedo and climate while changes in ocean circulation and dust deposition support the glacial $pCO_2$ draw-down and are largely responsible for the rapid deglacial rise in atmospheric $pCO_2$. The records of atmospheric $pCO_2$ and eustatic sea-level change (diagrams in the upper left corner) reflect the internal non-linear dynamics of the Earth system (as described above) and its response to external insolation forcing.

termination is induced by an increase in pelagic carbonate accumulation at the deep-sea floor. It creates a small $pCO_2$ rise which is drastically amplified by the abrupt decrease in iron fertilization and increase in deep ocean ventilation. The rapid deglacial $pCO_2$ rise is followed by a brief interglacial period until the cycle starts again with the glacial inception. The model system continues to oscillate for an unlimited period of time without any form of external forcing. The $\delta^{13}C$ value of carbon in the ocean/atmosphere system calculated by the model (Fig. 2) is consistent with the benthic $\delta^{13}C$ record. However, the simulated $^{13}C$ depletion in the glacial ocean is not driven by the decline in terrestrial carbon stocks but by sea-level change controlling the rates of organic carbon burial and weathering at continental margins. The $pCO_{2A}$- and $\delta^{13}C$ oscillations develop without any form of external Milankovitch forcing. They are induced and maintained by $pCO_2$-controlled sea-level change generating persistent imbalances in the marine carbon and phosphorus budgets. Self-sustained oscillations are also obtained when sea-level change is allowed to lag temperature with a realistic time scale for ice sheet adjustment.

## 4. Conclusions

The model shows that a significant part of the glacial climate and $pCO_2$ record can be explained by the internal non-linear dynamics of the earth system. However, the signature of Milankovitch forcing can be clearly resolved in the climate record and the formation and melting of continental ice sheets is strongly influenced by high latitude summer insolation (Fig. 3). It is thus very likely that the 100 ka cycle is the result of the internal non-linear dynamics of the earth system overprinted and supported by Milankovitch forcing (Fig. 3).

### *References*

Broecker, W. S.: Glacial to interglacial changes in ocean chemistry. Progr. Oceanogr. *11*, 151–197 (1982)

Wallmann, K.: Is late Quaternary climate change governed by self-sustained oscillations in atmospheric $CO_2$? Geochimica et Cosmochimica Acta *132*, 413 – 439 (2014)

Prof. Dr. Klaus Wallmann
GEOMAR Helmholtz Centre for Ocean Research Kiel
Wischhofstraße 1–3
Room 8D-102
24148 Kiel
Germany
Phone: +49 431 6002287
Fax: +49 431 6002928
E-Mail: kwallmann@geomar.de

Nova Acta Leopoldina NF *121*, Nr. 408, 247–251 (2015)

# Southern Ocean Overturning, Controlled by Wind or Buoyancy Flux? Unterstanding the Link between Antarctic Temperatures and Atmospheric $CO_2$

Andrew J. Watson,[1] Geoffrey K. Vallis,[2] and Maxim Nikurashin[3]

## 1. Introduction

The Antarctic ice-core record provides compelling evidence for the importance of the Southern Ocean in controlling atmospheric $CO_2$ on glacial-interglacial timescales. The close correspondence between Antarctic temperature and atmospheric $CO_2$ concentrations persists over the last ~ 800 ka (Petit et al. 1999, Siegenthaler et al. 2005), while the shape of the temperature changes and their phase relative to $CO_2$ indicate specifically a link with southern, as distinct from mid- or northern latitudes (Shakun et al. 2012).

From our basic knowledge of the carbon cycle, we understand why this should be, but still the mechanisms so far studied do not provide a satisfactory description for the full magnitude of atmospheric $CO_2$ change, or a rationale for why it should be so closely tied to conditions over the Southern Ocean. However, over the last decade or so there has been a paradigm shift in our understanding of what controls the overturning circulation of the Southern Ocean – a shift which seems to have gone largely unnoticed by paleoceanographers. Our contention is that this new understanding of the physics, in combination with simple representation of the carbon cycle, leads to a revised and clearer understanding of the influence of Antarctic conditions on atmospheric $CO_2$.

The Southern Ocean is the dominant location in the world's oceans for upwelling of dense abyssal water to the surface, and also the site of formation of much of the deep water, both Antarctic Bottom Water (AABW) and Antarctic Intermediate Water (AAIW). These, together with North Atlantic Deep Water (NADW) make up most of the volume of the oceans. The dissolved inorganic carbon in this deep ocean water is by far the largest reservoir for labile carbon available at the Earth surface. Any process, acting at the surface of the Southern Ocean, that alters the partitioning of $CO_2$ into the source waters for the deep ocean water masses, will affect the natural concentration of atmospheric $CO_2$.

1 College of Life and Environmental Sciences, University of Exeter, Laver Building, North Park Road, Exeter EX4 4QE, UK.

2 College of Engineering, Mathematics and Physics, University of Exeter, Harrison Building, North Park Road, Exeter EX4 4QF, UK.

3 Institute for Marine and Antarctic Studies, University of Tasmania, Private Bag 129, Hobart, TAS 7001, Australia, and ARC Centre of Excellence for Climate System Science, Sydney, New South Wales, Australia.

## 2. Preformed Nutrient, Biological and Physical Timescales

Under rather general assumptions, (broadly, conservation of carbon and nutrients, and constant carbon-to-nutrient ratio), the "preformed" macronutrient content of deep waters sourced in the Southern Ocean controls atmospheric $CO_2$ concentrations (Ito and Follows 2005). Preformed nutrient is the concentration of phosphate (and/or nitrate) left unused by marine biology when the water leaves the surface. Preformed nutrient in southern-sourced deep waters is today high – biology is inefficient at removing carbon and nutrient. This is due to a combination of physical and biological processes: the locations of upwelling and deep water source are quite close together, so the vigorous overturning circulation means that there is only a short residence time of water at the surface between upwelling and downwelling. Biological processes also play a role, because phytoplankton in the region is limited by lack of iron and light in the winter. The time scale for water subduction is therefore comparable or shorter than the response time of the biota, and much of the nutrient brought to the surface by upwelling is unused when the water is returned to depth. In glacial time, a speeding up the biological response (for example, by iron fertilization) or a slowing of the renewal of surface water (reducing the overturning) could have altered this balance resulting in lower preformed nutrient, and lower atmospheric $CO_2$. Proxies for nutrient utilization are usually interpreted to support the idea that at last glacial maximum there was greater utilization of nutrients in Southern Ocean waters (Robinson and Sigman 2008). However, increasing the biological productivity while retaining the same overturning circulation as today goes against evidence that, in the polar Southern Ocean at least, productivity was lower during glacial time. A role for a reduced overturning circulation is therefore indicated.

## 3. Influencing the Rate of Overturning: Winds or Buoyancy?

The motive power of the Southern Ocean meridional circulation comes from the circumpolar westerly winds. Following the suggestion (Toggweiler et al. 2006) that northward shifting of these winds, and/or a weakening of them, could have been responsible for lower glacial atmospheric $CO_2$ by reducing the overturning, there have been a number of studies using GCMs to examine the response of $CO_2$ to shifted or reduced westerlies (Tschumi et al. 2008, Völker and Köhler 2013). Overall, these studies have not been very supportive of the idea: with reasonable magnitude of change in the westerlies, only small changes in atmospheric $CO_2$ are found.

However, the wind stress over the Southern Ocean is not the only variable that influences the character of the ocean overturning there. The circulation is expected also to respond to buoyancy forcing (e. g. heat, fresh water, and ice formation/melt fluxes) from the surface. This has become clear over the last decade, with the application of residual circulation theory, first developed for the atmosphere (Andrews and Mcintyre 1976) to the Southern Ocean (see e. g. Karsten and Marshall 2002, Marshall and Speer 2012). Deep water upwells in the Southern Ocean, under the influence of the westerly winds which cause an Ekman drift to the north in the surface there. This drift causes the isopycnals to tilt up towards the south, and the Antarctic Circumpolar Current (ACC) is the result of geostrophic adjustment to this forcing. Baroclinic instability in the current generates eddies which mediate a net flux to the south near the surface, tending to flatten the isopycnals. At steady state, the net residual overturning is the difference between northward wind-driven and southward eddy fluxes, and is

constrained by the requirement that the buoyancy budget is balanced (Marshall and Speer 2012). If upwelling water reaching the surface becomes lighter because heat or freshwater is added to it from the atmosphere then this balance will be satisfied by an increased net northward flow. Conversely, if upwelling water loses buoyancy on reaching the surface, by cooling and/or sea ice formation and brine rejection, then we expect enhanced near surface flow south due to enhanced eddy transport. Wind forcing is therefore not the only factor determining how tracers are advected by the MOC: the buoyancy budget strongly influences how much upwelling occurs, and whether upwelled water joins the upper or the lower overturning cell. As a result, the buoyancy budget will also have a strong influence on atmospheric $CO_2$ (Watson and Naveira Garabato 2006).

We can be reasonably certain that the net buoyancy fluxes over the Southern Ocean were substantially different in glacial time than they are to today. We know for example, that in winter the sea ice extent was much greater, about twice the area covered today (Gersonde et al. 2005). This suggests a greater area of buoyancy loss than today, and also weaker net buoyancy fluxes, which are small once ice has formed. Today, much of the water that upwells in the Southern Ocean moves north on reaching the surface to join the upper overturning cell which eventually sinks again in the North Atlantic to form NADW. Since diapycnal mixing in the interior ocean is weak, much of this NADW formation is effectively "pulled" by the Southern Ocean upwelling through isocpycnal transport. Thus NADW formation is responsive to the conditions in the Southern Ocean: the implication of the weaker "Glacial North Atlantic Intermediate Water" circulation at LGM, is that there was also weaker upwelling in the Southern Ocean.

## 4. Initial Model Results

To gauge the potential of changes in buoyancy forcing to impact atmospheric $CO_2$, we have adapted the 2-D residual circulation model of the interhemispheric overturning described by Nikurashin and Vallis (2012). The model solves the equations of momentum, buoyancy and mass conservation in the Transformed Eulerian Mean formulation, in a rectangular latitude-depth domain. The domain is 4 km deep and consists of a re-entrant channel 2000 km wide, representing the Southern Ocean, joined at its northern edge to a closed basin 15,000 km in length, representative of the Atlantic/Pacific. Forced with prescribed wind stress and buoyancy across the southern channel, and buoyancy loss at the northern end of the closed basin, it reproduces an upper NADW overturning, and a lower AABW cell, as described by Nikurashin and Vallis (2012). To this physical model is added a very simple biogeochemical scheme in which marine phosphate, DIC and total alkalinity are advected by the model circulation. The marine biota remove nutrients, carbon and alkalinity in Redfield ratios from the surface 100 m on a time scale of 1 year, appropriate to the Southern Ocean. The resulting particulate material is instantaneously remineralized in the underlying water column with a scale depth of 500 m, with any material that reaches the bottom of the domain being remineralized there, so that there is no loss of nutrient or carbon from the system. A single well-mixed reservoir represents atmospheric carbon dioxide. The surface partial pressure of $CO_2$ is computed using standard chemical constants, and the flux between surface and atmosphere is calculated using a fixed air-sea gas transfer velocity.

For realistic variation in the buoyancy forcing over the southern channel, with other forcing kept constant, the model produces changes in atmospheric $CO_2$ of between 30 and 70 ppm. Atmospheric $CO_2$ decreases with weaker buoyancy forcing shifted northwards, because the upwelling is slowed and moved northward away from the Antarctic continent. Water upwelling and travelling south has further to go before it reaches the southern boundary, where most of the deep water formation of the AABW cell occurs. The residence time of this water in the surface is therefore longer and the marine biota can remove more carbon and nutrient from it. With the addition of other known influences (such as iron fertilization, a direct effect of temperature on $CO_2$ solubility, and possibly also "carbonate compensation", an influence of this size is more than sufficient to explain the glacial to interglacial $CO_2$ variation.

The model shows a number of encouraging features. In particular, the weakening and retreat from the Southern Ocean of the NADW cell is reproduced, which is in agreement with proxy data (Curry and Oppo 2005). Southern Ocean productivity decreases and the zone of maximum productivity moves northward, again in agreement with proxies. The model shows clearly that buoyancy forcing is critical in diagnosing the strength of the Southern Ocean overturning, both in the paleo-and the modern day context, and we believe it is solving the fundamental equations for the most important processes that set that circulation, albeit in a much simplified formulation.

## *References*


Andrews, D. G., and Mcintyre, M. E.: Planetary waves in horizontal and vertical shear: the generalized Eliassen-Palm relation and the mean zonal acceleration. J. Atmos. Sci. *33*, 2031–2048 (1976)

Curry, W. B., and Oppo, D. W.: Glacial water mass geometry and the distribution of $\delta^{13}C$ of $\Sigma CO_2$ in the Western Atlantic Ocean. Paleoceanography *20*, doi:10.1029/2004PA00102 (2005)

Gersonde, R., Crosta, X., Abelmann, A., and Armand, L.: Sea-surface temperature and sea ice distribution of the Southern Ocean at the EPILOG Last Glacial Maximum – A circum-Antarctic view based on siliceous microfossil records. Quat. Sci. Rev. *24*/7, 869 – 896 (2005)

Ito, T., and Follows, M. J.: Preformed phosphate, soft tissue pump and atmospheric $CO_2$. J. Marine Res. *63*/4, 813 – 839 (2005)

Karsten, R. H., and Marshall, J.: Constructing the residual circulation of the ACC from observations. J. Phys. Oceanogr. *32*/12, 3315 –3327 (2002)

Marshall, J., and Speer, K.: Closure of the meridional overturning circulation through Southern Ocean upwelling. Nature Geosci. *5*/3, 171–180 (2012)

Nikurashin, M., and Vallis, G.: A theory of the interhemispheric meridional overturning circulation and associated stratification. J. Phys. Oceanogr. *42*/10, 1652–1667 (2012)

Petit, J.-R., Jouzel, J., Raynaud, D., Barkov, N., Barnola, J.-M., Basile, I., Bender, M., Chappellaz, J., Davis, M., and Delaygue, G.: Climate and atmospheric history of the past 420,000 years from the Vostok ice core, Antarctica. Nature *399*, 6735, 429 – 436 (1999)

Robinson, R. S., and Sigman, D. M.: Nitrogen isotopic evidence for a poleward decrease in surface nitrate withing the ice age Antarctic. Quat. Sci. Rev. *27*, 1076 –1090 (2008)

Shakun, J. D., Clark, P. U., He, F., Marcott, S. A., Mix, A. C., Liu, Z. Y., Otto-Bliesner, B., Schmittner, A., and Bard, E.: Global warming preceded by increasing carbon dioxide concentrations during the last deglaciation. Nature *484*/7392, 49 –54 (2012)

Siegenthaler, U., Stocker, T. F., Monnin, E., Lüthi, D., Schwander, J., Stauffer, B., Raynaud, D., Barnola, J. M., Fischer, H., Masson-Delmotte, V., and Jouzel, J.: Atmospheric science: Stable carbon cycle-climate relationship during the late pleistocene. Science *310*/5752, 1313 –1317 (2005)

Toggweiler, J. R., Russell, J. L., and Carson, S. R.: Midlatitude westerlies, atmospheric $CO_2$, and climate change during the ice ages. Paleoceanography *21* (2 Art. no. Pa2005) (2006)

Tschumi, T., Joos, F., and Parekh, P.: How important are Southern Hemisphere wind changes for low glacial carbon dioxide? A model study. Paleoceanography *23*/4, doi:10.1029/2008PA001592 (2008)

Völker, C., and Köhler, P.: Responses of ocean circulation and carbon cycle to changes in the position of the Southern Hemisphere westerlies at Last Glacial Maximum. Paleoceanography *28*/4, 726–739 (2013)

Watson, A. J., and Naveira Garabato, A. C.: The role of Southern Ocean mixing and upwelling in glacial-interglacial atmospheric $CO_2$ change. Tellus B *58*/1, 73–87 (2006)

Prof. Andrew J. Watson, Ph.D.
College of Life and Environmental Sciences
University of Exeter
Laver Building
Office 709
North Park Road
Exeter EX4 4QE
UK
Phone: +44 1392 723792
E-Mail: andrew.watson@exeter.ac.uk

Nova Acta Leopoldina NF *121*, Nr. 408, 253–255 (2015)

# Deep Atlantic Carbon Sequestration and Atmospheric $CO_2$ Decline during the Last Glaciation

Jimin Yu (Canberra, Australia)

With 1 Figure

Ice core records show that atmospheric $CO_2$ concentrations during full glacials were ~ 30 % lower than the levels during interglacial periods. The terrestrial biosphere carbon stock was likely reduced during glacials, and increased carbon storage in the deep ocean is thought to play an important role in lowering glacial atmospheric $CO_2$ (Sigmann and Boyle 2000). However, ambiguity remains to use available proxy data to evaluate the carbon storage changes in the deep ocean. Furthermore, it has been suggested that Atlantic Meridional Overturning Circulation decoupled with the carbon cycle, showing a time lag of up to ~2,500 years, during the last glaciation (Piotrowski et al. 2005).

To provide new constraints on the deep ocean carbon cycle, we here present deep water carbonate ion reconstructions for extensive cores widely distributed in the Atlantic Ocean. Our results show that seawater carbonate ion concentration in the deep Atlantic (>~ 3km water depth) declined by ~20 mmol/kg from the Marine Isotope Stage 5a to 4 (Fig. 1).

Because ocean alkalinity likely increased during the last glaciation, this carbonate ion decline must reflect acidification due to increased carbon sequestration in the deep Atlantic, which possibly contributed to the contemporary atmospheric $CO_2$ decrease. The carbonate records allow us to estimate the minimum carbon storage increase in the deep Atlantic Ocean during the last glaciation. Our calculation suggests that, despite its relative small volume, the deep Atlantic Ocean may contribute significantly to past atmospheric $CO_2$ variations at major climate transitions. Moreover, a direct comparison of deep water carbonate ion (benthic foraminiferal B/Ca) and ocean circulation (benthic neodymium isotopes) proxies from the same high-resolution sediment core suggests a strong coupling of ocean circulation and carbon cycle in the deep Atlantic during the last glaciation.

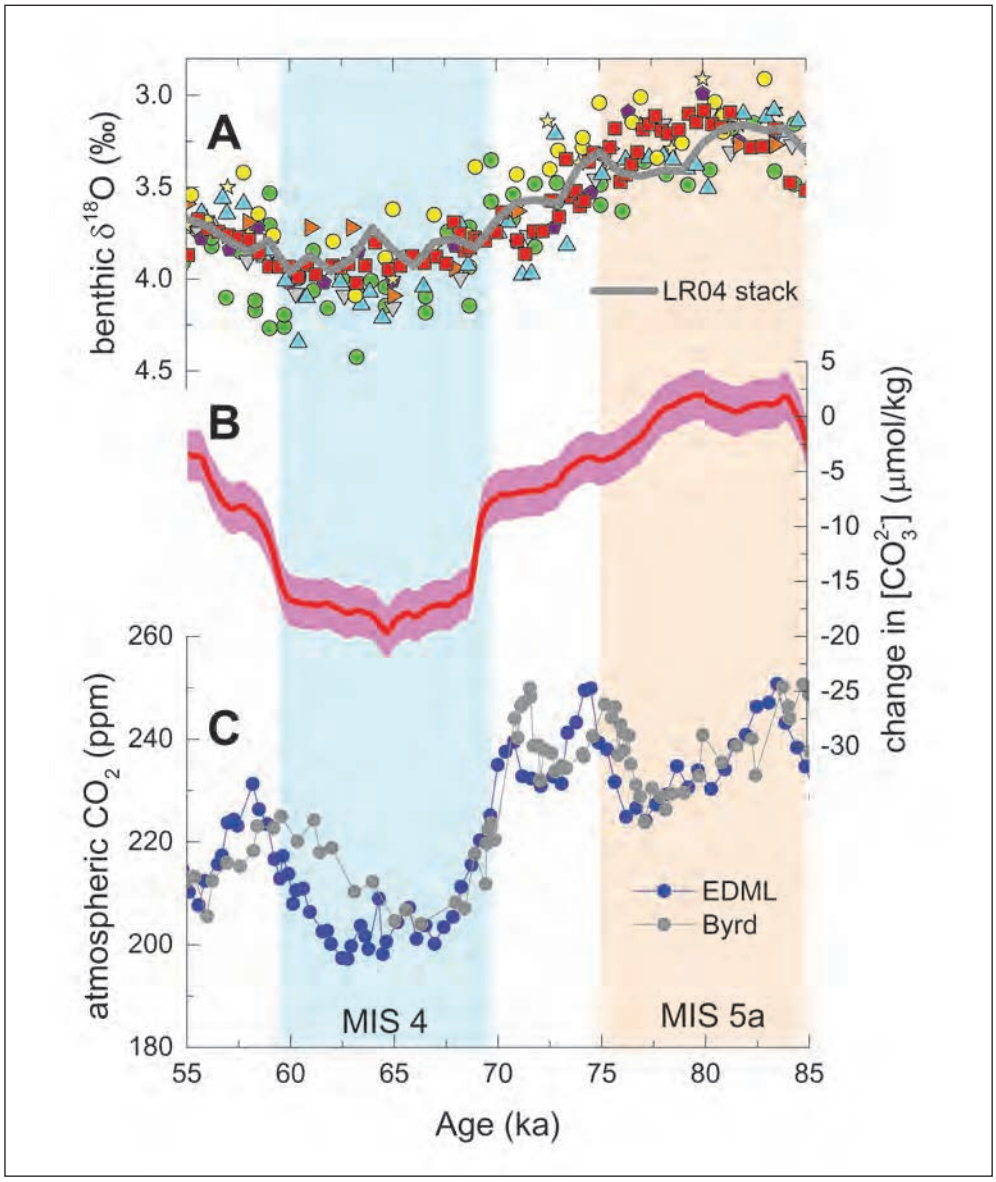


Fig. 1 Deep Atlantic carbonate ion compared with atmospheric $CO_2$ across MIS5a to 4. (*A*) Benthic $\delta^{18}O$ for studied cores as an age control. (*B*) Mean carbonate ion concentration changes (based on reconstructions for 8 cores) in the deep Atlantic Ocean. (*C*) Atmospheric $CO_2$ (Ahn and Brook 2008, Bereiter et al. 2012).

## *References*

Ahn, J., and Brook, E. J.: Atmospheric $CO_2$ and climate change on millennial time scales during the last glacial period. Science *322*, 83–85 (2008)

Bereiter, B., Lüthi, D., Siegrist, M., Schupbach, S., Stocker, T. F., and Fischer, H.: Mode change of millennial $CO_2$ variability during the last glacial cycle associated with a bipolar marine carbon seesaw. Proc. Natl. Acad. Sci. USA *109*, 9755–9760; doi:10.1073/pnas.1204069109 (2012)

Piotrowski, A., Goldstein, S. J., Hemming, S. R., and Fairbanks, R. G.: Temporal relationships of carbon cycling and ocean circulation at glacial boundaries. Science *307*, 1933–1938 (2005)

Sigman, D. M., and Boyle, E. A.: Glacial/interglacial variations in atmospheric carbon dioxide. Nature *407*, 859–869 (2000)

Dr. Jimin Yu
Research School of Earth Sciences
The Australian National University
Canberra
ACT 0200
Australia
Phone: +61 2 61259967
E-Mail: jimin.yu@anu.edu.au

# Poster

Nova Acta Leopoldina NF *121*, Nr. 408, 259–260 (2015)

# Deglacial Surface-Water Reservoir Ages from Key Positions in the Subtropical and Tropical Atlantic

Sven Balmer and Michael Sarnthein ML (Kiel)

With 1 Figure

Surface-water reservoir ages are considered as almost constant near ~400 years through time. This paradigm is slowly changing, since increasing evidence suggests surface water reservoir ages that changed through time and amongst different locations. In recent years, the "$^{14}$C plateau-tuning technique" formed an important tool to deduce surface water reservoir ages from

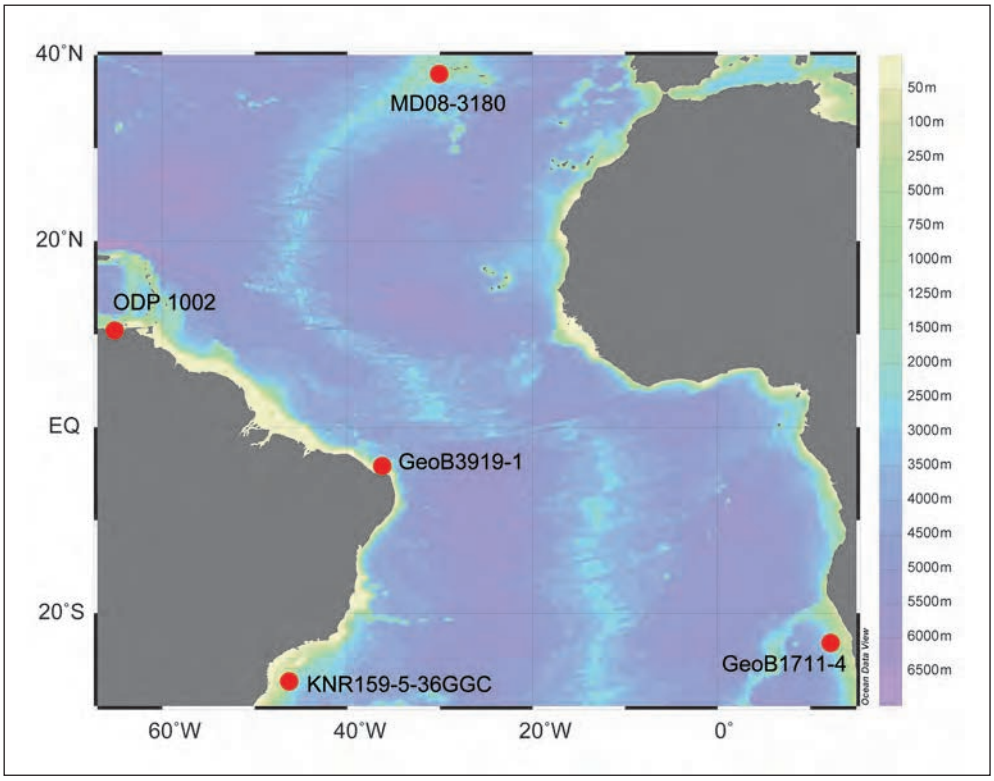


Fig. 1 Equatorial and South Atlantic core locations, where deglacial reservoir ages of surface waters have been reconstructed.

planktic $^{14}C$ records. We employed this technique on planktic $^{14}C$ records from four/five sediment cores retrieved at key positions in the subtropical and tropical Atlantic to monitor glacial and deglacial surface-water reservoir-age changes and to broaden the data set of planktic reservoir ages in the South Atlantic, in particular, from southwest off the Azores Islands, from offshore Namibia and northern and southern Brazil, and from the Cariaco Basin.

Reservoir ages from the Azores region were low (320–600 $^{14}C$ years) near the end of the Last Glacial Maximum (LGM), while high values of 1210 and 1610 $^{14}C$ years persisted over HS-1, prior to a sharp drop to 320 $^{14}C$ years at the onset of B/A. Offshore Namibia planktic reservoir ages range from 730–1080 $^{14}C$ years at the end of the LG) and continue at a high level of 940 $^{14}C$ years over the onset of HS-1, prior to a drop to ~410 $^{14}C$ years near its end and a subsequent rise to 880 $^{14}C$ years near the onset of B/A. Off northern Brazil reservoir ages show an ongoing low of 170–590 $^{14}C$ years over HS-1 and one of 260–280 $^{14}C$ years at the onset of B/A. Off southern Brazil sediments reveal high values of 750 to 870 $^{14}C$ years over the LGM and a drop from 750 to 170 $^{14}C$ years during HS-1. The B/A is marked by 230 $^{14}C$ years, while the onset of the YD shows an extreme low of 100 $^{14}C$ years.

These findings approve the $^{14}C$ plateau-tuning technique as reliable tool to deduce surface-water reservoir-ages from planktic $^{14}C$ records that were subject to significant and, in terms of paleoceanography, meaningful changes on spatial and temporal scales. High reservoir-ages near the Azores clearly depict the short-lasting influence of HS-1 meltwaters. High reservoir-ages offshore Namibia were induced by the Benguela upwelling regime, where old, hence $^{14}C$-depleted intermediate-waters are advected to the sea surface. In contrast, a reservoir-age of 410 $^{14}C$ years at the end of HS-1 suggests a short-lasting complete breakdown in coastal upwelling. In contrast to temporarily high reservoir-ages off Namibia the continuously low reservoir ages along the Brazilian margin suggest quasi-perfect stratification, thus a lack of old subsurface waters admixed to the sea surface, which presents a general characteristics of western ocean margins.

Sven Balmer
Institute for Geosciences
University of Kiel
Olshausenstraße 40
24098 Kiel
Germany
Phone: +49 431 8802928
Fax: +49 431 8804376
E-Mail: balmer@gpi.uni-kiel.de

Nova Acta Leopoldina NF *121*, Nr. 408, 261–264 (2015)

# Revision of the EPICA Dome C $CO_2$ Record from 800 to 600 ka BP

Bernhard Bereiter,[1] Sarah S. Eggleston,[1] Jochen Schmitt,[1] Christoph Nehrbass-Ahles,[1] Thomas F. Stocker,[1] Hubertus Fischer,[1] Sepp Kipfstuhl,[2] and Jérôme Chappellaz[3]

With 1 Figure

## 1. Background[4]

The EPICA (European Project for Ice Coring in Antarctica) Dome C (EDC) ice core provides the oldest samples of atmospheric air, allowing for the reconstruction of $CO_2$ concentrations as far back as 800 ka BP (thousand years before present, where present is defined as 1950) (Siegenthaler et al. 2005, Lüthi et al. 2008). To date, the EDC $CO_2$ record is the only record available for the period from 450 – 800 ka BP. In more recent time periods where overlaps exists between different ice core records, the EDC and other ice core $CO_2$ records generally confirm each other within the uncertainty boundaries. However, single records show systematic offsets of a few ppm relative to the other records that are beyond calibration issues (e.g. Bereiter et al. 2012, Marcott et al. 2014). For the older part of the EDC $CO_2$ record, the quality of the data cannot be independently verified with measurements on other ice cores that have been drilled to date.

## 2. Aim

We performed extensive re-measurements in order to test the integrity of the oldest/deepest part of this record, where $CO_2$ concentrations were found that were lower than expected from the $CO_2$-temperature correlation (Lüthi et al. 2008). Since we were able to identify an analytical artefact in the deepest/oldest section of the EDC ice core, we aim to come up with a correction for the previously published $CO_2$ record published by Siegenthaler et al. (2005) and Lüthi et al. (2008), discuss possible underlying mechanisms, and revisit the conclusions drawn by Lüthi et al. (2008).

1 Climate and Environmental Physics, Physics Institute, University of Bern, Sidlerstrasse 5, CH-3012 Bern, Switzerland, and Oeschger Centre for Climate Change Research, University of Bern, Switzerland.
2 Alfred Wegener Institute (AWI), Helmholtz Centre for Polar and Marine Research, P.O. Box 12 01 61, 27515 Bremerhaven, Germany.
3 CNRS, LGGE, F-38000 Grenoble, France; Univ. Grenoble Alpes, LGGE, F-38000 Grenoble, France.
4 This poster presentation is based on Bereiter et al. 2015.

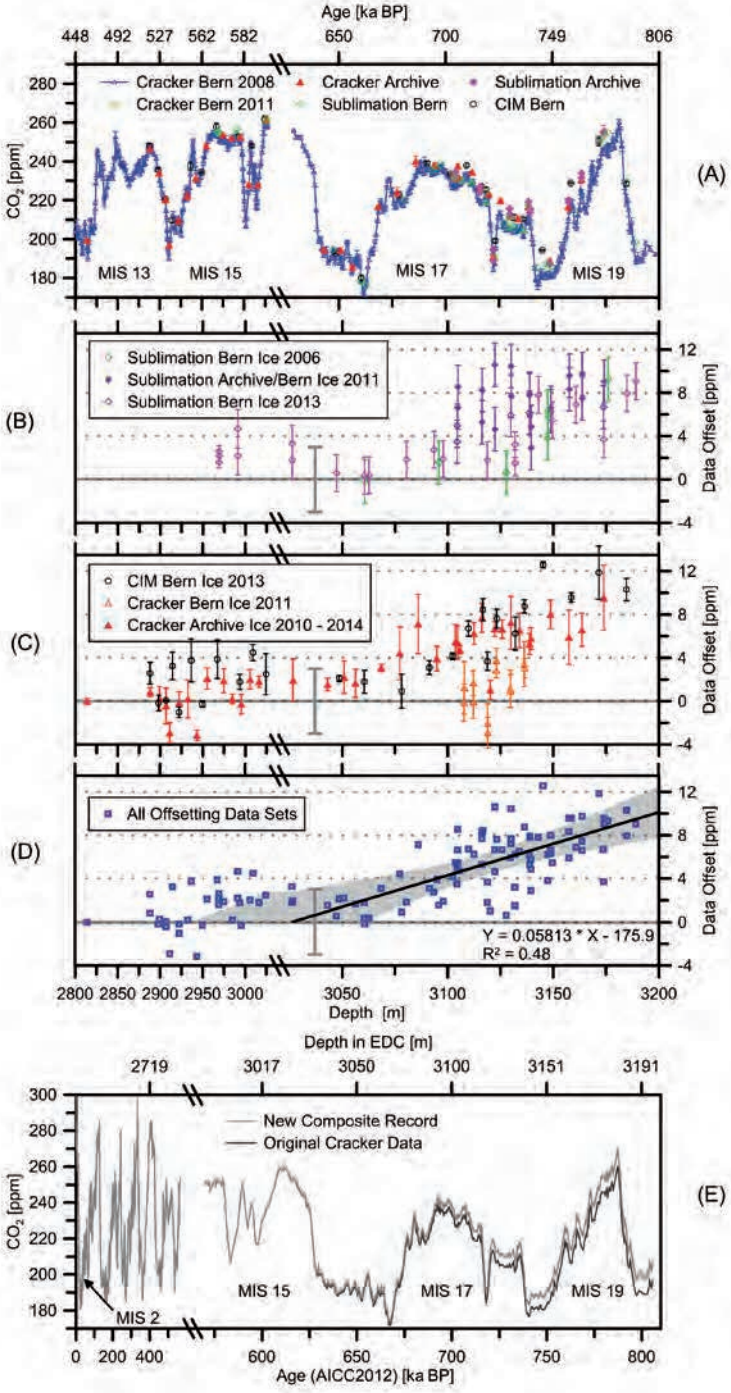
Age [ka BP]
448 492 527 562 582 650 700 749 806
Cracker Bern 2008
Cracker Bern 2011
Cracker Archive
Sublimation Bern
Sublimation Archive
CIM Bern
CO2 [ppm]
MIS 13
MIS 15
MIS 17
MIS 19
(A)
Sublimation Bern Ice 2006
Sublimation Archive/Bern Ice 2011
Sublimation Bern Ice 2013
(B)
CIM Bern Ice 2013
Cracker Bern Ice 2011
Cracker Archive Ice 2010 - 2014
(C)
All Offsetting Data Sets
(D)
Data Offset [ppm]
Y = 0.05813 * X - 175.9
R² = 0.48
2800 2850 2900 2950 3000 3050 3100 3150 3200
Depth [m]
Depth in EDC [m]
2719 3017 3050 3100 3151 3191
New Composite Record
Original Cracker Data
MIS 2
(E)
0 200 400 600 650 700 750 800
Age (AICC2012) [ka BP]

## 3. Methods

We used three independent devices – using different dry extraction principles – to remeasure the deepest 400 m (442–816 ka BP) of the EDC ice core: (*i*) the standard cracker device which was (among others) originally used for the oldest part of the EDC $CO_2$ record (Siegenthaler et al. 2005, Lüthi et al. 2008), (*ii*) a sublimation device primarily built for $\delta^{13}C(CO_2)$ analysis in ice cores (Schmitt et al. 2011), (*iii*) a new device called Centrifugal Ice Microtome (CIM) (Bereiter et al. 2013). We investigated two different, axially parallel pieces of the originally cylindrical ice core and performed 107 re-measurements in total. The so-called "Gas Cut" was shipped to Europe shortly after drilling and stored ever since in a freezer at –22.5 ± 2.5 °C (here referred to as "Bern Ice"). The other part was stored in Antarctica in a snow cave nearby the drilling camp with annual mean temperature of –53.5 °C ("Archive Ice") and shipped to Europe just before the measurements.

## 4. Results

All records that were measured either with a sublimation system or the CIM show significantly higher values relative to the original "Bern Ice" data below 3150 m depth. The same holds true for the data originating from the cracker in combination with "Archive Ice". Only the combination of "Bern Ice" and the cracker system shows reproducible low values within this depth range, even 5 years after the original data were obtained (Fig. 1 *A–C*).

It appears that the "Bern Ice" has passed through an alteration after the drilling such that only the low efficiency extraction with the cracker results in depleted values relative to the effectively trapped $CO_2$ concentration in this ice. The new data indicate a linearly increasing offset with depth from about 3027 m downwards reaching a maximum of about 10 ppm. All records that show an offset relative to the original data are used for a linear regression (Fig. 1*D*), which is subsequently used to correct the EDC $CO_2$ record below a depth of 3027 m (approx. 614 ka BP; Fig. 1*E*).

## 5. Conclusion

This study shows that $CO_2$ measurements obtained from extraction systems with incomplete gas extraction should be carefully checked and validated with devices allowing quantitative extraction. Based on the corrected data here, the average value from 650–799 ka BP (MIS 16–19) is 216.4 ppm, which is 5.6 ppm higher than the previous value reported by Lüthi et al. (2008). The lowest atmospheric $CO_2$ concentration ever found in an ice core changes only slightly by 2.1 ± 1.9 ppm to 173.7 ppm and remains the record lowest value. The correction we apply here does not fully resolve the anomalously low $CO_2$ values found for MIS 16–17.

---

Fig. 1 (*A*) Comparison of the original data published by Siegenthaler et al. (2005) and Lüthi et al. (2008) (blue) and re-measurements of this study (see methods and legend). (*B–D*) Offsets between original EDC $CO_2$ records and re-measurements in this study. (*E*): Comparison of the original record (black line) and the corrected record of this study (grey line, see (*D*) for applied correction curve) and its 95 % uncertainty range (light grey area behind).

The relationship between $CO_2$ and Antarctic temperatures is still significantly different for the affected period compared to what was found earlier. The cause of the analytical offset found here is still an open question but might be related to the extraction efficiency of the extraction device, ice properties in the deepest/oldest section (e.g. grain sizes or in-situ temperature), and/or storage history of the core sections and therefore potentially faster relaxation of the warmer-stored ice.

## *References*

Bereiter, B., Eggleston, S., Schmitt, J., Nehrbass-Ahles, C., Stocker, T. F., Fischer, H., Kipfstuhl, S., and Chappellaz, J.: Revision of the EPICA Dome C $CO_2$ record from 800 to 600 kyr before present. Geophys. Res. Lett. *42*, 542–549 (2015)

Bereiter, B., Lüthi, D., Siegrist, M., Schüpbach, S., Stocker, T. F., and Fischer, H.: Mode change of millennial $CO_2$ variability during the last glacial cycle associated with a bipolar marine carbon seesaw. Proc. Natl. Acad. Sci. USA *109*, 9755–9760 (2012)

Bereiter, B., Stocker, T. F., and Fischer, H.: A centrifugal ice microtome for measurements of atmospheric $CO_2$ on air trapped in polar ice cores. Atmospheric Measurement Techniques *6*, 251–262 (2013)

Lüthi, D., Le Floch, M., Bereiter, B., Blunier, T., Barnola, J.-M., Siegenthaler, U., Raynaud, D., Jouzel, J., Fischer, H., Kawamura, K., and Stocker, T. F.: High-resolution carbon dioxide concentration record 650,000-800,000 years before present. Nature *453*, 379–382 (2008)

Marcott, S. A., Bauska, T. K. Buizert, C., Steig, E. J., Rosen, J. L., Cuffey, K. M., Fudge, T. J., Severinghaus, J. P., Ahn, J., Kalk, M. L., McConnell, J. R., Sowers, T., Taylor, K. C., White, J. W. C., and Brook, E. J.: Centennial-scale changes in the global carbon cycle during the last deglaciation. Nature *514*, 616–619 (2014)

Schmitt, J., Schneider, R., and Fischer, H.: A sublimation technique for high-precision measurements of $\delta^{13}C$ ($CO_2$) and mixing ratios of $CO_2$ and $N_2O$ from air trapped in ice cores. Atmospheric Measurement Techniques *4*, 1445–1461 (2011)

Siegenthaler, U., Stocker, T. F., Monnin, E., Lüthi, D., Schwander, J., Stauffer, B., Raynaud, D., Barnola, J.-M., Fischer, H., Masson-Delmotte, V., and Jouzel, J.: Stable carbon cycle-climate relationship during the late Pleistocene. Science *310*, 1313–1317 (2005)

Christoph Nehrbass-Ahles
Climate- and Environmental Physics
Physics Institute and
Oeschger Centre for Climate Change
Research
University of Bern
CH–3012 Bern
Switzerland
Phone: +41 31 631 44 66
E-Mail: nehrbass@climate.unibe.ch

Nova Acta Leopoldina NF *121*, Nr. 408, 265–268 (2015)

# A Comprehensive Database for the Most Commonly Measured Paleoceanographic Proxies: Evaluating Global Organic Carbon Burial Variations over the Last Glacial Cycle

Olivier Cartapanis,[1,2] Daniele Bianchi,[1,3] and Eric Galbraith[1]

With 2 Figures and 1 Table

The paleoceanographic community has measured the physical and chemical properties of thousands of sediment cores, in order to reconstruct past oceanic conditions across a wide range of timescales. Most of these datasets were archived in online data repositories, in order to facilitate later analysis. However, the diversity of proxy types and heterogeneous reporting standards hindered the analysis of globally distributed paleoceanographic time series, despite the tremendous potential utility of large datasets. In order for the existing archives of paleoceanographic data to contribute towards important unanswered issues, the datasets must be readily accessible in an organized structure, with an appropriate unified age model for each sediment site.

Here we present a comprehensive database, built using MATLAB structure, for the most commonly measured proxies in marine sediment cores and surface sediment samples. These include the concentrations of carbonate, organic matter, opal and barium, density of the sediment, the oxygen and carbon isotopic composition of benthic and planktonic foraminifera, sea surface temperature estimates, as well as chronological constraints. The records were downloaded from the PANGAEA and the NOAA databases and multiple records from the same sediment core were grouped together, allowing age models to be shared between records. The resulting database consists of more than 30,000 different sites, facilitating rapid and accurate mapping of sediment composition for selected time periods, and retrieving and plotting time series.

The greatest hurdle identified in building a unified data product of this type is inconsistency in the reporting of depth measurements and chronological information. In our view, standardized reporting practices would greatly assist in developing global quantitative analysis, and requires community-wide action. We suggest that the development of a unified global sediment core registry, including metadata and chronological information for all marine sediment cores, should be a high priority for the paleoceanographic community.

As a first application of our global database, we have reconstructed global changes in the accumulation rate of organic carbon in deep-sea sediments over the last glacial cycle. Our

1 Department of Earth and Planetary Science, McGill University, Montreal, QC, Canada.
2 Oeschger Centre for Climate Change Research, Institute of Geological Sciences, University of Bern, 3012 Bern, Switzerland.
3 School of Oceanography, University of Washington, Seattle, WA, USA.

strategy consists of three consecutive steps. *First*, to produce a global map of modern organic carbon burial in the sediment. *Second*, to subdivide the ocean into provinces with consistent biogeochemical properties. *Third*, to modulate the modern burial in each province over time, according to the mean changes in burial rates calculated using sediment cores from the same province.

Global maps of modern organic carbon accumulation rates were calculated using previously published maps of the TOC content of surface sediment and mass accumulation rates. The TOC map was generated by combining the map of SEITER et al. (2004), updated with

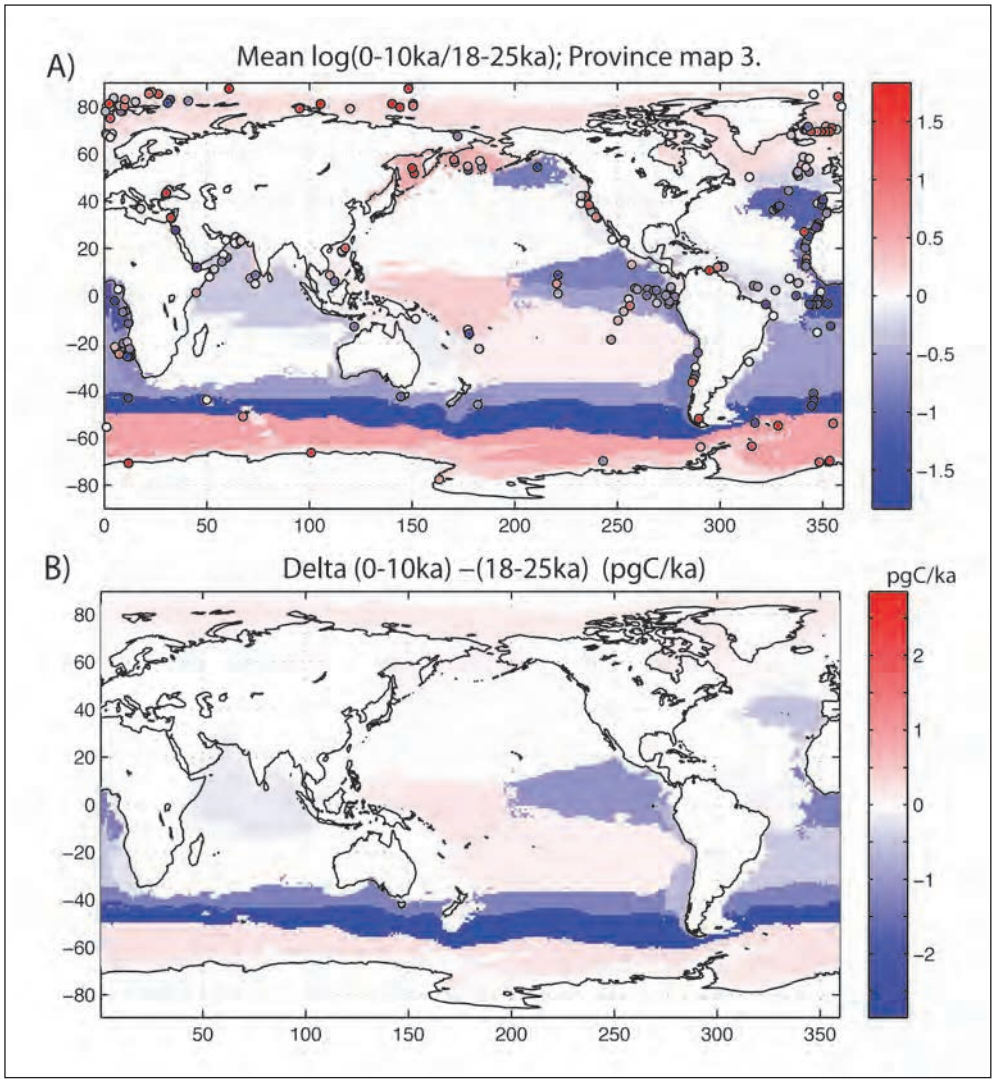


Fig. 1 Holocene to glacial burial rate ratio for sedimentary record and mean value in each provinces using the Longhurst province map (log(0–10 ka/18–25 ka)). Difference between Holocene and LGM burial rates in each provinces (pgC/ka).

other unpublished data, while the mass accumulation rate map was derived from the geometric mean of two preexisting maps (Jahnke 1996, and other unpublished data, see details in Dunne et al. 2007). In order to take into account the geographic and bathymetric variability in global organic carbon burial variations, we need to divide the world into provinces; however, any such division is sure to introduce some kind of bias. In an attempt to account for this bias, we used a total of seven different strategies to subdivide the world into provinces, and compare the results obtained using the different strategies. The first two strategies simply take the major ocean basins as provinces (map 1), as well as finer subdivisions of the oceans into seas (map 2), based on International Hydrographic Organization definition (1953). Next, based on the assumption that the large-scale ocean features driving biogeochemical cycles in the modern world have been relatively stationary over time, we used the annual climatology of the ocean biogeochemical provinces based on Longhurst (1995), and updated by Reygondeau et al. (2013). This map describes 56 coherent provinces from a biogeochemical point of view (map 3). In order to adapt the subdivision of the ocean to our sample distribution, the Longhurst map was redrawn and simplified into two different maps with respectively 30 (map 4) and 15 different provinces (map 6). Then, these two maps were used to create two new sets of maps by dividing each province into a shallow and a deep component using the 1500 m isobaths (map 5 and 7).

Downcore mass accumulation rate variations were calculated using organic carbon content, sedimentation rates and dry bulk density when available, for hundreds of sediment cores. Recent age models with larger numbers of tie point were preferred, and composite age models were created for some records. For each province map, the mean Holocene to Last Glacial Maximum (LGM) ratio of sedimentary records was calculated in each province, and used to estimate LGM TOC burial (Fig. 1). LGM global burial rate was then obtained from the sum of the calculated burial in each province (Tab. 1). The same procedure was used to calculate global TOC burial rate over 150 ka with a 1 ka time step (Fig. 2).

Tab. 1 Calculated Holocene and LGM deep ocean burial flux for the different provinces map. Subdivision of the provinces following the 1500 m isobaths was added for province map e. and g.

| Province map | Holocen flux (PgC/ka) | LGM flux (PgC/ka) | LGM/Holocene (%) | Provinces number |
|---|---|---|---|---|
| 1. Ocean | 17.1 | 21.1 | 123.27 | 7 |
| 2. Seas | 17.1 | 22.9 | 134.14 | 101 |
| 3. Longhurst (L.) | 16.8 | 28.2 | 167.57 | 56 |
| 4. Modified L. 1 | 17.1 | 23.8 | 139.48 | 30 |
| 5. Modified L. 1 + depth. | 17.1 | 24.1 | 140.97 | 60 |
| 6. Modified L. 2 | 17.1 | 29.5 | 172.70 | 15 |
| 7. Modified L. 2 + depth. | 17.1 | 33.4 | 195.72 | 30 |
| mean | | 26.1 | 153.41 | |
| std dev | | | 25.79 | |

Our results indicate that organic carbon burial was higher during the LGM (≈ 153 % ± 25 % of Holocene value), especially in the Atlantic, Southern Ocean and Eastern Equatorial Pacific. The sum of reconstructed regional TOC burial rates shows a pronounced peak during both the LGM (MIS2) and MIS6 (Fig. 2), and lower values during the interglacial, independently

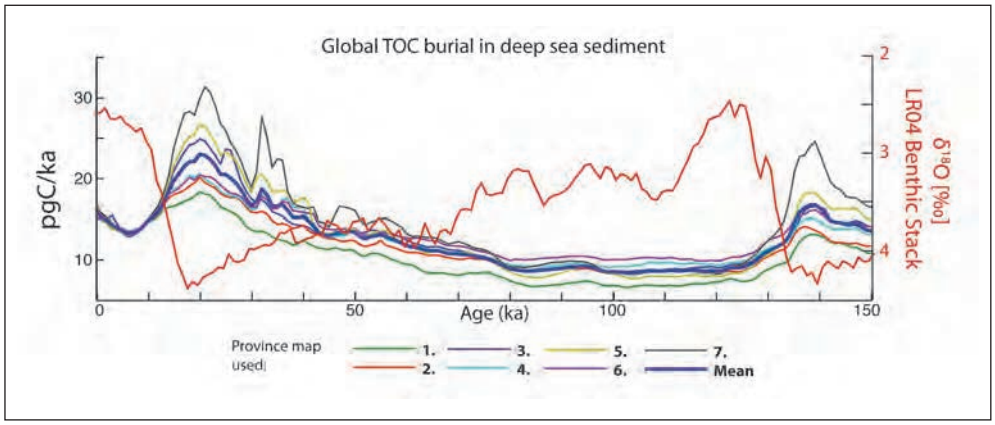


Fig. 2 Global deep sea burial rate variations over the last 150 ka calculated using different province map.

of the province map used. Glacial TOC burial represents a removal of approximately 200 PgC over the last glacial period, compared to the interglacial baseline burial flux. Peak TOC burial during the last glacial was likely caused by increased export production and/or better preservation due to reduced oxygenation, and is consistent with enhanced carbon storage in the deep sea during glacial periods.

## *Reference*

Dunne, J. P., Sarmiento, J. L., and Gnanadesikan, A.: A synthesis of global particle export from the surface ocean and cycling through the ocean interior and on the seafloor. Global Biogeochem. Cycles *21*, GB4006; doi:10.1029/2006GB002907 (2007)

*International Hydrographic Organization*: Limits of Oceans and Seas. Bremerhaven 1953

Jahnke, R. A.: The global ocean flux of particulate organic carbon: Areal distribution and magnitude. Global Biogeochem. Cycles *10*, 71–88; doi:10.1029/95GB03525 (1996)

Longhurst, A.: Seasonal cycles of pelagic production and consumption. Progr. Oceanogr. *36*, 77–167, http://dx.doi.org/10.1016/0079-6611(95)00015-1 (1995)

Reygondeau, G., Longhurst, A., Martinez, E., Beaugrand, G., Antoine, D., and Maury, O.: Dynamic biogeochemical provinces in the global ocean. Global Biogeochem. Cycles *27*, 1046–1058; doi:10.1002/gbc.20089 (2013)

Seiter, K., Hensen, C., Schröter, J., and Zabel, M.: Organic carbon content in surface sediments – defining regional provinces. Deep-Sea Res. Part I Oceanogr. Res. Pap. *51*, 2001–2026, http://dx.doi.org/10.1016/j.dsr.2004.06.014 (2004)

Olivier Cartapanis, Ph.D.
Institute of Geological Sciences and
Oeschger Centre for Climate Change
Research
University of Bern
Baltzerstr. 3
CH–3012 Bern
Switzerland
Phone: +41 31 631 8770
E-Mail: olivier.cartapanis@geo.unibe.ch; olivier.cartapanis@mail.mcgill.ca

Nova Acta Leopoldina NF *121*, Nr. 408, 269–273 (2015)

# Comparison of $[CO_2]$ and $\delta^{13}C_{atm}$ Measurements from Antarctic Ice Cores during Marine Isotope Stages 2 and 4

Sarah S. Eggleston, Jochen Schmitt, Fortunat Joos, and Hubertus Fischer (Bern, Switzerland)

With 2 Figures

Antarctic ice cores provide an archive of a plethora of climate data from the past 800 ka, including concentrations of atmospheric gases as well as proxies for Antarctic temperatures, dust flux to the Southern Ocean, and many others. Coupled with data from marine sediment cores as well as terrestrial records, it is possible to reconstruct a large suite of parameters characterizing the climate of the past. One of the most prominent features of such records is the approximately 100 ka cycle of glacial inceptions and terminations. Although much research has been devoted to better understanding the precise mechanisms involved in the abrupt rise in temperature, greenhouse gases, and rapid changes seen in many other parameters at glacial terminations, the relative importance and timing of these mechanisms remains debated in proxy as well as in modeling studies.

As the second most important greenhouse gas after water vapor, it is known that $CO_2$ plays an important role in these terminations. It is therefore of great interest to gain a better understanding of the global carbon cycle during such transitions. Measurements of the stable carbon isotope of atmospheric $CO_2$, $\delta^{13}C_{atm}$, provide a valuable constraint for this system, allowing us to better approximate carbon fluxes between the atmospheric, terrestrial, oceanic, and sedimentary reservoirs on glacial-interglacial as well as on shorter timescales. Previous studies of $\delta^{13}C_{atm}$ have used this parameter coupled with others to demonstrate that a combination of processes is as work during a glacial termination (Schmitt et al. 2012, Schneider et al. 2013). However, the $\delta^{13}C_{atm}$ record demonstrates that such a suite of processes may have also been active during the glacial period. At the end of Marine Isotope Stage (MIS) 4, a signal is clearly visible in the stable isotope record that matches the amplitude of that at termination 1 (T1; see Fig. 1 and 2). Thus, in addressing the question as to what causes a termination, we can alternatively ask the question what does *not* lead to a termination? Here, we attempt to answer this by assessing the similarities and differences in ($CO_2$) and $\delta^{13}C_{atm}$ at the MIS 4/3 and MIS 2/1 transitions.

Not only the $\delta^{13}C_{atm}$ signal but also that of several other parameters is similar at these two transitions. Iron fluxes (e.g. Vallelonga et al. 2013, Martínez-García et al. 2011) were elevated during MIS 2 and 4 and declined as the climate warmed. This supports the iron fertilization hypothesis (Martin et al. 1988), in which iron is becoming a limiting nutrient to marine productivity, corroborated by the increase in atmospheric $[CO_2]$ and decrease in $\delta^{13}C_{atm}$ at these times. Opal flux records from a Southern Ocean core, an indication of upwelling in this region, show marked increases at the terminations of each of these cold periods (An-

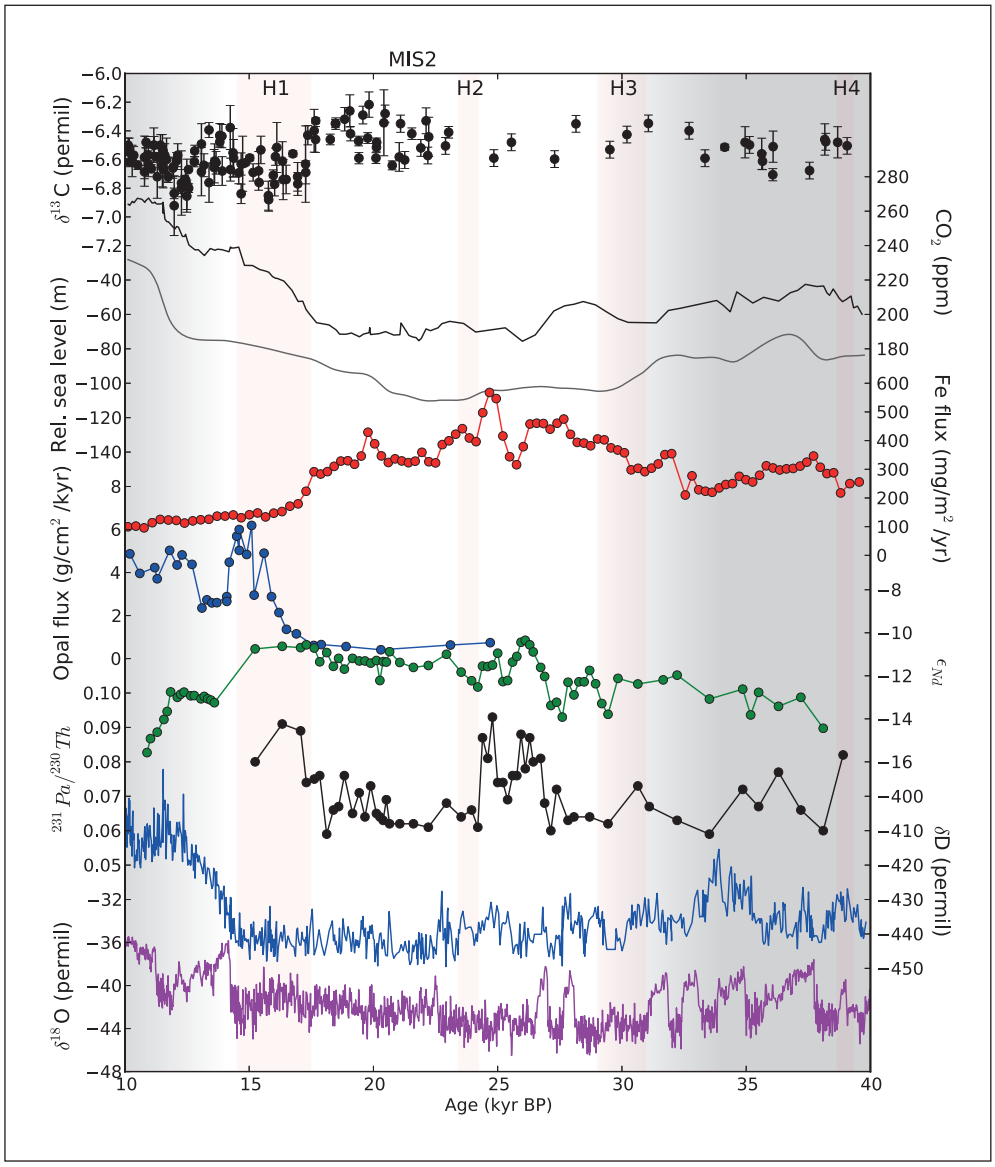


Fig. 1 Records of $\delta^{13}C_{atm}$ (Schmitt et al. 2012) and [$CO_2$] (Monnin et al. 2001, Ahn and Brook 2008, Bereiter et al. 2012) from Antarctic ice cores, Red Sea relative sea level (Grant et al. 2012), iron flux measured at marine core 1090 in the Southern Ocean (Martínez-García et al. 2011), opal flux measured at marine core TN057 in the Southern Ocean (Anderson et al. 2009, Jaccard et al. in prep), $\varepsilon_{Nd}$ and Pa/Th measured at marine core 1063 in the North Atlantic (Böhm et al. 2014), δD from EPICA Dome C (Jouzel et al. 2007), and $\delta^{18}O$ from NGRIP (NGRIP Community Members) during MIS 2 and termination 1. Vertical bars show Heinrich events as evidenced by IRD.

derson et al. 2009, Jaccard et al., in prep). Upwelling of deep, carbon-rich water from the Southern Ocean, which is also depleted in $^{13}C$, has been proposed to play an important role in the termination sequence; indeed, modelling studies indicate that this could have a significant

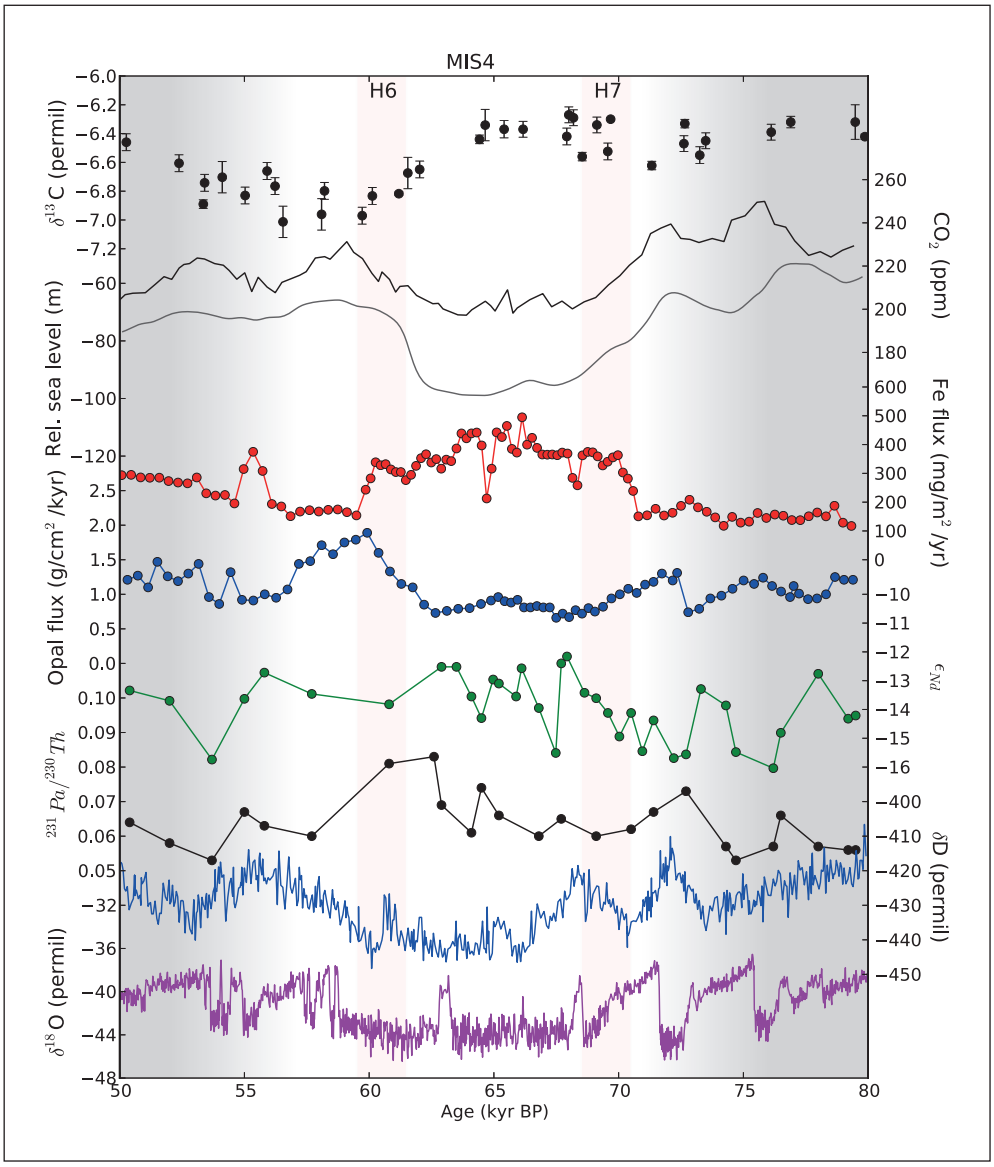


Fig. 2 Same as Figure 1 for MIS 4; note the different scales on the y-axes.

impact on $\delta^{13}C_{atm}$ (Köhler et al. 2010, Menviel et al. 2012, Tschumi et al. 2011). The cause of the upwelling (wind or buoyancy forcing), however, is still debated, although a substantial influence of changing winds appears increasingly unlikely (Tschumi et al. 2008, Schmittner and Lund 2014). Sea level, while not vital to explaining $\delta^{13}C_{atm}$, can have an impact on [$CO_2$] through e.g. increased weathering rates at low stand when more rock is exposed to the atmosphere, and MIS 4 and 2 are the two periods during the last glacial cycle that are most similar in terms of mean sea level (Grant et al. 2012).

Despite the many similarities, MIS 4 and 2 also differ in important respects. Firstly, the summer insolation in the Northern Hemisphere was even more significantly reduced in MIS 4 as in MIS 2. Additionally, a recent study of $\varepsilon_{Nd}$ and Pa/Th, proxies for southern sourced water at a given marine core site and Atlantic Meridional Overturning Circulation (AMOC) strength, respectively, shows a marked difference between these periods in these parameters (Böhm et al. 2014). These data indicate that the AMOC was strong during the Eemian and gradually weakened over the course of the glacial inception, finally switching to the "off" mode during the Last Glacial Maximum. Thus, the structure of water masses in the North Atlantic may have been quite different in MIS 4 compared to MIS 2, which would have implications for the nutrient and DIC content of the water in the deep Atlantic, thus affecting estimates of the effect of upwelling on parameters such as $\delta^{13}C_{atm}$ and on processes such as enhancement of the marine biological pump in response to the upwelling of nutrients. In addition, terminations are unique in that they are periods of warming in the Southern Hemisphere that proceed much longer without interruption by warming in the Northern Hemisphere, identified by Dansgaard-Oeschger (D-O) events. Wolff et al. (2009) proposed that this delayed sudden NH warming, potentially connected to the larger ice sheets in the North, could be the reason that a full termination is only achieved at the end of MIS 2.

In summary, to gain a better grasp on the factors leading to a glacial termination, the best comparison during the last glacial cycle is the MIS 4/3 transition, where many parameters show a similar behaviour to the beginning of the last deglacial. Important differences which could have led to a full deglacial transition only at the end of MIS 2 include the specific orbital parameters, the composition of water masses in the North Atlantic, the strength of the AMOC, and/or the lack of D-O events to "interrupt" the warming trend in the Southern Hemisphere.

## *References*


Ahn, J., and Brook, E. J.: Atmospheric $CO_2$ and climate on millennial time scales during the last glacial period. Science *322*, 83–85 (2008)

Anderson, R. F., Ali, S., Bradtmiller, L. I., Nielsen, S. H. H., Fleisher, M. Q., Anderson, B. E., and Burckle, L. H.: Wind-driven upwelling in the Southern Ocean and the deglacial rise in atmospheric $CO_2$. Science *323*, 1443–1448 (2009)

Bereiter, B., Lüthi, D., Siegrist, M., Schüpbach, S., Stocker, T. F., and Fischer, H.: Mode change of millennial $CO_2$ variability during the last glacial cycle associated with a bipolar marine carbon seesaw. Proc. Natl. Acad. Sci. USA *109*, 9755–9760 (2012)

Böhm, E., Lippold, J., Gutjahr, M., Frank, M., Blaser, P., Antz, B., Fohlmeister, J., Frank, N., Andersen, M. B., and Deininger, M.: Strong and deep Atlantic meridional overturning circulation during the last glacial cycle. Nature *517*, 73–76 (2014)

Grant, K. M., Rohling, E. J., Bar-Matthews, M., Ayalon, A., Medina-Elizalde, M., Ramsey, C. B., Satow, C., and Roberts, A. P.: Rapid coupling between ice volume and polar temperature over the past 150,000 years. Nature *491*, 744–747 (2012)

Jouzel, J., Masson-Delmotte, V., Cattani, O., Dreyfus, G., Falourd, S., Hoffmann, G., Minster, B., Nouet, J., Barnola, J. M., Chappellaz, J., Fischer, H., Gallet, J. C., Johnsen, S., Leuenberger, M., Loulergue, L., Luethi, D., Oerter, H., Parrenin, F., Raisbeck, G., Raynaud, D., Schilt, A., Schwander, J., Selmo, E., Souchez, R., Spahni, R., Stauffer, B., Steffensen, J. P., Stenni, B., Stocker, T. F., Tison, J. L., Werner, M., and Wolff, E. W.: Orbital and millennial Antarctic climate variability over the past 800,000 years. Science *317*, 793–796 (2007)

Köhler, P., Fischer, H., and Schmitt, J.: Atmospheric $\delta^{13}CO_2$ and its relation to $pCO_2$ and deep ocean $\delta^{13}C$ during the late Pleistocene. Paleoceanography *25*, doi:10.1029/2008PA001703 (2010)

Martin, J. H., and Fitzwater, S. E.: Iron deficiency limits phytoplankton growth in the north-east Pacific subarctic. Nature *331*, 341–343 (1988)

Martínez-García, A., Rosell-Mele, A., Jaccard, S. L., Geibert, W., Sigman, D. M., and Haug, G. H.: Southern Ocean dust-climate coupling over the past four million years. Nature *476*, 312–315 (2011)

Menviel, L., Joos, F., and Ritz, S.: Simulating atmospheric $CO_2$, $\delta^{13}C$ and the marine carbon cycle during the last glacial–interglacial cycle: possible role for a deepening of the mean remineralization depth and an increase in the oceanic nutrient inventory. Quat. Sci. Rev. *56*, 46 C68 (2012)

Monnin, E., Indermühle, A., Dällenbach, A., Flückiger, J., Stauffer, B., Stocker, T. F., Raynaud, D., and Barnola, J.-M.: Atmospheric $CO_2$ concentrations over the last glacial termination. Science *291*, 112–114 (2001)

Schmitt, J., Schneider, R., Elsig, J., Leuenberger, D., Lourantou, A., Chappellaz, J., Köhler, P., Joos, F., Stocker, T. F., Leuenberger, M., and Fischer, H.: Carbon isotope constraints on the deglacial $CO_2$ rise from ice cores. Science *336*, 711–714 (2012)

Schmittner, A., and Lund, D. C.: Carbon isotopes support Atlantic meridional overturning circulation decline as a trigger for early deglacial $CO_2$ rise. Clim. Past Discuss. *10*, 2857–2893 (2014)

Schneider, R., Schmitt, J., Köhler, P., Joos, F., and Fischer, H.: A reconstruction of atmospheric carbon dioxide and its stable carbon isotopic composition from the penultimate glacial maximum to the last glacial inception. Clim. Past *9*, 2507 C2523 (2013)

Tschumi, T., Joos, F., Gehlen, M., and Heinze, C.: Deep ocean ventilation, carbon isotopes, marine sedimentation and the deglacial $CO_2$ rise. Clim. Past *7*, 771–800 (2011)

Tschumi, T., Joos, F., and Parekh, P.: How important are Southern Hemisphere wind changes for low glacial carbon dioxide? A model study. Paleoceanography *23* (2008)

Vallelonga, P., Barbante, C., Cozzi, G., Gabrieli, J., Schüpbach, S., Spolaor, A., and Turetta, C.: Iron fluxes to Talos Dome, Antarctica, over the past 200 kyr. Clim. Past *9*, 597–604 (2013)

Wolff, E. W., Fischer, H., and Röthlisberger, R.: Glacial terminations as southern warmings without northern control. Nature Geosci. *2*, 206–209 (2009)

Sarah S. Eggleston
Climate and Environmental Physics
Physics Institute & Oeschger
Centre for Climate Change Research
University of Bern
Sidlerstrasse 5
CH-3012 Bern
Switzerland
Phone: +41 31 6318639
Fax: +41 31 6318742
E-Mail: eggleston@climate.unibe.ch

Nova Acta Leopoldina NF *121*, Nr. 408, 275–278 (2015)

# Mitigation Potential, Risks, and Side-Effects of Ocean Alkalinity Enhancement

Miriam Ferrer-Gonzalez and Tatiana Ilyina (Hamburg)

With 2 Figures

Increasing atmospheric carbon dioxide ($CO_2$) levels due to human activities leads to climate change and ocean acidification (decline in ocean pH). In order to tackle these issues and due to the lack of effective mitigation actions, a great variety of geo-engineering techniques have been suggested, however, knowledge about their effectiveness and collateral effects remains sparse (*Royal Society* 2009). In 1995, Kheshgi proposed the carbon dioxide removal (CDR) method of artificial ocean alkalinization (AOA) (Kheshgi 1995). This is one of the ocean-based CDR methods that aims at enhancing the natural and slow (geological timescales of tens to hundreds of thousands of years) process of weathering by which $CO_2$ is taken out of the atmosphere. Alkalinity is the charge balance of ions in water and it determines the $CO_2$ oceanic uptake and storage as well as the buffering capacity of the seawater to inhibit changes in pH. It has been claimed that ocean alkalinity might have played a key role in glacial-interglacial cycles. For instance, Broecker and Peng (1989) proposed an increase in the alkalinity of polar surface waters as driver of the last glacial to interglacial atmospheric $CO_2$ changes. Ocean alkalinity might be artificially increased by injecting the dissolution products of alkaline minerals into the seawater (e. g. calcium hydroxide). This geo-engineering technique would not only tackle climate change, but also ocean acidification, which has been found to accelerate climate change (Six et al. 2013) and it possess a serious risk for marine organisms (Doney et al. 2009). Ocean acidification not only leads to changes in physiology and reproduction of living organisms, it also threats ocean biota due to the decrease of the mineral saturation state of calcium carbonate ($CaCO_3$), commonly known as omega.

Few studies exist that address the method of alkalinity enhancement. Kheshgi (1995) proposed this geo-engineering technique and carried out a preliminary analysis of its potential and limitations. He concluded that ocean alkalinization might enhance marine storage of atmospheric $CO_2$ but its implementation would be an energy-intensive process. Using the carbon-cycle model LOSCAR, Paquay and Zeebe (2013) studied the impact of this method on ocean pH and atmospheric $pCO_2$ during the time span 2020 to 2400. From this study, they came to the conclusion that large scale implementation of ocean alkalinization might stabilize ocean acidification but $CO_2$ atmospheric levels would remain higher than pre-industrial levels. Ilyina and colleagues also carried out research on this matter using HAMOCC (Ilyina et al. 2013), they implemented and examined different alkalinity enhancement scenarios. In these scenarios, alkalinity was added to the ocean in proportional amounts to $CO_2$ emissions. They show that this method, under the scenario where two moles of alkalinity per mol of emitted $CO_2$ are dis-

tributed widely into the ocean, does have the potential to stabilize (at current levels) ocean pH and the saturation state of carbonate minerals. Regarding the atmospheric $CO_2$ concentration, this method under the same scenario would only lead to a reduction of 300 ppm with respect to the unmitigated scenario by 2100. The novelty of our research relies on the fact that none of previous studies have addressed this topic with a fully coupled Earth system model of such a level of complexity. Fully coupled set-ups (*versus* box-models or forced subsystems) hold the potential of revealing new features within the Earth system dynamics. Coupled models provide a more complete approach because box models are limited by simplified formulations of the underlying processes. Besides, since climate engineering research is a new scientific field, many aspects of ocean-based carbon dioxide removal methods remain still unanswered. Our research might bring new insights into the link of deglacial changes with ocean dynamics and atmospheric $CO_2$ through a better understanding of the underlying mechanisms. This project belongs to the German Research Foundation (DFG) priority program (SPP) 1689 that examines the risks and side-effects of different climate engineering technologies from a multidisciplinary perspective. Thus, it will be part of a comparative assessment of potential impacts, side-effects and uncertainties of different climate engineering measures.

We use the Max Planck Institute Earth System Model (MPI-ESM) based on the Coupled Model Intercomparison Project Phase 5 version with low-resolution (MPIOM: 1.5. horizontal resolution and 40 vertical layers; ECHAM: 1.9. horizontal resolution and 47 levels) (Giorgetta et al. 2013). Fossil fuel $CO_2$ emissions follow the pathway of scenario RCP8.5. Model scenarios of alkalinity enhancement (from 2006 until 2100) are designed to keep the atmospheric $CO_2$ concentrations similar to values of the stabilization scenario RCP4.5, whilst fossil

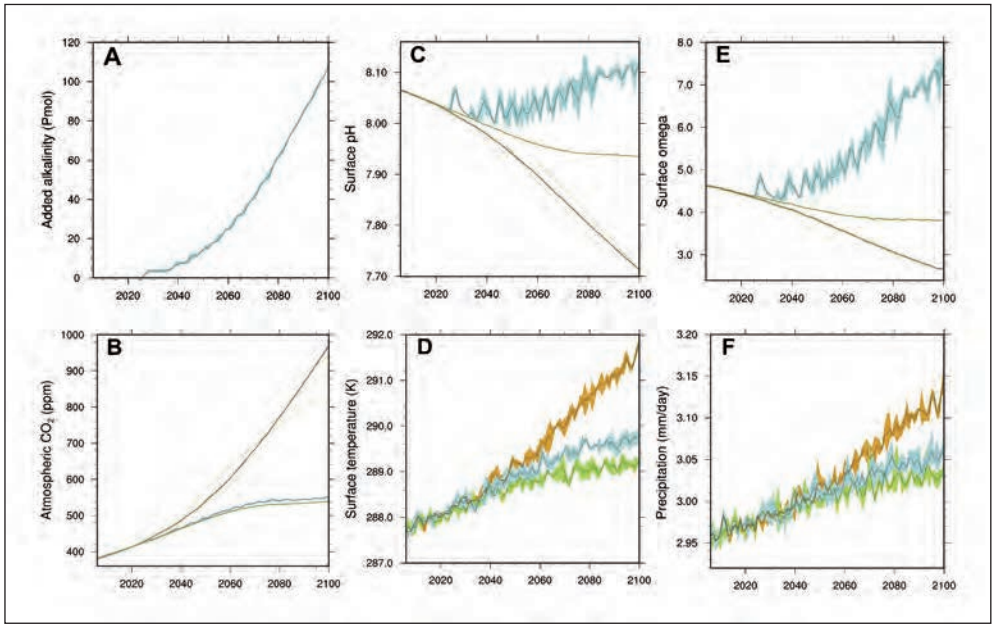


Fig. 1 Time series of globally averaged annual means for scenarios: RCP8.5, AOA and RCP4.5. Coloured area is model internal variability based on 3 ensemble members. Solid lines show 5-year-running means.

fuel emissions follow the pathway of the scenario RCP8.5. Alkalinity is added globally into the upper 12 meters of the ocean in different seasons and years. Note that this CE method addresses only atmospheric $CO_2$ reduction, therefore, land use, air pollutants, and other greenhouse gases (GHGs) remain unchanged with the values of the RCP8.5 emission scenario.

In order to maintain atmospheric $CO_2$ at RCP4.5 levels under the high emission scenario RCP8.5 (Fig. 1*B*), alkalinity was added in the upper ocean (Fig. 1*A*). In total, approximately 105 Petamol would be needed until the year 2100. Compared to the unmitigated scenario (RCP8.5) this AOA scenario leads to a reduction in the annual global mean of air surface temperature of around 1.5 K (Fig. 1*D*), following more closely the RCP4.5. The slightly higher temperature (0.5 K) of AOA compared to RCP4.5 is due to the radiative forcing effect of other GHGs (e. g. $N_2O$, $CH_4$ and halogenated GHGs). AOA strongly mitigates ocean acidification leading to higher pH and omega (calcite) values than those associated with the RCP4.5 scenario and preindustrial values over the whole period (Fig. 1*C* and *E*). Largest changes of pH occur in the Arctic ocean where values higher than 8.4 are reached (see Fig. 2). This AOA

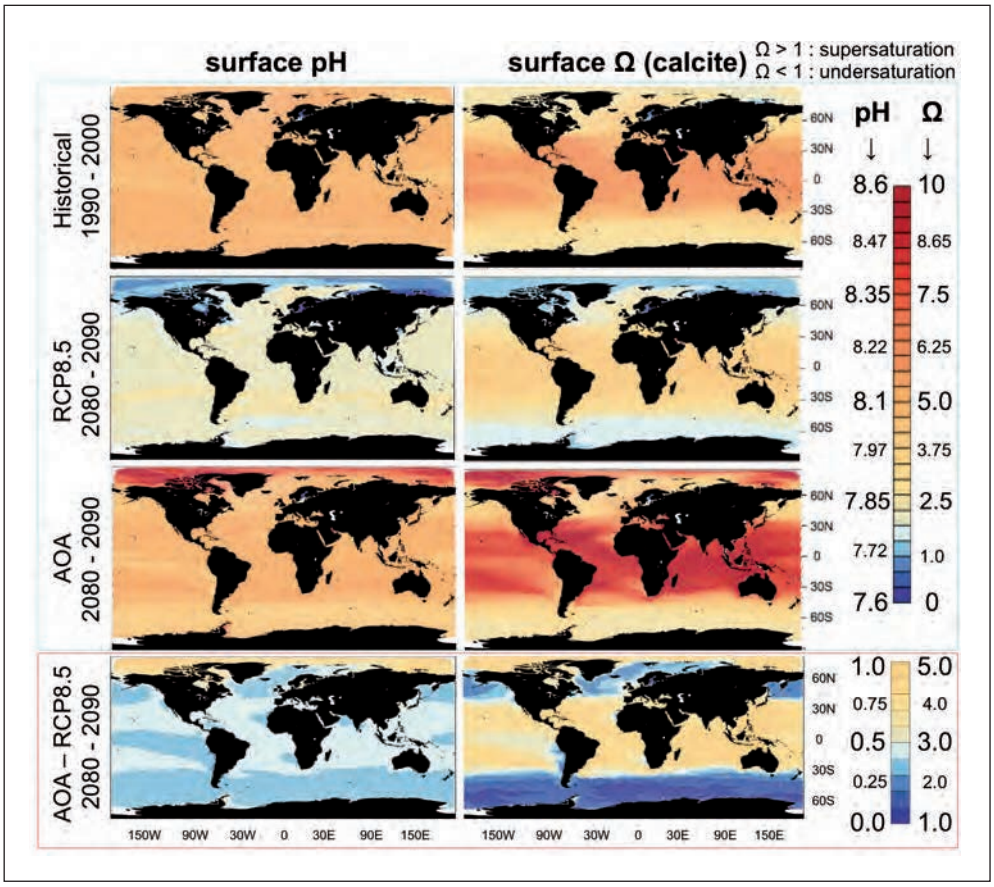


Fig. 2 Averages of 10-year periods of pH (*left*) and the saturation state of carbonate minerals (Ω, calcite) (*right*) for different time intervals.

scenario leads to changes in different properties of the climate system which are noticeable within centennial timescale. For instance, in global precipitation (Fig. 1*F*). Despite model internal variability, it is clear that state of the Earth system is similar to the RCP4.5 scenario. However, mitigating atmospheric $CO_2$ alone does not lead to an identical climate state.

Averages of a 10-year period of pH (*left*) and the saturation state of carbonate minerals (Ω, calcite) (*right*) for different time intervals are shown in Figure 2. By the end of this century, whilst global values of pH (see Fig. 1*C*) would be similar to preindustrial levels, regional values would differ and that has a strong impact on the ocean biogeochemistry. This AOA implementation scenario would prevent the extreme ocean acidification projected for the unmitigated scenario (RCP8.5); however, high pH and Ω values would be reached leading to a potential impact on marine biota (Cripps et al. 2013).

## *References*


Broecker, W. S., and Peng, T.-H.: The cause of the glacial to interglacial atmospheric $CO_2$ change: A polar alkalinity hypothesis. Global Biogeochem. Cycles *3*/3, 215–239 (1989)

Cripps, G., Widdicombe, S., Spicer, J. I., and Findlay, H. S.: Biological impacts of enhanced alkalinity in Carcinus maenas. Marine Pollution Bull. *71*/1–2, 190–198 (2013)

Doney, S. C., Fabry, V. J., Feely, R. A., and Kleypas, J. A.: Ocean acidification: The other $CO_2$ problem. Annu. Rev. Marine Sci. *1*/1, 169–192 (2009)

Giorgetta, M. A., Jungclaus, J., Reick, C. H., Legutke, S., Bader, J., Böttinger, M., Brovkin, V., Crueger, T., Esch, M., Fieg, K., Glushak, K., Gayler, V., Haak, H., Hollweg, H. D., Ilyina, T., Kinne, S., Kornblueh, L., Matei, D., Mauritsen, T., Mikolajewicz, U., Mueller, W., Notz, D., Pithan, F., Raddatz, T., Rast, S., Redler, R., Roeckner, E., Schmidt, H., Schnur, R., Segschneider, J., Six, K. D., Stockhause, M., Timmreck, C., Wegner, J., Widmann, H., Wieners, K. H., Claussen, M., Marotzke, J., and Stevens, B.: Climate and carbon cycle changes from 1850 to 2100 in MPI-ESM simulations for the coupled model intercomparison project phase 5. J. Adv. Model. Earth Systems *5*/3, 572–597 (2013)

Ilyina, T., Wolf-Gladrow, D., Munhoven, G., and Heinze, C.: Assessing the potential of calcium-based artificial ocean alkalinization to mitigate rising atmospheric $CO_2$ and ocean acidification. Geophys. Res. Lett. *40*, 1–6 (2013)

Kheshgi, H. S.: Sequestering atmospheric carbon dioxide by increasing ocean alkalinity. Energy *20*/9, 915–922 (1995)

Paquay, S., and Zeebe, R. E.: Assessing possible consequences of ocean liming on ocean pH, atmospheric $CO_2$ concentration and associated costs. Int. J. Greenhouse Gas Control *17*/0, 183–188 (2013)

*Royal Society*: Geoengineering the Climate: Science, Governance and Uncertainty. London: Royal Society 2009

Six, K. D., Kloster, S., Ilyina, T., Archer, S. D., Zhang, K., and Maier-Reimer, E.: Global warming amplified by reduced sulphur fluxes as a result of ocean acidification. Nature Clim. Change *3*/11, 975–978 (2013)



Miriam Ferrer-Gonzalez
Max Planck Institute for Meteorology
Bundesstraße 53
B117
20146 Hamburg
Germany
Phone: +49 40 41173193
Fax: +49 40 41173298
E-Mail: miriam.ferrer-gonzalez@mpimet.mpg.de

Dr. Tatiana Ilyina
Max Planck Institute for Meteorology
Bundesstraße 53
B218
20146 Hamburg
Germany
Phone: +49 40 41173164
Fax: +49 40 41173298
E-Mail: tatiana.ilyina@mpimet.mpg.de

Nova Acta Leopoldina NF *121*, Nr. 408, 279–282 (2015)

# Radiocarbon Evidence of Ocean Circulation Change over the Last Deglaciation

Emma Freeman, and Luke C. Skinner (Cambridge, UK)

With 1 Figure

Understanding the cause of the ~ 90 ppm difference in atmospheric $CO_2$ during glacial *versus* interglacial periods remains a major challenge for palaeoclimate scientists. Whilst the cause is almost certainly related to a greater storage of carbon in the ocean, the mechanism remains unsolved. Radiocarbon based ventilation ages could shed light on this problem by helping to determine the distribution of carbon in the ocean as well as the partitioning of carbon between the ocean and the atmosphere. Despite this, deglacial Atlantic radiocarbon ventilation is very poorly constrained. Emerging new data, however, suggest an interesting story with a significant role for the Atlantic Ocean both in storing carbon during the Last Glacial Maximum (LGM) and by triggering major releases of carbon over the last deglaciation.

During the LGM, atmospheric $CO_2$ concentrations were around 80 ppm lower than pre-industrial levels, and ocean circulation was altered (e.g. McManus et al. 2004). Radiocarbon based ventilation ages (Freeman et al., in prep., Keigwin and Schlegel 2002, Skinner et al. 2010, 2014) suggest at least some of this atmospheric $CO_2$ decrease could have been due to greater storage of carbon in the deep Atlantic Ocean (>2.5 km) as a direct result of changes in the overturning circulation. All of these records show that the deep Atlantic Ocean was more poorly ventilated at the LGM compared to today. This is likely to be associated with increased carbon storage due to reduced release of $CO_2$ to the atmosphere from a deep ocean that was receiving a continuous input of carbon *via* the biological pump. Ventilation ages at the LGM were up to 2.5-times modern values, reaching 2500 years offset from the atmosphere in the deep equatorial Atlantic. In the deep South Atlantic they reached over 3500 years, significantly older than any waters in the deep oceans today (Skinner et al. 2010). Low $\delta^{13}C$ values are also recorded in the deep Atlantic at this time suggesting the poorly ventilated deep waters contained a greater proportion of southern sourced water (Freeman et al., in prep, Curry and Oppo 2005). This is also supported by εNd data from the Blake Ridge that show an increased influence of southern sourced waters below 3.4 km during the LGM (Gutjahr et al. 2008). The very high ventilation ages in the deep glacial Atlantic exceed those of southern sourced bottom waters today. This indicates not only a change in the proportion of northern *versus* southern sourced waters but also a change in end-member ventilation ages, a significant increase in the mean transit time or a combination of the two. Pa/Th data hint at a slowdown in the deep water transport, but additional data from the South Atlantic are required to confirm this (Lippold et al. 2012). High ventilation ages are seen in the deep South Atlantic close to the source region suggesting the increase is due, at least in part, to an elevated ventilation age

at the formation site (Skinner et al. 2010). This is most likely due to reduced air-sea exchange as a result of increased sea-ice cover, rather than very sluggish overturning. Increased ventilation ages at the site of southern deep water formation would also affect the Pacific and Indian Oceans, further increasing the deep ocean carbon storage at the LGM (Skinner et al. 2015).

LGM ventilation ages from shallower depths (<2.5 km) are close to modern values indicating a vigorous upper circulation cell that was well equilibrated with the atmosphere was maintained at this time. This is in agreement with the idea of shoaled North Atlantic deep water (NADW), often referred to as glacial North Atlantic intermediate water (GNAIW), which was well ventilated throughout the LGM. Further support for this is provided by Pa/Th data that shows intermediate water transport was at least as strong during the LGM as deep water transport is today (Lippold et al. 2012). A fast overturning upper cell overlying a sluggish deep cell is also supported by additional Pa/Th data (Bradtmiller et al. 2014) as well as numerous other palaeoceanographic records which show a chemical divide in the glacial Atlantic at around 2.5 km (e.g. Curry and Oppo 2005, Marchitto et al. 2006)

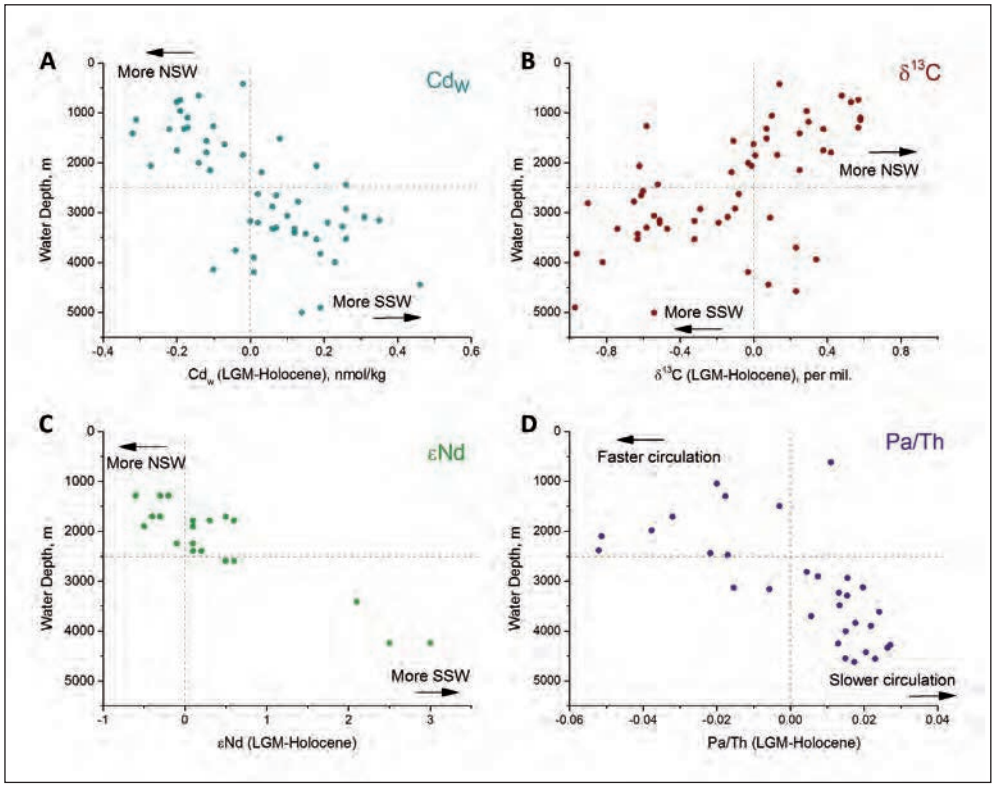


Fig. 1 LGM-Holocene depth profiles in the Atlantic Ocean showing an opposite sense of change above and below around 2.5 km in various proxies: (*A*) $Cd_W$ of benthic foraminifera (Marchitto et al. 2006), (*B*) $\delta^{13}C$ measured on *Cibicidoides* (Marchitto et al. 2006), (*C*) Authigenic Nd isotope signal (Gutjahr et al. 2008), (*D*) $^{231}Pa/^{230}Th$ data (Lippold et al. 2012). An increased presence of 'sluggish' southern sourced waters (SSW) below 2.5 km is seen during the LGM, with shoaled northern sourced waters (NSW) above.

Over the last deglaciation, atmospheric $CO_2$ concentrations increased both in gradual and rapid steps. Three main steps have recently been identified at 16.3, 14.8 and 11.7 ka BP in a high-resolution $CO_2$ record from the West Antarctic Ice Sheet (Marcott et al. 2014). During these steps, increases in $pCO_2$ of 10–15 ppm occurred in just 100–200 years. The rapidity of these $CO_2$ increases, strongly points to a release of $CO_2$ from the ocean, potentially caused by the resumption and/or deepening of Atlantic overturning circulation. Whilst foraminifera radiocarbon records are not typically of high enough resolution to resolve oceanic changes over these rapid $CO_2$ increases, a growing number of records show a sharp decrease in ventilation age at the transition from Heinrich stadial 1 to the Bølling-Allerød, around 14.8 ka BP (Freeman et al., in prep, Barker et al. 2008, Skinner et al. 2010, 2014). A ventilation pulse of the entire intermediate and deep Atlantic (>1000 m) looks to occur synchronously with the rapid increase in $pCO_2$. The Atlantic Ocean was as well or even better ventilated than the modern ocean at all depths at the peak of this ventilation pulse. We therefore propose that it was during this transition that the reduced/shoaled AMOC observed at the LGM and most likely accentuated over Heinrich stadial 1 (e.g. Bradtmiller et al. 2014) was reinvigorated and deepened resulting in the rapid release of deeply sequestered carbon to the atmosphere. Ocean circulation similar to modern may have been established at this time.

## *References*


Barker, S., Broecker, W., Diz, P., Vautravers, M., and Hall, I.: Deglacial variations in South Atlantic deep water ventilation. Nature *457*/7233, 1097–1102 (2008)

Bradtmiller, L. I., McManus, J. F., and Robinson, L. F.: $^{231}Pa/^{230}Th$ evidence for a weakened but persistent Atlantic meridional overturning circulation during Heinrich stadial 1. Nature Comm. *5*, 5817 (2014)

Curry, W. B., and Oppo, D. W.: Glacial water mass geometry and the distribution of $\delta^{13}C$ of $\Sigma CO_2$ in the western Atlantic Ocean. Paleoceanography *20*/1 (2005)

Gutjahr, M., Frank, M., Stirling, C. H., Keigwin, L. D., and Halliday, A. N.: Tracing the Nd isotope evolution of North Atlantic deep and intermediate waters in the western North Atlantic since the last glacial maximum from Blake Ridge sediments. Earth Planet. Sci. Lett. *266*/1, 61–77 (2008)

Keigwin, L. D., and Schlegel, M. A.: Ocean ventilation and sedimentation since the glacial maximum at 3 km in the western North Atlantic. Geochem. Geophys. Geosyst. *3*/6, 1034 (2002)

Lippold, J., Luo, Y., Francois, R., Allen, S. E., Gherardi, J., Pichat, S., Hickey, B., and Schulz, H.: Strength and geometry of the glacial Atlantic meridional overturning circulation. Nature Geosci. *5*/11, 813–816 (2012)

Marchitto, T. M., and Broecker, W. S.: Deep water mass geometry in the glacial Atlantic ocean: A review of constraints from the paleonutrient proxy Cd/Ca. Geochem. Geophys. Geosyst. *7*/12, Q12003 (2006)

Marcott, S. A., Kalk, M. L., McConnell, J. R., Sowers, T., Taylor, K. C., White, J. W. C., Brook, E. J., Bauska, T. K., Buizert, C., Steig, E. J., Rosen, J. L., Cuffey, K. M., Fudge, T. J., Severinghaus, J. P., and Ahn, J.: Centennial-scale changes in the global carbon cycle during the last deglaciation. Nature *514*/7524, 616–619 (2014)

McManus, J. F., Francois, R., Gherardi, J.-M., Keigwin, L. D., and Brown-Leger, S.: Collapse and rapid resumption of Atlantic meridional circulation linked to deglacial climate changes. Nature *428*/6985, 834–837 (2004)

Skinner, L. C., Fallon, S., Waelbroeck, C., Michel, E., and Barker, S.: Ventilation of the deep Southern Ocean and deglacial $CO_2$ rise. Science *328*/5982, 1147–1151 (2010)

Skinner, L. C., Waelbroeck, C., Scrivner, A. E., and Fallon, S. J.: Radiocarbon evidence for alternating northern and southern sources of ventilation of the deep Atlantic carbon pool during the last deglaciation. Proc. Natl. Acad. Sci. USA *111*/15, 5480 (2014)

Skinner, L., McCave, I. N., Carter, L., Fallon, S., Scrivner, A. E., and Primeau, F.: Reduced ventilation and enhanced magnitude of the deep Pacific carbon pool during the last glacial period. Earth Planet. Sci. Lett. *411*, 45–52 (2015)

Emma Freeman
University of Cambridge
Godwin Laboratory for Palaeoclimate Research
Department of Earth Sciences
Downing Site / N324
Cambridge, CB2 3EQ
UK
Phone: +44 1223 768342
Fax: +44 1223 333450
E-Mail: ef276@cam.ac.uk

Dr. Luke C. Skinner
University of Cambridge
Godwin Laboratory for Palaeoclimate Research
Department of Earth Sciences
Downing Site / N339
Cambridge, CB2 3EQ
UK
Phone: +44 1223 764912
Fax: +44 1223 333450
E-Mail: lcs32@cam.ac.uk

Nova Acta Leopoldina NF *121*, Nr. 408, 283–289 (2015)

# Characterizing Deep Circulation in the Northeast South China Sea Using Dissolved Inorganic Radiocarbon

Pan Gao,[1] Liping Zhou,[2] Xiaomei Xu,[3] and Kexin Liu[4]

With 4 Figures

## 1. Introduction

As a semi-closed marginal sea, the circulation pattern of the South China Sea (SCS) is highly complex. Much is known about the surface current flows and about the sills around the basin (Qu et al. 2006). The deepest sill (~ 2500 m) is located in the Luzon Strait between Taiwan and the Philippines, where the Pacific water is known to enter the SCS although its specific source(s) is still ambiguous. The fate of the deep water and mixing processes remains as a mystery. With many unknowns in vertical mixing processes, our knowledge of water column structure at different parts of the SCS is still patchy. Such a gap in our understanding of the deep circulation and the mixing processes of water masses leads to large uncertainty in the estimation of the residence time of the deep water and turnover time of the SCS. Without a good knowledge of the fundamental oceanographic processes which determine the distribution of heat and nutrients, it would be hard for us to understand the SCS's role in climate change and in global biogeochemical cycles, not only for the present but also for the past and the future.

In order to improve our understanding on the deep processes in the SCS, we have started a project which involves measurements of radiocarbon ($^{14}C$) in the dissolved inorganic carbon (DIC) of the seawater. The objective of the study is to characterize the structure of the water columns at different parts of the SCS, to identify the source of the Pacific inflow, and in particular to study the transport pathways of deep water and the mixing processes of water masses. Radiocarbon has been widely used as a tracer for characterizing large-scale circulation and subsequently in modelling ocean circulation, as in the GEOSECS and WOCE projects conducted in the later part of the 20$^{th}$ century. However, the SCS has not been visited during these previous cruise expeditions and only a few studies have examined the variation of $^{14}C$ of seawater in the SCS. Here we report preliminary results of this study including a new method of sample preparation for dissolved inorganic carbon in seawater for $^{14}C$ analysis by accelerator mass spectrometry (AMS) and our DI$^{14}C$ records obtained in the northeast SCS and Luzon Strait.

1 Department of Geography, Peking University, Beijing, 100871, China; E-Mail: pangao@pku.edu.cn.
2 Institute of Ocean Research, Peking University, Beijing, 100871, China, E-Mail: lpzhou@pku.edu.cn.
3 Department of Earth System Science, University of California, Irvine, CA 92697-3100, USA, E-Mail: xxu@uci.edu.
4 School of Physics, Peking University, Beijing, 100871, China, E-Mail: kxliu@pku.edu.cn.

## 2. Seawater DI$^{14}$C Sample Preparation

Seawater samples from 21 stations located at the northeast SCS were collected during March to May, 2013; another station located at the Manila trench (E3) was occupied in July, 2014 (Fig. 1). A SBE 911plus CTD attached with twenty four 12-liter Carousel Water Sampler was used for seawater collection. About 100 ml of seawater samples were collected at multiple depths for each station and poisoned with 50 μL of saturated $HgCl_2$ solution right after collection.

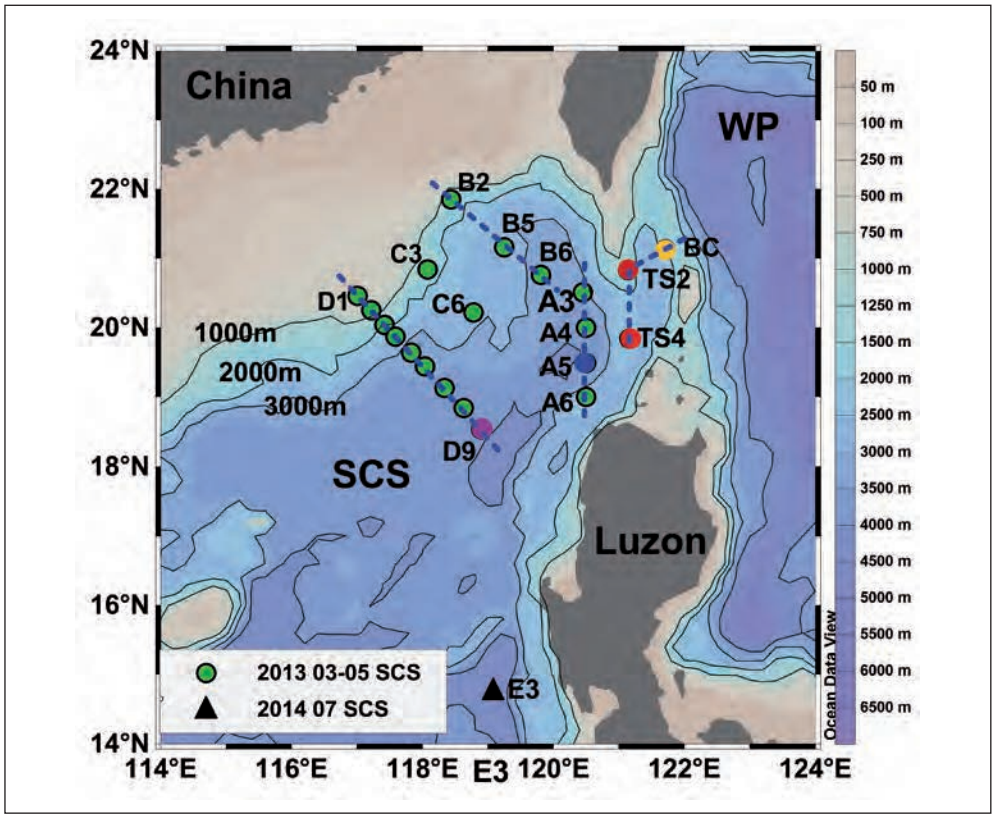


Fig. 1 Seawater DI$^{14}$C sampling station distribution in the South China Sea; dashed lines show the selected sections presented in Figure 4.

For analysis of DI$^{14}$C, seawater samples were processed using the headspace-extraction method developed by Gao et al. (2014) at the cosmogenic nuclide sample preparation laboratory of Peking University. Sample $CO_2$ was extracted from 30 ml seawater after acidifying with $H_3PO_4$, then cryogenically purified on a vacuum line and graphitized by Zn reduction method (Xu et al. 2007), and pressed into an aluminium target and submitted for AMS $^{14}$C measurements in PKUAMS facility (Liu et al. 2007).

Systematic investigations have shown that the headspace-extraction method does not introduce contaminants that could bias the $^{14}$C measurements and that the $^{14}$C results for stand-

ards are consistent with their consensus values. Large numbers of duplicate measurements have established a precision of 1.7 ‰ for modern samples with an average background of ~43,400 radiocarbon years for graphite target samples > 0.3 mg carbon.

## 3. Seawater DI$^{14}$C Profiles in the Northeast SCS

The DI$^{14}$C values of seawater samples collected from the SCS range from 53.5 ±3.2‰ (at 200 m depth) to –235.5 ± 2.8‰ (at 3000 m) (Fig. 2). The average DI$^{14}$C value remains high in the surface layer (40.6 ± 4.2 ‰; n = 22) and increases slightly to 44.4 ± 5.9 ‰ (n = 12) at 100 m depth, then quickly decreases to an average low of –223.9 ± 4.6 ‰ (n = 14) at 2000 m depth. Below 2000 m depth, the average DI$^{14}$C values remain relatively constant around –225.1 ± 4.1 ‰ (n = 59). As shown in the DI$^{14}$C spatial distribution (Fig. 3), the DI$^{14}$C spatial difference among stations is about 25 ‰ between 5–100 m depth. Significant difference is found between 200 and 1000 m depth in the range of 40–75 ‰, with the largest variation reaching ~ 75 ‰ on 300 m depth (from 44.8 ± 1.8 ‰ to –28.3 ± 2.3 ‰). Note that below 1500 m depth, the DI$^{14}$C differences become smaller than 25 ‰.

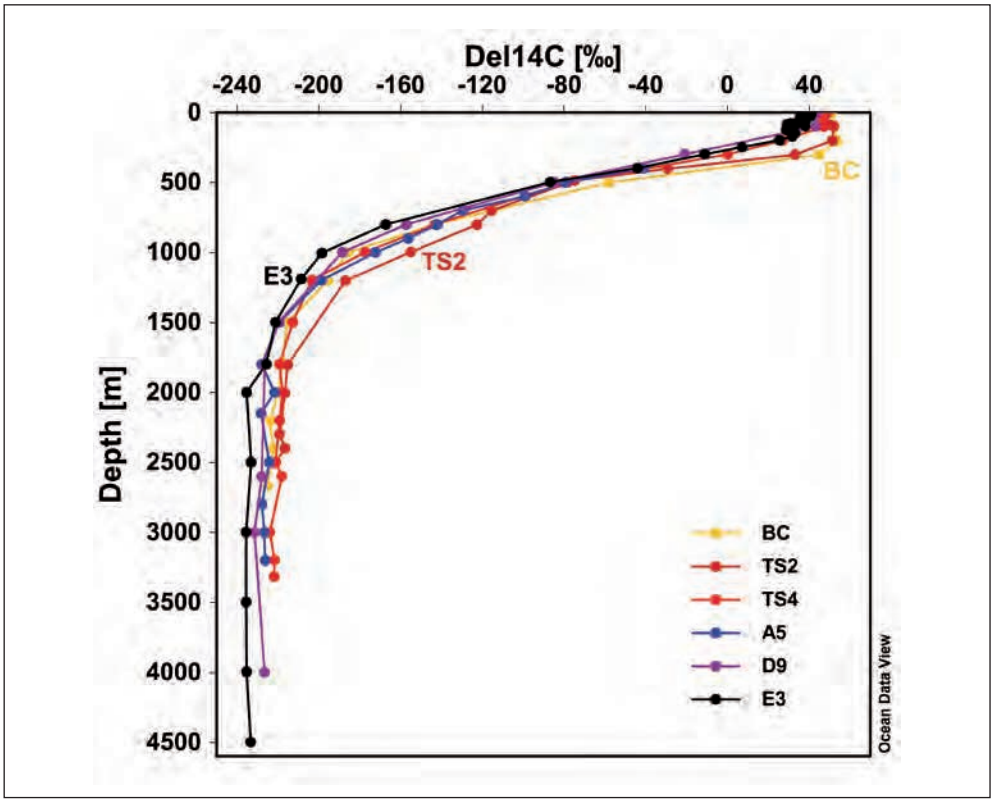


Fig. 2. DI$^{14}$C depth profiles of selected stations (BC, TS2, TS4, A5, D9, E3), which contain the extreme values among all stations.

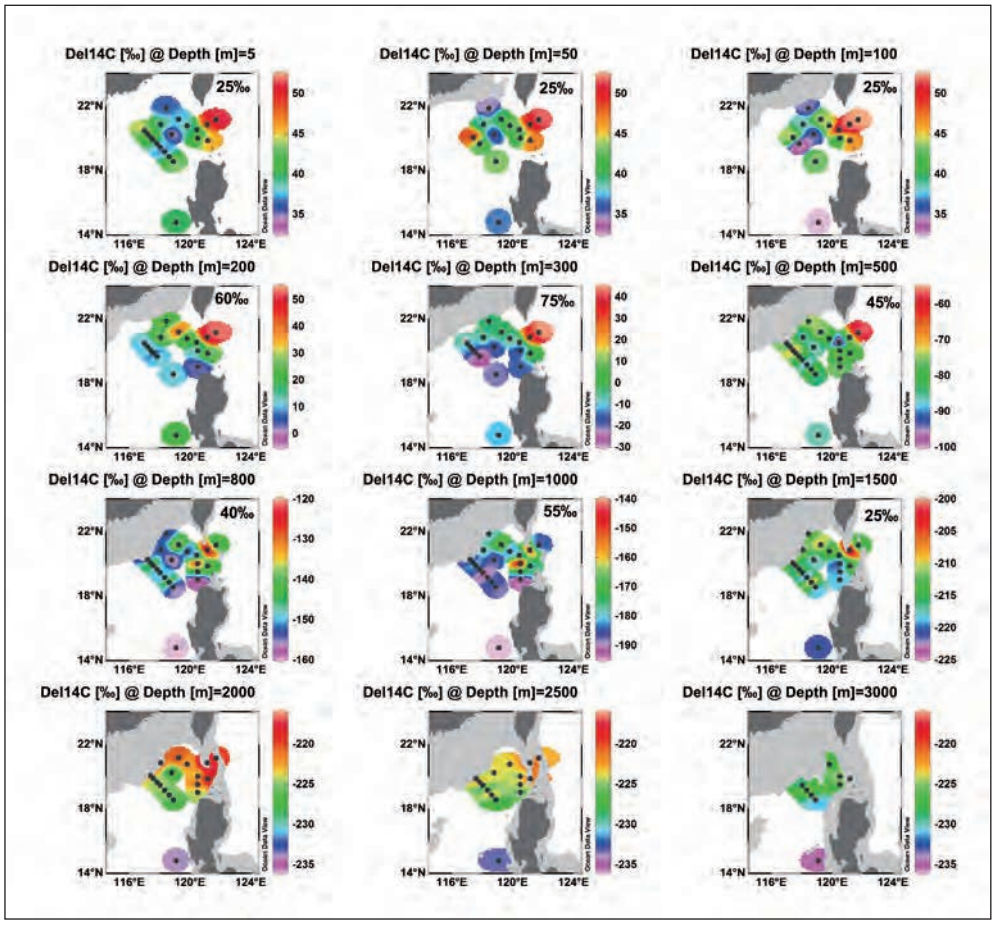


Fig. 3 $DI^{14}C$ spatial distribution of 2013–2014 SCS seawater samples at 5, 50, 100, 200, 300, 500, 800, 1000, 1500, 2000, 2500 and 3000 m depths. The $DI^{14}C$ scale differences on each depth are shown in the upper right corner of each plot, except for 2000–3000 m depth, the $DI^{14}C$ scale is fixed to –216 ~ –236 ‰.

Compared to the previous $DI^{14}C$ profile measured in the western Pacific by WOCE P09 cruise in July to August, 1994 (GLODAP Bottle Data, Key et al. 2004), SCS surface $\Delta^{14}C$ values are about 70–80‰ lower. An average decrease of $DI^{14}C$ values is observed at a rate of about 3–4‰ per year between 1994 and 2014. Bomb carbon penetration depth in the Northeast South China Sea and Luzon Strait is 500–650 m.

Between 5–500 m depth, stations inside SCS always show relatively lower $DI^{14}C$ value compared to the stations located in Luzon (BC, TS2, TS4; Fig. 3). This is probably because that as a marginal sea, the SCS basin has overall enhanced diapycnal mixing process in the upper layer compared to the open western Pacific, thus bomb radiocarbon signal is more diluted inside the SCS. Hydrological characters of the upper layer waters in Luzon are more influenced by the Pacific water through ocean circulation processes such as Kuroshio Current, which brings relatively high $DI^{14}C$ signals.

Relatively high $DI^{14}C$ water masses are found along Luzon Strait and the SCS northeast continental slope between 800–2000 m, with some extremely high points at Stations TS2 and A4 on certain depths (Fig. 3); while the $DI^{14}C$ values of water masses in the southern parts of the study area are much lower, especially for Stations D9 and E3. The possible mechanism of this might be the enhanced diapycnal mixing processes caused by the strong internal waves which frequently happen in Luzon Strait and the SCS continental slope (Tian et al. 2009).

Physical oceanography observation in Luzon Strait has shown that the North Pacific deep water (NPDW) enters the SCS between 1900–2600 m depth through the Luzon Strait (Zhao

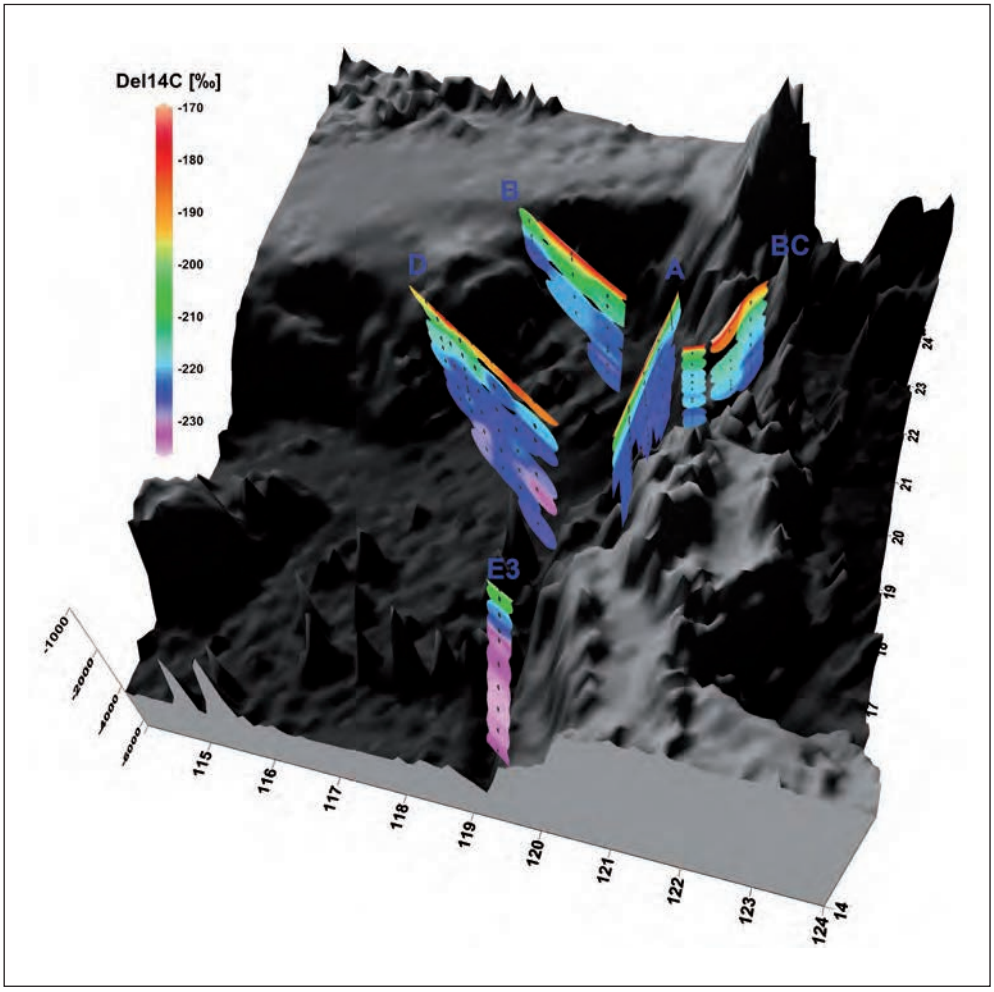


Fig. 4 3D map of $DI^{14}C$ distribution below 1000 m depth in the northeast SCS. The detailed positions of these sections (BC, A, B and D section) are shown in Figure 1.

et al. 2014). The NPDW undergoes strong diapycnal mixing inside Luzon Strait and quickly enters the SCS. The average $DI^{14}C$ value of the SCS waters deeper than 2500 m is –225.1 ± 4.1 ‰ (n = 59), which is consistent with the previously measured average $DI^{14}C$ values in the western Pacific between 2000–2500 m depth by WOCE P09 cruise (GLODAP Bottle Data; Key et al, 2004). In addition, the smallest $DI^{14}C$ variation appears on 2500 m depth by ~ 5 ‰ (range from –220.7 ± 1.4 ‰ to –226.5 ± 1.8 ‰) and trend to have a very uniform spatial distribution pattern in the northeast SCS (Fig. 3). These all point to the rapid invasion of the NPDW through Luzon Strait and its important influence on northeast SCS deep water in this depth range. Figure 4 shows the 3D distribution map of the SCS $DI^{14}C$ below 1000 m depth.

$DI^{14}C$ variation range of station BC is –185.6 ± 1.7 to –225.1 ± 1.5 ‰ and is most influenced by the NPDW. TS stations showed highest $DI^{14}C$ values (especially for TS2, ranges from –154.9 ± 2.0 ‰ to –221.5 ± 2.0 ‰) compare to the rest stations, which reveals that strong diapycnal mixing process inside Luzon Strait brings high $DI^{14}C$ signal down to the deep layer. Sections A, B and D located in-between the transition of Luzon Strait and SCS and show moderate $DI^{14}C$ values. The $DI^{14}C$ of E3 is the lowest (ranges from –198.4 ± 1.8 ‰ to –235.5 ± 2.8 ‰) and better represents the deep water characters inside SCS basin. Compared to E3, there are relatively high $DI^{14}C$ (–225 ‰) and uniform water masses from the passageway of Luzon Strait to the continental slope of northeast SCS between 2200–2800 m depth (Fig. 3 and 4), which may indicate the flow path of the NPDW along the SCS northeast continental slope and the resulting SCS deep western boundary current. The average $DI^{14}C$ difference of A5 and E3 is ~ 9 ± 3 ‰, which represents an apparent deep water age difference of about 90 ± 30 a between these two stations.

## 4. Summary

Our $DI^{14}C$ data point to a strong diapycnal mixing inside Luzon Strait within the range of 1000–2500 m. Relatively high $DI^{14}C$ (–225 ‰) are found from Luzon Strait to SCS northeast continental slope between 2200–2800 m depth, which may indicate the flow path of the NPDW after entering the SCS. The average $DI^{14}C$ difference between the stations located to the exit of Luzon (A5) and inside SCS basin (E3) showed an apparent deep water age difference of about 90 ± 30 a below 2000 m depth.

### *References*

Gao, P., Xu, X., Zhou, L. P., Pack, M. A., Griffin, S., Santos, G. M., Southon, J. R., and Liu, K.: Rapid sample preparation of dissolved inorganic carbon in natural waters using a headspace-extraction approach for radiocarbon analysis by accelerator mass spectrometry. Limnol. Oceanogr. Methods *12*, 172–188 (2014)

Key, R. M., Kozyr, A., Sabine, C. L., Lee, K., Wanninkhof, R., Bullister, J. L., Feely, R. A., Millero, F. J., Mordy, C., and Peng, T.-H.: A global ocean carbon climatology: Results from Global Data Analysis Project (GLODAP). Global Biogeochem. Cycles *18*, GB4031 (2004)

Liu, K. X., Ding, X. F., Fu, D. P., Pan, Y., Wu, X., Guo, Z., and Zhouet, L.: A new compact AMS system at Peking University. Nucl. Instrum. Methods Phys. Res. Sect. B *259*, 23–26 (2007)

Qu, T. D., Du, Y., and Sasaki, H.: South China Sea throughflow: A heat and freshwater conveyor. Geophys. Res. Lett. *33*/23, L23617 (2006)

Tian, J. W., Yang, Q. X., and Zhao, W.: Enhanced diapycnal mixing in the South China Sea. J. Phys. Oceanogr. *39*, 3191–3203 (2009)

Xu, X., Trumbore, S. E., Zheng, S. H., Southon, J. R., McDuffee, K. E., Luttgen, M., and Liu, J. C.: Modifying a sealed tube zinc reduction method for preparation of AMS graphite targets: Reducing background and attaining high-precision. Nucl. Instrum. Methods Phys. Res. Sect. B. *259*, 320–329 (2007)

Zhao, W., Zhou, C., Tian, J. W., Yang, Q., Wang, B., Xie, L., and Qu, T.: Deep water circulation in the Luzon Strait. J. Geophys. Res. – Oceans *119*/2, 790–804 (2014)

Dr. Pan Gao (Postdoctoral Fellow)
Department of Geography
Peking University
Beijing, 100871
China
Phone: +86 138 11483808
Fax: +86 010 62754411
E-Mail: pangao@pku.edu.cn

Nova Acta Leopoldina NF *121*, Nr. 408, 291–295 (2015)

# What Caused Enhanced Export Production in the Sub-Antarctic Zone during Glacial Intervals?

Robert M. Graham,[1,2] Agatha M. de Boer,[1,2] Karen E. Kohfeld,[3] and Christian Schlosser[4]

With 3 Figures

There is wide spread evidence from sediment records in the Southern Ocean that export production was enhanced in the Sub-Antarctic Zone during glacial intervals (Fig. 1; Kohfeld et al. 2013). The lithogenic fraction of material in these sediment records was also higher during periods when export production was enhanced (Ziegler et al. 2013, Anderson et al. 2014, Lamy et al. 2014, Martínez-García et al. 2014). Coincident with the increase in export production, ice core records from Antarctica show that dust fluxes were more than 20-times greater than today during glacial intervals and atmospheric carbon dioxide concentrations decreased (Petit et al. 1990). These records have led many studies to the conclusion that enhanced export production in the Sub-Antarctic Zone during glacial intervals was driven primarily by an increase in the supply of iron from dust, which is a limiting micronutrient in the Southern Ocean, and that this enhanced export production helped lower atmospheric carbon dioxide concentrations (Martin 1990, Ziegler et al. 2013, Anderson et al. 2014, Lamy et al. 2014, Martínez-García et al. 2014).

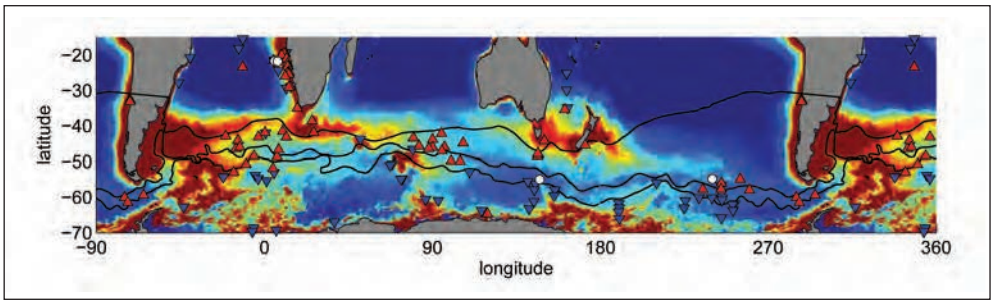


Fig. 1 Present day, mean annual chlorophyll concentrations for years 1999–2009 (colour scale, mg $m^{-3}$), and export production anomalies at the Last Glacial Maximum (red higher, blue lower). Black lines are the Orsi et al. (1995) Subtropical, Sub-Antarctic and Polar Fronts. Export production data were compiled by Kohfeld et al. (2013). The Sub-Antarctic Zone is the region between the Subtropical and Sub-Antarctic Front. (Figure is by Graham 2014.)

1 Stockholm University, Sweden.
2 Bolin Centre for Climate Research, Sweden.
3 Simon Fraser University, Canada.
4 GEOMAR, Germany.

Recent studies have shown that productivity in the modern day Southern Ocean is relatively insensitive to iron supplied by dust (Mackie et al. 2008, Wagener et al. 2008, Tagliabue et al. 2014). For example, Mackie et al. (2008) showed that there was no evidence of enhanced chlorophyll concentrations in the Southern Ocean following the deposition of dust from major dust storms from Australia. Similarly Tagliabue et al. (2014) showed in a modelling study that export production changed by approximately 1 % when all dust sources of iron

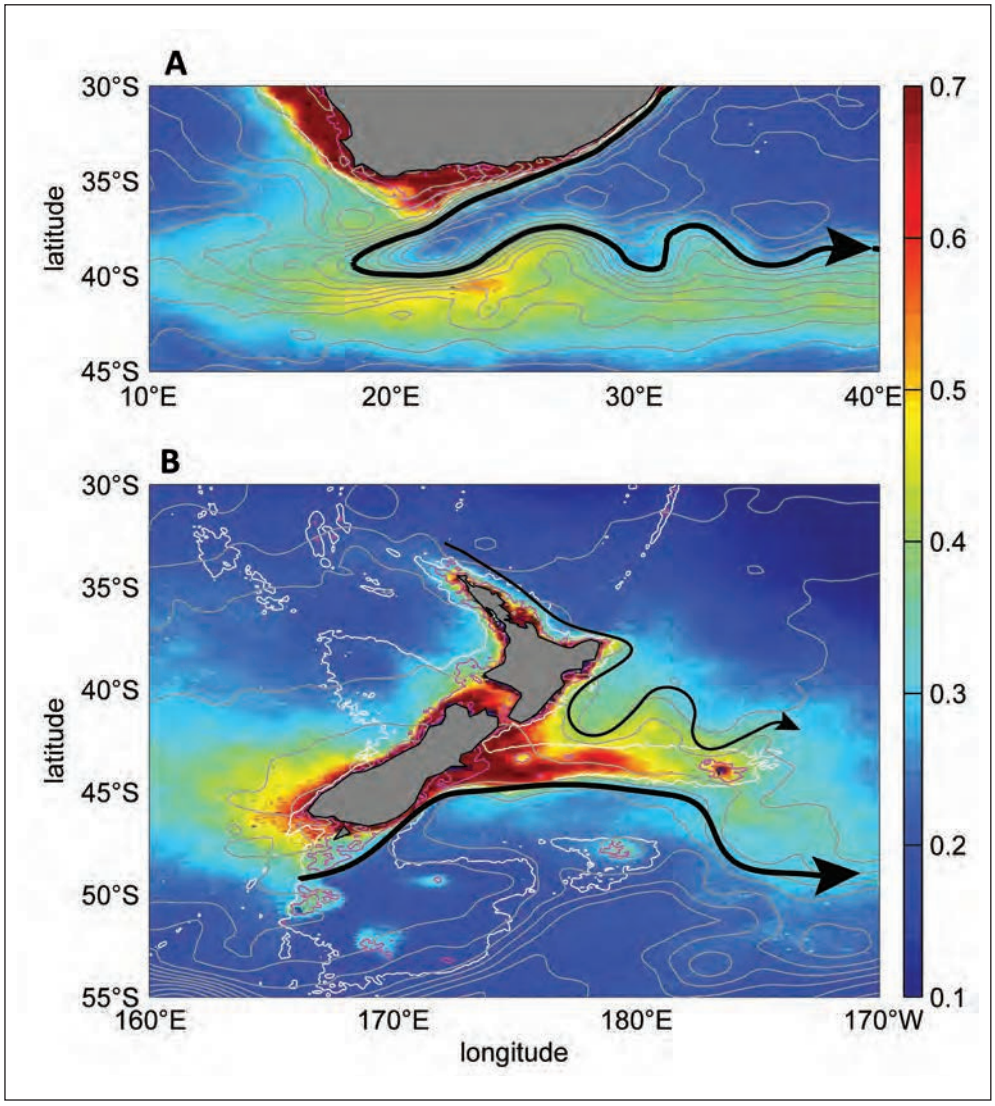


Fig. 2 Mean annual chlorophyll concentration for 1999–2009 (colour scale, $mgm^{-3}$). Grey contours are the sea surface height field for 1999–2009. White contours are the 1000 m isobaths, and pink the 200 m isobaths. Hand drawn black arrows illustrate the path of the western boundary currents and Dynamical Subtropical Front. (*A*) South Africa. (*B*) New Zealand and the Campbell Plateau. (Figure is by Graham et al. in review, Deep-Sea Res.-Part I.)

were removed. In contrast, when sedimentary iron sources were removed, export production decreased by approximately 7 % and atmospheric carbon increased by 14.5 ppm (Tagliabue et al. 2014). Given these recent findings, we argue that the possibility should be considered that Southern Ocean export production anomalies may have been driven by changes to the supply of shelf sediment iron rather than just dust. Shelf sediments are thought to represent one of the largest sources of iron to the global ocean (Johnson et al. 1999, Elrod et al. 2004).

Here we study the chlorophyll blooms in the modern day Sub-Antarctic Zone, which are situated over a number of sediment records used in paleo archives (Fig. 1). These blooms are very tightly related to the sea surface height field that indicates the horizontal flow in the ocean (Fig. 2 and 3). In particular, these chlorophyll blooms are associated with western boundary current extensions from the Atlantic, Indian and Pacific Oceans (Fig. 2 and 3). These currents are known collectively as the Dynamical Subtropical Front (Graham and de Boer 2013).

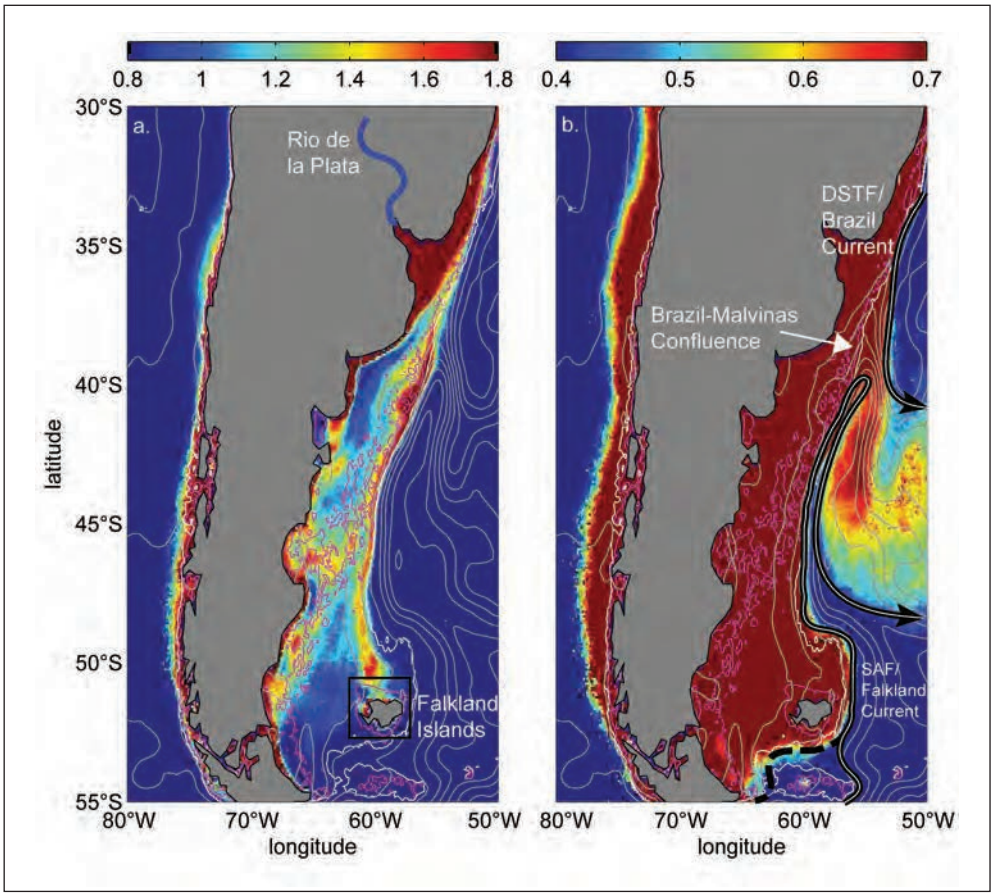


Fig. 3 Mean annual chlorophyll concentrations for years 1999–2009 (colour scale, note different scale between figures, $mgm^{-3}$). Grey contours are the sea surface height field for 1999–2009. White contours are the 400 m isobaths, and pink contours the 120 m isobaths (indication for glacial coastline). Hand drawn black arrows illustrate the path of the western boundary currents, Sub-Antarctic Front and Dynamical Subtropical Front in (*B*). Location of the Rio de la Plata estuary is shown by the blue line in (*A*). (Figure is by Graham et al. in review, Deep-Sea Res.-Part I.)

We suggest that present day chlorophyll blooms in the Sub-Antarctic Zone are stimulated by an off shelf transport of shelf sediment iron by the Dynamical Subtropical Front, rather than iron supplied by dust or open ocean upwelling. Shelf sediment iron is entrained into western boundary currents as they run parallel to the continental shelf. This iron is then advected downstream into the Sub-Antarctic Zone along the Dynamical Subtropical Front.

Most biogeochemical models prescribe a shelf sediment iron source uniformly through the sea floor over all areas of shelf where the water depth is shallower than 1000 m (Moore et al. 2004, Aumont and Bopp 2006). However, the chlorophyll data analysed in our study indicate that the largest shelf sediment iron fluxes are concentrated around coastal margins, rather than spread evenly over continental shelves (Fig. 3*A*). This could be due to higher sedimentation rates and input of organic material in coastal environments from processes such as fluvial transport and coastal erosion. This would help promote the establishment of anoxic conditions in coastal sediments and the reduction of iron oxide.

At the Last Glacial Maximum sea levels were approximately 120 m lower than today (Peltier and Fairbanks 2006). We calculate that a uniform drop in sea level of 120 m would reduce the area of continental shelves between the depths of 0 and 1000 m by approximately 50 %. For many biogeochemical models this would result in a ~50 % decrease in the shelf sediment flux of dissolved iron (Moore et al. 2004, Aumont and Bopp 2006). The findings from Tagliabue et al. (2014) suggest this would lead to a substantial reduction in export production and increase atmospheric carbon dioxide concentrations. However, various paleo records show that export production increased in the Sub-Antarctic Zone and atmospheric carbon dioxide decreased during glacial intervals when sea levels were lower (Ziegler et al. 2013, Anderson et al. 2014, Lamy et al. 2014, Martínez-García et al. 2014).

If the shelf sediment iron flux is not spread evenly across continental shelves, but instead concentrated along coastal margins, a reduction in sea level would shift the location of the major iron flux closer towards the western boundary currents (Fig. 3, pink contour). This may have increased the fraction of iron that was entrained into western boundary currents and transported into the Sub-Antarctic Zone. This mechanism would be more consistent with suggestions that sediment transport by ocean currents, rather than dust, are substantial contributors to the increased lithogenic fraction recorded in ocean sediment cores from the Agulhas Region and Antarctic Peninsula during glacial periods (Diekmann and Kuhn 2002, Latimer et al. 2006, Noble et al. 2012).

## *References*

Anderson, R. F., Barker, S., Fleisher, M., Gersonde, R., Goldstein, S. L., Kuhn, Mortyn, P. G., Pahnke, K., and Sachs, J. P.: Biological response to millennial variability of dust and nutrient supply in the Subantarctic South Atlantic Ocean Phil. Trans. Royal Soc. A *372*, doi:10.1098/rsta. (20130054) (2014)

Aumont, O., and Bopp, L.: Globalizing results from ocean in situ iron fertilization studies. Global Biogeochem. Cycles *20*/2, doi:10.1029/2005GB002591 (2006)

Diekmann, B., and Kuhn, G.: Sedimentary record of the mid-Pleistocene climate transition in the southeastern South Atlantic (ODP Site 1090). Palaeogeogr. Palaeoclimatol. Palaeoecol. *182*, 241–258 (2002)

Elrod, V. A., Berelson, W. M., Coale, K. H., and Johnson, K. S.: The flux of iron from continental shelf sediments: A missing source for global budgets. Geophys. Res. Lett. *31*/12, L12307; doi:10.1029/2004GL020216 (2004)

Graham, R. M.: The role of Southern Ocean fronts in the global climate system. PhD Thesis in Marine Geology at Stockholm University (2014)

Graham, R. M., and Boer, A. M. de: The Dynamical Subtropical Front. J. Geophys. Res. – Oceans *118*, doi:10.1002/jgrc.20408 (2013)

Graham, R. M., Boer, A. M. de, Kohfeld, K. E., van Sebille, E., and Schlosser, C.: Inferring potential source regions and transport pathways of iron in the Southern Ocean from satellite chlorophyll data. Deep-Sea Res. Part I (in review)

Johnson, K. S., Chavez, F. P., and Friederich, G. E.: Continental-shelf sediment as a primary source of iron for coastal phytoplankton. Nature *398*, 697–700; doi:10.1038/19511 (1999)

Kohfeld, K. E., Graham, R. M., Boer, A. M. de, Sime, L. C., Wolff, E. W., Le Quéré, C., and Bopp, L.: Southern Hemisphere westerly wind changes during the Last Glacial Maximum: paleo-data synthesis. Quat. Sci. Rev. *68*, 76–95; doi:10.1016/j.quascirev.2013.01.017 (2013)

Lamy, F., Gersonde, R., Winckler, G., Esper, O., Jaeschke, A., Kuhn, G., Ullermann, J., Martínez-García, A., Lambert, F., and Kilian, R.: Increased dust deposition in the Pacific Southern Ocean during glacial periods. Science *343*/6169, 403–407; doi:10.1126/science.1245424 (2014)

Latimer, J. C., Filippelli, G. M., Hendy, I. L., Gleason, J. D., and Blum, J. D.: Glacial-interglacial terrigenous provenance in the southeastern Atlantic Ocean: The importance of deep-water sources and surface currents. Geology *34*/7, 545; doi:10.1130/G22252.1 (2006)

Mackie, D. S., Boyd, P. W., McTainsh, G. H., Tindale, N. W., Westberry, T. K., and Hunter, K. A.: Biogeochemistry of iron in Australian dust: From eolian uplift to marine uptake. Geochem. Geophys. Geosyst. *9*/3, doi:10.1029/2007GC001813 (2008)

Martin, J.: Glacial-interglacial $CO_2$ change: The iron hypothesis. Paleoceanography *5*/1, 1–13 (1990)

Martínez-García, A., Sigman, D. M., Ren, H., Anderson, R. F., Straub, M., Hodell, D. A., Jaccard, S. L., Eglinton, T. I., and Haug, G. H.: Iron fertilization of the Subantarctic Ocean during the last ice age. Science *343*/6177, 1347–1350; doi:10.1126/science.1246848 (2014)

Moore, J. K., Doney, S. C., and Lindsay, K.: Upper ocean ecosystem dynamics and iron cycling in a global three-dimensional model. Global Biogeochem. Cycles *18*/4, doi:10.1029/2004GB002220 (2004)

Noble, T. L., Piotrowski, A. M., Robinson, L. F., McManus, J. F., Hillenbrand, C.-D., and Bory, A. J.-M.: Greater supply of Patagonian-sourced detritus and transport by the ACC to the Atlantic sector of the Southern Ocean during the last glacial period. Earth Planet. Sci. Lett. *317/318*, 374–385; doi:10.1016/j.epsl.2011.10.007 (2012)

Orsi, A., Whitworth, T., and Nowlin, W. D. Jr.: On the meridional extent and fronts of the Antarctic Circumpolar Current. Deep-Sea Res. Part I *42*/5, 641–673; doi:10.1016/0967-0637(95)00021-W (1995)

Peltier, W. R., and Fairbanks, R. G.: Global glacial ice volume and Last Glacial Maximum duration from an extended Barbados sea level record. Quat. Sci. Rev. *25*/23, 24, 3322–3337; doi:10.1016/j.quascirev.2006.04.010 (2006)

Petit, J., Mourner, L., Jouzel, J., Korotkevich, Y., Kotlyakov, V., and Lorius, C.: Palaeoclimatological and chronological implications of the Vostok core dust record. Nature *343*, 56–58; doi:10.1038/343056a0 (1990)

Tagliabue, A., Aumont, O., and Bopp, L.: The impact of different external sources of iron on the global carbon cycle. Geophys. Res. Lett. *41*, 920–926; doi:10.1002/2013GL059059 (2014)

Wagener, T., Guieu, C., Losno, R., Bonnet, S., and Mahowald, N.: Revisiting atmospheric dust export to the Southern Hemisphere ocean: Biogeochemical implications. Global Biogeochem. Cycles *22*/2, doi:10.1029/2007GB002984 (2008)

Ziegler, M., Diz, P., Hall, I. R., and Zahn, R.: Millennial-scale changes in atmospheric $CO_2$ levels linked to the Southern Ocean carbon isotope gradient and dust flux. Nature Geosci. *6*/6, 457–461; doi:10.1038/ngeo1782 (2013)

Robert M. Graham
Department of Geological Sciences
Bolin Centre for Climate Research
Stockholm University
106 91 Stockholm
Sweden
E-Mail: r.graham.1007@gmail.com

Nova Acta Leopoldina NF *121*, Nr. 408, 297–300 (2015)

# Paleoceanographic Evolution of the Atlantic Sector of the Antarctic Southern Ocean across the Mid-Pleistocene Transition

Adam P. Hasenfratz,[1] Alfredo Martínez-García,[1] Samuel L. Jaccard,[2] David A. Hodell,[3] Derek Vance,[1] Stefano Bernasconi,[1] Mervyn Greaves,[3] Helga (Kikki) F. Kleiven,[4] and Gerald H. Haug[1]

With 1 Figure

The mid-Pleistocene transition (MPT; 1.25 – 0.7 Ma) marked a fundamental change in the periodicity of the climate cycles, shifting from a 41-ka to a high-amplitude, asymmetric, 100-ka cycle without any significant change in orbital forcing. This change in the dominant periodicity comes along with a gradual increase in the glacial $\delta^{18}O$ of benthic foraminiferal tests, implying larger ice volume and/or cooler deep ocean temperatures. Hypotheses to explain the MPT involve changes in glacial dynamics, non-linear responses to orbital forcing, and internal changes in the carbon cycle (e.g. Clark et al. 2006). Specifically, a decrease in $pCO_2$ during peak ice age conditions and the associated global cooling, more pronounced during glacials, is often proposed as one of the possible triggers for the MPT (Hönisch et al. 2009, McClymont et al. 2013).

The most promising explanations for the bulk of the $pCO_2$ variations in the Pleistocene involve ocean biogeochemistry and its interaction with the physical circulation. It was recognized early on that the high-latitude oceans, specifically the Southern Ocean, exert a dominant influence on the partitioning of $CO_2$ between the ocean interior and the atmosphere through their leverage on the efficiency of the biological pump. In the modern Southern Ocean, the low efficiency of the biological pump allows for the evasion of deeply sequestered $CO_2$ back to the atmosphere. Previous results have indicated that the Southern Ocean leak in the biological pump may have been reduced during ice ages (e.g. Sigman et al. 2010) contributing to sequester carbon into the ocean interior.

Although the two regions of the Southern Ocean, the Antarctic Zone (AZ) and the Subantarctic Zone (SAZ) south and north of the Antarctic Polar Front (APF), respectively, are both thought to contribute to the $pCO_2$ decrease during ice ages, their biogeochemical signature and timing is very different. Export of organic carbon from surface waters of the AZ decreased during ice ages, whereas nutrient utilization increased, indicating reduced exposure of nutrient-rich subsurface waters (Francois et al. 1997, Jaccard et al. 2013). In contrast, in the SAZ, export production and nutrient consumption both increased during the later stages of glaciations, which, together with the concomitant increase in atmospheric dust loading,

1 Geological Institute, Department of Earth Sciences, Sonneggstraße 5, ETH Zurich, Switzerland.
2 Institute of Geological Sciences and Oeschger Center for Climate Change Research, University of Bern, Switzerland.
3 Godwin Laboratory for Paleoclimate Research, Department of Earth Sciences, University of Cambridge, UK.
4 Department of Earth Science, University of Bergen and Bjerknes Centre for Climate Research, Norway, and Uni Climate, Uni Research, University of Bergen and Bjerknes Centre for Climate Research, Norway.

suggests iron fertilization of phytoplankton (Martínez-García et al. 2014). Together, they provide a coherent two-part Southern Ocean mechanism for the timing and amplitude of the glacial/interglacial $pCO_2$ variations (Hain et al. 2010, Jaccard et al. 2013). However, there is still much uncertainty and debate regarding the response of the Southern Ocean biogeochemistry to the changes invoked by the MPT, and its contribution to the proposed $pCO_2$ variations.

It was suggested that atmospheric $pCO_2$ was ~30 ppm higher during glacial stages before the MPT, but interglacial values were similar to those of the late Pleistocene (Hönisch et al. 2009). During this transition, glacial dust fluxes to the SAZ of the Southern Ocean doubled, suggesting that an increase in iron availability may have potentially contributed to explain the $pCO_2$ shift across the MPT (Martínez-García et al. 2011). The importance of the Antarctic Southern Ocean in explaining the glacial/interglacial $pCO_2$ variations suggests that the gradual decrease in glacial $pCO_2$ across the MPT may be potentially influenced by mechanisms occurring in the AZ as well. However, most of the paleoceanographic reconstructions focus on the SAZ, partly due to the scarcity of calcite-producing organisms south of the APF that are required by many of the biogeochemical tools. The few existing records from the AZ that trace changes in the rate of overturning are mostly restricted to the last glacial cycle or the last one million years (e.g. Jaccard et al. 2013), or have a low temporal resolution (Hillenbrand and Fütterer 2001). Hence, the role of the AZ in contributing to explain the glacial $pCO_2$ decrease across the MPT remains elusive.

Here, we show 1.5 Ma-long highly-resolved records of export production, sedimentary $CaCO_3$ and planktonic (*N. pachyderma*) and benthic (*Cibicidoides*) foraminiferal stable isotopes from ODP Site 1094. The site is located in the Atlantic sector of the Antarctic Southern Ocean south of the present-day position of the APF (Fig. 1). The new age model is largely based on tuning of the new *Cibicidoides* $\delta^{18}O$ record to the LR04 benthic $\delta^{18}O$ stack (Lisiecki and Raymo 2005).

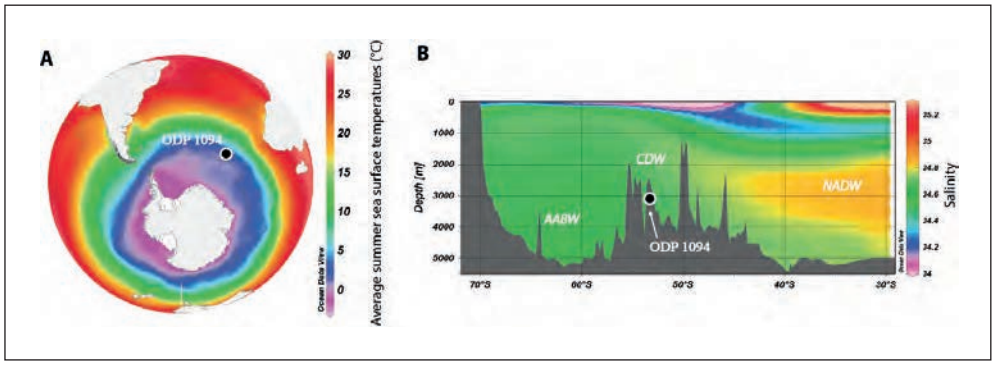


Fig. 1 Location of ODP Site 1094 in the Atlantic sector of the Antarctic Southern Ocean (53.2°S S, 5.1°E; water depth of 2807m) (*A*) on the January to March sea surface temperature field and (*B*) on a latitudinal salinity transect centered at ~10°E.

In order to trace variations in export production and sedimentary $CaCO_3$ across the MPT, the 1 Ma-long Ba/Fe and Ca/Fe records by Jaccard et al. (2013) have been extended to the base of the core, corresponding to an age of 1.5 Ma. Barite ($BaSO_4$) forms in seawater and its flux

to the seafloor is linked to integrated surface productivity (Francois et al. 1995). Biogenic barite (bioBa) precipitation is thought to accompany phytoplankton decay and may, therefore, represent a reliable proxy for integrated organic carbon export from the photic zone. As downcore pore-water profiles at ODP Site 1094 never reached sulfate-reducing conditions, the variations in bioBa are unaffected by bacterially mediated sulfate reduction and associated diagenetic barite dissolution. Assuming that sedimentary iron is exclusively of detrital origin, Ba abundance normalized by Fe is a proxy for the sedimentary concentration of bioBa, and hence export production. Similarly, Ca normalized to Fe yields the sedimentary concentration of biogenic $CaCO_3$ (Jaccard et al. 2013).

The 1 Ma-long stable isotope records of the left-coiling planktonic foraminifera *N. pachyderma* (Hodell et al. 2003, Kleiven and Jansen 2003) were likewise prolonged to the base of the ODP core. Considering the modern mixed layer depth of the Southern Ocean (~100–200 m) and the typical depth habitat of *N. pachyderma* (upper ~130 m), its $\delta^{18}O$ can be interpreted as reflecting changes in sea surface conditions (temperature, salinity) and global ice volume. The $\delta^{18}O$ record corresponds well to Antarctic temperature (Lüthi et al. 2008) over the last 800 ka, and its downcore evolution records climatic changes in the Antarctic realm also beyond the time frame covered by ice cores. Paired measurements of $\delta^{18}O$ and Mg/Ca on *N. pachyderma* allow us to calculate $\delta^{18}O$ of seawater that is known to vary linearly with salinity in the modern ocean.

## *References*


Clark, P. U., Archer, D., Pollard, D., Blum, J. D., Rial, J. A., Brovkin, V., Mix, A. C., Pisias, N. G., and Roy, M.: The middle Pleistocene transition: characteristics, mechanisms, and implications for long-term changes in atmospheric $pCO_2$. Quat. Sci. Rev. *25*/23, 3150–3184 (2006)

Francois, R., Honjo, S., Manganini, S. J., and Ravizza, G. E.: Biogenic barium fluxes to the deep sea: Implications for paleoproductivity reconstruction. Global Biogeochem. Cycles *9*/2, 289–303 (1995)

Francois, R., Altabet, M. A., Yu, E.-F., Sigman, D. M., Bacon, M. P., Frank, M., Bohrmann, G., Bareille, G., and Labeyrie, L. D.: Contribution of Southern Ocean surface-water stratification to low atmospheric $CO_2$ concentrations during the last glacial period. Nature *389*/6654, 929–935 (1997)

Hain, M. P., Sigman, D. M., and Haug, G. H.: Carbon dioxide effects of Antarctic stratification, North Atlantic inter-mediate water formation, and subantarctic nutrient drawdown during the last ice age: Diagnosis and synthesis in a geochemical box model. Global Biogeochem. Cycles *24*/4, GB4023 (2010)

Hillenbrand, C.-D., and Fütterer, D.: Neogene to Quaternary deposition of opal on the continental rise west of the Antarctic Peninsula, ODP Leg 178, Sites 1095, 1096, and 1101. In: Barker, P. F., Camerlenghi, A., Acton, G. D., and Ramsay, A. T. S. (Eds.): Proceedings of the Ocean Drilling Program. Scientific Results Vol. *178*; pp. 1–33. College Station TX, USA 2001

Hodell, D. A., Charles, C. D., Curtis, J. H., Mortyn, P. G., Ninnemann, U. S., and Venz, K. A.: Data report: Oxygen isotope stratigraphy of ODP Leg 177 Sites 1088, 1089, 1090, 1093, and 1094. In: Gersonde, R., Hodell, D. A., Blum, P., et al. (Eds.): Proceedings of the Ocean Drilling Program. Scientific Results Vol. *177*, Ch. 9; pp. 1–26. College Station TX, USA 2003

Hönisch, B., Hemming, N. G., Archer, D., Siddall, M., and McManus, J. F.: Atmospheric carbon dioxide concentration across the mid-Pleistocene transition. Science *324*/5934, 1551–1554 (2009)

Jaccard, S. L., Hayes, C. T., Martínez-García, A., Hodell, D. A., Anderson, R. F., Sigman, D. M., and Haug, G. H.: Two modes of change in Southern Ocean productivity over the past million years. Science *339*/6126, 1419–1423 (2013)

Kleiven, H. F., and Jansen, E.: Data Report: Early-mid-Pleistocene oxygen isotope stratigraphy from the Atlantic sector of the Southern Ocean: ODP Leg 177 Sites 1094 and 1091. In: Gersonde, R., Hodell, D. A., and Blum, P., et al. (Eds.): Proceedings of the Ocean Drilling Program. Scientific Results Vol. *177*, Ch. 12, pp. 1–20. College Station TX, USA 2003

Lisiecki, L. E., and Raymo, M. E.: A Pliocene – Pleistocene stack of 57 globally distributed benthic $\delta^{18}O$ records. Paleoceanography *20*/1, PA1003 (2005)

Lüthi, D., Le Floch, M., Bereiter, B., Blunier, T., Barnola, J.-M., Siegenthaler, U., Raynaud, D., Jouzel, J., Fischer, H., Kawamura, K., and Stocker, T. F.: High-resolution carbon dioxide concentration record 650,000–800,000 years before present. Nature *453*/7193, 379–382 (2008)

Martínez-García, A., Rosell-Melé, A., Jaccard, S. L., Geibert, W., Sigman, D. M., and Haug, G. H.: Southern Ocean dust-climate coupling over the past four million years. Nature *476*/7360, 312–315 (2011)

Martínez-García, A., Sigman, D. M., Ren, H., Anderson, R. F., Straub, M., Hodell, D. A., Jaccard, S. L., Eglinton, T. I., and Haug, G. H.: Iron fertilization of the Subantarctic Ocean during the last ice age. Science *343*/6177, 1347–1350 (2014)

McClymont, E. L., Sosdian, S. M., Rosell-Melé, A., and Rosenthal, Y.: Pleistocene sea-surface temperature evolution: Early cooling, delayed glacial intensification, and implications for the mid-Pleistocene climate transition. Earth Sci. Rev. *123*, 173–193 (2013)

Sigman, D. M., Hain, M. P., and Haug, G. H.: The polar ocean and glacial cycles in atmospheric $CO_2$ concentration. Nature *466*/7302, 47–55 (2010)

Adam P. Hasenfratz
Department of Earth Sciences
Geological Institute
NO E 27
Sonneggstrasse 5
8092 Zürich
Switzerland
Phone: +41 44 6326975
E-Mail: adam.hasenfratz@erdw.ethz.ch

Nova Acta Leopoldina NF *121*, Nr. 408, 301–303 (2015)

# Effects of Changing Ocean Circulation on the Marine Carbon Cycle during the Paleocene-Eocene Thermal Maximum

Mathias Heinze and Tatiana Ilyina (Hamburg)

With 2 Figures

The Paleocene-Eocene Thermal Maximum (PETM) was a transient global warming event, which occurred 56 million years ago. During this period of abrupt environmental change the climate underwent a significant transformation within short geological timescales (<10 ka, Zeebe et al. 2009). The PETM is globally recorded in proxy-data by a negative $\delta^{13}C$ carbon isotope excursion and carbonate dissolution in the ocean, suggesting that the occurred warming was caused by massive carbon release. Despite several plausible hypotheses, the exact rate of carbon release and the ultimate location of the carbon source remain unknown. The deep ocean conditions must have been inhospitable to marine organisms, since PETM sediment records indicate a mass extinction of benthic foraminifera and vast dissolution of $CaCO_3$ sediments. Both, ocean circulation and marine biogeochemistry must have been affected by the carbon perturbation of the PETM.

Until now, however, modelling studies did not consider the changes in the ocean circulation together with the changes in ocean biogeochemistry. As ocean circulation state is the key in shaping the marine carbon cycle, the current interpretation of the PETM proxy record may be incomplete. To address this issue, we simulate the late Paleocene background climate and the onset of the PETM with the state of the art Earth System Model of the Max Planck Institute (MPI-ESM). The model has a horizontal resolution of ~3.5°. The atmospheric model is represented by 31 and the ocean model by 40 vertical levels. For the first time the onset of the PETM is simulated with a complex ESM, including a comprehensive ocean biogeochemistry model.

The late Paleocene background climate state is based on an atmospheric $CO_2$ concentration of 560 ppm, which is producing a global mean SST of ~24 °C (Heinze and Ilyina 2015). Unlike today, the main area of deep water formation is located in the Pacific and Indian sector of the Southern Ocean. Our model does not predict any deep water formation in the North Atlantic, which is consistent with proxy reconstructions (Tripati and Elderfield 2005, Thomas et al. 2003).

Starting from this already warmer background climate than present, we increase the atmospheric $CO_2$ concentration by 0.5 ppm $a^{-1}$ (equivalent to emission of 1 Gt C) over a period of 1300 years. Following the atmospheric $CO_2$ increase phase, the simulation is run for another 1700 years with fixed atmospheric $CO_2$ concentrations of 1173 ppm. Due to rising atmospheric $CO_2$, the global SST increases by 6 °C over the whole simulation period. The meridional temperature gradient flattens and the hydrological cycle intensifies, leading to in-

creased freshwater input in the deep water formation areas. As a consequence, the deep water formation is reduced and the vertical stratification of the ocean is increased (Fig. 1). Surface waters are facing low nutrient concentrations and reduced biological production because of weaker upwelling of nutrient rich waters. Consistent with recent boron isotope reconstructions (Penman et al. 2014), the surface ocean pH decreases by 0.28 in our simulation.

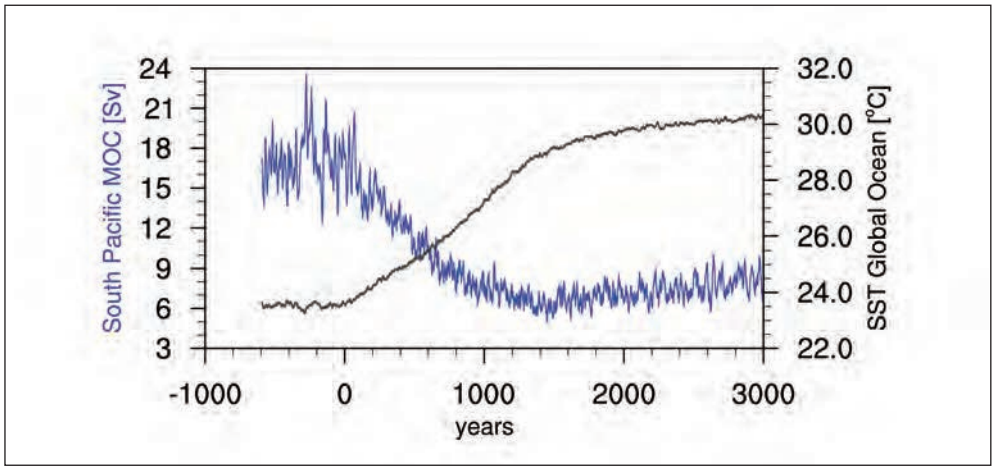


Fig. 1 Timeseries (10 year running mean) of the maximum MOC, below 1000 m depth in the South Pacific (blue line) and the SST (global, black line) for the PETM $CO_2$ emission scenario. Negative values on the x-axis correspond to the steady state in the control run.

Our results indicate that the significantly weakened deep-ocean ventilation is the key mechanism to reproduce the $CaCO_3$ dissolution pattern of the PETM, suggested by the proxy record. Transport of carbon to depth by physical processes is strongly reduced due to the increased ocean stratification. However, the increased respiration of organic matter and the accumulation of its remnants drive the deoxygenation and acidification of the mid and deep ocean instead. The reduced ocean ventilation causes the products of organic matter remineralization

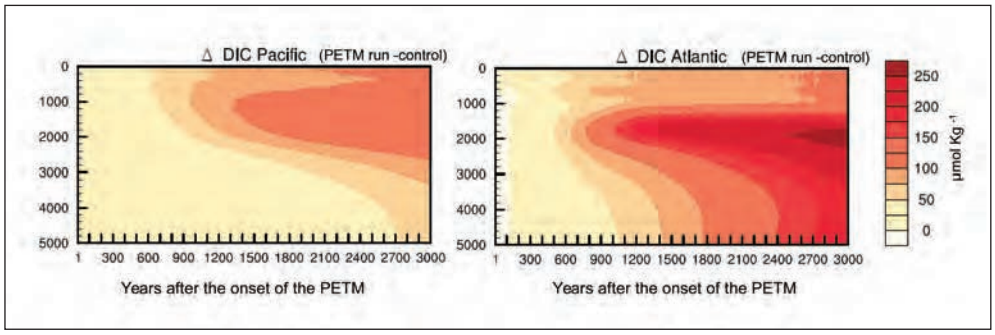


Fig. 2 Temporal evolution of anomaly (PETM run-control) in DIC concentrations, integrated over the whole Pacific (*left*) and Atlantic (*right*) basin.

(releasing $PO_4$, $CO_2$ and consuming $O_2$) to be trapped in intermediate waters (Fig. 2). Thereby carbon accumulates and triggers dissolution of $CaCO_3$ throughout the water column and the sediment. In terms of ocean acidification this long-term effect, occurring over timescales of several 1000 years, seems to be of high relevance also for future climate under rising $CO_2$.

In conclusion, our study highlights the role of changing ocean circulation on the carbon cycle during the PETM. Although we are focusing in our study on this warm period, similar processes could have played a crucial role during glacial cycles, controlling carbon exchange between surface and deep ocean.

## *References*

Heinze, M., and Ilyina, T.: Ocean biogeochemistry in the warm climate of the late Paleocene. Clim. Past. *11*, 63–79 (2015)

Penman, D. E., Hönisch, B., Zeebe, R. E., Thomas, E., and Zachos, J. C.: Rapid and sustained surface ocean acidification during the Paleocene-Eocene Thermal Maximum. Paleoceannography *29*, doi: 10.1002/2014PA002621 (2014)

Thomas, D. J., Bralower, T. J., and Jones, C. E.: Neodymium isotopic reconstruction of late Paleocene-early Eocene thermohaline circulation. Earth Planet. Sci. Lett. *209*, 309–322 (2003)

Tripati, A., and Elderfield, H.: Deep-sea temperature and circulation changes at the PETM. Science *308*, 1894–1898 (2005)

Zeebe, R. E., Zachos, J. C., and Dickens, G. R.: Carbon dioxide forcing alone insufficient to explain PETM warming. Nature Geosci. *2*, 576–580 (2009)

Mathias Heinze
Max Planck Institute for Meteorology
Bundesstraße 53
B207
20146 Hamburg
Germany
Phone: +49 40 41173150
Fax: +49 40 41173298
E-Mail: mathias.heinze@mpimet.mpg.de

Dr. Tatiana Ilyina
Max Planck Institute for Meteorology
Bundesstraße 53
B218
20146 Hamburg
Germany
Phone: +49 40 41173164
Fax: +49 40 41173298
E-Mail: tatiana.ilyina@mpimet.mpg.de

Nova Acta Leopoldina NF *121*, Nr. 408, 305–309 (2015)

# New Carbonate System Proxies: Foram Culturing and Pteropod Potentials

Nina Keul, Gerald Langer, Lennart de Nooijer, Gernot Nehrke, Gert-Jan Reichart, Jelle Bijma, and Ralph Schneider (Kiel)

Global climate change is one of the most pressing challenges our society is facing currently. Climate sensitivity due to atmospheric $CO_2$ doubling will most likely increase global temperatures by 2.0–4.5 °C (*IPCC* 2007). While some direct effects of increasing $CO_2$ are straightforward (e.g. ocean acidification, atmospheric temperature rise), the mid- and long-term impacts of increasing $CO_2$ levels are less easily predicted due to poorly qualified contribution from various potential positive and negative feedbacks in the climate system. Palaeoreconstructions combining temperature reconstructions and atmospheric paleo-$CO_2$ levels are necessary to validate models that aim at predicting future global temperature increases. Reconstructions of atmospheric $CO_2$ from ice-cores are confined to the last 800 ka (Lüthi et al. 2008), while reconstruction of atmospheric $pCO_2$ on longer timescales rely largely on marine sedimentary archives (e.g. Hönisch et al. 2012). Within the latter, foraminifera play a central role, since the chemical and isotopic composition of their shells reflect the physicochemical properties of the seawater that these organisms grew in (Emiliani 1955). Palaeo atmospheric $CO_2$ concentrations can be estimated from past seawater $CO_2$ (aq), which in turn can be reconstructed when two out of six parameters are known of the oceans carbonate system ("C system"; $CO_2$, $HCO_3^-$, $CO_3^{2-}$, pH, DIC [dissolved inorganic carbon] and total alkalinity).

Currently established, foraminifera-based C system proxies include boron isotopes (pH), B/Ca ($CO_3^{2-}$) or the reconstruction of total alkalinity *via* salinity variations (Hemming and Hanson 1992, Hönisch and Hemming 2005, Hönisch et al. 2009, Sanyal et al. 1995, Yu et al. 2010). However, these proxies do not allow the reconstruction of the complete C system by themselves, due to various limitations and uncertainties associated with the different methods used (e.g. Yu and Elderfield 2007). Despite much recent progress in the field of paleoclimatology aiming at overcoming these limitations and uncertainties, accurate and precise reconstructions of past $pCO_2$ levels remains challenging. Here we present the potential of culturing studies with foraminifera and field studies using pteropods to establish new C system proxy relationships.

Culturing living foraminifera is a valuable tool to precisely calibrate new and existing proxies. In some species, asexual reproduction can be triggered in the laboratory, resulting in 50 to 300 one-chambered juveniles that can be placed into experiments under controlled conditions (e.g. various pH's, [DIC]s, TAs). After maintaining them at a range of environmental conditions until they have grown into maturity, the resulting isotope and element composition of their calcium carbonate can be measured and related to these environmental conditions.

Through careful selection of culturing conditions, where values can be tweaked far beyond to what is found in nature to get a good handle on the correlation between the seawater parameters and the proxy, it is thus possible to establish new proxy relationships. With respect to carbonate chemistry it is important to be able to know whether the proxy-carbonate system parameter correlation represents a causal relationship or solely an accidental regularity due to the covariation of the C system parameters. Experiments need therefore be constructed in a way that the individual parameters of the C system are deconvolved and varied independently. The classical C system manipulation approaches are therefore inappropriate as parameters are changing simultaneously (e.g. Smith and Roth 1979). For example, changes in pH and carbonate ion concentration are correlated in classical C system manipulations, so that an observed effect cannot be traced back to an individual parameter and hence prevents separating the sole impact of e.g. pH on carbonate chemical composition.

To overcome this problem, we conducted C system culturing experiments on the benthic foraminifer *Ammonia* sp. (molecular type T6, Hayward et al. 2004) where the classical approach (covariation of parameters, e.g. pH and $[CO_3^{2-}]$) is combined with a manipulation, where pH and $[CO_3^{2-}]$ are varied independently (pH was kept constant, $[CO_3^{2-}]$ was allowed to vary). The experimental setup used allows us hence to independently quantify effects of pH, $[CO_3^{2-}]$ and DIC on foraminiferal calcite chemistry. Due to its shallow water habitat *Ammonia* sp. is not commonly used in palaeo-oceanographic studies, however, its abundance, good accessibility and tolerance of broad ranges of environmental parameters make it a suitable candidate when determining new potential proxy relationships and can thus serve as a model species.

## 1. Sr/Ca as a Proxy for DIC?

Sr/Ca is a widely measured parameter and has been used in a variety of organisms to reconstruct various parameters such as temperature in corals (Smith and Roth 1979). Foraminiferal Sr/Ca has been shown to be influenced by growth rates, temperature, salinity and pH (Kisakürek et al. 2008, Lea et al. 1999). With respect to the latter, it has been demonstrated by several studies that foraminiferal Sr/Ca varies with seawater carbonate chemistry (e.g. Lea et al. 1999, Raitzsch et al. 2011, Russell et al. 2004). However, due to the co-variation of the C system parameters in these studies, it remained inconclusive to isolate the impact of each parameter of the C system to incorporation of Sr in foraminiferal calcite. To solve this problem, we measured shell Sr/Ca using LA-ICP-MS (laser ablation inductively coupled plasma mass spectrometry) on shells from C system manipulations, where the parameters were varied independently (see above, and also Keul et al. 2013 for a full description of the experimental procedures). Linear regression analyses were performed to analyse the correlation between individual C system parameters and foraminiferal Sr/Ca. Since the carbonate system parameters covary differently in the two experimental approaches, it is possible to exclude certain parameters of the C system as (primary) causes for the observed changes in Sr/Ca, namely $pCO_2$, pH, $[HCO_3]$ and $[CO_3^{2-}]$. This leaves TA and DIC as potential parameters that primarily affect Sr incorporation. The importance of TA on Sr/Ca is less likely, since it is an artificially constructed dimension, leaving DIC as the most likely parameter that determines foraminiferal Sr/Ca. The influence of DIC on Sr/Ca can be explained if one assumes that foraminifera need to keep Omega in the calcification environment stable ("Omega

homeostasis"). The high DIC in our experiments (up to 3-times higher than normal oceanic levels) leads to an influx of $pCO_2$ into the foraminiferal cell, since $CO_2$ in its gaseous form can easily diffuse across cell membranes. This $CO_2$ will be transformed into carbonate and bicarbonate ions both in the cell and in the calcification environment, which leads to an increase in Omega. To achieve Omega homeostasis, the foraminifera will need to adjust Ca. This decrease in Ca concentration would thusly cause an increase of the Sr/Ca concentration in the calcifying fluid and consequently also in the foraminiferal shell.

Martin and colleagues (2000) have reported Sr/Ca oscillations in foraminiferal calcite over glacial-interglacial (G-IG) cycles, which seems to be a common phenomenon across species and ocean basins. It was demonstrated, that these oscillations cannot be explained by temperature effects or dissolution, also salinity and pH had to be ruled out since the magnitude of these changes was too small. While the authors have convincingly described how changes in the mean ocean Sr/Ca could be causing the oscillation in foraminiferal Sr/Ca over G-IG cycles, we will explore the potential role of DIC on foraminiferal Sr/Ca. In the above-mentioned C system manipulation experiments we found the following correlation between DIC and Sr/Ca:

$$\mathrm{Sr/Ca} = 1.168\text{e-}04 \times \mathrm{DIC} + 1.083 \ (p < 0.001, R^2 = 0.65, \text{Keul et al., in prep.}). \quad [1]$$

Assuming a G-IG change in DIC of 130 mmol/kg-sw, the resulting change in Sr/Ca would be 1.2 %. While the direction of the change is correct, the magnitude is too small to account for the full oscillation (ca. 4 %). Allen and co-authors (in prep.) have performed a similar calibration study with the planktonic species *G. sacculifer*, where the slope of the calibration was twice as steep. Applying this linear equation would lead to a change in Sr/Ca of 4.2 %, which is in the order of the reported changes over G-IG cycles. The slope of a calibration is usually species-specific, so that it is likely that the absolute change in foraminiferal Sr/Ca as a response to the same environmental change will vary among species, which is shown here by the difference in slope of the *Ammonia* sp. calibration and that of *G. sacculifer*.

## 2. U/Ca as a Proxy for Carbonate Ion Concentration

The U/Ca ratio of benthic and planktonic foraminifera has been shown to correlate with carbonate system parameters ($[CO_3^{2-}]$ and pH; Raitzsch et al. 2011, Russell et al. 2004). In order to quantify the impact of each individual parameter (pH, $[CO_3^{2-}]$) on foraminiferal U/Ca, LA-ICP-MS measurements were carried out on the foraminifera from the above mentioned culture experiments. The correlation of U/Ca and the carbonate system parameters were analysed by means of regression analysis. Since the carbonate system parameters co-vary differently in the two experimental approaches (see Keul et al. 2013 for a detailed description of the experiments), it is possible to exclude certain parameters of the C system as causes for the observed changes in U/Ca. This approach points to $[CO_3^{2-}]$ as the sole parameter primarily affecting U/Ca ratios in *Ammonia* sp. The correlation between U/Ca and $[CO_3^{2-}]$ can be explained in terms of uranium speciation in seawater, as uranium easily complexes with carbonate ions (Markich 2002). Speciation depends strongly on $[CO_3^{2-}]$: free uranium forms complexes with carbonate ions, consequently decreasing the amount of free uranium with increasing $[CO_3^{2-}]$. It has been shown by Markich (2002) that free Uranium forms are taken up by algae cells. Our findings suggest that this might also be the case in *Ammonia*

sp., since similar to the content of free uranium in the seawater, the U/Ca content in the shell clearly decreases with increasing $[CO_3^{2-}]$:

$$\text{Log U/Ca} = 2.42 - 2.65 \times 10^{-3} \times [CO_3^{2-}] \; (R^2 = 0.65,\ p > 0.001;\ \text{Keul et al. 2013}). \quad [2]$$

Fractionation against trace elements in foraminifera is species-specific, causing the U/Ca content to be different among foraminiferal species and underlines the necessity for species-specific calibrations when applying U/Ca to reconstruct past carbonate ion concentrations. Based on the described correlation we can infer that a glacial-interglacial decrease of 100 µmol/kg-sw in carbonate ion concentration would result in a 54 % increase in foraminiferal U/Ca. With the great analytical precision associated to (LA-)ICP-MS, the glacial to interglacial changes can be resolved within 95 % confidence intervals.

## 3. Assessing the Proxy Potential of Pteropods

Another opportunity to establish new C system proxies is to examine the potential of pteropod shells. Pteropods are ideal candidates: they are abundant in all major ocean bodies (Lalli and Gilmer 1989), and their physiology is known to be highly sensitive to climate change (Ocean Acidification and Ocean Warming; Lischka et al. 2011). Pteropods are pelagic molluscs, producing shells made out of aragonite, a metastable form of calcium carbonate, which is more soluble than calcite in seawater. This make pteropods an interesting subject in the development of new proxies: since presence of pteropods in the underlying sediments is governed by the corrosiveness of the water column, pteropods can be used as a "double archive" as they offer the unique chance, to quantify both, the characteristics of the water column at the time of biomineralization (as imprinted in the trace elemental incorporation in the pteropod shell) and the corrosiveness of the water column (through their presence/absence/fragmentation in the sediment). It has been shown that pteropods are an excellent recorder of the aragonite saturation of bottom waters (Mekik 2013). Through a combination of analyses on open-ocean, cultured and down core pteropods we are currently analysing the proxy potential of pteropods with a special regard on carbonate system proxies. Preliminary results will be presented. This includes a trace-elemental-calibration from a culturing study (under changing C system parameters and temperature) and the variability of trace elemental incorporation from a 10-year sediment trap study.

### *References*

Emiliani, C.: Pleistocene temperatures. J. Geol. *63*, 538–578 (1955)

Hayward, B. W., Holzmann, M., Grenfell, H. R., Pawlowski, J., and Triggs, C. M.: Morphological distinction of molecular types in Ammonia – towards a taxonomic revision of the world's most commonly misidentified foraminifera. Marine Micropaleontol. *50*/3, 4, 237–271 (2004)

Hemming, N. G., and Hanson, G. N.: Boron isotopic composition and concentration in modern marine carbonates. Geochim. Cosmochim. Acta *56*/1, 537–543 (1992)

Hönisch, B., Ridgwell, A., Schmidt, D. N., Thomas, E., Gibbs, S. J., Sluijs, A., Zeebe, R., Kump, L., Martindale, R. C., Greene, S. E., Kiessling, W., Ries, J., Zachos, J. C., Royer, D. L., Barker, S., Marchitto, T. M., Moyer, R., Pelejero, C., Ziveri, P., Foster, G. L., and Williams, B.: The geological record of ocean acidification. Science *335*/6072, 1058–1063 (2012)

Hönisch, B., Hemming, N. G., Archer, D., Siddall, M., and McManus, J. F.: Atmospheric carbon dioxide concentration across the mid-Pleistocene transition. Science *324*/5934, 1551–1554 (2009)

Hönisch, B., and Hemming, N. G.: Surface ocean pH response to variations in $pCO_2$ through two full glacial cycles. Earth Planet. Sci. Lett. *236*, 305–314 (2005)

*IPCC* (Intergovernmental Panel on Climate Change): Climate Change 2007: Synthesis Report. Contribution of Working Groups I, II and III to the Fourth Assessment Report of the Intergovernmental Panel on Climate Change. Geneva, Switzerland: IPCC 2007

Keul, N., Langer, G., Nooijer, L. J. de, Nehrke, G., Reichart, G.-J., and Bijma, J.: Incorporation of uranium in benthic foraminiferal calcite reflects seawater carbonate ion concentration. Geochem. Geophys. Geosyst. *14*, 102–111 (2013)

Kisakürek, B., Eisenhauer, A., Böhm, F., Garbe-Schönberg, D., and Erez, J.: Controls on shell Mg/Ca and Sr/Ca in cultured planktonic foraminiferan, Globigerinoides ruber (white). Earth Planet. Sci. Lett. *273*, 260–269 (2008)

Lalli, C. M., and Gilmer, R.W.: Pelagic Snails: The Biology of Holoplanktonic Gastropod Mollusks. Palo Alto, CA, USA: Stanford University Press 1989

Lea, D. W., Mashiotta, T., and Spero, H.: Controls on magnesium and strontium uptake in planktonic foraminifera determined by live culturing. Geochim. Cosmochim. Acta, *63*/16, 2369–2379 (1999)

Lischka, S., Büdenbender, J., Boxhammer, T., and Riebesell, U.: Impact of ocean acidification and elevated temperatures on early juveniles of the polar shelled pteropod Limacina helicina: mortality, shell degradation, and shell growth. Biogeosciences *8*, 919–932 (2011)

Lüthi, D., Le Floch, M., Bereiter, B., Blunier, T., Barnola, J.-M., Siegenthaler, U., Raynaud, D., Jouzel, J., Fischer, H., Kawamura, K., and Stocker, T. F.: High-resolution carbon dioxide concentration record 650,000–800,000 years before present. Nature *453*/7193, 379–382 (2008)

Markich, S.: Uranium Speciation and Bioavailability in Aquatic Systems: An Overview. Scientific World J. *2*, 707–729 (2002)

Martin, P. A., Lea, D. W., Mashiotta, T. A., Papenfuss, T., and Sarnthein, M.: Variation of foraminiferal Sr/Ca over Quaternary glacialinterglacial cycles: Evidence for changes in mean ocean Sr/Ca? Geochem. Geophys. Geosyst. *1*/1, 1004 (2000)

Mekik, F.: Abstract. American Geophysical Union Fall Meeting (2013)

Raitzsch, M., Kuhnert, H., Hathorne, C., Groeneveld, J., and Bicker, T.: U/Ca in benthic foraminifers: A proxy for the deep-sea carbonate saturation. Geochem. Geophys. Geosyst. *12*/6, Q06019 (2011)

Russell, A. D., Hönisch, B., Spero, H. J., and Lea, D. W.: Effect of seawater carbonate ion concentration and temperature on shell U, Mg, and Sr in cultured planktonic foraminifera. Geochim. Cosmochim. Acta *68*/21, 4347–4361 (2004)

Sanyal, A., Hemming, N. G., Hanson, G. N., and Broeker, W. S.: Evidence for a higher ph in the glacial ocean from boron isotopes in foraminifera. Nature *373*/6511, 234–236 (1995)

Smith, A. D., and Roth, A. A.: Effect of carbon dioxide concentration on calculation in the red coralline alga Bossiella orbigniana. Marine Biol. *52*, 217–225 (1979)

Yu, J., and Elderfield, H.: Benthic foraminiferal B/Ca ratios reflect deep water carbonate saturation state. Earth Planet. Sci. Lett. *258*, 73–86 (2007)

Yu, J., Foster, G. L., Elderfield, H., Broecker, W. S., and Clark, E.: An evaluation of benthic foraminiferal B/Ca and delta B-11 for deep ocean carbonate ion and pH reconstructions. Earth Planet. Sci. Lett. *293*, 114–120 (2010)

Dr. Nina Keul
University of Kiel
Institute for Geosciences
Ludewig-Meyn-Straße 10
Room 12
24118 Kiel
Germany
Phone: +49 431 8803253
Fax: +49 431 8801912
E-Mail: nina.keul@gmail.com

Nova Acta Leopoldina NF *121*, Nr. 408, 311–314 (2015)

# Sensitivity of Open-Ocean Convection to Ice Sheet Melting: A Regional Modelling Approach

Annegret Krandick,[1,2] André Paul,[1] Shawn J. Marshall,[3] and Michael Schulz[1]

With 2 Figures

During the last glacial period abrupt climate changes occurred that were accompanied by variations in the flux of ice sheet-derived meltwater to the North Atlantic Ocean. These events, especially during Heinrich stadial 1, presumably affected the formation of North Atlantic Deep Water (NADW) (e.g. Sarnthein et al. 2001) and led to changes in the strength of the Atlantic Meridional Overturning Circulation (AMOC). However, the associated meltwater may have been largely entrained in coastal currents along the continental shelves (see Fig. 1) and not reached the convection sites in the subarctic North Atlantic Ocean (e.g. Stigebrandt 1985, Myers 2005, Condron et al. 2009). Thus, the key hypothesis to be tested is that entrainment of freshwater in a coastal current renders open-ocean convection and the AMOC less sensitive to meltwater input than in traditional "water-hosing" experiments with coarse-resolution, global climate models. To understand the role of meltwater runoff and its effect on the ocean circulation, especially the AMOC, is also very important with regard to the future if the Greenland ice sheet melts (e.g. Hu et al. 2011).

To this end, a regional sea ice-ocean model is being set up with different horizontal resolutions and forced by global climate model output and specially designed meltwater runoff scenarios. The model domain includes the Arctic Ocean, the Bering Strait and the Atlantic Ocean down to about 10°N (see Fig. 2). The numerical ocean model is based on the Massachusetts Institute of Technology general circulation model (MITgcm) with an embedded sea-ice component (Adcroft et al. 2004, Losch et al. 2010).

An advantage of the MITgcm in modelling the Arctic Ocean is the possibility of using the so-called latitude-longitude-cap grid (llc), whereby the Arctic is covered by a cap, by which the convergence of the meridians towards the North Pole can be avoided. The singularities at the cap corners are located on land (see Fig. 2). This grid configuration is also used globally in the ECCO (Estimating the Circulation & Climate of the Ocean) version 4 project (Forget et al., in prep.). A horizontal resolution of 1° on this grid ranges from 111 km at the equator to 20 km in the Arctic. Due to the fact that the mean eddy-deformation radius in the Arctic Ocean ranges from 5–10 km (e.g. Manley and Hunkins 1985, Chelton et al. 1998) it is not possible to resolve the coastal current system with regard to the key hypothesis. Thus, we

1 MARUM – Center for Marine Environmental Sciences, University of Bremen, Germany.
2 Department of Geosciences, Klagenfurter Straße, 28359 Bremen, Germany.
3 Department of Geography, University of Calgary, Canada.

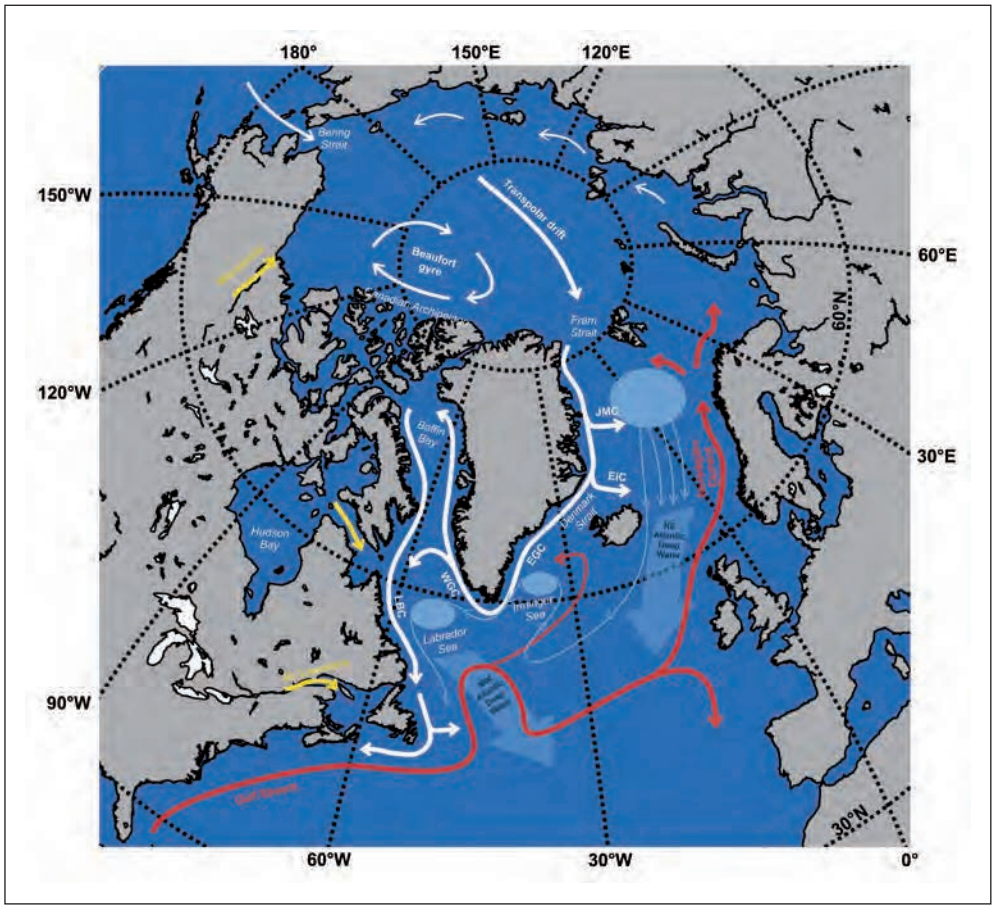


Fig. 1 Map of the current system in the Arctic and possible meltwater pathways (yellow arrows). EIC = East Icelandic Current, JMC = Jan Mayen Current, EGC = East Greenland Current, WGC = West Greenland Current, LBC = Labrador Current (prepared on the basis of Colling 2001, Condron and Winsor 2009).

are also going to set-up a model on a llc-grid with a horizontal resolution of 1/3°. As a long-term objective it is planned to set-up an eddy-resolving model with a horizontal resolution of up to 1/12°.

To investigate the sensitivity of open-ocean convection to ice sheet-melting, meltwater runoff scenarios will be designed from modelling the Northern Hemisphere ice sheets during the last glacial cycle (Marshall and Clarke 1999), likely focusing on Heinrich stadial 1. To trace the freshwater spreading we plan to implement stable water isotopes as passive tracers as well in the MITgcm (see abstract of Rike Völpel) as in the ice sheet model.

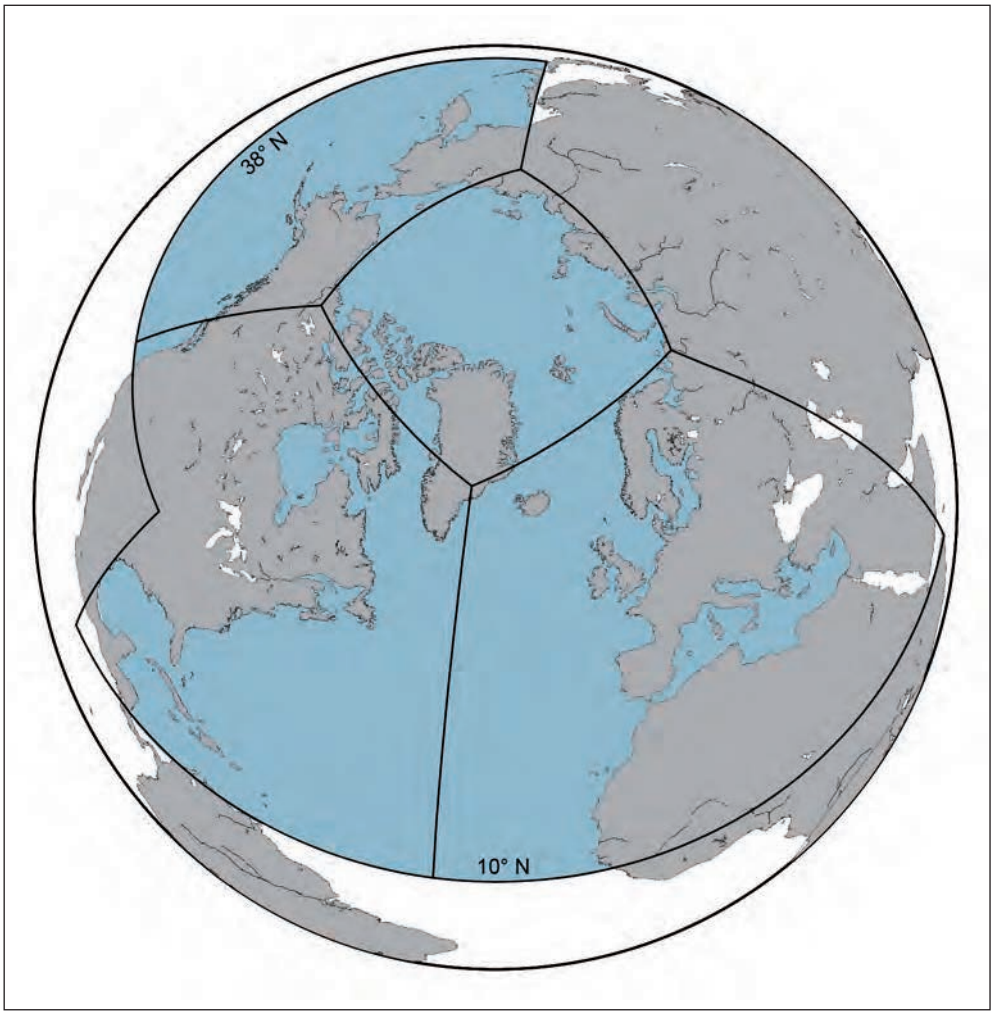


Fig. 2 Map of the regional model area (blue) on the latitude-longitude-cap grid. The Arctic cap of the 1° llc-grid contains 90 × 90 grid points.

## *References*

ADCROFT, A., HILL, C., CAMPIN, J.-M., MARSHALL, J., and HEIMBACH, P.: Overview of the formulation and numerics of the MITgcm. In: Proceedings of the ECMWF Seminar Series on Numerical Methods. Recent Developments in Numerical Methods for Atmosphere and Ocean Modelling. 2004

CHELTON, D. B., DESZOEKE, R. A., SCHLAX, M. G., EL NAGGAR, K., and SIWERTZ, N.: Geographical variability of the first baroclinic Rossby radius of deformation. J. Phys. Oceanogr. *28*/3, 433–460 (1998)

COLLING, A. (Ed.): Ocean Circulation. Oxford: Butterworth-Heinemann 2001

CONDRON, A., WINSOR, P., HILL, C., and MENEMENLIS, D.: Simulated response of the Arctic freshwater budget to extreme NAO wind forcing. J. Climate *22*, 2422–2437 (2009)

Condron, A., and Winsor, P.: Meltwater routing and the younger Dryas. Proc. Natl. Acad. Sci. USA *109*/49, 1–6 (2012)

Forget, G., Heimbach, P., Campin, J.-M., Hill, C., Giering, R., Ponte, R., Fukumori, I., Lee, T., and Wunsch, C.: ECCO version 4: A global ocean modeling and state estimation framework. Geoscientific Model Development (2015, in prep.)

Hu, A., Meehl, G. A., Han, W., and Yin, J.: Effect of the potential melting of the Greenland Ice Sheet on the Meridional Overturning Circulation and global climate in the future. Deep-Sea Res. Part II *58*/17–18, 1914–1926 (2011)

Losch, M., Menemenlis, D., Campin, J-M., Heimbach, P., and Hill, C.: On the formulation of sea-ice models. Part 1: Effects of different solver implementations and parameterizations. Ocean Modelling *33*, 129–144 (2010)

Manley, T. O., and Hunkins, K.: Mesoscale eddies of the Arctic Ocean. J. Geophys. Res. Oceans (1978–2012), *90*/C3, 4911–4930 (1985)

Marshall, S. J., and Clarke, G. K. C.: Modeling North American freshwater runoff through the last glacial cycle. Quat. Res. *52*, 300–315 (1999)

Myers, P. G.: Impact of freshwater from the Canadian Arctic archipelago on Labrador Sea water formation. Geophys. Res. Lett. *32*/6, doi:10.1029/2004GL022082 (2005)

Sarnthein, M., Stattegger, K., Dreger, D., Erlenkeuser, H., Grootes, P., Haupt, B., Jung, S., Kiefer, T., Kuhnt, W., Pflaumann, U., Schäfer-Neth, C., Schulz, H., Schulz, M., Seidov, D., Simstich, J., van Kreveld, S., Vogelsang, E., Völker, A., and Weinelt, M.: Fundamental modes and abrupt changes in North Atlantic circulation and climate over the last 60 ky – Concepts, reconstruction and numerical modeling. In: Schäfer, P., Ritzrau, W., Schlüter, M., and Thiede, J. (Eds.): The Northern North Atlantic: A Changing Environment; pp. 365–410. Berlin, Heidelberg: Springer 2001

Stigebrandt, A.: On the hydrographic and ice conditions in the Northern North Atlantic during different phases of a glaciation cycle. Palaeogeogr. Palaeoclimat. Palaeoecol. *50*, 303–321 (1985)

Annegret Krandick
MARUM – Center for Marine Environmental Sciences
University of Bremen
PO Box 330 440
28334 Bremen
Germany
Phone: +49 421 21865456
Fax: +49 421 21865456
E-Mail: akrandick@marum.de

Nova Acta Leopoldina NF *121*, Nr. 408, 315–319 (2015)

# Deglacial History of the Subarctic North Pacific Oxygen Minimum Zone – Implications for Ocean Dynamics

Hartmut Kuehn,[1,2] Lester Lembke-Jene,[1] Rainer Gersonde,[1,2] Oliver Esper,[1,2] Frank Lamy,[1,2] Helge Arz,[3] Gerhard Kuhn,[1] and Ralf Tiedemann[1]

With 2 Figures

A characteristic of the last glacial termination is the widespread decrease of mid-depth oxygen concentrations in the upper world ocean (Jaccard and Galbraith 2012). The resulting expansion of oxygen minimum zones (OMZs) fostered the deposition of laminated sediments throughout the subarctic North Pacific. Such sediments are found in the Gulf of California (e.g. Zheng et al. 2000), the Santa Barbara Basin (e.g. Behl and Kennett 1996), near the island of Hokkaido (e.g. Ikehara et al. 2006), the Alaska margin (e.g. Davies et al. 2011) and in the Bering Sea (e.g. Cook et al. 2005). Laminations occur when oxygen contents in the water column fall below 0.1 ml/l and therefore can be seen as a direct indicator for extreme changes in ocean ventilation. For the deglacial subarctic North Pacific region it is controversially discussed if these ventilation variations might be coupled to changes in the age of mid-depth water masses, e.g. North Pacific Intermediate Water (NPIW) and/or connected with higher export productivity (e.g. Kennett and Ingram 1995, Mix et al. 1999). However, knowledge of the driving forcing mechanism and the timing for OMZ strengthening is of particular importance, as it has influence on the global carbon budget, e.g. *via* effect of the biological pump. Here, laminated sediments provide the unique opportunity to study ocean dynamics in exceptional detail, possible on decadal timescales.

From a collection of sediment cores retrieved in 2009 during R/V *Sonne* cruise SO202 INOPEX (Innovative NOrth Pacific EXperiment; Gersonde 2012), we selected two partly laminated, mid-depth sediment records (1100 m water depth) from the northern Bering Shelf slope (Fig. 1), to investigate ocean dynamics and OMZ development during termination I (Kuehn et al. 2014). We performed layer countings, AMS $^{14}C$ measurements and a correlation to the NGRIP Greenland $\delta^{18}O$ ice core record. Additional high resolution XRF data with a resolution of up to 200 µm, X-ray images, geochemical data and diatom counts gave information about the processes that led to single lamina formation.

During the correlation to the NGRIP record and the layer countings it became obvious that (*i*) the presence of laminations is tightly coupled to submillennial, short-term warm phases, especially during the Bølling-Allerød (B/A), (*ii*) that the correlation to the NGRIP record is possible on decadal timescales and (*iii*) that the laminations represent annual layered sedi-

1 Alfred Wegener Institute, Helmholtz Centre for Polar and Marine Research, Bremerhaven, Germany.
2 MARUM – Center for Marine Environmental Sciences, University of Bremen, Germany.
3 IOW – Leibniz Institut für Ostseeforschung, Warnemünde, Germany.

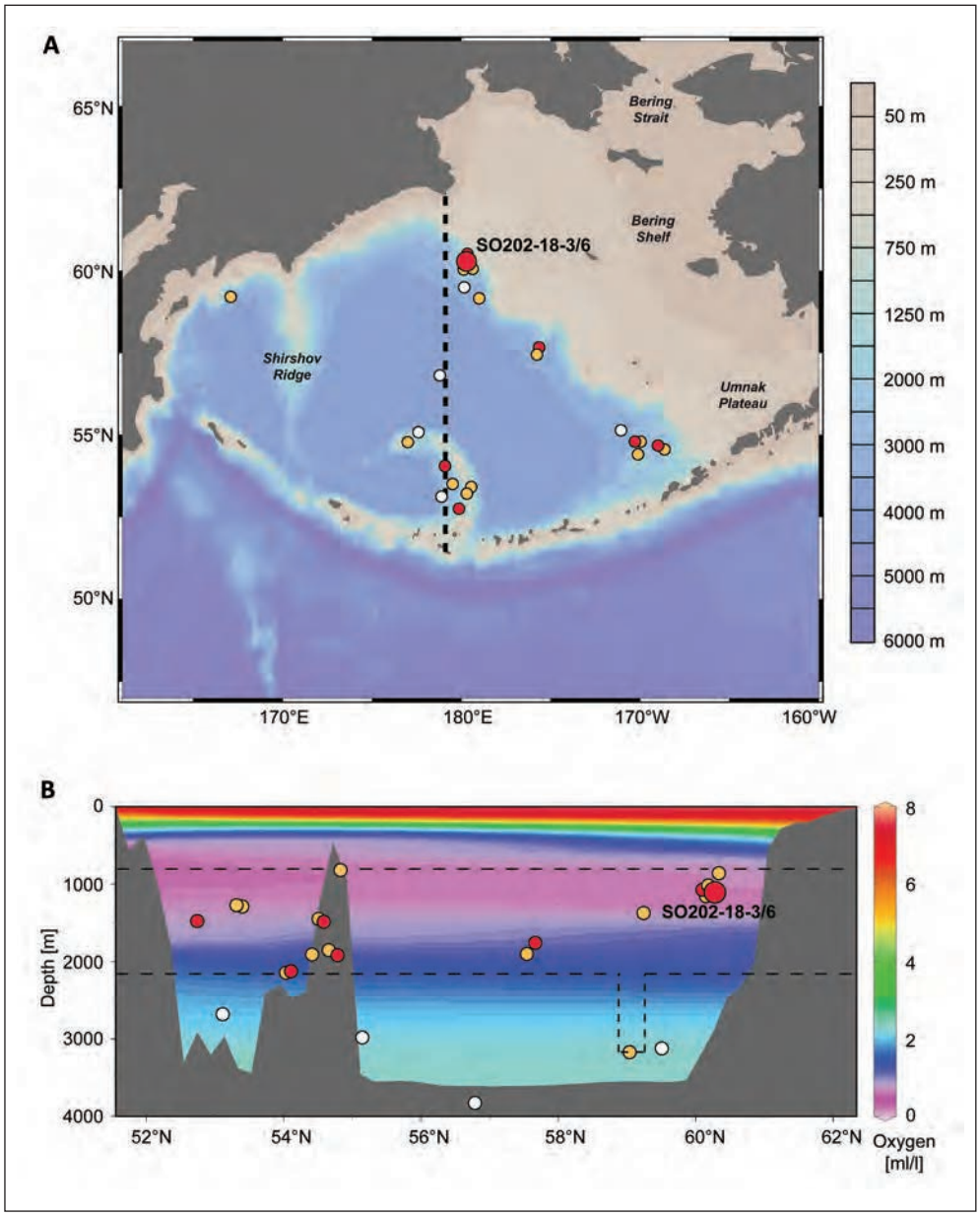


Fig. 1 Position of laminated and non-laminated INOPEX cores with red circles and white circles respectively. The position of studied cores SO202-18-3/6 is marked by a large red circle. Orange circles mark positions of published sediment records, containing laminations during the last deglaciation. (*A*) Bathymetric map of the Bering Sea region. The position of the transect shown in (*B*) is indicated by a vertical dashed line. (*B*) Transect showing the annual mean oxygen concentrations in the Bering Sea. Dashed lines indicate the vertical expansion of the oxygen minimum zone during the last deglaciation, based on the occurrence of laminated sediment cores. Pictures modified from KUEHN et al. 2014.

ments (varves). The point (*ii*) strongly argues for a atmospheric teleconnection between the North Atlantic and the North Pacific, and our observed changes in the mid-depth ocean ventilation occur faster than previously published results. In those studies variations of the OMZ were observed only on millennial timescales (e.g. Kennett and Ingram 1995). This means that the Bering Sea and its OMZ is a highly sensitive system reacting almost instantaneously to small temperature changes and therefore has the potential to influence the global carbon budget on short timescales. Another important outcome of our correlation approach was an absolute age model, in large parts independent from radiocarbon ages. This makes our core one of the few marine sediment records where it is possible to directly calculate planktic reservoir ages. Reservoir ages at our core location vary between 730–1100 years during the B/A to Preboreal and confirm studies that argue for varying reservoir ages during the last deglaciation (e.g. Sarnthein et al. 2007).

To further investigate the mechanisms for lamina formation, we calculated benthic-planktic ventilation age differences. These show only smaller variations between 470–700 $^{14}C$ years (Fig. 2) and, therefore, do not support the influence of old and oxygen poor water masses. However, higher Si/Ti ratios from XRF measurements and high biogenic opal mass accumulation rates during times of lamina formation point to increased seasonal export production (Fig. 2). By combining this evidence with detailed sedimentological analysis we suggest two processes that contribute to the OMZ strengthening in the Bering Sea. Firstly, our constant ventilation ages argue for millennial-scale changes in oxygen concentration of mid-depth

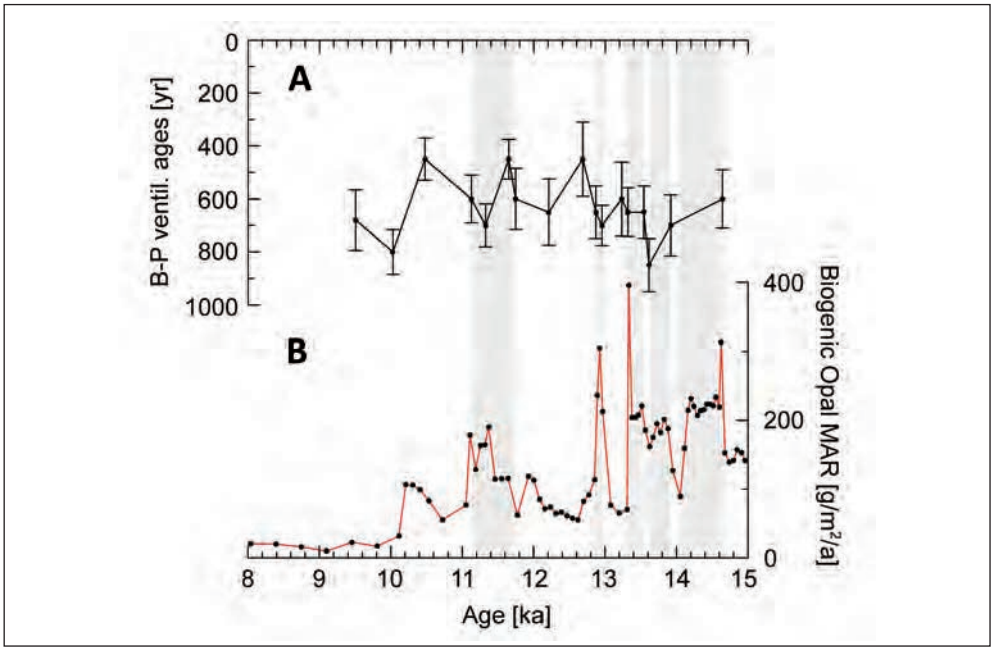


Fig. 2 (*A*) Benthic-planktic (B-P) ventilation ages and (*B*) biogenic opal mass accumulation rate (MAR) of cores SO202-18-3/6 from the northern Bering Slope. Vertical bars in (*A*) show errors from radiocarbon datings and the gray boxes mark the occurrence of prominent laminated sections, identified in our sediment cores. (Pictures modified from Kuehn et al. 2014.)

water masses without changes in their formation rate, and secondly we see higher regional export production.

During the last deglaciation the Bering Sea-OMZ also showed an increased vertical expansion. Based on a collection of published marine sediment records containing laminations we see a deepening of the OMZ to 2100 m water depth in most parts of the Bering Sea and at one location to more than 3100 m (Fig. 1). This is much deeper than today's core of the OMZ, which lies between 900–100 m water depth and has also implications for the carbon storage capacity of the Bering Sea during those times.

Looking at single laminae high resolution XRF data and diatom counts showed that the laminations represent an alternation of pure diatom ooze and rather terrigenous sedimentation. Compared to the terrigenous laminae, the diatomaceous laminae have high Si/Ti ratios in the XRF data, a lower density and diatom counts showed high amounts of well preserved sea-ice- and cold-water-related species like *Fragilariopsis oceanica*, *F. cylindrus* and *Bacterosira bathyomphala*. We therefore interpret the biogenic laminae as a diatom-dominated productivity event related to the spring/summer sea-ice break-up and the terrigenous laminae as the background sedimentation during autumn/winter.

## *References*


Behl, R. J., and Kennett, J. P.: Brief interstadial events in the Santa Barbara basin, NE Pacific, during the past 60 kyr. Nature *379*, 243–246 (1996)

Cook, M. S., Keigwin, L. D., and Sancetta, C. A.: The deglacial history of surface and intermediate water of the Bering Sea. Deep-Sea Res. Part II: Topical Studies in Oceanography *52*, 2163–2173; doi:10.1016/j.dsr2.2005.07.004 (2005)

Davies, M. H., Mix, A. C., Stoner, J. S., Addison, J. A., Jaeger, J., Finney, B., and Wiest, J.: The deglacial transition on the southeastern Alaska Margin: Meltwater input, sea level rise, marine productivity, and sedimentary anoxia. Paleoceanography *26*, PA2223; doi:10.1029/2010PA002051 (2011)

Gersonde, R.: The expedition of the research vessel "Sonne" to the Subpolar North Pacific and the Bering Sea in 2009 (SO202-INOPEX). Reports on Polar and Marine Research. 323 pp. Bremerhaven: Alfred Wegener Institute 2012

Ikehara, K., Ohkushi, K., Shibahara, A., and Hoshiba, M.: Change of bottom water conditions at intermediate depths of the Oyashio region, NW Pacific over the past 20,000 yrs. Global and Planetary Change *53*, 78–91; doi:10.1016/j.gloplacha.2006.01.011 (2006)

Jaccard, S. L., and Galbraith, E. D.: Large climate-driven changes of oceanic oxygen concentrations during the last deglaciation. Nature Geosci. *5*, 151–156; doi:10.1038/ngeo1352 (2012)

Kennett, J., and Ingram, B.: A 20,000 year record of ocean circulation and climate change from the Santa Barbara Basin. Nature *377*, 510–514 (1995)

Kuehn, H., Lembke-Jene, L., Gersonde, R., Esper, O., Lamy, F., Arz, H., Kuhn, G., and Tiedemann, R.: Laminated sediments in the Bering Sea reveal atmospheric teleconnections to Greenland climate on millennial to decadal timescales during the last deglaciation. Clim. Past *10*, 2215–2236; doi:10.5194/cp-10-2215-2014 (2014)

Mix, A., Lund, D., Pisias, N., Boden, P., Bornmalm, L., Lyle, M., and Pike, J.: Rapid climate oscillations in the northeast Pacific during the last deglaciation reflect Northern and Southern Hemisphere sources. In: Clark, P. U., Webb, R. S., and Keigwin, L. D. (Eds.): Mechanisms of Global Climate Change at Millennial Time Scales. Geophys. Monograph Series; pp. 127–148. Washington, D.C.: American Geophysical Union 1999

Sarnthein, M., Grootes, P. M., Kennett, J. P., and Nadeau, M.: $^{14}C$ reservoir ages show deglacial changes in ocean currents and carbon cycle. In: Schmittner, A., Chiang, J., and Hemming, S. (Eds.): Ocean Circulation: Mechanisms and Impacts. 1st ed. Geophys. Monograph Series 173; pp. 175–196. Washington, USA: American Geophysical Union 2007

Zheng, Y., Van Geen, A., Anderson, R. F., Gardner, J. V., and Dean, W. E.: Intensification of the northeast Pacific oxygen minimum zone during the Bølling-Allerød warm period. Paleoceanography *15*, 528–536 (2000)

Hartmut Kuehn
Alfred Wegener Institute
Helmholtz Centre for Polar and Marine Research
Am Alten Hafen 26
Building D-1190
27568 Bremerhaven
Germany
Phone: +49 471 48312043
Fax: +49 471 48311149
E-Mail: hartmut.kuehn@awi.de

Nova Acta Leopoldina NF *121*, Nr. 408, 321–325 (2015)

# Maximum Drawdown of Atmospheric $CO_2$ due to Biological Uptake in the Ocean

Malin Ödalen,[1] Jonas Nycander,[1] Kevin Oliver,[2] Johan Nilsson,[1] and Laurent Brodeau[1]

With 3 Figures

During each of the last four glacial cycles, there has been a lowering of atmospheric $CO_2$ of about 1/3 (~90 ppm) and, considering the relative sizes of the carbon reservoir in the ocean compared to those of the atmosphere and the terrestrial biosphere, it is likely that ocean processes caused most of this $CO_2$ drawdown. It has, however, proved to be difficult to put constraints on the relative effects of different processes contributing to this oceanic uptake (Kohfeld and Ridgwell 2009, and references therein). In this work, we attempt to constrain the maximum $CO_2$ drawdown that can be achieved by biological uptake in the ocean, by examining the consequences of 100 % nutrient utilization efficiency of biology using an Earth System Model of Intermediate Complexity (EMIC) called cGENIE (Ridgwell et al. 2007, Cao et al. 2009). Similar computations of the abiotic $CO_2$ equilibrium have previously been made for a variety of box models and GCMs by Archer et al. (2000).

By using an EMIC of this type, which is not very computationally demanding, we are able to do an ensemble of long simulations where we allow the model to reach steady state for the carbon system. This would not be feasible if we were using a GCM. Still, the model keeps a higher system complexity than box models. The cGENIE model is the carbon system centric version of the physical framework of the GENIE-1 model described in Ridgwell et al. (2007). The physical framework is comprised of a reduced physics (frictional geostrophic) 3-D ocean circulation model, which is coupled to a 2-D energy-moisture balance model (EMBM) of the atmosphere and a dynamic-thermodynamic sea-ice model. The spatial resolution in the ocean is a 36-by-36 equal-area grid in the horizontal and 16 levels in the vertical. In this case, we start our simulations from a preindustrial *spin-up* of the carbon system as described in Cao et al. (2009).

When biology is as efficient as it can be, hence using all available nutrients to produce new organic material, a maximum amount of carbon will be "trapped" in the biological cycle as soft organic material. This soft tissue carbon can be considered to no longer be a part of the chemical equilibrium between the atmosphere and the surface ocean. As a result, the atmospheric $pCO_2$, which is determined by this chemical equilibrium, will stabilize at a lower level than it does when biology is less efficient. Our work aims to determine this new equilibrium in the model.

1 Department of Meteorology Stockholm University, 10691 Stockholm, Sweden.
2 Ocean and Earth Science, National Oceanography Centre Southampton, University of Southampton Waterfront Campus, European Way, Southampton SO14 3ZH, United Kingdom.

Our calculations of the efficiency of the biological (soft tissue) pump are based on the framework presented in Ito and Follows (2005), using the tracer $P^*$ as an indicator for the nutrient utilization efficiency. $P^*$ is defined as the quota between regenerated phosphate, $P^{reg}$, originating from decomposition of organic material, and total phosphate, $P^{tot}$. Since phosphate is the main limiting nutrient in the global ocean, it is used as a proxy for nutrient availability in general. $P^{reg}$ is calculated from the Apparent Oxygen Utilization (AOU), which is approximately the difference between the observed oxygen concentration, $O_2^{obs}$, and the saturation concentration for oxygen, $O_2^{sat}$, at the observed salinity and potential temperature, by using the adjusted Redfield ratio between P and $O_2$, $R_{P:O2}$, of 1/–170 (Anderson and Sarmiento 1994). The concentration of soft tissue carbon, $C^{soft}$, can be calculated in a similar manner from $P^{reg}$ and the Redfield ratio of C and P, $R_{C:P}$, which is 117/1 (Anderson and Sarmiento 1994). The separation between the biological cycle and the chemical equilibrium when $P^* = 1$, and the calculation framework for the biological cycle are shown in the schematic in Figure 1.

The state we aim to reach in the model is when $P^* = 1$, thus when all nutrients in the surface ocean are instantly utilized by biology and no nutrients are brought into the deep ocean without being trapped in biological tissue. As an example, shown in Figure 2*A* is $P^*$ for a longitudinal cross-section through the Atlantic as calculated using data from World Ocean

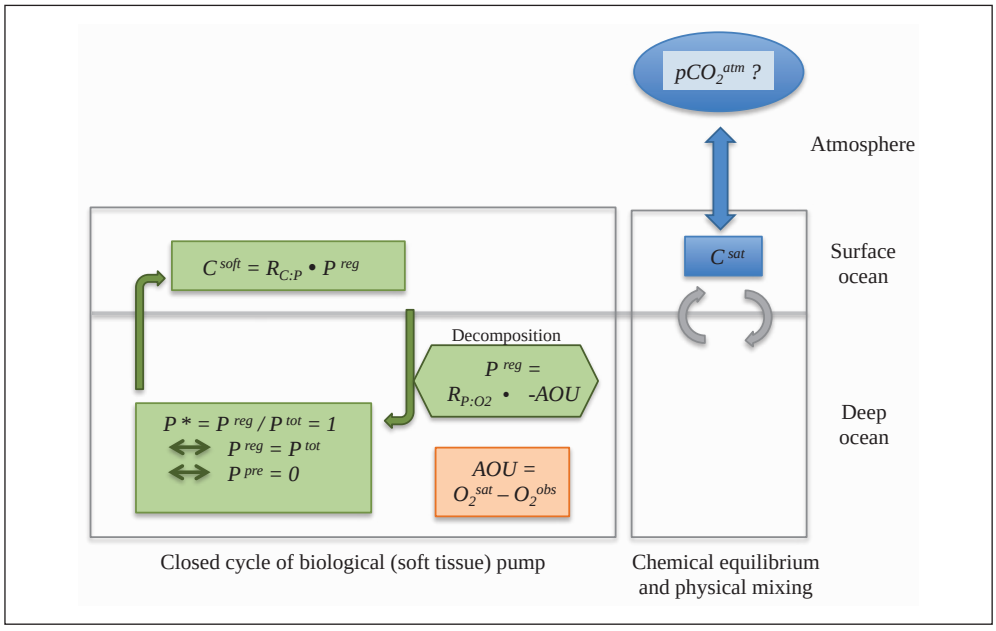


Fig. 1 Schematic describing the state where biology achieves 100 % nutrient uptake efficiency, which we aim to simulate in the cGENIE model to find the upper limit for $CO_2$ drawdown due to increased efficiency of biology. In this state, the biological (soft tissue) pump is detached from the (abiotic) chemical equilibrium. Here, $C^{soft}$ is the concentration of soft tissue carbon, $P^{reg}$ is regenerated phosphate, $P^{tot}$ is total phosphate, $O_2^{obs}$ is observed oxygen concentration, $O_2^{sat}$ is saturation concentration for oxygen at the observed salinity and potential temperature, AOU is Apparent Oxygen Utilization, $R_{P:O2} = 1/-170$ is the adjusted Redfield ratio between P and $O_2$, and $R_{C:P} = 117/1$ is the adjusted Redfield ratio of C and P (Anderson and Sarmiento 1994).

Atlas 2013 (Garcia et al. 2014a, b, Locarnini et al. 2013, Zweng et al. 2013). Typical values in the deep ocean are between 0.3 and 0.4. Hence, in the deep Atlantic, the soft tissue pump is only working at 30–40 % of its maximum theoretical capacity. This agrees well with the global calculation by Ito and Follows (2005) of 36 % efficiency for the modern ocean. Figure 2*B* shows similar numbers for $P^*$ in the Atlantic for the preindustrial *spin-up* made with the Cao et al. (2009) configuration of cGENIE.

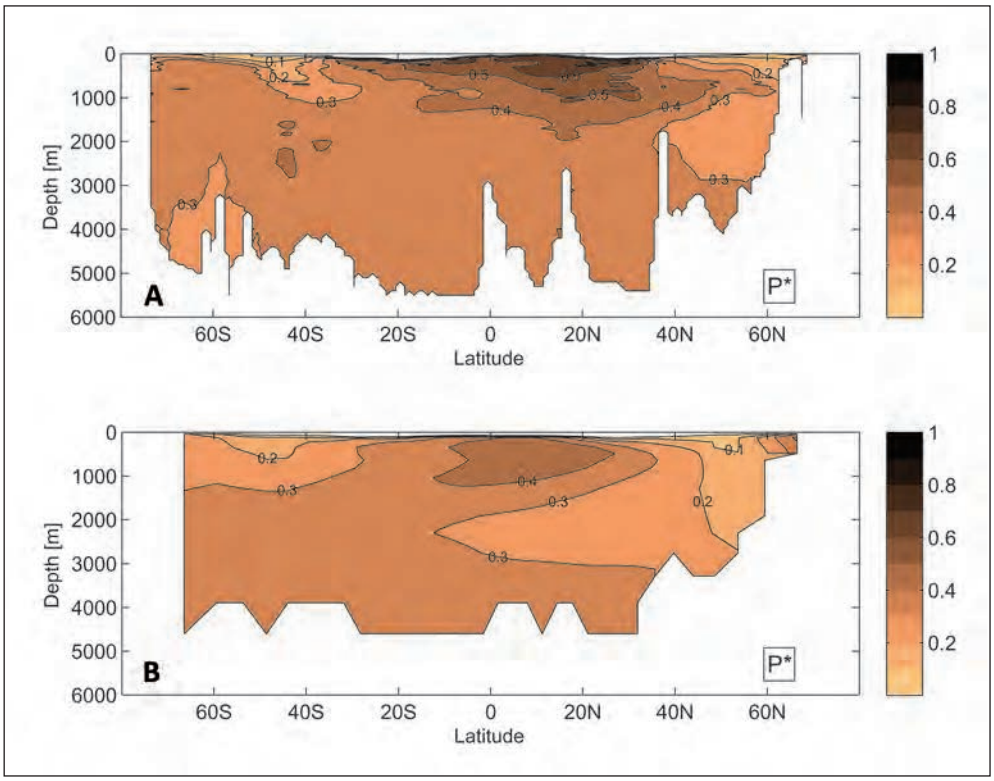


Fig. 2 Nutrient utilization, $P^*$, calculated from apparent oxygen utilization (AOU) and total phosphate using data for a longitudinal transect along 25°W through the Atlantic Ocean from (*A*) World Ocean Atlas 2013 (Garcia et al. 2014a, b, Locarnini et al. 2013, Zweng et al. 2013), (*B*) the preindustrial spin-up of cGENIE (Cao et al. 2009).

When $P^* = 1$, there are no preformed nutrients (phosphate), $P^{pre}$, in the deep ocean. Shown in Figure 3*A*, preformed phosphate in the deep Atlantic Ocean is currently about 0.8 µM in the northern parts and is higher than 1.6 µM when entering the Southern Ocean (calculated using data from World Ocean Atlas 2013: Garcia et al. 2014a, b, Locarnini et al. 2013, Zweng et al. 2013). Thus, vast amounts of unutilized nutrients are currently being subducted into the deep ocean. Therefore, increasing the efficiency of the biological soft tissue pump does have the potential to significantly affect the ocean-atmosphere $CO_2$ equilibrium. When comparing the model data (examples shown in Fig. 2*B* and 3*B*) to the climatological data, we see similar patterns of $P^*$ and $P^{pre}$. For a model of such low resolution, the representation of the nutrient

utilization is reasonably good and should be sufficient for our purposes. To achieve $P^* = 1$ in the model we will use restoring of surface nutrients (to 0) and remove a corresponding amount of dissolved inorganic carbon from the surface ocean. Interactive sediments and remineralization will be switched off.

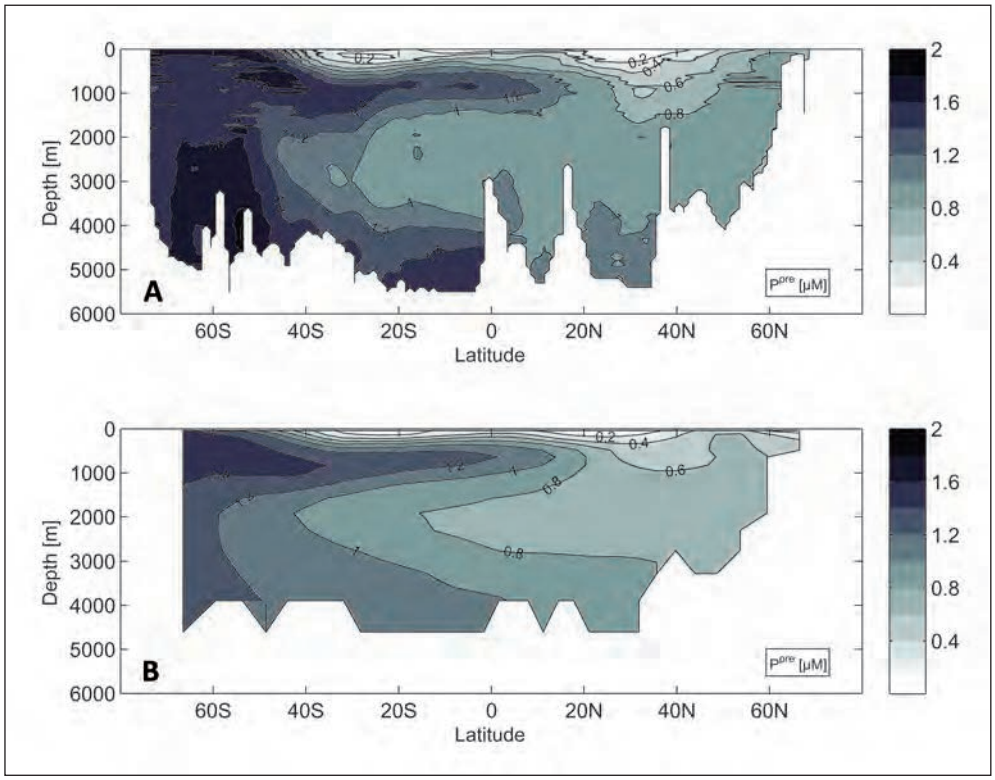


Fig. 3 Preformed phosphate, $P^{pre}$, calculated from apparent oxygen utilization (AOU) and total phosphate using data for a longitudinal transect along 25°W through the Atlantic Ocean from (*A*) World Ocean Atlas 2013 (Garcia et al. 2014a, b, Locarnini et al. 2013, Zweng et al. 2013), (*B*) the preindustrial spin-up of cGENIE (Cao et al. 2009).

It should be pointed out that the theoretical maximum limit where $P^* = 1$ is indeed a theoretical limit and an extreme upper bound for the capacity of $CO_2$ drawdown through increased efficiency of the biological pump. According to the theory presented by Ito and Follows (2005), the potential is ~30 ppmv of $pCO_2$ for an increase of 0.1 in $P^*$. It is yet too early to predict how big the potential effect in cGENIE is. In reality, deep water formation dynamics will prevent $P^*$ from exceeding values of ~0.55 (Ito and Follows 2005). Another important factor influencing the abiotic equilibrium and atmospheric $pCO_2$ is the temperature effect, where the distribution of SST influences the global mean ocean temperature (Goodwin et al. 2011) and hence the solubility of $CO_2$ in seawater. This effect will also be investigated in the model.

## *References*


Anderson, L. A., and Sarmiento, J. L.: Redfield ratios of remineralization determined by nutrient data analysis. Global Biogeochem. Cycles *8*/1, 65–80 (1994)

Archer, D. E., Eshel, G., Winguth, A., Broecker, W., Pierrehumbert, R., Tobis, M., and Jacob, R.: Atmospheric $pCO_2$ sensitivity to the biological pump in the ocean. Global Biogeochem. Cycles *14*/4, 1219–1230 (2000)

Cao, L., Eby, M., Ridgwell, A., Caldeira, K., Archer, D., Ishida, A., Joos, F., Matsumoto, K., Mikolajewicz, U., Mouchet, A., Orr, J. C., Plattner, G.-K., Schlitzer, R., Tokos, K., Totterdell, I., Tschumi, T., Yamanaka, Y., and Yool, A.: The role of ocean transport in the uptake of anthropogenic $CO_2$. Biogeosciences *6*/3, 375–390 (2009)

Garcia, H. E., Locarnini, R. A., Boyer, T. P., Antonov, J. I., Baranova, O. K., Zweng, M. M., Reagan, J. R., and Johnson, D. R.: World Ocean Atlas 2013. Vol. *3*. Dissolved Oxygen, Apparent Oxygen Utilization, and Oxygen Saturation. In: Levitus, S. (Ed.), and Mishonov, A. (Technical Ed.): NOAA Atlas NESDIS *75*, 27 pp. (2014a)

Garcia, H. E., Locarnini, R. A., Boyer, T. P., Antonov, J. I., Baranova, O. K., Zweng, M. M., Reagan, J. R., and Johnson, D. R.: World Ocean Atlas 2013. Vol. *4*. Dissolved Inorganic Nutrients (Phosphate, Nitrate, Silicate). In: Levitus, S. (Ed.), and Mishonov, A. (Technical Ed.): NOAA Atlas NESDIS *76*, 25 pp. (2014b)

Goodwin, P., Oliver, K. I. C., and Lenton, T. M.: Observational constraints on the causes of Holocene $CO_2$ change. Global Biogeochem. Cycles *25*, GB3011; doi:10.1029/2010GB003888 (2011)

Ito, T., and Follows, M. J.: Preformed phosphate, soft tissue pump and atmospheric $CO_2$. J. Marine Res. *63*/4, 813–839 (2005)

Kohfeld, K. E., and Ridgwell, A.: Glacial-interglacial variability in atmospheric $CO_2$. In: Quéré, C. L., and Saltzman, E. S. (Eds.): Surface Ocean-Lower Atmosphere Processes; pp. 251–286; doi:10.1029/2008GM000845. Washington, D. C.: American Geophysical Union 2009

Locarnini, R. A., Mishonov, A. V., Antonov, J. I., Boyer, T. P., Garcia, H. E., Baranova, O. K., Zweng, M. M., Paver, C. R., Reagan, J. R., Johnson, D. R., Hamilton, M., and Seidov, D.: World Ocean Atlas 2013. Vol. *1*. Temperature. In: Levitus, S. (Ed.), and Mishonov, A. (Technical Ed.): NOAA Atlas NESDIS *73*, 40 pp. (2013)

Ridgwell, A., Hargreaves, J. C., Edwards, N. R., Annan, J. D., Lenton, T. M., Marsh, R., Yool, A., and Watson, A.: Marine geochemical data assimilation in an efficient Earth System Model of global biogeochemical cycling. Biogeosciences *4*/1, 87–104 (2007)

Zweng, M. M, Reagan, J. R., Antonov, J. I., Locarnini, R. A., Mishonov, A. V., Boyer, T. P., Garcia, H. E., Baranova, O. K., Johnson, D. R., Seidov, D., and Biddle, M. M.: World Ocean Atlas 2013. Vol. *2*. Salinity. In: Levitus, S. (Ed.), and Mishonov, A. (Technical Ed.): NOAA Atlas NESDIS *74*, 39 pp. (2013)



Malin Ödalen
Department of Meteorology
Stockholm University
106 91 Stockholm
Sweden
Phone: +46 8 162416
Fax: +46 8 157185
E-Mail: malin.odalen@misu.su.se

Nova Acta Leopoldina NF *121*, Nr. 408, 327–329 (2015)

# New Data of DIC Radiocarbon in the Eastern Equatorial Indian Ocean

Na Qian,[1] Liping Zhou,[2] and Pan Gao[3]

With 2 Figures

Radiocarbon ($^{14}C$) in ocean has long been used as a tracer to study the processes of air-sea $CO_2$ exchange, mixing and ocean circulation at different timescales (e.g. Dutta and Bhushan 2012). The early measurements of $^{14}C$ in dissolved inorganic carbon ($DI^{14}C$) in the northeastern Indian Ocean were carried out during the GEOSECS expeditions of 1978 (Stuiver and Östlund 1983) and WOCE expedition of 1995 (Key et al. 2004). More recently, Bhushan et al. (2000, 2003, 2008), and Dutta et al. (2010, 2012) reported $DI^{14}C$ measurements at several other locations in the northern Indian Ocean. These studies provided valuable information about the distribution and temporal changes of $DI^{14}C$ in Indian Ocean, and some of them revealed high bomb radiocarbon inventories in equatorial Indian Ocean that is partly attributed to the influence of different water masses exchange between different ocean basins, such as Indonesian Throughflow (ITF) from Pacific and mode water from the southern gyre of the Indian Ocean.

Given the potential of radiocarbon in addressing a range of scientific questions related to the global carbon cycle change and ocean circulation process, we have started a project which involves collection of seawater for measurements of $DI^{14}C$ from the Eastern Equatorial Indian Ocean. Here we report our initial $DI^{14}C$ data of some seawater samples collected onboard R/V SHIYAN 1 in 2014 (Fig. 1). The headspace-extraction method developed by Gao et al. (2014) was used for sample preparation and AMS $^{14}C$ measurements were made in the Institute of Heavy Ion Physics, Peking University. Our main observations are as follows:

– The $\Delta^{14}C$ values of measured stations range from –205.3 to 72.1 ‰, and the depth profiles show an overall similar pattern. The surface $DI^{14}C$ varies from 22.7–72.1 ‰. On the sub-surface depth (25–100 m), it reaches a maximum value of 28.3–69.2 ‰ (except for Station I512), and then gradually decreases to about 190.5±10.0 ‰ (n = 5) at 2000 m. Below 2000 m, the $DI^{14}C$ values remain almost constant around 221.0 ± 4.9 ‰ (n = 9). The $\Delta^{14}C$ records from different stations are quite complex in the upper 200 m water column.
– In the reoccupation station I401 (GEOSECS 448, WOCE 302) and I316 (GEOSECS 449, WOCE 316) (Fig. 2), the surface $\Delta^{14}C$ values decrease to a level of 25.5 ± 4.0 ‰ (n = 2), while the bomb radiocarbon penetration depths increase significantly, showing the tem-

1 Department of Geography, Peking University, Beijing, 100871, China, E-Mail: qianna@pku.edu.cn.
2 Institute of Ocean Research, Peking University, Beijing, 100871, China, E-Mail: lpzhou@pku.edu.cn.
3 Department of Geography, Peking University, Beijing, 100871, China, E-Mail: pangao@pku.edu.cn.

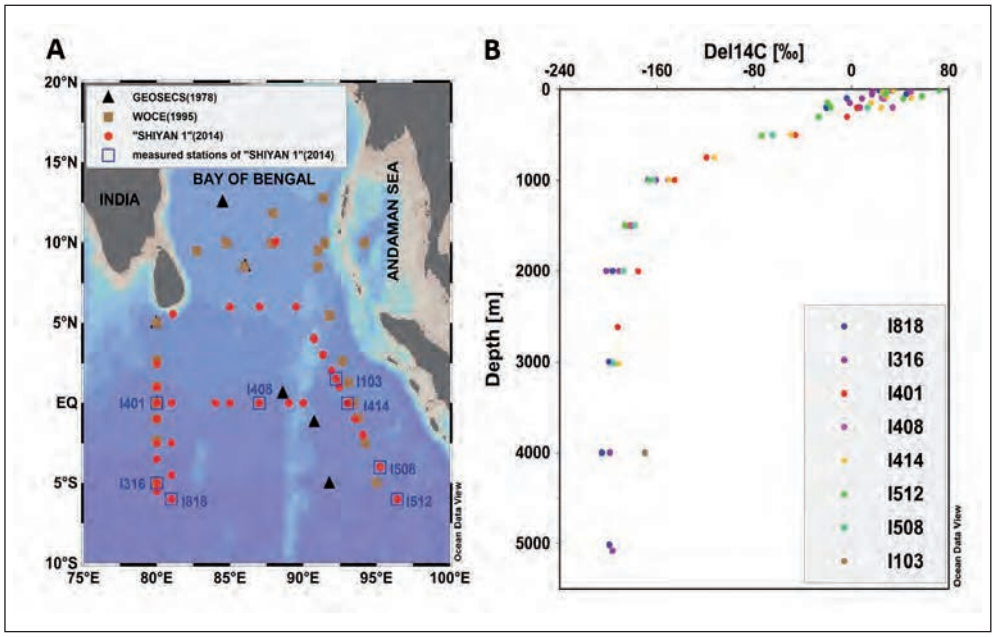


Fig. 1 (*A*) Distribution of DI$^{14}$C sampling stations in northeastern Indian Ocean from GEOSECS, WOCE and our R/V SHIYAN 1 expedition. (*B*) Depth profile of $\Delta^{14}$C values obtained in this study.

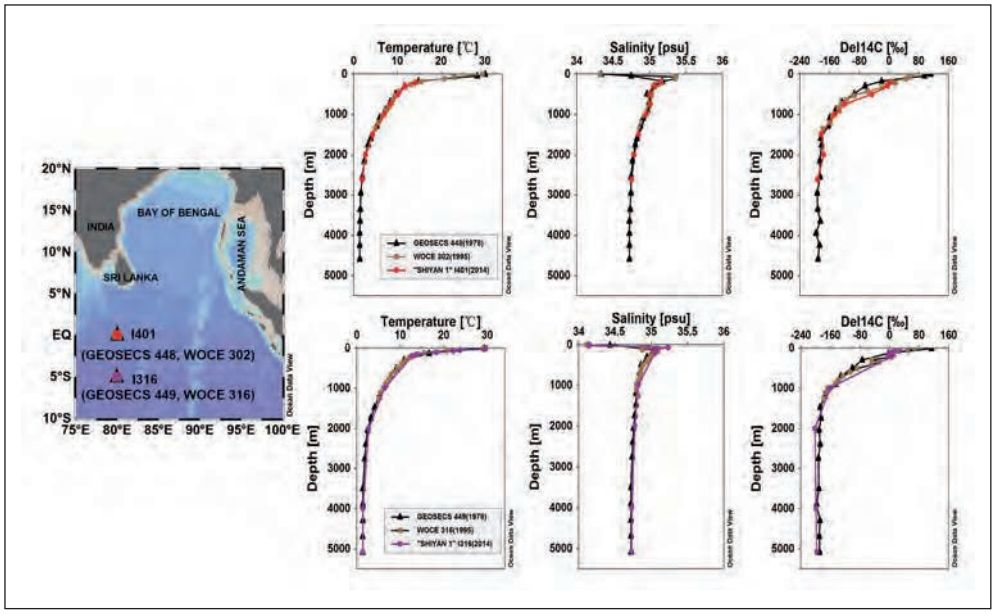


Fig. 2 Depth profiles of temperature, salinity, and DI$^{14}$C at the reoccupation station I401 and I316. Filled black triangles and grey squares are the data from GEOSECS and WOCE expeditions, respectively. Filled red dots are the results obtained in this study.

poral variation of bomb-$^{14}C$ penetration through downward transfer mixing with deeper waters between 1978 to 2014.

– The maximum $\Delta^{14}C$ value and corresponding depth varies a lot among stations, e.g. the surface $\Delta^{14}C$ value of station I512 (72.1 ‰) is much higher than other stations (22.7–34.5 ‰), which may indicate the lateral advection of $^{14}C$-enriched waters from the Pacific Ocean through the Indonesian Throughflow (ITF).

## *References*


Bhushan, R., Dutta, K., Mulsow, S., Povinec, P. P., and Somayajulu, B. L. K.: Distribution of natural and man-made radionuclides during the reoccupation of GEOSECS stations 413 and 416 in the Arabian Sea: temporal changes. Deep-Sea Res. II *50*, 2777–2784 (2003)

Bhushan, R., Dutta, K., and Somayajulu, B. L. K.: Estimate of upwelling rates in the Arabian Sea and the equatorial Indian Ocean based on bomb radiocarbon. J. Environm. Radioactivity *99*, 1566–1571 (2008)

Bhushan, R., Somayajulu, B. L. K., Charkraborty, S., and Krishnaswami, S.: Radiocarbon in the Arabian Sea water column: Temporal variations in bomb $^{14}C$ inventory since the GEOSECS and $CO_2$ air-sea exchange rates. J. Geophys. Res. *105*, 14273–14282 (2000)

Dutta, K., and Bhushan, R.: Radiocarbon in the Northern Indian Ocean two decades after GEOSECS. Global Biogeochem. Cycles *26*, GB2018 (2012)

Dutta, K., Ravi Prasad, G. V. R., Ray, D. K., and Raghav, S.: Decadal changes of radiocarbon in the surface Bay of Bengal: three decades after GEOSECS and one decade after WOCE. Radiocarbon *52*, 1191–1196 (2010)

Gao, P., Xu, X., Zhou, L. P., Pack, M. A., Griffin, S., Santos, G. M., Southon, J. R., and Liu, K.: Rapid sample preparation of dissolved inorganic carbon in natural waters using a headspace-extraction approach for radiocarbon analysis by accelerator mass spectrometry. Limnol. Oceanogr. Methods *12*, 172–188 (2014)

Key, R. M., Kozyr, A., Sabine, C. L., Lee, K., Wanninkhof, R., Bullister, J. L., Feely, R. A., Millero, F. J., Mordy, C., and Peng, T.-H.: A global ocean carbon climatology: Results from Global Data Analysis Project (GLODAP). Global Biogeochem. Cycles *18*, GB4031 (2004)

Stuiver, M., and Östlund, H. G.: GEOSECS Indian Ocean and mediterranean radiocarbon. Radiocarbon *25*, 1–29 (1983)



Na Qian, Ph.D. candidate
Department of Geography, Yifu second building, Room 3501
Peking University, No 5, Yiheyuan Road, Haidian District
Beijing, 100871
China
Phone: +86 18618475538
Fax: +86 0106275117
E-Mail: qianna@pku.edu.cn

Nova Acta Leopoldina NF *121*, Nr. 408, 331–335 (2015)

# Northern Source for Deglacial and Holocene Deep Water Composition Changes in the Eastern North Atlantic Basin

Janne Repschläger,[1] Mara Weinelt,[2] Nils Andersen,[3]
Dieter Garbe-Schönberg,[1] and Ralph Schneider[1] (Kiel)

With 2 Figures

Over the last decades extensive research has been carried out on changes in the Atlantic Meridional Overturning Circulation (AMOC) and its role during the last deglaciation. At present, only a few high-resolution data sets from the deep eastern North Atlantic (NA) exist for this period. It, therefore, remains uncertain whether deep water changes in the Eastern North Atlantic Basin were governed by alternating contributions of northern and southern deep water or whether the Eastern North Atlantic Basin reflects changes in the initial composition and source of NA deep water only. Furthermore, it is still debated whether such changes are triggered by Northern or Southern Hemisphere climatic changes.

In this study we investigate centennial to decadal scale changes in deep water composition of the Eastern North Atlantic Basin over the last 15 ka BP. We used sediment cores GEOFAR KF16 and MD08-3180 (37.984°N; 31.118°W, wd. 3050 m/37.999°N; 31.134°W, wd 3064 m), obtained from a small basin at the eastern flank of the Mid Atlantic Ridge (MAR) south of the Azores Islands. Under modern conditions the coring site is situated at the boundary between southern Lower Deep Water (LDW) and northern Eastern North Atlantic Deep Water (ENADW) consisting of Iceland Scotland Overflow Water (ISOW) and Labrador Sea Water (LSW) (Fig. 1). Distinct differences between the three water masses in terms of ventilation state, temperature, and salinity signatures are ideal for tracking changes in the deglacial NA deep water distribution. For these reconstructions we use paired benthic foraminifera stable isotope ($\delta^{13}C$, $\delta^{18}O$) and Mg/Ca bottom water temperature (BWT) reconstructions, including salinity estimates using $\delta^{18}O$ values corrected for ice volume changes ($\delta^{18}O_{ivc}$) and temperature changes ($\delta^{18}O_{w\text{-}ivc}$).

The results show a close coupling of low BWT (1.5 °C) and $\delta^{13}C$ (0–0.5 ‰) values during the end of cold Heinrich event 1 (H1), the Younger Dryas (YD) and the Preboreal (PB), that were coeval with a major decrease of $\delta^{18}O_{w\text{-}ivc}$ values that can be associated with a freshening of the deep water. These subtropical ENADW changes are in phase with the NGRIP Greenland ice core $\delta^{18}O$ record (Andersen et al. 2006) and with subpolar NADW changes. The $\delta^{13}C/\delta^{18}O_{ivc}$ signatures from our coring site (Fig. 2) are similar to those from the subpolar

1 Institute of Geosciences, University of Kiel, Ludewig-Meyn Straße 10, 24118 Kiel, Germany.
2 Institute of Prehistoric and Protohistoric Archaeology, University of Kiel, Johanna-Mestorf-Straße 2–6, 24118 Kiel, Germany.
3 Leibniz Laboratory for Radiometric Dating and Stable Isotope Research, University of Kiel, Max-Eyth-Str. 11–13, 24118 Kiel, Germany.

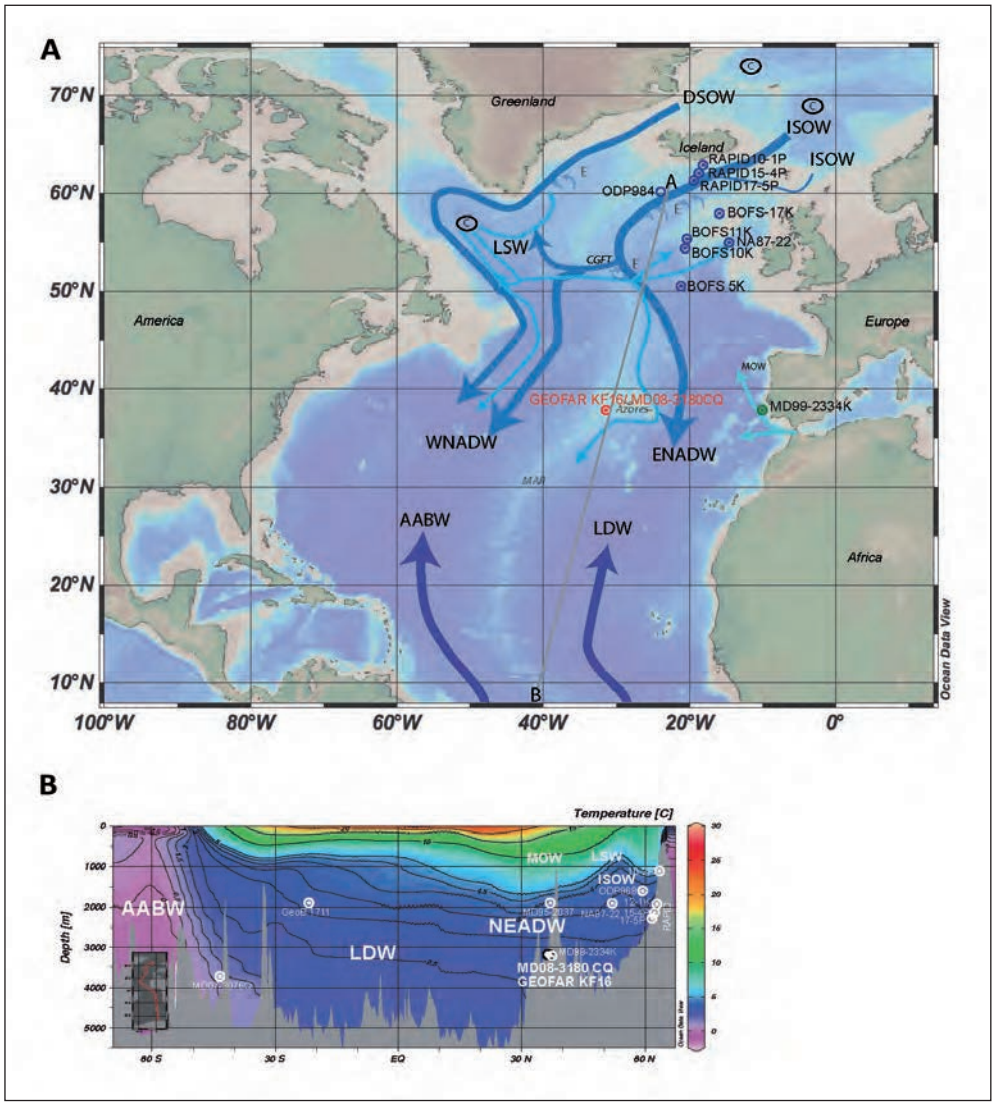


Fig. 1 Overview of the modern deep water hydrography at the Azores coring site (GEOFAR16/ MD08-3180) (red dot) (Repschläger et al. 2015a). Additional cores (Skinner et al. 2003, Thornalley et al. 2010, Waelbroeck et al. 2011, Yu et al. 2008) used in this study are indicated in blue dots. (*A*) Map with the main deep water currents of the NA modified after Schott et al. (2004). (*B*) Temperature cross-section of the Eastern North Atlantic Basin, cores used in this study are indicated. Both figures are based on Ocean Data View. © Deep water convection areas. Abbreviations: NAC North Atlantic Current; ISOW Iceland-Scotland Overflow Water; DSOW Denmark-Strait-Overflow-Water; LSW Labrador-Sea Water; MOW Mediterranean Overflow Water; ENADW Eastern North Atlantic Deep Water; WNADW Western North Atlantic Deep Water; LDW Lower Deep Water; AABW Antarctic Bottom Water, CGFT Charlie- Gibbs-Fracture-Zone, E Entrainment

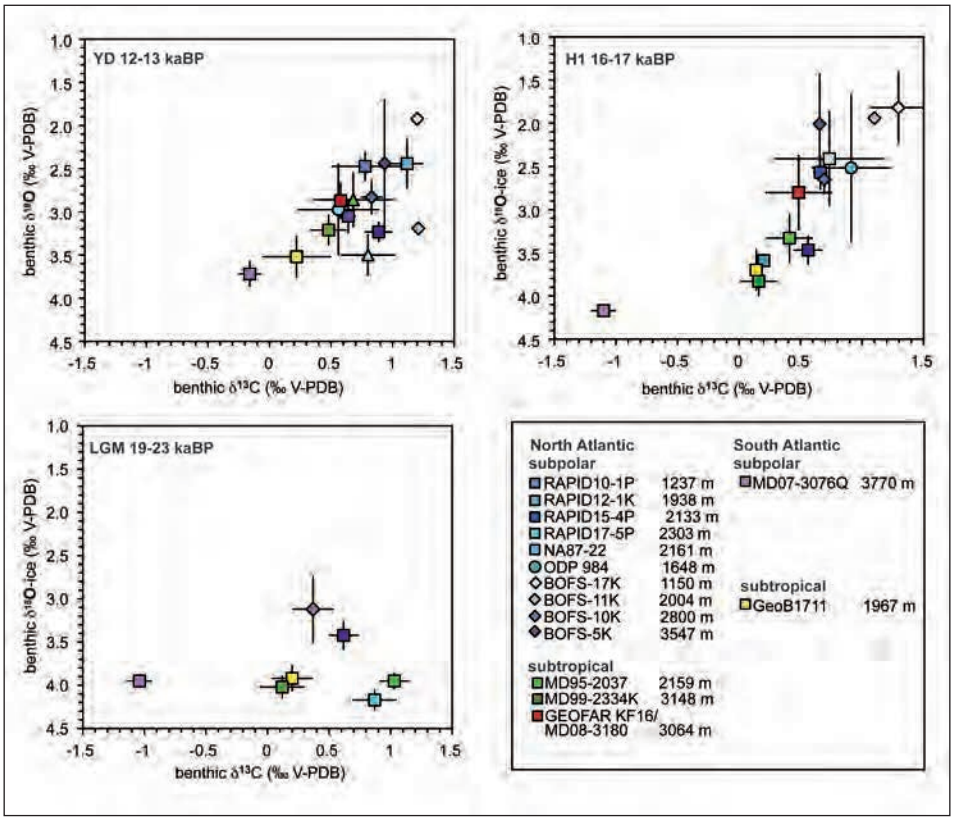


Fig. 2 Three deglacial time slices (modified after Repschläger et al. 2015a) showing $\delta^{13}C/\delta^{18}O_{-ice}$ cross plots comparing cores GEOFAR KF16/MD08-3180 from the Azores coring site with records obtained from the Eastern Atlantic Basin (Waelbroeck et al. 2011), supplemented with four RAPID cores from the South Iceland Rise (Thornalley et al. 2010), BOFS cores from the supolar ENAB (Yu et al. 2008 and citations therein), and core ODP 986 from the Reykjanes Ridge (Praetorius et al. 2008). The cross-plots indicate that changing contributions and compositions of northern and southern sourced deep water can explain the deglacial deep water changes. Azores $\delta^{13}C$ data obtained from *C. wuellerstorfi* published in Repschläger et al. (2015b).

North Atlantic, becoming more negative during the Deglacial. This cannot be explained by a deep water intrusion of southern origin reaching northward towards the Azores coring site, as the AABW $\delta^{18}O$ signature was more positive during the Deglacial than the Northern Hemisphere end-member.

Thus we assume a northern origin of the cold, less saline, low $\delta^{13}C$ deep water that is observed at the Azores coring site during the H1 and the YD. This assumption contradicts the classical interpretation of deglacial $\delta^{13}C$ and Pa/Th data sets (e.g. Gherardi et al. 2009, Mcmanus 2004, Piotrowski et al. 2012, Roberts et al. 2010, Sarntheim et al. 1994) and requires a process, which can explain a dominance of a deep water mass with a more negative $\delta^{13}C$ produced in northern high latitudes. We assume that the low $\delta^{13}C$ signature is related to the existence of a third deglacial water mass, e.g., a glacial lower NADW (Yu et al. 2008), that extended down to 3060 m wd at 38°N. The influence of brine water formation as postulated

to have caused $\delta^{13}C$ changes within the Nordic Seas (e.g. Meland et al. 2008, Thornalley et al. 2010, Waelbroeck et al. 2011) could not be proofed by our data.

The Northern Hemisphere governance of the deep water composition changes instead of a N-S see-saw mechanism also seems to be evident over the early Holocene under stepwise increasing $\delta^{13}C$ values that suggest increasing ENADW production with minor but distinct interruptions (at 10.8, 10.6, 9.1, 8.4, 8.1 and 7.2 ka BP), which were most probably also triggered in the subpolar NA.

Our new dataset indicates that deglacial deep water changes are governed by changes in NADW composition instead of changing contributions of northern and southern sourced deep water. Thus it is likely that the deglacial deep water changes were triggered by changes in the Northern Hemisphere. Furthermore, our results strengthen the arguments that deep water convection remained active in the Nordic Seas over the Deglacial (e.g. Dokken and Jansen 1999, Meland et al. 2008), and supports the existence of glacial lower NADW (Yu et al. 2008) during the Deglacial. Our data implies that this water mass that is characterized by low $CO_3^{2-}$ concentrations, extended further southward and at least 200 m deeper than previously expected. As already suggested by Yu et al. (2008) this deep reaching glacial lower NADW could result in a decrease of carbon sequestration in the deep North Atlantic.

## *References*


Andersen, K. K., Svensson, A., Johnsen, S., Rasmussen, S. O., Bigler, M., Röthlisberger, R., Ruth, U., Siggaard-Andersen, M.-L., Steffensen, J. P., Dahl-Jensen, D., Vinther, B. M., and Clausen, H. B.: The Greenland ice core chronology 2005, 150-0 ka. Part 1: Constructing the time scale. Quat. Sci. Rev. *25*/23–24, 3246–3257 (2006)

Dokken, T., and Jansen, E.: Rapid changes in the mechanism of ocean convection during the last glacial period. Nature *401*, 458–461 (1999)

Gherardi, J. M., Labeyrie, L., Nave, S., Francois, R., McManus, J. F., and Cortijo, E.: Glacial-interglacial circulation changes inferred from $^{231}Pa/^{230}Th$ sedimentary record in the North Atlantic region. Paleoceanography *24*/2, PA2204 (2009)

McManus, J. F., Francois, R., Gherardi, J. M., Keigwin, L. D., and Brown-Leger, S.: Collapse and rapid resumption of Atlantic meridional circulation linked to deglacial climate changes. Nature *428*/6985, 834–837 (2004)

Meland, M. Y., Dokken, T. M., Jansen, E., and Hevroy, K.: Water mass properties and exchange between the Nordic seas and the northern North Atlantic during the period 23-6 ka: Benthic oxygen isotopic evidence. Paleoceanography *23*/1, 19 (2008)

Piotrowski, A. M., Galy, A., Nicholl, J. A. L., Roberts, N., Wilson, D. J., Clegg, J. A., and Yu, J.: Reconstructing deglacial North and South Atlantic deep water sourcing using foraminiferal Nd isotopes. Earth Planet. Sci. Lett. *357*/358(0), 289–297 (2012)

Praetorius, S. K., McManus, J. F., Oppo, D. W., and Curry, W. B.: Episodic reductions in bottom-water currents since the last ice age. Nature Geosci. *1*/7, 449–452 (2008)

Repschläger, J., Weinelt, M., Andersen, N., Garbe-Schönberg, D., and Schneider, R.: Northern source for Deglacial and Holocene deepwater composition changes in the Eastern North Atlantic Basin. Earth Planet. Sci. Lett. (in review) (2015a)

Repschläger, J., Weinelt, M., Kinkel, H., Andersen, N., Blanz, N., and Schwab, C.: Response of the central subtropical North Atlantic surface hydrography on Deglacial and Holocene AMOC changes. Paleoceanography (in review) (2015b)

Roberts, N. L., Piotrowski, A. M., McManus, J. F., and Keigwin, L. D.: Synchronous deglacial overturning and water mass source changes. Science *327*/5961, 75–78 (2010)

Sarnthein, M., Winn, K., Jung, S. J. A., Duplessy, J.-C., Labeyrie, L., Erlenkeuser, H., and Ganssen, G.: Changes in east Atlantic deepwater circulation over the last 30000 years: Eight time slice reconstructions. Paleoceanography *9*/2, 209–267 (1994)

Schott, F., Zantopp, R., Stramma, L., Dengler, M., Fischer, J., and Wibaux, M.: Circulation and deep-water export at the western exit of the subpolar North Atlantic. J. Phys. Oceanogr. *34*, 817 (2004)

Skinner, L. C., Shackleton, N. J., and Elderfield, H.: Millennial-scale variability of deep-water temperature and $\delta^{18}O_{dw}$ indicating deep-water source variations in the Northeast Atlantic, 0–34 cal. ka BP. Geochem. Geophys. Geosyst., *4*/12; 1098; doi:10.1029/2003GC000585 (2003)

Thornalley, D., Elderfield, H., and McCave, I. N.: Intermediate and deep water paleoceanography of the northern North Atlantic over the past 21,000 years. Paleoceanography *25*/1, PA1211 (2010)

Waelbroeck, C., Skinner, L. C., Labeyrie, L., Duplessy, J. C., Michel, E., Vazquez Riveiros, N., Gherardi, J. M., and Dewilde, F.: The timing of deglacial circulation changes in the Atlantic. Paleoceanography *26*/3, PA3213 (2011)

Yu, J., Elderfield, H., and Piotrowski, A. M.: Seawater carbonate ion-$\delta^{13}C$ systematics and application to glacial-interglacial North Atlantic ocean circulation. Earth Planet. Sci. Lett. *271*/1,4, 209–220 (2008)

Janne Repschläger
University of Kiel
Institute for Geosciences
Ludewig-Meyn-Straße 10
Room 11
24118 Kiel
Germany
Phone: +49 431 8802884
Fax: +49 431 8801912
E-Mail: jr@gpi.uni-kiel.de

Nova Acta Leopoldina NF *121*, Nr. 408, 337–339 (2015)

# Implementing Water Isotopes in the MIT Ocean General Circulation Model (MITgcm)

Rike Völpel,[1, 2] André Paul,[1, 2] Annegret Krandick,[1, 2] Stefan Mulitza,[1] and Michael Schulz[1,2]

With 1 Figure

During the last deglaciation large amounts of freshwater, emanating from the continental ice sheets over the Northern Hemisphere, entered the North Atlantic and likely affected the Atlantic Meridional Overturning Circulation (AMOC – e.g. Clark et al. 2002). Since glacial meltwater has a very characteristic water isotopic signature, water isotope ratios can be used to trace the meltwater signal in the ocean.

In the present study, we include the water isotopes $H_2{}^{16}O$, HDO and $H_2{}^{18}O$ as passive tracers in the MIT ocean general circulation model (MITgcm), which enables the investigation of present and past states of ocean circulation and a direct comparison with proxy data (oxygen-isotopes in foraminiferal calcite – $\delta^{18}O_c$). The MITgcm is used in a global configuration (Marshall et al. 1997, Adcroft et al. 2004) with a horizontal resolution of approximately 2.8° and 15 levels in the vertical, ranging in thickness from 50 m at the surface and 690 m at depth, giving a maximum model depth of 5200 m. We use a nonlinear free surface in combination with the real freshwater flux as a natural boundary condition (Huang 1993). Special care is given to an annual balanced freshwater flux by implementing a correction factor for precipitation.

To perform a pre-industrial (PI) experiment, the model is forced with the isotopic content of precipitation and water vapor obtained from an atmospheric general circulation model (NCAR IsoCAM – Tharammal et al. 2013), while the kinetic fractionation during evaporation is treated explicitly in the MITgcm. Fractionation during the formation of sea ice is neglected, because it is very small and leads to no observable effect on the isotopic composition of sea water ($\delta^{18}O_w$ – Craig and Gordon 1965). Furthermore, the isotopic composition of river runoff is set to 0 ‰ with reference to the V-SMOW (Vienna Standard Mean Ocean Water), whereby no difference between river runoff in low and high latitudes occurs.

Comparing the resulting distribution of $\delta^{18}O_w$ to the NASA GISS Global Seawater Oxygen-18 Database (Schmidt et al. 1999), we obtain a good agreement between the simulated and observed values (Fig. 1). General pattern and latitudinal gradients at the sea surface as well as in the deep ocean are faithfully reproduced. However, the sea surface in northern high latitudes is enriched in $^{18}O$, which is caused by insufficient river runoff.

1 MARUM – Center for Marine Environmental Sciences, University of Bremen, 28359 Bremen, Germany.
2 Department of Geosciences, University of Bremen, Klagenfurter Straße, 28359 Bremen, Germany.

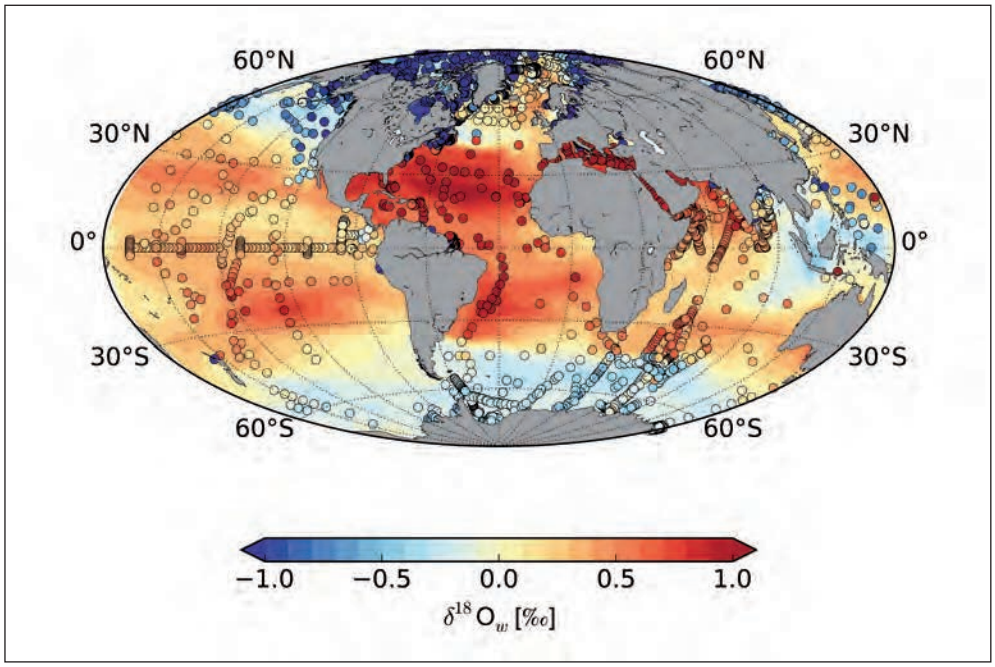


Fig. 1 Preliminary result of modelled sea surface $\delta^{18}O_w$ compared to the NASA GISS Global Seawater Oxygen-18 Database (colored circles – Schmidt et al. 1999).

Hence, as a next step, river runoff with a reasonable isotopic composition will be implemented in the ocean model. Further, surface boundary conditions will be derived from output of the NCAR IsoCAM to simulate water isotopes during the LGM and last deglaciation. For comparison with proxy data, we compile a synthesis of benthic foraminiferal $\delta^{18}O_c$ for the Atlantic Ocean.

## *References*

Adcroft, A., Hill, C., Campin, J., Marshall, J., and Heimbach, P.: Overview of the formulation and numerics of the MIT GCM. In: Proceeding of the ECMWF Seminar Series on Numerical Methods, Recent Developments in Numerical Methods for Atmosphere and Ocean Modelling, ECMWF; pp.139–149 (2004)

Clark, P. U., Pisias, N. G., Stocker, T. F., and Weaver, A. J.: The role of the thermohaline circulation in abrupt climate change. Nature *415*, 863–869 (2002)

Craig, H., and Gordon, L. I.: Deuterium and oxygen-18 variations in the ocean and the marine atmosphere. In: Tongiogi, E. (Ed.): Stable Isotopes in Oceanographic Studies and Paleotemperatures. Spoleto, Italy, 9–130 (1965)

Huang, R. X.: Real freshwater flux as a natural boundary condition for the salinity balance and thermohaline circulation forced by evaporation and precipitation. J. Phys. Oceanogr. *23*, 2428–2446 (1993)

Marshall, J., Adcroft, A., Hill, C., Perelman, L., and Heisey, C.: A finite-volume, incompressible Navier Stokes model for studies of the ocean on parallel computers. J. Geophys. Res. *102*/C3, 5753–5766 (1997)

Schmidt, G. A., Bigg, G. R., and Rohling, E. J.: Global Seawater Oxygen-18 Database – v1.21. http://data.giss.nasa.gov/o18data/ (1999)

Tharammal, T., Paul, A., Merkel, U., and Noone, D.: Influence of Last Glacial Maximum boundary conditions on the global water isotope distribution in an atmospheric general circulation model. Clim. Past *9*, 789–809 (2013)

Rike Völpel
University of Bremen
MARUM – Center for Marine Environmental Sciences
Postfach 330 440
28334 Bremen
Germany
Phone: +49 421 21865456
Fax: +49 421 21865456
E-Mail: rvoelpel@marum.de

Nova Acta Leopoldina NF *121*, Nr. 408, 341–344 (2015)

# Simulating Holocene Variations of the Eastern Tropical South Pacific Oxygen Minimum Zone

Xu Xu,[1] Birgit Schneider,[2] and Wonsun Park[3]

With 2 Figures

The distribution of dissolved oxygen in the ocean is controlled by ocean transport and biogeochemical cycling. Oxygen is considered a key parameter of biogeochemical cycles, and especially in areas of low oxygen concentrations it has strong relevance for nutrient cycling and eventually the global carbon system (Bopp et al. 2002). Oxygen minimum zones (OMZs) are located at subsurface ocean, mainly in the tropics, where ventilation by ocean circulation is rather sluggish and/or oxygen consumption due to the decomposition or organic matter is relatively high. Although the tropical OMZs constitute only ~1 % of global ocean volume, they have profound impact on the oceanic nutrient budgets, and thus global biological productivity and $CO_2$-fixation (Stramma et al. 2010). Modern observations indicate an expansion/intensification of OMZs, probably caused by climate change (Stramma et al. 2008), so that it can be assumed that OMZs also must have exhibited significant variations over geological times, including implications for oceanic carbon and nutrient cycling (Meissner et al. 2005). For more reliable future projections of oceanic oxygen distributions, it is important to better understand their sensitivity to climate variability and climate change.

The climate of the Holocene, the current warm period, is globally relative stable, which means that Holocene climate change is more characterized by pronounced reorganizations of seasonal and interannual variability and rather regional long-term trends. Therefore, this epoch provides an ideal scenario to assess both the impact of internal climate variability and climate change on OMZ.

In our study, we use an atmosphere-ocean-sea ice general circulation model, the Kiel Climate Model (KCM, Park et al. 2009) in combination with a marine biogeochemical model PISCES (Aumont and Bopp 2006) to simulate oceanic dissolved oxygen, nutrients and marine productivity in the early (9.5 ka BP), middle (6 ka BP), and late Holocene (preindustrial). We developed an anomaly method that considers climate model biases, which are common in the state-of-the-art non-flux corrected model. The method uses KCM circulation anomalies between 6 K and preindustrial (0 K) as well as 9.5 K and 0 K, and those anomalies are added on a reference ocean circulation field (NEMO standalone) to form a new ocean field for early Holocene and mid-Holocene. The PISCES simulation with the chosen reference ocean

1 Institute of Geosciences, University of Kiel, Kiel, Germany; E-Mail: xu@gpi.uni-kiel.de.
2 Institute of Geosciences, University of Kiel, Kiel, Germany; E-Mail: Bschneider@gpi.uni-kiel.de.
3 GEOMAR Helmholtz Centre for Ocean Research Kiel, Kiel, Germany, E-Mail: wpark@geomar.de.

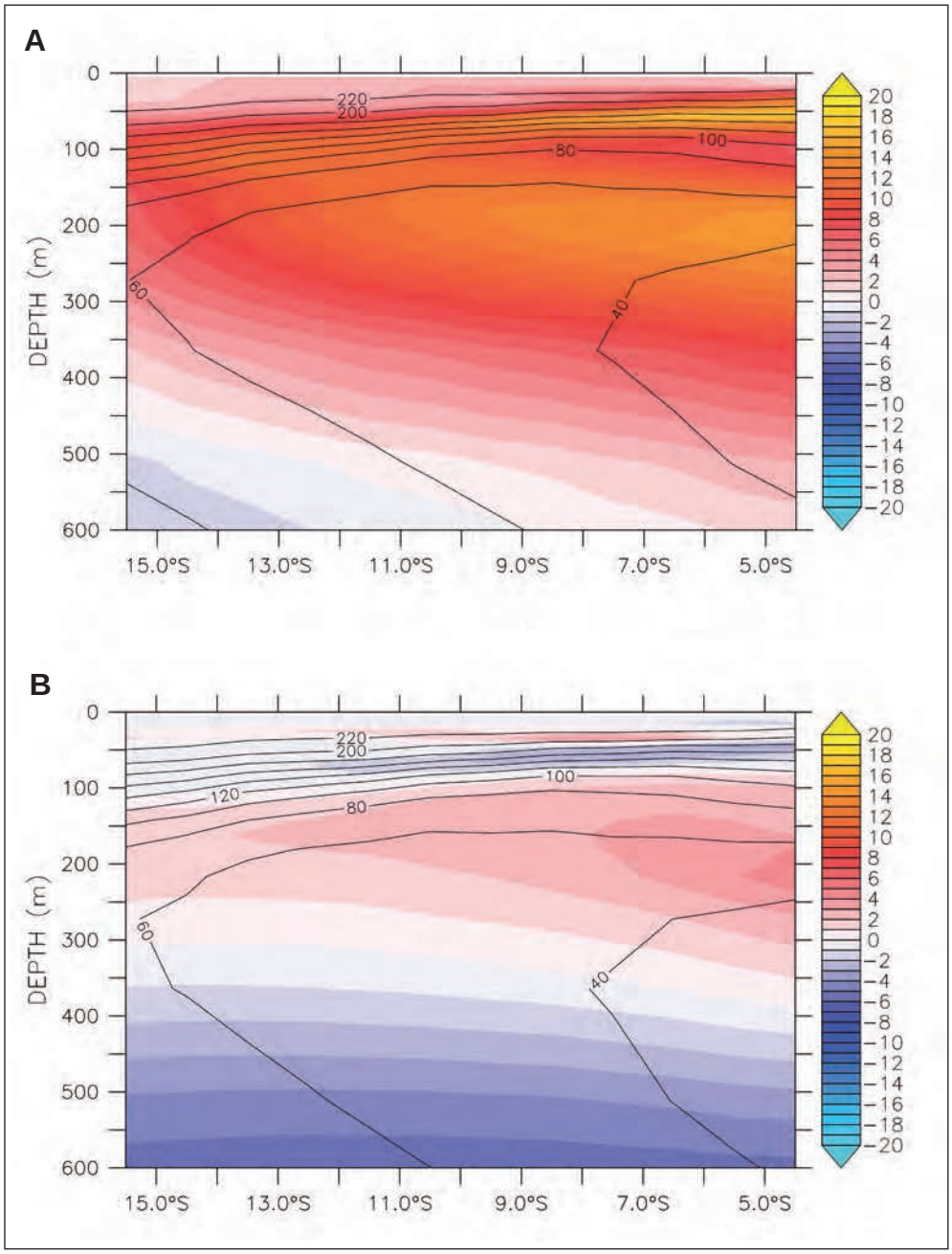


Fig. 1 6 K to 0 K (*A*) and 9.5 K to 6 K (*B*) oxygen change (shade, µmol/L) and dissolved oxygen concentration (contour, µmol/L) average between 90W and 75W.

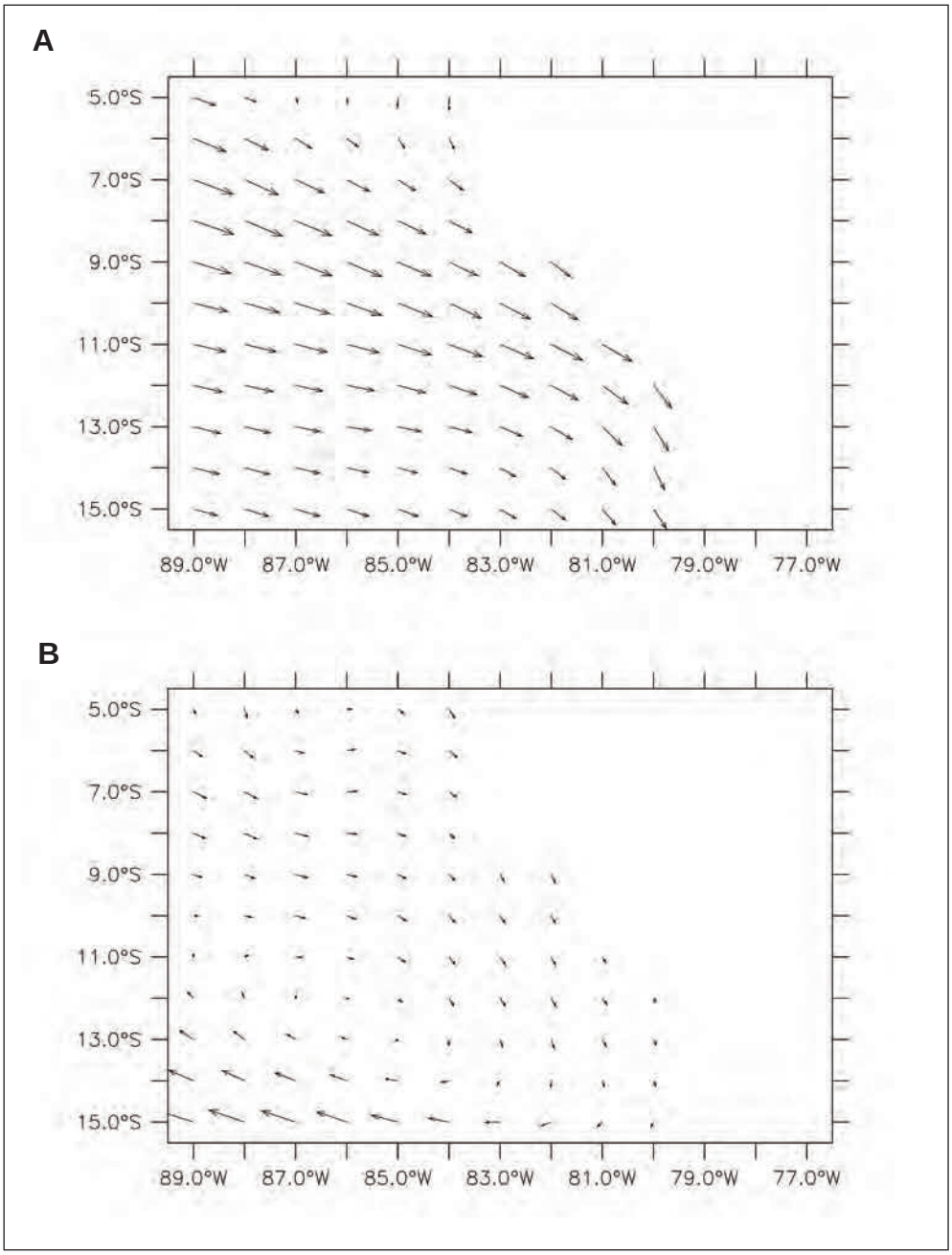


Fig. 2 Maps of 6 K to 0 K (*A*) and 9.5 K to 6 K (*B*) oxygen transport change (arrow, mmol/m$^2$s) averaged over 100 m to 600 m

circulation field is in fairly good agreement with observation and performs as well as other Earth System Models.

In our analysis we focus on the Eastern Tropical South Pacific (5S–15S and 75W–90W). Despite the relatively stable global climate conditions of the Holocene, here the changes in oxygen concentration are up to 10 %. We find an intensification of low oxygen conditions over the Holocene, while the early Holocene trend (9.5 K to 6 K) is less pronounced than the late Holocene trend (6 K to preindustrial) (Fig. 1). The analysis of oxygen transport between 100 m and 600 m depth in this area (Fig. 2) reveals a stronger south-east ward oxygen transport at middle Holocene than preindustrial. Therefore, the mid-Holocene relaxation of the OMZ off Peru is mostly due to better oxygen ventilation.

## *References*

Aumont, O., and Bopp, L.: Globalizing results from ocean in situ iron fertilization studies. Global Biogeochem. Cycles *20*, GB2017; doi:10.1029/2005GB002591 (2006)

Bopp, L., Quéré, C. L., Heimann, M., and Manning, A. C.: Climate-induced oceanic oxygen fluxes: Implications for the contemporary carbon budget. Global Biogeochem. Cycles *16*/2, 1022; doi:10.1029/2001GB001445 (2002)

Meissner, K. J., Galbraith, E. D., and Völker, C.: Denitrification under glacial and interglacial conditions: A physical approach. Paleoceanography *20*, PA3001; doi:10.1029/2004PA001083 (2005)

Park, W., Keenlyside, N., Latif, M., Ströh, A., Redler, R., Roeckner, E., and Madec, G.: Tropical Pacific climate and its response to global warming in the Kiel climate model. J. Climate *22*, 71–92; http://dx.doi.org/10.1175/2008JCLI2261.1 (2009)

Stramma, L., Johnson, G. C., Sprintall, J., and Mohrholz, V.: Expanding oxygen minimum zones in the tropical oceans. Science *320*, 655–685 (2008)

Stramma, L., Schmidtko, S., Levin, L. A., and Johson, G. C.: Ocean oxygen minima expansions and their biological impacts. Deep-Sea Res. *I*, doi:10.1016/j.dsr.2010.01.005 (2010)

Dr. Xu Xu
Institute of Geosciences
University of Kiel
Ludewig-Meyn-Straße 10
Room 114
24118 Kiel
Germany
Phone: +49 431 8802947
Fax: +49 431 8801912
E-Mail: xu@gpi.uni-kiel.de

Nova Acta Leopoldina NF *121*, Nr. 408, 345–350 (2015)

# Changes in the Terrestrial Carbon and Nitrogen Cycles since the Last Glacial Maximum

Sönke Zaehle,[1] Joy S. Singarayer,[2] and Pierre Friedlingstein[3]

With 3 Figures and 1 Table

From the time of the Last Glacial Maximum (LGM, 21 ka BP) to the pre-industrial era (0 ka BP) the volume mixing ratio of $CO_2$ in the atmosphere increased by about 100 ppm (from 184 to 278 ppm). The magnitude of oceanic carbon (C) release required to explain this rise and the concurrent isotopic changes of atmospheric $CO_2$ depends on estimates of changes in terrestrial C. However, a comprehensive understanding of the terrestrial carbon dynamics during the transition from glacial to pre-industrial conditions is still lacking (Ciais et al. 2011). Estimates of the changes in terrestrial C pools are either inferred from $^{13}C$ isotope data and mass-balance approaches, or based on the application of process-based ecosystem models; and typically range between 0 Pg C and 700 P g C (Bird et al. 1996, Köhler and Fischer 2004, Ciais et al. 2011). Terrestrial biosphere models used in studies of the LGM carbon cycle generally do not take account of the wide-spread nitrogen (N) limitation of temperate, boreal, and arctic ecosystems. Models not accounting for these limitations tend to overestimate the productivity of vegetation, and – in consequence – carbon storage in these ecosystems (Zaehle et al. 2010, Zaehle 2013).

Here, we investigate the effects of the carbon-nitrogen cycle coupling on projections of the terrestrial C storage increase between 21 ka and 0 ka by applying the terrestrial biosphere model O-CN (Zaehle and Friend 2010, Zaehle et al. 2011). O-CN has been developed from the land surface model ORCHIDEE (Krinner et al. 2005), and describes the nitrogen and carbon fluxes and stocks of vegetation and soil organic matter for 10 natural plant functional types at a half hourly timescale. Nitrogen availability directly controls photosynthesis and respiration of vegetation through tissue nitrogen concentrations, which are varying in time according to N availability, and effects on plant allocation (e. g. the root, shoot ratio), and thus foliage area and root growth. Nitrogen availability also affects the temperature-sensitive rate of organic matter decomposition and the net mineralization of nitrogen. The modelled ecosystem receives inputs from biological N fixation and atmospheric N deposition, and simulates losses of N to leaching and volatilization based on the process-based simulation of nitrification and denitrification. The biogeochemical fluxes are tightly coupled to the calculations of the terrestrial energy and water balance.

1 Biogeochemical Integration Department, Max Planck Institute for Biogeochemistry, Hans-Knöll-Straße 10, 07745 Jena, Germany; E-Mail: szaehle@bgc-jena.mpg.de.
2 Centre for Past Climate Change and Department of Meteorology, University of Reading, UK.
3 CEMPS, Earth System Science, University of Exeter, UK.

To isolate the effects of N dynamics, the O-CN model has been run twice, once with explicit accounting for N dynamics (referred to as CN cycle), and once with N concentrations set to global averages of observed values (referred to as C cycle), such that plant productivity and soil organic matter decomposition correspond to an ecosystem with average N availability, not taking account of the spatial-temporal patterns of N availability. A key uncertainty in these simulations is the response of biological N fixation to the differing climatic and atmospheric conditions between 0 and 21 ka. We therefore conducted two experiments with the CN cycle model: one, in which biological N fixation was derived from an empirical relationship between actual evapotranspiration and biological N fixation (referred to as pre-calculated BNF, Cleveland et al. 1999), and another one, in which biological N-fixation was calculated dynamically based on the non-structural carbohydrate reserve of the plant, its N stress, as well as the C cost of N fixation, which varies with temperature (referred to as dynamic BNF, Houlton et al. 2008). Both approaches yielded comparable global vegetation production and ecosystem carbon storage, despite an about 25 % lower global nitrogen fixation in the dynamic case.

Driving data for O-CN, i.e. the climate forcing, as well as associated information on atmospheric $CO_2$ volume mixing ratios, orbital parameters, land-sea mask, and vegetation distribution, were obtained from 21 ka, 6 ka and 0 ka snapshot simulations using the Hadley Centre climate model, HadCM3 (Singarayer and Valdes 2010). The O-CN model was applied at the spatial resolution of the climate model (i.e. 3.25° × 2.5°). A weather generator (Krinner et al. 2005) was used to dis-aggregate monthly climate model output to half-hourly values. Simulations were made for each time slice from bare ground and until an equilibrium state of the terrestrial C cycle was obtained. That is to say, that the simulations do not account for transient changes in vegetation and soil C following deglaciation, nor the transient effects of biome shifts.

The O-CN simulations show that net primary production, vegetation and soil C storage were greatly reduced north of 40°N under LGM conditions, but that lower biomass densities and soil C storage also occured in tropical regions (Fig. 1). In concert with these C cycle changes, also biological N-fixation was considerably lower in these regions at this time. Globally integrated, net primary production was 15 Pg C $a^{-1}$ (Tab. 1) lower in LGM conditions (34 Pg C $a^{-1}$) relative to pre-industrial conditions (48 Pg C $a^{-1}$), which is comparable to changes inferred with the C cycle version of the O-CN model, and previous studies (Köhler and Fischer 2004).

Tab. 1 Key carbon and nitrogen cycle properties and their change between 21 ka and 0 ka derived from the C cycle and the CN cycle version with dynamic biological N fixation (BNF).

| | | C cycle | | | CN cycle | | |
|---|---|---|---|---|---|---|---|
| **Parameter** | **Units** | **21 ka** | **0 ka** | **0 ka–21 ka** | **21 ka** | **0 ka** | **0 ka–21 ka** |
| NPP | Pg C $a^{-1}$ | 35.8 | 52.4 | 16.6 | 33.6 | 48.2 | 14.6 |
| Vegetation C | Pg C | 261 | 616 | 355 | 232 | 548 | 316 |
| Soil C | Pg C | 699 | 1203 | 504 | 586 | 960 | 375 |
| **Total Land C** | **Pg C** | **960** | **1819** | **859** | **818** | **1508** | **691** |
| BNF | Tg N $a^{-1}$ | n.a. | n.a. | n.a. | 73,1 | 98.3 | 25.1 |

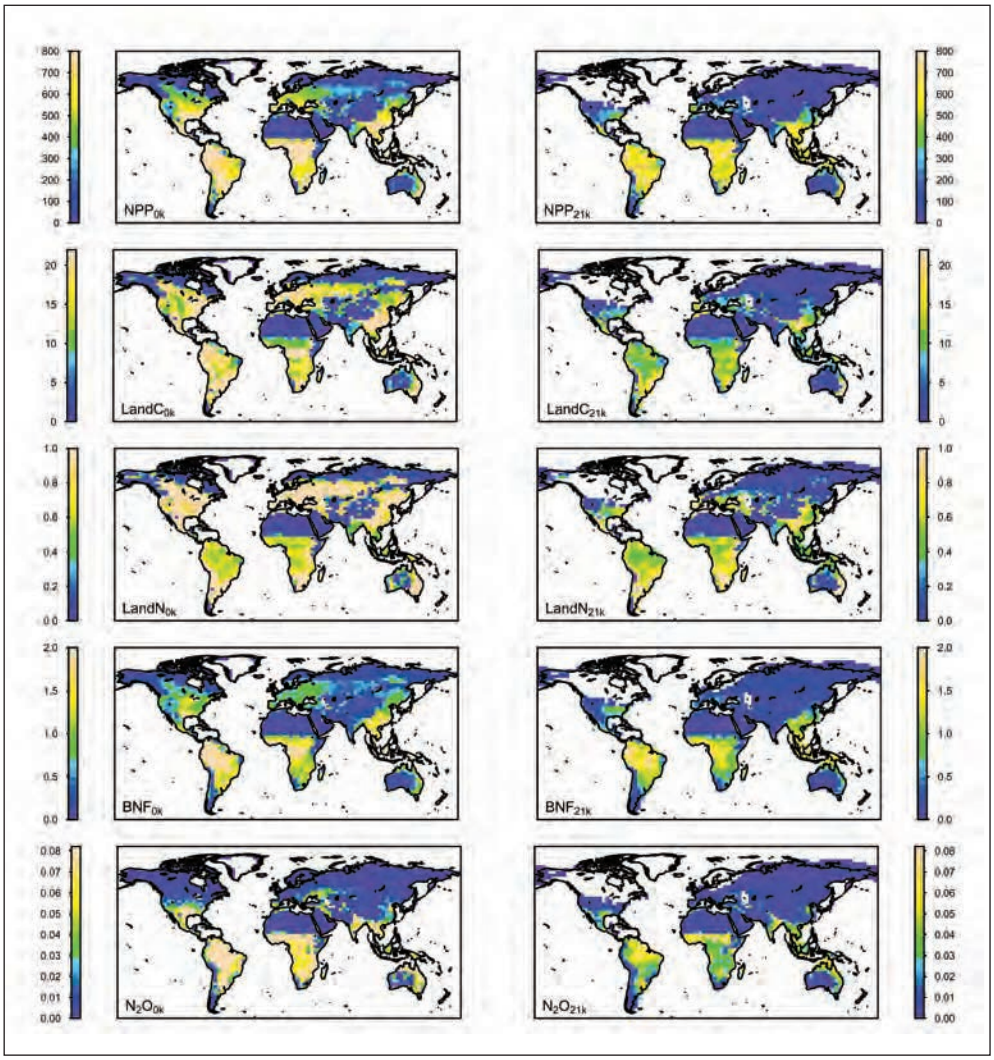


Fig. 1 Simulated net primary production (NPP; g C $m^{-2}$ $a^{-1}$), ecosystem C storage (LandC; kg C $m^{-2}$), ecosystem N storage (LandN; kg N $m^{-2}$), biological N fixation (g N $m^{-2}$ $a^{-1}$), and terrestrial $N_2O$ emissions ($N_2O$; g N $m^{-2}$ $a^{-1}$) derived from the dynamic BNF run with O-CN for the time slice of 21 ka and 0 ka.

The increases in atmospheric $CO_2$ and the concurrent climate change between LGM, 6 ka, and 0 ka has caused net primary production and ecosystem C storage to increase (Fig. 2). Interestingly, the relative increase in net vegetation production (NPP; 43 %) is larger than the relative increase in biological N fixation (34 %), indicating that – assuming equilibrium – the colder LGM conditions do – globally – not lead to increased N limitation of vegetation production, probably because the direct effect of changes in the atmospheric $CO_2$ mixing ratio on photosynthesis is larger than the indirect effect of temperature (and plant net primary production) on biological N fixation. This finding is robust between the two CN cycle model ver-

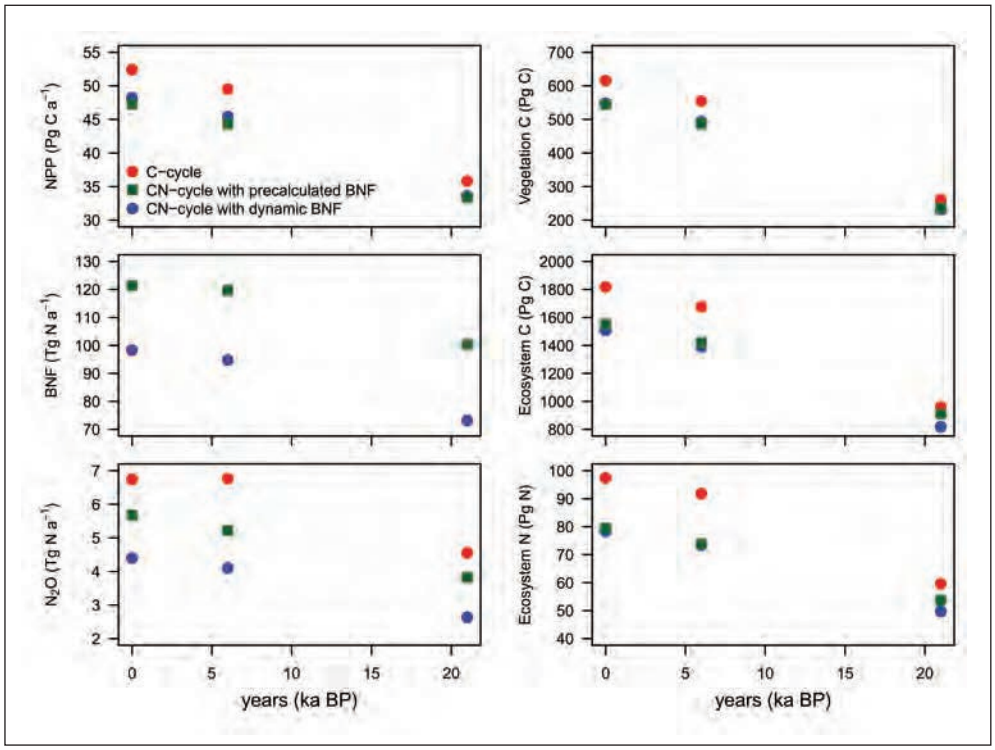


Fig. 2 Simulated global net primary production (NPP), vegetation and ecosystem C storage, ecosystem N storage, biological N fixation, and terrestrial $N_2O$ emissions for the time slices of 21 ka, 6 ka, and 0 ka. Models used: the carbon-cycle only version (C cycle), the carbon-nitrogen cycle version with prescribed BNF (CN cycle with pre-calculated BNF), as well as the carbon-nitrogen cycle version with dynamic BNF (CN cycle with dynamic BNF).

sions applied here: despite a difference in biological N fixation between the two versions of the CN cycle model, projected changes in the terrestrial carbon and nitrogen pools are fairly similar, and diverge notably from the projections of the C cycle version of the model (Fig. 2).

The C cycle model projects a larger difference in terrestrial C and N between LGM and pre-industrial than the CN cycle models (Tab. 1 and Fig. 2). Most of these differences result from strongly attenuated net primary production and terrestrial C storage in the boreal and arctic zone due to N constraints (Fig. 3). Tropical regions are not strongly impacted by nitrogen dynamics, consistent with the observation that tropical ecosystems are typically not strongly limited by N availability (Zaehle 2013). The difference between C cycle and CN cycle models is consistent with earlier studies, showing that not accounting for N availability results in larger estimates boreal vegetation cover, production and biomass. For the O-CN model, earlier studies have shown that accounting for N constraints improved the performance of the model under modern conditions (Zaehle et al. 2010). In total, the differences between the C cycle and CN cycle predictions is 178 Pg C. While this is a significant (and robust) difference, both estimates clearly fall into the range of uncertainty of previous studies.

Our simulations also suggest nearly a doubling of terrestrial $N_2O$ emissions from around 2.5 Tg N a$^{-1}$ to 4.4 Tg N a$^{-1}$, which is commensurate with the total change in atmospheric $N_2O$

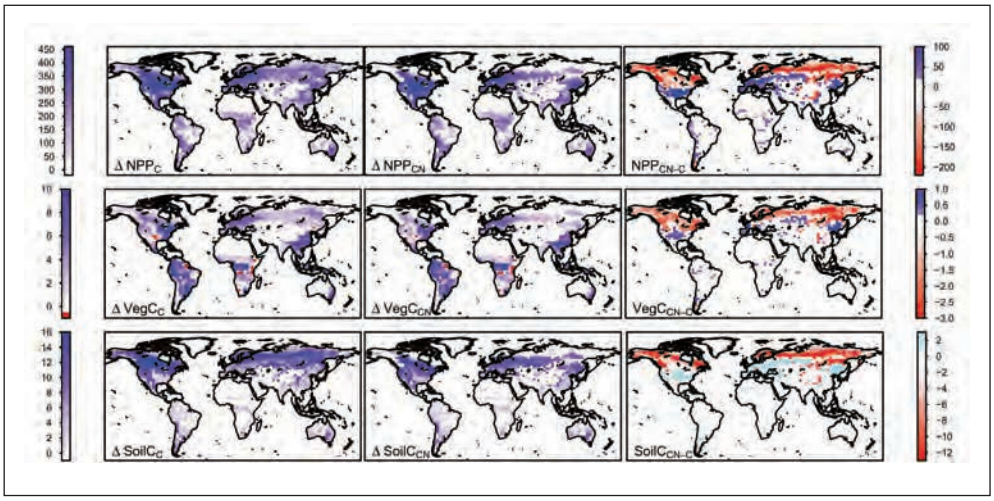


Fig. 3 Simulated change in net primary production (NPP; g C m$^{-2}$ a$^{-1}$), vegetation C (VegC; kg C m$^{-2}$) and soil C (SoilC; kg C m$^{-2}$) between 21 ka and 0 ka for left: the C cycle version, middle: the CN cycle version with dynamic BNF. The right hand side shows the difference between the C-cycle and CN-cycle versions.

volume mixing ratios observed in the ice core records, however, larger than the estimates reported in the recent study of Schilt et al. (2014), and potentially conflicting with the isotopic evidence presented there.

Our results are preliminary because we assumed steady-state for all time slices, therefore omitting the time-lag between melting and vegetation regrowth on carbon sequestration. Likely, this would tend to increase the gap between the C cycle and CN cycle model versions. We also did not account for the potential presence of old, inactive C (Ciais et al. 2011), which, if melting and becoming an active part of the terrestrial C and N cycle might stimulate vegetation regrowth and reduce the difference between the C cycle and CN cycle versions. Future work will therefore be to investigate include dynamic changes in vegetation between the time slices, so as to account for the succession of ecosystems from bare ground to fully developed under N constraints.

## *References*

Bird, M. I., Lloyd, J., and Farquhar, G. D.: Terrestrial carbon-storage from the last glacial maximum to the present. Chemosphere *33*, 1675–1685 (1996)

Ciais, P., Tagliabue, A., Cuntz, M., Bopp, L., Scholze, M., Hoffmann, G., Lourantou, A., Harrison, S. P., Prentice, I. C., Kelley, D. I., Koven, C., and Piao, S. L.: Large inert carbon pool in the terrestrial biosphere during the Last Glacial Maximum. Nature Geosci. *5*, 74–79 (2011)

Cleveland, C. C., Townsend, A. R., Schimel, D. S., Fisher, H., Howarth, R. W., Hedin, L. O., Perakis, S. S., Latty, E. F., Fischer, J. C. von, Elseroad, A., and Wasson, M. F.: Global patterns of terrestrial biological nitrogen (N-2) fixation in natural ecosystems. Global Biogeochem. Cycles *13*, 623–645 (1999)

Houlton, B. Z., Wang, Y. P., Vitousek, P. M., and Field, C. B.: A unifying framework for dinitrogen fixation in the terrestrial biosphere. Nature *454*, 327–330 (2008)

Köhler, P., and Fischer, H.: Simulating changes in the terrestrial biosphere during the last glacial/interglacial transition. Global and Planetary Change *43*, 33–55 (2004)

Krinner, G., Viovy, N., Noblet-Ducoudré, N. de, Ogée, J., Friedlingstein, P., Ciais, P., Sitch, S., Polcher, J., and Prentice, I. C.: A dynamic global vegetation model for studies of the coupled atmosphere-biosphere system. Global Biogeochem. Cycles *19*, GB1015 (2005)

Schilt, A., Brook, E. J., Bauska, T. K., Baggenstos, D., Fischer, H., Joos, F., Petrenko, V. V., Schaefer, H., Schmitt, J., Severinghaus, J. P., Spahni, R., and Stocker, T. F.: Isotopic constraints on marine and terrestrial N. Nature *516*, 234–237 (2014)

Singarayer, J. S., and Valdes, P. J.: High-latitude climate sensitivity to ice-sheet forcing over the last 120 kyr. Quat. Sci. Rev. *29*, 43–55 (2010)

Zaehle, S.: Terrestrial nitrogen-carbon cycle interactions at the global scale. Phil. Trans. Royal Soc. Series B – Biol. Sci. *368*, 20130125 (2013)

Zaehle, S., and Friend, A. D.: Carbon and nitrogen cycle dynamics in the O-CN land surface model: 1. Model description, site-scale evaluation, and sensitivity to parameter estimates. Global Biogeochem. Cycles *24*, GB1005 (2010)

Zaehle, S., Ciais, P., Friend, A. D., and Prieur, V.: Carbon benefits of anthropogenic reactive nitrogen offset by nitrous oxide emissions. Nature Geosci. *4*, 601–605 (2011)

Zaehle, S., Friend, A. D., Friedlingstein, P., Dentener, F., Peylin, P., and Schulz, M.: Carbon and nitrogen cycle dynamics in the O-CN land surface model: 2. Role of the nitrogen cycle in the historical terrestrial carbon balance. Global Biogeochem. Cycles *24* (2010)

Dr. Sönke Zaehle
Department Biogeochemical Integration
Max Planck Institute for Biogeochemistry
Hans-Knöll-Straße 10
Room: C3.015
07745 Jena
Germany
Phone: +49 3641 576230
Fax: +49 3641 577200
E-Mail: szaehle@bgc-jena.mpg.de

# Rolle der Wissenschaft im Globalen Wandel

Vorträge anlässlich der Jahresversammlung
vom 22. bis 24. September 2012 in Berlin

Nova Acta Leopoldina N. F. Bd. *118*, Nr. 400
Herausgegeben von Detlev Drenckhahn (Würzburg) und
Jörg Hacker (Halle/Saale, Berlin)
(2013, 396 Seiten, 123 Abbildungen, 27 Tabellen, 29,95 Euro,
ISBN: 978-3-8047-3210-0)

Gesellschaftliche Probleme verlangen heute sehr häufig eine Widerspiegelung im Bereich der Wissenschaften. Als Nationale Akademie der Wissenschaften ist die Leopoldina in zunehmendem Maße gefordert, auch Beratung bei Fragen zu liefern, die über Länder und Kontinentgrenzen hinausgreifen: Klimawandel, der Einsatz erneuerbarer Energien, Fragen der Gesundheitsversorgung, die Einrichtung einer effektiveren Landwirtschaft zur Bekämpfung von Hunger in Krisengebieten und die sich wandelnde Altersstruktur von Bevölkerungen in vielen Staaten sind nur einige Beispiele für entsprechende Gebiete mit dringendem Forschungsbedarf. Sie bilden Herausforderungen für die Gesellschaften, die nur in internationaler, oft globaler Zusammenarbeit zu bewältigen sein werden. Daher wählte die Leopoldina 2012 das Thema „Rolle der Wissenschaft im Globalen Wandel“ für ihre Jahresversammlung. Der Band umfasst Beiträge zu den Themenkomplexen „Die Erde im Globalen Wandel“, „Herausforderungen des Globalen Wandels“ und „Lösungswege von Problemen des Globalen Wandels“ sowie zu den gesellschaftlichen und politischen Implikationen der mit dem globalen Wandel verbundenen Prozesse.

*Wissenschaftliche Verlagsgesellschaft Stuttgart*

# Russian-German Synergies in the Scientific Exploration of Northern Eurasia and the Adjacent Arctic Ocean

Leopoldina-Symposium in Zusammenarbeit mit der
Sankt Petersburger Staatlichen Universität
10.–12. September 2012 in Sankt Petersburg

Nova Acta Leopoldina N. F. Bd. *117*, Nr. 399
Herausgegeben von Jörn THIEDE (Kiel) und Wolf Dieter BLÜMEL (Stuttgart)
(2014, 198 Seiten, 73 Abbildungen, 7 Tabellen, 23,95 Euro,
ISBN: 978-3-8047-3242-1)

Der Band behandelt die deutsch-russische Zusammenarbeit bei der wissenschaftlichen Erforschung Nordostsibiriens und des angrenzenden arktischen Meeres. Die wissenschaftlichen Beziehungen in dieser Forschungsregion besitzen eine lange Tradition, die in einem ausführlichen historischen Essay von Jörn THIEDE dargestellt wird. Die kurzen Forschungsbeiträge stammen überwiegend von jungen Wissenschaftlern und sind in Gemeinschaftsarbeit von russischen und deutschen Forschern entstanden. Sie umfassen grundlegende Fragen der Geographie und Geologie des nordöstlichen Sibiriens.

*Wissenschaftliche Verlagsgesellschaft Stuttgart*

ISSN: 0369-5034
ISBN: 978-3-8047-3433-3